

Anisotropic Elasticity of Composite Molecular Networks Formed from Non-Gaussian Chains

K. J. SMITH, JR., A. CIFERRI, and J. J. HERMANS, *Chemstrand Research Center, Inc., Research Triangle Park, Durham, North Carolina*

Synopsis

The theory of composite networks by Berry, Scanlan, and Watson was generalized so as to include the case in which the elasticity of the chains is described by non-Gaussian statistics. For this purpose, existing theories of non-Gaussian networks had to be critically reviewed and a new simple treatment is presented here. This new treatment yields substantially the same results as that obtained from the more complex theory of Wang and Guth. Results obtained from the simple three-chain model for the network, as described by Treloar, were also shown to be in satisfactory agreement with both the new treatment and that of Wang and Guth. The generalized theory of composite networks predicts anisotropic elastic behavior; the tensile force at a given strain should be generally higher for elongation in the direction parallel to orientation than in the direction perpendicular to it. However, depending upon details pertaining to the preparation of the networks (ratio of first and second stage crosslinks and elongation at which the latter are introduced), the tensile force required for elongation in the direction perpendicular to orientation may be higher. It appears that the isotropic elastic behavior, predicted by previous theories of composite networks, is merely a consequence of the use of the Gaussian approximation.

I. INTRODUCTION

When a strip of crosslinked rubber is held stretched at sufficiently high temperatures, a permanent increase of the unstrained length is observed on releasing the stress. Andrews, Tobolsky, and Hanson¹ postulate that this "set" is due to a partial degradation of the initial network and concurrent formation of new chains unstrained at the stretched length. The set network was thus visualized as a "composite" network, the set length resulting from the balancing of the retractive force of one network (unstrained at the original length and characterized by the number of "first stage" crosslinks left unbroken) and the extensive force of a second network (unstrained at the stretched length and characterized by the number of "second stage" crosslinks introduced).

The theory of elasticity of a particular type of composite network (one in which crosslinkage formation in the strained state is unaccompanied by rupture of first stage crosslinks) was formulated by Berry, Scanlan, and Watson.² More complex cases were subsequently treated by others,³ but the main conclusions of the theory of Berry, Scanlan, and Watson were

not modified. According to these authors, the composite network should display isotropic elasticity (relative to the state of ease of the set material) and the shape of the stress-strain isotherm in simple elongation should be given by the familiar strain function of the simple theory of rubber elasticity. However, while isotropic elastic behavior can be expected for networks formed when the rubber is in an isotropic state, it may not be intuitively obvious that a network formed in a state of strain, such as the composite network, should display isotropic elasticity. In fact, experimental evidence clearly indicates anisotropic elastic behavior for networks which had been formed by crosslinking fibrous natural rubber.³ The increase of length on swelling in the direction perpendicular to orientation was up to 15% larger than the corresponding increase in the direction parallel to orientation. A definite interpretation of this effect was not given; however, it was indicated that the tendency of this highly set sample toward oriented recrystallization (accompanied by spontaneous re-elongation) could be responsible. The composite networks prepared by Berry, Scanlan, and Watson² did not exhibit such large sets, and incidence of oriented crystallization was also not apparent. Yet, variations up to 4% of the linear swelling ratios in the directions parallel and perpendicular to orientation were observed while, using the same technique adopted by Berry, Scanlan, and Watson,² it was shown later³ that for networks crosslinked in the isotropic state the linear swelling ratio was effectively the same in all directions.

The existence of anisotropic elasticity in a rubberlike material crosslinked in the oriented state having thus been reported, and the origin of it being unclear, it seemed desirable to reconsider existing theories of polymer networks crosslinked in states of strain, with particular emphasis on their prediction of isotropic elasticity. A recent work by Lodge⁴ unequivocally shows that in the Gaussian approximation, a rubberlike material is necessarily isotropic, irrespective of the fact that some of the crosslinks may be introduced in a state of strain. Since Gaussian statistics were used in the derivations of all present theories of composite networks, the prediction of isotropic elasticity therefore appears obvious. These facts prompted us to generalize the theory of Berry, Scanlan, and Watson to the more accurate non-Gaussian statistical theory which takes into account the finite extensibility of the chains and hence of the network.⁵

The non-Gaussian aspects of a polymeric network have been described by essentially two theoretical treatments; one, an approximate method, which treats the network as a system of three sets of independent chains was originally given by James and Guth⁶ and later by Treloar,⁵ and another, more accurate treatment, based upon the series development of the chain vector distribution function as described by Wang and Guth.⁷ Ishihara, Hashitsume, and Tatibana⁸ have also investigated non-Gaussian behavior but unfortunately certain coefficients appearing in their equations are left undetermined.

The three-chain model⁵ is the simplest approach and has the advantage

of yielding expressions which are written in a closed form. On the other hand, it suffers from the fact that the network model is too idealized, i.e., the reduction of the real network to one consisting of three independent sets of chains having their displacement vectors parallel to the axes of the coordinate system appears unrealistic.

The Wang and Guth⁷ treatment appears far more elegant than the three-chain model, but it yields expressions which cannot be written in closed form and therefore, must be presented by means of a series expansion of terms involving the three strain invariants given by Rivlin.⁵ Furthermore, close examination of Wang and Guth's result reveals certain inconsistencies in their approach which are subject to reexamination; notably, the neglect of certain terms which are, in some cases, more significant than some of those retained. In addition, they found it necessary to replace the real network with one whose network junctions (crosslinkages) were fixed in space at their most probable positions. We deem it desirable, therefore, to present a different theoretical approach to non-Gaussian elasticity, the results of which will be shown to differ slightly from those of Wang and Guth.

Accordingly, the ensuing sections will be concerned first with the development of a suitable expression describing the entropy change, upon deformation, of a network composed of non-Gaussian chains, and later, the application of this result to determine the elastic behavior of composite networks. A subsequent section presents results obtained by utilizing the three-chain model.

For convenience, the principal symbols used throughout are grouped in the appendix.

II. ELASTIC ENTROPY OF A NON-GAUSSIAN NETWORK

We consider a network composed of G flexible chains (a chain being defined as that portion of a polymeric molecule having both ends attached to a crosslink), each containing N statistical links of length b , and make the customary assumptions that the general nature of the result is not seriously altered by the omission of excluded volume effects and chain connectivity patterns. These chains are able to undergo numerous changes in conformation subject only to the condition that no conformation can exceed in length that of the fully extended chain Nb , thus contrasting sharply with Gaussian chains for which there is no ultimate limit of extension.

The general function describing the end-to-end vector distribution for flexible chains has been given by Chandrasekhar⁹ but cannot be immediately used in the form as presented. Wang and Guth,⁶ however, expanded this result so as to obtain a distribution [eq. (1)] which is useful for small deviations from Gaussian behavior and applied the result to their theory of non-Gaussian networks. The first term of their expansion corresponds to the well known Gaussian approximation, whereas the remaining ones represent the leading correction terms of the series. Wang and Guth's

expansion is (retention of additional terms, though possible, is of increasingly doubtful significance):

$$\begin{aligned} \psi_0(\mathbf{r})d\tau &= (3/2\pi Nb^2)^{3/2} d\tau \exp \left\{ -3r^2/2Nb^2 \right\} [1 - 15/20N \\ &\quad + 30r^2/20N^2b^2 - 9r^4/20N^3b^4 + \dots] \quad (1) \\ r^2 &= \sum_{i=1}^3 X_i^2 \\ d\tau &= \prod_{i=1}^3 dX_i \end{aligned}$$

$\psi_0(\mathbf{r})d\tau$ represents the probability that the displacement vector, \mathbf{r} , lies in the interval between X_i and $X_i + dX_i$ ($i = 1, 2, 3$).

A network of chains described by eq. (1), upon deformation, undergoes an entropy change of an amount approximated by¹⁰

$$\Delta S/k = G \int d\tau \psi(\mathbf{r}) \ln [\psi_0(\mathbf{r})/\psi(\mathbf{r})] \quad (2)$$

where $\psi(\mathbf{r})d\tau$ represents the vector distribution in the deformed state and k is Boltzmann's constant. Following the method proposed by Wall¹¹ the expression is maximized under the conditions

$$\int \psi(\mathbf{r})d\tau = 1 \quad (3)$$

$$\int X_i^2 \psi(\mathbf{r}) d\tau = K\lambda_i^2 \quad i = 1, 2, 3 \quad (4)$$

where K is a constant and λ_i^2 is the deformation ratio along the i th coordinate. Use of Lagrangian multipliers affords an easy solution to this problem, the result being

$$\psi(\mathbf{r}) = B\psi_0(\mathbf{r}) \exp \left\{ \sum_i (3/2Nb^2 - p_i)X_i^2 \right\}$$

The quantities B and p_i contain the undertermined multipliers, and the summations are performed over the three coordinate axes.

On performing the integrations of eqs. (2), (3), and (4) we obtain, respectively,

$$-\Delta S/k = G[\ln B - K \sum_i (p_i - 3/2Nb^2)\lambda_i^2] \quad (6)$$

$$B = (2Nb^2/3)^{3/2} (\prod_i p_i)^{1/2} [1 - 3/4N + \epsilon] \quad (7)$$

$$2Kp_i\lambda_i^2 = 1 + \epsilon_i \quad (8)$$

where

$$\begin{aligned} \epsilon &= (3/4N^2b^2) \sum_i p_i^{-1} - (9/40N^3b^4) [(3/2) \sum_i p_i^{-2} + \sum_{i < k} p_i^{-1} p_k^{-1}] \\ \epsilon_i &= (3/2N^2b^2 p_i) \left\{ 1 - (3/10Nb^2) [2p_i^{-1} + \sum_j p_j^{-1}] \right\} \quad (9) \end{aligned}$$

Since $p_i = 3/2Nb^2$ when $\lambda_i = 1$, the value of K is determined to be $Nb^2/3$.

Substitution of eqs. (7) and (8) into eq. (6) yields

$$\Delta S/Gk = -\left(\sum_i \lambda_i^2 - 3\right)/2 - 3/4N + \ln \left(\prod_i \lambda_i\right) + \epsilon$$

Since terms of order $1/N^2$ are neglected, $1/p_i$ in the expression for ϵ may be replaced by $2K\lambda_i^2$ with the result

$$\begin{aligned} \Delta S/Gk = \ln \prod_i \lambda_i - 1/2(1 - N^{-1}) \left[\sum_i \lambda_i^2 - 3 \right] - 3 \left[\sum_i \lambda_i^4 - 3 \right] / 20N \\ - \left[\sum_{i < k} \lambda_i^2 \lambda_k^2 - 3 \right] / 10N \quad (10) \end{aligned}$$

This result differs from that given by Wang and Guth⁶ in two respects. First, the logarithmic term appearing in eq. (10) is totally lacking in their treatment. The presence of this term is purely a consequence of the particular distribution function utilized for $\psi(\mathbf{r})d\tau$ and has been thoroughly discussed in connection with Gaussian networks;¹⁰ therefore, aside from pointing out that so long as the volume remains constant this term is of no consequence, it is felt that no further elaboration is required at this time. The second difference is found in the coefficient of the second term in eq. (10). We obtain a factor $(1-1/N)$ which compares with the factor $(1 + 1/4N)$ in the treatment of Wang and Guth. Similar differences would have been observed in the higher order terms if they had been retained. In view of the fact that the quantities $1/N$ and $1/4N$ are small in comparison to unity, such differences between the theories are clearly of secondary importance. This is particularly attractive in view of the simplicity of our approach as compared to that of Wang and Guth. The fact that the quantity $1/4N$ is small compared to unity prompted Wang and Guth to neglect it altogether. This, however, appears inconsistent since, in the case of simple extension, the term in $1/4N$ exceeds the last term in our eq. (10) which they retain. It is to be noted that eq. (10) also coincides with one obtained by Kuhn and Gr \ddot{u} n¹² following a somewhat less rigorous approach.

By introducing the strain invariants⁵

$$\begin{aligned} I_1 &= \sum \lambda_i^2 - 3 \\ I_2 &= \sum_{i < k} \lambda_i^2 \lambda_k^2 - 3 \\ I_3 &= \prod \lambda_i^2 \end{aligned}$$

eq. (10) may be written as

$$\Delta S/Gk = 1/2 G [\ln I_3 - (1 + 4/5N)I_1 - 3I_1^2/10N + 2I_2/5N] \quad (11)$$

It may be noted that results identical to eqs. (10) or (11) are obtained when an affine transformation is assumed, i.e., when one assumes that in the deformed state

$$\psi(X_1, X_2, X_3) = \psi_0(X_1/\lambda_1, X_2/\lambda_2, X_3/\lambda_3)$$

III. COMPOSITE NETWORK

Along the lines followed by Berry, Scanlan, and Watson² it will be assumed that the formation of the second stage network does not alter in any manner the primary structure, and that the entropy of a composite network may be equated to the sum of the entropies of the separate networks. For simplicity, we will restrict the treatment to ideal elastomers, i.e., those for which the internal energy does not depend upon strain.^{3,5} However, the treatment of a non-Gaussian network displaying conformational energy effects will be discussed in full detail in a later publication.¹³

a. Determination of the Set Length

If the second stage crosslinkages are introduced at the deformation ratio λ_i° and the length of the composite network is described by the strain variable λ_i^* , the total entropy of the system will be, according to eq. (10),

$$\Delta S/k = G_1 \ln \prod_i \lambda_i^* + G_2 \ln \prod_i (\lambda_i^*/\lambda_i^\circ) - G_1 A_1 - G_2 A_2 \quad (12)$$

$$A_1 = \frac{1}{2}(1 - N_1^{-1}) \left[\sum_i \lambda_i^{*2} - 3 \right] + 3 \left[\sum_i \lambda_i^{*4} - 3 \right] / 20N_1 \\ + \left[\sum_{i < k} \lambda_i^{*2} \lambda_k^{*2} - 3 \right] / 10N_1$$

$$A_2 = \frac{1}{2}(1 - N_2^{-1}) \left[\sum_i (\lambda_i^{*2}/\lambda_i^{\circ 2}) - 3 \right] + 3 \left[\sum_i (\lambda_i^{*4}/\lambda_i^{\circ 4}) - 3 \right] / 20N_2 \\ + \left[\sum_{i < k} (\lambda_i^{*2} \lambda_k^{*2} / \lambda_i^{\circ 2} \lambda_k^{\circ 2}) - 3 \right] / 10N_2$$

where the subscripts 1 and 2 attached to the quantities G and N refer to the first and second stage networks respectively.

If the X_1 direction is arbitrarily assigned as the direction of orientation (i.e., the direction along which the first stage network is elongated during formation of the second stage network), the condition of maximum entropy is

$$(\partial \Delta S / \partial \lambda_1^*)_{\lambda_i^\circ} = 0 \quad (13)$$

Furthermore, the condition of constant volume requires that

$$\lambda_2^* = \lambda_3^* = 1/\lambda_1^{*1/2} = 1/\lambda_*^{1/2} \\ \lambda_2^\circ = \lambda_3^\circ = 1/\lambda_1^{\circ 1/2} = 1/\lambda_0^{1/2}$$

Maximization of eq. (12) in accordance with eq. (13) yields after a simple rearrangement

$$\lambda_*^3 = \lambda_\infty^3 [1 + \delta \lambda_\infty^{-2} (G_1 + G_2/\lambda_0^2)^{-1}] \quad (14)$$

where λ_∞ is the value of λ_* in the limit of the Gaussian approximation ($N \rightarrow \infty$) and δ is composed of the remaining terms, omitting quantities of order $1/N^2$

$$\lambda_\infty^3 = (G_1 + \lambda_0 G_2) / (G_1 + G_2/\lambda_0^2)$$

$$\begin{aligned} \delta = & (G_1/N_1) [(\lambda_\infty^2 - \lambda_\infty^{-1}) - 3(\lambda_\infty^4 - \lambda_\infty^{-2})/5 - (\lambda_\infty - \lambda_\infty^{-2})/5] \\ & + (G_2/N_2) [(\lambda_\infty^2 \lambda_0^{-2} - \lambda_0 \lambda_\infty^{-1}) - 3(\lambda_\infty^4 \lambda_0^{-4} - \lambda_0^2 \lambda_\infty^{-2})/5 \\ & - (\lambda_\infty \lambda_0^{-1} - \lambda_0^2 \lambda_\infty^{-2})/5] \quad (15) \end{aligned}$$

b. Retractive Force

For a subsequent deformation of the composite network the deformation entropy will be uniquely defined by a strain variable λ_i (λ_i = deformation ratio of the composite network referred to the set dimensions).

$$\begin{aligned} \Delta S/k = & (G_1 + G_2) \ln \lambda_1 \lambda_2 \lambda_3 - G_1 A_1^* - G_2 A_2^* + \text{constant} \quad (16) \\ A_1^* = & 1/2(1 - N_1^{-1}) [\lambda_1^2 \lambda_*^{-2} + (\lambda_2^2 + \lambda_3^2) \lambda_*^{-1}] + 3[\lambda_1^4 \lambda_*^4 \\ & + (\lambda_2^4 + \lambda_3^4) \lambda_*^{-2}]/20N_1 + [(\lambda_2^2 + \lambda_3^2) \lambda_1^2 \lambda_* + \lambda_2^2 \lambda_3^2 \lambda_*^{-2}]/10N_1 \\ A_2^* = & 1/2(1 - N_2^{-1}) [\lambda_1^2 \lambda_*^2 \lambda_0^{-2} + (\lambda_2^2 + \lambda_3^2) \lambda_0 \lambda_*^{-1}] + 3[\lambda_1^4 \lambda_0^{-4} \lambda_*^4 \\ & + (\lambda_2^4 + \lambda_3^4) \lambda_0^2 \lambda_*^{-2}]/20N_2 + [(\lambda_2^2 + \lambda_3^2) \lambda_1^2 \lambda_* \lambda_0^{-1} + \lambda_2^2 \lambda_3^2 \lambda_0^2 \lambda_*^{-2}]/10N_2 \end{aligned}$$

On substitution of eq. (15) into eq. (16) and neglecting orders of magnitude smaller than $1/N$ we obtain

$$\begin{aligned} \Delta S/k = & (G_1 + G_2) \ln \lambda_1 \lambda_2 \lambda_3 - G_1 A_1^\infty - G_2 A_2^\infty - (2\lambda_1^2 - \lambda_2^2 - \lambda_3^2) \delta/6 \\ & + \text{constant} \quad (17) \end{aligned}$$

$$\begin{aligned} A_1^\infty = & 1/2(1 - N_1^{-1}) [\lambda_1^2 \lambda_\infty^2 + (\lambda_2^2 + \lambda_3^2) \lambda_\infty^{-1}] + 3[\lambda_1^4 \lambda_\infty^4 \\ & + (\lambda_2^4 + \lambda_3^4) \lambda_\infty^{-2}]/20N_1 + [(\lambda_2^2 + \lambda_3^2) \lambda_1^2 \lambda_\infty + \lambda_2^2 \lambda_3^2 \lambda_\infty^{-2}]/10N_1 \\ A_2^\infty = & 1/2(1 - N_2^{-1}) [\lambda_1^2 \lambda_\infty^2 \lambda_0^{-2} + (\lambda_2^2 + \lambda_3^2) \lambda_0 \lambda_\infty^{-1}] + 3[\lambda_1^4 \lambda_\infty^4 \lambda_0^{-4} \\ & + (\lambda_2^4 + \lambda_3^4) \lambda_0^2 \lambda_\infty^{-2}]/20N_2 + [(\lambda_2^2 + \lambda_3^2) \lambda_1^2 \lambda_\infty \lambda_0^{-1} + \lambda_2^2 \lambda_3^2 \lambda_0^2 \lambda_\infty^{-2}]/10N_2 \end{aligned}$$

In the case of simple elongation along the X_1 axis at constant volume (i.e., parallel to the direction of orientation) $\lambda = L/L_*$ and

$$\lambda_2 = \lambda_3 = 1/\lambda_1^{1/2} = 1/\lambda^{1/2}$$

The retractive force will be given by

$$f' = -(T/L_*) (\partial \Delta S / \partial \lambda)_{P,T}$$

Therefore, eq. (17) yields

$$\begin{aligned} f' = & (kT/L_*) [G_1 C_1' + G_2 C_2' + (2\lambda + \lambda^{-2})\delta/3] \quad (18) \\ C_1' = & (1 - N_1^{-1}) [\lambda \lambda_\infty^2 - \lambda^{-2} \lambda_\infty^{-1}] + 3[\lambda^3 \lambda_\infty^4 - \lambda^{-3} \lambda_\infty^{-2}]/5N_1 \\ & + [\lambda_\infty - \lambda^{-5} \lambda_\infty^{-2}]/5N_1 \\ C_2' = & (1 - N_2^{-1}) [\lambda \lambda_\infty^2 \lambda_0^{-2} - \lambda_0 \lambda^{-2} \lambda_\infty^{-1}] + 3[\lambda^3 \lambda_\infty^4 \lambda_0^{-4} \\ & - \lambda_0^2 \lambda^{-3} \lambda_\infty^{-2}]/5N_2 + [\lambda_\infty \lambda_0^{-1} - \lambda_0^2 \lambda^{-3} \lambda_\infty^{-2}]/5N_2 \end{aligned}$$

However, if the subsequent elongation occurs along either of the other two axes, say X_3 , then

$$\lambda_1 = \lambda_2 = 1/\lambda_3^{1/2} = 1/\lambda^{1/2}$$

and

$$f'' = 1/2(kT/L_*)[G_1C_1'' + G_2C_2'' - (2\lambda + \lambda^{-2})\delta/3] \quad (19)$$

$$C_1'' = (1 - N_1^{-1}) [2\lambda\lambda_\infty^{-1} - (\lambda_\infty^2 + \lambda_\infty^{-1})\lambda^{-2}] + 3 [2\lambda^3\lambda_\infty^{-2} - (\lambda_\infty^4 + \lambda_\infty^{-2})\lambda^{-3}]/5N_1 + [\lambda_\infty^{-2} - 2\lambda_\infty\lambda^{-3} + \lambda_\infty]/5N_1$$

$$C_2'' = (1 - N_2^{-1}) [2\lambda\lambda_0\lambda_\infty^{-1} - (\lambda_\infty^2\lambda_0^{-2} + \lambda_0\lambda_\infty^{-1})\lambda^{-2}] + 3 [2\lambda^3\lambda_0^2\lambda_\infty^{-2} - (\lambda_\infty^4\lambda_0^{-4} + \lambda_0^2\lambda_\infty^{-2})\lambda^{-3}]/5N_2 - (\lambda_\infty^4\lambda_0^{-4} + \lambda_0^2\lambda_\infty^{-2})\lambda^{-3}]/5N_2 + [\lambda_0^2\lambda_\infty^{-2} - 2\lambda_\infty\lambda^{-3}\lambda_0^{-1} + \lambda_\infty\lambda_0^{-1}]/5N_2$$

The quantities f' and f'' represent the retractive forces when elongation occurs respectively parallel or perpendicular to the direction of orientation.

As $N \rightarrow \infty$ either eq. (18) or (19) yields the expression derived by Berry, Scanlan, and Watson,² i.e.,

$$f = (kT/L_*)(G_1 + \lambda_0G_2)^{2/3} (G_1 + G_2/\lambda_0^2)^{1/3} (\lambda - \lambda^{-2})$$

c. Dimensional Changes in Swollen Systems

The above considerations can be extended to the case where a deformation, subsequent to the formation of the composite network, is accomplished through the action of a swelling liquid. Since the X_2 and X_3 vectors are identical when the direction of orientation is along the X_1 axes, the value of the deformation ratio λ_2 will equal λ_3 , and

$$\lambda_2 = \lambda_3 = 1/\phi^{1/2}\lambda_1^{1/2}$$

where ϕ is the volume fraction of polymer. Accordingly the elastic component of the swelling entropy may be written as a function of ϕ and λ_1 or λ_2 (say λ_1); therefore,

$$dS_{e1} = (\partial S_{e1}/\partial \lambda_1)_\phi d\lambda_1 + (\partial S_{e1}/\partial \phi)_{\lambda_1} d\phi$$

At equilibrium swelling the quantity $(\partial S_{e1}/\partial \phi)_{\lambda_1}$ equals zero, and the equilibrium value of λ_1 is determined from

$$(\partial S_{e1}/\partial \lambda_1)_\phi = 0$$

S_{e1} , the elastic component of the swelling entropy, is given by eq. (16). Therefore, we obtain

$$G_1D_1 + G_2D_2 + (2\lambda_1 + \phi^{-1}\lambda_1^{-2})\delta/3 = 0 \quad (21)$$

$$D_1 = (1 - N_1^{-1})[\lambda_1\lambda_\infty^2 - \phi^{-1}\lambda_\infty^{-1}\lambda_1^{-2}] + 3[\lambda_1^3\lambda_\infty^4 - \phi^{-2}\lambda_\infty^{-2}\lambda_1^{-3}]/5N_1 + [\lambda_\infty\phi^{-1} - \phi^{-2}\lambda_\infty^{-2}\lambda_1^{-3}]/5N_1$$

$$D_2 = (1 - N_2^{-1})[\lambda_1\lambda_\infty^2\lambda_0^{-2} - \lambda_0\phi^{-1}\lambda_\infty^{-1}\lambda_1^{-2}] + 3[\lambda_1^3\lambda_\infty^4\lambda_0^{-4} - \lambda_0^2\phi^{-2}\lambda_\infty^{-2}\lambda_1^{-3}]/5N_2 + [\lambda_\infty\phi^{-1}\lambda_0^{-1} - \lambda_0^2\phi^{-2}\lambda_\infty^{-2}\lambda_1^{-3}]/5N_2$$

By neglecting orders of magnitude smaller than $1/N$, eq. (21) can be rearranged to read

$$\lambda_1 = \phi^{-1/3} \left\{ 1 - (1 - \phi^{2/3}) 3^{-1} \lambda_{\infty}^{-2} (t_1 + (t_2/\lambda_0^2)^{-1}) [(t_1(\lambda_{\infty}^2 - \lambda_{\infty}^{-1})/N_1 + (t_2(\lambda_{\infty}^2 \lambda_0^{-2} - \lambda_0 \lambda_{\infty}^{-1})/N_2 - \delta)] \right\} \quad (22)$$

From eq. (22) the λ_1 value for a given value of ϕ can be determined. In the Gaussian approximation, obtained by letting $N \rightarrow \infty$, eq. (22) predicts isotropic swelling, i.e., $\lambda_1 = \lambda_2 = \lambda_3 = \phi^{-1/3}$.

IV. THREE-CHAIN MODEL

In this section the three-chain model for the network will be used in order to obtain the expression for the retractive force of a composite network.

The three-chain model has the advantage of simplicity and permits the results to be written in closed form. Therefore expressions derived by the use of this model may be used to explore the general features of the network even when deviations from non-Gaussian behavior becomes large while the elastic entropy calculated in section II is valid only for small deviations from Gaussian behavior. Comparison of the results obtained from the use of the three-chain model and from the more exact treatment of section II, in the range of small deviations from Gaussian behavior, will be made in the next section.

The three-chain model, as proposed by Treloar, reduces the real network to one consisting of three independent sets of chains having their displacement vectors parallel to the axes of the coordinate system. Thus, the total entropy of the network is given by

$$S = (G/3) [s(r_{x1}) + s(r_{x2}) + s(r_{x3})]$$

The chain entropy expression, $s(r)$, employed in this model is approximated by

$$s(r) = \text{const.} - Nk [(r/Nb)\beta + \ln (\beta/\sinh\beta)]$$

where β is the inverse Langevin function

$$\beta = L^{-1}(r/Nb)$$

Making the same assumptions as used earlier the entropy of the composite network may be expressed as

$$S = -(k/3) \left\{ G_1 N_1 \sum [\lambda_i \lambda_i^* r_{i1} / N_1 b + \ln (\beta_{i1} / \sinh \beta_{i1})] + G_2 N_2 \sum [\lambda_i \lambda_i^* r_{i2} / \lambda_i^{\circ} N_2 b + \ln (\beta_{i2} / \sinh \beta_{i2})] \right\} + \text{const.}$$

where the subscripts 1 and 2 refer to the first and second stage networks, respectively, and,

$$\beta_{i1} = L^{-1} (\lambda_i \lambda_i^* r_{i1} / N_1 b)$$

$$\beta_{i2} = L^{-1} (\lambda_i \lambda_i^* r_{i2} / \lambda_i^{\circ} N_2 b)$$

By making the assumption that r may be replaced by the root-mean-square value of a free chain⁵ ($r = N^{1/2}b$), and employing the conditions of constant volume given in section III, the retractive forces parallel and perpendicular to the direction of orientation (f', f'') are found to be

$$f' = (kT/3L_*) \left\{ G_1 [(\lambda_* N_1^{1/2})\beta'_{11} - (N_1/\lambda^3\lambda_*)^{1/2}\beta'_{21}] + G_2 [(\lambda_* N_2^{1/2}/\lambda_0)\beta'_{12} - (\lambda_0 N_2/\lambda^3\lambda_*)^{1/2}\beta'_{22}] \right\} \quad (23)$$

$$\beta'_{11} = L^{-1} (\lambda\lambda_*/N_1^{1/2})$$

$$\beta'_{21} = L^{-1} [(1/\lambda\lambda_*N_1)^{1/2}]$$

$$\beta'_{12} = L^{-1} (\lambda\lambda_*/\lambda_0N_2^{1/2})$$

$$\beta'_{22} = L^{-1} [(\lambda_0/\lambda\lambda_*N_2)^{1/2}]$$

$$f'' = (kT/3L_*) \left\{ G_1 [(N_1/\lambda_*)^{1/2}\beta''_{31} - 1/2(N_1/\lambda^3\lambda_*)^{1/2}\beta''_{21} - 1/2(\lambda_*^2N_1/\lambda^3)^{1/2}\beta''_{11}] + G_2 [(\lambda_0N_2/\lambda_*)^{1/2}\beta''_{32} - 1/2(\lambda_0N_2/\lambda^3\lambda_*)^{1/2}\beta''_{22} - 1/2(\lambda_*^2N_2/\lambda^3\lambda_0^2)^{1/2}\beta''_{12}] \right\} \quad (24)$$

$$\beta''_{31} = L^{-1} [(\lambda^2/\lambda_*N_1)^{1/2}]$$

$$\beta''_{21} = L^{-1} [(1/\lambda\lambda_*N_1)^{1/2}]$$

$$\beta''_{11} = L^{-1} [(\lambda_*^2/\lambda N_1)^{1/2}]$$

$$\beta''_{32} = L^{-1} [(\lambda^2\lambda_0/\lambda_*N_2)^{1/2}]$$

$$\beta''_{22} = L^{-1} [(\lambda_0/\lambda\lambda_*N_2)^{1/2}]$$

$$\beta''_{12} = L^{-1} [(\lambda_*^2/\lambda\lambda_0N_2)^{1/2}]$$

The value of λ_* , obtained by placing $f = 0$ and $\lambda = 1$ in either eq. (23) or (24), may be determined from the equation

$$G_1 [(\lambda_*N_1^{1/2})\beta_{11}^* - (N_1/\lambda_*)^{1/2}\beta_{21}^*] + G_2 [(\lambda_*N_2^{1/2}/\lambda_0)\beta_{12}^* - (\lambda_0N_2/\lambda_*)^{1/2}\beta_{22}^*] = 0 \quad (25)$$

$$\beta_{11}^* = L^{-1} (\lambda_*/N_1^{1/2})$$

$$\beta_{21}^* = L^{-1} [(1/\lambda_*N_1)^{1/2}]$$

$$\beta_{12}^* = L^{-1} (\lambda_*/\lambda_0N_2^{1/2})$$

$$\beta_{22}^* = L^{-1} [(\lambda_0/\lambda_*N_2)^{1/2}]$$

If the β^* 's are expanded in eq. (25) and only the first two terms of each expansion are retained, then after rearrangement λ_* becomes

$$\lambda_*^3 = \lambda_\infty^3 [1 + (3/5)\eta\lambda_\infty^{-2}(G_1 + G_2/\lambda_0^2)^{-1}] \quad (26)$$

where

$$\eta = -(G_1/N_1)[\lambda_\infty^4 - \lambda_\infty^{-2}] - (G_2/N_2)[\lambda_\infty^4\lambda^{-4} - \lambda_0^2\lambda_\infty^{-2}]$$

and λ_∞ has the same meaning as before.

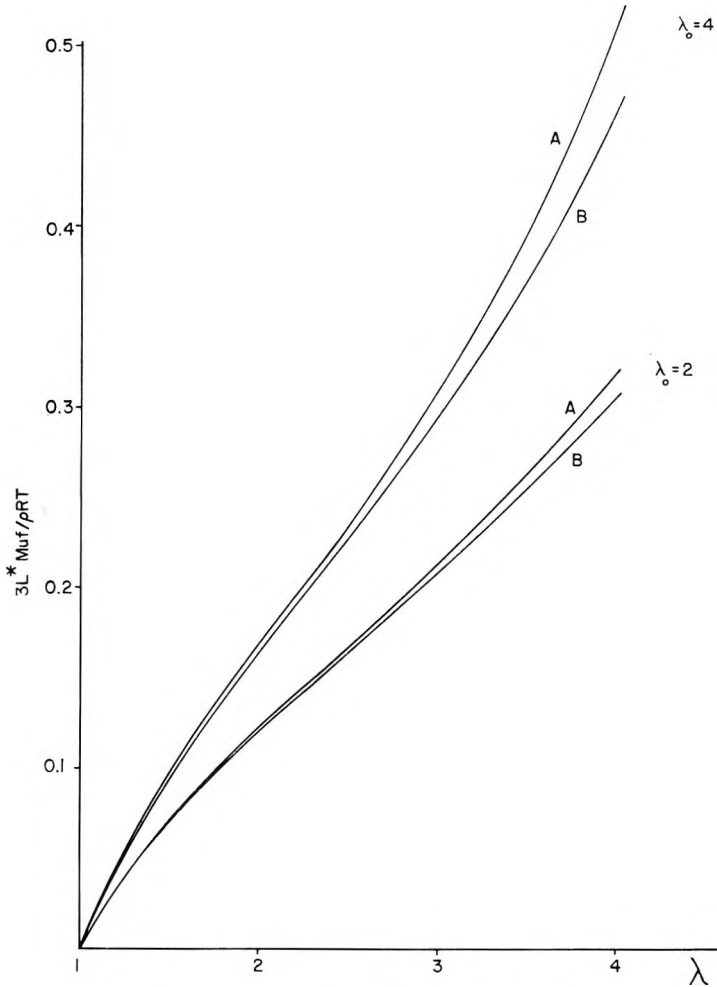


Fig. 1. *A* and *B* vs. λ . Values calculated from eqs. (28) and (29) for $N_1 = N_2 = 100$. λ_* corresponding to curves for $\lambda_0 = 4$ was equal to 1.674, while λ_* corresponding to curves for $\lambda_0 = 2$ was 1.338. λ_* was calculated from eq. (25).

In the limit of infinite chain length, eqs. (23), (24), and (25) yield the corresponding equations derived from Gaussian statistics.

An approximate graphical representation of eqs. (23) and (24) may be obtained by using the familiar expression for the number of chains:⁵

$$G_1 = \rho N_a / M_\mu N_1 \tag{27}$$

$$G_2 = \rho N_a / M_\mu N_2$$

แผนกห้องสมุด กรมวิทยาศาสตร์
 กระทรวงอุตสาหกรรม

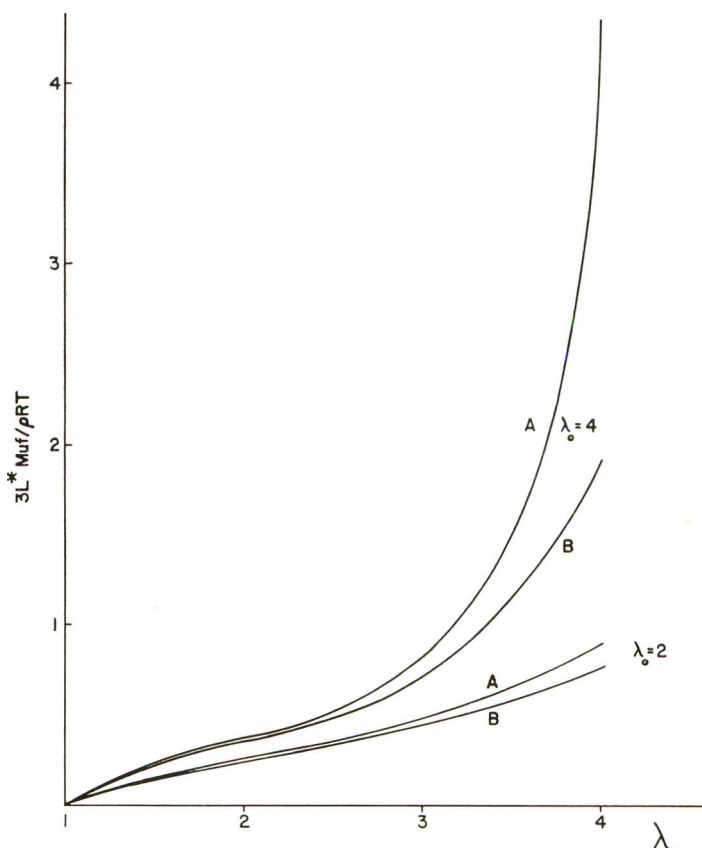


Fig. 2. A and B vs. λ . Values calculated from eqs. (28) and (29) for $N_1 = N_2 = 50$. λ_* corresponding to curves for $\lambda_0 = 4$ was equal to 1.671, while λ_* corresponding to curves for $\lambda_0 = 2$ was 1.337. λ_* was calculated from eq. (25).

where ρ is the density of the sample, N_a is Avogadro's number, and M_μ is the molecular weight of a statistical link. Accordingly, the quantities

$$A = 3L^*M_\mu f' / \rho RT \quad (28)$$

$$B = 3L^*M_\mu f'' / \rho RT \quad (29)$$

calculated from eqs. (23) and (24), using eq. (25), are plotted as a function of λ for several values of the variables N_1 , N_2 , and λ_0 in Figures 1-3.

V. DISCUSSION

If eqs. (23) and (24) are expanded and only the first two terms retained we find, after substitution of eq. (26), that the three-chain model treatment yields:

$$f' = (kT/L_*)[G_1 E'_1 + G_2 E'_2 - (2\lambda + \lambda^{-2})\eta/5] \quad (30)$$

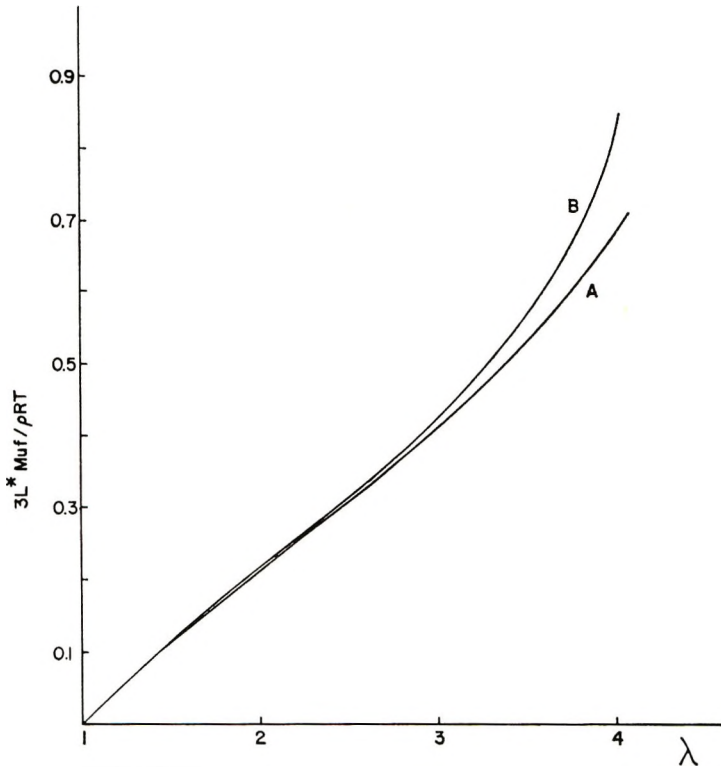


Fig. 3. *A* and *B* vs. λ . Values calculated from eqs. (28) and (29) for $\lambda_0 = 4$, $N_1 = 150$, $N_2 = 50$. λ^* calculated from eq. (25) was equal to 2.222.

$$E'_1 = (\lambda \lambda_{\infty}^{-2} - \lambda^{-2} \lambda_{\infty}^{-1}) + 3(\lambda^3 \lambda_{\infty}^{-4} - \lambda^{-3} \lambda_{\infty}^{-2}) / 5N_1$$

$$E'_2 = (\lambda \lambda_{\infty}^{-2} \lambda_0^{-2} - \lambda_0 \lambda^{-2} \lambda_{\infty}^{-1}) + 3(\lambda^3 \lambda_{\infty}^{-4} \lambda_0^{-4} - \lambda_0^2 \lambda^{-3} \lambda_{\infty}^{-2}) / 5N_2$$

$$f'' = 1/2(kT/L^*) [G_1 E''_1 + G_2 E''_2 + (2\lambda + \lambda^{-2})\eta/5] \quad (31)$$

$$E''_1 = (2\lambda \lambda_{\infty}^{-1} - \lambda_{\infty}^{-2} \lambda^{-2} - \lambda^{-2} \lambda_{\infty}^{-1}) + 3(2\lambda^3 \lambda_{\infty}^{-2} - \lambda_{\infty}^{-4} \lambda^{-3} - \lambda^{-3} \lambda_{\infty}^{-2}) / 5N_1$$

$$E''_2 = (2\lambda \lambda_0 \lambda_{\infty}^{-1} - \lambda_{\infty}^{-2} \lambda^{-2} \lambda_0^{-2} - \lambda_0 \lambda^{-2} \lambda_{\infty}^{-1}) + 3(2\lambda^3 \lambda_0^2 \lambda_{\infty}^{-2} - \lambda_{\infty}^{-4} \lambda^{-3} \lambda_0^{-4} - \lambda_0^2 \lambda^{-3} \lambda_{\infty}^{-2}) / 5N_2$$

Comparison of eqs. (30) and (31) with eqs. (18) and (19) reveals that the more exact treatment yields several terms in powers of $1/N$ that are lacking in the three-chain treatment. However, these terms are small and tend to balance one another, while the predominant terms appearing in the more exact eqs. (18) and (19) are exactly those appearing in eqs. (30) and (31). We can thus conclude that the three-chain model treatment can be regarded as a satisfactory approximation.

From Figures 1, 2, and 3 it is apparent that, once the assumption of Gaussian behavior is removed, the composite network displays anisotropic

elasticity. It is also evident that, if we define the quantity Δ as the $A - B$ difference [eqs. (28), (29)], Δ may be positive or negative, depending upon the particular network. We interpret the presence of anisotropy in non-Gaussian networks and the variations in Δ as follows.

When a composite network is at rest, the distribution of internal stresses can be visualized in terms of the deformations of the two interpenetrating model networks. The first network is elongated in the direction parallel to orientation, where the fractional extension of its chains is $\lambda_*/N_1^{1/2}$, and compressed in a direction perpendicular to orientation, where the fractional extension of chains is $(1/\lambda_*N_1)^{1/2}$. The second network is compressed in the direction of orientation, where the fractional extension of its chains is $\lambda_*/\lambda_0N_2^{1/2}$, and extended in the direction perpendicular to orientation, where the fractional extension is $(\lambda_0/\lambda_*N_2)^{1/2}$. When the composite network is stretched, the largest contribution to the retractive force will arise from the further elongation of the first network, if stretching is in the direction parallel to orientation, or from the further elongation of the second network, if stretching is in the direction perpendicular to orientation. The term $\lambda_*/N_1^{1/2}$ carries therefore the larger contribution to A [eq. (23)], while the term $(\lambda_0/\lambda_*N_2)^{1/2}$ carries the larger contribution to B [eq. (24)]. The character of the Gaussian approximation is such that the sum of the terms contributing to A always equals the sum of the terms contributing to B . However, in the more precise expression derived from non-Gaussian statistics, the contributions of the terms due to the larger fractional extensions are magnified through the inverse Langevin function. The magnification is introduced in order to account for the finite extensibility of the chains. The result is that, in general, $A \gtrsim B$ if, correspondingly $\lambda_*/N_1^{1/2} \gtrsim (\lambda_0/\lambda_*N_2)^{1/2}$. Detailed inspection of eqs. (30) and (31) confirms this interpretation. Whether $A \gtrsim B$ thus depends upon details such as N_1 , N_2 , and λ_0 which pertain to the formation of a particular composite network.

We can obtain an approximate relationship among Δ , λ_0 , and N_1/N_2 by substituting eqs. (27), (30), and (31) into eqs. (28) and (29). Thereby we obtain

$$\Delta = (9N_2/5N_1F)(\lambda_0^3 - 1)[2\lambda^4(\lambda^2 - 1) - (\lambda - 1)][\lambda_0 - (N_1/N_2)^2] \quad (32)$$

$$F = \lambda^3\lambda_0^{1/3}(\lambda_0^2N_2 + N_1)^{4/3}(N_2 + \lambda_0N_1)^{2/3}$$

Use of the more exact expressions, eqs. (18) and (19), in lieu of eqs. (30) and (31) yields

$$\Delta' = \Delta + (3/10N_2H)(\lambda_0^3 - 1)[\lambda^3(2\lambda - 1) + (\lambda - 2)][\lambda_0 - (N_2/N_1)] \quad (33)$$

$$H = \lambda^3\lambda_0^{4/3}(\lambda_0^2N_2 + N_1)^{1/3}(N_2 + \lambda_0N_1)^{2/3}$$

where Δ is given by eq. (32).

Because of the inherent approximation, neither eq. (32) nor (33) can be expected to be accurate for large values of λ_∞ , λ , and degrees of cross-linking. They show, however, that for composite networks characterized by a ratio $(N_1/N_2)^2 \leq 1$, Δ (and approximately Δ') is positive for all λ_0 values exceeding unity, while if $(N_1/N_2)^2 > 1$, Δ will be negative when $\lambda_0 < (N_1/N_2)^2$.

The only available experimental data for which the present theory can be tested are those of Berry, Scanlan, and Watson.² By using their reported values of λ_0 and approximating the values of N_1 and N_2 through the use of their observed moduli it is possible to show, from eqs. (20) and (22), that (under the experimental conditions adopted) the linear swelling ratio in the direction parallel to orientation could not have differed more than one per cent from the corresponding ratio measured in the direction perpendicular to orientation. Therefore, we conclude that: (1) their equilibrium swelling data are not adequate to detect anisotropic elasticity; (2) their reported differences (up to 4%) of the increase in length in the direction parallel and perpendicular to orientation are not explainable merely in terms of non-Gaussian behavior; and (3) new experimental data appear desirable, preferably those obtained by the much more sensitive load-elongation techniques, for networks which encompass a wider range of the variables N_1 , N_2 , and λ_0 .

A crucial test of the present theory would be the analysis of the predicted change of sign of Δ as a function of λ_0 when $N_1/N_2 > 1$. The peculiarity of this prediction is such that it may be used for an experimental investigation of non-Gaussian behavior in general. In fact, no adequate experimental description of non-Gaussian behavior has been so far given owing to complications arising from the onset of stress-induced crystallization.⁵

Very pleasantly we acknowledge the interest and cooperation of A. Greene in the performance of the lengthy calculations.

APPENDIX

Glossary of Principal Symbols

- λ_i^* Ratio of the length of the set network to the rest length of the first stage network.
- λ_* The value of λ_i^* in simple elongation.
- λ_∞ The value of λ_* in the limit of the Gaussian approximation.
- λ_i° Ratio of the rest length of second stage network to the rest length of the first stage network.
- λ_0 The value of λ_i° in simple elongation.
- λ_i In section II: deformation ratio of non-Gaussian network; in all other sections: deformation ratio of the composite network referred to the set dimension.
- λ The value of λ_i in simple elongation.
- l_* Rest length of the set network.
- G Number of chains in a network.
- N Number of statistical links in a chain.
- N_a Avogadro's number.
- r Root-mean-square end-to-end distance of a chain.
- b Length of a statistical link.

- ρ Density of sample.
 f' Retractive force when elongation occurs parallel to the direction of orientation.
 f'' Retractive force when elongation occurs perpendicular to the direction of orientation.
 ϕ Volume fraction of polymer in a swollen system.

References

1. Andrews, R. D., A. V. Tobolsky, and E. E. Hanson, *J. Appl. Phys.*, **17**, 352 (1946).
2. Berry, J. P., J. Scanlan and W. F. Watson, *Trans. Faraday Soc.*, **52**, 1137 (1956).
3. For more details and extensive reference list see: A. Greene and A. Ciferri, *Kolloid-Z.*, **186**, 1 (1962).
4. Lodge, A. S., *Kolloid Z.*, **171**, 46 (1960).
5. Treloar, L. R. G., *The Physics of Rubber Elasticity*, Oxford University Press, 1958.
6. James, H. M., and E. Guth, *J. Chem. Phys.*, **11**, 445 (1943).
7. Wang, M. C., and E. Guth, *J. Chem. Phys.*, **20**, 1144 (1952).
8. Ishihara, A., N. Hashitsume, and M. Tatibana, *J. Chem. Phys.*, **19**, 1508 (1952).
9. Chandrasekhar, S., *Revs. Mod. Phys.*, **15**, 1 (1943).
10. Hermans, J. J., *J. Polymer Sci.*, **59**, 191 (1962).
11. Wall, F. T., *J. Chem. Phys.*, **11**, 527 (1943).
12. Kuhn, W., and F. Gr \ddot{u} m, *J. Polymer Sci.*, **1**, 183 (1946).
13. Smith, K. J., Jr., A. Greene, and A. Ciferri, paper presented at the Fourth International Congress on Rheology, Brown University, Providence, R. I., 1963, to be published.

Résumé

On a généralisé la théorie des réseaux mixtes par Berry, Scanlan et Watson, afin d'inclure le cas dans lequel on décrit l'élasticité des chaînes par des statistiques non-gaussiennes. Dans ce but, on a critiqué les théories existantes des réseaux non-gaussiens et on présente ici un nouveau traitement simple. Ce nouveau traitement rend substantiellement les mêmes résultats que ceux obtenus à partir de la théorie plus complexe de Wang et Guth. Les résultats obtenus à partir du modèle simple à trois chaînes pour le réseau, comme décrit par Treloar, sont aussi en bon accord avec à la fois le nouveau traitement et celui de Wang et Guth. La théorie généralisée des réseaux mixtes prévoit un comportement élastique anisotrope; la résistance à la traction d'une tension donnée doit être généralement plus élevée pour l'élongation dans la direction parallèle à l'orientation que dans la direction perpendiculaire à cette orientation. Cependant, suivant certains détails dus à la préparation de réseaux (rapport de premier et second stade de pontage et l'élongation à laquelle on effectue ce dernier), on peut élever la résistance à la traction requise pour l'élongation dans la direction perpendiculaire à l'orientation. Il apparaît que le comportement élastique isotrope, prédit par les théories prévues des réseaux mixtes, est purement une conséquence de l'emploi de l'approximation gaussienne.

Zusammenfassung

Die Theorie zusammengesetzter Netzwerke von Berry, Scanlan und Watson wurde zur Erfassung des Falles einer Kettenelastizität nach nicht-Gauss'scher Statistik verallgemeinert. Zu diesem Zweck wurde eine kritischer Überblick über die bekannten Theorien Gauss'scher Netzwerke gegeben und eine neue, einfache method angegeben. Diese neue Methode liefert im wesentlichen die gleichen Ergebnisse, wie sie nach der komplizierteren Theorie von Wang und Guth erhalten werden. Die mit Hilfe des einfachen Drei-Ketten-Modells von Treloar erhaltenen Ergebnisse standen ebenfalls mit der neuen Methode und mit der von Wang und Guth in befriedigender Übereinstimmung. Die verallgemeinerte Theorie zusammengesetzter Netzwerke lässt ein

anisotropes elastisches Verhalten erwarten; die Zugkraft bei gegebener Verformung sollte im allgemeinen für eine Dehnung parallel zur Orientierungsrichtung höher sein als für eine solcher senkrecht dazu. Es kann jedoch je nach der Herstellung der Netzwerke (Verhältnis der Vernetzungsstellen in der ersten und zweiten Stufe und Dehnung, bei welcher die letzteren eingeführt werden) die für eine Dehnung senkrecht zur Orientierungsrichtung erforderliche Zugkraft höher sein. Es scheint, dass das von den älteren Theorien für zusammengesetzte Netzwerke geforderte isotrope elastische Verhalten bloss durch die Verwendung der Gauss'schen Näherung bedingt ist.

Received January 16, 1963

Cold-Drawing of Acetone-Crystallized Polyethylene Terephthalate

P. R. BLAKEY and R. P. SHELDON, *Institute of Technology, Bradford, England*

Synopsis

The room-temperature cold-drawing behavior of acetone-crystallized polyethylene terephthalate film has been compared with that of amorphous and heat-crystallized film. X-ray diffraction photographs give good resolution in the case of the acetone-crystallized sample with evidence of molecular orientation in every case. The order of the magnitudes of the yield stresses is acetone-crystallized < amorphous < heat-crystallized. Heating of the drawn samples produces disorientation for the amorphous drawn film with an improved resolution of the diffraction photograph for the heat-crystallized film. It is suggested that the results are in agreement with a picture of a drawing mechanism involving molecular mobility in the amorphous regions and that acetone influences the yield stress by lowering the softening temperature.

INTRODUCTION

It is well known that, under certain conditions, a number of amorphous and semicrystalline polymers exhibit the phenomenon of cold-drawing at a well defined neck under the further influence of a critical stretching force. In the case of amorphous polyethylene terephthalate, a detailed investigation of the process has been made by Marshall and Thompson,¹ and in a largely rheological interpretation they conclude that the mechanism involves a local heating effect in the region of the neck in the nature of a thermal wave front which has a velocity fixed by the imposed rate of extension. Perhaps a more specific suggestion has been made by Jackel,² who considers that the temperature in the flow-zone of the neck must be equal to, or slightly in excess of, the softening temperature which is itself generally associated with an increase of molecular mobility in the amorphous rather than the crystalline regions of the polymer. In a more recent study of the problem with particular reference to nylon 66, Hookway³ has attempted to unify the various theories of cold-drawing and concludes that the critical stretching force which is identical with the yield stress in a particular polymer is closely related to molecular mobility within the amorphous regions, and that in this instance the results are more consistent with a picture of crystallite stripping as proposed by Bunn and Alcock,⁴ this conclusion being further supported by the evidence that an increase of

moisture content is accompanied by a lowering of the yield stress, the moisture presumably reducing interchain attraction in the amorphous regions.

In the present paper a description is given of a preliminary study which has been made of the drawability of acetone-crystallized polyethylene terephthalate. In order to see how the observed behavior is accommodated by current theories, a simultaneous comparison has been made with measurements relating to the cold-drawing of both amorphous and crystalline polymer.

EXPERIMENTAL

Materials

The polyethylene terephthalate was in the form of essentially amorphous film (see Table II) which has a thickness of 2.0×10^{-2} cm. The acetone was of analytical reagent quality.

Procedure

A weighed strip of film was crystallized by immersion in acetone for 24 hr. at room temperature.⁵ After extraction the strip was air-dried for 2 hr., when the weight loss due to acetone evaporation had become immeasurably small over a long period of time. The weight was again recorded. A number of dumbbell-shaped specimens of stem width equal to 3 mm. were cut for tensile testing in an extensometer. In one instance a test piece was reweighed so that an extrapolation could be made in order to calculate the original dry weight. The test pieces were extended at a rate of approximately 0.003 ft./sec. and the yield loads noted. The weighed test piece was given a rolling treatment with a serrated roller and then a heat treatment at 140°C. for 30 min. in an oven. Weighings were again made after each of these operations. Use of the serrated roller was made simply in order that rolled and unrolled portions could be obtained on the same specimen.

X-ray diffraction photographs were obtained after the drawing, rolling, and heat treatment stages.

Yield load measurements were made on untreated amorphous polymer, and x-ray diffraction photographs were again taken after drawing and after similar rolling and heat treatments as described above.

A third sample of film was heat-crystallized at 130°C. for 30 min., and similar test pieces were cut for yield load evaluations. X-ray diffraction photographs were obtained after drawing, and after heating at 140°C. for 30 min. as described previously, and also after heating a separate drawn sample at 130°C. for 30 min. under constant strain conditions in which the sample was held in a stretching frame.

Another sample of heat-crystallized film was immersed in boiling acetone for 3 hr. before test pieces were cut as before for yield load measurements. The sample was weighed before and after the acetone immersion.

RESULTS

The weight history of an acetone-crystallized test piece is given in Table I. It should be pointed out that, because of the elapse of a period of 2 days between the drawing and rolling treatments the test piece had lost weight merely by evaporation of acetone with time.

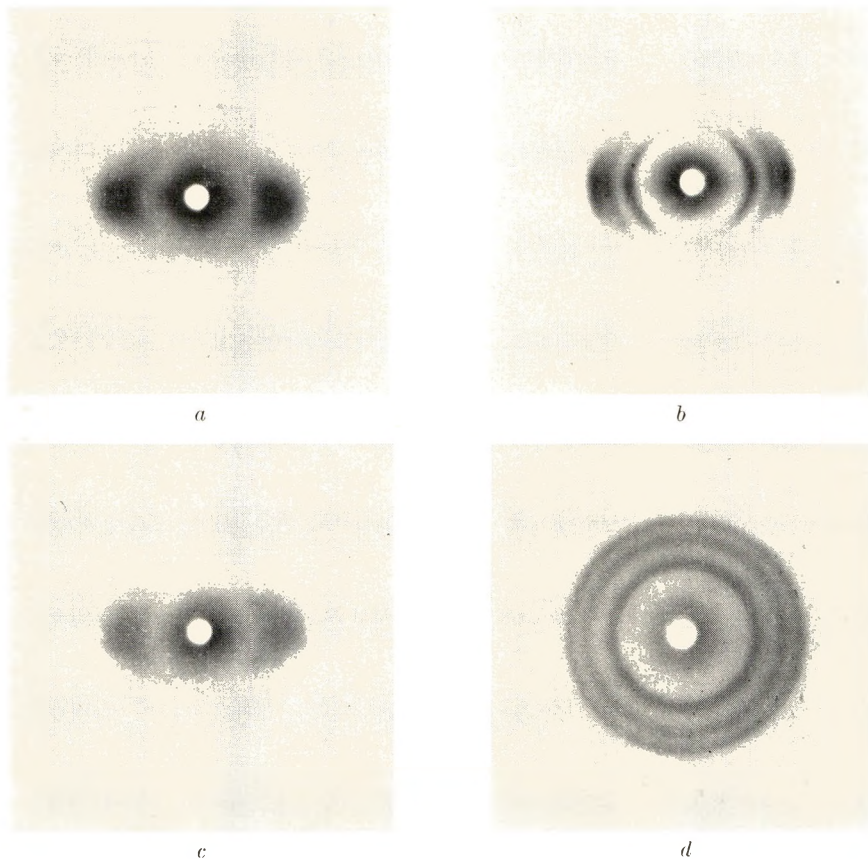


Fig. 1. X-ray diffraction photographs of polyethylene terephthalate: (a) amorphous, cold-drawn; (b) crystallized with acetone, cold drawn; (c) heat-crystallized, cold-drawn; (d) heat-crystallized, undrawn. $\text{CuK}\alpha$ radiation, specimen-film distance 3 cm.

Table II gives the values of the densities of the various samples of polymer prior to drawing, a correction being made for imbibed acetone in the case of the acetone-crystallized sample.⁵ Bearing in mind that the amorphous density and the crystalline unit cell density are reported to be 1.335 and 1.455 g./c.c., respectively,^{6,7} the density values give a general indication of the extent of crystallization. The yield loads recorded are taken from the average of at least three repeated measurements which in themselves agreed to within ± 0.25 lb.

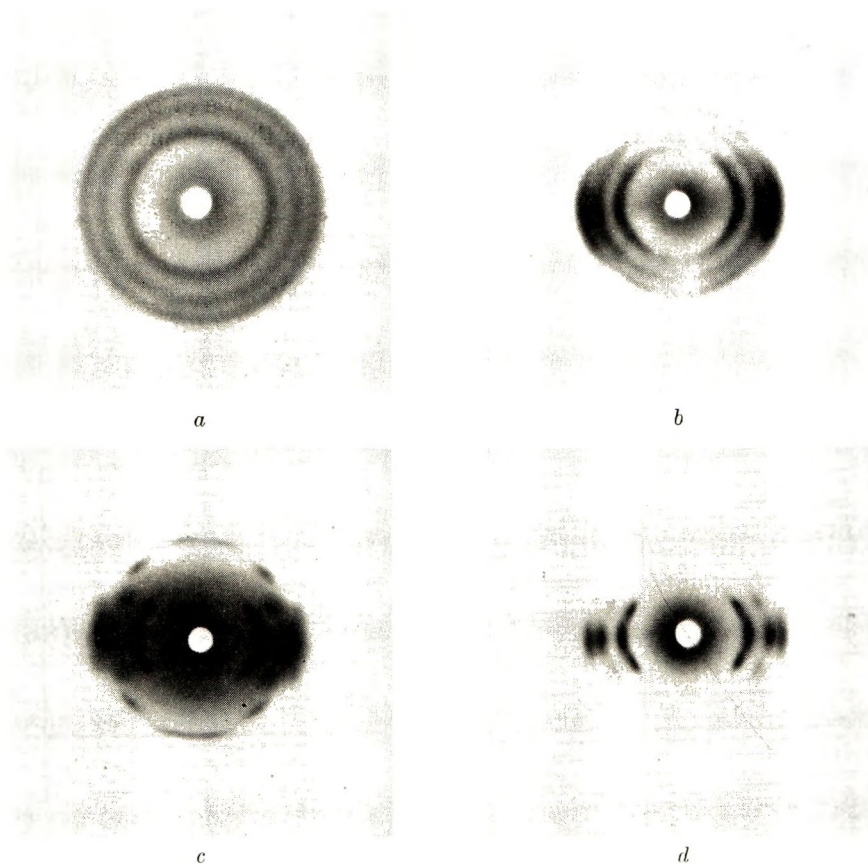


Fig. 2. X-ray diffraction photographs of polyethylene terephthalate: (a) amorphous, cold-drawn, heat-treated 30 min., 140°C.; (b) acetone-crystallized, cold-drawn, heat-treated 30 min., 140°C.; (c) heat-crystallized, cold-drawn, heat-treated 30 min., 130°C., constant strain; (d) heat-crystallized, cold drawn, heat-treated 30 min., 130°C., no tension. $\text{CuK}\alpha$ radiation, specimen-film distance 3 cm.

The increase in weight of the acetone-treated, heat-crystallized sample was 2% of the original dry weight.

Figure 1 shows the x-ray diffraction photographs of the cold-drawn

TABLE I
Weight of Acetone-Crystallized Test Piece after Various Treatments

Condition	Wt., g.
Original	0.2630
After crystallization	0.2807
After drawing	0.2807
Before rolling	0.2782
After rolling	0.2782
After 30 min. at 140°C.	0.2633

TABLE II
Densities and Yield Loads of Various Samples

Sample	Density, g./cc.	Yield load, lb.
Amorphous	1.338	3.5
Acetone-crystallized	1.400	2.5
Heat-crystallized	1.377	6.5
Heat-crystallized (acetone-treated)	—	5.5

regions of the test pieces, together with a photograph of the heat-crystallized piece before drawing.

Figure 2 gives the corresponding patterns after the heat treatment at 140°C. and of the heat-crystallized sample subsequently annealed at constant strain. Photographs obtained from the rolled portions of the films are not reproduced but are described in the following discussion.

DISCUSSION

The x-ray diffraction photographs shown in Figure 1 indicate that molecular orientation has occurred in every case of cold-drawing. For the amorphous polymer (Fig. 1*a*), orientation without resolution between the main equatorial reflections is observed, whereas with the acetone-crystallized sample (Fig. 1*b*) good resolution as well as orientation is apparent. The heat-crystallized specimen (Fig. 1*c*) shows orientation with loss of resolution when compared with the undrawn sample (Fig. 1*d*). This suggests that disruption of the crystalline region has occurred on drawing. In the case of the acetone-crystallized test piece, if crystallite breakdown has also taken place during the drawing process, then it is evident that this has been on a smaller scale or that recrystallization occurs after drawing. An alternative suggestion that the latter observation may be explained by a mechanism involving fibrillar slip was rejected since not only has the acetone-crystallized material an identical unit cell as the heat-crystallized, but in each case the preferred orientation is the same.

Rolling of the film gave little change in the x-ray diffraction photographs for either the amorphous, drawn material or the drawn, acetone-crystallized sample. In the latter case an improved optical clarity was obtained which can be understood if we assume cavitation has occurred during drawing and that collapse of the voids takes place on rolling.

Heating of the test pieces produced complete disorientation for the unrolled part of the amorphous cold-drawn sample but with good resolution on the x-ray diffraction photograph (Fig. 2*a*). When the acetone-crystallized sample was heated, the bulk of the imbibed acetone was lost and the molecular orientation was retained (Fig. 2*b*), suggesting that the crystallinity acts as a stabilizer against disorientation. Subsequent heat treatment of the drawn, heat-crystallized specimen produces an improved resolution again with a retention of orientation (Fig. 2*c*), while heating at constant strain produces good resolution with an increase in orientation (Fig. 2*d*).

The results of Table I at first sight appear to be contrary to the conclusions of previous workers and in particular to the observations of Marshall and Thompson,¹ who reported that a definite hot-spot could be detected at the neck, and if this were the case in these studies it might be imagined that this would tend towards loss of acetone on drawing. A possible explanation of the present observations may be that there is a lowering of the softening temperature by the acetone, thus providing for the necessary mobility in the amorphous regions at a lower temperature. This would be in agreement with the observed fall in yield load in heat-crystallized polyethylene terephthalate which has been later treated with acetone and with the results of Hookway³ in connection with the effect of moisture on the yield stress of nylon 66. In fact, the results are in agreement in many ways with the conclusions of the latter author and therefore in support of a crystallite stripping process as the basis of crystallite breakdown.

In conclusion we can say that acetone-crystallized polyethylene terephthalate, and presumably polymer crystallized with other liquids as a separate observation with benzene-crystallized polymer has shown,⁸ is capable of being cold-drawn at ambient temperatures to a highly oriented and crystalline condition under relatively small stretching forces.

We wish to thank I. C. I. Ltd., for kindly supplying film used in these studies and to the Plastics Engineering Research Committee of this Institute for arranging facilities.

References

1. Marshall, I., and A. B. Thompson, *Proc. Roy. Soc. (London)*, **A221**, 541 (1954).
2. Jackel, K., *Kolloid-Z.*, **137**, 130 (1954).
3. Hookway, D. C., *J. Textile Inst.*, **49**, 292 (1958).
4. Bunn, C. W., and T. C. Alcock, *Trans. Faraday Soc.*, **41**, 323 (1945).
5. Kolb, H. J., and E. F. Izard, *M. Appl. Phys.*, **20**, 571 (1949); W. R. Moore, D. O. Richards, and R. P. Sheldon, *J. Textile Inst.*, **51**, 438 (1960); P. R. Blakey and R. P. Sheldon, *Nature*, **195**, 175 (1962).
6. Bunn, C. W., in *Fibres from Synthetic Polymers*, R. Hill, Ed., Elsevier, Amsterdam 1953.
7. Thompson, A. B., and D. W. Woods, *Nature*, **176**, 78 (1955).
8. Cottam, L., and R. P. Sheldon, unpublished results.

Résumé

On a comparé le comportement du téréphthalate de polyéthylène cristallisé dans l'acétone pendant l'étirement à froid, à température de chambre, à celui des films de téréphthalate de polyéthylène amorphe ou cristallisé à chaud. Les spectres de diffraction des rayons-X montrent une bonne résolution pour l'échantillon cristallisé dans l'acétone et une orientation moléculaire évidente dans toutes les expériences. La grandeur des forces obtenues est dans l'ordre suivant: cristallisé dans l'acétone < amorphe < cristallisé à chaud. Le réchauffement des échantillons étirés donne lieu à une désorientation dans le film étiré amorphe, et une amélioration de la résolution du spectre de diffraction dans le film cristallisé à chaud. On admet que les résultats sont en accord avec une représentation d'un mécanisme d'étirement dans lequel il existe une mobilité moléculaire dans les régions amorphes et dans lequel l'acétone influence la tension interne obtenue en diminuant la température de ramollissement.

Zusammenfassung

Das Verhalten eines aus Aceton kristallisierten Polyäthylenterephthalatfilmes bei der Kaltreckung bei Raumtemperatur wurde mit dem eines amorphen und wärme-kristallisierten Filmes verglichen. Röntgenbeugungsaufnahmen geben im Falle der aus Aceton kristallisierten Probe gute Auflösung und in allen Fällen Anzeichen für Molekülorientierung. Die Reihenfolge der Grösse der Bruchspannung ist: aceton-kristallisiert < amorph < wärme-kristallisiert. Erhitzen der gereckten Proben erzeugt beim amorphen gereckten Film Desorientierung mit einer verbesserten Auflösung der Beugungsaufnahme beim wärme-kristallisierten Film. Die Ergebnisse entsprechen dem Bild eines Reckungsmechanismus mit Molekülbeweglichkeit in den amorphen Bereichen und der Annahme, dass Aceton die Bruchspannung durch Erniedrigung der Erweichungstemperatur beeinflusst.

Received January 18, 1963

Aromatic Polysulfonates: Preparation and Properties

DAVID W. THOMSON and GERHARD F. L. EHLERS, *Air Force Materials Laboratory, Research and Technology Division, Wright-Patterson Air Force Base, Ohio*

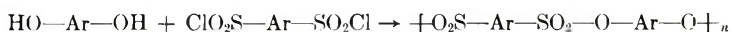
Synopsis

Aromatic polysulfonates of high molecular weight and purity can easily be prepared by interfacial polycondensation of the disulfonyl chlorides with diphenols. The polymers were found to have a low degree of crystallinity, softening ranges in the region 200–250°C., molecular weights up to 50,000 and a thermal stability under nitrogen to above 300°C.

Introduction

It has been known for some time that aromatic polymers which incorporate sulfur-containing groups into the chain can often show excellent thermal stability. Especially noted for this property are the aromatic polysulfones¹ and polysulfides.²

In searching for new polymers which might also show evidence of high thermal stability, the preparation and characterization of a series of aromatic polysulfonates was explored. It was found that high molecular weight polymers, free from impurities, could be obtained from interfacial polycondensation of aromatic disulfonyl chlorides with the corresponding diphenols according to the reaction:



where Ar represents benzene 1,3-, biphenyl 4,4'-, diphenyl ether 4,4'-, diphenyl methane 4,4'-, and diphenyl sulfone 4,4'-. In addition, a polymer was prepared from the condensation of 1,3,5-benzenetrisulfonyl chloride with 4,4'-biphenol.

Discussion

The preparation of the polymers was accomplished by standard interfacial polycondensation methods, both at room temperature and at 70°C. It was found that the molecular weights were significantly increased when the polymers were prepared at elevated temperatures. The higher molecular weight material obtained in this manner was found to possess increased thermal stability.

In addition to elemental analysis, the polymers were characterized by infrared spectra correlations. The stretching vibrations attributed to the

TABLE I
Physical Properties of Polysulfonates

Repeat unit	Reaction temp., °C.	η_{inh}^a	Reaction solvents	Softening range, °C.	Infection point of TGA curve, °C.
	25	0.14	C ₆ H ₆ H ₂ O	150-160	335
	25	0.42	C ₆ H ₆ H ₂ O	190-200	330
	70	0.62	C ₆ H ₆ H ₂ O	250-260	365
	70	0.37	C ₆ H ₆ H ₂ O	270-280	310
	25	0.10	CH ₂ Cl ₂ H ₂ O	180-190	270
	70	0.31	CH ₂ Cl ₂ H ₂ O	200-210	305
	70	0.20	CH ₂ Cl ₂ H ₂ O	170-180	290
	70	0.45 ^b	CH ₂ Cl ₂ H ₂ O	190-200	370

^a For 0.25 g. sample in 100 ml. of *N,N*-dimethylformamide. Measurements were made at 30°C.

^b Soluble fraction.

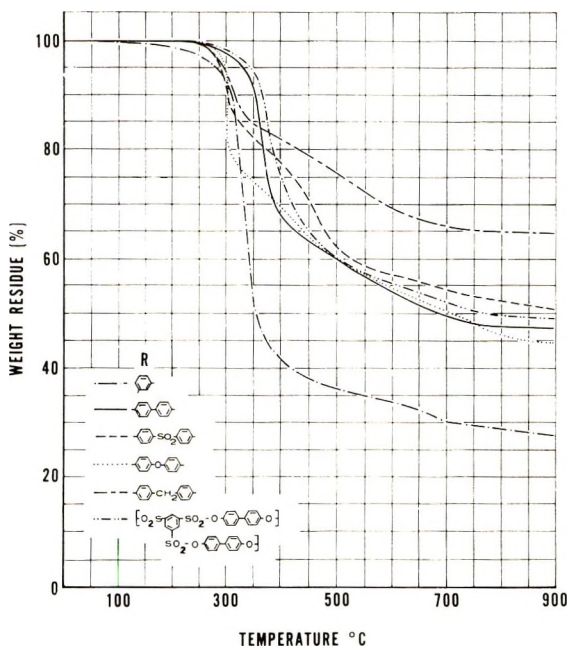


Fig. 1. TGA curves of polysulfonates $[\text{O}_2\text{S}-\text{R}-\text{SO}_2-\text{O}-\text{R}-\text{O}]_n$.

sulfonate linkage ($-\text{SO}_2-\text{O}-$) can be readily distinguished in the polymer spectra, absorption occurring at both $1200\text{--}1145\text{ cm.}^{-1}$ and $1420\text{--}1330\text{ cm.}^{-1}$.³

Inherent viscosities of the respective polymers suggested high molecular weights. In order to verify this, a sample of a polysulfonate containing the biphenylene unit ($\eta_{\text{inh}} = 0.42$) was subjected to a molecular weight determination by light scattering. The value for \bar{M}_w was found to be on the order of 50,000.

X-ray powder diagrams show a low degree of crystallinity in all of the polymers. The physical properties of the polymers are summarized in Table I. The polymers show limited solubility in common organic solvents; *N,N*-dimethylformamide was found to be the best solvent. A softening range was determined for each polymer in a modified Vicat apparatus and was found to occur within ten degrees in the region of $200\text{--}250^\circ\text{C}$.

Thermal gravimetric analysis (TGA) in a nitrogen atmosphere was used to evaluate the thermal stability of the respective polysulfonates. Figure 1 shows the curves obtained from the various polymers. A fairly sharp onset of weight loss is noted around 300°C ., which levels off at 500°C ., leaving approximately 50% residue up to 900°C .. Since the majority of the polymers show loss of weight in the $300\text{--}340^\circ\text{C}$. region, the upper limits of stability appear to be governed by the stability of the sulfonate linkage. The polymer melt decomposes rapidly with the evolu-

tion of sulfur dioxide, indicating that the sulfonate linkage is the weak spot in the chain. The contribution from the aromatic unit appears to be responsible for only a slight increase or decrease in overall stability. In terms of weight loss, the diphenylmethane polysulfonate appears to be the most resistant to thermal degradation (Fig. 1). However, the weight residue obtained from this polymer can be explained by the benzylic nature of the methylene linkage. Following decomposition of the sulfonate linkage, hydrogen abstraction could occur which would result in a highly crosslinked residue. This residue, consisting of aromatic rings for the most part, would be expected to show little weight loss at elevated temperatures.

The polymers of highest molecular weight and thermal stability were obtained from the more rigid aromatic structures, such as biphenyl and diphenyl sulfone. In other cases, high molecular weight polymer could be obtained only under more severe reaction conditions. Normal conditions gave polymers of very low molecular weight ($\eta_{inh} = 0.10-0.05$). This may indicate that the more flexible monomers are cyclizing rather than growing linearly. The cyclic trimers and tetramers have molecular weights of approximately 1500 and 2000, respectively.

All of the polymers were found to be hydrolytically stable to both acid and base at room temperatures. Concentrated solutions, when heated for 24 hr., produced polymers which were only slightly decreased in viscosity.

Experimental

A general method of preparation of the polysulfonates is as follows. To a solution of 0.1 mole of the diphenol in 500 ml. of water were added 0.1 g. of sodium carbonate and 0.1 g. of sodium lauryl sulfate. With rapid stirring, a solution of 0.1 mole of the disulfonyl chloride in 500 ml. of either benzene or methylene chloride was added. The reaction mixture was stirred for 30 min., followed by addition of 500 ml. of methanol. The white polymer was filtered, washed with methanol, and dried under vacuum.

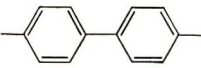
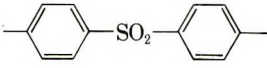
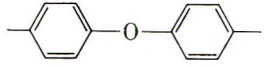
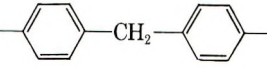
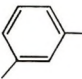
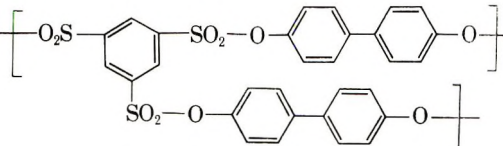
Elemental analyses of the polymers are presented in Table II.

Infrared spectra were obtained on all monomers and polymers. In addition to absorptions attributed to the sulfonate linkage, those occurring at 1240 cm.^{-1} (aromatic ether), 1440 cm.^{-1} (methylene), $1600-1550\text{ cm.}^{-1}$ (biphenyl doublet), and $1160-1140$ and $1350-1300\text{ cm.}^{-1}$ (sulfone) were valuable in establishing the presence of these groups in the respective polymers.³

Light-scattering molecular weight measurements were made with the use of a Brice-Phoenix light-scattering photometer, Universal 1000 Series. The scattering intensities were determined on carefully filtered *N,N*-dimethylformamide solutions of the polymer contained in a cylindrical cell having the dimensions 75×26 mm. The refractive index increment for a wavelength of $436\text{ m}\mu$ was 0.236 ml./g. at $25.00 \pm 0.05^\circ\text{C.}$, obtained through the use of a Brice-Phoenix Model BP-1000-U differential refractom-

eter. The data obtained were interpreted through the use of a Zimm plot. The weight-average molecular weight was found to be $52,000 \pm 5,000$.

TABLE II
Elemental Analyses for $+O_2S-Ar-SO_2-O-Ar-O+$

Ar	Element	Analyses, %	
		Calc.	Found
	C	62.07	61.40
	H	3.45	3.48
	S	13.81	13.86
	C	48.65	48.61
	H	2.70	2.79
	S	21.62	21.80
	C	58.06	57.32
	H	3.63	3.83
	S	12.90	12.78
	C	63.41	62.96
	H	4.07	4.18
	S	13.01	12.30
	C	46.15	45.76
	H	2.58	2.67
	S	20.53	19.30
	C	61.54	61.75
	H	3.30	3.23
	S	11.72	12.91

Thermal gravimetric analysis in a nitrogen atmosphere was obtained in a Chevenard thermobalance. Samples were heated to 900°C . at a programmed rate of $150^\circ\text{C}/\text{hr}$.

References

1. Kreuchunas, A., U. S. Pat. 2,822,351 (Feb. 4, 1958).
2. Lenz, R. W., and C. E. Handlovits, *J. Polymer Sci.*, **43**, 167 (1960).
3. Bellamy, L. J., *The Infra-red Spectra of Complex Molecules*, 2nd Ed., Methuen, London, 1959, pp. 13, 65, 115, 350.

Résumé

Des polysulfonates aromatiques très purs et de poids moléculaires élevés peuvent facilement être préparés par polycondensation interfaciale des chlorures de disulfonyle avec les diphénoles. Les polymères possèdent un faible degré de cristallinité, un point de ramollissement se situant dans la région $200-250^\circ\text{C}$, des poids moléculaires supérieurs à 50.000 et une stabilité thermique sous azote supérieure à 300°C .

Zusammenfassung

Hochmolekulare aromatische Polysulfonate von hoher Reinheit können durch Grenzflächenpolykondensation von Disulfonylchloriden mit Diphenolen leicht dargestellt werden. Die Polymeren besitzen einen niedrigen Kristallinitätsgrad, einen Erweichungsbereich im Gebiet von 200–250°C, Molekulargewichte bis hinauf zu 50000 und eine thermische Stabilität unter Stickstoff bis oberhalb 300°C. fin.

Received January 18, 1963

Evaluation of Molecular Weight Averages Resulting from Random Chain Scission Process for Wide Distributions as in Polyolefins

A. M. KOTLIAR, *Esso Research & Engineering Company,
Enjay Laboratories Division, Linden, New Jersey*

Synopsis

The effects of random degradation on the molecular weight averages for broad Schulz-Zimm and Wesslau type distributions are evaluated by blending two most probable Flory type distributions so that the $\bar{M}_n : \bar{M}_w : \bar{M}_z$ ratios of the blend were equal to that of the distribution models for any particular \bar{M}_w/\bar{M}_n ratio. The results indicate a rather extreme sensitivity of broad Wesslau distributions to small degrees of degradation and suggest that this function is not a good description for polyolefins.

Introduction

The general theoretical developments for changes in the various molecular weight averages of polymers undergoing random chain scission have been described and evaluated for specific distribution models.¹⁻²⁰ However, present experimental methods of determining wide molecular weight distributions are rather crude, and the most we may say at present is that a particular distribution will behave like a particular theoretical model. This is equivalent to knowing the ratios $\bar{M}_n : \bar{M}_w : \bar{M}_z$, but not the actual differential molecular weight distribution. Although these parameters do not completely specify the differential distribution, it is reasonable to assume that they may characterize a polymer sufficiently well to permit practical correlations with rheological behavior and mechanical and vulcanizate properties. The simplest method for evaluating the effects of random scission on wide molecular weight distributions having a given $\bar{M}_n : \bar{M}_w : \bar{M}_z$ is to consider the distribution as a blend of two most probable (Flory) distributions since (1) a most probable distribution remains most probable after being subjected to a random degradation process; (2) the linear superposition of two most probable distributions yields a single peak differential distribution under certain constraints (see Appendix); (3) the resulting molecular weight averages are related to the initial values by a factor $1 + s$, where s is the scission index (the number of bonds broken per original number-average molecule).

Theory

The weight fraction, $W(P)$ of a polymer species of size P in the range dP for a most probable distribution is given by

$$W(P)dP = y^2 P e^{-yP} dP \quad (1)$$

where

$$y = \frac{1}{\bar{P}_n} = \frac{2}{\bar{P}_w} = \frac{3}{\bar{P}_z}$$

For a linear superposition of two such species

$$W(P)dP = (g_1 y_1^2 P e^{-y_1 P} + g_2 y_2^2 P e^{-y_2 P}) dP \quad (2)$$

where g_1 and g_2 are the weight fractions of the species and

$$g_1 + g_2 = 1 \quad (3)$$

Setting

$$\bar{P}_{n_2} = m \bar{P}_{n_1} \quad (4)$$

yields

$$\bar{P}_n = \frac{m \bar{P}_{n_1}}{1 - g_1(1 - m)} \quad (5)$$

for the number-average,

$$\bar{P}_w = 2[g_1 + m(1 - g_1)] \bar{P}_{n_1} \quad (6)$$

for the weight-average, and

$$\bar{P}_z = \frac{3[g_1 + (1 - g_1)m^2] \bar{P}_{n_1}}{g_1 + m(1 - g_1)} \quad (7)$$

for the z-average.

Then

$$\bar{P}_w / \bar{P}_n = \frac{2[g_1 + m(1 - g_1)][1 - g_1(1 - m)]}{m} \quad (8)$$

This yields

$$g_1 = \frac{1 \pm [1 - 4m(\bar{P}_w/2\bar{P}_n - 1)/(1 - m)^2]^{1/2}}{2} \quad (9)$$

the choice of sign being determined by

$$\bar{P}_z / \bar{P}_w = \frac{3[g_1 + (1 - g_1)m^2]}{2[g_1 + m(1 - g_1)]} \quad (10)$$

Setting $\bar{P}_{n_1} > \bar{P}_{n_2}$ and neglecting m^2 terms, since m will be necessarily small for wide distributions, yields, by combining eqs. (9) and (10),

$$m \cong \frac{3\bar{P}_w/2\bar{P}_z - (3\bar{P}_w/2\bar{P}_z)^2}{1 + \bar{P}_w/2\bar{P}_n - 3\bar{P}_w/\bar{P}_z} \quad (11)$$

Equations (9) and (11) can then be readily solved for m and g_1 for particular values of \bar{P}_w/\bar{P}_n and \bar{P}_z/\bar{P}_w .

The number of bonds broken per original number-average molecule of each component is

$$s_1 = s\bar{P}_{n_1}/\bar{P}_n \quad (12)$$

$$s_2 = s\bar{P}_{n_2}/\bar{P}_n \quad (13)$$

where s is the number of bonds broken per original number-average of the whole polymer.

For a most probable distribution, it may be readily shown that

$$\bar{P}_{ns} = \bar{P}_{n,0}/1 + s \quad (14)$$

$$\bar{P}_{ws} = \bar{P}_{w,0}/1 + s \quad (15)$$

$$\bar{P}_{zs} = \bar{P}_{z,0}/1 + s \quad (16)$$

$$[\eta]_s = [\eta]_0/(1 + s)^\alpha \quad (17)$$

where α is the Mark-Houwink exponent. Using the above relationships, the results for the blend are

$$P_{ns} = \frac{1}{(g_1/\bar{P}_{n_1s}) + (g_2/\bar{P}_{n_2s})} = P_{n0}/1 + s \quad (18)$$

$$\bar{P}_{ws}/P_{w0} = \left(\frac{g_1}{1 + s_1} + \frac{mg_2}{1 + s_2} \right) \left(\frac{1}{g_1 + mg_2} \right) \quad (19)$$

$$P_{zs}/P_{z0} = \left[\frac{\frac{g_1}{(1 + s_1)^2} + \frac{g_2m^2}{(1 + s_2)^2}}{\frac{g_1}{1 + s_1} + \frac{g_2m}{1 + s_2}} \right] \left[\frac{g_1 + g_2m}{g_1 + g_2m^2} \right] \quad (20)$$

$$[\eta]_s/[\eta]_0 = \left[\frac{g_1}{(1 + s_1)^\alpha} + \frac{g_2m^\alpha}{(1 + s_2)^\alpha} \right] \left(\frac{1}{g_1 + g_2m^\alpha} \right) \quad (21)$$

The resulting differential molecular weight distribution is

$$W(P_s)dP = (y_{1s}^2Pe^{-y_{1s}P} + y_{2s}^2Pe^{-Py_{2s}})dP \quad (22)$$

where

$$y_{1s} = y_1(1 + s_1)$$

and

$$y_{2s} = y_2(1 + s_2)$$

TABLE I
Schulz-Zimm Type Distributions^a

a	s	$M_{n,s}$		$M_{w,s}$		$M_{z,s}$		$M_{n,s}$		$M_{w,s}$		$M_{z,s}$		$[\eta]_s/[\eta]_0$					
		$M_{n,0}$	$M_{w,0}$	$M_{z,0}$	$M_{w,0}$	$M_{z,0}$	$M_{n,s}$	$M_{w,s}$	$M_{z,s}$	$M_{n,s}$	$M_{w,s}$	$M_{z,s}$	$M_{n,s}$	$M_{w,s}$	$M_{z,s}$	$\alpha = 0.5$	$\alpha = 0.6$	$\alpha = 0.7$	$\alpha = 0.8$
0.05	0.00	1.000	1.000	1.000	21.00	41.00	1.000	1.000	1.000	1.000	1.000	1.000	1.000	1.000	1.000	1.000	1.000	1.000	1.000
0.05	0.02	0.980	0.786	0.783	16.83	32.75	0.783	0.890	0.890	0.868	0.847	0.826	0.805	0.890	0.868	0.847	0.826	0.805	0.805
0.05	0.04	0.962	0.647	0.644	14.14	27.43	0.644	0.811	0.811	0.775	0.741	0.708	0.677	0.811	0.775	0.741	0.708	0.677	0.677
0.05	0.06	0.943	0.551	0.546	12.26	23.71	0.546	0.751	0.751	0.705	0.663	0.623	0.586	0.751	0.705	0.663	0.623	0.586	0.586
0.05	0.08	0.926	0.479	0.474	10.87	20.97	0.474	0.703	0.703	0.651	0.603	0.558	0.517	0.703	0.651	0.603	0.558	0.517	0.517
0.05	0.10	0.909	0.425	0.418	9.81	18.86	0.418	0.663	0.663	0.606	0.554	0.507	0.464	0.663	0.606	0.554	0.507	0.464	0.464
0.05	0.20	0.833	0.271	0.263	6.82	12.95	0.263	0.536	0.536	0.467	0.407	0.355	0.310	0.536	0.467	0.407	0.355	0.310	0.310
0.05	0.40	0.714	0.158	0.150	4.65	8.62	0.150	0.416	0.416	0.343	0.283	0.233	0.192	0.416	0.343	0.283	0.233	0.192	0.192
0.05	0.60	0.625	0.113	0.105	3.78	6.86	0.105	0.354	0.354	0.282	0.224	0.178	0.142	0.354	0.282	0.224	0.178	0.142	0.142
0.05	0.80	0.556	0.088	0.080	3.32	5.91	0.080	0.315	0.315	0.244	0.189	0.146	0.113	0.315	0.244	0.189	0.146	0.113	0.113
0.05	1.00	0.500	0.072	0.065	3.03	5.31	0.065	0.286	0.286	0.218	0.165	0.125	0.095	0.286	0.218	0.165	0.125	0.095	0.095
0.05	1.50	0.400	0.050	0.044	2.64	4.49	0.044	0.241	0.241	0.177	0.129	0.094	0.069	0.241	0.177	0.129	0.094	0.069	0.069
0.05	2.00	0.333	0.039	0.033	2.44	4.06	0.033	0.213	0.213	0.152	0.108	0.077	0.055	0.213	0.152	0.108	0.077	0.055	0.055
0.05	3.00	0.250	0.027	0.022	2.26	3.64	0.022	0.179	0.179	0.123	0.084	0.058	0.039	0.179	0.123	0.084	0.058	0.039	0.039
0.05	6.00	0.143	0.014	0.011	2.09	3.24	0.011	0.131	0.131	0.084	0.054	0.035	0.022	0.131	0.084	0.054	0.035	0.022	0.022
0.10	0.00	1.000	1.000	1.000	11.00	21.00	1.000	1.000	1.000	1.000	1.000	1.000	1.000	1.000	1.000	1.000	1.000	1.000	1.000
0.10	0.02	0.980	0.878	0.876	9.85	18.77	0.876	0.940	0.940	0.927	0.914	0.902	0.890	0.940	0.927	0.914	0.902	0.890	0.890
0.10	0.04	0.962	0.783	0.779	8.96	17.01	0.779	0.889	0.889	0.867	0.845	0.824	0.803	0.889	0.867	0.845	0.824	0.803	0.803
0.10	0.06	0.943	0.706	0.701	8.24	15.61	0.701	0.897	0.897	0.817	0.788	0.759	0.732	0.897	0.817	0.788	0.759	0.732	0.732
0.10	0.08	0.926	0.644	0.637	7.65	14.45	0.637	0.810	0.810	0.774	0.740	0.706	0.674	0.810	0.774	0.740	0.706	0.674	0.674
0.10	0.10	0.909	0.591	0.584	7.16	13.49	0.584	0.778	0.778	0.737	0.697	0.660	0.625	0.778	0.737	0.697	0.660	0.625	0.625
0.10	0.20	0.833	0.421	0.411	5.56	10.36	0.411	0.662	0.662	0.605	0.553	0.505	0.461	0.662	0.605	0.553	0.505	0.461	0.461

0.10	0.40	0.714	0.269	0.257	4.14	7.56	0.535	0.467	0.407	0.355	0.309
0.10	0.60	0.625	0.199	0.186	3.50	6.26	0.464	0.392	0.331	0.279	0.236
0.10	0.80	0.556	0.158	0.146	3.13	5.52	0.416	0.344	0.283	0.233	0.192
0.10	1.00	0.500	0.132	0.120	2.89	5.03	0.381	0.309	0.250	0.202	0.163
0.10	1.50	0.400	0.093	0.083	2.57	4.34	0.324	0.253	0.198	0.154	0.120
0.10	2.00	0.33	0.073	0.063	2.40	3.97	0.287	0.219	0.166	0.126	0.096
0.10	3.00	0.250	0.051	0.043	2.23	3.60	0.241	0.177	0.130	0.095	0.070
0.10	6.00	0.143	0.027	0.022	2.08	3.24	0.177	0.122	0.084	0.058	0.040
0.20	0.00	1.000	1.000	1.000	6.00	11.00	1.000	1.00	1.000	1.000	1.000
0.20	0.02	0.980	0.932	0.930	5.71	10.42	0.967	0.960	0.953	0.946	0.939
0.20	0.04	0.962	0.873	0.869	5.45	9.93	0.937	0.924	0.911	0.898	0.886
0.20	0.06	0.943	0.821	0.816	5.22	9.50	0.910	0.892	0.874	0.856	0.838
0.20	0.08	0.926	0.775	0.769	5.02	9.11	0.886	0.863	0.840	0.818	0.796
0.20	0.10	0.909	0.734	0.727	4.85	8.77	0.863	0.836	0.809	0.783	0.758
0.20	0.20	0.833	0.581	0.570	4.19	7.50	0.772	0.730	0.690	0.652	0.616
0.20	0.40	0.714	0.412	0.397	3.46	6.10	0.655	0.598	0.545	0.497	0.452
0.20	0.60	0.625	0.320	0.304	3.08	5.34	0.581	0.517	0.459	0.407	0.361
0.20	0.80	0.556	0.263	0.246	2.84	4.86	0.528	0.460	0.401	0.348	0.303
0.20	1.00	0.500	0.223	0.206	2.68	4.53	0.489	0.419	0.358	0.306	0.261
0.20	1.50	0.400	0.163	0.157	2.44	4.04	0.420	0.348	0.288	0.239	0.197
0.20	2.00	0.333	0.129	0.114	2.31	3.77	0.375	0.304	0.245	0.198	0.160
0.20	3.00	0.250	0.091	0.079	2.19	3.48	0.317	0.248	0.194	0.151	0.117
0.20	6.00	0.143	0.049	0.042	2.07	3.20	0.234	0.172	0.126	0.092	0.092

^a Schulz-Zimm distribution

$$W(P) = \frac{y^a + 1}{\Gamma(a + 1)} P^a e^{-yP}$$

where $W(P)dP$ is the weight fraction of material of size P in the range dP and $y = a/\bar{P}_n = (a + 1)/\bar{P}_w = (a + 2)/\bar{P}_z$.

TABLE II
Wesslau Type Distributions*

β	s	$\frac{M_{n,s}}{M_{n,0}}$	$\frac{M_{w,s}}{M_{w,0}}$	$\frac{M_{z,s}}{M_{z,0}}$	$\frac{M_{m,s}}{M_{m,0}}$	$[\eta]_s/[\eta]_0$					
						$\alpha = 0.5$	$\alpha = 0.6$	$\alpha = 0.7$	$\alpha = 0.8$	$\alpha = 0.9$	
2.47	0.00	1.000	1.000	1.0000	21.00	441.00	1.000	1.000	1.000	1.000	1.000
2.47	0.02	0.980	0.302	0.1907	6.46	85.77	0.763	0.660	0.554	0.455	0.370
2.47	0.04	0.962	0.206	0.0918	4.49	42.10	0.703	0.585	0.466	0.360	0.273
2.47	0.06	0.943	0.167	0.0566	3.71	26.48	0.671	0.546	0.424	0.317	0.231
2.47	0.08	0.926	0.145	0.0396	3.29	18.88	0.649	0.522	0.398	0.291	0.207
2.47	0.10	0.909	0.131	0.0300	3.03	14.54	0.632	0.503	0.379	0.274	0.191
2.47	0.20	0.833	0.099	0.0132	2.50	7.00	0.580	0.449	0.328	0.227	0.152
2.47	0.40	0.714	0.076	0.0070	2.22	4.29	0.522	0.393	0.279	0.187	0.121
2.47	0.60	0.625	0.064	0.0052	2.14	3.66	0.483	0.358	0.249	0.164	0.104
2.47	0.80	0.556	0.055	0.0043	2.09	3.41	0.453	0.331	0.227	0.147	0.092
2.47	1.00	0.500	0.049	0.0037	2.07	3.28	0.428	0.309	0.209	0.134	0.083
2.47	1.50	0.400	0.039	0.0029	2.04	3.15	0.381	0.269	0.178	0.111	0.067
2.47	2.00	0.333	0.032	0.0023	2.03	3.10	0.347	0.240	0.156	0.096	0.056
2.47	3.00	0.250	0.024	0.0017	2.02	3.06	0.300	0.202	0.127	0.076	0.043
2.47	6.00	0.143	0.014	0.0010	2.01	3.03	0.227	0.144	0.086	0.048	0.026
2.19	0.00	1.000	1.000	1.0000	11.00	121.00	1.000	1.000	1.000	1.000	1.000
2.19	0.02	0.980	0.582	0.4553	6.53	56.19	0.861	0.816	0.758	0.697	0.638
2.19	0.04	0.962	0.437	0.2782	4.99	35.01	0.808	0.735	0.657	0.578	0.504
2.19	0.06	0.943	0.362	0.1939	4.22	24.87	0.769	0.686	0.598	0.512	0.432
2.19	0.08	0.926	0.316	0.1460	3.75	19.08	0.740	0.651	0.558	0.468	0.386
2.19	0.10	0.909	0.284	0.1158	3.44	15.41	0.719	0.625	0.529	0.437	0.355

2.19	0.20	0.833	0.206	0.0551	2.73	8.00	0.650	0.547	0.446	0.353	0.273
2.19	0.40	0.714	0.151	0.0282	2.33	4.77	0.577	0.471	0.371	0.283	0.204
2.19	0.60	0.625	0.125	0.0202	2.20	3.92	0.531	0.425	0.328	0.244	0.177
2.19	0.80	0.556	0.108	0.0164	2.13	3.56	0.496	0.391	0.297	0.218	0.155
2.19	1.00	0.500	0.095	0.0140	2.10	3.38	0.468	0.365	0.274	0.198	0.139
2.19	1.50	0.400	0.075	0.0105	2.05	3.18	0.416	0.316	0.231	0.163	0.112
2.19	2.00	0.333	0.062	0.0085	2.03	3.03	0.378	0.282	0.203	0.140	0.094
2.19	3.00	0.250	0.046	0.0063	2.02	3.00	0.327	0.237	0.165	0.111	0.082
2.19	6.00	0.143	0.026	0.0035	2.01	3.00	0.246	0.169	0.111	0.071	0.043
1.89	0.00	1.000	1.000	1.000	6.00	36.00	1.000	1.000	1.000	1.000	1.000
1.89	0.02	0.980	0.816	0.718	4.99	26.38	0.942	0.921	0.897	0.871	0.844
1.89	0.04	0.962	0.701	0.552	4.37	20.67	0.900	0.866	0.827	0.786	0.744
1.89	0.06	0.943	0.622	0.444	3.96	16.95	0.868	0.824	0.776	0.725	0.673
1.89	0.08	0.926	0.564	0.369	3.66	14.35	0.841	0.791	0.736	0.679	0.621
1.89	0.10	0.904	0.520	0.315	3.43	12.46	0.819	0.763	0.704	0.642	0.580
1.89	0.20	0.833	0.392	0.179	2.82	7.73	0.743	0.673	0.600	0.527	0.457
1.89	0.40	0.714	0.287	0.099	2.41	4.97	0.657	0.576	0.496	0.420	0.349
1.89	0.60	0.625	0.235	0.071	2.25	4.10	0.602	0.517	0.436	0.361	0.293
1.89	0.80	0.556	0.201	0.057	2.17	3.71	0.561	0.475	0.394	0.321	0.256
1.89	1.00	0.500	0.177	0.049	2.13	3.49	0.529	0.442	0.362	0.290	0.229
1.89	1.50	0.400	0.138	0.036	2.07	3.25	0.469	0.382	0.305	0.238	0.183
1.89	2.00	0.333	0.114	0.029	2.04	3.15	0.426	0.340	0.266	0.204	0.154
1.89	3.00	0.250	0.084	0.021	2.02	3.07	0.368	0.285	0.216	0.161	0.118
1.89	6.00	0.143	0.048	0.012	2.01	3.01	0.277	0.203	0.146	0.102	0.071

^a $W(P) = (1/\beta P \pi^{1/2}) \exp\{- (1/\beta^2) \ln^2 P/P_0\}$ where $W(P)dP$ is the weight fraction of material of size P in the range dP and $\bar{P}_n = P_0 e^{-\beta^2/4}$; $\bar{P}_w = P_0 e^{+\beta^2/4}$; $\bar{P}_w/\bar{P}_n = \bar{P}_z/\bar{P}_w = e^{\beta^2/2}$.

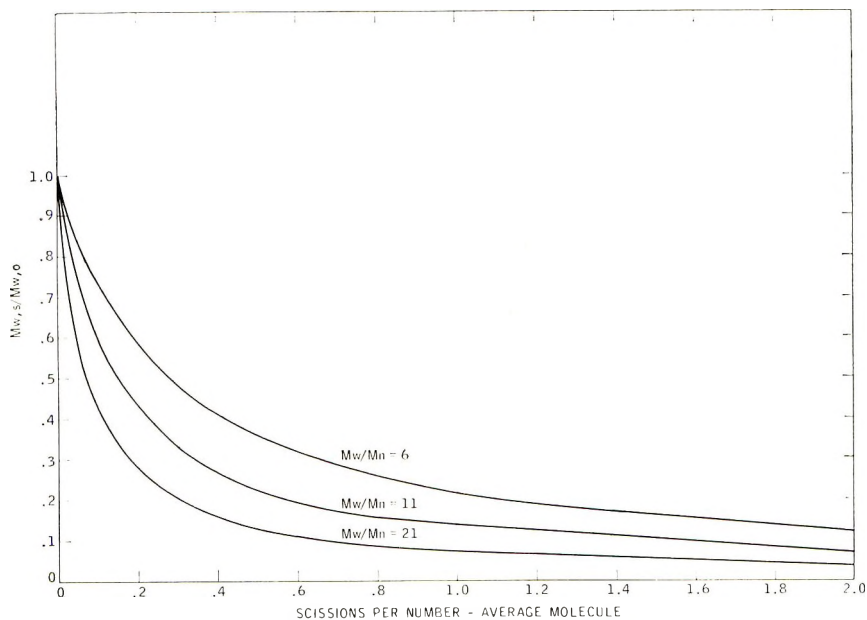


Fig. 1. Random degradation of Schulz-Zimm type distributions.

Results and Discussion

The results of random degradation of wide Schulz-Zimm²¹ and Wesslau²² like distributions are listed in Tables I and II with typical results shown in Figures 1 and 2. It can be seen that by proper curve fitting one may distinguish not only \bar{M}_w/\bar{M}_n , but also \bar{M}_z/\bar{M}_w . In Figure 3, a comparison is shown of Schulz-Zimm and Wesslau like distributions each having a \bar{M}_w/\bar{M}_n of 11. The rather extreme sensitivity of wide Wesslau distributions to small degrees of random degradation indicates that this function is not a good description for polyolefins. This is in contradiction to recent claims²³⁻²⁸ based on fractionation data. A recent analysis²⁹ of column elution and precipitation fractionation data based on the Flory-Huggins theory shows that the Schulz-Dinglinger approximation, namely

$$I(P) = W_j/2 + \sum_{j=1}^{j=1} W_i \quad (23)$$

where $I(P)$ is the cumulative weight and $w_{j,i}$ are the respective weight fractions of the collected samples, is a poor approximation for wide distributions. The fact that one finds a fair fit of the data on a Wesslau plot, which is generally poor at the low and high molecular weight ends with the computed \bar{M}_w generally being about 20% different than the measured value, is poor justification for assuming that the distribution is a Wesslau type. It is indeed justification for assuming that these distributions are not of the Wesslau type, the pseudo straight line on a Wesslau plot being a result of the methods employed.

When it is known that the distribution about the maximum is significantly narrower than the superposition of two most probable distributions or that the distribution has more than one significant peak, e.g., blending

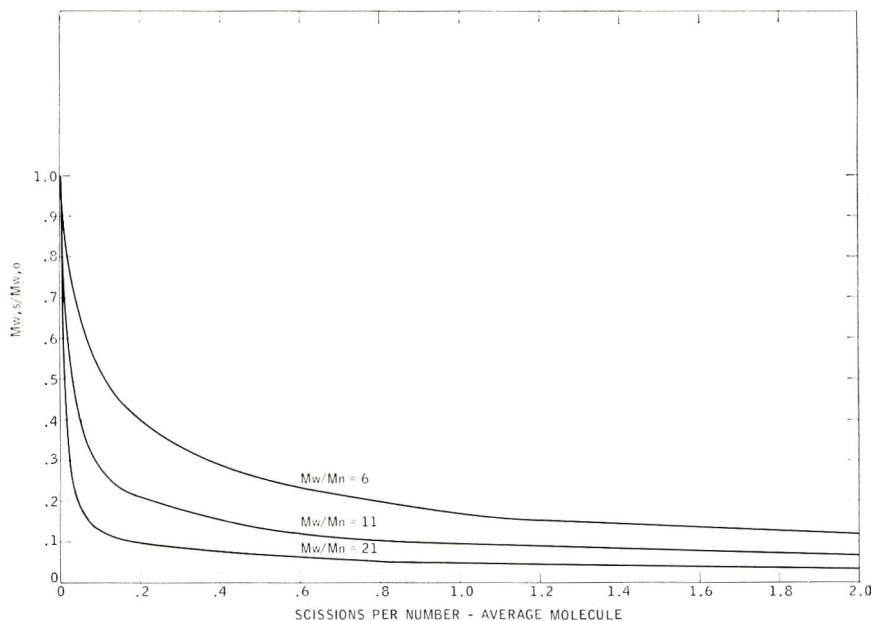


Fig. 2. Random degradation of Wesslau type distributions.

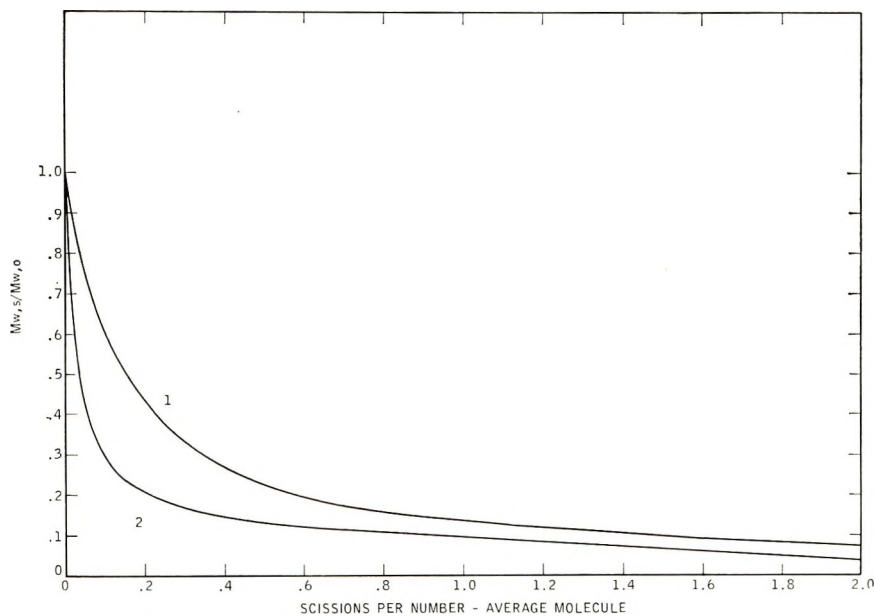


Fig. 3. Effect of distribution type on the ratio $M_{w,s} / M_{w,0}$ for (1) Schulz-Zimm and (2) Wesslau types having $M_{w,0} / M_{n,0} = 11$.

of fractionated samples, the above method can be readily extended using the calculations of Kotliar and Anderson¹⁴ or Inokuti³⁰ on random degradations of narrow molecular weight distributions, i.e., $\bar{M}_w/\bar{M}_n < 2$.

The author gratefully acknowledges the helpful discussions with Dr. John Rehner, Jr., and the assistance of Miss Diana Mahon and Mr. Howard Oakley in the computer calculations.

APPENDIX

The conditions under which a blend of two most probable distribution exhibits more than one maximum may be evaluated by differentiating eq. (2) with respect to P yielding

$$dW(P)/dP = g_1 y_1^2 e^{-y_1 P} (1 - y_1 P) + g_2 y_2^2 (1 - y_2 P) \quad (24)$$

and

$$d^2W(P)/dP^2 = g_1 y_1^3 e^{-y_1 P} (y_1 P - 2) + g_2 y_2^3 e^{-y_2 P} (y_2 P - 2) \quad (25)$$

Equating eqs. (24) and (25) to zero and solving for P yields

$$P = \frac{1 + b \pm \sqrt{1 - 6b + b^2}}{2y_1} \quad (26)$$

where

$$b = 1/m$$

For real value of P

$$b = 3 \pm 2\sqrt{2}$$

and the maximum value for m where an inflection point exists is

$$m = 3 - 2\sqrt{2}$$

and is independent of g_1 or g_2 . The existence of an inflection point, for $m \geq 0.172$, reduces the two possible maxima values for P to only a single maximum. For m values less than 0.172, two maxima may exist, depending on the ratio of g_1/g_2 . When $g_1 = g_2$, two maxima exist for values of m less than about 0.075. The conclusion of Billmeyer and Stockmayer³¹ that the distribution possesses but a single maximum, whatever the value of m , when $g_1 = g_2 = 0.5$ is therefore in error.

References

1. Kuhn, W., *Ber.*, **63**, 1503 (1930).
2. Montroll, D. W., and R. Simha, *J. Chem. Phys.*, **8**, 721 (1940).
3. Simha, R., *J. Appl. Phys.*, **12**, 569 (1941).
4. Sakurada, I., and S. Okamura, *Z. Physik. Chem.*, **A187**, 389 (1940).
5. Schultz, G. V., *Z. Physik. Chem.*, **352**, 50 (1942).
6. Flory, P. J., *J. Am. Chem. Soc.*, **63**, 3905 (1940).
7. Stockmayer, W. H., *J. Chem. Phys.*, **12**, 125 (1944).

8. Charlesby, A., *J. Polymer Sci.*, **11**, 513 (1953); *Proc. Roy. Soc. (London)*, **A222**, 60 (1954); *ibid.*, **A222**, 542 (1954); *ibid.*, **A224**, 120 (1954); *ibid.*, **A231**, 521 (1956).
9. Small, P. A., *J. Polymer Sci.*, **18**, 431 (1955).
10. Horikx, M. M., *J. Polymer Sci.*, **19**, 445 (1956).
11. Saito, O., *J. Phys. Soc. Japan*, **13**, 198 (1958); *ibid.*, **13**, 1451 (1958); *ibid.*, **13**, 1465 (1958).
12. Kilb, R. W., *J. Phys. Chem.*, **63**, 1838 (1959).
13. Inokuti, M., and K. Katsuura, *J. Phys. Soc. Japan*, **14**, 1379 (1959).
14. Kotliar, A. M., and A. D. Anderson, *J. Polymer Sci.*, **45**, 541 (1960).
15. Kotliar, A. M., *J. Polymer Sci.*, **51**, 363 (1961).
16. Kotliar, A. M., *J. Polymer Sci.*, **61**, 525 (1962).
17. Kotliar, A. M., *J. Polymer Sci.*, **62**, S98 (1962).
18. Kotliar, A. M., *J. Polymer Sci.*, **1**, 3175 (1963).
19. Kotliar, A. M., and S. Podgor, *J. Polymer Sci.*, **55**, 423 (1961).
20. Inokuti, M., *J. Chem. Phys.*, **33**, 1607 (1960).
21. Schultz, G. V., *Z. Physik. Chem.*, **B43**, 25 (1939); B. H. Zimm, *J. Chem. Phys.*, **16**, 1099 (1948).
22. Wesslau, H., *Makromol. Chem.*, **20**, 111 (1950).
23. Henry, M. P., *J. Polymer Sci.*, **36**, 3 (1959).
24. Kenyon, A. S., and I. O. Salyer, *J. Polymer Sci.*, **43**, 427 (1960).
25. Davis, T. E., and R. L. Tobias, *J. Polymer Sci.*, **50**, 227 (1961).
26. Francis, P. S., R. C. Cooke, Jr., and J. H. Elliott, *J. Polymer Sci.*, **31**, 453 (1958).
27. Shyluk, S., preprint, papers presented to Division of Polymer Chemistry, **2**, 133 (1960), 138th Meeting, American Chemical Society, New York, N. Y., September 1960.
28. Tung, L. H., *J. Polymer Sci.*, **26**, 333 (1957).
29. Kotliar, A. M., to be published.
30. Inokuti, M., and M. Dole, private communication.
31. Billmeyer, F. W., Jr., and W. H. Stockmayer, *J. Polymer Sci.*, **5**, 121 (1950).

Résumé

On évalue les effets de la dégradation statistique sur le poids moléculaire moyen pour des larges distributions du type Schulz-Zimm et Wesslau en mêlant deux distributions du type Flory les plus probables de sorte que les rapports $\bar{M}_w : \bar{M}_n : \bar{M}_z$ du mélange soient égaux à celui des modèles de distribution pour chaque rapport \bar{M}_w/\bar{M}_n particulier. Les résultats indiquent une sensibilité assez forte des larges distributions Wesslau aux faibles degrés de dégradation, ce qui suggère que cette fonction n'est pas adéquate pour des polyoléfines.

Zusammenfassung

Der Einfluss eines statistischen Abbaus auf die Molekulargewichtsmittelwerte für breite Verteilungen vom Schulz-Zimm- und Wesslau-Typ wird durch Mischung zweier wahrscheinlichster Verteilungen vom Flory-Typ in der Weise, dass das $\bar{M}_w : \bar{M}_n : \bar{M}_z$ Verhältnis der Mischung gleich dem der Modellverteilung für irgend ein spezielles \bar{M}_w/\bar{M}_n -Verhältnis ist, ermittelt. Die Ergebnisse zeigen eine extrem grosse Empfindlichkeit breiter Wesslau-Verteilungen für geringe Abbaugrade, so dass diese Funktion zur Beschreibung von Polyolefinen nicht gut geeignet ist.

Received January 21, 1963

Photosensitized Polymerization of Acrylic Monomers.

II. Kinetics of Polymerization in the Presence of Oxygen

G. DELZENNE,* W. DEWINTER, S. TOPPET, and G. SMETS,
*Laboratoire de Chimie Macromoléculaire, University of Lowain,
Belgium*

Synopsis

The kinetics of the photopolymerization of acrylamide and methacrylic acid in aqueous and semi-organic solutions have been examined; the initiating redox system used in the presence of oxygen were eosin-thiourea, eosin-1-ascorbic acid, or in some cases riboflavine. The rates of photopolymerization were determined by measuring the thermal rise of the reaction cell using a thermistor technique. In aqueous and in semi-organic solutions, the rate is proportional to the square of the monomer concentration in both cases. Below a critical concentration of sensitizer the rate of polymerization of monomers is proportional to the square root of sensitizer concentration (acrylamide in the presence of riboflavine, methacrylic acid in the presence of eosin-ascorbic acid); above it, the rate becomes inversely proportional to the square root of the sensitizer concentration. With respect to the reducing agent concentration, the exponent for thiourea is located between 0.5 and 1 in the case of acrylamide and 0.5 for methacrylic acid. Finally with respect to the oxygen concentration the rates are proportional to the square root of its concentration, at least below a given oxygen-concentration where the induction period becomes predominant. These results are interpreted assuring a participation of the monomer in the initiation step, and a low initiation efficiency of the primary radicals (cage recombination). A kinetic scheme is presented and the experimental results discussed on the basis of it.

INTRODUCTION

The photosensitized polymerization of vinyl compounds has been intensively studied during the last few years. Several sensitizing systems based on the use of dyestuffs were described for polymerization as well as for grafting reactions.¹⁻¹³ The initiation mechanism proposed by these authors are widespread and take into account not only the formation of radicals by photolysis of the sensitizer but also the more energy transfer processes. In this particular case the excited triplet state of the sensitizer seems to play a very important role. These systems however are characterized by the necessity of an oxygen-free reaction medium and by a rather low quantum yield for monomer conversion.

The sensitizing systems described by Oster et al.,¹⁴⁻²⁶ on the other hand,

* Present address: Gevaert Photoproducten N. V., Mortcel-Antwerp, Belgium.

are very active in the presence of oxygen and give rise to high quantum yields for monomer conversion. The essential feature of these systems is the simultaneous action of a sensitizing dye and a mild reducing agent. Their use has also been extended to the photosensitization of grafting reactions.²⁷ The initiation is produced by the action of a redox system formed during the photoreduction step of the sensitizer which occurs simultaneously. During this reaction hydrogen peroxide is formed by reoxidation of the photoreduction products. This has already been described for sensitizing dyes of the xanthene and acridine types.²⁸

The present work is devoted to the kinetic study of the photopolymerization of acrylamide and methacrylic acid in aqueous and semiorganic solutions. The photosensitizing systems tetrabromofluorescein (eosin)/thiourea, eosin/*l*(+)-ascorbic acid and in some cases, riboflavin, were used in the presence of oxygen.

EXPERIMENTAL

Materials

Riboflavin was pure commercial product from Light and Co. (England). Tetrabromofluorescein (eosin) was obtained from Biological Michrome reagents (E. Gurr, Ltd., London).

Thiourea and *l*(+)-ascorbic acid were Merck analytical grade reagents. Pure acrylamide was used after recrystallization from methylene chloride. Pure methacrylic acid was obtained by alkaline hydrolysis of methyl methacrylate. It was used after distillation under reduced pressure (b.p.: 163°C.). Distilled water saturated with air at atmospheric pressure and other organic solvents (analytical grade) were used without any further purification.

Procedure

Photopolymerization Technique. The solutions containing dye, reducing agent, and monomer in the appropriate concentrations for each experiment were placed in a cylindrical reaction cell having a diameter of 2 cm. and a total volume capacity of 30 ml. The volume of the solutions used throughout the experiments was 15 ml. The reaction cell was placed in a double-walled calorimeter and exposed, through an adequate aperture in the walls, to the light emitted by a 500-w. Episcopo Philips projector lamp with tungsten filament. The lamp output was stabilized by an automatic Sola voltage stabilizer. A parabolic mirror incorporated in the lamp concentrated the light beam on the lens. The parallel beam was passed through a water-cell with parallel plane faces in order to remove the greatest part of the infrared radiations. The irradiation system was fixed on an optical bench.

Polymerization Rate Measurements. The polymerization rates were measured on the basis of thermal rise accompanying the reaction by the use of a thermistor technique. The thermistor was a MBL E code B8/32003 P, 2.200-ohm gauge incorporated in the center of the reaction cell

and connected to one arm of a measuring Wheatstone bridge. The temperature rise during the reaction was followed by galvanometric recording of the resistivity changes in the gauge. The galvanometric measurements were converted into polymer yields by means of a conversion factor previously determined gravimetrically. The results were finally corrected for a slight temperature rise due to the irradiation of the cell. The rates were furthermore determined from a constant initial temperature on a small range in order to minimize the effects of temperature rise on the reaction itself and of the lack of adiabatic character of the system. The conversion factor used throughout this work for acrylamide in aqueous solution was:

$$(\Delta T)_{1^{\circ}\text{C.}} = 0.915 \times 10^{-3} \text{ mole/15 ml.}$$

In some cases the rate was measured gravimetrically after precipitation of the polymer in acetone, drying, and weighing.

Actinometry. The total incident light intensity was determined by the actinometric procedure of Parker and Hatchard.^{29,30} This method is based on the photolysis of the potassium ferrioxalate complex in acid solution. The ferrous ion concentration was determined colorimetrically by means of the complex formed with *o*-phenanthroline under well defined experimental conditions. The colorimetric measurements were carried out with an Eppendorf-Netheler colorimeter with a cadmium light source.

RESULTS

A. Influence of the Monomer Concentration

The influence of the monomer concentration on the rate of photopolymerization of acrylamide and methacrylic acid was determined at constant

TABLE I
Influence of the Acrylamide Concentration on the Rate of Polymerization^a

Solvent	Eosin, moles/l. $\times 10^5$	Reducing agent and concn., moles/l. $\times 10^3$	Monomer, moles/l.	Rate of polymerization moles/l./min.
Water	0.4	Ascorbic acid, 3	1.41	0.022
			2.82	0.093
			4.23	0.21
Water	1.44	Ascorbic acid, 5.7	2.81	0.016
			4.22	0.044
			5.62	0.1
Water	0.55	Thiourea, 92	2.82	0.105
			3.24	0.15
			3.52	0.2
			4.22	0.285
Water- ethanol, 75/25	0.4	Ascorbic acid, 3	5.63	0.45
			1.41	0.032
			2.82	0.122
			4.23	0.266

^a $I_0, 6.3 \times 10^{-6}$ Einsteins/hr./10 ml.

TABLE II
Influence of the Acrylamide Concentration on the Rate of Polymerization^a

Monomer, moles/l.	Rate of polymerization, moles/l./min.			
	Water	Water-dioxane, 70/30	Water-ethanol, 70/30	Water-methanol, 80/20
0.705	0.0007 ^b			
1.04	0.0026 ^b			
1.408	0.0057 ^b			
1.41	0.028	0.046	0.05	
2.11	0.018 ^b	0.1	0.1	
2.82	0.1	0.155	0.158	0.075
4.23	0.23	0.353	0.356	0.152
5.63	0.583			0.285

^a Except where otherwise noted, $I_0 = 6.3 \times 10^{-6}$ Einsteins/hr./10 ml., riboflavin, 1.54×10^{-4} moles/l., thermometric method.

^b I_0° , 3.66×10^{-6} Einsteins/hr./10 ml., riboflavin, 2.6×10^{-4} moles/l.; gravimetric method.

TABLE III
Influence of the Methacrylic Acid Concentration on the Rate of Polymerization^a

Monomer, moles/l.	Rate of polymerization, moles/l./min.
1.16	0.006
2.33	0.022
3.49	0.05
4.65	0.086

^a I_0 , 6.3×10^{-6} Einsteins/hr./10 ml.; eosin, 0.8×10^{-4} moles/l.; thiourea, 0.158 moles/l.; solvent: H₂O-C₂H₅OH, 70/30.

sensitizer and reducing agent concentrations and at constant light intensity. The sensitizing systems used were riboflavin, eosin-thiourea, and eosin-ascorbic acid. From the results summarized in Tables I-III and graphically represented in Figure 1, a dependence of the polymerization rate on the square of the monomer concentration can be concluded for both monomers as well in aqueous as in semiorganic solution. The results are in good agreement with the work of Oster et al.¹⁵ and will be discussed later. The kinetic dependence on monomer concentration in pure organic solution, however, could not be determined because of the insolubility of the polymer.

B. Influence of the Sensitizer Concentration

The influence of the sensitizer concentration on the polymerization rate was determined for riboflavin and eosin at constant monomer and reducing agent concentration and constant light intensity. The existence of a critical sensitizer concentration can be concluded from the experimental results. At this concentration the total incident light intensity is absorbed, and the polymerization rate passes through a maximum value. The results obtained for acrylamide in aqueous and semiorganic solutions sensi-

tized by riboflavin are summarized in Table IV. From a logarithmic plot of the rates of polymerization versus the sensitizer concentration (Fig. 2) the order of reaction has been determined and found to be equal to 0.5 below and to -0.5 above this critical concentration. The influence of the eosin concentration on the polymerization rate was studied for acrylamide in aqueous solution in the presence of thiourea, and for methacrylic acid

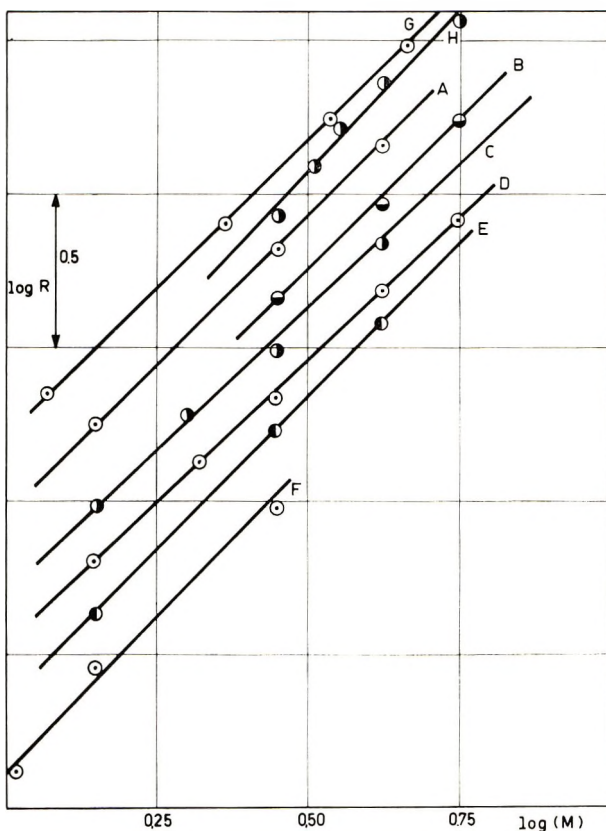


Fig. 1. Influence of the monomer concentration: (A) acrylamide in ethanol-water (25/75), eosin + ascorbic acid redox system. (B) acrylamide in methanol-water (20/80) riboflavin; (C) acrylamide in ethanol-water (30/70), riboflavin; (D) acrylamide in dioxane-water (30/70), riboflavin; (E) (F) acrylamide in water, riboflavin; (G) methacrylic acid in ethanol-water (30/70), eosin + thiourea; (H) acrylamide in water, eosin + thiourea.

in semiorganic solution in the presence of ascorbic acid and of thiourea. From the results summarized in Table V for eosin concentrations below the critical value (about 1.41×10^{-5} moles/l. in aqueous solution and 8×10^{-5} moles/l. in semiorganic solution) a 0.5 value was found for the concentration exponent in the case of the polymerization of methacrylic acid with ascorbic acid as reducing agent (Fig. 2). For acrylamide, on the other hand, the eosin concentration exponent was found to be 0.65 below and

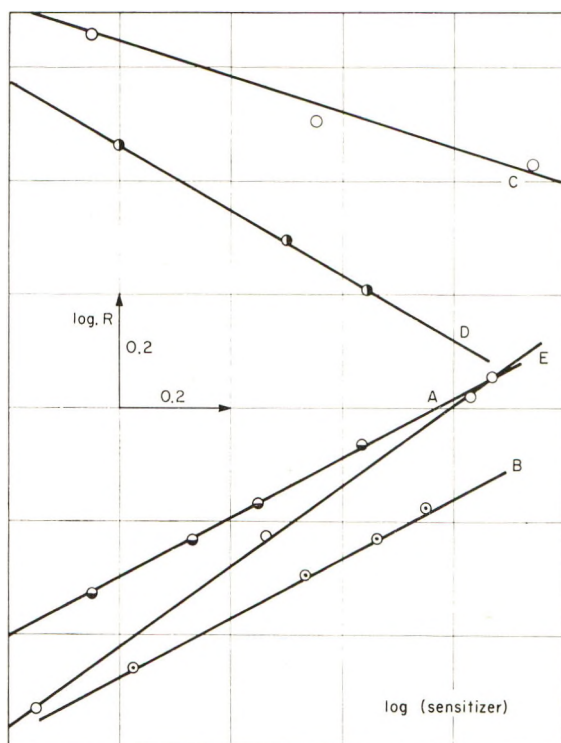


Fig. 2. Influence of the sensitizer concentration: (A) acrylamide in water-dioxane (50/50), riboflavin redox system; (B) methacrylic acid in water/ethanol (50/50), eosin + ascorbic acid; (C) acrylamide in water, eosin + thiourea; (D) acrylamide in water, riboflavin; (E) acrylamide in water, eosin + thiourea.

TABLE IV
Influence of Riboflavin Concentration on the Rate of Photopolymerization^a

Solvent	I_0 , Einsteins \times 10^6 /l./min.	Riboflavin, moles/l. $\times 10^4$	Rates of polymer- ization, moles/l./min.	Measuring technique
Water	6.1	2.6	0.01	Gravimetric
		1.5	0.0135	
		1.12	0.0165	
Water- dioxane	10.5	0.56	0.024	Thermo- metric
		0.5	0.062	
		0.77	0.077	
		1	0.09	
		1.54	0.118	
		1.86	0.117	
		2.5	0.1	
5	0.046			
7.5	0.037			

^a Acrylamide, 2.82 moles/l.

TABLE V
Influence of the Eosin Concentration on the Rate of Photopolymerization of Acrylamide and Methacrylic Acid^a

Monomer and concn., moles/l.	Reducing agent and concn., moles/l. $\times 10^3$	Eosin, moles/l. $\times 10^5$	Rate of polymerization, moles/l./min.	Solvent
Acrylamide, 4.22	Thiourea, 66	0.036	0.02	Water
		0.09	0.04	
		0.217	0.07	
		0.361	0.09	
		0.563	0.1	
		1.41	0.2	
		3.53	0.14	
		8.82	0.1	
Methacrylic acid, 3.49	Ascorbic acid, 3	21.8	0.08	Water-ethanol, 50/50
		2.4	0.05	
		4.8	0.075	
		6.4	0.087	
		8	0.1	
		9.6	0.05	
	12	0.012		

^a I_0 , 1.05×10^{-5} Einsteins/l./min.; thermometric method.

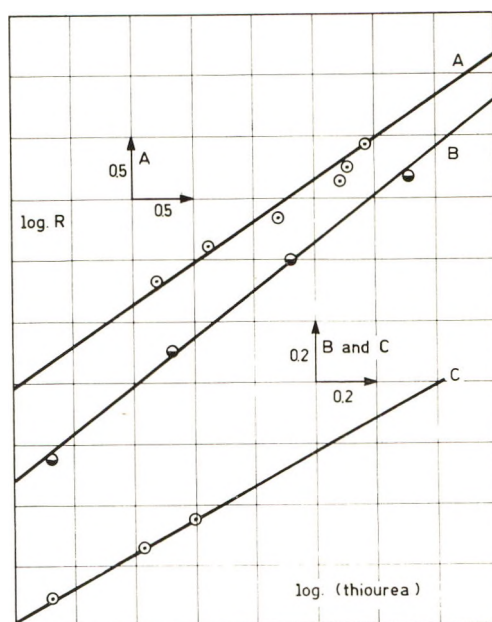


Fig. 3. Influence of the concentration of thiourea: (A) acrylamide in water, eosin, 0.55×10^{-5} moles/l.; (B) acrylamide in water, eosin, 22×10^{-5} moles/l.; (C) methacrylic acid in ethanol/water (30/70), eosin, 24×10^{-5} mole/l.

TABLE VI
 Influence of the Reducing Agent Concentration (Thiourea) on the Rate of Polymerization of Acrylamide and Methacrylic Acid^a

Monomer and concn., moles/l.	Eosin, moles/l. $\times 10^3$	Solvent	Reducing agent: moles/l. $\times 10^2$	Rates of polymerization, moles/l./min.	$\Delta \log$ rate	
					$\Delta \log$ (thiourea)	$\Delta \log$ (thiourea)
Acrylamide, 4.22	0.55	Water	0.67	0.012	0.75	
			1.67	0.027		
			4.2	0.053		
			10.5	0.096		
Acrylamide, 4.22	22	Water	0.592	0.013	0.66	
			1.265	0.022		
			3.68	0.034		
			9.2	0.06		
			10.5	0.074		
Methacrylic acid, 2.33	24	Water- methanol, 70/30	13.15	0.1	0.5	
			5.3	0.035		
			10.5	0.05		
			15.8	0.062		

^a I_0 , 1.05×10^{-5} Einsteins/l./min.; thermometric technique.

-0.35 above the critical concentration when thiourea was used as reducing agent (Fig. 2).

C. Influence of the Reducing Agent Concentration

The influence of the reducing agent concentration on the rate of photopolymerization of acrylamide and methacrylic acid was determined by means of systems containing eosin and thiourea. It is well known that this mild reducing agent exists in a tautomeric equilibrium between the thioamide and the thiol form of which the potential action as transfer agent must be taken into account. The rates were measured for increasing reducing agent concentrations at constant eosin and monomer concentrations and at constant light intensity. The rate values obtained for the photopolymerization of acrylamide and methacrylic acid in aqueous and semi-organic solutions are summarized in Table VI. The order of the reaction with respect to the reducing agent concentration can be determined from the slopes of the logarithmic plots in Figure 3. For eosin concentrations below and above the critical concentration the exponent of the thiourea concentration is situated between 0.5 and 1 in the case of the polymerization of acrylamide, whereas a value of 0.5 is found for the polymerization of methacrylic acid.

For the photopolymerization of acrylamide in aqueous solution sensitized by the system eosin-ascorbic acid a maximum rate was observed for a reducing agent concentration of $0.135 \pm 0.035 \times 10^{-2}$ moles/l. (Fig. 4). This behavior agrees with the results of Takayama²⁵ obtained for the photopolymerization of vinyl acetate sensitized by the system acriflavin-ascorbic acid. The influence of the reducing agent concentration could not be

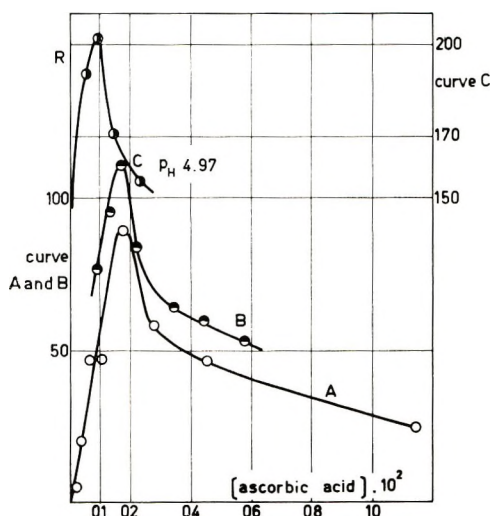


Fig. 4. Influence of the concentration of ascorbic acid on the rate of polymerization of acrylamide $[M] = 4.22$ moles/l.: (A) eosin, 0.722×10^{-5} mole/l., unbuffered; (B) eosin, 0.232×10^{-5} mole/l., unbuffered; (C) eosin 0.4×10^{-5} mole/l., pH 4.97.

studied for the sensitization by riboflavin; indeed, in this particular case the reducing ribityl group is stoichiometrically bound to the flavin residue.

D. Influence of the Oxygen Concentration

The influence of the oxygen concentration on the rate of polymerization was studied at constant monomer and eosin concentrations (acrylamide, 4.22 moles/l.; eosin, 0.4×10^{-5} moles/l.). Three series were carried out

TABLE VII
Influence of the Oxygen Concentration on the Rate of Photopolymerization of Acrylamide^a

Serial No.	O ₂ , %	Rate of polymerization, moles/l./min.	Period of inhibition, sec.	Ascorbic acid, moles/l. $\times 10^2$
D3	10	0.117	255	0.171
E3	19	0.16	307.5	0.171
F3	29.4	0.218	322.5	0.171
H3	37.6	0.261	382.5	0.171
I3	60.25	0.34	630	0.171
B4	8.85	0.147	315	0.057
A4	20	0.246	510	0.057
D4	27.6	0.285	690	0.057
C4	41.2	0.328	1155	0.057
D6	3.9	0.08	225	0.0456
C6	18.1	0.2	540	0.0456
B6	20.2	0.21	600	0.0456
E6	31	0.205	1035	0.0456

^a Solvent, water; acrylamide, 4.22 moles/l.; eosin, 0.4×10^{-5} moles/l.; I_0 , 6.3×10^{-6} Einsteins/hr./10 ml.

at different ascorbic acid concentrations. The variation of the oxygen concentrations was obtained by bubbling different gaseous mixtures (N₂/O₂) through a special set-up of the reaction cell. The results are expressed in function of the oxygen percentage in the various mixtures accord-

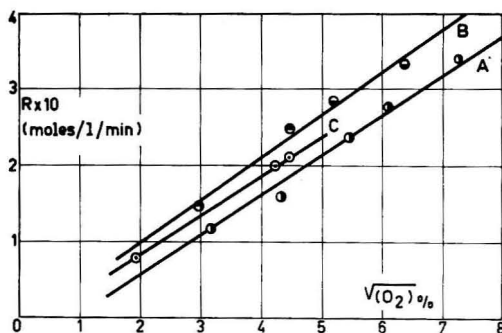


Fig. 5. Influence of the oxygen concentration (eosin), 0.4×10^{-5} moles/l.; acrylamide, ≈ 4.22 moles/l.: (A) ascorbic acid, 0.171×10^{-2} moles/l.; (B) ascorbic acid; 0.057×10^{-2} moles/l.; (C) ascorbic acid, 0.045×10^{-2} moles/l.

ing to the law of Henry. The results are summarized in Table VII and Figure 5. The rates are proportional to the square root of the oxygen concentration, at least below a given concentration where the induction period becomes very important and makes the rate determination inaccurate.

DISCUSSION

The dye-sensitized photopolymerization of acrylic monomers described in the present work is a consequence of the presence of the free radicals produced during the primary photoreduction step of the sensitizer and subsequent oxidation of the reduction products by molecular oxygen. The dye undergoes first a transition to the excited singlet state, the fluorescence of the solution being produced by the radiative return to the ground state. However a definite probability exists for a radiationless transition to a longer-lived, metastable excited triplet state which can be photoreduced in the presence of a hydrogen donor to the semiquinone radical and even to the leuco derivative. In the presence of oxygen, a reoxidation of the photoreduction products occurs with formation of hydrogen peroxide as already described.²⁸

The interaction of this peroxide and reducing agents gives rise to a redox initiating system, which is very important for the polymerization of acrylic monomers. The other radicals formed during the earlier steps could also contribute, although to a smaller part, to the initiation of the polymer chains.

The rate of monomer conversion is proportional to the square of the monomer concentration as well for acrylamide as for methacrylic acid in both aqueous and semi-organic solutions, in agreement with the results of Oster et al.¹⁵

Taking the participation of the monomer into account for the formation of the initiating radicals on the basis of kinetic evidences,³¹ the dependence on the square of the monomer concentration can be explained by assuming a low initiating efficiency of the radicals.³⁶ This hypothesis already proposed by Oster et al. is supported by the high molecular weight of the polymers obtained in these reactions. The reaction scheme is then given by eqs. (1)–(5).

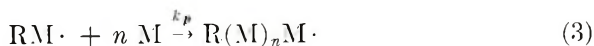
Formation of initiating radicals:



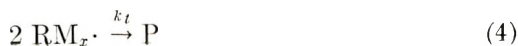
Activation:



Propagation:



Termination:



"Cage" recombination of primary radicals:



The initiator includes simultaneously the dye-sensitizer, the reducing agent, and the oxygen present in the solution. According to this scheme and assuming steady-state conditions, the following rate expression can be obtained:

$$-d[M]/dt = k_p[M] \left(\frac{k_i k_a [\text{Initiator}][M]^2}{k_a[M] + k_5} \right)^{1/2} \quad (6)$$

If k_a can be neglected with respect to k_5 assuming a low efficiency, the rate becomes:

$$-d[M]/dt = k_p[M]^2 (k_i k_a / k_5)^{1/2} [\text{Initiator}]^{1/2} \quad (7)$$

The square root dependence with respect to the sensitizer concentration has been demonstrated in the case of the sensitized polymerization of acrylamide and methacrylic acid (eosin and riboflavin). Above a critical sensitizer concentration the formal kinetics are completely modified on account of the total absorption of the incident light within a path l negligible with respect to the total length of the reaction cell. This front-effect can be expressed as follows:

$$R = (l/L) (k/n) [A_0]^m (\epsilon' [B_0]^{n-1}) I_0^n \quad (8)$$

where R is the mean specific polymerization rate, L the length of the reaction vessel, $[A_0]$ the concentration of nonabsorbing species, ϵ' the molar extinction coefficient of the sensitizer, $[B_0]$ the initial sensitizer concentration, I_0 the incident light intensity, and m and n are the concentration exponents for the formal kinetics in the absence of any front-effect.³³

An inverse proportionality to the square root of the sensitizer concentration was indeed observed at high sensitizer concentration in the case of the polymerization of acrylamide with riboflavin and of methacrylic acid with eosin.

In the case of the eosin-sensitized polymerization of acrylamide with thiourea as reducing agent, an exponent between 0.5 and 1 was observed both for the sensitizer and for the reducing agent concentrations. This behavior can be explained by assuming a partial degradative chain transfer reaction with the thiol tautomer of thiourea.³⁴ This substance behaves as a powerful reducing agent and transfers a hydrogen atom to a growing chain.

The corresponding $\cdot S-C(NH_2) = NH$ radicals are resonance-stabilized and will only reinitiate a polymeric chain in the presence of highly reactive monomers, as methacrylic acid, for which equation (7) remains valid. For less reactive monomers, as acrylamide,³⁴ the rate is no longer proportional to the square root of the thiourea concentration, as a consequence of this partial degradative chain transfer process, and the exponent becomes intermediate between 0.5 and 1.

With ascorbic acid as reducing agent, a rate maximum is obtained rapidly

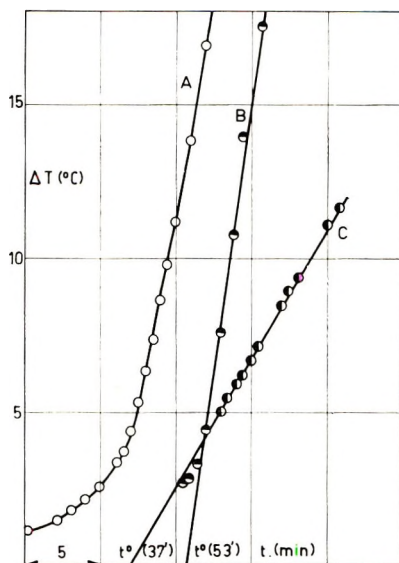


Fig. 6. Post-effect and preirradiation (eosin, 0.784×10^{-5} moles/l.; ascorbic acid, 0.171×10^{-2} moles/l.; acrylamide, 4.22 moles/l.: (A) photopolymerization; (B) polymerization with preirradiated solution; (C) post-effect (after 4 min. irradiation).

(Fig. 4), making the determination of the order of reaction with respect to its concentration very difficult. This effect was attributed to the powerful reducing capacity of ascorbic acid towards eosin, with progressive formation of the leuco derivative with increasing concentration of ascorbic acid. Considering that the leuco derivative is much more difficult to re-oxidize than the semiquinone intermediate, a smaller amount of initiating radicals will be produced as soon as the ascorbic acid concentration becomes important, and consequently the rate of polymerization drops.

The square root dependence of the polymerization rate of acrylamide with respect to the riboflavin concentration is directly related to the intramolecular photoreduction process, the reducing ribityl group being chemically bounded to the flavin dye residue in stoichiometrically well determined proportions.³⁵

The influence of oxygen was found to be in good agreement with the proposed mechanism, at least in a given range of concentration; at higher oxygen concentrations the inhibition period becomes, however, too important and makes any rate determination inaccurate. In the absence of oxygen and the presence of reducing agent, no important polymerization could be detected. The anaerobic sensitization of polymerization by eosin in reducing agent-free solutions will be studied in a forthcoming publication.

The light intensity exponent was found by Oster et al. to be 0.5 according to the proposed reaction mechanism. Finally the redox initiation in the case of the eosin-ascorbic acid system was confirmed by the very important post-effect and by the possibility of initiating the polymerization

by addition of the monomer to a preilluminated sensitizer solution (Fig. 6). The experimental evidence can be explained by the initiation due to the homolytic decomposition of the hydrogen peroxide-ascorbic acid system built up during the photoreduction step.

The authors are indebted to the IRSIA (Institut National de la Recherche Scientifique pour l'Industrie et l'Agriculture) and to Gevaert Photoproducten (Antwerp) for financial support of this research of the Centre d'Etudes des hauts Polymères, and to the IRSIA for a fellowship to two of them (W. D. W.) (S. T.).

References

1. Miyama, H., *Nippon Kagaku Zasshi*, **77**, 691 (1956); *ibid.*, **76**, 1013 (1956).
2. Watanabe, A., and M. Koizumi, *Bull. Chem. Soc. Japan*, **28**, 141 (1955); *ibid.*, **28**, 136 (1955); *ibid.* **34**, 1086 (1961).
3. Watanabe, A., *Bull. Chem. Soc. Japan*, **32**, 557 (1959).
4. Koizumi, M., A. Watanabe, and Z. Kuroda: *Nature*, **175**, 770 (1955).
5. Koizumi, M., *J. Inst. Polytech. Osaka City Univ. Ser. C*, **2**, 1 (1951).
6. Kuroda, Z., and M. Koizumi, *J. Inst. Polytech. Osaka City Univ., Ser. C*, **5**, 135 (1956).
7. Bamford, C. H., and M. S. S. Dewar, *Nature*, **163**, 214 (1949).
8. Ueberreiter, G. S., *Z. Elektrochem.*, **57**, 795 (1953).
9. Uri, N., *J. Am. Chem. Soc.*, **74**, 5808 (1952).
10. Whyte, R. B., and H. W. Melville, *J. Soc. Dyers Colourists*, **65**, 703 (1949).
11. Korsunovskii, G. A., *Zhur. Fiz. Khim.*, **32**, 1926 (1958).
12. Yoshida, Z., and K. Maeda, *Kogyo Kagaku Zasshi*, **60**, 1161 (1957).
13. Geacintov, N., V. Stannett, and E. W. Abrahamson, *Makromol. Chem.*, **36**, 52 (1959); *J. Appl. Polymer Sci.*, **3**, 54 (1960).
14. Oster, G., *Nature*, **173**, 300 (1954).
15. Oster, G. K., G. Oster, and G. Prati, *J. Am. Chem. Soc.*, **79**, 595 (1957).
16. Oster, G., and M. Taniyama, *Bull. Chem. Soc. Japan*, **30**, 856 (1957).
17. Oster, G., and Y. Mizutani, *J. Polymer Sci.*, **22**, 173 (1956).
18. Oster, G., *Phot. Sci. Eng.*, **4**, 237 (1960).
19. Oster, G. K., and G. Oster, *J. Polymer Sci.*, **48**, 321 (1960).
20. Klaus, C. J., I. T. Krohn, and P. C. Swanton, *Phot. Sci. Eng.*, **5**, 211 (1961).
21. Oster, G., U. S. Pat. 2,875,047 (Feb. 24, 1959).
22. Oster, G., U. S. Pat. 2,850,445 (Sept. 2, 1958).
23. Oster, G., Germ. Pat. 1,009,914, Jan. 18, 1956-June 6, 1957.
24. Nishijima, Y., *Kyoto Daigaku Nippon Kagakuseni Kenkyusho Koenshu*, **16**, 141 (1959); *Chem. Abstr.*, **54**, 8616f (1960).
25. Takayama, G., *Kobunshi Kagaku*, **17**, 644 (1960).
26. Oba, H., and I. Fujita, *Kobunshi Kagaku*, **15**, 445 (1958).
27. Smets, G., S. Dewinter, and G. Delzenne, *J. Polymer Sci.*, **55**, 767 (1961).
28. Delzenne, G., S. Toppet, and G. Smets, *J. Polymer Sci.*, **48**, 347 (1960).
29. Parker, C. A., *Proc. Roy. Soc. (London)*, **A220**, 104 (1953).
30. Parker, C. A., and C. G. Hatchard, *Proc. Roy. Soc. (London)*, **A235**, 518 (1956).
31. Delzenne, G., S. Toppet, and G. Smets, unpublished results.
32. Jungers, J. C., *Cinétique chimique appliquée*, Société des éditions Technic, Paris, 1958, p. 580.
33. Allen, P. W., F. M. Merrett, and J. Scanlan: *Trans. Faraday Soc.*, **51**, 95 (1955).
34. Crauwels, K., and G. Smets, *Bull. Soc. Chim. Belg.*, **59**, 443 (1950).
35. Oster, G., J. S. Bellin, and B. Holmström, *Experientia*, **18**, 249 (1962).
36. Noyes, R. M., *J. Am. Chem. Soc.*, **77**, 2042 (1955).

Résumé

On a étudié la cinétique de photopolymérisation de l'acrylamide et de l'acide méthacrylique en solution aqueuse et solution semi-organique; les systèmes initiateurs oxydoréducteurs utilisés en présence d'oxygène étaient l'éosine-thiouree, éosine-acide ascorbique-1, ou, dans certains cas, la riboflavine. La vitesse de photopolymérisation était déterminée en mesurant l'effet thermique de la polymérisation grâce à une technique au thermistor. En milieu aqueux et semi-organique, la vitesse est proportionnelle au carré de la concentration en monomère dans les deux cas. En dessous d'une concentration critique en sensibilisateur, la vitesse de polymérisation du monomère est proportionnelle à la racine carrée de la concentration en sensibilisateur (riboflavine pour l'acrylamide, eosine-acide ascorbique pour l'acide méthacrylique); au-dessus de cette concentration critique, la vitesse devient inversement proportionnelle à la racine carrée de la concentration en sensibilisateur. Par rapport à la concentration en réducteur, l'exposant de la thiouree est intermédiaire entre 0.5 et 1 dans le cas de l'acrylamide, et 0.5 pour l'acide méthacrylique. Finalement, en ce qui concerne la concentration en oxygène, la vitesse est proportionnelle à la racine carrée de sa concentration, du moins en-dessous d'une certaine concentration en oxygène à partir de laquelle la période d'induction devient trop importante. Ces résultats sont interprétés en admettant une participation du monomère à l'étape initiatrice, en une faible efficacité d'initiation pour les radicaux primaires (recombinaison en cage). Un schéma cinétique est présenté et les résultats expérimentaux discutés sur la base de celui-ci.

Zusammenfassung

Die Kinetik der Photopolymerisation von Acrylamid und Methacrylsäure in wässriger und semi-organischer Lösung wurde untersucht; als Redox-Startersystem wurde in Gegenwart von Sauerstoff Eosin-Thioharnstoff, Eosin-1-Ascorbinsäure oder in einigen Fällen Riboflavin verwendet. Die Geschwindigkeit der Photopolymerisation wurde durch Messung der Temperaturerhöhung der Reaktionszelle mit einem Thermistor bestimmt. In wässriger und semi-organischer Lösung ist die Geschwindigkeit in beiden Fällen dem Quadrat der Monomerkonzentration proportional. Unterhalb einer kritischen Sensibilisatorkonzentration ist die Geschwindigkeit der Polymerisation von Monomeren der Quadratwurzel aus der Sensibilisatorkonzentration proportional; (Acrylamid in Gegenwart von Riboflavin, Methacrylsäure in Gegenwart von Eosin-Ascorbinsäure); oberhalb derselben wird die Geschwindigkeit der Quadratwurzel aus der Sensibilisatorkonzentration umgekehrt proportional. In bezug auf die Konzentration des Reduktionsmittels liegt der Exponent für Thioharnstoff im Falle von Acrylamid zwischen 0,5 und 1 und für Methacrylsäure bei 0,5. Schliesslich ist die Geschwindigkeit, zumindest unterhalb einer gegebenen Sauerstoffkonzentration, wo die Induktionsperiode zu überwiegen beginnt, der Quadratwurzel aus der Sauerstoffkonzentration proportional. Die Ergebnisse werden unter Annahme einer Teilnahme des Monomeren am Startschritt und einer niedrigen Startausbeute der primären Radikale (Käfig-Rekombination) interpretiert. Ein kinetisches Schema wird aufgestellt und die Versuchsergebnisse auf seiner Grundlage diskutiert.

Received January 22, 1963

Amylose "V" Complexes: Low Molecular Weight Primary Alcohols*

ROBERT M. VALLETTA,† FELIX J. GERMINO, ROBERT E. LANG,
and RAYMOND J. MOSHY, *Research & Development Division, American
Machine & Foundry Company, Springdale Connecticut*

Synopsis

The methanol-, ethanol-, and 1-propanol-amylose "V" complexes have been prepared and their unit cell dimensions calculated from their x-ray powder patterns. The small unit cell (with 13.0 Å helix diameter), previously reported to occur only after the complete removal of water, has been observed for the wet methanol and ethanol complexes. In fact, a methanol complex containing as much as one mole of water per glucose residue had the small unit cell. Residual water and residual complexing agent analyses have shown that complexes dried to constant weight under stringent conditions retain as much as one mole of water and one-quarter mole of complexing agent per helix turn. It has been concluded that the specific organic complexing agent plays an important role in dictating the unit cell size.

INTRODUCTION

The physical configuration of the "V" form of amylose as the well-known, close-packed helices, containing six glucose residues per turn, has been a steadily evolving concept. Katz and Derksen¹ suggested that Katz's "V" (Verkleisterung) modification of starch represents an intermediate step between the pasted, or the "A," form of starch and the retrograded, or the "B," form of starch. Bear² reported that the x-ray diffraction patterns he obtained with methanol, ethanol, 1-propanol, 1-butanol, and acetone were indistinguishable.

Rundle and his co-workers^{3,4} have presented evidence that the unit cell of both the 1-butanol and the iodine amylose complexes is pseudohexagonal. Rundle⁵ has also shown that a structure based upon close packing of amylose helices, containing six glucose residues per turn, is consistent with the observed intensities in the x-ray patterns.

Although it was first reported⁴ that the "dried" 1-butanol and the anhydrous iodine complexes had different lattice constants (and different helix diameters), it was found⁵ that a more complete drying of the 1-bu-

* Presented in part at the Symposium on Starch Fractions and Their Characteristics at the 142nd Meeting of the American Chemical Society, Atlantic City, September 1962.

† Present address: International Business Machines Corp., Poughkeepsie, New York.

tanol complex resulted in equal lattice constants. This change in the helix diameter for the "dried" 1-butanol complex (now commonly called the hydrated "V" complex) from 13.7 Å. to 13.0 Å. for the completely dried complex (now commonly called the anhydrous "V" complex) was attributed⁵ to a complete removal of both water and 1-butanol.

Partial drying of the fatty acid complexes of amylose⁶ resulted in a diffraction pattern identical to the hydrated "V" complex. On the other hand, a thoroughly dried fatty acid complex (containing as much residual fatty acid as the partially dried one) had a helix diameter of 13.0 Å. but could be indexed only as an orthorhombic unit cell. Recently, Zaslow and Miller⁷ have shown that it is possible to reverse the dehydration process and form the hydrated "V" complex from the corresponding anhydrous form.

TABLE I
Unit Cells of Amylose "V" Complexes

Complexing agent	Hydration state	Lattice constants, Å.	Helix diameter, Å.	Unit cell type	Reference
Iodine	Wet	$a = 27.2$ $c = 8.01$	13.6	Hexagonal	7
Iodine	Dry	$a = 12.97$ $c = 7.91$	13.0	Pseudo-hexagonal	3
Butanol	Partially dried	$a = 27.4$ $c = 8.05$	13.7	Pseudo-hexagonal	4
Butanol	Dry	$a = 12.97$ $c = 7.91$	13.0	Pseudo-hexagonal	5
Fatty acids ^a	Wet	$a = 27.4$ $c = 8.05$	13.7	Pseudo-hexagonal	6
Fatty acids ^a	Dry	$a = 13.0$ $b = 23.0$ $c = 8.05$	13.0	Orthorhombic	6

^a Oleic, palmitic, and lauric acids.

The results of the past studies (summarized in Table I) indicate the major factor dictating the unit cell size and, specifically, the helix diameter of an amylose "V" complex is the presence or absence of water. The organic complexing agent would appear to be doing little more than distorting the unit cell, as evidenced by the change from pseudohexagonal to orthorhombic symmetry in the case of the fatty acid complexes.⁶ This result is surprising, since these complexing molecules are generally at least as large as the water molecule and it seems reasonable to expect that their presence in the structure would result in changes comparable to those noted for water.

An x-ray diffraction study of the amylose "V" complexes of methanol, ethanol, and 1-propanol was initiated in this laboratory to elucidate further the effect of the size as well as the role of the organic complexing agent. Since the amount of water present appears to be an important factor in the

structure, a drying rate study was also performed to establish criteria for the preparation of an anhydrous "V" complex. The water contents of the wet and dry methanol- and 1-propanol-amylose complexes were determined. The residual alcohol contents of the dry complexes were also determined.

EXPERIMENTAL

Preparation of Amylose "V" Complexes

The amylose "V" complexes of methanol, ethanol, and 1-propanol were prepared as follows. A 130-g. portion of potato amylose (Superlose, Stein, Hall and Co.) was solubilized in two liters of water by heating the mixture at 160°C. for 35 min. in a Parr reaction apparatus. The resulting solution was cooled to approximately 90°C. and the particular amylose complex was precipitated by the rapid addition of two liters of the corresponding alcohol. After waiting 5 min. for the crystals to form, the precipitate was filtered through a Buchner funnel, washed by dispersing the filter cake in the alcohol for 1 min. in a Waring Blendor, and then filtered. The washing step was repeated twice, and the final precipitate was used as the corresponding wet "V" complex. The wet "V" complexes were dried to constant weight at 113°C. over P_2O_5 *in vacuo* for 24 hr. Constant weight was attained in approximately 8 hr. The dried products were taken as the corresponding anhydrous "V" complexes.

Preparation of the Butanol Complex

The 1-butanol-amylose "V" complex had to be prepared differently, due to the partial immiscibility of water and 1-butanol. The wet methanol "V" complex, prepared as above, was dissolved in sufficient water to make a 1% solution. The solution was heated to 70°C. and the amount of 1-butanol, equivalent to 1% by volume of the above solution was added, and the whole heated at 75°C. for an additional 10 min. The resulting wet butanol complex was cooled to 30°C., filtered, and washed with butanol following the procedure above described for the other alcohols. The anhydrous complex was prepared by drying the wet complex as above.

The methanol-amylose complex was prepared by the same method as the preparation of the butanol-amylose complex, to establish that a methanol-amylose complex is actually formed. A wet methanol "V" complex, prepared as above, was dissolved in insufficient water to make 1% solution. The solution was heated to about 70°C. and sufficient methanol added to give a final solution which was 2% in methanol. The solution was cooled slowly to room temperature, whereupon a crystalline methanol-amylose complex precipitated.

Drying Rate Study

A detailed drying study was made by placing 185 g. of wet methanol complex in a one-liter flask maintained at 80°C., under vacuum, and ar-

ranged so that the distillate was collected in a Dry Ice-acetone trap. The drying was interrupted at intervals of 0.25, 0.75, 1.5, 3, 6, and 22 hr. to collect the condensate and to sample the complex. At each point, the entire condensate in the cold trap was removed and reserved for the methanol and water content analyses. The corresponding representative samples of the amylose complex were taken for x-ray analysis.

Methanol-Water Analysis

The methanol and water contents of the drying study condensates were determined by infrared absorption spectroscopy. It was found that the net absorbance of the 6.10 μ water band obeyed Beer's law in the range of 0-5 vol.-% of water in methanol with the 1% absorption coefficient being 10 ($A/\text{cm.}$). The net absorbance was obtained by:

$$A_{\text{net}} = A_{6.10} - (A_{5.25} + A_{6.75})/2$$

All analyses were made by scanning an aliquot of the condensate fraction over the range of 5.0-7.0 μ with the use of a Perkin-Elmer Model 21 infrared spectrophotometer with 0.1 mm. liquid cells with Irtran (Eastman Kodak) windows.

TABLE II
Unit Cells of "V" Complexes Found in These Studies

Complexing agent	State	Orthorhombic lattice constants, A.	Helix diameter, A.	Pseudo-hexagonal
Methanol	Dry	$a = 13.0$ $b = 22.8$ $c = 7.91$	13.0	No
Methanol	Wet	$a = 13.0$ $b = 22.8$ $c = 7.91$	13.0	Yes
Ethanol	Dry	$a = 13.0$ $b = 22.8$ $c = 7.91$	13.0	No
Ethanol	Wet	$a = 13.0$ $b = 22.8$ $c = 7.91$	13.0	No
Propanol	Dry	$a = 13.0$ $b = 23.0$ $c = 8.05$	13.0	No
Propanol	Wet	$a = 13.7$ $b = 23.8$ $c = 8.05$	13.7	Yes
Butanol	Wet	$a = 13.7$ $b = 23.8$ $c = 8.05$	13.7	Yes

Determination of X-Ray Patterns

The powder patterns of the complexes were obtained with a Norelco x-ray diffraction unit using Cu $K\alpha$ radiation and a 114.6 mm. powder camera. Exposure times were approximately 7 hr. at 45 kv. and 18 ma. The samples were prepared by packing the various complexes into 0.3 mm. i.d. Pyrex capillaries. All x-ray samples were run within 2 hr. from the time they were prepared and, in most cases, in duplicate.

Water Content of Amylose "V" Complexes

The water contents of the complexes were determined with the use of Karl Fisher reagent. An appropriately sized sample was weighed into a clean and dry titration flask, 50 ml. of anhydrous methanol was added, the slurry was stirred for 15 min. and titrated to an orange-red endpoint which persisted for at least 30 sec. The Karl Fisher reagent was standardized daily with a known water-methanol solution.

Residual Solvent Analyses of Amylose "V" Complexes

Amylose "V" complexes were prepared as outlined above using C^{14} -labelled methanol and 1-propanol having a specific activity of 2.5 $\mu\text{c./g.}$

TABLE III
Powder Diffraction Data for Wet Methanol and Iodine Complexes

Methanol				Iodine		
Inten- sity ^a	Ortho- rhombic	$\sin^2 \theta$ (obsd.)	$\sin^2 \theta$ (calcd.)	Inten- sity ^a	Hexag- onal	$\sin^2 \theta$ (obsd.)
m	(110)	0.0047	0.0045	vs	(100)	0.0047
m	(200)		0.0141		(110)	0.0141
	(111)	0.0142	0.0140	s	(101)	0.0142
vw	(140)		0.0195			
	(031)	0.0190	0.0185	m	(200)	0.0188
w	(230)		0.0232			
	(201)	0.0231	0.0236	vw	(111)	0.0237
vw	(150)		0.0286			
	(141)	0.0282	0.0291	vw	(201)	0.0275
	(221)		0.0277			
s	(310)		0.0328			
	(231)	0.0332	0.0327	vs	(210)	0.0329
					(300)	
					(311)	
				s	(102)	0.0423
vw	(170)		0.0527		(301)	
	(212)	0.0526	0.0531	vw	(112)	0.0520
					(220)	
				m	(202)	0.0565
				ms	(310)	0.0612
vw	(302)		0.0698		(311)	
	(421)	0.0704	0.0700	vw	(212)	0.0707

^a Intensity notation: s, strong; m, medium; w, weak; v, very.

TABLE IV
Powder Diffraction Data of Dry 1-Propanol-Amylose Complex

Intensity	Orthorhombic	$\sin^2 \theta$ (obsd.)	$\sin^2 \theta$ (calcd.)
s ⁺	(110)		0.0046
	(020)	0.0047	0.0045
vw	(030)		0.0101
	(011)	0.0113	0.0103
s	(200)		0.0143
	(130)		0.0136
	(021)	0.0142	0.0137
	(111)		0.0138
vw	(040)		0.0180
	(021)	0.0175	0.0172
w ⁺	(220)		0.0186
	(031)	0.0189	0.0193
m ⁺	(131)		0.0228
	(201)	0.0231	0.0232
m ⁺	(050)		0.0281
	(041)	0.0290	0.0277
	(221)		0.0277
s	(310)		0.0328
	(240)	0.0329	0.0320
vw	(320)		0.0361
	(002)	0.0369	0.0367
	(051)		0.0373
vw	(102)	0.0396	0.0402
vw	(250)		0.0422
	(330)	0.0426	0.0418
	(311)		0.0419
vw	(032)	0.0469	0.0468
w ⁺	(340)		0.0496
	(132)		0.0503
	(061)	0.0503	0.0496
	(331)		0.0509
w ⁺	(212)		0.0519
	(161)	0.0526	0.0531

(continued)

Approximately 0.1-g. samples of complex were weighed into 20 ml. low potassium glass vials (Wheaton Glass Co.); 20 ml. of liquid scintillator solution, consisting of toluene containing 4 g./l. of phenyl phenyloxazole and 100 mg./l. of 1,4-bis-2-(5-phenyloxazolyl)benzene, was added; the vial contents were shaken for 5 min. and placed in a Tracerlab liquid scintillation counter where they were held at the counting temperature for at least 1 hr. before counting. Sample activities were converted into per cent residual solvent by the following formula:

$$\text{Residual solvent} = 100A/CW$$

where A is the sample activity as measured, C is the conversion factor (or specific activity of the labelled solvent), and W is the sample weight.

TABLE IV (continued)

Intensity	Orthorhombic	$\sin^2 \theta$ (obsd.)	$\sin^2 \theta$ (calcd.)
vs	(070)		0.0550
	(260)		0.0545
	(042)	0.0547	0.0547
	(222)		0.0552
vw	(410)		0.0574
	(170)	0.0577	0.0586
	(142)		0.0582
vw	(430)		0.0664
	(411)	0.0661	0.0666
	(401)		0.0654
w ⁺	(421)	0.0706	0.0699
vw	(180)		0.0754
	(431)	0.0758	0.0756
vw	(162)		0.0806
	(081)	0.0811	0.0810
	(361)		0.0813
vw	(280)		0.0859
	(103)	0.0853	0.0861
	(181)		0.0846
vw	(033)		0.0927
	(402)	0.0927	0.0930
	(451)		0.0935
w	(530)		0.0980
	(511)	0.0990	0.0982
w	(082)		0.1086
	(362)	0.1092	0.1088
vw	(600)		0.1266
	(163)	0.1266	0.1265
vw	(621)		0.1403
	(382)	0.1403	0.1402
	(413)		0.1399
vw	(034)		0.1569
	(443)	0.1568	0.1568
	(491)		0.1564

RESULTS

The results of our x-ray investigations are presented in Table II. It will be noted that all of the patterns can be indexed using unit cell lattice constants previously reported by Rundle and his co-workers.³⁻⁶ However, there are some variations in the symmetry of the various unit cells. Although the unit cells of all the methanol and ethanol complexes are identical in size to that observed for the anhydrous iodine complex, the wet methanol complex is the only one with pseudohexagonal symmetry. The dry methanol complex and both ethanol complexes have lines which can only be indexed by orthorhombic indices. There is no corresponding set of pseudohexagonal indices for them. This could mean that the distortion

TABLE V
Analysis of the Water-Methanol Distillates

Fraction	Time, hr.	Weight of distillate, g.	Water concn., wt.-%
I	0.25	50	0.5
II	0.75	33	1.6
III	1.5	29	4.7
IV	3.0	15	14.1
V	6.0	2	87.5
VI	22.0	0	—

TABLE VI
Water and Solvent Content of Methanol and 1-Propanol "V" Complexes

Amylose complex	Sample state	Mole ratio water:glucose	Helix diameter, A.	Residual alcohol, %
Methanol	Wet	1:1.03	13.0	—
Methanol	Wet	1:2.1	13.0	—
1-Propanol	Wet	1:1.6	13.7	—
1-Propanol	Wet	1:0.92	13.7	—
Methanol	Dry	1:5.8	13.0	0.67
1-Propanol	Dry	1:6.2	13.0	1.4

required to change the symmetry is too small to affect the experimentally determined values for the lattice constants.

The patterns of the wet and dry complexes indicate a high degree of crystallinity. The overall particle size of the complex is 250 A. by the Scherrer formula.

The agreement between observed and calculated $\sin^2 \theta$'s for the wet methanol and the dry 1-propanol complexes is illustrated in Tables III and IV. These patterns represent the two extremes in symmetry in the unit cell. The data³ for the iodine complex are also given in Table III to show the pseudo-hexagonal symmetry of the wet methanol complex.

The weight and composition of the distillate fractions collected at various times when the wet methanol complex was dried under controlled conditions are presented in Table V.

Of the 185 g. of sample used for the drying rate study, depicted in Table V, 55 g. correspond to the solids content which, on a glucose basis, is 0.35 mole. The total water content of the distillate was 6 g., or 0.33 mole. Therefore, the water-glucose ratio in the wet methanol complex was equivalent to a glucose monohydrate.

The amount of water in some wet and dry methanol- and 1-propanol-amylose complexes was determined by Karl Fisher titrations. There was a good check obtained by the Karl Fisher versus the infrared water analysis. The Karl Fisher moisture data as well as the residual alcohol content of the dry methanol and 1-propanol complexes are given in Table VI. The residual alcohol was determined by C¹⁴ analyses.

It was also found that there was approximately one molecule of methanol

per seven glucose residues in the wet C^{14} -labeled methanol-amylose complex after it had been washed three times with carbon tetrachloride. Assuming that carbon tetrachloride does not exchange with methanol, the C^{14} analysis establishes the composition of the wet methanol-amylose complex and shows that an amylose-alcohol complex is formed by our method of preparation.

DISCUSSION

The present study shows the organic complexing agent affects the helix diameter of wet amylose "V" complexes.

The unit cell constants of the wet and dry methanol and ethanol complexes are similar to the anhydrous iodine complex and, in all cases, the helix diameter is 13.0 Å. The drying study clearly shows that washing the methanol complex with excess methanol does not extract all the water from the structure. In fact, the water content of one of our wet methanol complexes was equivalent to one water molecule per glucose residue. The water content of two different wet methanol-amylose complexes, as is shown in Table VI, approximate a glucose monohydrate and a glucose hemihydrate. A glucose monohydrate ratio agrees with the value determined by density measurements on the partially dry 1-butanol and fatty acid complexes.⁵ However, these monohydrates were reported to have helix diameters of 13.7 Å. The methanol-amylose complex shown in Table VI, with a glucose monohydrate ratio, as well as the methanol-amylose complex with a water to glucose ratio of 1:6 both have helix diameters of 13.0 Å.

The wet propanol complexes with helix diameters of 13.7 Å. are shown as the monohydrate, and a stage between the hemihydrate and monohydrate in the case of a water-glucose ratio of 1:1:6. Table VI thus presents two examples where there is at least a monohydrate ratio in the amylose "V" complexes, but where there are two different helix diameters. Therefore, it is safe to say that, at the very least, the organic solvent plays some determinant role in the helix diameter. Thus, the helix diameter of an amylose "V" complex can be 13.0 Å. and still contain as much as one water molecule per glucose unit, if the complex is formed with a small organic molecule such as methanol or ethanol.

In the cases of the dry methanol and 1-propanol complexes, the helix diameters are both 13.0 Å. The decrease in the helix diameter for the 1-propanol-amylose complex is presumably due to the removal of the 1-propanol from within the helix. This is borne out by the low level of residual solvent, as measured by C^{14} analyses. The residual methanol and 1-propanol levels are equivalent to a solvent to glucose ratio of about 1:25. In both cases the water level is equivalent to one water molecule for each 6 glucose units, or one water molecule per turn of the helix.

The ratio of residual alcohol to glucose in the dry methanol and 1-propanol-amylose complexes of 1:25 corresponds approximately to one-half mole of alcohol per orthorhombic unit cell, the cell in turn containing twelve glucose residues. Further, the dried complexes also contain the tena-

ciously held residual water content of one mole of water per helix, or six moles of glucose. One might conclude that these solvent or water residues, singly or in combination, account for the peaks observed in the centers of the helices of the Fourier projections of "anhydrous" 1-butanol "V" complex reported by Rundle.⁵

It is interesting to note that there is no smooth variation in the helix diameter. There is no increase in the diameter when one goes from a methanol to an ethanol complex. However, there is a sudden increase of 0.7 Å. when one goes from an ethanol to a 1-propanol complex. Apparently, the helix diameter does not gradually adjust to the size of the primary alcohol molecule. This suggests there is a distinct change in the arrangement of the glucose residues and not just a continuous distention of the helix to accommodate larger molecules.

The authors wish to thank Miss Patricia Beckman for her assistance in packing the x-ray samples and reading the power patterns reported in this paper.

References

1. Katz, J. R., and J. C. Derksen, *Z. Physik, Chem.*, **A167**, 129 (1933).
2. Bear, R. S., *J. Am. Chem. Soc.*, **64**, 1388 (1942).
3. Rundle, R. E., and D. French, *J. Am. Chem. Soc.*, **65**, 1707 (1943).
4. Rundle, R. E., and F. C. Edwards, *J. Am. Chem. Soc.*, **65**, 2200 (1943).
5. Rundle, R. E., *J. Am. Chem. Soc.*, **69**, 1769 (1947).
6. Mikus, F. F., R. M. Hixon, and R. E. Rundle, *J. Am. Chem. Soc.*, **68**, 1115 (1946).
7. Zaslów, B., and R. L. Miller, *J. Am. Chem. Soc.*, **83**, 4378 (1961).

Résumé

On a préparé les complexes "V" méthylique, éthylique, 1-propylique d'amylose et les dimensions de leur unité cellulaire ont été calculées par diffraction de rayons-X à partir d'échantillons en poudre. La petite unité cellulaire (de 13.0 Å de diamètre de l'hélice) qui a été antérieurement mentionnée ne se produit qu'après enlèvement complet de l'eau, a été observée dans des complexes méthylique et éthylique humides. En fait, un complexe méthylique contenant une môle d'eau par glucose restant présentait encore la petite unité cellulaire. Des analyses de l'eau et de l'agent complexant résiduaux ont montré que des complexes séchés jusqu'à poids constant sous des conditions sévères retiennent une môle d'eau et une môle un quart ($1\frac{1}{4}$) d'agent complexant par tour d'hélice. On en a déduit que la spécificité de l'agent organique complexant joue un rôle important dans la prédiction de la dimension de l'unité cellulaire.

Zusammenfassung

Die "V"-Komplexe von Methanol-, Äthanol und 1-Propanolamylose wurden dargestellt und ihre Elementarzeldimensionen aus den Röntgenpulverdiagrammen berechnet. Die früher nur nach vollständiger Entfernung von Wasser festgestellte kleine Elementarzelle (mit einem Helixdurchmesser von 13,0 Å) wurde an feuchten Methanol- und Äthanolkomplexen beobachtet. Sogar ein Methanolkomplex mit einem Mol Wasser pro Glukoserest besaß noch die kleine Elementarzelle. Bestimmung des Gehalts an Wasser und Komplexierungsmittel zeigte, dass scharf zur Gewichtskonstanz getrocknete Komplexe noch ein Mol Wasser und ein viertel Mol Komplexierungsmittel pro Schraubengang der Helix enthalten. Das spezifische organische Komplexierungsmittel spielt offenbar eine wichtige Rolle bei der Festlegung der Grösse der Elementarzelle.

Received December 13, 1962

Revised January 25, 1963

Free Volumes in Polystyrene and Polyisobutylene

A. A. MILLER, *General Electric Research Laboratory,
Schenectady, New York*

Synopsis

The melt viscosities of polystyrene and polyisobutylene fractions are expressed by a modified Arrhenius (M.A.) temperature equation, $\eta = A \exp \{B/(T - T_c)\}$, and by a free volume equation, $\eta = A \exp 1/\{f\}$, in which $f = v_f/v$, the free volume fraction. Thus, it is assumed that f , as defined, is a linear function of temperature, since $f = (T - T_0)/B$. By this method, the derived "occupied" volume, $v_o = v - v_f$, has a temperature dependence which is determined by the temperature coefficients of f and v (i.e., $1/B$ and α_l) and is not related to the experimental α_o value for the glass. For polyisobutylene, the temperature coefficient of v_o is positive, while for polystyrene it is slightly negative. Possible effects of liquid structure in determining the temperature behavior of v_o are suggested. Calculated viscosities and free volume fractions at the glass point, T_g , over a wide range of molecular weight, M , in both polymers lead to the conclusion that the glass transition is primarily an "iso-viscosity" ($\eta_g \simeq 10^{13}$ poise), rather than an "iso-free volume," state. However, in the two polymers, both conditions can exist simultaneously for similar values of M . Thus at equal M , $f_g = (T_g - T_0)/B$ is about the same for both polymers. For $M \simeq 100,000$, $f_g \simeq 0.031$. These observations support the view that the glass transition is primarily a kinetic, rather than a thermodynamic, phenomenon. The estimated time dependence of T_g is found to differ in the two polymers at equal M and to vary with M in each case.

Introduction

In previous papers^{1,2} it was shown that the melt viscosities of polystyrene and polyisobutylene fractions could be expressed by a modified Arrhenius (M.A.) equation, $\eta = A \exp \{B/(T - T_0)\}$, which could be related to the Williams-Landel-Ferry (W. L. F.) equation³ and to free volume approaches by these authors³ and by Williams.⁴ The basic principle which seems to unify all of these approaches is that the theoretical zero-point for free volume is at T_0 , as suggested by Cohen and Turnbull.⁵

In the present work, a more rigorous comparison between the Williams⁴ and the M.A. approach for polystyrene is made. In particular, the relationship of the temperature dependence of free volume to the temperature parameter, B , is considered.

Viscosities and free volumes at the glass point, T_g , are calculated for polystyrene and polyisobutylene fractions over broad ranges of molecular weight. On the basis of these, some conclusions regarding the nature of the glass transition in these polymers are presented.

Polystyrene

Following the Doolittle method,⁶ Williams⁴ defined a "relative free volume" as $f' = (v - v_0)/v_0$, in which the occupied volume, v_0 , remained temperature-invariant.* It was assumed that f' had the following temperature dependence:

$$f' = f'_g + \alpha(T - T_g) \quad (1)$$

The melt viscosities of twelve polystyrene fractions were then expressed by the Doolittle equation:

$$\log \eta = \log A + b/2.3f' \quad (2)$$

Williams pointed out that the derived value of $b = 0.91$, although it was essentially constant over the entire series, did not agree with the expected and previously assumed value of 1.00. It now appears that the Williams (or Doolittle) b is actually a correction factor, which reconciles the temperature dependence of f' (or, approximately, v_f) with the liquid expansion coefficient, α , under the arbitrarily imposed restriction that the occupied volume, v_0 , remain temperature-invariant.

If f' is replaced by a new function, $f = f'/b$, eq. (2) becomes:

$$\log \eta = \log A + 1/2.3f \quad (3)$$

Comparing this with the M.A. equation, $\log \eta = \log A + B/2.3(T - T_0)$, we find

$$f = (T - T_0)/B \quad (4)$$

Accordingly, f becomes zero at $T = T_0$ and $df/dT = 1/B$. From eq. (1), for $f' = 0$ at $T = T_0$,

$$T_g - T_0 = f'_g/\alpha \quad (5)$$

Also from eq. (1), $df'/dT = \alpha$. Comparison of the temperature derivatives of f' and f leads to

$$B = b/\alpha = 0.91/\alpha \quad (6)$$

Equations (5) and (6), which transform the Williams parameters into the present parameters, are the same as those derived in the previous paper.¹

For a polystyrene fraction with $M = 1675$, a plot of the viscosity data according to the M.A. equation¹ gave $T_0 = 5^\circ\text{C.}$ and $B(\ln) = 1430^\circ$. From eq. (5) with $f'_g = 0.0225$, $\alpha = 6.3 \times 10^{-4} \text{ deg.}^{-1}$, and $T_g = 40^\circ\text{C.}$,⁴ we find $T_0 = 4^\circ\text{C.}$, and from eq. (6), $B = 1440^\circ\text{C.}$

If the function f in eq. (3) is, in fact, the free volume fraction, $f = v_f/v$, the derived "occupied" volumes for the lowest ($M = 1675$) and the highest ($M = 134,000$) of the polystyrene fractions are as indicated in Figure 1.

* The Williams f is primed to differentiate it from another definition used in this paper.

The liquid specific volume lines, v , are based on values from Table I of the Williams paper.⁴ The occupied volumes, $v_s = v - v_f = (1 - f)v$, are derived from eq. (4). For $M = 134,000$, the Williams⁴ parameters, $f'_g = 0.0287$, $T_g = 99^\circ\text{C}$., and $\alpha = 5.85 \times 10^{-4} \text{ deg.}^{-1}$, give $B(\ln) = 1550^\circ$ and $T_0 = 50^\circ\text{C}$. by eqs. (5) and (6). As shown in Figure 1, the temperature coefficient of the occupied volume has a negative value which remains essentially constant, $-dv_s/dT \simeq 0.9 \times 10^{-4} \text{ cc./g./}^\circ$, over the entire molecular weight range from $M = 1675$ to $M = 134,000$.

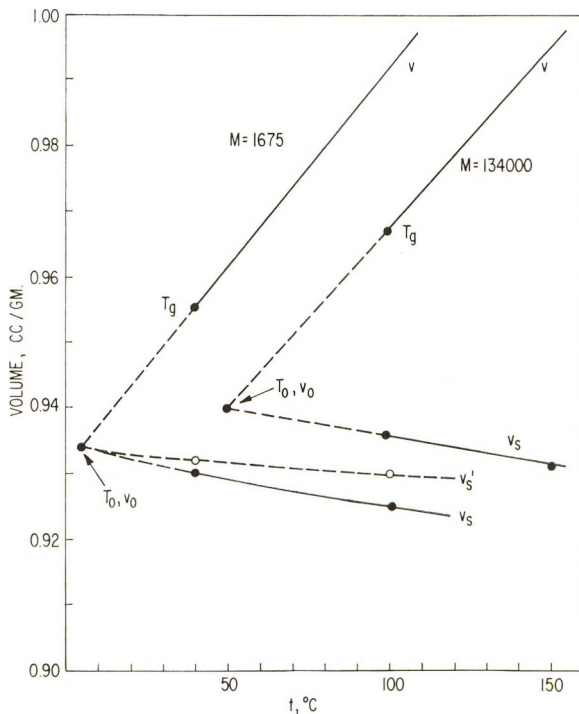


Fig. 1. Total and "occupied" volumes for low and high fractions of polystyrene. v_s and v'_s are occupied volumes, derived for the cases of f and v_f , respectively, linear in temperature.

It should be emphasized that the free volume interpretation depicted in Figure 1 is based on an assumed liquid expansion model: namely, that the free volume fraction, as defined by $f = v_f/v$, increases linearly with temperature. For an alternate model, in which v_f itself is made linear in temperature, we use $f = v_f/v_0$. For $M = 1675$, $v_0 = 0.934 \text{ cc./g.}$,⁴ giving an occupied volume designated by v'_s in Figure 1. For this case, $-dv'_s/dT \simeq 0.4 \times 10^{-4} \text{ cc./g./}^\circ$.

In either expansion model, the temperature dependencies of v_f and v_s are given more exactly by $df/dT = 1/B$, using the appropriate definitions of f indicated earlier.

Polyisobutylene

From the earlier work,² the M.A. parameters for higher molecular weight PIB fractions ($M > 5000$) are $T_0 = 123^\circ\text{K}$. and $B(\ln) = 2850^\circ$. In Figure 2, the line for the liquid specific volume is drawn according to the parameters^{2,7} $v(30^\circ\text{C.}) = 1.131$ cc./g. and $dv/dT = 6.0 \times 10^{-4}$ cc./g./ $^\circ$. The limiting ($M = \infty$) value of $T_g = 210^\circ\text{K}$.,^{2,7} with $v_g = 1.075$ cc./g., are also indicated. The line for the occupied volume, v_s , is derived by the method described in the previous section for polystyrene using the M.A.

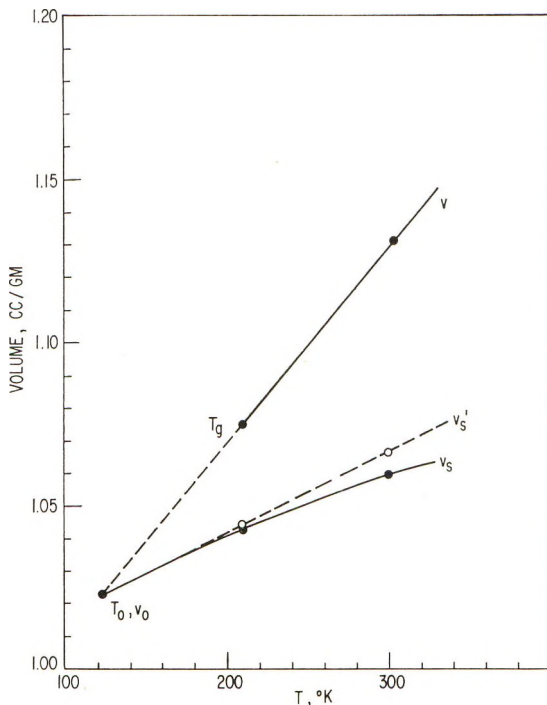


Fig. 2. Total and "occupied" volumes characteristic of high molecular weight polyisobutylene, $M > 50,000$. v_s and v_s' as for Fig. 1.

parameters listed above. In contrast to polystyrene, the occupied volume for PIB increases with temperature. The average slope between 123°K . (T_0) and 303°K . is $dv_s/dT = 2.1 \times 10^{-4}$ cc./g./ $^\circ$. The free volume fraction at the glass point, given by $f_g = (T_g - T_0)/B$, is found to be $f_g = 0.0306$. As before, v_s' represents the occupied volume for the alternate expansion model, in which v_f itself rather than f , is made linear with temperature.

It may be noted that if the Williams method, with a temperature-invariant v_0 , were applied to PIB, the derived Doolittle slope, $b = \alpha B$, would have a value of 1.7.²

Viscosity and Free Volume at the Glass Point

The viscosities of the series of twelve polystyrene fractions at their glass points may be calculated directly from Williams' results⁴ by eq. (2) or its equivalent, eq. (3): $\log \eta_g = \log A + 1/2.3f_g$, where $f_g = f'_g/0.91$. The $\log A$ values are given by eqs. (14) and (15) of ref. 4.*

$$\begin{aligned} \log A &= -7.08 + 1.12 \log M & M \leq 35,000 \\ \log A &= -17.32^* + 3.38 \log M & M \geq 35,000 \end{aligned}$$

These terms for the twelve polystyrene fractions are listed in Table I.

TABLE I
Parameters for Polystyrene Fractions at T_g

M	f_g	$1/2.3f_g$	$+\log A$	$\log \eta_g$
1,675	0.0247	17.6	-3.45	14.1
2,085	0.0270	16.2	-3.36	12.8
2,600	0.0261	16.8	-3.26	13.5
3,041	0.0282	15.4	-3.18	12.2
3,590	0.0294	14.8	-3.10	11.7
6,650	0.0257	16.9	-2.81	14.1
13,300	0.0269	16.1	-2.46	13.6
19,300	0.0269	16.1	-2.28	13.8
24,200	0.0303	14.3	-2.18	12.1
32,200	0.0317	13.8	-2.03	11.6
80,000	0.0328	13.2	-0.72	12.5
134,000	0.0316	13.8	+0.05	13.8

The free volume fraction at the glass point, f_g , shows an increasing trend with molecular weight. (The Williams values for f'_g , of course, increase proportionately the same, 0.0225 to 0.0287.) This trend is reflected in a decrease of about four decades in the viscosity term, $1/2.3f_g$, which is nearly balanced by a similar increase in the $\log A$ term. The $\log \eta_g$ values show no trend but rather irregular fluctuations and can be considered to be independent of M , with the mean value: $\log \eta_g = 12.9 (\pm 1)$.

Similar results are found for polyisobutylene fractions. For the range $M = 4170$ ($T_g = 193^\circ\text{K.}$) to $M = 80,000$ ($T_g = 209^\circ\text{K.}$), the $\log A$ term increases by about three decades.² The value of f_g , calculated from $f_g = (T_g - T_0)/B$, where $B = 2850^\circ$ and $T_0 = 123^\circ\text{K.}$,² increases from 0.0246 to 0.0302, giving a decrease of about three decades in the $1/2.3f_g$ viscosity term. For six PIB fractions within this molecular weight range, the mean value of $\log \eta_g$ is 13.3 (± 0.7), which is similar to the value found for polystyrene.

It is concluded from these observations that within a homologous poly-

* The value -12.32 in the second of the equations in the Williams paper is obviously in error. From Fig. 2 of that paper it appears that -17.32 is more nearly correct. This is confirmed by the M. A. parameters and equation for $M = 134,000$ at $t = 217^\circ\text{C.}$ and comparing with eq. (12) of ref. 4. Thus, $\log A = -17.43 + 3.4 \log M$.

mer series, the glass transition point is more nearly an "iso-viscous," rather than an "iso-free volume," condition and that these two conditions cannot exist simultaneously as M is varied.

However, it appears that for the same molecular weights, the two polymers may indeed have nearly equal values of f_g . For polystyrene⁴ and for polyisobutylene² at equal values of M above $M \simeq 5000$, the $\log A$ terms differ by only a half-decade. In the viscosity equation, $\log \eta_g = \log A + 1/2.3f_g$, this difference in $\log A$ produces only a 4% difference in f_g at constant η_g or, conversely, only a 3-fold difference in absolute viscosities, η , at constant f_g .

Time Dependence of T_g

On the basis that the glass point is a viscosity-controlled, kinetic phenomenon, the time dependence of T_g may be estimated for the range of polymer fractions being considered here.* If the viscosity and the time scale of the glass-point measurement are simultaneously increased n -fold, the system remains in a condition of the glass transition. In the viscosity equation, the $\log A$ term is invariant, so that the $1/2.3f_g$ viscosity term will increase by $\log n$ units. Thus, we find $-\Delta f_g = 2.3f_g^2 \log n / (1 + 2.3f_g \log n)$. From $f_g = (T_g - T_0)/B$, we obtain $\Delta T_g = B(\Delta f_g)$.

The results for the low and high fractions of polystyrene and polyisobutylene, based on the parameters given earlier, are listed in Table II for $n = 10$ and $n = 100$.

TABLE II
Time Dependence of T_g

	Polystyrene		Polyisobutylene	
M	1675	134,000	4170	80,000
$B, ^\circ$	1440	1550	2850	2850
f_g	0.0247	0.0316	0.0246	0.0302
$-\Delta f_g$				
$n = 10$	0.0013	0.0021	0.0013	0.0021
$n = 100$	0.0025	0.0040	0.0025	0.0039
$-\Delta T_g, ^\circ$				
$n = 10$	1.9	3.3	3.7	6.0
$n = 100$	3.6	6.2	7.1	11.0

The values for ΔT_g ($n = 10$) are consistent with the "universal" value, $\sim 3^\circ$, derived by the W. L. F. equation.³ However, more detailed effects are apparent from Table II. For example, it evolves that ΔT_g increases with molecular weight. Also, at approximately equal molecular weights, ΔT_g is about 2-fold greater for PIB, because of the greater B value. It is assumed that the theoretical lower limit for T_g at infinite equilibration times is T_0 . Thus, for these ranges of M , the limiting values of ΔT_g are 35–49° for polystyrene and 70–85° for polyisobutylene.

* The general approach will be the same as described in ref. 3, pp. 221–3.

Discussion

In previous approaches to free volume, as manifested by transport or relaxation processes in polymeric and nonpolymeric liquids, it has been assumed either that the occupied volume, v_0 , remains temperature-independent,^{4,6} or that the thermal expansion of the occupied volume is the same as that of the glass, α_g .^{2,3} For the latter case, the temperature dependence of the free volume has been represented as $\alpha_l - \alpha_g = \Delta\alpha$. From the present viewpoint, the free and occupied volumes in the liquid are determined by structural characteristics of the liquid itself and it is suggested that these are not related directly to experimentally determined parameters for the glass below T_g (i.e., v , α_g , etc.).

In the method described here, the temperature coefficient of the occupied volume, dv_s/dT , is found to be positive for polyisobutylene and slightly negative for polystyrene. Neither of these coefficients corresponds to reported α_g values: $1.0\text{--}1.5 \times 10^{-4}$ for PIB^{2,8} and 2.5×10^{-4} for polystyrene.⁹ In another paper,¹⁰ it is shown that the same approach (for the case of f linear in T) applied to an n -alkane, $C_{13}H_{28}$, leads to an even larger negative value $-dv_s/dT = 4 \times 10^{-4}$ cc./g./°.

If correct, a negative temperature coefficient for v_s can perhaps best be explained on the basis of molecular association. The "aggregates" resulting from such association would appear as "occupied volume" in the flow process and the degree of association would be expected to decrease with increasing temperature. (An extreme example of this effect is provided by a recent correlation of the viscosity and structure of liquid water.¹¹) This further suggests that the temperature behavior of v_s may be related to the tendency of the liquid to crystallize, rather than vitrify.

In the present view, T_0 is the theoretical zero-point for thermodynamic quantities measured in the liquid.* Presumably, it is the extrapolation of these below T_0 that leads to absurd values, as in the present case, a negative v_f .

This work suggests that at T_g , "iso-viscosity" and "iso-free volume" conditions cannot exist simultaneously as the molecular weight changes within a homologous series, but may exist simultaneously in different linear polymers at approximately equal values of M .

Simha and Boyer⁸ have reported a relationship between T_g and expansion coefficients, in which $f_g = (\alpha_l - \alpha_g)T_g \simeq 0.11$. This value is considerably greater than the "universal" $f_g = 0.025$, suggested by Williams, Landel, and Ferry.³ It will be recalled that by the present method, $f_g = (T_g - T_0)/B$, and for high molecular weight polystyrene and PIB, $f_g = 0.032$ and 0.031, respectively. In the Simha and Boyer correlation, the theoretical origin of the free volume is taken to be 0°K., while in the present method (also implied in the W. L. F. equation), the origin of v_f is T_0 .

Some comments, in addition to those already set forth by Williams,⁴ may be made regarding the pre-exponential term, A . This term represents the viscosity at infinite temperature and infinite free volume. The latter condition suggests that A is quite analogous to the intrinsic viscosity (i.e., viscosity at infinite dilution) in polymer solutions. For the two linear polymers examined thus far, the values of A at equal M are remarkably similar, below and above the chain-entanglement points. As mentioned earlier, for $M > 5000$ these values differ by only a factor of 3. This indicates that in these, and possibly other, linear polymers the A term is determined primarily by the molecular weight, rather than by the chemical structure. The latter is apparently important only for the remaining term, $1/f$ or $B/(T - T_0)$, in the viscosity equation.

References

1. Miller, A. A., *J. Polymer Sci.*, **A1**, 1857 (1963).
2. Miller, A. A., *J. Polymer Sci.*, **A1**, 1865 (1963).
3. See J. D. Ferry, *Viscoelastic Properties of Polymers*, Wiley, New York, 1961, Chap. 11.
4. Williams, M. L., *J. Appl. Phys.*, **29**, 1395 (1958).
5. Cohen, M. H., and D. Turnbull, *J. Chem. Phys.*, **31**, 1164 (1959).
6. Doolittle, A. K., *J. Appl. Phys.*, **22**, 1471 (1951).
7. Fox, T. G., and S. Loshaek, *J. Polymer Sci.*, **15**, 371 (1955).
8. Simha, R., and R. F. Boyer, *J. Chem. Phys.*, **37**, 1003 (1962).
9. Fox, T. G., and P. J. Flory, *J. Appl. Phys.*, **21**, 581 (1950).
10. Miller, A. A., *J. Phys. Chem.*, **67**, 1031 (1963).
11. Miller, A. A., *J. Chem. Phys.*, **38**, 1568 (1963).
12. Gibbs, J. H., and E. A. DiMarzio, *J. Chem. Phys.*, **28**, 373 (1958).
13. Gibbs, J. H., in *Unsolved Problems in Polymer Science*, N. R. C. Publication 995, Washington, D. C., 1962, p. 107; See also A. J. Kovacs, *ibid.*, p. 112, for a kinetic viewpoint.
14. W. Kauzmann, *Chem. Revs.*, **43**, 219 (1948).

* This was pointed out to the author by W. B. Hillig.

Résumé

On exprime les viscosités de fractions de polystyrène et de polyisobutylène fondus par une équation d'Arrhénius modifiée (M.A.), $\eta = A \exp \{B/(T - T_0)\}$, et par une équation du volume libre $\eta = A \exp \{1/f\}$, dans laquelle $f = V_f/V$, est la fraction de volume libre. On admet donc que f ainsi défini, est une fonction linéaire de la température vu que $f = (T - T_0)/B$. Par cette méthode, le volume "occupé" dérivé, $v_s = v - v_f$ dépend de la température par les coefficients de température de f et v (c.à.d. $1/B$ et α , et ce volume occupé n'est pas en relation avec la valeur expérimentale α_0 pour l'état vitreux. Dans le cas du polyisobutylène le coefficient de température de v_s est positif tandis que pour le polystyrène il est légèrement négatif. On suggère des effets possibles de la structure liquide sur la détermination du comportement de v_s vis-à-vis de la température. Les viscosités calculées et les fractions de volume libre au point de transition vitreuse, T_g , dans un large domaine de poids moléculaire, M , pour les deux polymères, nous mènent à la conclusion que la transition vitreuse est avant tout un état d'isoviscosité" ($\eta_0 \simeq 10^{13}$ poises), plutôt qu'un état de "même volume libre." Toutefois dans les deux polymères, les deux conditions peuvent exister simultanément pour des valeurs semblables de M . Ainsi à M égal, $f_g = (T_g - T_0)/B$ est à peu près le même pour les deux polymères. Pour $M \simeq 100.000$, $f_g = 0.031$. Ces observations confirment l'idée que la transition vitreuse est plutôt un phénomène cinétique que thermodynamique. On trouve que la dépendance de T_g vis-à-vis du temps diffère pour les deux polymères à M égal et varie avec M dans chaque cas.

Zusammenfassung

Die Schmelzviskosität von Polystyrol- und Polyisobutylfraktionen wird durch eine modifizierte Arrheniusgleichung (M.A.), $\eta = A \exp \{B/(T - T_0)\}$, und durch eine Freie-Volums-Beziehung, $\eta = A \exp \{1/f\}$, wo $f = v_f/v$, der Freie-Volums-Bruchteil ist, dargelegt. Somit wird angenommen, dass das so definierte f eine lineare Temperaturfunktion ist, da $f = (T - T_0)/B$. Das nach dieser Methode abgeleitete "besetzte" Volumen, $v_s = v - v_f$, besitzt eine Temperaturabhängigkeit, die durch den Temperaturkoeffizienten von f und v (d.h. $1/B$ und α_1) bestimmt ist und keine Beziehung zum experimentellen α_0 -Wert des Glases zeigt. Bei Polyisobutylen ist der Temperaturkoeffizient von v_s positiv, während er für Polystyrol schwach negativ ist. Mögliche Einflüsse der Flüssigkeitsstruktur auf die Temperaturabhängigkeit von v_s werden in Betracht gezogen. Für die Glasumwandlungstemperatur, T_g , in einem weiten Molekulargewichtsbereich, M , berechnete Viskositäts- und Freie-Volums-Bruchteilwerte führen bei beiden Polymeren zu dem Schluss, dass die Glasumwandlung primär ein "Iso-Viskositäts"-Phänomen ($\eta_0 \simeq 10^{13}$ Poise) und nicht ein "Iso-Freie-Volums"-Phänomen ist. Es können aber bei den zwei Polymeren beide Bedingungen gleichzeitig für ähnliche M -Werte erfüllt sein. So ist bei gleichem M , $f_g = (T_g - T_0)/B$ für beide Polymere etwa gleich. Bei $M \simeq 100.000$ ist $f_g \simeq 0,031$. Diese Beobachtungen bilden eine Stütze für die Ansicht dass die Glasumwandlung primär ein kinetisches, und nicht ein thermodynamisches Phänomen ist. Die Zeitabhängigkeit von T_g erweist sich bei den zwei Polymeren bei gleichem M als verschieden und ist in beiden Fällen von M abhängig.

Received January 28, 1963

Polymerization of Butyl Esters of Methacrylic Acid and Hydrolysis of the Polymers

KEI MATSUZAKI, TAKEHIKO OKAMOTO, AKIRA ISHIDA, and
HIROSHI SOBUE, *Faculty of Engineering, The University of Tokyo,
Tokyo, Japan*

Synopsis

tert-Butyl methacrylate was polymerized with Grignard reagent, benzoyl peroxide, and gamma rays as initiator. The infrared spectra of the polymers indicated that the polymer polymerized with Grignard reagent had an isotactic structure and those polymerized with benzoyl peroxide and gamma rays had syndiotactic structures. Hydrolysis of polymethyl methacrylates and poly-*tert*-butyl methacrylates with hydroiodic acid was attempted, and differences in the infrared spectra of the polymethacrylic acids obtained due to stereoregularity were discussed. No difference in the demethylation behavior due to stereoregularity of polymethyl methacrylates was observed. Heat treatment of polymethacrylic acids and poly-*tert*-butyl methacrylates showed that isotactic polymers form polymer anhydride faster than syndiotactic polymers.

INTRODUCTION

In a previous paper,¹ polymerization of *n*-butyl, isobutyl, and *sec*-butyl esters of methacrylic acid with Grignard reagent or benzoyl peroxide as initiator, and polymerization induced by gamma ray were reported. On the basis of a comparison of the infrared spectra of the polymers with those of polymethyl methacrylate,² it was suggested that polymers polymerized with a Grignard reagent as initiator have an isotactic structure, and those induced with gamma rays and those polymerized with benzoyl peroxide have a syndiotactic structure.

In this investigation, polymerization of the *tert*-butyl ester of methacrylic acid was attempted, and the infrared spectra of the polymers obtained were compared with those of the polymers of other butyl esters. Hydrolysis of poly-*tert*-butyl methacrylate and polymethyl methacrylate was carried out and the differences due to stereoregularity in the infrared spectra of the polymethacrylic acid obtained were discussed. Furthermore, differences due to stereoregularity in thermal behavior of poly-*tert*-butyl methacrylates and polymethacrylic acids were observed.

EXPERIMENTAL AND RESULTS

1. Preparation of *tert*-Butyl Methacrylate and Polymerization

tert-Butyl methacrylate³ was prepared from methacryloyl chloride and *tert*-butyl alcohol.

Grignard reagent (*sec*-butylmagnesium bromide) was prepared from 2.5 g. of magnesium and 13.7 g. of *sec*-butyl bromide in ether. Ether was replaced with 100 ml. of toluene by distillation of ether.

Polymerization with Grignard reagent in toluene was carried out in sealed tubes in a temperature range from -40 to 27°C ., as shown in Table I. The yield decreased as the temperature increased, as in the polymerization of other butyl methacrylates.¹

TABLE I
Polymerization of *tert*-Butyl Methacrylate with Grignard Reagent as Initiator^a

Polymerization temperature, $^{\circ}\text{C}$.	Yield, %	Melting point, $^{\circ}\text{C}$.
-40	43	95
-20	16.7	97
0	10.0	104
27	0	—

^a Monomer : initiator solution (*sec*-butylmagnesium bromide in toluene) = 1 : 1.

TABLE II
Polymerization of *tert*-Butyl Methacrylate with Gamma Rays^a

Polymerization temperature, $^{\circ}\text{C}$.	Yield, %	Solvent
-78	3.8	Toluene (1:1)
-20	68.5	Bulk
ca. 20	100	Bulk

^a Total dose 1.63×10^7 r, dose rate 2.3×10^5 r/hr.

TABLE III
Viscosity and Melting Point of Poly-*tert*-butyl Methacrylate

Initiator	Polymerization temperature, $^{\circ}\text{C}$.	$[\eta]$, 100 ml./g.	Melting point, $^{\circ}\text{C}$.
Grignard reagent	-40	0.055	ca. 100
Gamma rays	0	0.992	ca. 165
Benzoyl peroxide	80	0.336	ca. 150

Radiation-induced polymerization of the monomer in toluene or in bulk form was carried out at -78 , -20 , and at about 20°C . under vacuum (10^{-3} mm. Hg), as shown in Table II.

Solution polymerization in toluene with benzoyl peroxide as initiator was carried out in a sealed tube at $80 \pm 5^{\circ}\text{C}$. The yield was 10.8%.

The intrinsic viscosity and melting point of the poly-*tert*-butyl methacrylates are shown in Table III. Both the intrinsic viscosity and melting point of the polymers polymerized with Grignard reagent are rather low,

but the low melting point seems mainly due to steric structure of the polymers.

2. Infrared Spectra of Poly-*tert*-butyl Methacrylate

Infrared spectra of poly-*tert*-butyl methacrylates polymerized with gamma rays and Grignard reagent did not show appreciable change in a wide range of polymerization temperature. As shown in Figure 1, differences in the infrared spectra of the polymers polymerized with Grignard reagent and those polymerized with benzoyl peroxide or gamma rays were observed in the regions of 1060, 940–970, 870, 785, and 750 cm^{-1} . The latter have stronger absorptions at 1060, 870, and 750 cm^{-1} , weaker at 785 cm^{-1} , and two absorptions at 940 and 970 cm^{-1} , while the former has rather a broad absorption at 940–970 cm^{-1} . No differences between the

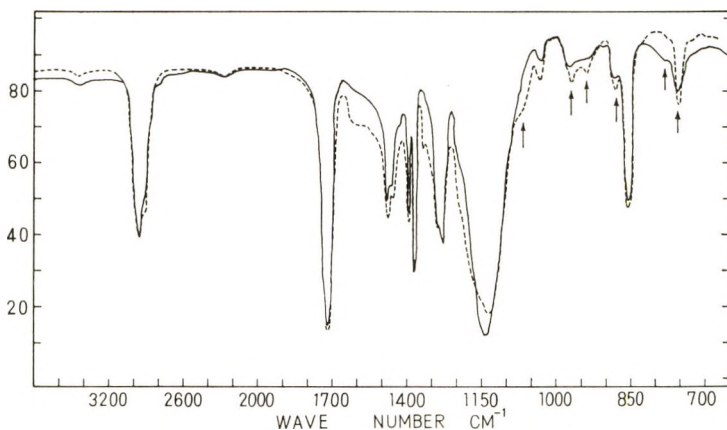


Fig. 1. Infrared spectra of poly-*tert*-butyl methacrylates: (—) polymerized with Grignard reagent at -40°C ., (- - -) (polymerized with gamma rays at 0°C .)

two types of polymers are observed in the region of 1450–1600 cm^{-1} , whereas in the polymers of other butyl esters, absorptions in this region varied according to the stereoregularity of the polymers as well as in polymethyl methacrylate. Absorptions in this region are usually assigned to deformation vibration of $\text{C}-\text{CH}_3$ or scissor vibration of $-\text{CH}_2-$. No differences in the infrared spectra of the two types of poly-*tert*-butyl methacrylates in this region may be due to overlapping of $\text{C}-\text{CH}_3$ vibration of *tert*-butyl groups to the absorption of $\text{C}-\text{CH}_3$ and $-\text{CH}_2-$ along the main chain.

As compared with polymethyl methacrylate² and polymers of other butyl esters of polymethacrylic acid,¹ the stronger absorptions at 1060 and 750 cm^{-1} suggest that poly-*tert*-butyl methacrylates polymerized with gamma rays or benzoyl peroxide have a syndiotactic structure and the polymer obtained with Grignard reagent has an isotactic structure.

3. Hydrolysis of Polymethyl Methacrylate and Poly-*tert*-butyl Methacrylate

In order to ascertain that polymethacrylic acid esters polymerized with Grignard reagent may have isotactic structure and those polymerized with benzoyl peroxide or with gamma rays a syndiotactic structure, hydrolysis of polymethacrylic acid esters was attempted.

First, polymethyl methacrylate was hydrolyzed. Samples used were isotactic polymer polymerized with *sec*-butylmagnesium bromide, syndiotactic polymer polymerized with tributylboron at -30°C ., and atactic polymers (commercial and gamma ray-induced at 0°C .). The polymers were hydrolyzed with hydroiodic acid (specific gravity 1.7) at 140°C . for 1 hr. in a Zeisel methoxyl determination apparatus. The results of determination are shown in Table IV. The hydrolyzed polymers were purified by repeated dissolution in methanol and reprecipitation with ether.

TABLE IV
Deesterification of Polymethacrylates and Polyacrylates

Sample	Initiator or stereoregularity	OCH ₃ , %	Yield of OCH ₃ , %	Purified polymer, %
Polymethyl methacrylate	Isotactic	21.0	67.7	61.8
	Syndiotactic	20.2	65.1	59.4
	Atactic (commercial)	18.2	58.7	53.6
	Atactic (gamma rays)	12.5	40.2	36.8
Polymethyl acrylate	Benzoyl peroxide	34.7	96.4	—
Poly- <i>tert</i> -butyl methacrylate	Grignard reagent	—	—	70.8
	Gamma rays	—	—	88.6

As shown in Table IV, polymethyl methacrylates could be hydrolyzed to 60–70% of the theoretical value in 1 hr. irrespective of the kind of stereoregularity, whereas polymethyl acrylate polymerized with benzoyl peroxide at 80°C . was easily hydrolyzed to 96%. Demethylation after 1 hr. was very slow; e.g., for atactic polymethyl methacrylate, 14.43% OCH₃ for the first hour and 0.81% OCH₃ for the next hour. The reason why the demethylation terminates at 60–70% of the theoretical value and does not depend on the stereoregularity, in contrast to other investigations,⁴ is not known.

Among the polymethacrylic acid butyl esters, polymers of *tert*-butyl ester were easily hydrolyzed. The reaction may be deisobutenation as in thermal degradation,⁵ since evolution of gas was observed in the treatment of the polymers with hydroiodic acid.

The infrared spectra of polymethacrylic acid obtained from polymethyl methacrylates are shown in Figure 2. The differences between the spectra of isotactic and syndiotactic polymers were observed in the regions of 930–980, 1020, 1460, 1490, and 1800 cm^{-1} . For isotactic polymer, the absorption at 930–980 cm^{-1} is broad, while for the syndiotactic polymer,

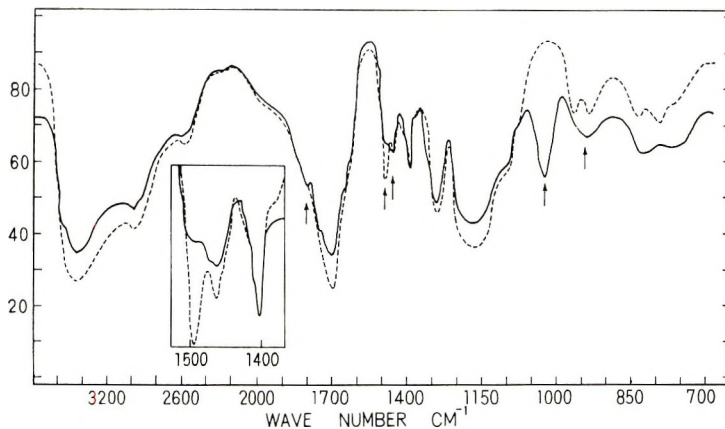


Fig. 2. Infrared spectra of polymethacrylic acids from polymethyl methacrylates: (—) isotactic; (---) syndiotactic.

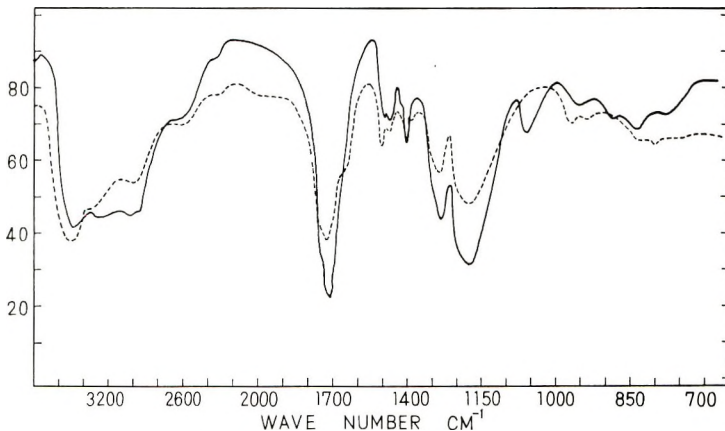


Fig. 3. Infrared spectra of polymethacrylic acids from poly-*tert*-butyl methacrylates: (—) polymerized with Grignard reagent at -40°C ., (---) polymerized with gamma rays at 0°C .

two distinct absorptions are observed. The absorption at 1460 cm^{-1} is stronger than that at 1490 cm^{-1} for isotactic polymer, while for syndiotactic polymer, the latter is stronger. The absorptions at 1020 and 1800 cm^{-1} disappeared on treatment of the polymers with hot water at 80°C . for 3 hr., showing that these absorptions probably attributable to the presence of anhydride groups.

In the above observations, absorptions at 1460 and 1490 cm^{-1} varied most with the stereoregularity (isotactic and syndiotactic) of the polymers. Therefore, it seems possible to determine the stereoregularity of polymethacrylic acid by the intensity ratio of these absorptions. Experiments on the problem are now in progress.

The infrared spectra of the hydrolyzates of poly-*tert*-butyl methacrylates are shown in Figure 3. Differences in the absorption of the two types of the polymers are similar to those in the polymethacrylic acids from polymethyl methacrylates, except for the absorption due to anhydride groups. The absorption at 1020 cm^{-1} in isotactic polymethacrylic acid from polymethyl methacrylate shifted to 1060 cm^{-1} in the acid from isotactic poly-*tert*-butyl methacrylate. In the acid from syndiotactic poly-*tert*-butyl methacrylate, no absorption at 1020–1060 cm^{-1} was observed.

From the above results, it is evident that on hydrolysis isotactic polymethyl and poly-*tert*-butyl methacrylates form anhydrides much more easily than syndiotactic polymers.

4. Thermal Treatment of Poly-*tert*-butyl Methacrylate

Grassie et al.⁵ showed that, when poly-*tert*-butyl methacrylate was heated, the polymer changed to polymethacrylic anhydride via polymethacrylic acid. Behavior of the two types of poly-*tert*-butyl methacrylate on heat treatment were observed; the change of weight with time is shown in Figure 4. The temperature was raised to 200°C. at a rate of ca. 2°C./min. and maintained at this temperature.

The polymer polymerized with Grignard reagent lost weight at 180–200°C., resulting in direct anhydride formation. For the polymer polymerized with gamma rays, the rate of weight loss was not only slow, but it

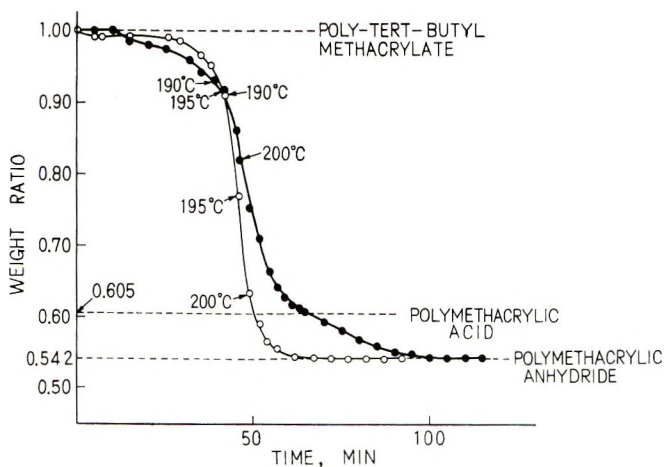


Fig. 4. Change of weight with time on heat treatment of poly-*tert*-butyl methacrylates: (O) polymerized with Grignard reagent at -40°C ., (●) polymerized with gamma rays at 0°C .

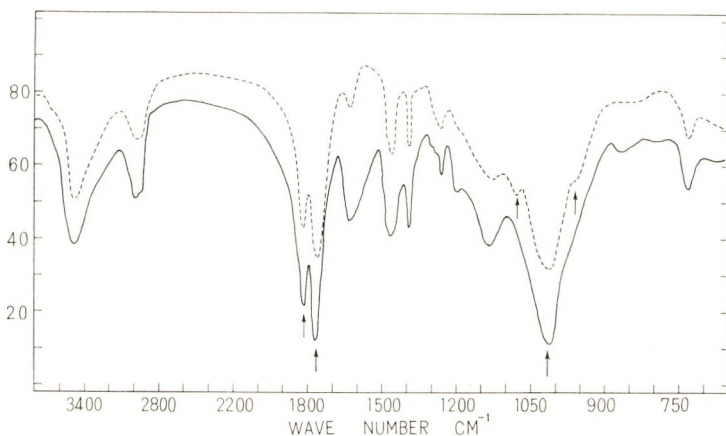


Fig. 5. Infrared spectra of poly-*tert*-butyl methacrylates after thermal treatment: (—) polymerized with Grignard reagent at -40°C ., (---) polymerized with gamma rays at 0°C .

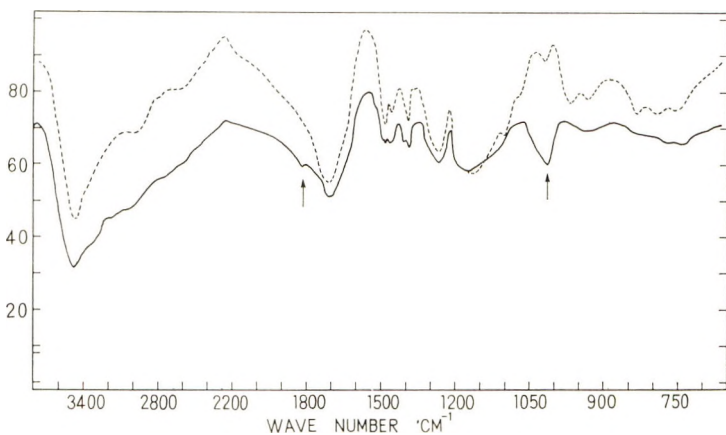


Fig. 6. Infrared spectra of polymethacrylic acids heated at 170°C . for 10 min.: (—) isotactic; (---) syndiotactic.

showed tendency for two-step reaction, that is, deesterification and subsequent anhydride formation.

The above observations suggest the following. In isotactic poly-*tert*-butyl methacrylate, as soon as carboxyl groups are formed by deesterification, they accelerate deesterification of adjacent ester groups and anhydride formation by the reaction between the adjacent carboxyl groups. In syndiotactic polymer, as the interaction between carboxyl groups formed by deesterification and unesterified ester groups is less than in isotactic polymer, the rate of deesterification and anhydride formation is slower, and a two-step reaction results. Faster anhydride formation of isotactic polymer suggests that the polymer has a zigzag *trans* structure rather than

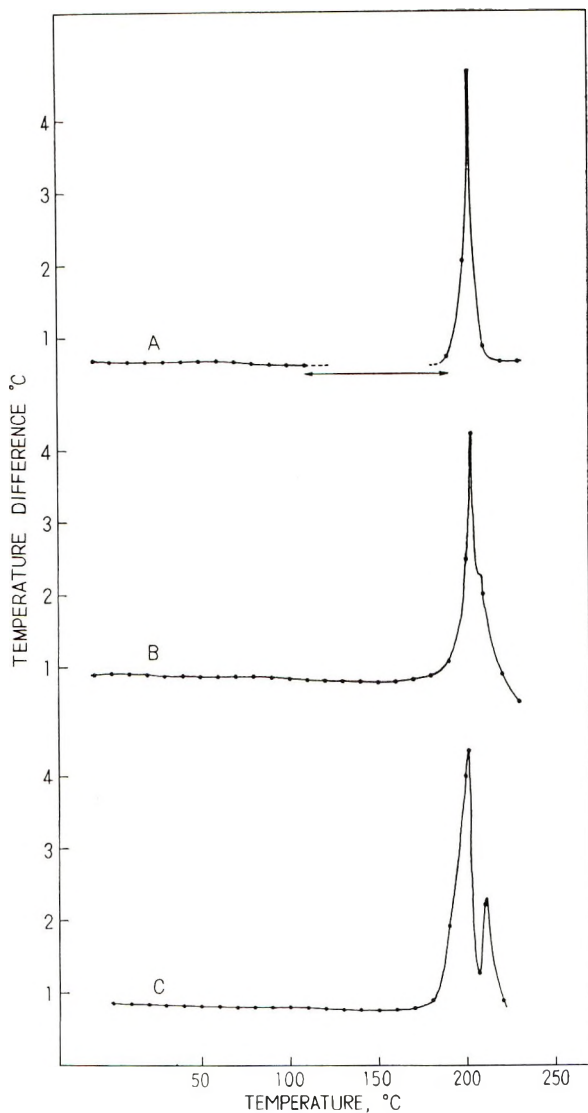


Fig. 7. Differential thermal analysis curves for poly-*tert*-butyl methacrylates: (A) polymer polymerized with Grignard reagent at -40°C .; (B) polymerized with benzoyl peroxide at 80°C ., (C) polymerized with gamma rays at 0°C .

the helical *trans-gauche* structure during this heat treatment and also in the hydrolysis reaction mentioned before.

The infrared spectra of the polymers after thermal treatment are shown in Figure 5. Strong absorptions assigned to anhydride groups are observed at 1022 , 1760 , and 1810 cm.^{-1} . Absorptions at 965 and 1085 cm.^{-1} are found only in the spectra of the heated polymer polymerized with gamma rays.

In order to confirm that isotactic polymethacrylic acid forms anhydride on heating much faster than syndiotactic polymer, isotactic and syndiotactic polymethacrylic acids from polymethyl methacrylates were heated at 170°C. for 10 min. The infrared spectra of the polymers after heating are shown in Figure 6. From the figure, it is evident that the isotactic polymer forms anhydride faster.

5. Differential Thermal Analysis of Poly-*tert*-butyl Methacrylate

Poly-*tert*-butyl methacrylates were analyzed by a differential thermal method. The apparatus was a differential thermal analyzer of Rigaku Denki Co. The temperature was raised at a rate of 3.6–4.1°C./min. The results are shown in Figure 7.

The main peak, which may be the decomposition temperature of the polymethacrylates, is the same for all the polymers, the maximum being at 202–203°C. A difference due to stereoregularity of the polymers is a small peak at 211°C. for the polymer polymerized with gamma rays and a shoulder at 210°C. for the polymer polymerized with benzoyl peroxide. It is interesting that the polymer polymerized with benzoyl peroxide at 80°C. behaves like an intermediate between the two other polymers (isotactic and syndiotactic). The small peak may be attributed to the formation of anhydride in syndiotactic polymer corresponding to the second reaction of the two-step reaction. Further investigation is necessary to confirm the above supposition.

We wish to thank Dr. T. Kawaguchi, Central Research Laboratory, Toyo Rayon Co. for his measurements of differential thermal analysis and Dr. H. Watanabe, Electrical Communication Laboratory, Nippon Telegraph and Telephone Public Corporation, for giving us a sample of syndiotactic polymethyl methacrylate.

References

1. Matsuzaki, K., H. Kubota, A. Ishida, K. Eto, K. Itagaki, and H. Sobue, *Kogyo Kagaku Zasshi*, **65**, 600 (1962).
2. Fox, T. G. et al., *J. Am. Chem. Soc.*, **80**, 1768 (1958); U. Baumann, H. Schreiber, and K. Tessmar, *Makromol. Chem.*, **36**, 81 (1959).
3. Heyboer, J., and A. J. Staverman, *Rec. Trav. Chim.*, **69**, 787 (1950).
4. Glavis, F. J., *J. Polymer Sci.*, **36**, 547 (1959); G. Smets, and W. de Loecker, *ibid.*, **45**, 461 (1960).
5. Grassie, N., *J. Polymer Sci.*, **48**, 79 (1960); D. H. Grant, and N. Grassie, *Polymer*, **1**, 125, 445 (1960).

Résumé

Le méthacrylate de *tertiobutyle* a été polymérisé en présence d'initiateurs tels que le réactif de Grignard, le peroxyde de benzoyle et le rayonnement gamma. Les spectres infra-rouges des polymères indiquent que le polymère obtenu au moyen du réactif de Grignard a une structure isotactique et que ceux obtenus au moyen du peroxyde de benzoyle et du rayonnement gamma ont une structure syndiotactique. L'hydrolyse des polyméthacrylates de méthyle et de *tertiobutyle* fut tentée au moyen d'acide iodhydrique et les différences dans les spectres infra-rouges dues à la stéréorégularité des acides polyméthacryliques obtenus ont été discutées. Il n'a guère été observé de différence

dans le comportement au point de vue stéréorégularité lors de la déméthylation des polyméthacrylates de méthyle. Les acides polyméthacryliques et les polyméthacrylates de *tertiobutyle* ont été soumis à un traitement thermique. Il a été trouvé que les polymères isotactiques forment des polyanhydrides plus rapidement que les polymères syndiotactiques.

Zusammenfassung

tert-Butylmethacrylat wurde mit Grignard-Reagens, Benzoylperoxyd und γ -Strahlen als Starter polymerisiert. Die Infrarotspektren der Polymeren zeigten, dass das mit Grignard-Reagens hergestellte Polymere isotaktische Struktur, das mit Benzoylperoxyd und π -Strahlen hergestellte syndiotaktische Struktur besitzt. Hydrolyse von Polymethylmethacrylaten und Poly-*tert*-butylmethacrylaten mit Jodwasserstoffsäure wurde versucht und die durch die Stereoregularität der erhaltenen Polymethacrylsäure verursachten Unterschiede in den Infrarotspektren diskutiert. Bei der Entmethylierung konnten keine durch die Stereoregularität von Polymethylmethacrylaten verursachten Unterschiede beobachtet werden. Eine Hitzebehandlung von Polymethacrylsäure und Poly-*tert*-butylmethacrylat wurde durchgeführt. Es wurde festgestellt, dass isotaktische Polymere rascher polymere Anhydride bilden als syndiotaktische.

Received January 28, 1963

Multicomponent Non-Fickian Diffusion through Inhomogeneous Polymer Membranes

H. L. FRISCH, *Bell Telephone Laboratories, Incorporated, Murray Hill, New Jersey*

Synopsis

We point out explicitly the dependence of the non-Fickian diffusive flows of low molecular weight penetrants through a polymer membrane possessing a gradient in internal composition or a local property, such as a stress, on the gradient of the chemical potential of the polymeric substance. The possibility of maintaining for sufficiently long times a gradient in internal composition or property in these substances is a consequence of the long relaxation times encountered in these substances. A number of ways are suggested for preparing such membranes. Certain consequences for the diffusive separation of penetrants by such membranes are noted.

This note is concerned with pointing out certain possible consequences of extremely long relaxation times encountered in macromolecular center of mass motions for low molecular weight penetrant diffusion through inhomogeneous polymer films and the diffusive separation of low molecular penetrants by such polymer membranes. For simplicity we restrict ourselves to isothermal diffusion, although for practical separations a temperature gradient may be desirable. In any case the extension for this eventuality is straightforward.¹

We consider a polymer (component 3) membrane, $0 < x < l$ in contact with two low molecular weight penetrant reservoirs at $x = 0$ and $x = l$, respectively. The penetrants (components 1 or 2) can dissolve in and diffuse through the polymer membrane. The flow of component i , defined with respect to the center of mass movement, in the ternary system (component 1-component 2-component 3), J_i ($i = 1, 2, 3$) can be shown to satisfy¹

$$\begin{aligned} J_1 &= L_{11} \frac{\partial}{\partial x} (\mu_3 - \mu_1) + L_{12} \frac{\partial}{\partial x} (\mu_3 - \mu_2) \\ J_2 &= L_{12} \frac{\partial}{\partial x} (\mu_3 - \mu_1) + L_{22} \frac{\partial}{\partial x} (\mu_3 - \mu_2) \\ J_3 &= - (J_1 + J_2), \quad (T \text{ constant}) \end{aligned} \quad (1)$$

where $\mu_i = \mu_i(x)$ is the chemical potential of component i and the $L_{ij} = L_{ji}$ are the Onsager coefficients. Denoting by \bar{J}_i the flows of component i

in the corresponding binary systems (component 1–component 3 and component 2–component 3) one can write

$$\begin{aligned}\bar{J}_1 &= L_{11} \frac{\partial}{\partial x} (\bar{\mu}_3 - \bar{\mu}_1) \\ \bar{J}_2 &= L_{22} \frac{\partial}{\partial x} (\bar{\mu}_3 - \bar{\mu}_1)\end{aligned}\tag{2}$$

respectively, with $\bar{\mu}_i = \bar{\mu}_i(x)$ the chemical potential of component i in the respective binary systems.

The main purpose of this note is to point out: (1) the explicit dependence of the diffusive flows given by eqs. (1) and (2) on the gradient of the chemical potential of the polymer component (i.e., component 3) and (2) the possibility of maintaining these gradients over time periods at least of the order of magnitude of that required to attain steady states in the flows of the low molecular weight penetrant(s) because of the large polymer center of mass motion or stress relaxation times, etc. In practice the gradient in the chemical potential of the “polymeric substance” (component 3) composing the membrane can be established by the variation in local composition of the “polymeric substance.” Such is the case with an effectively “bonded sandwich” membrane, in which the successive layers normal to the x -axis are composed of chemically different polymers (e.g., increasingly more polar ones) chemically bonded together (say by crosslinks) or a mutually “bonded” set of layers of different molecular weight fractions of the same polymer species. In some cases chemical bonding of the layers is not necessary if sufficiently stable graded heterogeneous mixtures of polymer molecules can be attained, held together by mutual entanglement, crystallites, etc. Alternatively, one can attempt initially to produce a gradient across the polymer membrane by dispersal of a relatively high molecular weight penetrant whose diffusion coefficient is negligible in comparison with those of the subsequently admitted low molecular weight components 1 or 2 or by varying degrees of reaction (with suitable reagents e.g., hydrolysis) of functional groups on the backbone chain of the polymer etc. Another method of establishing a gradient in the chemical potential of the polymeric component 3 is by a local, graded variation in a physical property such as a local stress. An example of the latter category would be a polymeric membrane, with a gradient in the degree of crystallinity or orientation or size distribution of crystallites in the amorphous matrix. Membranes of this type can conceivably result from anisotropically prestressing of the membrane or initially subjecting the membrane to permeation by suitable penetrants, etc.

While in all of these instances the term “polymeric substance” is widened beyond the accepted usage of the term chemical substance (i.e., a pure compound or element) we wish to point out that this is not necessarily thermodynamically inconsistent (if due precautions are taken). Indeed this is

generally done, at least implicitly, in many areas of colloid chemistry and in the very definition of polymeric substance in polymer chemistry.

The temporal evolution of these, in general, non-Fickian diffusion processes is obtained by substituting the flows given by eqs. (1) and (2) into the hydrodynamical continuity equation of component i (i.e., the condition of mass balance of component i). In what follows we restrict ourselves to stationary states of flow in which J_i is a constant in time and x . In the usual permeation experiments the boundary conditions under which eqs. (1) or (2) have to be integrated are those which correspond to the assumption of equilibrium at the faces of the membrane $x = 0$ and $x = l$; there the chemical potentials of the penetrant components are equal to the constant values assumed in the reservoirs. These constant values can be varied independently by suitable preparation of the reservoirs.

If we denote by

$$\begin{aligned}\bar{v}_{ij}(x) &= \mu_i(x) - \mu_j(x) \\ \bar{v}_{ij}(x) &= \tilde{\mu}_i(x) - \tilde{\mu}_j(x)\end{aligned}\quad (3)$$

and define the difference operator Δ acting on the function $A(x)$ to be such that

$$\Delta A(x) = A(l) - A(0) \quad (4)$$

then the integrals of eqs. (2) are

$$\left(\frac{\bar{J}_1 l}{\Delta \bar{v}_{31}}\right)_{1,3} = \bar{L}_{11} = \frac{\int_0^l L_{11} \frac{\partial}{\partial x} (\bar{\mu}_3 - \bar{\mu}_1) dx}{\Delta \bar{v}_{31}} \quad (5)$$

and

$$\left(\frac{\bar{J}_2 l}{\Delta \bar{v}_{32}}\right)_{2,3} = \bar{L}_{22} = \frac{\int_0^l L_{22} \frac{\partial}{\partial x} (\bar{\mu}_3 - \bar{\mu}_2) dx}{\Delta \bar{v}_{32}} \quad (6)$$

where the mean Onsager coefficients \bar{L}_{ij} are functions of the $\bar{\mu}_i(l)$ and the $\bar{\mu}_i(0)$. Only if the original Onsager coefficients L_{ij} are constants independent of the local parameters characterizing the system in $\bar{L}_{ij} = L_{ij}$. In what follows we shall assume for simplicity that all gradients are sufficiently small so that we can set the $\bar{L}_{ij} = L_{ij}$. The integrals of eq. (1) are then

$$\begin{aligned}J_1 l &= L_{11} \Delta v_{31} + L_{12} \Delta v_{32} \\ J_2 l &= L_{12} \Delta v_{31} + L_{22} \Delta v_{32}\end{aligned}\quad (7)$$

Concerning the Onsager coefficients the thermodynamics of irreversible processes¹ asserts that

$$\begin{aligned}L_{ij} &\geq 0 \\ L_{ji} &= L_{ij} \leq \sqrt{L_{ii} L_{jj}} \leq 1/2(L_{ii} + L_{jj})\end{aligned}\quad (8)$$

Furthermore the values of L_{11} and L_{22} can be found from measurement on the binary system [cf. eqs. (5) and (6)]. These coefficients can be directly related to the mass fixed binary diffusion coefficients, e.g., if c_1 is the ratio of the mass of component 1 to the total mass in the binary system component 1-component 3 and ρ_{13} is the inverse specific volume of the system, then¹

$$D_{13} = [L_{11} | \rho_{13}(1 - c_1)] \frac{\partial \bar{\mu}_1}{\partial c_1}, \text{ etc.} \quad (9)$$

From eq. (7), we find that L_{12} can be found from a measurement of the flows J_1 and J_2 , if L_{11} and L_{22} are known, since

$$L_{12} = \frac{J_1 L_{22} \Delta v_{32} - J_2 L_{11} \Delta v_{31}}{L_{22} (\Delta v_{32})^2 - L_{11} (\Delta v_{31})^2} \quad (10)$$

The implications of eq. (7) for the separation of penetrants 1 and 2 follow from the separation ratio x_{12}

$$x_{12} = \frac{J_1}{J_2} = \frac{(L_{11} + L_{12}) \Delta \mu_3 - L_{11} \Delta \mu_1 - L_{12} \Delta \mu_2}{(L_{22} + L_{12}) \Delta \mu_3 - L_{12} \Delta \mu_1 - L_{22} \Delta \mu_2} \quad (11)$$

We see from eq. (11) that this ratio depends explicitly on $\Delta \mu_3$, which can be varied, by certain procedures already indicated, to obtain optimum separation relative to the given constraints under which the separation is to be carried out. In particular we note that for the special case that $\Delta \mu_1 = \Delta \mu_2 = 0$ when $x_{12} = x_{12}^0$ we have

$$x_{12}^0 = \frac{L_{11} + L_{12}}{L_{22} + L_{12}} \quad (12)$$

Thus even in the absence of chemical potential differences of the penetrants across a suitably prepared membrane (i.e., one for which $\Delta \mu_3 \neq 0$ can be maintained) separation of the penetrants will occur with flows J_i^0 given by [cf. eq. (7)]

$$\begin{aligned} J_1^0 &= \frac{(L_{11} + L_{12}) \Delta \mu_3}{l} \\ J_2^0 &= \frac{(L_{22} + L_{12}) \Delta \mu_3}{l} \end{aligned} \quad (13)$$

In sufficiently dilute systems involving small penetrant molecules one could attempt to estimate the value of x_{12}^0 , J_i^0 ($i = 1, 2$), etc. for small $\Delta \mu_3$ by neglecting the cross-coefficient L_{12} in comparison with L_{11} or L_{22} , which in turn can be related to diffusion data in the binary systems (in particular D_{13} and D_{23}) by using eq. (9). The mean Onsager coefficients [cf. eqs. (5) and (6)] must replace the Onsager coefficients in the general case. In the case of components which are electrically charged or in the presence of a temperature gradient eqs. (2) and (3) have to be replaced by

eqs. (196) and (107) of reference 1, respectively. Alternatively, these relations for x_{12} suggest a possible way of measuring a gradient in μ_3 . It should be noted that our considerations are based on the validity of the thermodynamics of irreversible processes for the description of non-Fickian diffusion in these systems.

We wish to acknowledge helpful discussions with Drs. E. Helfand, F. Stillinger, and J. J. Hermans.

Reference

1. See, e.g., S. R. de Groot, *Thermodynamics of Irreversible Processes*, North Holland, Amsterdam, 1959.

Résumé

Nous signalons explicitement la dépendance des courants de diffusion qui ne suivent pas la loi de Fick pour des particules de bas poids moléculaire pénétrant à travers une membrane polymérique possédant un gradient dans la composition interne ou une propriété locale, telle qu'une force, sur le gradient du potentiel chimique de la substance polymérique. La possibilité de maintenir pendant un temps suffisamment long un gradient dans la composition interne ou propriété dans ces substances est une conséquence des temps de relaxation rencontré dans ces substances. Un nombre de manières de préparer ces membranes sont suggérées. Certaines conséquences pour la séparation par diffusion de corps pénétrants à travers de telles membranes sont signalées.

Zusammenfassung

Die Abhängigkeit des nicht-Fickschen Diffusionsflusses niedermolekularer Stoffe durch eine Polymermembrane mit einem Gradienten der inneren Zusammensetzung oder einer lokalen Eigenschaft, wie einer Spannung, vom Gradienten des chemischen Potentials der "polymeren Substanz" wird explizit angegeben. Die Möglichkeit, durch genügend lange Zeit einen Gradienten der inneren Zusammensetzung oder Eigenschaft bei diesen Substanzen aufrechtzuerhalten, ist eine Folge der bei ihnen auftretenden langen Relaxationszeiten. Eine Reihe von Herstellungsmöglichkeiten für solche Membranen werden vorgeschlagen. Gewisse Folgerungen werden für die Diffusionstrennung von Stoffen durch solche Membranen gezogen.

Received January 24, 1963

Molecular Weight Distributions in Equilibrium Polymerizations*

J. L. LUNDBERG, *Bell Telephone Laboratories, Incorporated, Murray Hill, New Jersey*

Synopsis

Molecular weight distributions at polymerization equilibria appear to fall between two limiting cases, one which gives a "most probable" distribution and one which gives a very broad distribution. The difference between the two results depends on whether entropies of pure, crystalline homopolymers or pure, unoriented liquid homopolymers are proportional to molecular size. The free energies of polymerization of liquid homopolymers of ethylene can be estimated from published thermodynamic data if the entropies of pure, disoriented, liquid homopolymers are assumed to be proportional to molecular size. This leads to the expectation that molecular weight distributions are very broad for equilibrium polymers. For polyethylenes at polymerization equilibria, weight-average/number-average degree of polymerization ratios of 6 to 33, high weight-average degrees of polymerization ($10^2 \leq \bar{n}_w \leq 10^{14}$), and equilibrium monomer fugacities from 10^{-10} to 10^2 atm. are predicted at temperatures of 300–600°K. and at total pressures in the $1-10^4$ atm. range. These results are consistent with molecular weights and molecular weight distributions found for nonequilibrium polyethylenes. This agreement indicates that ethylene polymerizations might be controlled in part by energetics and not by kinetics alone.

Flory¹ and Tobolsky's² estimates of molecular weight distributions at polymerization equilibria describe what appears to be one limit of a continuum of molecular weight distributions attainable in polymerizing systems moderately concentrated in polymer. A "most probable" distribution is expected at equilibrium in this limiting case. Harris³ has demonstrated the likelihood of small departures from a most probable distribution toward more broad distributions in other than very dilute polymerizing systems at equilibria by estimating partition functions for polymer and solvent molecules in dilute solutions. Extreme departures from a most probable distribution to a very broad molecular weight distribution at polymerization equilibrium are shown to be likely by describing another limiting case for polymerization to equilibrium in systems relatively concentrated in polymer.

The problem concerns the degree of order in a liquid and is one facet of the "communal entropy" problem that has bothered thermodynamicists for years.⁴ To describe the properties of a polymerizing system at equi-

* Presented in part before the Division of High Polymer Chemistry, 132nd Meeting, American Chemical Society, September 13, 1957, New York.

librium, the change in free energy of polymerization must be estimated. Polymerization from monomer to the equilibrium polymer consisting of a mixture (solution) of monomer, dimer, trimer, n -mer, etc., may be considered to be the sum of two processes, the polymerization of monomer to pure homopolymers and the mixing of the pure homopolymers in their polymerization equilibrium concentrations to form the equilibrium polymerization system. The free energies of formation, and hence, the free energies of polymerization, of pure gaseous monomer to form pure gaseous n -mer are expected to be proportional to molecular size, i.e., chain length, for an homologous series such as the polymerization of ethylene gas to the gaseous 1-alkenes.^{5,6} This is a consequence of assuming that vibrational, rotational, and translational motions of a molecule are independent of one another and that the partition function describing these motions may be written as the product of partition functions, each describing one type of motion.⁷ Thermodynamic tables for the gaseous hydrocarbons are constructed from spectral data on the basis of these assumptions.⁸ No serious question of the validity of these assumptions has been raised so as to be widely published.

The free energies of formation, and polymerization of gaseous or liquid monomer to form pure liquid n -mer homopolymer, may or may not be linear functions of molecular size depending upon the degree of order present in pure liquids. The difference in entropy between a rigid (crystalline) n -mer molecule and a flexible n -mer molecule is approximately⁹

$$S_{\text{flexible}} - S_{\text{rigid}} \leq k \ln(n) + k(n-1) \ln\left(\frac{z-1}{e}\right) \quad (1)$$

where k is Boltzmann's constant, n is the degree of polymerization, and z is the coordination number of a lattice approximating the structure of the liquid polymer. Equation (1) is derived by counting the number of ways that n links of a flexible n -mer molecule can be arranged in n subvolumes. (There are n ways for the first link, zg_2 for the second link, $(z-1)g_3$ for the third link, etc. The g 's are factors less than 1 allowing for the inability of two links to occupy the same subvolume and the lack of complete flexibility of the polymer chain. An upper limit for the entropy of disorder is found by taking all g 's equal to one.) A consequence of eq. (1) is the expectation that the free energies of formation and polymerization of monomer to pure liquid n -mer homopolymer may be expected to be linear functions of chain length n if the liquid is highly random, approximating the disorder of pure, dense gaseous n -mer, and to depart from linearity by approximately $kT \ln(n)$ per molecule if the liquid is highly ordered approaching the regularity of a crystal. That real liquid homopolymers are somewhere between these two extremes seems likely.

The analogy for small molecule systems is the "communal entropy" problem.⁴ Consider m molecules in volume V in the gaseous state and m molecules each in m subvolumes of volume V/m corresponding to the

crystalline state. The difference in configurational entropy between these two states is km or k per molecule. In the case where the liquid is highly disordered, little of this change in configurational entropy might be lost in condensing from gas to liquid and most of it might be expected to be lost in freezing from disordered liquid to the perfectly ordered crystal. On the other hand, if the liquid is highly ordered, most of this configurational entropy will be lost upon condensation from the disordered gas to the ordered liquid, and little will remain to be lost upon freezing the ordered liquid to the perfectly ordered crystal. Assigning the k entropy change to either the freezing point or the boiling point represents a limiting situation. Real liquids probably occupy a broad range between (but not including) these extremes, depending upon the degrees of order in the liquids.

The two limiting cases for polymerization equilibrium arise as follows:

1. Assume the free energies of formation and polymerization of monomer to pure, crystalline (perfectly oriented) n -mer homopolymers are linear functions of molecular size. Mix the monomer, dimer, trimer, n -mer, etc., to form the equilibrium polymer. This gives a "most probable" distribution at polymerization equilibrium.¹

2. Assume the free energies of formation and polymerization of monomer to pure, unoriented (randomly oriented) n -mer homopolymers are linear functions of molecular size. Mix the monomer, dimer, trimer, n -mer, etc., to form the equilibrium polymer. This gives a very broad molecular weight distribution at polymerization equilibrium.¹⁰

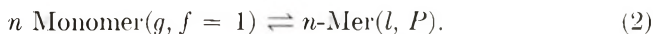
The latter case appears to be the more reasonable in view of the linear increase of entropy with chain length for an homologous series of hydrocarbons in the gas phase⁵ and the entropy of disorder of a polymer chain varying with the logarithm of chain length [eq. (1)]. The "third law" entropies of the normal alkanes through $C_{15}H_{34}$ have been measured.¹¹ No departure from linearity of entropy with chain length, aside from the even number-odd number of carbon atoms alternation, is apparent. Therefore, the free energies of formation and polymerization to form liquid alkanes (or 1-alkenes) may be expected to be linear functions of chain length. If normal alkanes are disoriented liquids, case 2 leading to a very broad molecular weight distribution at equilibrium is the more likely. If normal alkanes are highly ordered liquids, case 1 leading to a "most probable" molecular weight distribution at equilibrium may be correct in spite of the expectation that entropy of polymerization of monomer to pure oriented polymer might be nonlinear with chain length by the logarithm of chain length according to the estimate of disorder of a random polymer chain [eq. (1)].

In this paper, the equilibrium equations for case 2, leading to broad molecular weight distributions at polymerization equilibria, are given. Estimates of free energies of polymerization from gaseous ethylene to pure, unoriented, liquid, linear n -mer homopolymers are made using published free energies of formation in the ideal gas state, vapor pressure data, and molar volume data.⁵ Molecular weights and molecular weight distribu-

tions at equilibria for polyethylenes in bulk polymerizations are calculated from these free energy data.

I. Equilibrium Equations

Consider the polymerization of n gaseous monomer units at unit fugacity to form liquid n -mer in the equilibrium polymerization mixture under a total pressure P :



The activity product for this reaction may be written as

$$a_n/f_1^n = N_n\gamma(n)/f_1^n = e^{-\Delta F_p^\circ(n)/RT} \quad (3)$$

where f_1 = fugacity of monomer, a_n = activity of n -mer, N_n = mole fraction of n -mer, $\gamma(n)$ = activity coefficient of n -mer, and $\Delta F_p^\circ(n)$ = standard change in free energy of polymerization of gaseous monomer at unit fugacity to pure, unoriented, liquid, n -mer homopolymer at pressure P .

A bulk polymerization is a solution (mixture) of monomer, dimer, trimer, n -mer, etc. In such a system in the liquid phase, the activity coefficient $\gamma(n)$ is the departure of the activity a_n from that given by the ideal solution law, the mole fraction N_n . A good estimate for $\gamma(n)$ is given by Flory¹ whose eq. (14) may be recast as

$$\ln \gamma(n) = \ln \frac{n}{\bar{n}_n} + 1 - \frac{n}{\bar{n}_n} \quad (4)$$

where \bar{n}_n is the number-average degree of polymerization. Equation (4) can be deduced from Guggenheim's¹² eq. (8.7) by assuming a monomer molecule or a monomer unit in a polymer chain can occupy one site on a pseudolattice.

The entropies of homologous series of liquid hydrocarbons are proportional to molecular size.¹¹ The heats of combustion (and formation) of real polymers are proportional to molecular size.¹³ Thus, the standard changes in free energies of polymerization to pure liquid homopolymers may be expected to be given by

$$\Delta F_p^\circ(n) = \alpha + \beta n \quad (5)$$

where α and β are constants (dependent upon pressure and temperature) and n is the number of monomer units.

Substitution of eqs. (4) and (5) in eq. (3) gives

$$N_n = \exp \left\{ n \ln f_1 - \frac{\alpha + \beta n}{RT} - \ln \frac{n}{\bar{n}_n} - 1 + \frac{n}{\bar{n}_n} \right\} \quad (6)$$

for the mole fraction of n -mer at equilibrium. If eq. (6) is substituted in the equation

$$\sum_{n=1}^{n=\infty} N_n = 1 \quad (7)$$

for the sum of mole fractions, into the equation

$$\bar{n}_n = \sum_{n=1}^{n=\infty} n \cdot N_n \quad (8)$$

for the number-average degree of polymerization, and into the equation

$$\bar{n}_w = \frac{\sum_{n=1}^{n=\infty} n^2 \cdot N_n}{\sum_{n=1}^{n=\infty} n \cdot N_n} \quad (9)$$

for the weight-average degree of polymerization, if the summations are carried out, the resulting equations are, after simplifying,

$$N_n = \left(\frac{1}{\ln \bar{n}_w} \right) \frac{1}{n} \left(1 - \frac{1}{\bar{n}_w} \right)^n \quad (10)$$

for the mole fraction of n -mer,

$$\bar{n}_n = \frac{e^{\left(\frac{\alpha}{RT} + 1 \right)}}{\ln \left(1 + e^{\left(\frac{\alpha}{RT} + 1 \right)} \right)} = \frac{\bar{n}_w - 1}{\ln \bar{n}_w} \quad (11)$$

for the number-average degree of polymerization,

$$\bar{n}_w = e^{\left(\frac{\alpha}{RT} + 1 \right)} + 1 = 1 + \bar{n}_n \ln \bar{n}_w \quad (12)$$

for the weight-average degree of polymerization, and

$$f_1 = \left(\frac{\bar{n}_w - 1}{\bar{n}_w} \right) e^{\left(\frac{\beta}{RT} - 1/\bar{n}_w \right)} \quad (13)$$

for the fugacity of monomer at polymerization equilibrium.

An equation of the form of eq. 10, which gives a very broad molecular weight distribution at polymerization to equilibrium, can be derived by substituting Flory's¹ eq. (19) (which gives an estimate of the change in partial molal free energy when one mole of pure, disoriented, liquid, n -mer homopolymer is added to an infinite amount of solution of dimer, trimer, n -mer, etc.) in his eq. (37) (which gives the criterion for thermodynamic equilibrium accounting for changes in free energy due to mixing dimer, trimer, n -mer, etc., and due to polymerization of pure monomer in some standard state to pure, disoriented, liquid homopolymers, dimer, trimer, n -mer, etc.) Flory's eq. (37), thus substituted, and his eq. (38), a material balance requirement, can be solved using Lagrangian multipliers (exactly as Flory¹ has done for case 1 leading to the "most probable" molecular weight distribution at polymerization equilibrium).

The molecular weight distribution of an equilibrium polymer is given by eq. (10) is very broad. The mole fraction of n -mer is inversely proportional to chain length (which is to say the weight fraction of n -mer is independent of chain length) up to chain lengths of the order of the weight-average degree of polymerization. Characteristic of this broad molecular weight distribution is a large weight-average/number-average molecular weight

ratio which is [by eq. (11)] almost exactly equal to $\ln \bar{n}_w$. The difference between the treatments that lead to the "most probable" and the very broad molecular weight distributions at polymerization equilibrium does not involve directly the manipulation of solution theory of high polymers. Both treatments are equally dependent upon and use the athermal mixing theories in exactly the same manner. The difference arises in whether the entropies (and, hence, the free energies of formation and polymerization) of an homologous series of molecules (hydrocarbons) are proportional to (linear functions of) molecular size in the liquid state or in the solid state. For relatively disordered liquids, such as polymerizing, never frozen monoolefins, the liquid is perhaps best described as a dense gas as far as configurational entropy is concerned. In this case a broad molecular weight distribution at equilibrium might be expected. On the other hand, in a polymerizing system involving ionic species in a melt, a high degree of order is present and the system is probably best described as a crystalline system. In this case, a narrower molecular weight distribution, perhaps approaching a "most probable" distribution, might be expected.

II. Predicted Molecular Properties of Equilibrium Polyethylene

Molecular weights, molecular weight distributions, and monomer fugacities for equilibrium polyethylenes can be estimated if free energy data, vapor pressure data, and molar volume data for the 1-alkenes (and molar volume data for the normal alkanes) are manipulated so as to estimate the constants α and β in eq. (5) for the standard changes in free energies of polymerization of ethylene gas to pure, liquid polyethylene homopolymers (at various pressures and temperatures). (See Appendix.) These predictions are based on thermodynamic data for 1-alkenes; hence, the results are limited to linear polyethylenes, at least in principle. However, changes in standard free energies of isomerization per branch point are usually small (close to zero);¹⁴ therefore, these estimates should be equally valid for branched polyethylenes.

Polymerization to liquid polymer is assumed in developing these equations. The melting points of polyethylenes increase with increasing pressure;¹⁵ therefore, the stable forms of polyethylenes in much of the pressure-temperature region discussed are crystalline or partially crystalline forms. Neither polymerization or depolymerization are likely to occur in the crystalline state in view of the large heat of polymerization of ethylene.¹³ Depolymerization and polymerization at high pressures probably occur in undercooled liquids. Thus, these equations should be applicable in at least parts of the pressure-temperature region in which stable forms of polyethylenes are crystalline or partially crystalline. In any case, the estimates based upon these equations should be considered to be rough approximations only.

The predicted weight-average degrees of polymerization at equilibrium range from 10^{10} at 300°K. to 10^4 at 500°K. for polymerizations at 1-1000

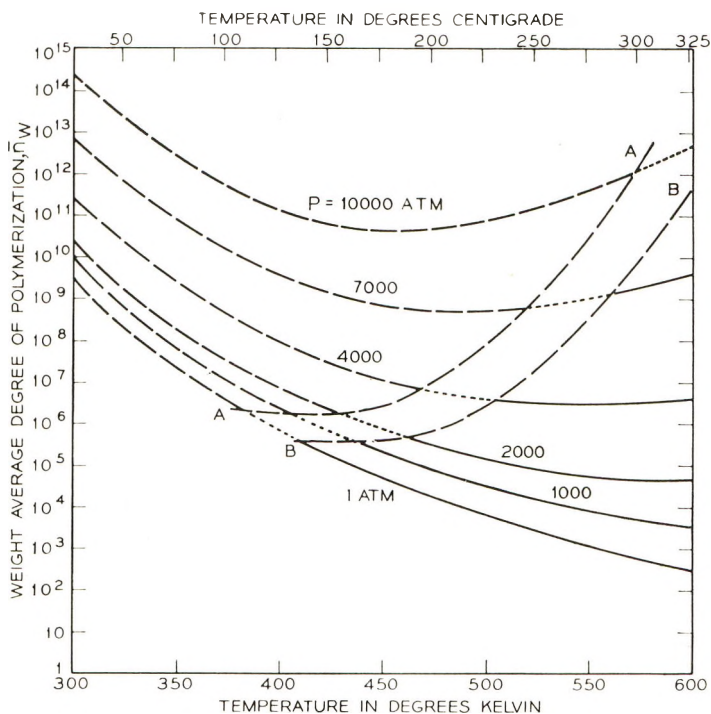


Fig. 1. Predicted weight-average degrees of polymerization of linear polyethylene at equilibrium with ethylene gas at various temperatures and pressures.

atm. However, if the polymerization pressure is increased to 10,000 atm., giant molecules having weight-average degrees of polymerization from 10^{14} at 300°K . to 10^{11} at 500°K . are predicted at equilibrium (Fig. 1). A molecule 10^{11} monomer units long would have an average end-to-end distance of 0.007 cm.¹⁶ That these extremely large equilibrium molecules might be reasonable is evidenced by reports of very large polyethylene molecules in high pressure polymers.¹⁷ Certainly, the predicted molecular sizes meet the requirement that they be at least as great as those observed for non-equilibrium polymers.^{18,19} In Figures 1, 3, and 4, the lines AA and BB are the freezing point versus pressure curves for branched and linear polyethylene respectively, based on the data and extrapolations of the data of Matsuoka.¹⁵ To the left of AA and BB are pressure-temperature regions wherein the stable states are partially crystalline polyethylenes, to the right, liquid polyethylenes.

The molecular weight distributions predicted for equilibrium polyethylenes prepared under various conditions of pressure and temperature are very similar at low molecular weights (Fig. 2). In each case, about 1 mole-% heptamer is predicted. Increasing pressure and decreasing temperature shift the molecular weight distributions only slightly toward lower mole fractions of low polymers; rather, the shift is toward producing additional large molecules which are few in number but significant in size and

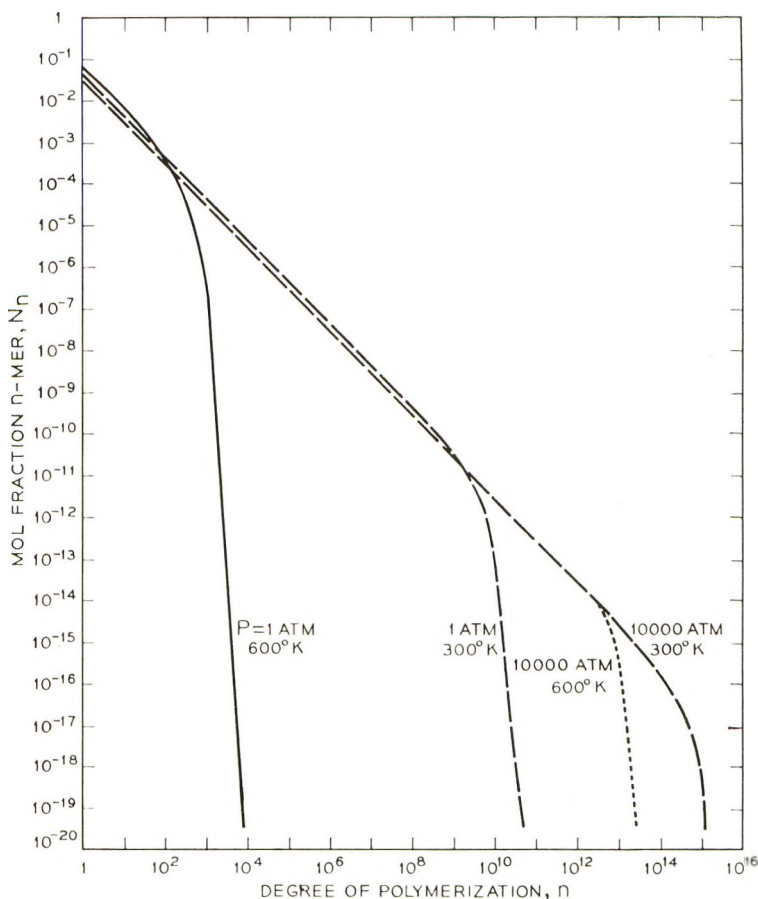


Fig. 2. Predicted mole fractions of n -mer of linear polyethylene at equilibrium with ethylene gas at various temperatures and pressures.

weight. The dependence upon chain length of this equilibrium molecular weight distribution [eq. (10)] is not inconsistent with most of the experimentally determined distributions of ordinary polyethylenes reported in the literature.¹⁸ Of the four distribution curves (Fig. 2) representing extremes of pressure-temperature conditions considered, only the one atmosphere 600°K. molecular weight distribution curve represents pressure-temperature conditions where the stable forms of both linear and branch polyethylenes are liquids. At 600°K. and 10,000 atm. the stable forms of branched polyethylenes may be liquids.

The weight-number average ratios, $\ln \bar{n}_w$ [eq. (12)], predicted for equilibrium polyethylenes range from 9 to 33 in the temperature interval 300–500°K. and pressure range of 1–10,000 atm. (Fig. 3). These predicted ratios are similar to those observed for most nonequilibrium polyethylenes. The exceptions are a few ratios greater than 33, as high as 300, and a few cases where ratios close to two are reported.^{18,19} Considering the difficulties

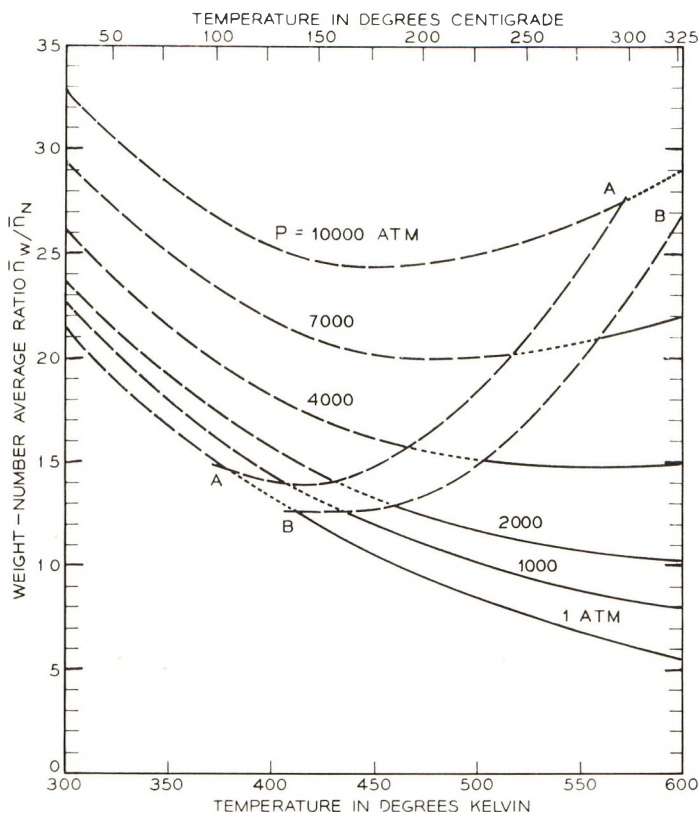


Fig. 3. Predicted weight-average/number-average molecular weight ratios of linear polyethylene at equilibrium with ethylene gas at various temperatures and pressures.

in molecular weight measurements on polyethylenes and the assumptions made in predicting these results, that only a small fraction of the reported weight-number ratios falls outside the predicted range is surprising.

Predicted ethylene fugacities at equilibrium increase with increasing pressure and increasing temperature (Fig. 4). In general, these fugacities are low, under 1 atm., except at high total pressures at temperatures above 435°K. These predicted fugacities are in agreement with the fact that in low pressure batch polymerizations ethylene pressures drop to very low pressures if a polymerization path is given the system.²⁰

The fugacities of ethylene at equilibrium with the polymerizing system are considerably less than the total pressures on the polymerizing system for which the fugacities are calculated. The vapor pressure of a polymerizing system at equilibrium is equal to the sum of the vapor pressures of monomer and all polymeric species (and solvent, if any is present). If the total pressure on the system is greater than the vapor pressure of the polymerizing system only condensed phases will exist. Polymerization to equilibrium can take place even if only one condensed phase exists. Only

if the vapor pressure is to be measured is it necessary to devise some semi-permeable membrane such that vapor pressure can be measured in the presence of a larger (than vapor pressure) applied pressure. If the total pressure on the polymerizing system is equal to the vapor pressure of the polymerizing system, two (or three) phases, one vapor and one (or two) condensed, coexist. A two-phase polymerizing system that contains nothing but a single kind of monomer and polymer of that monomer behaves at equilibrium as does a single component system. Such a two-phase system is monovariant at equilibrium. [That this is the case can be readily seen

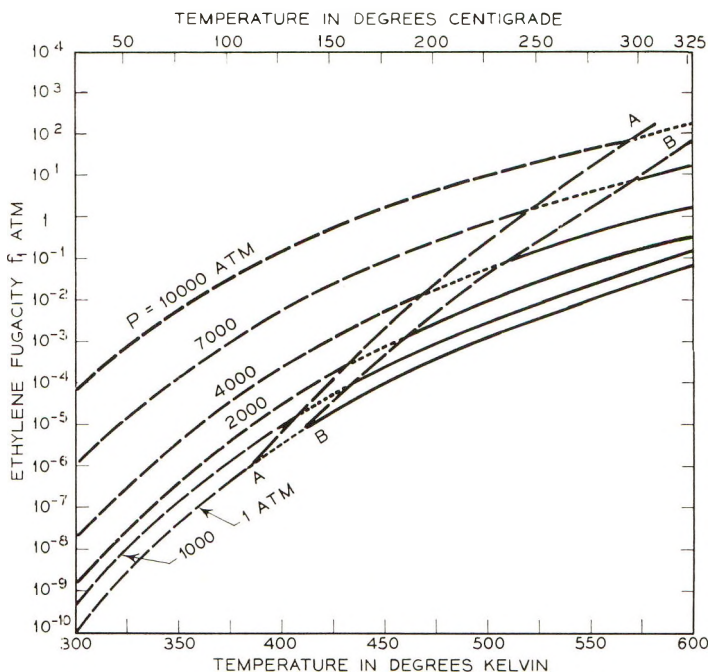


Fig. 4. Predicted fugacities of ethylene gas at equilibrium with linear polyethylene at various temperatures and pressures.

if a polymerizing system at equilibrium containing monomer, dimer, trimer, etc., up through and including n -mer is considered. Such a system has n components and, by the phase rule $n + 2 - P$ degrees of freedom, where P is the number of phases present. However, there are $n - 1$ polymerization equilibrium equations relating the n activities. Thus, there are actually $n + 2 - P - (n - 1) = 3 - P$ degrees of freedom for a system at polymerization equilibrium.] The fugacity of monomer at equilibrium in a polymerizing system is a slowly varying function of the total pressure (according to eqs. (13) and (21b), Appendix, as shown in Fig. 4), the ethylene fugacity in a polymerizing system at equilibrium under its own vapor pressure is very nearly equal to the ethylene fugacity in a polymerizing system at equilibrium at 1 atm. total pressure.

The predicted molecular weights and molecular weight distributions for equilibrium polyethylenes that are presented here must be considered as only approximate. The changes in standard free energies of polymerization are based on data from monomer through decamer in chain length. Extrapolation of these data to high degrees of polymerization would be prohibitively hazardous were it not that in eqs. (10), (11), and (12) for the molecular weight distribution and average degrees of polymerization only intercepts, not slopes, of the free energy-degree of polymerization relation, eq. (21), appear. The equilibrium fugacities estimated are more uncertain because these do depend upon the slope of eq. (21) (Appendix). Estimates at higher pressures, particularly at 10,000 atm. total pressure, probably err high for average degrees of polymerization because liquid alkenes were considered to be incompressible in developing the pressure dependence of free energy changes on polymerization [eqs. (17a) and (18) of Appendix].

III. Summary

For case 2, assuming the entropies of pure unoriented homopolymers are linear functions of degree of polymerization, the free energies of polymerization may be estimated empirically using ideal gas state free energy data and measured vapor pressures and molar volumes for the 1-alkenes. If observed molecular weights, weight-average/number-average ratios, and molecular weight distributions for ordinary polyethylenes are compared with these properties calculated for equilibrium polyethylenes using published thermodynamic data for the 1-alkenes, reasonable agreement is found. This indicates that polymerizations of ethylene, particularly by the "high pressure" process, may be controlled by energetics, at least in part, rather than by kinetics alone. A broad molecular weight distribution is predicted for an equilibrium polymer. Thus, if ethylene polymerizations are energetics-controlled (at least in part), the observed broad molecular weight distributions of polyethylenes are not anomalous but are to be expected for vinyl polymerizations in bulk if the reactions are carried on such as to approach equilibrium. Large equilibrium molecular weights are predicted for polyethylenes; large equilibrium molecular weights should be expected for most other vinyl polymers as well.

For case 1, assuming the entropies of pure oriented (crystalline) homopolymers are linear functions of degree of polymerization, estimation of the free energies of polymerization from ideal gas state free energy data appears to be imprudent because the crystalline state for 1-alkenes does not exist above about 137°C.²¹ at 1 atm. Thus, even with sufficient heat of fusion and heat capacity data, estimation of free energies of hypothetical crystals on the basis of extrapolations of heat capacities with temperature is hazardous. Therefore, numerical comparison of predicted molecular weight distributions and degrees of polymerization for case 1 and case 2 for polymerization of ethylene to equilibrium probably has no meaning.

Several systems apparently polymerize to equilibria.²² Investigation of molecular weight distributions at polymerization equilibria, with particular emphasis on monomer, dimer, and other low molecular weight species and with careful measurement of monomer activity (and dimer and trimer activity, if they be appreciable), should be particularly rewarding studies. An exact description of at least one equilibrium polymerization system seems important to our understanding of polymerization reactions. More important, within the limits of our knowledge of polymer solutions, the dependence of entropy upon molecular size of an homologous series probably can be estimated from equilibrium polymerization studies more easily and more accurately than from calorimetric study of several pure members of an homologous series.

Appendix

The standard changes in free energies of formation (and, hence, polymerization) for the 1-alkenes, the low polymers of ethylene, are tabulated for the ideal gas state.⁵ From these data we can calculate the standard changes in free energies of polymerization of gaseous monomer to pure liquid polymer.

Consider the reaction given by eq. (2) to be the sum of four processes:

1. Polymerization in the ideal gas state:



for which the standard changes in free energies of polymerization are given by linear equations.⁵

$$\Delta F_p^\circ(n) (f = 1) = A + Bn \quad (14a)$$

2. Expansion of n -mer from unit fugacity to the vapor pressure of n -mer



for which the free energy change is

$$\Delta F_{\text{exp}}(n) = RT \ln \frac{f_{P_{\text{vap}}}(n)}{f = 1} = RT \ln f_{P_{\text{vap}}}(n) \quad (15a)$$

3. Condensation of n -mer under its own vapor pressure



for which the free energy change is zero.

4. Change of pressure from the vapor pressure of liquid n -mer to the reaction pressure P of the system



for which the free energy change is

$$\Delta F_{\text{press}}(n) = \int_{P_{\text{vap}}(n)}^P V(n, P) dP \cong V(n) [P - P_{\text{vap}}(n)] \quad (17a)$$

TABLE I
 Constants Relating Thermodynamic Data to Molecular Size For the 1-Alkenes and Evaluation of Free Energy, Molecular Weight, and Monomer Fugacity Equations

$$\Delta F_p^\circ \frac{(n)(f=1)}{RT} = \frac{A + Bn}{RT}; \quad V(n) = a_0 + a_1n; \quad \ln P_{\text{vap}}(n) = b_0 + b_1n$$

Temp., <i>T</i> , °K.	$\frac{A}{RT}$	$\frac{B}{RT}$	a_0	a_1	b_0	b_1
300	14.78	-20.463	27.5 ± 0.4	32.71 ± 0.06	5.91 ± 0.12	-2.397 ± 0.023
400	6.68	-11.087	39.8 ^a	34.8 ^a	5.74 ± 0.05	-1.390 ± 0.007
500	1.80	-5.516	67.3 ^b	35.8 ^b	5.86 ± 0.12	-0.907 ± 0.017
600	-1.44	-1.807	116.2 ^b	37.6 ^b	6.01 ± 0.11	-0.640 ± 0.016
	$\frac{\alpha}{RT} = \frac{A}{RT} + b_0 + \frac{P_{a_0}}{RT}$	$\frac{\beta}{RT} = \frac{B}{RT} + b_1 + \frac{P_{a_1}}{RT}$	$e^{\left(\frac{\alpha}{RT} + 1\right)}$			$e^{\frac{\beta}{RT}}$
300	20.69 + 1.45 × 10 ⁻³ <i>P</i>	-22.860 + 1.33 × 10 ⁻³ <i>P</i>	2.6 × 10 ⁹ (10 ^{3.3} × 10 ⁻⁴ <i>P</i>)	-12.477 + 1.06 × 10 ⁻³ <i>P</i>	1.18 × 10 ⁻¹⁰ (10 ^{5.8} × 10 ⁻⁴ <i>P</i>)	3.8 × 10 ⁻⁶ (10 ^{4.6} × 10 ⁻⁴ <i>P</i>)
400	12.42 + 1.21 × 10 ⁻³ <i>P</i>	-6.423 + 0.87 × 10 ⁻³ <i>P</i>	6.7 × 10 ⁹ (10 ^{3.3} × 20 ⁻⁴ <i>P</i>)	-2.447 + 0.76 × 10 ⁻³ <i>P</i>	1.05 × 10 ⁻⁹ (10 ^{3.8} × 10 ⁻⁴ <i>P</i>)	8.7 × 10 ⁻² (10 ^{3.3} × 10 ⁻⁴ <i>P</i>)
500	7.66 + 1.64 × 10 ⁻³ <i>P</i>		5.8 × 10 ⁹ (10 ^{7.1} × 10 ⁻⁴ <i>P</i>)			
600	4.57 + 2.36 × 10 ⁻³ <i>P</i>		9.7 × 10 ⁹ (10 ^{1.0} × 10 ⁻⁴ <i>P</i>)			

^a Estimated from data on 1-alkenes and *n*-alkanes.

^b Estimated from data on *n*-alkanes.

where the molar volume $V(n)$ of liquid n -mer is assumed to be independent of pressure in making the approximation. Equation (5) is the sum of eqs. (14a), (15a), and (17a):

$$\Delta F_p^\circ(n) = \alpha + \beta \cong A + Bn + RT \ln f_{P_{\text{vap}}}(n) + V(n) [P - P_{\text{vap}}(n)] \quad (18)$$

Equation (18) can be simplified by replacing the fugacity at the vapor pressure of n -mer by the vapor pressure and noting that the vapor pressures of the 1-alkenes (and the normal alkanes)⁵ are given by equations of the form

$$\ln P_{\text{vap}}(n) = b_0 + b_1 n \quad (19)$$

where b_0 and b_1 are constants and n is the number of monomer units. Also, in eq. (18), the vapor pressure of n -mer is negligible compared to the polymerization pressure (which must be equal to or greater than the pressure of monomer and the partial pressures of dimer, trimer, and all other species present at equilibrium). The molar volumes of the 1-alkenes⁵ (and the normal alkanes) are proportional to molecular weight; thus,

$$V(n) = a_0 + a_1 n \quad (20)$$

where a_0 and a_1 are constants and n is the number of monomer units. Substituting eqs. (19) and (20) in eq. (18)

$$\Delta F_p^\circ(n) = \alpha + \beta n \cong A + Bn + RT(b_0 + b_1 n) + P(a_0 + a_1 n) \quad (21)$$

where

$$\alpha = A + RTb_0 + Pa_0 \quad (21a)$$

$$\beta = B + RTb_1 + Pa_1 \quad (21b)$$

The constants of eqs. (14a), (19), and (20) were evaluated by fitting data given in the A.P.I. Table.⁵ These constants and values of α/RT and β/RT are summarized in Table I.

The help and encouragement of colleagues, especially G. L. Baldwin, F. H. Winslow, and W. P. Slichter, of the Bell Telephone Laboratories, is appreciated. Review and criticism of early drafts of the manuscript by F. E. Harris and R. Ullman and of the final draft by E. A. DiMarzio were most helpful.

References

1. Flory, P. J., *J. Chem. Phys.*, **12**, 425 (1944).
2. Tobolsky, A. V., *J. Chem. Phys.*, **12**, 402 (1944); *Properties and Structure of Polymers*, Wiley, New York, 1960, p. 266.
3. Harris, F. E., *J. Polymer Sci.*, **18**, 351 (1955).
4. Hirschfelder, J. O., C. F. Curtiss, and R. B. Bird, *Molecular Theory of Gases and Liquids*, Wiley, New York, 1954, p. 273.
5. American Petroleum Institute Project 44, National Bureau of Standards, Selected Values of Hydrocarbons, Table Nos. 24-X, 24d-E, 24K, and 20K.
6. Jessup, R. S., *J. Chem. Phys.*, **16**, 661 (1948).

7. Born, M., and R. Oppenheimer, *Ann. Physik*, **84**, 457 (1927).
8. Kilpatrick, J. E., E. J. Prosen, K. S. Pitzer, and F. D. Rossini, *J. Res. Natl. Bur. Std.*, **36**, 559 (1946).
9. Flory, P. J., *Principles of Polymer Chemistry*, Cornell, Univ. Press, Ithaca, N. Y., 1953, p. 502.
10. Lundberg, J. L., Paper presented at 132nd Meeting, American Chemical Society, New York, September 8-13, 1957; *Abstracts*, p. 9t.
11. Finke, H. L., M. E. Gross, G. Waddington, and H. M. Huffman, *J. Am. Chem. Soc.*, **76**, 333 (1954).
12. Guggenheim, E. A., *Proc. Roy. Soc. (London)*, **A183**, 203 (1944).
13. Data of D. E. Roberts, cited in reference 6; F. S. Dainton and K. J. Ivin, *Experimental Thermochemistry*, Vol. 2, H. A. Skinner, Ed., Interscience (Wiley), New York, 1962, p. 253.
14. Prosen, E. J., K. S. Pitzer, and F. D. Rossini, *J. Research Natl. Bur. Stds.*, **34**, 255 (1945).
15. Matsuoka, S., *J. Polymer Sci.*, **57**, 569 (1962).
16. Flory, P. J., reference 9, p. 415.
17. Baker, W. O., W. P. Mason, and J. H. Heiss, *J. Polymer Sci.*, **8**, 129 (1952); L. T. Muus, and F. W. Billmeyer, Jr., *J. Am. Chem. Soc.*, **79**, 5079 (1957); L. Nicholas, *J. Polymer Sci.*, **29**, 191 (1958); W. M. D. Bryant, F. W. Billmeyer, Jr., L. T. Muus, J. T. Atkins, and J. E. Eldridge, *J. Am. Chem. Soc.*, **81**, 3219 (1959); L. D. Moore, Jr., and V. G. Peck, *J. Polymer Sci.*, **34**, 141 (1959).
18. Desreux, V., and M. C. Spiegels, *Bull. Soc. Chem. Belges*, **59**, 476 (1950); K. Ueberreiter, H. G. Orthmann, and G. Sorge, *Makromol. Chem.*, **8**, 21 (1952); A. C. Baskett and C. W. Miller, *Nature*, **174**, 364 (1954); L. Nicholas, *Compt. Rend.*, **242**, 2720 (1956); L. H. Tung, *J. Polymer Sci.*, **20**, 495 (1956); R. S. Aries and A. P. Sachs, *J. Polymer Sci.*, **21**, 551 (1956); H. Smith, *J. Polymer Sci.*, **21**, 563 (1956); H. Wesslau, *Makromol. Chem.*, **20**, 111 (1956); A. Nasini and C. Mussa, *Makromol. Chem.*, **22**, 59 (1957); L. H. Tung, *J. Polymer Sci.*, **24**, 333 (1957); H. S. Kaufman and E. K. Walsh, *J. Polymer Sci.*, **26**, 124 (1957); S. W. Hawkins and H. Smith, *J. Polymer Sci.*, **28**, 341 (1958); C. Mussa, *J. Polymer Sci.*, **28**, 587 (1958); P. S. Francis, R. C. Cooke, Jr., and J. H. Elliott, *J. Polymer Sci.*, **31**, 453 (1958); P. M. Henry, *J. Polymer Sci.*, **36**, 3 (1959); J. E. Guillet, R. L. Combs, D. F. Slonaker, and H. W. Coover, *J. Polymer Sci.*, **47**, 307 (1960).
19. Billmeyer, F. W., Jr., *J. Am. Chem. Soc.*, **75**, 6118 (1953); L. D. Moore, Jr., *J. Polymer Sci.*, **20**, 137 (1956); C. Mussa, *J. Polymer Sci.*, **23**, 877 (1957); Q. A. Trementozzi, *J. Polymer Sci.*, **23**, 887 (1957); T. Kobayashi, A. Chitale, and H. P. Frank, *J. Polymer Sci.*, **24**, 156 (1957); L. T. Muus and F. W. Billmeyer, Jr., *J. Am. Chem. Soc.*, **79**, 5079 (1957); L. Nicolas, *J. Polymer Sci.*, **29**, 191 (1958); N. K. Raman and J. J. Hermanns, *J. Polymer Sci.*, **35**, 71 (1959); Q. A. Trementozzi, **36**, 113 (1959); R. A. Mendelson, *J. Polymer Sci.*, **46**, 493 (1960); H. J. L. Schuurmans, *J. Polymer Sci.*, **57**, 557 (1962).
20. Ziegler, K., and H. G. Gellert, U. S. Pat. 2,699,457 (January 11, 1955).
21. Mandelkern, L., M. Hellmann, D. W. Brown, D. E. Roberts, and F. A. Quinn, Jr., *J. Am. Chem. Soc.*, **75**, 4093 (1953).
22. Dainton, F. S., and K. J. Ivin, *Quart. Revs.*, **12**, 61 (1958).

Résumé

Les distributions de poids moléculaire à l'équilibre de polymérisation se situent entre deux cas limites, le premier qui donne une distribution "la plus probable" et l'autre une distribution très large. La différence entre les deux résultats dépend de ce que les entropies des homopolymères cristallins purs ou des homopolymères liquides non-orientés purs sont proportionnelles à la dimension moléculaire. On peut estimer les énergies libres de polymérisation d'homopolymères liquides d'éthylène à partir des données

thermodynamiques publiées si les entropies des homopolymères liquides, désorientés, purs sont proportionnelles aux dimensions moléculaires. Ceci entraîne des distributions de poids moléculaire très larges pour des polymères à l'équilibre. Pour des polyéthylènes dans des conditions d'équilibre, on peut prévoir des rapports des degrés de polymérisation en poids et nombre de 6 à 33, des degrés de polymérisation moyens en poids élevés ($10^2 \leq \bar{n}_w \leq 10^{14}$) et des fugacités du monomère à l'équilibre de 10^{-10} à 10^2 atmosphères, à des températures de 300° à 600°K et des pressions totales variant de 1 à 10^4 atmosphères. Ces résultats sont en accord avec les poids moléculaires et les distributions de poids moléculaires trouvés pour des polyéthylènes qui ne sont pas à l'équilibre de polymérisation. Cet accord montre que les polymérisations d'éthylène peuvent être contrôlées en partie par des conditions énergétiques et non seulement par les conditions cinétiques.

Zusammenfassung

Molekulargewichtsverteilungen bei Polymerisationsgleichgewichten scheinen sich zwischen zwei Grenzfälle einordnen zu lassen, von denen der eine einer "wahrscheinlichsten" Verteilung, der andere einer sehr breiten Verteilung entspricht. Der Unterschied zwischen den beiden Fällen hängt davon ab, ob die Entropie reiner, kristalliner Homopolymerer oder reiner unorientierter flüssiger Homopolymerer der Molekulargröße proportional ist. Die freie Polymerisationsenergie flüssiger Äthylenhomopolymerer kann aus veröffentlichten thermodynamischen Daten unter der Annahme einer Proportionalität der Entropie reiner, nichtorientierter flüssiger Homopolymerer zur Molekülgröße bestimmt werden. Das lässt erwarten, dass die Molekulargewichtsverteilung bei Gleichgewichtspolymeren sehr breit ist. Für Polyäthylen lässt sich beim Polymerisationsgleichgewicht ein Verhältnis zwischen Gewichts- und Zahlenmittel des Polymerisationsgrades von 6 bis 33, ein hohes Gewichtsmittel des Polymerisationsgrades ($10^2 \leq \bar{n}_w \leq 10^{14}$), sowie eine Gleichgewichtsfugazität des Monomeren von 10^{-10} bis 10^2 Atmosphären bei Temperaturen von 300° bis 600°K und einem Gesamtdruck im Bereich von 1 bis 10^4 Atmosphären vorhersagen. Molekulargewichtsverteilungen, wie sie bei Nicht-Gleichgewichts-Polyäthylenen auftreten, stimmen mit diesen Voraussagen überein. Eine solche Übereinstimmung spricht dafür, dass für die Äthylenpolymerisation zum Teil auch die Energetik, und nicht die Kinetik allein, ausschlaggebend sein kann.

Received January 25, 1963

Aliphatic Polyhydrazides: A New Low Temperature Solution Polymerization

A. H. FRAZER and F. T. WALLENBERGER, *Pioneering Research Division, Textile Fibers Department, E. I. du Pont de Nemours & Company, Inc., Experimental Station, Wilmington, Delaware*

Synopsis

High molecular weight polyhydrazides have been prepared by a new low temperature polymerization technique from equimolar amounts of a dihydrazide and a dicarbonyl chloride in dialkyl amide solvents. All-aliphatic polyhydrazides were insoluble in dimethyl sulfoxide, had polymer melt temperatures ranging from 200 to 300°C. Films could be pressed and fibers could be pulled from the melt. Aliphatic-aromatic and oxalic-aromatic polyhydrazides which undergo dehydration at different rates had polymer melt temperatures ranging from 250 to 300°C. and inherent viscosities ranging from 0.3 to 1.5. They were soluble in dimethyl sulfoxide, a solvent from which tough films could be cast.

INTRODUCTION

Carboxylic hydrazides or symmetrical carboxylic dihydrazides have been prepared by the reaction between carboxylic acids,¹ esters,² anhydrides,² or carbonyl chlorides³ with hydrazine or carboxylic hydrazides, respectively. The reaction of esters with hydrazine or with 80–100% hydrazine hydrate is generally regarded to be quantitative while the other acid derivatives frequently lead to undesirable mixtures of mono-, di-, tri-, and tetraacyl hydrazines.^{2,4–6}

This monomeric model reaction has been adapted and applied to the preparation of polymers. A French patent,⁷ as early as 1942, discloses the condensation of hydrazine or with dicarboxylic acids in alcohol and the thermal treatment of the product to yield low melting polymeric materials presumed to be low molecular weight polyhydrazides. Moldenhauer and Bock⁸ obtained in similar reaction sequences polymer which supposedly could be melt spun to fibers or melt pressed to films. Pritchard⁹ described the melt polymerization of dihydrazides in the absence of dicarboxylic acid derivatives yielding unidentified polymer. Fisher,¹⁰ and later also Korshak, Chelnokova, and Shkoline¹¹ prepared well-defined polyaminotriazoles from two moles of hydrazine and one mole of a dibasic acid at elevated temperatures and pressures. McFarlane and Miller¹³ described the preparation of a series of polyhydrazides by a high temperature solution process. Most recently, Campbell, Foldi, and Farago¹² described the

preparation of well characterized polyurelenes and of poly(acyl semi-carbazides) from stoichiometric amounts of hydrazine or dihydrazides and diisocyanates.

Since polyhydrazides may also be considered as polyamides with hydrazine, as an inorganic diamine component, it was of interest to prepare well-defined, high molecular weight aliphatic, oxalic, alicyclic, homo- and hetero-aromatic polyhydrazides and copolyhydrazides, to study their solubilities and to evaluate their utility as films and fibers. The procedure of McFarlane and Miller¹³ which involves the reaction of stoichiometric amounts of dihydrazide with dicarboxylic acids, esters, or dicarbonyl chlorides in such solvents as nitrobenzene and mixed xylenols at temperatures of 170–200°C. appeared to be suited for our purposes. In the course of this investigation, we have developed a new low temperature polymerization method involving the reaction of a dicarbonyl chloride with hydrazine or a dihydrazide at low temperatures in a dialkyl amide solvent. Thus, this report not only describes the preparation and properties of the aliphatic polyhydrazide, but in addition, compares the results of this new synthetic route with those of prior work, specifically that by McFarlane and Miller.¹³ The description of all-aromatic polyhydrazides, as a new class of polymers, has been deferred for a separate discussion.¹⁴

EXPERIMENTAL

Polymer melt temperatures (PMT) and inherent viscosities (η_{inh}) were obtained by standard methods of polymer characterization as recommended by Beaman and Cramer¹⁵ and by Sorenson and Campbell.¹⁶

The system of codes used throughout this paper simplifies the writing of structures. It is extensively used in Tables I and II. Arabic numerals indicate the number of carbon atoms in a diacid component such as dihydrazides, diacid chlorides, or diesters. The following abbreviations have been used for other diacid portions: HT = hexahydroterephthalic acid, DP = dipicolinic acid, PY = 2,6-pyrazindicarboxylic, I = isophthalic, T = terephthalic. Zero (0), as abbreviation stands for the simplest diamine, hydrazine. A polymer code such as 0-2-0-I would, therefore, represent the ordered alternating polyhydrazide derived from oxalic acid and isophthalic acid.

Intermediates, such as diacids, diacid chlorides, and dialkyl esters were obtained by conventional methods.

1. Preparation of Dihydrazides^{1-6, 13}

A mixture of 1 mole of diethyl (or dimethyl) ester of a dibasic acid and 3 moles of hydrazine hydrate was refluxed in 500–1000 ml. of dry methanol for 4–24 hr. The solid dihydrazide which precipitates during the reaction is collected and recrystallized from water. In this manner, we have prepared isophthalic dihydrazide, azelaic dihydrazide and sebacic dihydrazide.

Oxalyl dihydrazide and hydrazine hydrate (Eastman Kodak), which are commercially available, were used as received.

2. Preparation of Polyhydrazides in Inert Solvents

McFarlane and Miller's method¹³ was used without change for the preparation of aliphatic polyhydrazides. A modification has also been reported by Frazer and Wallenberger.¹⁴

3. Preparation of Polyhydrazide in Amide Solvents

A solution of 0.01 mole of dicarboxylic acid dihydrazide and 20–30 ml. of *N*-methylpyrrolidone or hexamethylphosphoramide was placed in an ice-cooled reaction flask adapted with stirrer, nitrogen inlet and drying tube. To this was added portionwise over a period of ~15 min. 0.01 mole of a dicarbonyl chloride. The reaction mixture was stirred overnight, and the polymer precipitated with water. The isolated polymer was washed with ethanol and dried.

All-aliphatic polyhydrazides precipitated from the solution as the molecular weight solution viscosity increased. Aliphatic-aromatic and oxalic aromatic polyhydrazides remained in solution during the preparation.

RESULTS AND DISCUSSION

1. High Temperature Solution Preparation of Polyhydrazides

McFarlane and Miller¹³ described a high temperature solution (HTS) polymerization technique for the preparation of aliphatic and mixed aliphatic-aromatic copolyhydrazides. They reacted a diester, diacid chloride, or diacid component with hydrazine or an equimolar dihydrazide component in solvents such as mixed xyleneols or nitrobenzene at temperatures ranging from 170 to 200°C.

When these preparations¹³ were repeated, it was noted that the polymer melt temperatures of aliphatic polyhydrazides range from 185 to 328°C. (Table I) and that they were insoluble in a variety of polymer solvents including dimethyl sulfoxide. No self-supporting films and fibers were afforded by standard techniques.

The preparation of the heretofore unknown oxalic-aliphatic copolyhydrazides such as 0-2-0-6 (Table II, example 1b-1g) and the preparation of a series of aliphatic-aromatic polyhydrazides was attempted. However, only low molecular weight materials were obtained.

2. Low Temperature Solution Preparation of Polyhydrazides

Morgan, Tietz, and Sorenson,¹⁷ as well as Campbell, Foldi, and Farago¹² have studied the use of amide solvents in the preparation of condensation polymers. During this investigation, it was found that hydrazine or dihydrazides in hexamethylphosphoramide react with dicarbonyl chlorides smoothly to give high molecular weight polyhydrazides at room tempera-

TABLE I. Aliphatic Polyhydrazides

Polymer		Dicarboxylic intermediate				Method of polymerization ^b		M.P., °C.
No.	Code ^a	Acid ^a	Chloride ^a	Esters ^a	Hydrazide ^a		PMT, °C.	M.P., °C.
1	0-2			DiPh-2	2	HTS	380	
1a	0-2-0-6			DiEt-2	6	HTS		285 ^e
b				DiEt-2	6	HTS	300	
c			6		2	LTS	265	265 ^e
2a	0-2-0-7	2			9	HTS		
b				DiEt-2	9	HTS	295	
c		2			9	HTS	320	
d				DiEt-2	9	HTS	300	
3	0-2-0-10		10		2	LTS	300	
4	0-4-0-6	4			6	HTS		285 ^e
5	0-4-0-10	10			4	HTS		300 ^e
	0-6		6		6	LTS	328	
6a	0-6-0-9	9			6	HTS		300 ^e
b			6		9	LTS	318	
7a	0-6-0-10	10			6	HTS		295 ^e
b		10			6	HTS	325	
c			10		6	LTS	308	
8	0-6-0-HT	HT			6	HTS		300 ^e
9	0-9	9			9	HTS		215 ^e
10	0-9-0-10		10		9	LTS	280	
11	0-10		10		10	LTS	280	
12	0-13				13	Melt		185 ^d
13	0-18	18			0	Melt		high ^d

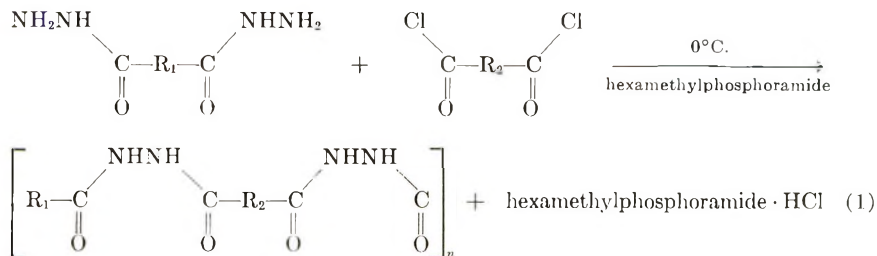
^a See experimental section for codes.^b HTS = High temperature solution polymerization; LTS = low temperature solution polymerization.^c Determination of McFarlane and Miller.¹³^d Determination of Moldenhauer and Bock.^{7,8}

TABLE II
 Aliphatic and Mixed Copolyhydrazides

Polymer		Dicarboxylic portion			Method of polymerization ^b		PMT, °C.	η_{inh} (DMSO)	Comments
No.	Code ^a	Acid ^a	Chlorides	Ester ^a	Hydrazide ^a				
a	0-2-0-I	I	I		2	LTS	342	1.43	Tough, clear films cast
b		I	I		2	HTS	290	0.12	—
c					2	HTS	310	Insoluble	—
d		2		DiMe-I	2	HTS	250	0.04	—
e			2		1	HTS	240	Insoluble	—
f			2		1	HTS	270	0.12	—
g				DiEt-2	1	HTS	210	0.10	—
	0-2-0-DP		DP		2	LTS	350	1.01	Strong films cast
	0-2-0-PY		PY		2	LTS	380	0.33	Clear yellow films
	0-6-0-I		I		6	LTS	290	0.60	Self-supporting films
a	0-6-0-T	T			6	HTS ^c	300	—	—
b		T			6	HTS	315	Insoluble	Brittle films pressed
	0-9-0-T	T			9	HTS	320	Insoluble	Brittle films pressed
	0-10-0-I		I		10	LTS	260	1.00	Strong films cast
	0-HT-0-I		HT		1	LTS	320	0.60	Tough films cast
	0-HI-0-I		HI		1	LTS	310	0.40	Tough films cast

^a See experimental section for codes.^b See footnote b in Table I.^c Preparation of McFarlane and Miller.¹³

ture or below. *N*-Methylpyrrolidone may be used as alternate solvent to give high molecular weight polyhydrazides. This condensation, a low temperature solution (LTS) polymerization, proceeds as shown in eq. (1).



In general, optimum molecular weight and yield of polyhydrazides were obtained when the intermediates and solvents were of the highest purity and moisture vigorously excluded. Surprisingly, film-forming molecular weight polymer could also be obtained with hydrazine *hydrate* in hexamethylphosphoramide as solvent. There is no apparent explanation for this anomalous behavior.

It was, however, noted that the first members of the homologous series of aliphatic dicarbonyl chlorides gave, in decreasing order, vigorous to mild reaction with the solvent. Thus, oxalyl, malonyl, succinyl, and glutaryl chloride could not be used for the preparation of high molecular weight polyhydrazides in amide solvents. Adipyl chloride was successfully employed if it was added dropwise and over prolonged periods of time to the dihydrazide in the amide solvent solution. In order to prepare copolyhydrazides with the radicals derived from oxalyl, malonyl, succinyl, and glutaryl chloride, it was necessary to prepare the corresponding dihydrazide and to react this with a diacid chloride. Based on our experimental data it would appear that there is no other restriction on the use of dicarbonyl chlorides as well as dihydrazides.

This new synthesis, therefore, affords high-molecular weight polyhydrazides, while the McFarlane-Miller¹³ procedure does not. The copolyhydrazide, for example, consisting of alternating portions of oxalic and isophthalic acids has been prepared by 7 different approaches (Table II, 1a-1g). Only the low temperature solution method gave high molecular weight film-forming polymers. Similarly, as shown in Table II, other film-forming aliphatic or mixed polyhydrazides were obtained only by the new synthesis.

3. Solubilities and Polymer Structure

Generally all of the copolyhydrazides (aliphatic-aromatic and oxalic-aromatic) are soluble in hot, and many in cold dimethyl sulfoxide. Aliphatic polyhydrazides are less soluble. They are either swollen or partly soluble in the hot solvent. Polyhydrazides are often soluble in hexamethylphosphoramide, and occasionally in hot tetramethylene cyclic sulfone.

The polymer solubility in a series of copolyhydrazides of 0-I/0-6 ranging in mole composition from 0.00/1.00 to 1.00/0.00, was found to vary markedly as the composition was varied. Solubilities and polymer melt temperatures of these copolymers are shown in Table III. The melting point-composition curve indicates that 0-I and 0-6 are isomorphous. The 0.5/0.5 copolymer, prepared by the reaction of isophthalyl chloride with adipyl dihydrazide, is soluble in both dimethyl sulfoxide and hexamethylphosphoramide. It is by virtue of its preparation an ordered copolymer. It should be noted, however, that a random copolymer which was prepared by the reaction of equivalent amounts of isophthalyl chloride and adipyl chloride with hydrazine was insoluble in DMSO.

TABLE III
0-I/0-6 Copolymers

Composition, mole-%	η_{inh} (DMSO)	PMT °C.	Solubility		Comment
			Dimethyl sulfoxide	Hexamethyl- phosphoramide	
0.00/1.00	—	290	Insoluble	Insoluble	No films
0.33/0.67	—	293	Insoluble	Insoluble	No films
0.50/0.50	0.45	322	Soluble	Soluble	Clear films
0.67/0.33	0.49	342	Soluble	Soluble	Tough films
1.00/0.00	1.00	380	Soluble	Soluble	Tough films

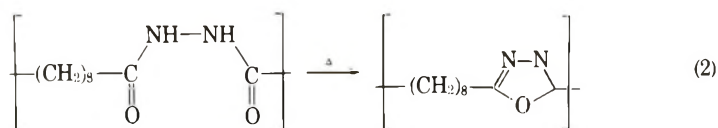
Of structural interest are the oxalic-aromatic polyhydrazides. They possess an unusually long and highly polar bishydrazide group



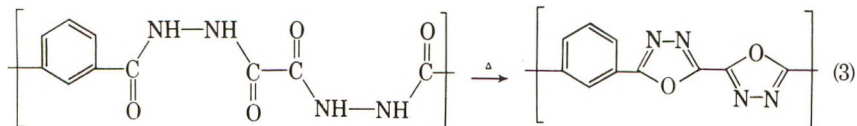
that provides the chain link within the aliphatic or aromatic polymer chain.

4. Post-Reactions and Polymer Structure

Dehydrations of a variety of monomeric polyhydrazides to give 2,5-disubstituted 1,3,4-oxadiazoles have been studied by Stolle.¹ We have applied this reaction quantitatively to prepare poly(1,3,4-oxadiazoles),¹⁴ but it seems appropriate to mention briefly the implications of this reaction which may occur as side reaction, when polyhydrazides are dried at elevated temperatures. Thus polyhydrazides may partially change into poly(1,3,4-oxadiazoles) which may be observed by slight changes in the microanalysis of dried polyhydrazides. For example, the polyhydrazide from sebacyl chloride and sebacic dihydrazide, 0-10, showed a noticeable tendency to lose water of reaction and change, at least partially into a polyoxadiazole structure [eq. (2)] upon drying above 150°C. (N₂).



Similar microanalytical evidence may be obtained for a change of oxalic acid containing polyhydrazides into the corresponding oxadiazoles. It was observed that the reaction proceeded at a faster rate. This may, at least in part, be due to the fact that a different type polyoxadiazole structure is formed during this cyclodehydration [eq. (3)] which contains adjacent



oxadiazole rings that separate the aliphatic or aromatic portion. This difference in reactivity and structure makes it advisable to distinguish aliphatic and aromatic polyhydrazides from those containing oxalic acid.

The authors wish to express their appreciation to Messrs. J. H. Curlett, W. F. Holley, and A. J. Prucino for their excellent technical assistance.

References

1. Stolle, R. (a) *Ber.*, **32**, 796 (1899); (b) *J. Prakt. Chem.* [2], **68**, 30 (1903).
2. Autenrieth, W., and P. Spiess, *Ber.*, **34**, 187 (1901).
3. Naegli, C., and G. Stefanovich, *Helv. Chim. Acta*, **11**, 609 (1928).
4. Suh, P. P. T., and C. L. Hsu, *Rec. Trav. Chim.*, **59**, 349 (1940).
5. Curtius, T., and A. Riedel, *J. Prakt. Chem.* [2], **76**, 238 (1907).
6. Curtius, T., and F. Bollenbeck, *J. Prakt. Chem.* [2], **76**, 281 (1907).
7. French Pat. 870,259 (3/6/42), to I. G. Farbenindustrie Aktiengesellschaft.
8. Moldenhauer, O., and H. Bock, U. S. Pat. 2,349,979 (5/30/44).
9. Pritchard, W. W., U. S. Pat. 2,395,642 (2/26/46), to Du Pont.
10. Fisher, J. W., U. S. Pat. 2,476,968 (7/26/49); U. S. Pat. 2,512,891 (6/27/50), to Celanese Corporation; *J. Appl. Chem.*, **4**, 212 (1954).
11. Korshak, V. V., G. N. Chelnokova, and M. A. Shkolina, *Izv. Akad. Nauk SSSR, Otdel. Khim. Nauk*, **1959**, 894, 925.
12. Campbell, T. W., V. S. Foldi, and J. Farago, *J. Appl. Polymer Sci.*, **5**, 155 (1959).
13. McFarlane, S. B., and A. L. Miller, U. S. Pat. 2,615,862 (10/28/52), to Celanese Corporation.
14. Frazer, A. H., and F. T. Wallenberger, *J. Polymer Sci.*, **A2**, 1147 (1964).
15. Beaman, R. G., and F. B. Cramer, *J. Polymer Sci.*, **21**, 223 (1956).
16. Sorenson, W. R., and T. W. Campbell, *Preparative Methods of Polymer Chemistry*, Interscience, New York, 1961, pp. 32-55.
17. Morgan, P. W., R. F. Tietz, and W. R. Sorenson, in preparation.
18. Borsche, W., W. Müller, and C. A. Bodenstein, *Ann.*, **475**, 120 (1929).

Résumé

On a préparé des polyhydrazides de haut poids moléculaire par une nouvelle technique de polymérisation à basse température à partir de quantités équimoléculaires d'un dihydrazide et d'un chlorure de dicarbone dans des solvants dialcyl-amide. Des polyhydrazides entièrement aliphatiques sont insolubles dans le diméthylsulfoxyde, ont un point de fusion qui varie de 200° à 300°. On peut presser des films et tirer des fibres au départ de la matière fondue. Les polyhydrazides aliphatiques-aromatiques et oxaliques, qui subissent une déshydratation à vitesses différentes, ont des points de fusion qui varient de 250° à 300°C, et des viscosités inhérentes variant de 0.3 à 1.5. Ils sont solubles dans le diméthyl sulfoxyde, solvant duquel on peut obtenir des films résistants.

Zusammenfassung

Hochmolekulare Polyhydrazide wurden nach einem neuen Tieftemperatur-Polymerisationsverfahren aus äquimolaren Mengen eines Dihydrazids und eines Dicarbonylchlorids in Dialkylamid-Lösungsmitteln hergestellt. Rein aliphatische Polyhydrazide waren in Dimethylsulfoxyd unlöslich und hatten Schmelztemperaturen im Bereich von 200 bis 300°. Aus der Schmelze konnten Filme gepresst und Fasern gezogen werden. Aliphatisch-aromatische und Oxalsäure-aromatische Polyhydrazide, die mit verschiedener Geschwindigkeit dehydratisieren, besaßen Polymerschmelztemperaturen im Bereich von 250 bis 300°C und Viskositätszahlen von 0,3 bis 1,5. Sie waren in Dimethylsulfoxyd löslich und aus der Lösung konnten zähe Filme gegossen werden.

Received January 31, 1963

Aromatic Polyhydrazides: A New Class of Highly Bonded, Stiff Polymers

A. H. FRAZER and F. T. WALLENBERGER, *Pioneering Research Division, Textile Fibers Department, E. I. du Pont de Nemours & Company, Inc., Experimental Station, Wilmington, Delaware*

Synopsis

High-molecular weight aromatic polyhydrazides have been prepared by using isophthalic, terephthalic, isocinchomeric, dipicolinic, 5-chloroisophthalic, 2,5-dichloroterephthalic, 5-*tert*-butylisophthalic, phenyl ether-4,4'-dicarboxylic, pyrazine-2,5-dicarboxylic, and thiophene-2,5-dicarboxylic acid as polymer intermediates. The polyhydrazides were prepared from equimolar amounts of diacid chloride and dihydrazide (or hydrazine) in hexamethylphosphoramide at room temperature. By contrast to aliphatic polyhydrazides, aromatic polyhydrazides were soluble in dimethyl sulfoxide and with few exceptions had polymer melt temperatures in the range of 350–400°C. Inherent viscosities ranged from 0.30 to 1.00 (in dimethyl sulfoxide). Tough films and strong fibers of these polymers could be fabricated.

INTRODUCTION

It has been long recognized that high polymer melt temperature is associated with two factors: strong intermolecular bonding, such as hydrogen bonding, and high chain stiffness such as derived from a plurality of carbocyclic or aromatic rings. The usual aliphatic polyamides, such as nylon 66, $[-NH-(CH_2)_6-NH-CO-(CH_2)_4-CO-]_n$ or aliphatic polyurethanes, such as $[-NH-(CH_2)_6-NH-CO-O-(CH_2)_4-O-CO-]_n$ have high intermolecular bonding but little chain stiffness, whereas aromatic polyesters and polycarbonates have little intermolecular bonding but high chain stiffness. However, the all-aromatic polyamides¹ possess a combination of strong intermolecular bonding and high chain stiffness. The resulting polymers have high melting points as well as other characteristics by which they differ markedly from aliphatic polyamides.

Since we have found a new synthetic route which affords high-molecular weight aliphatic polyhydrazides² it was of interest to synthesize all-aromatic polyhydrazides and to evaluate these polyhydrazides as a new class of polymers.

EXPERIMENTAL

Polymer melt temperature (PMT) and inherent viscosities (η_{inh}) were obtained by standard methods of polymer characterization as recommended by Beaman and Cramer³ and by Sorenson and Campbell.⁴

Intermediates such as diacids, diacid chlorides, dihydrazides,² and dialkyl esters were prepared by conventional methods. Physical constants of less common diacid chlorides and dihydrazides are listed in Table I.

The system of polymer codes used is given in another paper in this series,² which is concerned with aliphatic polyhydrazides.

TABLE I

Dicarboxylic acid	Diacid chloride		Dihydrazide	
	M.P., °C.	Ref.	M.P., °C.	Ref.
Isocinchomeric (2,5-Pyridine-)	58-59	5	268-269	10
Dinicotinic (3,5-Pyridine-)	110-111	6		
Dipicolinic (2,6-Pyridine-)	60-61	7	280-282	11
2,5-Pyrazine-	142-144	8	270-272	8
2,5-Thiophene-	45-46	9		
2,6-Naphthalene-	181-183	---		
5- <i>tert</i> -Butylisophthalic	44-46	---		
5-Chloroisophthalic	b.p. 140/5 mm.	---		

1. Preparation of Polyhydrazides in Inert Solvents

This high temperature solution (HTS) polymerization is an adaptation of the procedure given by McFarlane and Miller.¹² Dicarboxylic acids (dialkyl esters or diacid chlorides) were allowed to react in amounts or multiples of 0.025 mole with dicarboxylic acid dihydrazides in amounts or multiples of 0.025 mole. The reaction was carried out in 30 g. of nitrobenzene (Table II)

TABLE II
Preparative Attempts in Nitrobenzene

Polyhydrazide	Isophthalic dihydrazide plus	η_{inh} (DMSO)	PMT, °C.
Isophthalic	Isophthalic acid	0.08	250
Isophthalic	Isophthaloyl chloride	0.15	280
Isophthalic	Dimethyl isophthalate	0.14	260
Isophthalic-terephthalic	Terephthalic acid	0.06	290
Isophthalic-terephthalic	Dimethyl terephthalate	0.21	255

(or multiples thereof) at a temperature of 180°C. for a period of 3-4 hr. The reactions were heterogeneous, since at least the products, if not also the reactants, were insoluble in nitrobenzene and other inert solvents. The reaction mixture was poured into ethanol and the polymer was filtered. It was washed free of nitrobenzene with additional amounts of ethanol and dried.

2. Preparation of Polyhydrazides in Amide Solvents

The low temperature solution (LTS) polymerization is described in an earlier report by Frazer and Wallenberger² on aliphatic polyhydrazides.

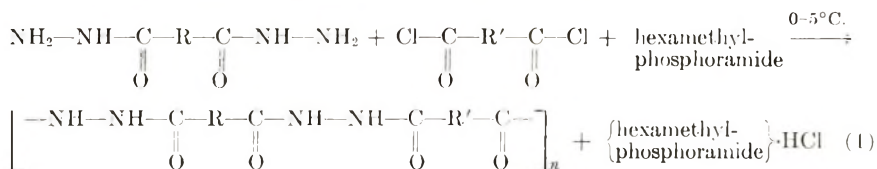
It was used in the successful preparation of aromatic polyhydrazides, as described herein, without modification.

RESULTS AND DISCUSSION

A series of experiments using the high temperature solution technique (HTS) of McFarlane and Miller¹² afforded only low molecular weight polymers as evidenced by the low polymer melt temperatures and low inherent viscosities (Table II). Aromatic polyhydrazides obtained in this manner were soluble in hot dimethyl sulfoxide but insoluble in a variety of polymer solvents. Since various changes in reaction conditions did not improve the resulting polymers, it was decided to use, exclusively, in this study the low temperature solution (LTS) polymerization which had previously² been found to afford high molecular weight aliphatic polyhydrazides.

1. Low Temperature Solution Polymerization

In accordance with this procedure, one or more diacid chlorides are combined to react with hydrazine or with one or more dihydrazides in a liquid basic medium which functions both as polymer solvent and also as an acid acceptor for the general reaction given in eq. (1).



Suitable solvents used successfully were hexamethylphosphoramide and *N*-methylpyrrolidone containing 5% lithium chloride. Although, in general, optimum molecular weight and yield of polyhydrazides were obtained when the intermediates and solvents were of the highest purity and moisture rigorously excluded, surprisingly film-forming molecular weight polymer was obtained with hydrazide hydrate and hexamethylphosphoramide as solvent. There is no apparent explanation for the anomalous behavior.

The reaction temperature was maintained at 0–15°C. In order to obtain

TABLE III
Effect of Reaction Time in Preparation of Poly(isophthalic Hydrazide)

From hydrazine		From hydrazide	
Time, hr.	η_{inh}	Time, hr.	η_{inh}
0.5	0.48	1	0.38
1	0.50	4	0.50
2	0.55	6	0.60
3	0.54	16	0.80

TABLE IV

Alternating polyhydrazide prepared from		η_{inh} (DMSO)	PMT, °C.	Comment
Dihydrazide	Dicarbonyl chloride			
1	Isophthalic	1.00	350	Tough films and strong fibers with excellent properties ¹³ Film, cast from DMSO Prepared by W. Sweeny for a detailed study ¹³ on poly(1,3,4-oxadiazoles) Transparent, yellow film Brittle film, from DMSO Soluble, but degraded in H ₂ SO ₄
2	Isophthalic	1.03	390	
3	Isophthalic	0.90	375	
4	Isophthalic	0.90	350	
5	Isophthalic	0.60	390	
6	Isophthalic	0.45	320	
7	Isophthalic	0.80	305	
8	Isophthalic	0.30	205	
9	Isophthalic	0.70	380	
10	Isophthalic	0.46	345	
11	Terephthalic	Insol.	>400	
12	Isocinchomeric	0.81	370	
13	Isocinchomeric	0.77	360	
14	Isocinchomeric	0.62	350	
15	Isocinchomeric	0.14	350	
16	Dipicolinic	0.72	360	
17	Pyrazine-2,5-	0.72	350	

maximum molecular weight, the reaction was allowed to proceed overnight. The effect of reaction time on molecular weight in hexamethylphosphoramide solutions is summarized in Table III.

2. Evaluation of Polymer Properties

All-aromatic (benzenoid or heterocyclic) polyhydrazides (Table IV) have been prepared with high inherent viscosities well above 0.3. They are soluble in cold dimethyl sulfoxide, and have very high polymer melt temperatures ranging from 350 to 400°C. These polyhydrazides give tough films when cast and yield excellent fibers when spun from dimethyl sulfoxide, dimethylacetamide, or *N*-methylpyrrolidone.

Pyrazine-containing polymers, particularly the alternating copolyhydrazide of pyrazine-2,5-dicarboxylic acid and isophthalic acid, have a yellow color. A film cast from dimethyl sulfoxide was yellow, clear-transparent, and tough.

The solubilities of aromatic polyhydrazides have been thoroughly investigated using a total of sixteen typical polymer solvents.

The two specific polyhydrazide solvents were tetramethylene cyclic sulfone and dimethyl sulfoxide. Dimethyl sulfoxide, at room temperature, dissolved all aromatic polyhydrazides except poly(terephthalic hydrazide). Tetramethylene cyclic sulfone near its boiling point generally dissolves aromatic polyhydrazides.

Strong acids such as sulfuric, formic, trifluoroacetic and dichloroacetic acid dissolved, but simultaneously degraded, all polyhydrazides. For example, alternating poly(isophthalic-terephthalic hydrazide) with an inherent viscosity of 1.03 in dimethyl sulfoxide when dissolved in concentrated sulfuric acid had inherent viscosities (H_2SO_4) ranging from 0.05 to 0.20. Polymer precipitated with water from such sulfuric acid solutions had inherent viscosities of 0.05 to 0.15 in dimethyl sulfoxide.

Chloroform, *m*-cresol, nitrobenzene, and trifluoropropanol were found to be typical nonsolvents. Other solvents such as trichloroethane, trichloroethane-formic acid (60:40), dimethylformamide-trichlorophenol (60:40), and *N*-methylpyrrolidone did affect partial solution or at least swelling of the polymer near boiling temperatures, or under conditions peculiar to the individual polymer.

3. Solubility and Polymer Structure

Of particular interest was the behavior of *N,N*-dimethylacetamide. The alternating copolyhydrazide from isophthalic dihydrazide and terephthaloyl chloride is soluble in *N,N*-dimethylacetamide at room temperature. However, if the solution is heated to temperatures of 120–130°C., the polymer precipitates from solution. A comparison of x-ray diffraction patterns (Fig. 1) of the polyhydrazide before solution and after precipitation clearly shows that the original, almost completely amorphous, poly-

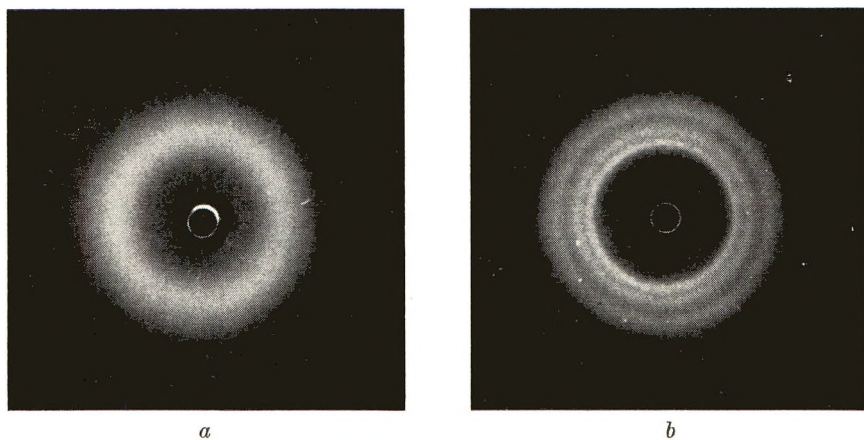
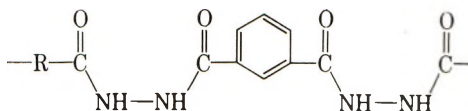


Fig. 1. X-Ray diffraction patterns of O-I-O-T, the polyhydrazide from isophthalic dihydrazide and terephthaloyl chloride, from dimethylacetamide solutions: (a) before thermal treatment; (b) after thermal treatment.

hydrazide (a) has been crystallized by the thermal treatment of the *N,N*-dimethylacetamide solution (b).

The alternating copolyhydrazide from equimolar amounts of isophthalic dihydrazide and terephthaloyl chloride is easily soluble in dimethyl sulfoxide, as are all alternating copolyhydrazides from isophthalic and any other diacid used thus far. This solubility behavior suggests that the solubility arises from the polymer structure,



where R is a residue from any diacid. In this structure the acid radicals are ordered with respect to each other.

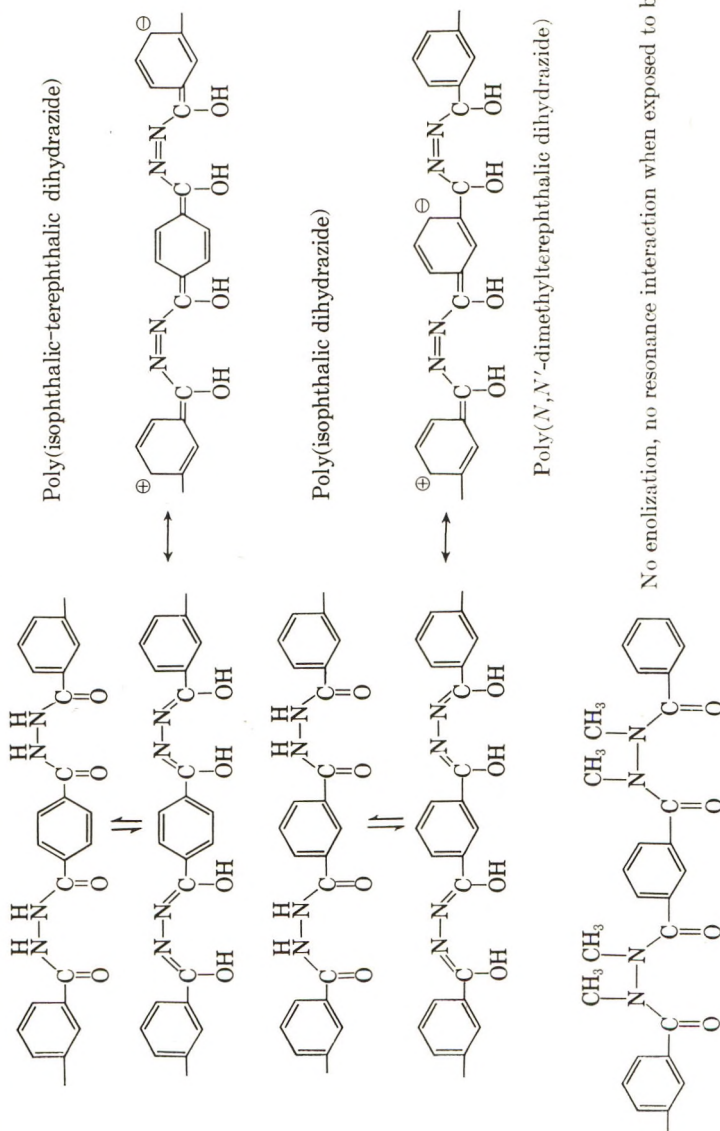
This study has shown that even an ordered copolyhydrazide containing $\frac{2}{3}$ poly(terephthalic dihydrazide) and $\frac{1}{3}$ poly(isophthalic dihydrazide) is still soluble in dimethyl sulfoxide, while a content of $\frac{3}{4}$ or more poly(terephthalic dihydrazide) renders the polymer insoluble.

It should be noted, however, that the random copolyhydrazide of equimolar portions of terephthalic and isophthalic acid which can be prepared by the reaction of terephthaloyl and isophthaloyl chlorides with hydrazine, is insoluble in dimethyl sulfoxide.

4. Conjugation and Resonance Stabilization

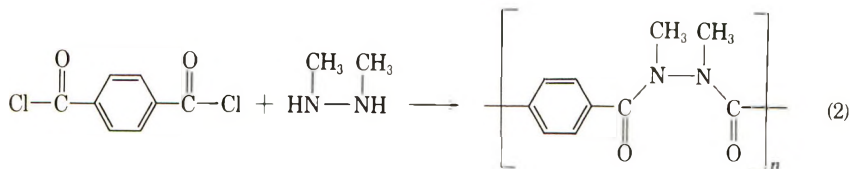
The hydrazide groups, adjoined by aromatic rings on either side, are capable of partaking in extended conjugation. Such resonance stabilized systems would involve aromatic portions and hydrazide portions (in enol form). Indeed, all polyhydrazides, most pronounced however, aromatic,

TABLE V
Types of Resonance Interactions



heterocyclic, and aromatic-heterocyclic polyhydrazides turn yellow when placed in basic solutions of pH 10–12 (Table V). (Polyhydrazides containing pyrazine as an intralinear ring become orange on exposure to base.) In general, these polyhydrazides revert to the original white (or yellow) color by changing back to neutral or acidic conditions.

This conjugation is apparently a unique feature of unsubstituted polyhydrazides and was not encountered with poly-(*N,N'*-dimethylterephthalic) hydrazide, which was especially prepared to test this hypothesis.



This *N,N*-disubstituted polyhydrazide, PMT 340°C., prepared from *N,N'*-dimethylhydrazine and terephthaloyl chloride showed no color change when exposed to base. Hence, no enolization and resonance interaction occurs.

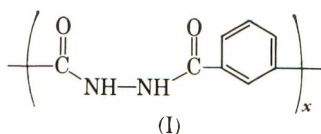
5. Fiber Properties of Aromatic Polyhydrazides

The high chain stiffness and strong intermolecular hydrogen bonding of these aromatic polyhydrazides are manifested in the properties of the fibers obtained from these polymers. In Table VI are summarized the

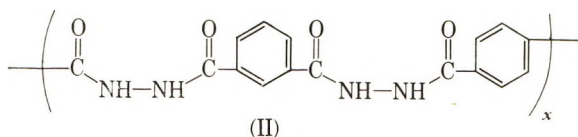
TABLE VI
Fiber Properties of Aromatic Polyhydrazides

Properties	I	II
Tenacity, g./den.	5.2	6.0
Elongation, %	14	8
Initial modulus, g./den.	115	151
Knot tenacity, g./den.	2.1	1.0
Knot elongation, %	7	4.2
Knot initial modulus, g./den.	50	90
Fiber stick temperature, °C.	320	335
Moisture regain	4.5	4.3
Density, g./cc.	1.443	1.452

properties of the fibers obtained from two aromatic polyhydrazides, polyisophthalic hydrazide (I),



and the alternating copolyhydrazide from terephthalic and isophthalic acids (II).



The high chain stiffness and strong intermolecular hydrogen bonding of these polymers are reflected in the high fiber stick temperatures and high initial moduli of these fibers. Similarly, the somewhat poor transverse properties (knot tenacity, etc.) reflect the reduced flexibility of the polymer chains. The low moisture regain of these fibers which are derived from polymer structures containing multiple hydrazide linkages could be explained on the basis of the good packing efficiency of these stiff linear polymer chains with increased steric hindrance of hydrogen bonding sites.

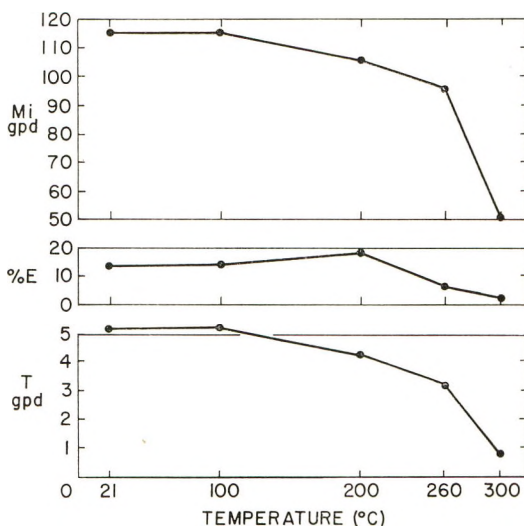


Fig. 2. Fiber properties (initial modulus M_i , elongation E , tenacity T) of I at elevated testing temperatures.

The high chain stiffness of these polymers is also reflected in the retention of fiber properties of elevated temperatures. In Figure 2 are plotted the fiber properties at various testing temperatures. It is apparent from an inspection of these data that the fiber properties are essentially unchanged up to temperatures of 200°C., and show only a small decrease in overall properties, up to temperatures of 260°C. Not unexpectedly at 300°C., which is only 20°C. below the fiber stick temperature of this fiber, the overall fiber properties are quite poor.

This work was carried out, in part, under Contract No. AF33(616)-8253, Project No. 7340 by the Directorate of Materials and Processes, ASD, Air Force Systems Command, Wright-Patterson Air Force Base, Ohio.

The authors wish to express their appreciation to Messrs. W. F. Holley and A. J. Prucino for their excellent technical assistance.

References

1. Flory, P. J., U. S. Pat. 2,244,192 (1938).
2. Frazer, A. H., and F. T. Wallenberger, *J. Polymer Sci.*, **A2**, 1137 (1964).
3. Beaman, R. G., and F. B. Cramer, *J. Polymer Sci.*, **21**, 223 (1956).
4. Sorenson, W. R., and T. W. Campbell, *Preparative Methods of Polymer Chemistry*, Interscience, New York, 1961, pp. 33-55.
5. Meyer, K., *Rec. Trav. Chim.*, **44**, 327 (1925).
6. Meyer, K., and D. Tropsch, *Monatsh.*, **35**, 207 (1914).
7. Meyer, K., and D. Tropsch, *Monatsh.*, **34**, 517 (1913).
8. Spoerri, P. E., and A. Erickson, *J. Am. Chem. Soc.*, **60**, 400 (1938).
9. Griffing, J. M., and L. F. Salisbury, *J. Am. Chem. Soc.*, **70**, 3416 (1948).
10. Meyer, K., and F. Staffen, *Monatsh.*, **34**, 517 (1913).
11. Meyer, K., *Monatsh.*, **24**, 205 (1903).
12. McFarlane, S. B., and A. L. Miller, U. S. Pat. 2,615,862 (10/28/52), to Celanese Corporation.
13. Frazer, A. H., W. Sweeny, and F. T. Wallenberger, *J. Polymer Sci.*, **A2**, 1157 (1964).

Résumé

On a préparé des polyhydrazides aromatiques de poids moléculaires élevés en employant comme intermédiaires polymériques les acides suivants: isophtalique, téréphtalique, isocinchoméronique, dipicolinique, 5-chloroisophtalique, 2,5-dichlorotéréphtalique, 5-tert-butylisophtalique, phényl'éther-4-4'-dicarboxylique, pyrazine-2,5-dicarboxylique, et thiophène-2,5-dicarboxylique. Les polyhydrazides sont obtenus en faisant réagir des parties équimoléculaires de chlorure de diacide et de dihydrazide (ou hydrazine) dans l'hexaméthylphosphoramidate et à température normale. Par opposition aux polyhydrazides aliphatiques, les polyhydrazides aromatiques étaient solubles dans le diméthylsulfoxyde et sauf quelques exceptions, ils fondaient tous à des températures entre 350 et 400°C. Les viscosités intrinsèques variaient entre 0,30 et 1 (dans le diméthylsulfoxyde). On pouvait transformer ces polymères en films durs et en fibres fortes.

Zusammenfassung

Hochmolekulare aromatische Polyhydrazide wurden ausgehend von Isophthal-, Terephthal-, Isocinchomeron-, Dipicolin-, 5-Chlorphthal-, 2,5-Dichlorterephthal-, 5-tert-Butylisophthal-, Phenyläther-4,4'-dicarbon-, Pyrazin-2,5-dicarbon- und Thiophen-2,5-dicarbonsäure dargestellt. Die Polyhydrazide wurden aus äquimolaren Mengen von Dicarbonsäurechloriden und Dihydrazid (oder Hydrazin) in Hexamethylphosphoramidat bei Raumtemperatur dargestellt. Im Gegensatz zu aliphatischen Polyhydraziden waren aromatische Polyhydrazide in Dimethylsulfoxyd löslich und besaßen mit wenigen Ausnahmen Polymerschmelztemperaturen von 350-400°C. Die Viskositätszahlen in Dimethylsulfoxyd lagen zwischen 0,30 und 1,00. Aus diesen Polymeren konnten zähe Filme und feste Fasern erzeugt werden.

Received January 31, 1963

Poly(1,3,4-Oxadiazoles): A New Class of Polymers by Cyclodehydration of Polyhydrazides

A. H. FRAZER, W. SWEENEY, and F. T. WALLENBERGER, *Pioneering Research Division, Textile Fibers Department, E. I. du Pont de Nemours & Company, Inc., Experimental Station, Wilmington, Delaware*

Synopsis

Thirteen aliphatic and aromatic polyhydrazides have been converted as bulk polymer by a unique polymer post reaction into high molecular weight poly(1,3,4-oxadiazoles). This reaction proceeds by thermal cyclodehydration at 170–280°C. with elimination of water. The resulting poly(1,3,4-oxadiazoles) have been characterized by microanalysis, inherent viscosity, x-ray diffraction patterns, and by infrared and ultraviolet absorption spectra. Films could be pressed from the melt of polyoxadiazoles melting below 350°C., while very high melting or infusible aromatic polyoxadiazoles could not be manufactured into films and fibers by conventional means. Such polymers are extremely thermally and oxidatively stable and decompose between 450 and 500°C.

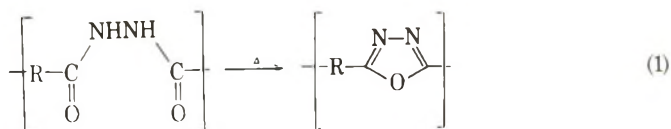
INTRODUCTION

Nearly all organic polymers of present commercial interest which can be manufactured into films, fibers, and molded objects are stable below a rather moderate temperature ceiling. Very high polymer melt temperatures are ordinarily not desirable and very high thermal stabilities are ordinarily not required.

Recent advances in technology, however, require thermally stable polymers and rapid development in the field of organic polymers has afforded two basic types of polymer structures with potentially high thermal resistance. Koton¹ has recently summarized our knowledge about such polymers containing fused cyclic ring systems (ladder polymers) and polymers containing only aromatic rings in the chain (polyphenylenes and analogs) but progress has already rendered his review incomplete.

In the recent work on new polymers consisting of only aromatic rings are the preparation of poly(*p*-phenylene) with molecular weights up to 10,000 by aromatization of poly(cyclohexadiene)² and a novel attempt to prepare this polymer by using the Wittig reaction.³ High molecular weight polybenzimidazoles which possess excellent thermal stabilities were prepared⁴⁻⁶ and were cast to yield tough films.⁶ Infusible and insoluble poly(1,3,4-oxadiazoles) have been obtained by the reaction of tetrazoles and acid chlorides.⁸ These polymers were thermally resistant but of limited molecular weight.

Poly(1,3,4-oxadiazoles) were also the subject of an extensive and independent investigation in our laboratory. We employed a different and novel synthetic route, the cyclodehydration of hydrazide links in polyhydrazides [eq. (1)]. This reaction is based on the preparation of 2,5-diaryl-1,3,4-oxadiazoles from diaryl hydrazine, which has been reported by Stolle.⁹



We wish therefore to report the preparation of well-defined, high molecular weight film-forming and fiber-forming¹⁰ poly(1,3,4-oxadiazoles) from high molecular weight aliphatic¹¹ and aromatic¹² polyhydrazides.

EXPERIMENTAL

Polymer melt temperatures (PMT) and inherent viscosities (η_{inh}) were obtained by standard methods of polymer characterization as recommended by Beaman and Cramer¹³ and by Sorenson and Campbell.¹⁴

The preparation of polyhydrazides suitable for the preparation of poly(1,3,4-oxadiazoles) has been described already. Generally equimolar amounts of diacid chloride and dihydrazide are combined in a suitable solvent and are allowed to react for 2–24 hr. The resulting polyhydrazide was precipitated from the polymer solution in an Osterizer with dry methanol and was washed several times with methanol and distilled water.

Conversion of Polyhydrazides

Suitable polyhydrazides (1-g. samples) were converted in muffle furnaces or in vacuum ovens at temperatures ranging from 170 to 280°C. The total weight loss of a sample when heated to constant weight includes loss of surface water and loss of water of reaction. In order to assess the water of reaction alone, samples were rigorously dried at 80–120°C. in a vacuum oven prior to quantitatively controlled conversion. Such dry samples could then be converted at 170–280°C. and the resulting weight loss could be compared with the theoretically calculated loss of water of reaction.

The significance of the interference of surface moisture may be seen in Figure 1, curve 1, which represents a programmed thermogravimetric analysis, TGA, using the polyhydrazide from isophthalic dihydrazide and terephthaloyl chloride (O—I—O—T). The initial weight loss is entirely due to loss of surface water (25–240°C.). It corresponds to about 10–12% of the initial weight. This is in agreement with the amount of surface moisture determined by independent means. The weight loss at higher temperatures, notably between 280 and 350°C., is due to conversion of polyhydrazide into poly(1,3,4-oxadiazole) with simultaneous loss of water of reaction which is theoretically 11.11%.

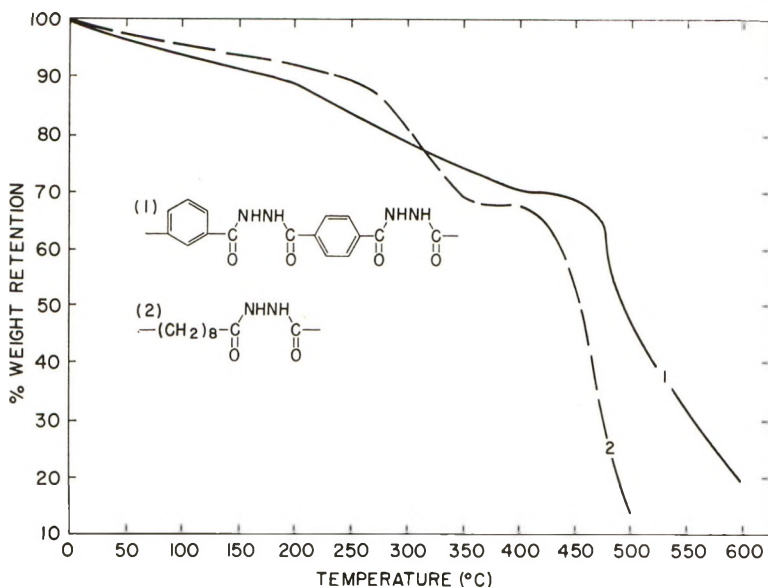


Fig. 1. Programed thermogravimetric analysis of polyhydrazides.

An even better distinction between surface water and water of reaction is obtained from the curve 2 in Figure 1 representing the weight loss of poly(octamethylene dihydrazide), 0–10. Between 25 and 225°C. there is a gradual smaller loss of surface water than in curve 1, while the water of reaction evolves between 250 and 350°C. Constant weight indicates the formation of poly(octamethylene-1,3,4-oxadiazole).

Reaction of *m*-Phenyleneditetrazole and Terephthaloyl Chloride

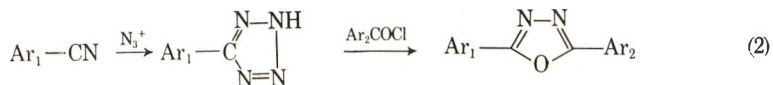
m-Phenyleneditetrazole was prepared by standard methods¹¹ from *m*-dicyanobenzene. It was recrystallized from ethanol, m.p. 266–267°C.

ANAL. Calcd. for C₈H₆N₆: C, 44.85%; H, 2.82% N, 52.32%. Found: C, 45.20% H, 2.92%; N, 52.00%.

Polymerization of equimolar amounts of ditetrazole and diacid chloride in hexamethylphosphoramide gave low molecular weight polymers ($\eta_{inh} = 0.04$ –0.1). Analysis indicated presence of poly(acyltetrazoles) and poly-oxadiazoles.

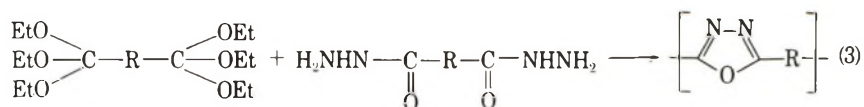
RESULTS AND DISCUSSION

Huisgen⁷ has reported extensively on the reaction of tetrazoles with acid chlorides, which gives 1,3,4-oxadiazoles in nearly quantitative yields [Eq. (2)]:



Using *p*-tetrazolylbenzoyl chloride (as AB monomer) he was the first to attempt the preparation of poly(1,3,4-oxadiazoles) by the tetrazole route. The attempt resulted in a product that was ascribed as containing a 9-ring structure. Abshire and Marvel⁸ attempted the preparation of poly(1,3,4-oxadiazoles) from *m*- and *p*-phenyleneditetrazole and terephthaloyl, isophthaloyl, oxalyl, azelayl, 4,4'-biphenyldicarbonyl, 2,2'-biphenyldicarbonyl, 3,5-pyridinedicarbonyl, and 2,6-pyridinedicarbonyl chlorides at elevated temperatures in pyridine. The resulting polymers had excellent thermal stabilities but inherent viscosities were less than 0.2 in sulfuric acid. We have obtained similar results with this variation of the original Huisgen reaction when the polymerization was attempted at low temperature in hexamethylphosphoramide.

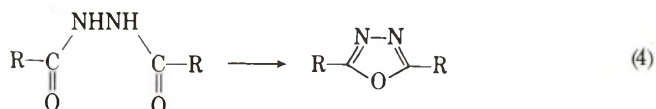
We have also briefly studied the reaction of bisorthoesters and dihydrazides in accordance to a model reaction reported by Ainsworth¹⁵ [eq. (3)]:



The preparation of bisorthoesters can be carried out by treating diiminoesters with absolute alkanols.¹⁶ The diethyl orthosuccinate was prepared with great difficulty in reasonably pure form from diethyl iminosuccinate^{17,18} and allowed to react with isophthalic dihydrazide. No high polymer resulted.

1. Thermal Cyclodehydration of Polyhydrazides

Stolle⁹ has extensively studied the reaction of hydrazides to give 2,5-disubstituted 1,3,4-oxadiazoles. The reaction proceeds at elevated temperature (thermal conversion) or in solution using chlorosulfonic acid, sulfonyl chloride, toluenesulfonic acid, tosyl chloride, organic anhydrides, or sulfuric acid as dehydrating agent.



Thermal conversion of polyhydrazides in solution and in the form of bulk polymer was given greatest attention in the present study because Pellizzare¹⁹ had found that dibenzoyl hydrazine, $\text{C}_6\text{H}_5\text{CONHNHCOC}_6\text{H}_5$, gave nearly quantitative conversion to the corresponding 2,5-diphenyl-1,3,4-oxadiazole when heated as solid below its melting point.

Thus, the prototype conversion experiment was carried out with bulk polymer, which was finely ground (40 mesh) and was heated in vacuum or in a muffle furnace (N_2) at temperatures ranging from 170 to 280°C. for 3–48 hr. For example, poly(isophthalic-terephthalic dihydrazide), O—I—O—T, the hydrazide derived from isophthalic dihydrazide and terephthal-

TABLE IA. Thermal Cyclodehydration: Polyhydrazides and Conversion Conditions

Polyhydrazide ^a	Analysis		PMT, °C.	η_{inh} (DMSO)	Temp., °C.	Time, hr.	Conversion wt. loss, %	Theor. wt. loss, %
	Calculated, %	Found, %						
I	C, 55.19	C, 54.74	318	insoluble	240	3	10.0	11.04
	H, 8.03	H, 8.06						
II	O, 19.61	O, 20.10	280	insoluble	200	2	8.5	9.08
	C, 60.58	C, 60.57						
III	H, 9.16	H, 9.06	350	1.0	240	3	13.0	14.45
	O, 16.14	O, 16.30						
IV	C, 43.37	C, 42.18	260	0.5	220	3	11.0	10.71
	H, 2.83	H, 3.64						
V	O, 25.68	O, 25.40	320	0.6	305	24	—	10.97
	C, 58.13	C, 59.36						
VI	H, 7.19	H, 6.97	325	1.5	277	12	11.0	11.11
	O, 19.03	O, 17.80						
VII	O, 19.50	O, 20.02	325	1.5	280	24	12.0	11.11
	O, 19.74	O, 19.50						
VIII	C, 59.25	C, 59.30	>375	0.6	260	24	12.5 ^b	9.16
	H, 3.73	H, 3.90						
IX	O, 19.74	O, 20.00	>400	0.3	200	2	9.0	6.29
	C, 48.87	C, 48.60						
X	H, 2.56	H, 3.02	205	0.7	240	3	10.0	10.29
	O, 18.04	O, 17.70						
XI	C, 67.12	C, 68.03	380	0.8	185	3	—	8.65
	H, 6.34	H, 6.58						
XII	O, 16.76	O, 16.70	290	0.60	255	4	—	10.80
	O, 18.27	O, 19.00						
XIII	O, 19.21	O, 19.20	342	1.43	265	20	—	14.58
	O, 21.05	O, 21.20						
	O, 25.81	O, 25.72						

^a See Table II for structures.^b Weight loss may still include some surface water.

TABLE IB
Thermal Cyclodehydration: Poly(1,3,4-oxadiazoles)

Poly(1,3,4-oxadiazole) ^a	Analysis		PMT, °C.	η_{inh} (H ₂ SO ₄)	Comments
	Calculated, %	Found, %			
I'	C, 62.05	C, 60.94	350	0.3	Polyoxadiazole became dark on conversion
	H, 7.64	H, 7.89			
	O, 11.02	O, 11.19			
II'	C, 66.63	C, 66.00	300	0.25	Conversion rate also followed by TGA
	H, 8.95	H, 9.00			
III'	C, 50.71	C, 49.86	350	0.1	—
	H, 1.42	H, 2.10			
IV'	O, 10.66	O, 11.00	350	0.4	—
V'	O, 10.94	O, 12.00	320	0.2	Films pressed and fibers pulled from melt; sol. in trifluoroacetic acid (TFA)
	O, 11.10	O, 11.60			
VI'	O, 11.10	O, 11.60	>400	0.6	Poly(1,3,4-oxadiazole) fiber from VI fiber
VII'	O, 11.10	O, 11.20	>400	0.5	Poly(1,3,4-oxadiazole) fiber from VII fiber
	C, 53.81	C, 53.08			
VIII'	H, 1.69	H, 2.11	>400	0.2	—
	O, 8.96	O, 9.14			
IX'	N, 10.45	N, 10.05	170	0.5	Films cast from TFA, and films melt pressed
	O, 11.93	O, 12.20			
X'	O, 10.20	O, 10.52	>400	0.6	—
XI'	O, 12.61	O, 13.00	305	1.45	Soluble in TFA and films melt pressed
XII'	O, 11.95	O, 12.10	>400	0.50	Soluble in TFA, and films cast from solution
	O, 15.09	O, 15.40			
XIII'	O, 15.09	O, 15.40	>400	0.60	Soluble in TFA, films cast from solution

^a See Table II for structures.

oyl chloride, was heated at 283°C. at 0.4 mm. for 48 hr. The resulting poly(1,3,4-oxadiazole) consisted of alternating oxadiazole, *m*-phenylene, and *p*-phenylene rings, analyzed correctly for such a structure as evidenced by carbon, hydrogen and oxygen analysis. Further work showed that most of the reaction occurs within the first 3–4 hr.

A large number of aliphatic and aromatic polyhydrazides were treated at temperatures given in Table I after appropriate drying. The weight loss was determined gravimetrically and initial and final structures were analyzed.

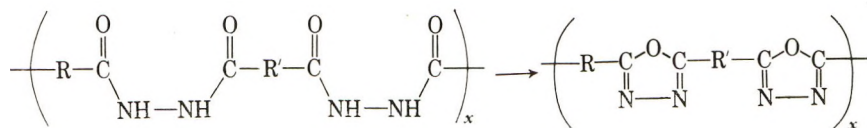
The weight losses correspond closely to the theoretically expected loss of water of reaction, except in the case of the reaction using the polyhydrazide derived from isophthalic and 2,5-dichloroterephthalic acid (0—I—0—2,5DCIT). In this case, even rigorous drying did not remove all the surface water, or the moisture regain was so rapid that the polymer picked up surface water on transfer from drying oven to muffle furnace.

2. Properties and Structure of High Molecular Weight Poly(1,3,4-oxadiazoles)

One of the most interesting facts of this study is the high molecular weight of the resulting polyoxadiazoles. The inherent viscosity ranges from 0.1 to 0.6 (H₂SO₄) with occasional values up to 0.9.

Such high molecular weights can be obtained only from high molecular polyhydrazides which in turn have been prepared by our low temperature solution polymerization.^{11,12} Only low molecular weight polyoxadiazoles

TABLE II
Polyhydrazide and Poly(1,3,4-oxadiazole) Structural Formulas



	R	R'
I → I'	1,4-Tetramethylene	1,7-Heptamethylene
II → II'	1,8-Octamethylene	1,8-Octamethylene
III → III'	2,6-Pyrazine	—
IV → IV'	1,3-Phenylene	1,8-Octamethylene
V → V'	1,3-Phenylene	1,4-Cyclohexyl
VI → VI'	1,3-Phenylene	1,3-Phenylene
VII → VII'	1,3-Phenylene	1,4-Phenylene
VIII → VIII'	1,3-Phenylene	2,5-Dichloro-1,4-phenylene
IX → IX'	1,3-Phenylene	1,3-C ₆ H ₄ -O-(CH ₂) ₁₀ -O-1,3-C ₆ H ₄ -
X → X'	1,3-Phenylene	2,6-Pyridine
XI → XI'	1,3-Phenylene	4,4'-Phenyl ether
XII → XII'	1,3-Phenylene	1,4-Tetramethylene
XIII → XIII'	1,3-Phenylene	—

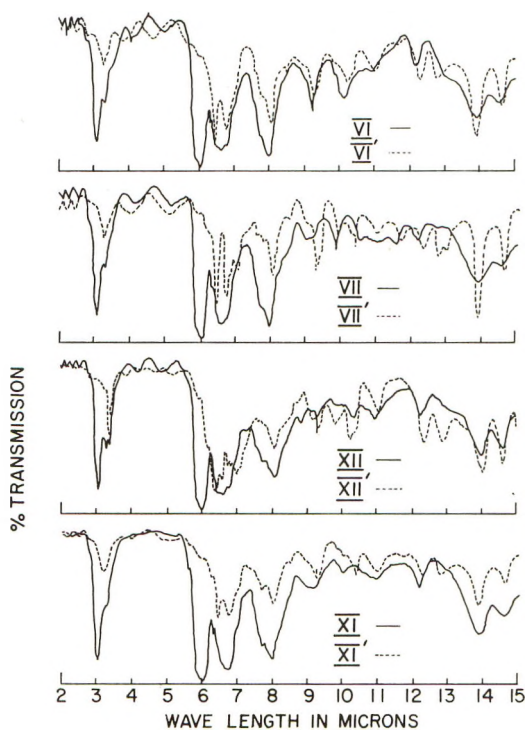


Fig. 2. Infrared spectra of (—) polyhydrazides and (- -) poly(1,3,4-oxadiazoles) as thin films, less than 1 mil.

resulted when polyhydrazides from other preparative routes²⁰ are used in the cyclodehydration. The inherent viscosities then range from 0.05 to 0.08.


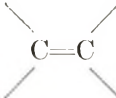

As shown in Table IB, last column, films could be pressed or fibers could be pulled from the melt from poly(1,3,4-oxadiazoles) which had melting points below 350°C. It appears that poly(1,3,4-oxadiazoles) containing aliphatic groups fall into this category. Aromatic poly(1,3,4-oxadiazoles), on the other hand, are very high melting (>400°C.) or infusible polymers and cannot be fabricated into films and fibers by conventional means. Indeed, aromatic poly(1,3,4-oxadiazole) fibers can be obtained only under controlled conditions when the cyclodehydration is carried out with polyhydrazide fiber.¹⁰

Although thirteen different poly(1,3,4-oxadiazole) structures (Table II) were prepared, only four structural types (VI', VII', XII', and XIII') were extensively studied.

These poly(1,3,4-oxadiazoles) represent a unique class of polymers containing intralinear carbocyclic and heterocyclic rings. In fact, in the case of the polyoxadiazoles VI', VII', and XIII', the polymer chains are made up exclusively of carbocyclic and heterocyclic rings. In VI' and VII', the polymer chain consists of alternating benzene and 1,3,4-oxadiazole

rings, and in XIII', the polymer chain consists of alternating benzene and bis(1,3,4-oxadiazole) rings.

The infrared spectra of these poly(1,3,4-oxadiazoles) (Fig. 2) were in agreement with the proposed structures (for comparison purposes the infrared spectra of the precursor polyhydrazides are also reproduced). In passing it is also of interest to point out that, in addition to the expected absorptions, common to all of these poly(1,3,4-oxadiazole) spectra were absorptions at 3.5 μ (aromatic —CH stretching; in the case of XII' also

aliphatic —CH stretching at 3.45 μ) in the 6.4–7.0 μ region ( C=N— and  C=C stretching) and in the 9.75–10.0 μ and 10.25–10.5 μ region ( =C—O—C= stretching).

Similarly, the ultraviolet absorption and fluorescent spectra of these poly(1,3,4-oxadiazoles) supported the proposed structures (Table III). A comparison of the spectral data (Table III) for VII', XII', and XIII'

TABLE III
Absorption and Fluorescence Spectral Data^a

Compounds or polymers ^b	Absorption λ_{\max} , m μ	Fluorescence Fl λ_{\max} , m μ
VI'	295, 224	380
XII'	248	380
XIII'	293, 231	420
VII'	306, 226	420
5,5'-Diphenyl-2,2'-bis(1,3,4-oxadiazole) ^c	298	370
2,2'-Phenylene-bis(5-phenyl-1,3,4-oxadiazole) ^c	315	390
2,5-Diphenyl-1,3,4-oxadiazole ^c	282	350

^a Solvent for both absorption and fluorescence spectra of poly(1,3,4-oxadiazoles) with H₂SO₄.

^b For polymer structures, see Table II.

^c Data of OH et al.²¹

with that of model compounds of similar structure gave agreement with the previous correlations of spectra with these structures.^{21,22} In the case of VI' the spectral data for the model compound, 2,2'-*m*-phenylene bis(5-phenyloxadiazole), were not available. However, a comparison of analogous model compounds, 2,2'-*m*-phenylene bis(5-phenyloxazole) and 2,2'-*p*-phenylene-bis(5-phenyloxazole), showed a shift of 40–50 m μ to a shorter wavelength for both absorption and fluorescent spectra in going from *para* to *meta* substitution. Such a shift in spectra is observed going from VII' (*para* substitution) to VI' (*meta* substitution in the chromophoric group). It is also of interest that the intensity of the fluorescence of

XII' was approximately $\frac{1}{3}$ of that observed for the other poly(1,3,4-oxadiazoles). A more complete discussion of the spectral characteristics of the poly(1,3,4-oxadiazoles) and related oligomers will be the subject of a separate publication.

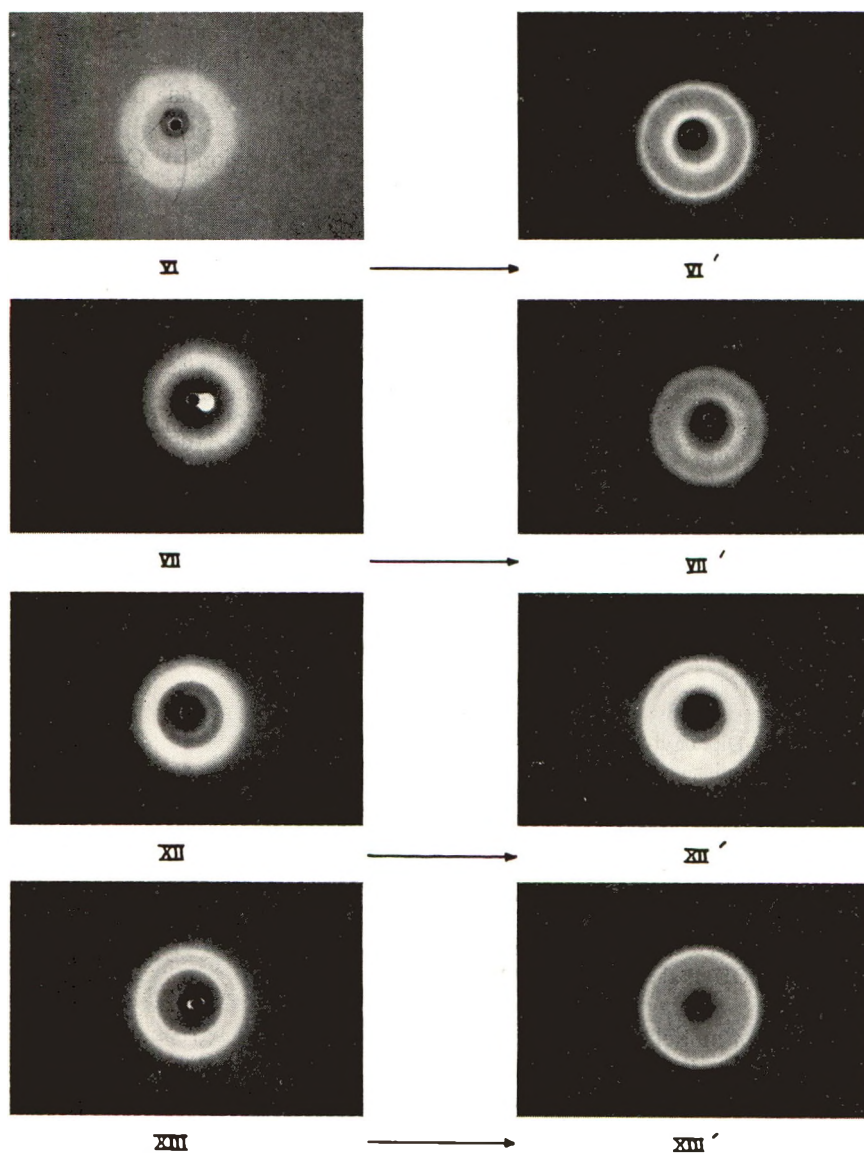


Fig. 3. X-ray diagrams of polyhydrazides and poly(1,3,4-oxadiazoles).

These novel polymer structures were expected to lead to novel properties of poly(1,3,4-oxadiazoles). All of the poly(1,3,4-oxadiazoles) were characterized by extremely high polymer melt temperatures, high inherent

viscosities in concentrated sulfuric acid, high crystallinity (Fig. 3), and excellent thermal, hydrolytic, and photostability.

Although the solubility of these poly(1,3,4-oxadiazoles) was extensively studied, only the strong acids, sulfuric and trifluoroacetic acids, were

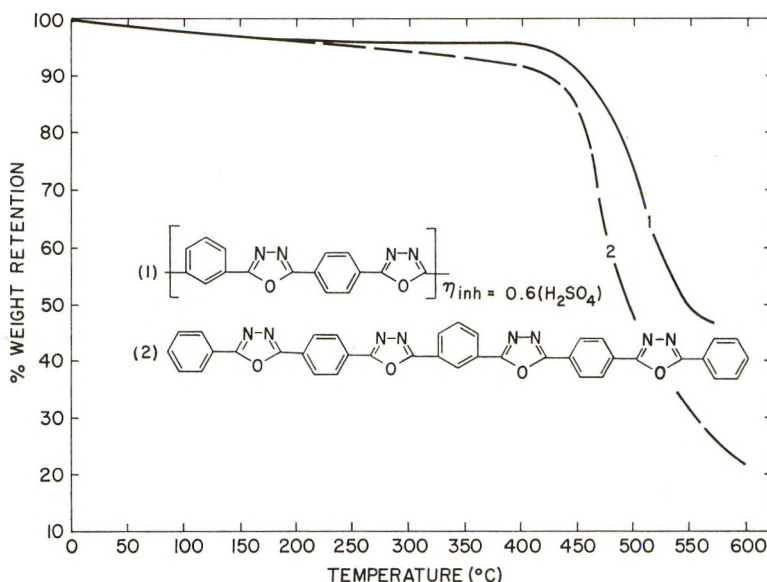


Fig. 4. Programed thermogravimetric analysis of polyoxadiazoles.

found to be solvents. Such typical polymer solvents as *m*-cresol, dimethylformamide, chloroform, nitrobenzene, formic acid, and tetrafluoropropanol were found to be ineffective as solvents.

3. Thermal Stabilities of Poly(1,3,4-oxadiazoles)

The thermal stability of poly(1,3,4-oxadiazoles) was investigated in order to compare structural differences and to assess more accurately their possible utility at elevated temperatures. This study was carried out on thermogravimetric balances, and the programed thermogravimetric analyses (TGA) are reproduced in Figure 4.

Curve 1 is reproduced from a programed TGA run (N_2) on poly-(1,3-/1,4-phenylene-2,5-(1,3,4-oxadiazole)] with $\eta_{inh} = 0.6$ (H_2SO_4). Curve 2 is a record of a TGA run with a 9-ring oligo-oxadiazole (M.W. 654.66).

To generalize, aromatic poly-1,3,4-oxadiazoles are extremely thermally stable and decompose between 450 and 500°C. Aliphatic polyoxadiazoles degrade between 400–450°C., as may be deduced from Figure 1 (curve 2), which shows the preparation of poly(octamethylene-1,3,4-oxadiazole) and finally its decomposition. Thus, there is a noticeable difference in thermal stability of aliphatic and aromatic species.

Since Huisgen⁷ has shown the spectral and electronic equivalence of the *p*-phenylene and the 1,3,4-oxadiazole rings, those poly(1,3,4-oxadiazoles)—VI' and VII'—in which the chain consists of alternating phenyl and 1,3,4-oxadiazole rings are indeed pseudo-polyphenyls in film- and fiber-forming molecular weight range.

This work was carried out, in part, under AF 33(616)8253, Project No. 7340 by the Directorate of Materials and Processes, ASD, Air Force Systems Command, Wright-Patterson Air Force Base, Ohio.

The authors wish to express their appreciation to Messrs. S. H. Catts, W. F. Holley and A. J. Prucino for their excellent technical assistance.

References

1. Koton, M. M., *J. Polymer Sci.*, **52**, 97 (1961).
2. Marvel, C. S., and G. E. Hartzel, *J. Am. Chem. Soc.*, **81**, 448 (1959).
3. McDonald, R. N., and T. W. Campbell, *J. Am. Chem. Soc.*, **82**, 4669 (1960).
4. Brinker, K. C., and I. M. Robinson, U. S. Pat. 2,895,948 (7/1/59), to Du Pont.
5. Vogel, H., and C. S. Marvel, *J. Polymer Sci.*, **50**, 511 (1961).
6. Vogel, H., and C. S. Marvel, *J. Polymer Sci.*, **A1**, 1531 (1963).
7. Sauer, J., R. Huisgen, and H. J. Sturm, *Tetrahedron*, **11**, 214 (1960).
8. Abshire, E. J., and C. S. Marvel, *Makromol. Chem.*, **44-46**, 388 (1961).
9. Stolle, R., *J. Prakt. Chem.* [2], **68**, 30 (1903).
10. Frazer, A. H., and F. T. Wallenberger, *J. Polymer Sci.*, **A2**, 1171 (1964).
11. Frazer, A. H., and F. T. Wallenberger, *J. Polymer Sci.*, **A2**, 1137 (1964).
12. Frazer, A. H., and F. T. Wallenberger, *J. Polymer Sci.*, **A2**, 1147 (1964).
13. Beaman, R. G., and F. B. Cramer, *J. Polymer Sci.*, **21**, 223 (1956).
14. Sorenson, W. R., and T. W. Campbell, *Preparative Methods of Polymer Chemistry*, Interscience, New York, 1961, pp. 32-55.
15. Ainsworth, C., *J. Am. Chem. Soc.*, **77**, 1148 (1955).
16. McElvain, S. M., and J. W. Nelson, *J. Am. Chem. Soc.*, **64**, 1825 (1942).
17. Pinner, A., *Chem. Ber.*, **16**, 352 (1885).
18. Luckenbach, G., *Chem. Ber.*, **17**, 1428 (1884).
19. N. Pellizzare, *Atti Reale Acad. Lincei Rend.*, **8**, I, 328 (1899).
20. McFarlane, S. B., and A. L. Miller, U. S. Pat. 2,615,862 (10/28/52), to Celanese Corporation.
21. Ott, D. G., V. N. Kerr, F. N. Hayes, and E. Hansbury, *J. Org. Chem.*, **25**, 872 (1960).
22. Ott, D. G., F. N. Hayes, E. Hansbury, and V. N. Kerr, *J. Am. Chem. Soc.*, **79**, 5448 (1957).
23. Klingsberg, E., *J. Org. Chem.*, **23**, 1086 (1958).

Résumé

Treize polyhydrazides aliphatiques et aromatiques ont été transformés en poly(1,3,4-oxadiazols) de poids moléculaires élevés par une réaction unique sur le polymère en masse. La réaction consiste en une cyclodéshydratation thermique à 170° à 280°C avec élimination d'eau. Les poly 1,3,4-oxadiazol formés ont été caractérisés par micro-analyse, la viscosité intrinsèque, la diffraction de rayons-X et les spectres I.R. et U.V. Les polyoxadiazols fondant au-dessous de 350°C pouvaient être laminés sous forme de films, tandis que les polyoxadiazols aromatiques infusibles ou fondant à une température très élevée ne pouvaient pas être transformés en films par les moyens habituels. Ces polymères résistent extrêmement bien à la température et à l'oxydation et se décomposent entre 450 et 500°C.

Zusammenfassung

Dreizehn aliphatische und aromatische Polyhydrazide wurden in Substanz durch eine ungewöhnliche Polymer-Nachreaktion in hochmolekulare Poly(1,3,4-oxadiazole) umgewandelt. Diese Reaktion verläuft bei 170° bis 280°C als thermische Cyclodehydratisierung. Die resultierenden Poly(1,3,4-oxadiazole) wurden durch Mikroanalyse, Viskositätszahl, Röntgendiagramm und Infrarot- und UltraviolettabSORPTIONSSPEKTRUM charakterisiert. Bei den unterhalb 50°C schmelzenden Polyoxadiazolen konnten aus der Schmelze Folien gepresst werden, während sehr hochschmelzende oder unschmelzbare aromatische Polyoxadiazole mit konventionellen Mitteln nicht zu Folien oder Fasern verarbeitet werden konnten. Solche Polymere sind thermisch und gegen Oxydation äusserst stabil und zersetzen sich zwischen 450 und 500°C.

Received January 31, 1963

Poly(1,3,4-Oxadiazole) Fibers: New Fibers with Superior High Temperature Resistance

A. H. FRAZER and F. T. WALLEMBERGER, *Pioneering Research Division, Textile Fibers Department, E. I. du Pont de Nemours & Company, Inc., Experimental Station, Wilmington, Delaware*

Synopsis

A polyoxiadiazole fiber, alt. poly[1,3-/1,4-phenylene-2,5-(1,3,4-oxadiazole)], with excellent thermal stability was prepared from poly(isophthalic-terephthalic hydrazide) fiber by thermal cyclodehydration. Conversion of this polyhydrazide fiber proceeded at 280°C. in a muffle furnace under positive nitrogen pressure and was completed in 48-72 hr., as evidenced by elemental analyses. The resulting polyoxadiazole fiber had the following typical fiber properties: $T/E/Mi/den. = 2.6/3.1/124/3.1$. It was thermally stable when exposed for prolonged periods of time at temperatures of 400°C. During heat treatment between 300 and 400°C. the initial polyoxadiazole fiber undergoes a structural change and final properties were: $T/E/Mi/den. \sim 1.5/1.5/90/3.0$. The polyoxadiazole structure was found to degrade severely at 450°C.

INTRODUCTION

The knowledge about films that retain useful properties after prolonged exposure at temperatures between 300 and 400°C. is very limited. Only few examples of such materials have been reported. One example is a film based on poly(2,2'-(*m*-phenylene)-5,5'-bibenzimidazole)^{1,2} which was found³ to exhibit excellent film properties after 150 hr. exposure at 300°C. in air. A fiber with excellent thermal stability which has become known in detail⁴ is Fiber AF (Black-Orlon fiber, Du Pont's acrylic fiber). It possessed useful fiber properties upon prolonged exposure at 250°C., and was found to retain its structural integrity when exposed for short periods of time to an open flame at temperatures in excess of 500°C.

Our preparations of poly(1,3,4-oxadiazoles)⁵ from aliphatic⁶ and aromatic⁷ polyhydrazide bulk polymer indicated that at least all-aromatic poly(1,3,4-oxadiazoles) would not decompose below 450°C. and would thus be potentially useful in high temperature applications, provided they could be manufactured into fibers. Since no useful spinning solvents were available, it was of interest to prepare polyhydrazide fiber⁷ and to convert this into poly(1,3,4-oxadiazole) fiber. This paper represents a report of such an unusual polymer post reaction on fiber.

EXPERIMENTAL

Codes and Abbreviations

Two fibers used for the present study were alt. poly(isophthalic-terephthalic dihydrazide) fiber (coded O—I—O—T fiber in agreement⁶ with previously used polyhydrazide codes) and alt. poly[1,3-/1,4-phenylene-2,5-(1,3,4-oxadiazole)] fiber coded PODZ fiber. Yarn properties used to characterize the fibers were tenacity T (g./den.), per cent elongation E , initial modulus M_i (g./den.), and denier.

Heating Cycles at Elevated Temperature

Fiber samples of O—I—O—T fiber, 2–12 in. length, were wound around small perforated metal bobbins in relaxed condition and were exposed to conversion conditions. Samples in individual runs, comprising 3–6 bobbins, were periodically withdrawn in order to follow the progress of the reaction with time.

Vacuum Conversions. Conversions were carried out at temperatures ranging from 222 to 283°C. The bobbins were placed in a tube which was evacuated and then heated in a vapor bath of refluxing methyl salicylate (222°C.), methyl naphthalene (242°C.), diphenylmethane (265°C.), or diphenylethane (283°C.).

Conversion in Solvent Vapors. A small number of conversions were carried out by exposing either bobbins carrying the fiber or fiber wound around Teflon (du Pont's TFE-fluorocarbon resin) bars to solvent vapors of diphenylmethane (263°C.), or diphenylethane (283°C.) at reflux. One larger sample, consisting of about 5 g. of O—I—O—T fiber was also converted under these conditions.

Conversions in Nitrogen. This type of conversion was carried out with commercial muffle furnaces. The heating elements were connected with Pyr-O-Vane thermoregulator (Minneapolis-Honeywell) for accurate temperature control. The size of the heating area allowed heating of fiber samples ranging from a few inches in length to samples weighing up to about 5 g. The conversion of O—I—O—T fiber samples were carried out at 280°C. under slight nitrogen pressure. Samples of PODZ fiber were periodically withdrawn and were analyzed. Constant microanalytical analyses indicated completion of conversion. Fiber properties of PODZ fiber were then recorded.

Thermal Stability of PODZ Fiber. The thermal stability of PODZ fiber was likewise determined in muffle furnaces at temperatures ranging from 300 to 450°C. for indicated periods of time. The temperature was controlled by means of a Pyr-O-Vane thermoregulator with a thermocouple leading into the center of the heating area of the furnaces. A second thermocouple was also installed in the center of the heating area and was used for independent temperature readings.

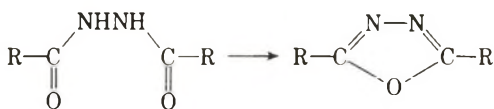
PODZ fiber samples (10–12 in.) with known fiber properties were wound

loosely around perforated metal bobbins and were placed in the center of the heating area.

No effort was made to measure or to correct for the temperature gradient which is known to exist in heating areas of muffle furnaces and may amount to $\pm 30^\circ\text{C}$. since not only the fibers (on bobbins) but also the two, and independent, sets of thermocouples were located in the center of the heating area.

RESULTS AND DISCUSSION

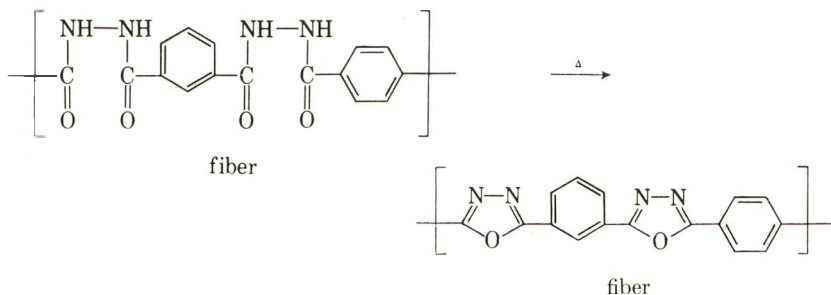
Stolle⁸ discovered that 2,5-disubstituted 1,3,4-oxadiazoles can be prepared from diaroyl or diacyl hydrazines by thermal or by chemical cyclodehydration.



This reaction was applied to the preparation⁵ of poly(1,3,4-oxadiazoles) from aliphatic⁶ and aromatic⁷ polyhydrazides. It was noted that chemical conversion, using agents such as sulfuric acid, acid chlorides or acid anhydrides, which gave best results on the monomeric scale, degraded the polyhydrazides which were used as starting materials. The best method for polymer reactions⁵ was the thermal cyclodehydration which allowed quantitative conversion and gave well-defined poly(1,3,4-oxadiazoles).

1. Thermal Cyclodehydration

Thermal cyclodehydrations can be carried out in vacuum, in nitrogen, or more directly by exposing fiber samples to solvent vapors at reflux. These methods have been studied and the results are discussed in the following paragraphs.



A number of conversions were carried out *in vacuum* as described in the Experimental section, and cyclodehydration on O-I-O-T fiber was attempted 222, 242, 265, and 283°C. No reaction occurred at 222°C. within 72 hr. as evidenced by virtually unchanged oxygen analyses. However, the yarn properties changed from $T/E = 5.2/20$ to 2.6/9. At 242°C.

TABLE I
 Initial Poly-1,3,4-oxadiazole (PODZ) Fiber Properties

Property	
Straight	
$T/E/M_i$	2.6/3.1/124
Denier	3.0
Loop	
T/E	1.8/2.8
Denier	3.9
Knot	
$T/E/M_i$	2.3/2.8/79
Denier	3.0
X-Ray crystallinity (amount/perfection)	low/low
X-Ray Orientation (degrees)	31-38
Oxygen analysis (theor. 11.10%), %	12.10

 TABLE II
 Initial Polyoxadiazole Tensile Properties

$T/E/M_i$ /Den.	O, %	Note
2.6/3.1/124	12.10	Converted in boiling diphenylmethane, 265°C.
2.4/6.6/102/3.5	12.40	Converted in N ₂ at 280°C.
3.0/3.2/149/2.8	11.89	Cyclized in furnace (N ₂ , 280°C.) Sample contained ash.
3.2/7.4/140/3.5	12.20	Courtesy of W. Sweeny and C. Smullen Sample contained ash.

there was a slow conversion, estimated by oxygen analysis to be 50% in about 48 hr. The yarn properties gradually changed from $T/E = 5.2/20$ to 1.9/5. At 265°C. the yarn conversion proceeded with noticeable rate but within 30 hr. the yarn properties had changed from $T/E = 5.2/20$ to 0.7/0.6. After 72 hr. at 283°C. the same result ($T/E = 1.0/1.0$) was observed with nearly complete conversion to PODZ.

Conversion studies in vacuum were cumbersome and gave inhomogeneous PODZ fiber possibly because of poor heat transfer. It was believed that *solvent vapors* at temperatures ranging from 270 to 290°C. would provide better heat transfer. A number of experiments were therefore carried out at 265, 273, and 283°C. with skeins of O—I—O—T wound around Teflon bars, thus avoiding metal bobbins which might cause contamination of polyhydrazides on the metal surface. A larger sample of O—I—O—T, after conversion at 273°C., was subsequently used for thermal stability studies at even higher temperatures. This effectively provided a second heating cycle. The initial polyoxadiazole properties are given in Table I.

Six samples of polyhydrazide fiber were heated in a steel bomb with high pressure steam at 254°C. Steam at this temperature did not effect cyclization, and the fiber degraded badly, presumably due to a hydrolytic degradation reaction.

In order to obtain large samples and to circumvent the cumbersome procedure of exposing fibers to solvent vapors (under these conditions solvents and polymer quite often show signs of degradation or discoloration), it was decided to use *muffle furnaces* (with N_2 bleeds) for conversion of O—I—O—T fibers at 280°C.

Fibers obtained by cyclodehydration in solvent vapors had properties similar to those obtained by carrying out this reaction in muffle furnaces (Table II).

2. Thermal Stability of Poly(1,3,4-oxadiazole) Fibers

The thermal stability of poly(1,3,4-oxadiazoles) has been determined^{5,9} and it was found that all-aromatic bulk polymer was thermally stable up to 450°C. and decomposed at 500°C. Aliphatic poly(1,3,4-oxadiazoles) were found to degrade at 400–450°C.

In the context of the present study it was of interest to determine the retention of fiber properties (1) at elevated testing temperatures and (2) after air aging for long periods of time at temperatures of 300°C. and above.

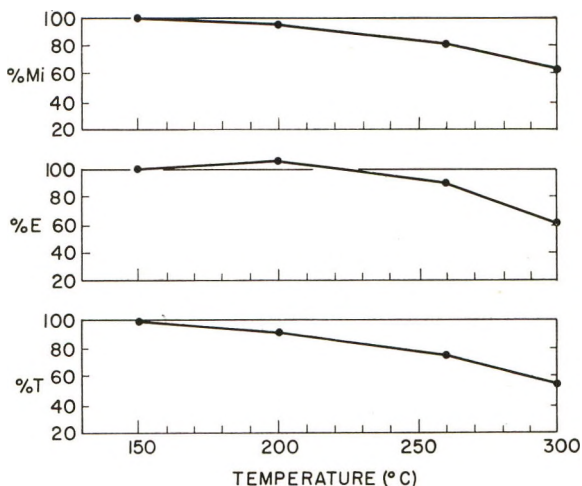


Fig. 1. Retention of poly(1,3,4-oxadiazole) fiber properties at elevated testing temperatures.

In Figure 1, the retentions of fiber properties, expressed as percentages of room temperature properties, are plotted against testing temperature. It is apparent from an inspection of these data that the poly(1,3,4-oxadiazole) fiber shows essentially no change in properties up to testing temperatures of 200°C. and retains 60% or better of room temperature properties even at temperatures of 300°C. This remarkable behavior reflects the high chain stiffness and stability arising from the alternating benzene and 1,3,4-oxadiazole rings along the polymer chain.

TABLE III
Retention of Fiber Properties of PODZ Fiber after Exposure at Elevated Temperatures

Thermal treatment			$T/E/M_i/\text{den.}$	Per cent retention $\%T/\%E/\%M_i^a$
Temp., °C.	Medium	Time, hr.		
300	Air	6	2.6/3.2/103/3.0	100/100/81.2
		96	1.2/1.2/87/2.7	46.2/38.1/70.0
		168 ^b	1.2/1.2/112/2.7	46.2/38.1/90.3
350	Air	24	2.1/2.2/103/2.7	80.8/71.0/83.1
		48	2.1/2.2/93/2.9	80.8/67.7/91.1
		96 ^c	1.1/1.1/102/3.3	42.3/32.3/82.3
375	Air ^d	4	1.9/2.2/72/2.8	73.1/71.0/58.1
		6	1.7/1.7/66/2.7	64.4/54.8/53.2
		48 ^c	1.6/1.3/100/2.7	61.5/41.9/80.6
400	Air	4	2.1/1.9/81/2.5	80.8/61.3/65.3
		24	2.5/2.6/67/2.6	96.2/83.9/54.0
		40 ^c	1.8/1.8/84/2.8	69.2/58.0/67.7
450	Air	>1	Disintegration of fiber	
300	N ₂	2	2.7/4.2/104/3.3	>100/>100/84.0
		24	2.3/2.4/107/2.9	92.5/77.5/86.5
		150 ^c	1.7/1.6/87/2.9	65.4/51.6/70.0
350	N ₂	24	2.3/2.2/132/2.9	88.5/71.0/>100
		48	2.8/2.6/128/2.8	96.2/83.9/>100
		96 ^c	1.2/1.2/83/2.7	46.2/38.7/66.9
375	N ₂	6	1.2/1.2/97/3.3	46.2/38.7/78.2
		24	1.6/1.4/112/2.7	61.5/45.2/90.3
		48 ^c	1.3/1.1/92/3.0	50.0/35.5/74.2
400	N ₂	4	1.7/1.8/100/3.0	65.8/58.1/80.6
		6	1.6/1.5/89/2.9	59.6/48.4/71.8
		24 ^c	1.3/1.2/102/2.8	50.4/38.7/82.3
450	N ₂	>1	Disintegration of fiber	

^a Retention of properties expressed as per cent of initial properties (Table I) for straight PODZ fiber ($T/E/M_i = 2.6/3.1/124$).

^b Fiber was too brittle to test in duplicate experiment.

^c Longer exposure produced fiber which was too brittle to test.

^d Fiber samples degraded partially in duplicate runs due to uneven heating.

The results of the study to determine effect of air aging of fibers for long periods of time at temperatures of 300°C. on fiber properties are summarized in Table III.

Inspection of these data shows that measurable fiber properties were obtained even after 168 hr. exposure to 300°C. or 24–40 hr. at 400°C. In agreement with observations on bulk polymer it was found that the PODZ fibers disintegrated upon short exposure >400°C., with complete loss of fiber properties.

The temperature gradient within muffle furnaces may vary $\pm 30^\circ\text{C.}$, so that reproducibility should be considered to lie within such limits. For example, once a sample was found too brittle to test after 168 hr. at 300°C. and in another instance a sample had measurable fiber properties after 48 hr. at 400°C. ($T/E/M_i/\text{den.} = 2.1/1.8/136/3.6$). In a third instance a

TABLE IV
 Final Polyoxadiazole Tensile Properties

Thermal treatment			O, %	$T/E/M_t/\text{den.}$
Time, hr.	Temp., °C.	Medium		
52	300	Air	11.57	1.1/1.1/93/3.2
168	300	Air	11.80	1.2/1.2/112/2.7
48	400	Air	11.64	2.1/1.8/136/3.6
48	375	N ₂	11.40	1.3/1.1/92/3.0

batch partially degraded at 375°C. in short time, probably due to local overheating.

Initial polyoxadiazole fiber properties thus are found to decrease from $T/E/M_t = 2.6/3.1/124$ to final fiber properties such as $T/E/M_t \sim 1.5/1.5/90$ on prolonged heating at temperatures ranging from 300 to 400°C. It should be noticed that even those fibers which have been exposed at elevated temperatures for long periods of time have a slightly high oxygen analysis (calcd: 11.10%). This fact, which is specifically borne out by inspection of Table IV, remains unexplained.

The change in fiber properties during heating cycles above 300°C. may be due to three factors: (a) final completion of conversion, (b) a structural change to a thermally more stable but stiffer fiber structure, and (c) a process of thermal aging.

The x-ray diffraction patterns for (1) O—I—O—T fiber, (2) PODZ fiber obtained therefrom by heating at 280°C. for 72 hr., and (3) for PODZ fiber that was exposed to an additional heating cycle of 7 days at 300°C. are shown in Figure 2a, 2b, and 2c, respectively. While there is a remarkable change in going from the O—I—O—T x-ray diagram to the PODZ diagram, there is no noticeable change in diffractions on additional heating. The final change in fiber properties is, therefore, most likely due to a combination of thermal aging accompanied by completion of the thermal cyclodehydration reaction.

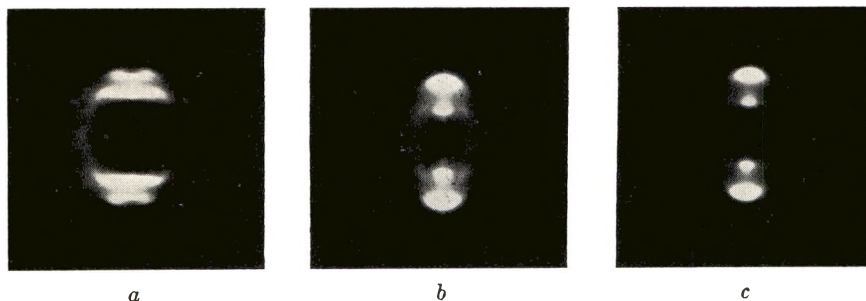


Fig. 2. X-ray diffraction patterns: (a) O—I—O—T fiber before conversion; (b) PODZ fiber after conversion (72 hr. at 280°C.); (c) PODZ fiber after additional thermal treatment (168 hr. at 300°C.).

The final, stiffer structure, however, possessing lower elongations and still high moduli, is entirely in accordance with a structure expected for a polymer consisting exclusively of intralinear aromatic and heterocyclic rings in the polymer chain. Recently, Huisgen and co-workers¹⁰ have shown that the oxadiazole ring is spectrally and electronically equivalent to a *p*-phenylene structure. Hence fiber consisting of exclusively benzene rings in the polymer chain would be expected to possess properties similar to those of PODZ fiber. Poly(*p*-phenylene) has been prepared¹¹ and was found to possess thermal properties resembling those of aromatic poly-(1,3,4-oxadiazoles), but no fiber could be prepared from this relatively low molecular weight polymer. Thus, PODZ fiber may be regarded as a *pseudopolyphenylene* fiber.

This work was carried out, in part, under Contract No. AF33(616)-8253, Project No, 7340 by the Directorate of Materials and Processes, ASD, Air Force Systems Command, Wright-Patterson Air Force Base, Ohio.

The authors wish to express their appreciation to Messrs. S. H. Catts, W. F. Holley, and A. J. Prucino for their excellent technical assistance.

References

1. Brinker, K. C., and I. M. Robinson, U. S. Pat. 2,895,948 (7/1/59), to Du Pont Company.
2. Vogel, H., and C. S. Marvel, *J. Polymer Sci.*, **154**, 511 (1961).
3. Vogel, H., and C. S. Marvel, *J. Polymer Sci.*, **A1**, 1531 (1963).
4. Vosburgh, W., *Textile Res. J.*, **30**, 882 (1960).
5. Frazer, A. H., W. Sweeny, and F. T. Wallenberger, *J. Polymer Sci.*, **A2**, 1157 (1964).
6. Frazer, A. H., and F. T. Wallenberger, *J. Polymer Sci.*, **A2**, 1137 (1964).
7. Frazer, A. H., and F. T. Wallenberger, *J. Polymer Sci.*, **A2**, 1147 (1964).
8. Stolle, R., *J. Prakt. Chem.* [2], **68**, 30 (1903).
9. Abshire, E. J., and C. S. Marvel, *Makromol. Chem.*, **44-46**, 388 (1961).
10. Sauer, J., R. Huisgen, and H. J. Sturm, *Tetrahedron*, **11**, 214 (1960).
11. Marvel, C. S., and G. E. Hartzel, *J. Am. Chem. Soc.*, **81**, 448 (1959).

Résumé

On a préparé une fibre de polyoxadiazol, alt. poly[1,3-/1,4-phénylène-2,5-(1,3,4-oxadiazol)] avec une stabilité thermique excellente à partir d'une fibre de polyisothalotéréphthalo hydrazide par cyclodéshydratation thermique. La conversion de cette fibre de polyhydrazide se passe à 250°C. dans un four à moufle sous une pression d'azote et elle était achevée en 48-72 H. comme prouvé par analyse élémentaire. La fibre du polyoxadiazol qui résulte, a les propriétés typiques suivantes: $T/E/M_i/\text{den} = 2,6/3,1/124/3,1$. Elle est thermostable quand on l'expose à des températures de 400°C. Pendant un traitement entre 300 et 400°C, la fibre initiale de polyoxadiazol subit un changement de structure et les propriétés finales sont: $T/E/M_i/\text{den} \sim 1,5/1,5/90/3,0$. On a trouvé qu'à 450°C on a une dégradation de structure importante.

Zusammenfassung

Eine Polyoxadiazolfaser, alt. Poly[1,3-1,4-phenylen-2,5-(1,3,4-oxadiazol)] mit ausgezeichneter thermischer Stabilität wurde aus einer Poly(isophthal-terephthalhydrazid)-Faser durch thermische Cyclodehydratisierung dargestellt. Die Umwandlung dieser Polyhydrazidfaser erfolgte bei 280°C in einem Muffelofen unter positivem Stickstoff-

druck und war in 48–72 Stunden vollständig, wie die Elementaranalyse zeigte. Die resultierende Polyoxadiazolfaser besass folgende typische Fasereigenschaften: T/E/ M_t /Den. = 2,6/3,1/124/3,1. Sie war bei Temperaturen von 400°C durch längere Zeiten thermisch stabil. Während einer Wärmebehandlung zwischen 300° und 400°C erleidet die zunächst gebildete Polyoxadiazolfaser eine strukturelle Veränderung und die endgültigen Eigenschaften sind: T/E/ M_t /Den. \sim 1,5/1,5/90/3,0. Die Polyoxadiazolstruktur wird bei 450°C tiefgreifend abgebaut.

Received January 31, 1963

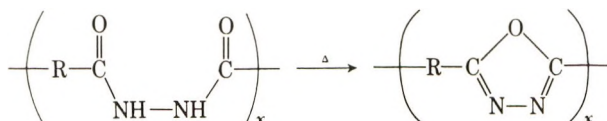
Poly(1,3,4-Oxadiazolidine)

A. H. FRAZER and F. T. WALLENBERGER, *Pioneering Research Division, Textile Fibers Department, E. I. du Pont de Nemours & Company, Inc., Experimental Station, Wilmington, Delaware*

Synopsis

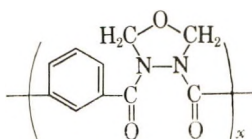
Poly(3,4-isophthaloyl-1,3,4-oxadiazolidine) was prepared from poly(isophthalic dihydrazide) by treatment by reaction with formic acid in dimethylsulfoxide as high-molecular weight film-forming polymer. Under thermal treatment with the evolution of formaldehyde and water, high yields of chemically pure poly[1,3-phenylene-2,5-(1,3,4-oxadiazole)] were obtained.

In the course of the investigation of the thermal cyclodehydration of polyhydrazides to poly(1,3,4-oxadiazoles),¹ it was of interest to determine the contribution of the enol form of the hydrazide structure in this cyclization reaction.



One approach to this problem was to compare the rates of conversion to poly(1,3,4-oxadiazole) of a polyhydrazide with that of a poly(1,3,4-oxadiazole) precursor which could not enolize.

The purpose of this paper is to report the synthesis of such a non-enolizable poly(1,3,4-oxadiazole) precursor, poly(3,4-isophthaloyl-1,3,4-oxadiazolidine):

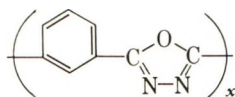


RESULTS AND DISCUSSION

The reaction of poly(isophthalic dihydrazide) with an excess of trioxane in dimethylsulfoxide/formic acid solution yielded a product which had a polymer melt temperature of 400°C. from which clear films could be obtained by casting from dimethylsulfoxide solutions. The infrared

spectra of these films showed little or no NH or OH absorption but definite bands at 8.45 and 9.00 μ which were attributed to a cyclic $-\text{CH}_2-\text{O}-\text{CH}_2-$ structure. This, in conjunction with elemental analyses, strongly favors the assignment of a poly(1,3,4-oxadiazolidine) structure to this reaction product.

When this poly(1,3,4-oxadiazolidine) was heated, formaldehyde and water were evolved, and the residual polymer was insoluble in dimethylsulfoxide but soluble in concentrated sulfuric acid. That this polymer was poly[1,3-phenylene-2,5-(1,3,4-oxadiazole)]



was conclusively shown by the identity of its infrared spectrum with that of the same poly(1,3,4-oxadiazole) from the cyclodehydration of poly(isophthalic hydrazide) and by elemental analyses.

EXPERIMENTAL

1. Preparation of Poly(3,4-isophthaloyl-1,3,4-oxadiazolidine)

A 20-g. sample of poly(isophthalic dihydrazide) was dissolved in 200 ml. of a solution containing 85 parts of dimethylsulfoxide and 15 parts of formic acid and was allowed to react with 30 g. of trioxane for 18 hr. at room temperature. The reaction mixture was diluted with 500 ml. of methanol, and the precipitated polymer was collected by filtration. The isolated polymer was repeatedly washed with methanol and dried to give 23.7 g. (90%) of product, η_{inh} in dimethylsulfoxide = 0.74. (ANAL.: Calcd. for poly(1,3,4-oxadiazolidine) structure: O, 23.5%, N, 13.7%. Found: O, 23.5%, N, 13.6%.)

Infrared spectra of thin films of this product show no absorption in 2.8–3.2 μ region (NH or OH), but definite bands at 5.9 to 6.2 μ (carbonyl) and 8.45 and 9.00 μ (cyclic $-\text{CH}_2-\text{O}-\text{CH}_2-$).

2. Preparation of Poly[1,3-phenylene-2,5-(1,3,4-oxadiazole)]

A 10-g. sample of poly(3,4-isophthaloyl-1,3,4-oxadiazolidine) was heated at 265°C. under less than 1 mm. pressure for 6 hr. Vigorous effervescence occurred and the gases which evolved were identified as formaldehyde and water vapor. After cooling under nitrogen, 6.4 g. (92%) of residual polymer was obtained, η_{inh} in concentrated sulfuric acid = 0.25. (ANAL.: Calcd. for poly(1,3,4-oxadiazole) structure: O, 11.10%; Found: O, 11.85%.)

Infrared spectrum of this product was identical with that of poly[1,3-phenylene-1,3,4-(oxadiazole)].

Reference

1. Frazer, A. H., W. Sweeny, and F. T. Wallenberger, *J. Polymer Sci.*, **A2**, 1137, 1147, 1157, 1171 (1964).

Résumé

La poly(3,4-isophthaloyl)-1,3,4-oxadiazolidine a été préparée à partir du polyisophthalodihydrazide en la traitant par l'acide formique dans le diméthyl-sulfoxyde; on obtient ainsi un polymère filmogène de poids moléculaire élevé. Par traitement thermique accompagné de dégagement de formaldéhyd et d'eau, on obtient de hauts rendements de poly[1,3-phénylène-2,5-(1,3,4-oxadiazol)] chimiquement pur.

Zusammenfassung

Poly(3,4-isophthaloyl-1,3,4-oxadiazolidin) wurde aus Poly(isophthalaldihydrazid) durch Behandlung mit Ameisensäure in Dimethylsulfoxyd als hochmolekulares, filmbildendes Polymeres dargestellt. Bei thermischer Behandlung wurden unter Entwicklung von Formaldehyd und Wasser hohe Ausbeuten an chemisch reinem Poly[1,3-phenylen-2,5-(1,3,4-oxadiazol)] erhalten.

Received January 31, 1963

Thiaalkyl Polyacrylates: The Influence of Sulfur in the Side Chain

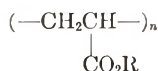
RICHARD M. McCURDY and JULIANNE H. PRAGER, *Central Research Laboratories, Minnesota Mining and Manufacturing Company, St. Paul, Minnesota*

Synopsis

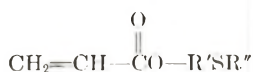
A series of acrylic esters containing a thio ether atom in the side chain has been prepared and polymerized. The glass transition temperatures and swelling volumes are reported as follows: 3-thiabutyl polyacrylate, T_g -60°C ., 9% volume swell in 70:30 isooctane-toluene; 3-thiapentyl polyacrylate, -71°C ., 31%; 4-thiapentyl polyacrylate, -65°C ., 32%; 4-thiahexyl polyacrylate, -76°C ., 36%; 5-thiahexyl polyacrylate, -70°C ., 36%. These data are compared with those for certain other polyacrylates; the relation between the structure and the properties of these materials is discussed.

INTRODUCTION

It is possible to alter the properties of polyacrylates over a wide range by varying the substituents in the group R:



Investigations have been carried out in various laboratories of polyacrylates containing one or more of the following substituents in the alcohol moiety: halogen,¹⁻⁴ nitro,^{2,5} nitrate,⁶ nitrile,^{1,2,7} ether oxygen,^{4,7,8} and amine.⁹ Much of this research has been directed toward an elastomer combining low-temperature flexibility with resistance to swelling by common fuels and lubricants. This paper reports the synthesis and polymerization of a number of acrylate esters having a thio ether atom in the side chain,



R' and R'' being unbranched hydrocarbon chains. (The following paper in this series¹⁰ reports the preparation and polymerization of a series of cyanothiaalkyl acrylates.)

TABLE I
Physical Properties and Analyses of Thiaalkanols

Formula	B.P., °C./mm.	n_D^{20}	Yield, %	Carbon, %		Hydrogen, %		Sulfur, %	
				Calc.	Found	Calc.	Found	Calc.	Found
$\text{HO}(\text{CH}_2)_2\text{SCH}_3$	74-78/23	1.4891	76	39.1	38.2	8.8	9.1	34.8	34.2
$\text{HO}(\text{CH}_2)_3\text{SCH}_2\text{CH}_3$	78-81/20	1.4841	81	45.2	45.1	9.5	9.5	30.2	29.7
$\text{HO}(\text{CH}_2)_3\text{SCH}_3$	52-55/1.5	1.4859	83	45.2	45.4	9.5	9.5	30.2	30.1
$\text{HO}(\text{CH}_2)_3\text{SCH}_2\text{CH}_3$	85-86/5	1.4830	87	50.0	49.4	10.1	9.8	26.7	26.4
$\text{HO}(\text{CH}_2)_4\text{SCH}_3$	81-85/3	1.4856	64	50.0	49.2	10.1	10.0	26.7	26.8

TABLE II
Physical Properties and Analyses of Thiaalkyl Acrylates, $\text{CH}_2=\text{CHCO}_2\text{R}$

R Group	B.P., °C./mm.	n_D^{20}	Yield, %	Carbon, %		Hydrogen, %		Sulfur, %	
				Calc.	Found	Calc.	Found	Calc.	Found
$-(\text{CH}_2)_2\text{SCH}_2$	60/4	1.4790	75	49.3	49.5	6.9	6.8	21.9	21.7
$-(\text{CH}_2)_2\text{SCH}_2\text{CH}_3$	83-85/7	1.4763	74	52.5	52.6	7.6	7.5	20.0	20.1
$-(\text{CH}_2)_3\text{SCH}_3$	52-55/1.3	1.4778	82	52.5	52.7	7.6	7.6	20.0	20.0
$-(\text{CH}_2)_3\text{SCH}_2\text{CH}_3$	63-65/3	1.4770	58	55.1	55.1	8.1	7.9	18.4	18.4
$-(\text{CH}_2)_4\text{SCH}_3$	81-85/3	1.4856	55	55.1	55.2	8.1	8.0	18.4	18.5

EXPERIMENTAL

Preparation of Thiaalkanols

Method A. The thiaalkanols in which R" is methyl were prepared substantially by the method of Windus and Shildneck¹¹ from the corresponding chloroalkanol and sodium methyl mercaptide. It was found advantageous to prepare the other thiaalkanols in aqueous solution (method B).

Method B. To the ice cold alkyl mercaptan was added dropwise with stirring 1.25 moles of a 25% aqueous solution of sodium hydroxide. To the resulting clear solution was added 1.3 moles of the desired chloroalkanol, at such a rate that the temperature of the reaction did not exceed 60°C. Stirring was continued at room temperature for about four hours, after which the organic layer was taken up in two volumes of benzene, washed with 25% sodium hydroxide and with water, dried over calcium sulfate, and fractionally distilled under reduced pressure.

Properties. The properties of these alcohols are given in Table I.

Preparation of Thiaalkyl Acrylates

To a stirred, cooled solution of the thiaalkanol (1.0 mole) and anhydrous triethylamine (1.2 moles) in five volumes of dry benzene was added a solution of acrylyl chloride (1.2 moles) in five volumes of dry benzene, at a rate such that the temperature of the reaction mixture did not exceed 30°C. The mixture was then washed with one-fourth volumes each of water, 10% sodium carbonate solution, 5% hydrochloric acid solution, and finally water. After being dried over calcium sulfate, the product was fractionally distilled in the presence of a suitable polymerization inhibitor. The data summarizing the properties of these acrylates are reported in Table II.

Polymerization of the Monomers

All of the monomers polymerized smoothly to high polymers. The emulsion type recipe given in Table III was used.

TABLE III
Polymerization Recipe

Component	Parts by weight
Monomer	100
Water	180
Sodium lauryl sulfate	5
Sodium persulfate	0.5
Sodium bisulfite	0.5

Polymerization was essentially complete after 4 hr. at 50°C.

TABLE IV
Comparison of the Thiaalkyl Polyacrylates with Various Other Polyacrylates
($-\text{CH}_2\text{CH}-$)
|
 CO_2R

R Group	Thiaalkyl polyacrylates ($\text{X}=\text{S}$)			Oxaalkyl polyacrylates ($\text{X}=\text{O}$)			Alkyl Polyacrylates ($\text{X}=\text{CH}_2$)			
	No.	T_g , °C.	Swell in 70:30 iso- octane- toluene, vol.-%	No.	T_g , °C.	Swell in 70:30 iso- octane- toluene, vol.-%	No.	T_g , °C.	Swell in 70:30 iso- octane- toluene, vol.-%	Ref.
$-\text{CH}_2\text{CH}_2\text{NCH}_3$	I	-60	9%	VI	-50	30%	X	-70	>200%	^a
$-\text{CH}_2\text{CH}_2\text{NCH}_2\text{CH}_3$	II	-71	31%	VII	-50	50%	XI	-76	>200%	^e
$-\text{CH}_2\text{CH}_2\text{CH}_2\text{NCH}_3$	III	-65	32%	VIII	-58	50%				
$-\text{CH}_2\text{CH}_2\text{CH}_2\text{N}-\text{CH}_2\text{CH}_3$	IV	-76	36%	IX	-55	130%	XII	-80	>200%	^e
$-\text{CH}_2\text{CH}_2\text{CH}_2\text{CH}_2\text{N}-\text{CH}_3$	V	-76	36%							

^a Data of Bovey and Abere.⁴

^b Determined by Paul I. Roth in this laboratory.

^c Data of Wiley and Brauer.¹²

^d Estimated from glass transition temperature data on related alkyl polyacrylates.

^e Estimated from swelling data on related alkyl polyacrylates.

POLYMER PROPERTIES

The glass transition temperatures and swelling data of these thiaalkyl polyacrylates are reported in Table IV. A modified Abbé refractometer was used to measure polymer glass transition temperatures by the method of Wiley and Brauer.¹³ The estimated error for this type of measurement is $\pm 5^\circ\text{C}$. Swelling volumes were calculated from the increase in length of 10-cm. strips of gum stock which had been lightly vulcanized by heating the rubber with three parts of Di-Cup 40C (40% dicumyl peroxide supported on precipitated calcium carbonate, Hercules Powder Co., Wilmington, Delaware). In all cases the gum vulcanizate was allowed to swell 72 hr. at room temperature and appeared to reach equilibrium in that time.

These data may be compared with those reported for certain oxalkyl polyacrylates and for some unsubstituted polyacrylates. Swelling data on the hydrocarbon and oxygen ether polymers were obtained on gum vulcanizates cured with a silicate recipe. However, a comparison of the three types is felt to be valid, since the level of crosslinking was comparable and low in all cases.

RESULTS

A comparison of the glass transition temperatures and swelling volumes of the oxalkyl and thiaalkyl polyacrylates can be made on isosteric members of each series. From Table IV it can be seen that the substitution of $-\text{S}-$ for $-\text{OCH}_2-$ brings about a very appreciable reduction in affinity for aromatic fuels, while the glass temperature T_g is held constant or even lowered slightly.

Thus, a comparison of the data on 3-thiabutyl polyacrylate (I) with that on the isosteric oxapentyl polyacrylates (VII and VIII) shows that the sulfur-containing type has a slightly lower glass temperature (-60°C . versus -50°C . and -58°C .) and is less affected by solvent as well (9% versus 50%). Similarly, the thiapentyl polyacrylates (II and III) may be compared with an oxahexyl polyacrylate (IX) to demonstrate again that the thiaalkyl polyacrylates exhibit lower glass temperatures (-71°C . and -65°C . versus -55°C .) and also decreased swells (31% and 32% versus 130%). The hydrocarbon polyacrylates have the lowest glass temperatures of the three types, but are highly swollen by the hydrocarbon solvent.

DISCUSSION

The effect of the nature of the side chain on the swelling behavior and modulus-temperature characteristics of acrylate polymers has been discussed.⁴ The factors which influence the solvent affinity and modulus-temperature characteristics of polyacrylates are the length, polarity,

shape, and flexibility of the side chain. All four of these factors affect the mobility of the polymer molecules and hence the glass temperature of the polymer. The solubility characteristics are influenced particularly by the first two.

Methyl polyacrylate has a low affinity for hydrocarbon solvents and a relatively high glass temperature (9°C.).¹⁴ The moderately strong intermolecular forces induced by the polar ester groups increase the hydrocarbon resistance of the polymer but also act to restrict free molecular movement. As longer hydrocarbon chains are attached to the polyacrylate structure, the ester groups become shielded, and dipole-dipole interactions are diminished. When the hydrocarbon groups are unbranched, as is the case here, there is apparently a considerable increase in free volume also. Both the reduced dipolar interactions and the increased free volume promote polymer mobility and thus result in lowered glass temperatures. The dilution of the ester group with progressively longer hydrocarbon side chains, however, also leads to decreased hydrocarbon resistance. The substitution of a quite different type of shielding side chain for the hydrocarbon type, i.e., replacement with a fluorinated side chain as in the fluorinated polyacrylates, brings about an increase both in hydrocarbon resistance and in glass temperature. The increase in T_g is believed to be due in large measure to the greater stiffness of the fluorocarbon chain relative to a hydrocarbon one. As can be seen from Table V, fluorocarbons have considerably higher energy barriers to rotation than do their hydrocarbon analogs.

The availability of polyacrylates containing the thio ether atom in the side chain offers the opportunity to study the effect of the incorporation of this substituent in the alcohol moiety. By substituting —S— for a —CH₂CH₂— group, we can investigate the effect of altering the polarity and flexibility of the polyacrylate side chain while keeping its length and shape substantially constant. Since the oxaalkyl polyacrylates are also known,

TABLE V
Energy Barriers to Rotation in Some Small Molecules

Formula	Energy barrier to rotation, kcal./mole
CH ₃ —S—CH ₃	2.0 ^a
CH ₃ —O—CH ₃	2.7 ^b
CH ₃ CH ₂ CH ₃	3.4 ^c
CH ₃ —CH ₂	2.75 ^d
CF ₃ —CF ₃	4.35 ^e

^a Data of Osborne et al.¹⁰

^b Data of French and Rasmussen.¹⁷

^c Data of Pitzer.¹⁸

^d Data of Kistiakowsky et al.¹⁹

^e Data of Pace and Aston.²⁰

it is possible to compare all three types of systems. Simple oxygen ethers exhibit dipole moments of 1.15–1.3 D., sulfides 1.4–1.6 D.¹⁵ Accompanying this change, there is a decrease in the energy barrier to rotation in going from C—C—C to C—O—C to C—S—C. Table V gives energy barrier data for some illustrative small molecules.

The effect on the properties of thiaalkyl polyacrylates of their increased polar character, on the one hand, and their reduced torsional resistance, on the other, is rather interesting. The sulfur-containing polyacrylates, which have the strongest intermolecular forces of the three classes of polymers, also have the greatest hydrocarbon resistance. As far as molecular mobility and the glass temperature are concerned, the hydrocarbon polyacrylates, in which dipolar interactions are at a minimum, show the lowest glass temperature of the three classes, while the thiaalkyl polyacrylates, which have the greatest degree of rotational freedom, have glass temperatures higher than those of the hydrocarbon type, but lower than those containing the oxygen ether substituent. It would seem that the stiffening effect brought about by the introduction of the polar thiaalkyl system is counterbalanced to a considerable extent by the reduced torsional resistance.

The authors wish to express appreciation to Dr. George B. Rathmann for many helpful discussions.

The authors wish to thank Paul I. Roth of these laboratories for transition temperature determinations.

References

1. Mast, W. C., C. E. Rehberg, T. J. Dietz, and C. H. Fisher, *Ind. Eng. Chem.*, **36**, 1022 (1944).
2. Rehberg, C. E., M. B. Dixon, and W. A. Faucette, *J. Am. Chem. Soc.*, **72**, 5199 (1950).
3. Bovey, F. A., J. F. Abere, G. B. Rathmann, and C. L. Sandberg, *J. Polymer Sci.*, **15**, 520 (1955).
4. Bovey, F. A., and J. F. Abere, *J. Polymer Sci.*, **15**, 537 (1955).
5. Marans, N. S., and R. P. Zelinski, *J. Am. Chem. Soc.*, **72**, 2125 (1950).
6. Marans, N. S., and R. P. Zelinski, *J. Am. Chem. Soc.*, **72**, 5330 (1950).
7. Butler, J. M. (to Monsanto Chemical Company), U. S. Pat. 2,720,512 (October 11, 1955).
8. Rehberg, C. E., and W. A. Faucette, *J. Org. Chem.*, **14**, 1094 (1949).
9. Rehberg, C. E., and W. A. Faucette, *J. Am. Chem. Soc.*, **71**, 3164 (1949).
10. Prager, J. H., R. M. McCurdy, and G. B. Rathmann, *J. Polymer Sci.*, in press.
11. Windus, W., and P. R. Shildneck, *Organic Syntheses*, Coll. Vol. II, Wiley, New York, 1943, p. 345.
12. Wiley, R. H., and G. M. Brauer, *J. Polymer Sci.*, **3**, 647 (1948).
13. Wiley, R. H., and G. M. Brauer, *J. Polymer Sci.*, **3**, 455 (1948).
14. Wood, L. A., *J. Polymer Sci.*, **28**, 319 (1958).
15. Wesson, L. G., *Tables of Electric Dipole Moments*, Technology Press, Cambridge, Mass.
16. Osborne, D. W., R. N. Doescher, and D. M. Yost, *J. Am. Chem. Soc.*, **64**, 196 (1946).
17. French, F. A., and R. S. Rasmussen, *J. Chem. Phys.*, **14**, 389 (1946).

18. Pitzer, K. S., *J. Chem. Phys.*, **12**, 310 (1944).
19. Kistiakowsky, C. B., J. R. Lacher, and F. Stitt, *J. Chem. Phys.*, **7**, 289 (1939).
20. Pace, E. L., and J. G. Aston, *J. Am. Chem. Soc.*, **70**, 566 (1948).

Résumé

On a préparé une série d'esters acryliques qui possèdent dans la chaîne latérale un atome de soufre du type éther, et on a effectué la polymérisation. On a trouvé les températures de transition vitreuse et les volumes de gonflement suivants: le polyacrylate de 3-thiabutyle T_g -60°C et 9% en volume de gonflement dans le milieu isoocetane-toluène 70/30; le polyacrylate de 3-thiapentyle -71°C , 31%; le polyacrylate de 4-thiapentyle, -65°C , 32%; le polyacrylate de 4-thiahexyle, -76°C , 36%; le polyacrylate de 5-thiahexyle -70°C , 36%. On a comparé ces valeurs à celles d'un certain nombre d'autres polyacrylates et on a étudié la relation entre la structure et les propriétés de ces matériaux.

Zusammenfassung

Eine Reihe von Acrylsäureestern mit einer Thioäthergruppierung in der Seitenkette wurde hergestellt und polymerisiert. Es werden folgende Glasumwandlungstemperaturen und Quellvolumina angegeben: 3-Thiabutylpolyacrylat T_g -60°C , 9% Volums-
quellung in einem 70:30 Isooctan-Toluolgemisch; 3-Thiapentylpolyacrylat -71°C , 31%; 4-Thiapentylpolyacrylat -65°C , 32%; 4-Thiahexylpolyacrylat -76°C , 36%; 5-Thiahexylpolyacrylat -70°C , 36%. Diese Daten werden mit denjenigen für gewisse andere Polyacrylate verglichen. Die Beziehung zwischen Struktur und Eigenschaften dieser Stoffe wird diskutiert.

Received January 22, 1963

Water Cocatalysis in the Polymerization of Benzene by Ferric Chloride*

PETER KOVACIC, FRED W. KOCH, and CHARLES E. STEPHAN,
Department of Chemistry, Case Institute of Technology, Cleveland, Ohio

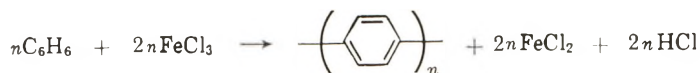
Synopsis

The influence of change in water cocatalyst concentration on polymer yield and composition, and on reaction rate was investigated in the benzene–ferric chloride system. For short reaction times, polymer yield passes through a maximum at a $\text{H}_2\text{O}/\text{FeCl}_3$ molar ratio of 1. The most rapid rate of hydrogen chloride evolution was observed at this same ratio. The data suggest that ferric chloride monohydrate constitutes the active catalyst–cocatalyst complex. With more prolonged reaction times, the yield maximum shifted to lower values of $\text{H}_2\text{O}/\text{FeCl}_3$, accompanied by a progressive increase in polymer yield. As evidenced by the $\text{C}/(\text{H} + \text{Cl})$ atomic ratio, *p*-polyphenyl formation is favored by short reaction times at $\text{H}_2\text{O}/\text{FeCl}_3$ ratios of 0, 1, and 2. Longer reaction times, gave $\text{C}/(\text{H} + \text{Cl})$ ratios greater than 1.5 for the polymer, indicating the presence of polynuclear structures. An increase in chlorine content attended the rise in $\text{C}/(\text{H} + \text{Cl})$ ratio. Interpretations of the data are presented.

INTRODUCTION

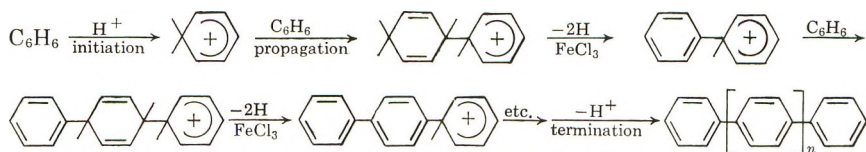
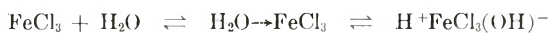
Recently, a new type of polymerization has been reported involving the system, aromatic monomer–Lewis acid catalyst–oxidant.¹ For example, benzene was converted under mild conditions to *p*-polyphenyl on treatment with aluminum chloride–cupric chloride.^{1,2} Molybdenum pentachloride³ and ferric chloride⁴ have also proved to be effective agents for the polymerization of benzene. In the case of these two salts, the metal halide apparently assumes the dual role of catalyst and oxidant, and, in addition, readily converts the initially formed *p*-polyphenyl to material containing polynuclear structures.

The evidence indicates that the initial reaction with ferric chloride proceeds according to the equation,⁴



* Paper V, Polymerization of Aromatic Nuclei; from the forthcoming Ph.D. thesis of F. W. Koch, and the B.S. thesis of C. E. Stephan, 1960.

It was shown previously that Brönsted acids, such as water, acetic acid, and nitroethane, exert a cocatalytic effect with ferric chloride.⁵ An oxidative cationic mechanism has been proposed for the polymerization.^{1,4}



This investigation concerns the influence of change in water cocatalyst concentration on polymer yield and composition, and on reaction rate in the benzene–ferric chloride system.

RESULTS AND DISCUSSION

Yield

Figure 1 illustrates the effect of change in the $\text{H}_2\text{O}/\text{FeCl}_3$ molar ratio and reaction time on polymer yield. The polymerizations were carried out at the reflux temperature under nitrogen with a $\text{C}_6\text{H}_6/\text{FeCl}_3$ molar ratio of 2. When the reactions were terminated at the end of 0.5 hr., the yield passed through a maximum at a $\text{H}_2\text{O}/\text{FeCl}_3$ ratio of 1. A similar result was observed with shorter periods of time (Table I). Since the reaction

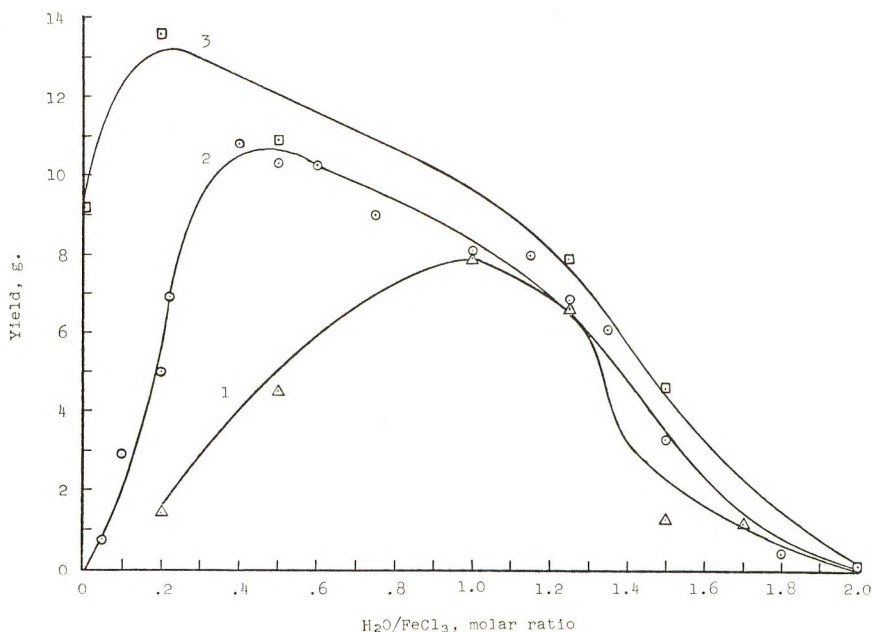


Fig. 1. Polymer yield vs. $\text{H}_2\text{O}/\text{FeCl}_3$; (1) 0.5 hr., (2) 2 hr., (3) 9–14 hr.

mixture is heterogeneous, the influence of metal halide particle size was investigated. Essentially the same type of curve was obtained with ferric chloride which had been subjected to blender action. Furthermore, hydrogen chloride was evolved at the most rapid rate with $\text{H}_2\text{O}:\text{FeCl}_3$ in 1:1 ratio (Fig. 2).

The data suggest that ferric chloride monohydrate constitutes the most active catalyst-cocatalyst complex. At the smaller ratios, the decreased

TABLE I
Polymer Yield and Composition

$\text{H}_2\text{O}/\text{FeCl}_3$, molar ratio	Time, hr.	Polymer yield, g.	Polymer analysis				C/ (H + Cl) molar ratio
			C, %	H, %	Cl, %	Fe, %	
0	28	9.12	75.05	1.96	20.15	0	2.47
	15	9.2	77.16	1.86	19.08	0	2.68
	2	0.13	85.08	3.89	8.78	0.24	1.71
0.05	2	0.77	82.94	2.88	12.86	0	2.13
0.1	2	2.8	80.52	2.27	14.48	1	2.50
0.2	14	13.8	79.96	2.22	16.92	0	2.47
	2	5.0	81.20	2.42	14.68	0.12	2.39
	0.5	1.45	83.79	2.98	11.16	0	2.12
	0.25	1.05	85.15	3.44	11.48	0	1.88
0.4	2	10.8	81.74	2.52	14.70	0.28	2.32
0.5	14	10.9	79.38	2.06	17.79	0.69	2.58
	2	10.5	81.36	2.50	15.12	0	2.32
	0.5	4.5	84.66	3.32	11.32	0	1.94
	0.083	3.15	86.60	3.87	9.46	0	1.74
0.6	2	10.3	82.76	2.64	14.15	0	2.27
0.75	2	9.2	82.70	2.83	12.96	0.06	2.16
1	2	8.12	84.23	3.43	11.35	0.02	1.87
	0.5	7.91	85.62	3.56	11.04	0	1.84
	0.25	6.54	86.46	3.74	8.75	0	1.80
	0.083	5.62	88.08	4.34	7.44	0	1.61
	0.017	5.0	88.56	4.72	6.50	0	1.50
	0.003	3.75	88.82	4.75	5.69	0	1.51
1.15	2	8.0	85.69	3.76	10.70	0	1.76
	0.017	2.65	88.36	4.32	7.06	0.63	1.62
1.25	14	7.9	82.88	3.50	10.14	0	1.82
	2	6.85	84.70	3.99	10.84	0	1.64
	0.5	6.71	87.10	4.09	8.37	0	1.67
	0.017	2.7	86.40	4.64	9.18	0	1.47
1.35	2	6.1	83.86	3.77	11.85	0	1.74
1.5	9	4.6	81.06	2.96	14.20	0	2.01
	2	3.3	81.22	2.80	14.03	0.17	2.11
	0.5	1.23	82.46	3.19	12.26	0.19	1.94
1.7	0.5	1.2	84.42	3.65	9.50	0.35	1.79
1.8	2	0.35	78.74	3.10	14.82	0.57	1.86
2	14	0.05	74.79	2.74	18.85	0	1.90
	2	0.13	75.98	3.11	15.16	2.3	1.79
	0.5	0.2	79.64	3.70	13.44	1.3	1.63

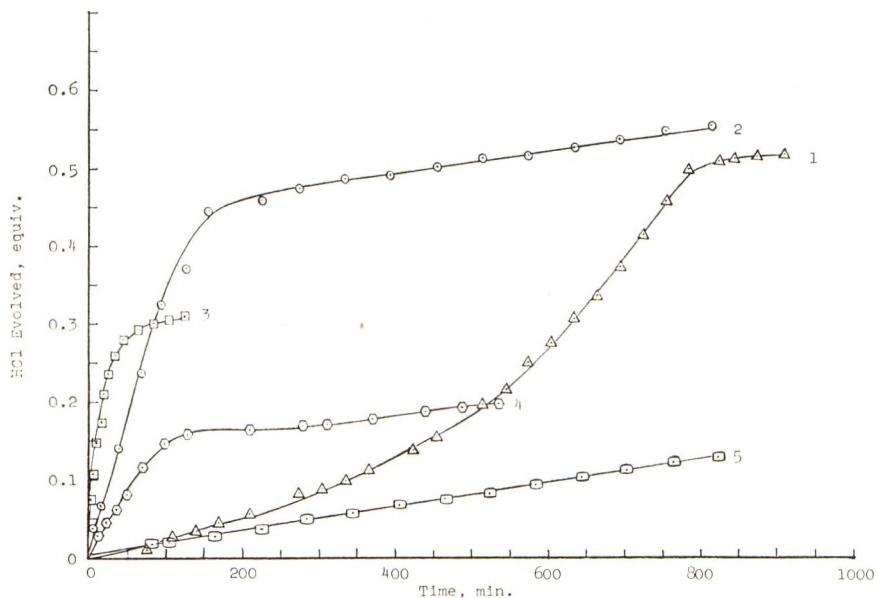


Fig. 2. Hydrogen chloride evolution as a function of time at various $\text{H}_2\text{O}/\text{FeCl}_3$ molar ratios: (1) 0, (2) 0.5, (3) 1, (4) 1.5, (5) 2.

polymer yield apparently derives from a lowered concentration of the active complex. It would seem that ferric chloride is converted to less active hydrates at the higher ratios. In comparison with the monohydrate, the polyhydrates should possess hydrogens of decreased acidity.

It is important to note that the position of the yield maximum shifts to lower values of $\text{H}_2\text{O}/\text{FeCl}_3$ with more prolonged reaction times. Simultaneously, this trend is accompanied by a progressive increase in the total yield of polymer. As reaction proceeds, more and more of the remaining unreduced ferric chloride would be converted to the inactive dihydrate form. Therefore, the greater the quantity of water in the system initially, the smaller is the amount of ferric chloride actually available for polymerization. With the lower concentrations of active catalyst, a longer time is required to attain maximum yield. It should be borne in mind that part of the weight increase in the long-term reactions is due to polynuclear formation and chlorination. The polymer yield data versus time correlate very nicely with the corresponding results for evolved hydrogen chloride.

Alternatively, one might suppose that water can effectively destroy ferric chloride by hydrolysis under the standard conditions. This hypothesis was discarded since only a very small amount of hydrogen chloride was generated from a mixture of ferric chloride (1 mole) and water (1 mole) in *o*-dichlorobenzene during 2 hr. at about 80°C .

The need for cocatalysis by water or other Brönsted acids is well established for many olefin-Lewis acid catalyst systems.^{6,7} The importance of the degree of solvation of the catalyst by the cocatalyst in the cationic

polymerization of olefins has been pointed out previously. For example, the idea was advanced by Pepper^{7b} and by Norrish and Russell⁸ that there is an optimum quantity of cocatalyst, and that additional amounts merely reduce the concentration of the active catalyst-cocatalyst complex through formation of less active, more highly solvated entities. Several experimental investigations contained in the literature provide support for these postulates. With a fixed quantity of water and increasing amounts of stannic chloride, the rate curve for isobutylene polymerization leveled out at approximately equimolar proportions of the catalyst and cocatalyst.⁸ Overberger, Ehrig, and Marcus⁹ determined the effect of variation in water concentration on rate in the polymerization of styrene by stannic chloride. In a 30/70% mixture of nitrobenzene and carbon tetrachloride, the rate increased as the concentration of water was increased, attaining a maximum at a 1:1 catalyst/cocatalyst molar ratio, and then decreasing with further addition of water. A similar result is reported for polymerization in the system, styrene-boron trifluoride-water.^{67a}

In a related area, Fairbrother and Frith^{10a} have provided evidence which suggests the existence of aluminum bromide monohydrate. Furthermore, water also appears to function as a cocatalyst in the Scholl reaction.^{10b}

Polymer Structure

The nature of the organic product varied with alteration in certain reaction variables, e.g., time and the $\text{H}_2\text{O}/\text{FeCl}_3$ molar ratio. When the reaction of benzene with ferric chloride (1:1) was carried out for a very

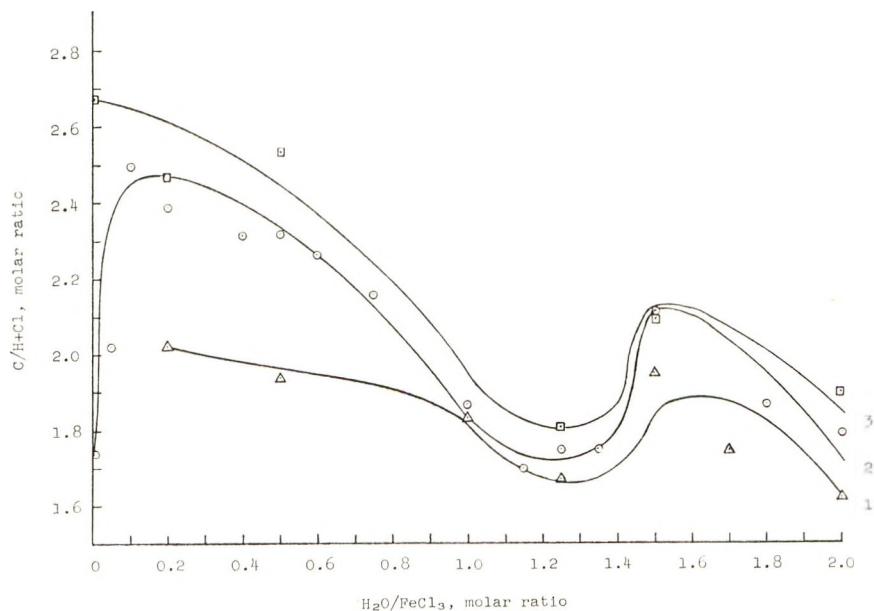


Fig. 3. Polymer $C/(H + Cl)$ vs. $\text{H}_2\text{O}/\text{FeCl}_3$; (1) 0.5 hr., (2) 2 hr., (3) 9-14 hr.

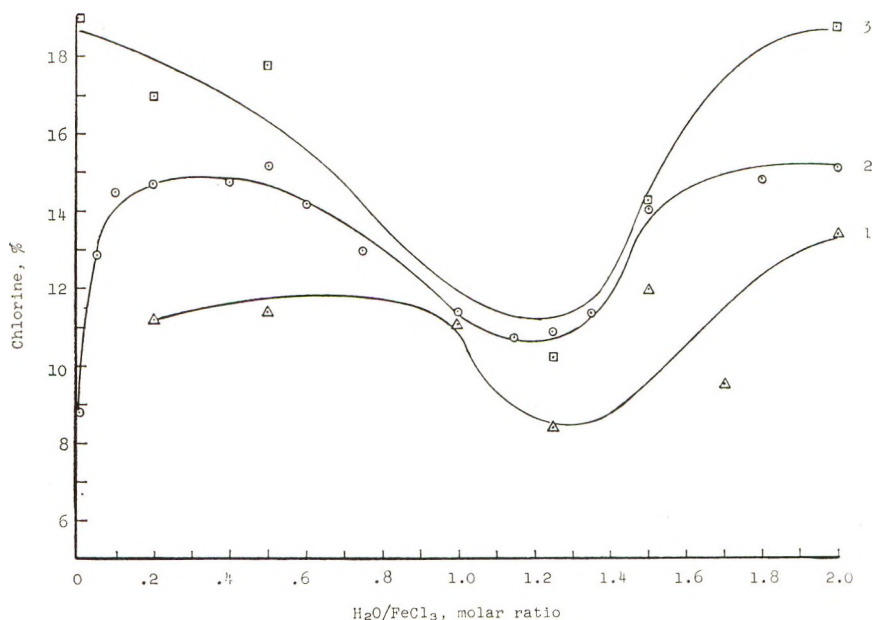


Fig. 4. Chlorine content of polymer vs. $\text{H}_2\text{O}/\text{FeCl}_3$; (1) 0.5 hr., (2) 2 hr., (3) 9-14 hr.

short period (< 1 min.) at the reflux temperature, *p*-polyphenyl was formed (Table I). The $\text{C}/(\text{H} + \text{Cl})$ atomic ratio of 1.5 is in excellent agreement with the limiting theoretical value of 1.5 for polyphenyl. The $\text{C}/(\text{H} + \text{Cl})$ atomic ratio is equal to the C/H ratio for the parent hydrocarbon on the assumption that chlorine is introduced by replacement of hydrogen. Therefore, this value provides information concerning the molecular weight and structure of the product. Characterization of the polymer by elemental analyses, infrared spectrum, x-ray diffraction pattern, pyrolysis products, and oxidative degradation is reported in detail elsewhere.⁴ The rust-colored product contained a small amount of chlorine, and possibly other structural irregularities, such as side-chains, crosslinks or polynuclear sites.

When the reaction time was increased to 2-14 hr. at the various water concentrations, the polymers became darker in color (black) and exhibited an increased $\text{C}/(\text{H} + \text{Cl})$ ratio (1.8-2.7) (Fig. 3). The data indicate the product now incorporates some polynuclear regions. There is evidence in support of the premise that the initially formed *p*-polyphenyl combines subsequently with benzene-ferric chloride in a reaction leading to polynuclear structures.⁴ Since treatment of *p*-polyphenyl with benzene-ferric chloride-water did not produce a product of increased $\text{C}/(\text{H} + \text{Cl})$ ratio, apparently water, at the level used, does not promote the *p*-polyphenyl transformation reaction.

The precise shape of the curves is difficult to interpret since the picture is a complicated one, with some facets little understood at present. Never-

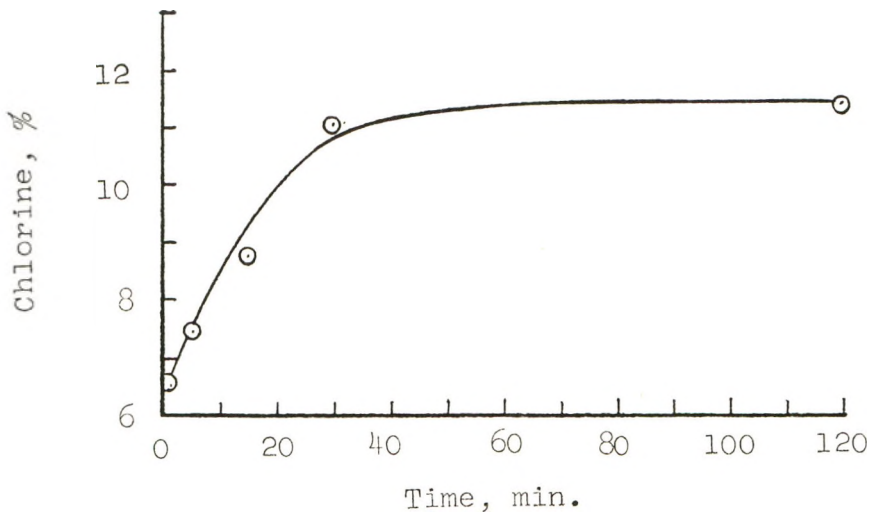


Fig. 5. Chlorine content of the polymer as a function of reaction time, $\text{H}_2\text{O}/\text{FeCl}_3$ molar ratio of 1.

theless, several working hypotheses have been formulated. Low $\text{C}/(\text{H} + \text{Cl})$ ratios are associated with those polymers formed in the rapid polymerizations, i.e., at the highest concentrations of the active catalyst-cocatalyst complex. Seemingly, the somewhat slower reactions permit subsequent conversion of the *p*-polyphenyl before the ferric chloride is consumed in the initial polymerization. For the two hour reactions, low $\text{C}/(\text{H} + \text{Cl})$ ratios are also identified with very slow rates (no added water and $\text{H}_2\text{O}/\text{FeCl}_3 = 2$). These correlations may arise from an unfavorable polymer concentration effect in relation to subsequent transformation of the *p*-polyphenyl. There is a greater degree of uncertainty associated with the analytical data for the low yield polymers since contaminant may now represent an appreciable per cent of the total.

The chlorine content varied from 5.7% for the product formed in the short-term reaction with ferric chloride-water (1:1) to 20.1% for the polymer obtained on prolonged heating with no added cocatalyst (Fig. 4). Since ferric chloride is known to halogenate aromatic compounds, the presence of chlorine is easily rationalized.¹¹ It is significant that the plots of chlorine content (Figs. 4 and 5) and $\text{C}/(\text{H} + \text{Cl})$ (Figs. 3 and 6) versus time and $\text{H}_2\text{O}/\text{FeCl}_3$ are very similar. Apparently, the increase in polynuclear composition is accompanied by a corresponding rise in the per cent chlorine. This correlation is understandable since, in general, a fused ring aromatic, e.g., naphthalene is more susceptible to substitution than the linear benzene analog, i.e., biphenyl.¹²

It should be noted that polymerization can be effected at room temperature provided the reaction is prolonged. The polymer produced displayed a $\text{C}/(\text{H} + \text{Cl})$ ratio of 2.28.

Attention was also devoted to the question of a possible relationship between water content and the nature and frequency of termination. In previous work which bears on this point, Biddulph and Plesch,¹³ as well as Russell,¹⁴ differentiated, on the basis of kinetic data,^{8,13} between the comparatively slow polymerization of isobutylene catalyzed by stannic chloride and the fast reaction induced by titanium tetrachloride. It was postulated that stannic chloride monohydrate is a very effective chain-terminating agent, but a poor initiator, whereas for the titanium tetrachloride complex, termination is relatively slow and initiation fast.¹³ For the polymerization of isobutylene by stannic chloride-water, the average molecular weight

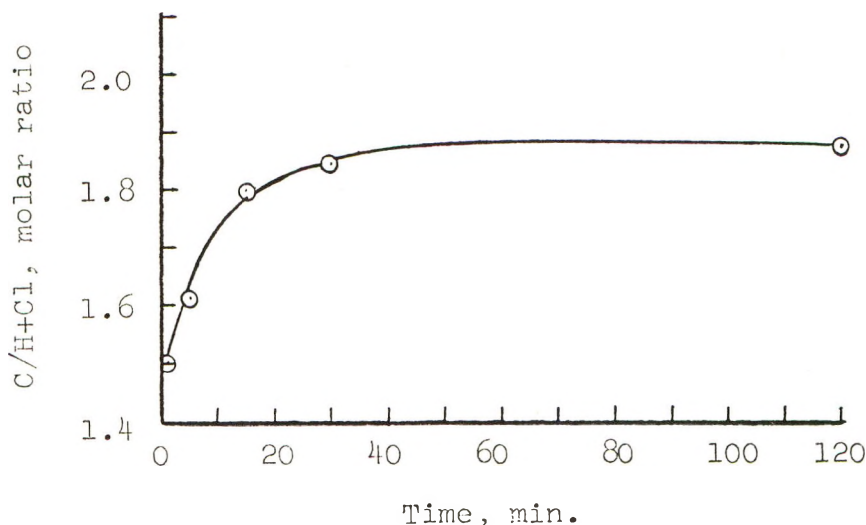


Fig. 6. Polymer $C/(H + Cl)$ as a function of reaction time, $H_2O/FeCl_3$ molar ratio of 1.

was almost inversely proportional to the amount of added water.⁸ Similarly, a decrease in polymer molecular weight with increasing water concentration was observed for polymerization effected either by stannic chloride⁹ or boron trifluoride.¹⁰

We were unable to obtain molecular weight data on the benzene polymer since the extreme insolubility precludes determination by the usual solution techniques. In the benzene polymerizations, water might participate in termination through solvation of the eliminated proton. On the other hand, oxygen could conceivably be incorporated by reaction of the growing carbonium ion with water. Unfortunately, because of the erratic results from oxygen analyses (0–3.7% range), no valid conclusions could be drawn. In some cases, the presence of small amounts of iron contaminant, possibly in oxide form, further complicates the situation, as does the increased susceptibility of the polynuclear polymer, *vis-à-vis* *p*-polyphenyl, to air oxidation at elevated temperatures.⁴

EXPERIMENTAL

Oxygen analyses (Unterzaucher indulin method) were performed by Geller Laboratories, Bardonia, N. Y., and the other elemental analyses by Drs. Weiler and Strauss, Oxford, Eng.

Materials

Benzene, reagent-grade, thiophene-free, Mallinckrodt Chemical Works, dried over sodium and redistilled; and ferric chloride, anhydrous reagent, sublimed powder, Matheson Coleman and Bell, or Fisher Scientific Co. were used.

Benzene and Ferric Chloride: General Procedure

Benzene (2 moles) and anhydrous ferric chloride (1 mole) were quickly weighed in air and placed in a 500-ml. flask equipped with a paddle stirrer. In those reactions involving a $\text{H}_2\text{O}/\text{FeCl}_3$ ratio of 0.05 or less, the apparatus was first flamed and the weighing, as well as the charging, was performed in a dry box.

Water cocatalyst was then added dropwise under nitrogen (sulfuric acid dried) with stirring and cooling below 25°C . The rate of addition and cooling were adjusted so that the temperature at the end was about 25°C . The reaction mixture was then heated to the reflux temperature during about 20 min. and kept at $79\text{--}81^\circ\text{C}$. for 2 hr. In certain cases the evolved gas was titrated with standard caustic.

After the mixture was quickly cooled and filtered, the residue was washed with benzene, stirred with dilute hydrochloric acid and ice, filtered, and triturated repeatedly with boiling hydrochloric acid until the filtrate was colorless. Following treatment with boiling 2*M* sodium hydroxide, the polymer was again triturated with boiling acid until the filtrate was colorless. Finally, the solid was washed with water until the filtrate was neutral, and then dried at $140\text{--}150^\circ\text{C}$. for 2–3 hr. Particular care was taken to avoid contamination.

For runs entailing extended or abbreviated times, the ferric chloride was weighed in a dry box. In the short term experiments, zero time was marked by the first sign of hydrogen chloride evolution if this occurred below the reflux temperature. Duplicate runs, made in almost all cases for the 2 hr. reactions, yielded data which checked satisfactorily, and for which the average values are listed. The results (averages) of the elemental analyses are tabulated in Table I.

In a modification of the standard procedure, the reaction mixture was stirred for 1 day at room temperature and then allowed to stand for 2 days. Work-up yielded 7.8 g. of polymer.

ANAL. Found: C, 86.54%; H, 2.98%; Cl, 9.88%.

The C/(H + Cl) ratio was calculated to be 2.28.

Benzene-Ferric Chloride-Water: Effect of Blending

A Ferric chloride (162 g.) was weighed out quickly in the air and mixed with benzene (100 g.) in a Waring blender for 2 min. After the mixture was placed in the reaction flask and cooled in an ice-water bath, water was added dropwise with stirring. The cold reaction mixture was blended for 2 min., additional benzene (56 g.) was added, and the reaction mixture was heated for 0.5 hr. as described in the general procedure. The data are summarized in Table II.

TABLE II
Benzene-Ferric Chloride-Water: Effect of Blending

H ₂ O/FeCl ₃ molar ratio	Polymer			C/(H + Cl), atomic ratio	
	Wt., g.	C, %	H, %		Cl, %
0.5	4.3	83.34	3.36	11.60	1.88
1	7.7	84.23	3.50	11.34	1.84
1.5	2.8	84.99	3.54	11.38	1.83

B Benzene (2 moles), ferric chloride (1 mole), and water (1 mole) were allowed to react for 0.5 hr. according to the standard procedure. Hydrogen chloride (0.23 mole) was evolved. The reaction mixture was cooled, mixed in a Waring blender for 3 min., and then reintroduced into the reaction flask. An additional 0.5 hr. of heating produced 0.04 mole of hydrogen chloride. Work-up yielded 7.9 g. of black powder.

p-Polyphenyl-Benzene-Ferric Chloride-Water

A mixture of *p*-polyphenyl² [4 g., C/(H + Cl) atomic = 1.47], benzene (156 g.), ferric chloride (162 g.), and water (36 g.) was stirred at reflux under nitrogen for 28 hr. Work-up gave a gray powder, 5.37 g.

ANAL. Found: C, 78.58%; H, 4.07%; Cl, 16.83%.

The data correspond to a C/(H + Cl) atomic ratio of 1.45.

Susceptibility of Ferric Chloride to Hydrolysis

A mixture of ferric chloride (162 g., 1 mole), water (18 g., 1 mole), and *o*-dichlorobenzene (294 g.) was heated at 80 ± 5°C. for 2 hr. according to the general procedure. Hydrogen chloride (0.013 mole) was evolved at a slow, almost constant rate.

We gratefully acknowledge support of this work by the National Science Foundation.

References

1. Kovacic, P., and A. Kyriakis, *Tetrahedron Letters*, **1962**, 467.
2. Kovacic, P., and A. Kyriakis, *J. Am. Chem. Soc.*, **85**, 454 (1963).
3. Kovacic, P., and R. M. Lange, *J. Org. Chem.*, **28**, 968 (1963).
4. Kovacic, P., and F. W. Koch, *J. Org. Chem.*, **28**, 1864 (1963).
5. Kovacic, P., and C. Wu, *J. Polymer Sci.*, **47**, 45 (1960).

6. Plesch, P. H., *Polymerisation and Related Complexes*, Heffer, Cambridge, England, 1953.
7. Pepper, D. C. (a) *Quart. Revs.*, **8**, 88 (1954); (b) ref. 6, p. 70.
8. Norrish, R. G. W., and K. E. Russell, *Trans. Faraday Soc.*, **48**, 91 (1952).
9. Overberger, C. G., R. J. Ehrig, and R. A. Marcus, *J. Am. Chem. Soc.*, **80**, 2456 (1958).
10. (a) Fairbrother, F., and W. C. Frith, *J. Chem. Soc.*, **1953**, 2975; (b) J. C., Earl, and W. A. Kable, *Chem. Ind.*, **1934**, 475.
11. Kovacic, P., C. Wu, and R. W. Stewart, *J. Am. Chem. Soc.*, **82**, 1917 (1960); Kovacic, P., and N. O. Brace, *ibid.*, **76**, 5491 (1954).
12. De La Mare, P. B. D., and J. H. Ridd, *Aromatic Substitution. Nitration and Halogenation*, Academic Press, New York, 1959, pp. 157, 176.
13. Biddulph, R. H., and P. H. Plesch, *J. Chem. Soc.*, **1960**, 3913.
14. Russell, K. E., ref. 6, p. 114.

Résumé

On étudie l'influence de la variation de concentration en cocatalyseur-eau sur le pourcentage et la composition du polymère, et sur la vitesse de réaction dans le système benzène-chlorure ferrique. Pour des courts temps de réaction le pourcentage de polymère passe par un maximum à un rapport molaire $H_2O/FeCl_3$ de 1. On observe à ce même rapport, la vitesse la plus rapide de formation d'HCl. Ces résultats indiquent que le chlorure ferrique monohydrate constitue le complexe catalyseur-cocatalyseur actif. Avec des temps de réaction plus longs, le pourcentage maximum recule vers de plus faibles valeurs de $H_2O/FeCl_3$, accompagné par une augmentation progressive du pourcentage polymérique. Comme le montre le rapport atomique $C/(H + Cl)$, la formation de *p*-polyphényle est favorisée par de faibles temps de réaction à des rapports $H_2O/FeCl_3$ de 0,1 et 2. De plus longs temps de réaction, particulièrement à d'autres concentrations en eau, donnent des rapports $C/(H + Cl)$ plus grands qu'à 1,5 pour le polymère, indiquant la présence de structures polynucléaires. Une augmentation dans le contenu en chlore provoque une augmentation dans le rapport $C/(H + Cl)$. On propose des explications de ces résultats.

Zusammenfassung

Der Einfluss der Konzentration von Wasser als Cokatalysator auf Polymerausbeute und -zusammensetzung und auf die Reaktionsgeschwindigkeit wurde am System Benzol-Eisen(III)-chlorid untersucht. Bei kurzer Reaktionsdauer ging die Polymerausbeute bei einem Molverhältnis $H_2O/FeCl_3$ von 1 durch ein Maximum. Bei diesem Verhältnis ist auch die Geschwindigkeit der HCl-Entwicklung am grössten. Diese Daten weisen drauf hin, dass der aktive Katalysator-Cokatalysator-Komplex Eisen(III)-chlorid-Monohydrat enthält. Bei längerer Reaktionsdauer verschiebt sich die Lage des Ausbeutemaximums unter fortschreitender Zunahme der Polymerausbeute zu kleineren Werten von $H_2O/FeCl_3$. Aus dem Atomverhältnis $C/(H + Cl)$ geht hervor, dass bei $H_2O/FeCl_3$ -Verhältnissen von 0, 1 und 2 durch kurze Reaktionsdauer die Bildung von *p*-Polyphenyl begünstigt wird. Längere Reaktionsdauer führte, besonders bei anderen H_2O -Konzentrationen, zu Polymeren mit $C/(H + Cl)$ -Verhältnissen grösser als 1,5, was die Anwesenheit vielkerniger Strukturen erkennen lässt. Die Erhöhung des $C/(H + Cl)$ -Verhältnisses war von einem Ansteigen des Chlorgehaltes begleitet. Eine Diskussion der Ergebnisse wird durchgeführt.

Received January 10, 1963

Light-Scattering Study of the Oxidative Degradation of Polystyrene*

JAMES C. SPITSBERGEN and HAROLD C. BEACHELL, *Department of Chemistry, University of Delaware, Newark, Delaware*

Synopsis

An investigation into the nature of the structural and molecular changes during the bulk oxidation of polystyrene has been conducted by light-scattering and viscometric methods. Oxidations were conducted on films in an air oven at 0, 2, 4, and 5 hr. at 200°C. The oxidized films were dissolved and various parameters obtained on the resulting solutions. Fractionation of unoxidized and oxidized thermally polymerized polystyrene showed a narrowing of the molecular weight distribution during oxidation. The weight-average molecular weight decreased from 1,090,000 to 33,000. That of an unfractionated commercial polystyrene, Styron 683K, decreased from 281,000 to 16,000. These results show that random chain scission of oxidized polymer occurs along with the formation of carbonyl groups giving polymer molecules of shorter chain length most of which probably retain the initial linear random coil structure. In addition to the chain scission, branching and crosslinking are indicated by the distortion of Zimm plots by microgel.

INTRODUCTION

Although the oxidation of polystyrene has received considerable study, little information is available pertaining to the structural changes which occur, previous studies having been concentrated on mechanism and rates of oxidation. This study presents the details of the changes which occur until the polymer no longer has useful commercial properties.

Previous to this study, the characterization of polystyrene oxidized in bulk or film phase was limited to viscometric studies.^{1,2} Although the large viscosity reductions obtained at 200°C. and above are indicative that chain scission occurs, they cannot be considered as conclusive inasmuch as viscosity measures only the size and shape of molecules and not the molecular weight. Factors such as branching, a decrease in polydispersity, or the lower solubility of the oxidized product would also reduce viscosity. Certainly no clear picture can be obtained, since these latter effects can be combined with chain scission to obscure the overall structural changes. Light scattering, since it is an absolute method of determining molecular weight, gives a clearer picture of these changes.

* Taken in part from the Ph.D. Dissertation of James C. Spitsbergen, submitted to the faculty of the University of Delaware, June 1962.

EXPERIMENTAL

Instrumentation

For the light-scattering determinations a Brice-Phoenix light-scattering photometer, Series 1440, was used. The shielded signal from the photomultiplier tube was amplified by a Leeds and Northrup Model 9835B amplifier, the output of which was sent to a Varian G-10 recorder. A Sorensen Model 100 voltage regulator controlled all input power lines.

The instrument was calibrated by using the standard opal provided. The calibration was checked by using, as a secondary standard, freshly filtered thiophene-free benzene. The benzene had been first distilled to separate from impurities, the fraction boiling at $80.1 \pm 1^\circ\text{C}$. collected, and then slowly redistilled without boiling to separate from dust. An average value for Rayleigh's ratio of 48.8×10^{-6} at 28°C . for unpolarized light of 4358 Å. was obtained with the large dissymmetry cell (D-101). Optical alignment was checked and adjusted according to the recommendations of the manufacturer.³

The solutions were measured using vertically polarized light of 4358 Å. wavelength in the cylindrical cell designed by Witnauer and Scherr.⁴ It had been found to be symmetrical from 35° to 135° by Carlson.⁵ This was confirmed by the constancy of the turbidity of benzene from 35° to 135° except for higher values around 100° caused by reflections from the edge of the small cell table diaphragm.

For the determination of the refractive index increment, dn/dc , a differential refractometer designed by Dr. F. W. Billmeyer was used. The light source was an AH-1 mercury lamp equipped with a filter which passed only the 4358 Å. wavelength. The differential cell was housed in a metal compartment which was held at a constant temperature of $28 \pm 0.05^\circ\text{C}$. by means of a doubly wound mantle. The instrument was calibrated by the method of Halwer.⁶ The value of dn/dc for polystyrene in benzene was found to be 0.113 ± 0.002 ml./g. which compares well with typical literature values of 0.1117 and 0.1151.⁸ The determination was made on the undiluted solutions.

For viscometry a size 25 Ubbelohde dilution viscometer was used. The temperature was held at $28 \pm 0.03^\circ\text{C}$. It was necessary to use nitrogen pressure which was passed through sintered glass for dilution and raising the liquid level to eliminate dust. The determination was made by diluting the highest concentration of polymer after the light-scattering determinations were made. The flow time exceeded 300 sec. for the solvent.

The infrared spectra were run on a Perkin-Elmer Model 421 spectrophotometer using films cast on rock salt.

Clarification

Benzene was doubly distilled and filtered through clean Selas FD 54 grade 03 porous porcelain filter candles, under no greater than 2 psi pres-

sure of nitrogen. Polymer solutions were filtered similarly in separate filter devices. Before an undiluted solution was filtered benzene was passed through the filter five to ten times until the scattering envelope from 30° to 135° was within 1% of the same benzene which had been filtered through the filter reserved for benzene. Solvent and solution were inspected in a cleaned cell at a low angle to an intense beam of light from a mercury lamp with a strong lens to determine effectiveness of filtration. Generally, only a few notes could be observed.

In certain cases where sufficient clarification was not possible with filtration, it was found necessary to ultracentrifuge. In this case a Beckman-Spinco ultracentrifuge, Model L was used. The solvent or solution was centrifuged an average of 55,000 or 151,000G for 4–5 hr. in stainless steel tubes with aluminum caps sealed with polyvinyl alcohol gaskets. The centrifuged liquid was transferred by means of a syringe to the cell.

Method of Oxidation

The oxidation studies consist of two parts: (1) the oxidation of an unfractionated commercial polystyrene, Styron 683K, manufactured by the Dow Chemical Company, Midland, Michigan, and (2) a thermally polymerized polystyrene which was fractionated before and after oxidation.

1. Styron 683K. A polymer solution of 0.5 g./100 ml. was made, filtered, and divided into 50 ml. portions. These 50 ml. portions were placed in dust-free 100 ml. beakers and covered with glass fiber filter paper which had been washed with benzene. The filter paper was fastened securely with copper wire to prevent entry of dust. The solutions, along with a benzene control, were heated to 70°C. to evaporate the benzene slowly, resulting in the formation of a thin film. The beakers were placed in a Precision Scientific circulating air oven at $200 \pm 3^\circ\text{C.}$ for 0, 2, 4, and 5 hr. After cooling the films were dissolved overnight in benzene. Each solution was then transferred to a 50 ml. volumetric flask, the beaker rinsed several times with benzene, the rinsings combined with the solution, and the flask made up to the mark.

The value of the photometer constant a was found before the determination of data for each oxidation. The value of R_{90} was checked for the benzene used to dilute each solution. The same benzene was used for all dissolving and diluting for the same solution. The value for the highest of four concentrations was determined first, followed by dilution in the cell. The solute turbidities were determined by subtracting the proportionally averaged turbidities of the control and dilution benzene from the apparent turbidities. The depolarization values were calculated similarly, except that the subtraction was made using the arbitrary intensities obtained.

Infrared spectra on films cast on rock salt from the solutions showed the expected formation of carbonyl in the oxidized polymer. To obtain better control over thickness so that a differential analysis could be made between oxidized and unoxidized Styron 683K, films were cast by placing a few drops of 10% Styron 683K in benzene on a flat plate and sliding a mandrel

with an indentation over the drops. In this manner films of 0.022 ± 0.001 mm. thickness could be cast. The films were transferred to rock salt and placed in a vacuum oven at 95°C . overnight to remove the solvent. One of these films was oxidized in the air oven for 2 and 4 hr. A progressively larger carbonyl band absorption was easily detected with $5\times$ expansion. A sufficiently even thickness could not be obtained, however, to determine definitely whether any other changes occurred.

2. Thermally Polymerized Polystyrene. Polystyrene was prepared by polymerizing freshly distilled styrene, which had been sealed under nitrogen in approximately 100 ml. reaction tubes, in a constant temperature bath set at $78.9 \pm .05^{\circ}\text{C}$. for 168 hr. The polystyrene was obtained as a mixed granular and fibrous white product which was vacuum-dried at 95°C . to constant weight. In general, the procedure recommended by Sorenson was followed.⁹

Since fractionation was planned the method used for the Styron 683K was not practical. In this case an approximately 2.5 g. sample was placed in a four-liter beaker and dissolved in 250 ml. of singly distilled benzene. The benzene was slowly evaporated so that a clear film was cast on the bottom of the beaker of approximately the same thickness as previously. The beaker was then covered with a watch glass and oxidized as previously. After oxidation the brittle film, now a light yellowish tan, was redissolved in 250 ml. of singly distilled benzene and fractionated.

For the fractionation, the method of Hall¹⁰ was generally followed, the main deviation being that precipitated polymer was separated by removing the supernatant layer through a filter stick. A viscous, gelatinous precipitate was obtained for the unoxidized polymer, whereas for the oxidized polymer the precipitate was mostly in the form of a transparent, oillike film. The precipitate was reprecipitated with methanol, filtered, washed and dried to constant weight. A total of eight fractions was obtained. The final fraction was obtained by evaporating the supernatant layer from the seventh fraction by means of a vacuum and slight heating. The unoxidized polymer fractions were obtained as a white, essentially granular, product, while the fractions obtained from the oxidized polymer, although slightly cream-colored when precipitated, gradually became a mixture of cream to very light yellowish to greenish-tan lumps as they were dried.

The light-scattering data were obtained in the same manner as the Styron 683K except that the dilutions were made in volumetric flasks, each dilution being clarified by filtration before it was placed in the cell. Further, the concentration was determined by weight. Five of the oxidized fractions were clarified by ultracentrifugation.

DISCUSSION OF RESULTS

The first part of this study concerns the measurement of the structural changes in unfractionated Styron 683K. From the turbidity and depolarization measurements the weight-average molecular weight \bar{M}_w , the root-

TABLE I
Oxidation of Styron 683K: Experimental Results from Light Scattering

Time at 200°C., hr.	Zimm method			Dissymmetry method		Intrinsic viscosity, dl./g.
	$\bar{M}_w \times 10^{-6}$	$\bar{s}_z^2 \times 10^{-5}, \text{A}^2$	$\bar{s}_w^2 \times 10^{-5}, \text{A}^2$	$A_2 \times 10^4$	$\bar{M}_w \times 10^{-5}$ $(\bar{r}_w^2)^{1/2}, \text{A}.$	
0*	2.86	0.985	0.660	5.90	2.81	0.860
0	2.90	0.940	0.625	5.82	2.81	0.850
2	1.88	0.580	0.385	6.54	1.96	—
2	1.83	0.530	0.355	6.06	1.91	0.650
4	0.46	0.12	0.078	9.6	0.53	0.239
4	0.36	0.086	0.057	13	0.40	0.186
5	0.18	—	—	33	0.23	0.127
A. Covered with filter paper; unfiltered after oxidation						
4	0.53	0.13	0.089	9.0	0.54	0.269
4	0.35	0.060	0.040	7.3	0.38	0.197
5	0.25	—	—	29	0.26	0.142
B. Covered with filter paper; filtered after oxidation						
4	0.15	—	—	13	0.16	0.112
4	0.16	—	—	14	0.17	0.121
C. Not covered with filter paper; filtered after oxidation						

* Unevaporated; Zimm plot determined with three angles.

mean-square z -average radius of gyration $(\bar{s}_z^2)^{1/2}$, and the second virial coefficient A_2 were determined by Zimm plots.¹¹ Further, by making an assumption as to the breadth of the molecular weight distribution and further assuming that the polymer has a generalized exponential distribution of molecular weights, $(\bar{s}_w^2)^{1/2}$, the root-mean-square weight-average radius of gyration, was calculated. A further assumption of a linear chain with random configurations obeying Gaussian statistics allowed calculation of $(\bar{r}_w^2)^{1/2}$, the root-mean-square end-to-end distance.¹²

Comparison of the results given in Table I shows not only the occurrence of considerable chain scission but also, by the increase in the second virial coefficient, an increase in the solubility in benzene. This trend continues over the whole oxidation period studied thus definitely showing that chain scission is the main structural change which occurs.

In addition to the results by the Zimm method the same parameters were calculated by the dissymmetry method. In this case the intercept of the $\theta = 90^\circ$ line of the Zimm plot with the $\sin^2 \theta/2 + 100c = 0.5$ ordinate is equal to $1/\bar{M}_w P(\theta)$. The factor $P(\theta)$ was determined from the tables of Beattie and Booth¹² by taking the value for the intrinsic dissymmetry $[f_z]$ corresponding to the estimated polydispersity of $b = 1.0$ and assuming a linear coil with a random configuration. The intrinsic dissymmetry was determined by the method of Cleverdon,¹³ which consists of an extrapolation of f_z to zero turbidity of a plot of f_z versus solute turbidity.

As the oxidation proceeds past 2 hr. the Zimm plots become distorted. \bar{M}_w values calculated from the final slopes of the distorted Zimm plots show that the molecular weight of the main component continues to decline from chain scission. The method of calculation will be discussed later.

Filtration of the oxidized polymer was avoided so that if large crosslinked particles were formed they would not be removed and thus undetected. Since even with the greatest of care a certain amount of dust enters the solution several comparisons of unfiltered and filtered solutions of oxidized polystyrene were made. Actually the increase in turbidity of the control benzene over freshly filtered benzene was only 0 to 3% even at an angle of 30° . The results in part B of Table I show that, although the amount of distortion was reduced slightly, filtration does not change the results. Another important fact revealed by the unfiltered runs was that dn/dc remains constant during the oxidation. Apparently whatever increase in refractive index that occurs by incorporation of the polar carbonyl groups is balanced by the lower molecular weight.

In part C of Table I are shown results of oxidations conducted without a filter paper cover. These results show that the filter paper retarded the oxidation rate slightly.

In Table II the values for various ratios which would remain constant if no structural change other than scission occurred are shown. However, \bar{M}_w/\bar{r}_w^2 would remain constant only in a theta solvent. Otherwise, the ratio \bar{M}_w/\bar{r}_w^2 normally increases with a decrease in molecular weight since the probability that segments will occupy an already filled space will

TABLE II
 Oxidation of Styron 683K: Theoretical Calculations

Time at 200°C., hr.	Zimm method				$\phi \times 10^{-21}$ (Dissymmetry method)
	$\frac{\bar{M}_w}{\bar{v}_w^2}$	$\phi \times 10^{-21}$	$\frac{A_2 \bar{M}_w}{[\eta]}$	$\frac{A_2 \bar{M}_w^2}{(\bar{v}_w^2)^{3/2}}$ $\times 10^{-24}$	
A. Covered with filter paper; unfiltered after oxidation					
0 ^a	0.727	1.8	2.0	5.2	2.1
0	0.770	2.0	2.0	5.7	2.0
2	0.817	2.0	1.9	5.6	1.9
2	0.865	2.2	1.7	5.6	1.8
4	1.1	2.0	1.8	5.4	0.52
4	1.1	1.9	2.5	7.2	0.45
5	—	—	4.7	—	0.80
B. Covered with filter paper; filtered after oxidation					
4	1.0	2.2	1.7	5.7	0.44
4	1.5	3.4	1.3	6.5	0.43
5	—	—	4.9	—	0.37
C. Not covered with filter paper; filtered after oxidation					
4	—	—	1.7	—	0.27
4	—	—	1.9	—	0.29

^a Unevaporated; Zimm plot determined with three angles.

decrease with molecular weight. These values were calculated from the results in Table I. The results for each oxidation run are in the same vertical order as Table I. The constants θ and $A_2 \bar{M}_w^2 / (\bar{v}_w^2)^{3/2}$ have been corrected for an assumed polydispersity of $b = 1$ by the method of Shultz.¹⁴ Flory's θ and the ratio $A_2 \bar{M}_w^2 / (\bar{v}_w^2)^{3/2}$ are shown to remain constant. The value of θ will increase either if branched molecules are formed or if there is a decrease in polydispersity.¹⁵ Although its constancy appears to indicate that as the oxidation proceeds there is no change in polydispersity, it will be shown later that a decrease occurs. The decrease in θ for the dissymmetry method reflects the effect of distortion on the dissymmetry ratio. It shows the hazards of calculating coil dimensions by this method. The ratio $A_2 \bar{M}_w / [\eta]$ appears to increase as the oxidation proceeds past 5 hr. This seems to reflect a change in the solubility or shape characteristic of the oxidized molecule.

A limited attempt was made to measure the polydispersity by the viscometric method of Frisch and Lundberg.¹⁶ In their relation the polydispersity, which equals $(\bar{M}_w / \bar{M}_n) - 1$, is obtained from $\delta_{\tau,s} = (\bar{M}_{v(\tau)} / \bar{M}_{v(s)} - 1$ where $\bar{M}_{v(\tau)}$ and $\bar{M}_{v(s)}$ are the molecular weight in the solvents with the higher (benzene for the present study) and the lower (2-butanone) values, respectively, for a in the relation $[\eta] = KM^a$. The viscosity-molecular weight relationships as determined by Ewart and Tingey given by Boundy and Boyer¹⁷ of $[\eta] = 0.97 \times 10^{-4} \bar{M}_v^{0.74}$ and $[\eta] = 3.06 \times$

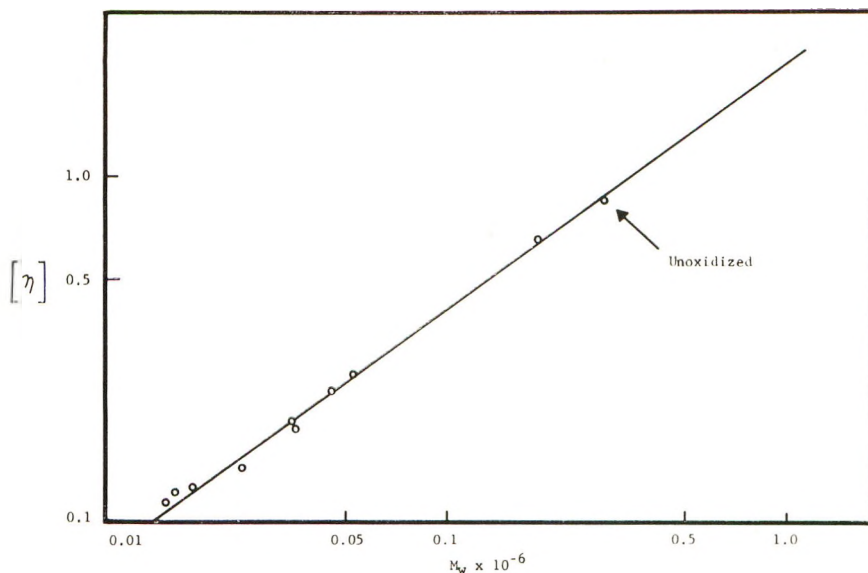


Fig. 1. Viscosity-molecular weight relationship for oxidized Styron 683K.

$10^{-4}\bar{M}_v^{0.60}$ were used for the calculation of $\bar{M}_{v(r)}$ and $\bar{M}_{v(s)}$, respectively. For 2 hr. at 200°C. \bar{M}_w/\bar{M}_n was calculated to be 3.2, which seems to be high. For 5 hr. at 200°C. an impossible negative value was obtained. Apparently the method does not apply in this case.

A viscosity-molecular weight plot of the data shown in Figure 1 gives a

TABLE III
Oxidation of Thermally Polymerized Polystyrene: Experimental Results

Frac- tion	Light scattering (Zimm method)				A_2 $\times 10^4$	Intrinsic viscosity, dl./g.
	\bar{M}_w $\times 10^{-6}$	\bar{s}_z^2 $\times 10^{-6}, A.^2$	\bar{s}_w^2 $\times 10^{-6}, A.$	$(\bar{r}_w^2)^{1/2}$, A.		
Unoxidized						
E-1	2.50	0.738	0.681	2010	5.11	3.79
E-2	1.54	0.345	0.318	1380	4.52	3.70
E-5	0.976	0.222	0.205	1110	4.97	2.56
E-7	0.503	0.105	0.0968	760	5.40	1.73
Oxidized 4 hr. at 200°C.						
F-1 ^a	0.097	0.013	0.012	270	2.5	0.376
F-2	0.057	0.0040	0.0037	150	8.1	0.273
F-3 ^a	0.061	0.012	0.011	260	7.0	0.257
F-3	0.042	—	—	—	7.4	0.239
F-4	0.033	0.0035	0.0032	140	8.8	0.194
F-6	0.016	—	—	—	13.3	0.128
F-7 ^a	0.017	—	—	—	10	0.112

^a Values determined by extrapolation of final slopes of Zimm plots.

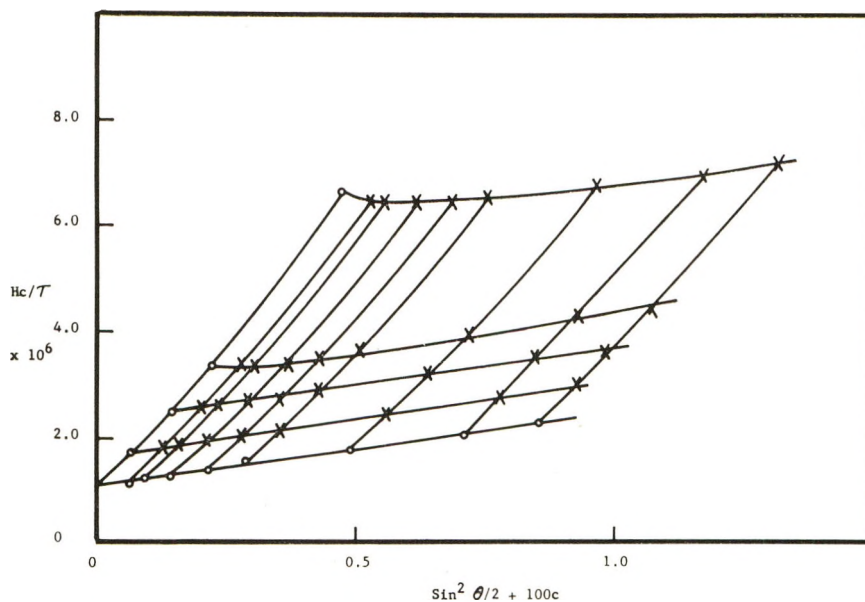


Fig. 2. Zimm plot for fraction E-5 of unoxidized polystyrene.

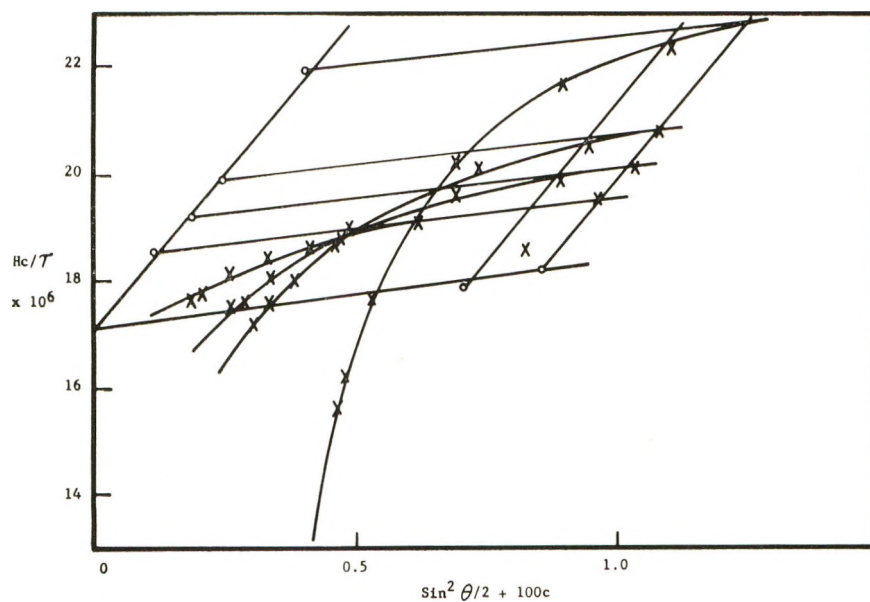


Fig. 3. Zimm plot for fraction F-3 of oxidized polystyrene.

straight line, indicating that essentially no long-chain branching occurs. The equation for the line is $[\eta] = 1.0 \times 10^{-4} \bar{M}_w^{0.72}$.

The oxidation of the thermally polymerized polystyrene (hereafter referred to as polystyrene) was conducted without the filter paper cover so that the retardation effect would not occur in order that the results

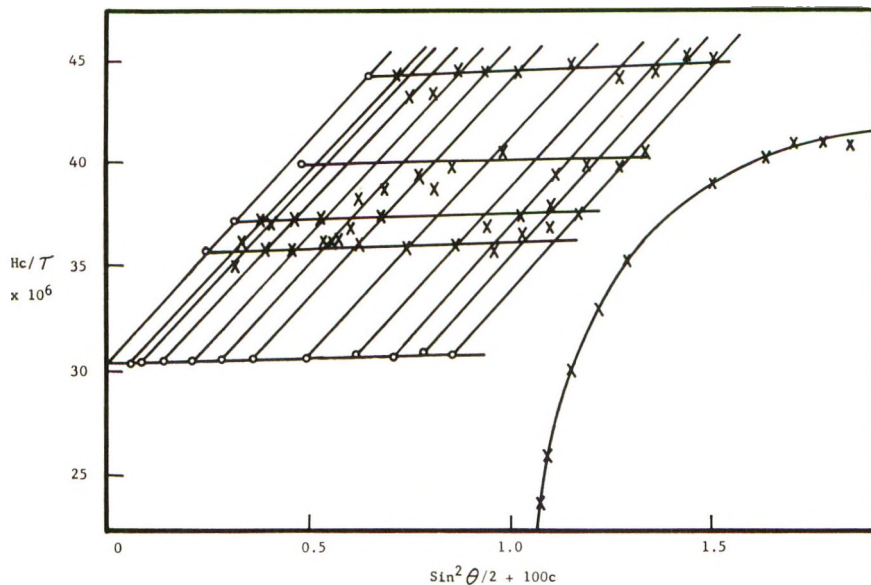


Fig. 4. Zimm plot for fraction F-4 of oxidized polystyrene clarified by ultracentrifugation at 151,000G; curved line denotes ultracentrifugation at 55,000G.

would be comparable with most film studies where the polymer is openly exposed. The calculations and methods were the same except for the method of dilution and in a few cases the method of clarification. The experimental results are shown in Table III. Comparison of the results shows the considerable chain scission that occurs. The results for each fraction have been derived from the Zimm plots as previously. For the unoxidized polymer normal plots were obtained. A typical plot is shown in Figure 2.

Figure 3 is a typical distorted Zimm plot caused by the presence of microgel in the oxidized polystyrene. These distorted plots are similar in shape to those obtained by others.^{18,19} Also shown are the extrapolations of the final slopes to obtain the molecular weight and radius of gyration. These, of course, are not as accurate as a complete Zimm plot. A less distorted Zimm plot was obtained for fraction F-7 which had been clarified by ultracentrifugation in the size 30 rotor with an average gravitational force of 55,000G. This resulted from less microgel in the fraction since the same conditions of centrifugation had little effect on fraction F-4. It was only by ultracentrifugation at an average 151,000G with the size 50 rotor that conditions were sufficient to remove the distorting particles.

Peebles¹⁸ and Muus and Billmeyer,¹⁹ who in their studies of polyacrylonitrile and polyethylene, respectively, had similar results, attribute the distortion to the presence of microgel. The scattering from spherical particles such as microgel no longer follows the Rayleigh-Gans relation,

$$Hc/\uparrow = 1/MP(\theta)$$

TABLE IV
Oxidation of Thermally Polymerized Polystyrene: Theoretical Calculations

Fraction	$\frac{\bar{M}_w}{\bar{r}_w^2}$	$\phi \times 10^{-21}$	$\frac{A_2 \bar{M}_w}{[\eta]}$	$\frac{A_2 \bar{M}_w^2}{(\bar{v}_w^2)^{3/2} \times 10^{-24}}$
Unoxidized polystyrene				
E-1	0.617	1.0	4.0	5.7
E-2	0.785	2.1	1.9	5.8
E-5	0.807	1.8	1.9	5.0
E-7	0.867	2.0	1.6	4.5
Oxidized polystyrene				
F-1 ^a	1.2	1.8	0.6	1.5
F-2	2.5	4.8	1.7	11
F-3 ^a	0.9	0.9	1.7	2.2
F-3	—	—	1.4	—
F-4	1.7	2.4	1.5	5.1
F-6	—	—	1.7	—
F-7 ^a	—	—	1.5	—

^a Values determined by extrapolation of final slopes of Zimm plots.

when $nD/\lambda > 0.26$, where D is the diameter (750 Å. in diameter under the present experimental conditions). When the diameter is larger than this, the dissymmetry of the scattering envelope is greater than what the Rayleigh-Gans relation predicts. Since the diameter of microgel can be well above this, it is assumed then that microgel is causing the distortion. The presence of microgel in the polyacrylonitrile solutions of Peebles has been confirmed by Heyn with electron micrographs.²⁰

With the elimination of the microgel, which represents only a small part of the polymer present, the normal Zimm plot shown in Figure 4 was obtained. Due to limited material and low molecular weight, it was not possible to obtain a sufficient turbidity so that individual points are somewhat scattered. Also a slightly higher dust level than usual was present for this determination due to the difficulties in transferring from the six small stainless steel tubes which were necessary in order to have a sufficient volume of polymer solution for measurements. In two cases sufficient dust was present to cause curvature in two of the concentration lines as an angle of 30° was approached. Since one of these cases occurred for the lowest concentration, the solution was reclarified by filtration. This removed the dust and consequently the curvature. The sharply curved line is a determination on a concentration which was clarified at 55,000G. It clearly shows the increased force necessary to remove the microgel. It further indicates that the amount of microgel originally present in fraction F-7 was less than for the other fractions. Ultracentrifugation at 151,000G of fractions F-2, F-6, and part of F-3 along with filtration of every dilution before placing it in the cell gave normal Zimm plots. In the case of Styron 683K the amount of distortion was slight compared to polystyrene.

TABLE V
Data and Calculations for the Determination of Integral and Differential Molecular Weight Distribution Curves^a

Fraction	Wt., g.	Cumulative % original	w_x	W_x	$\bar{M}_w \times 10^{-6b}$
Unoxidized polystyrene, $\Sigma w_x \bar{M}_w = 1.09 \times 10^6$					
E-1	0.4946	19.01	0.1889	1.0000	2.15
E-2	0.3194	31.28	0.1220	0.8110	1.54
E-3	0.2147	39.53	0.0810	0.6891	1.29
E-4	0.2546	49.32	0.0972	0.6074	1.12
E-5	0.2776	59.99	0.1060	0.5099	0.976
E-6	0.2626	70.08	0.1003	0.4040	0.755
E-7	0.3962	85.30	0.1512	0.3037	0.503
E-8	0.3992	100.64	0.1524	0.1524	0.195
Oxidized polystyrene, $\Sigma w_x \bar{M}_w = 0.033 \times 10^{-6}$					
F-1	0.2396	8.71	0.0911	1.0000	0.072
F-2	0.2113	16.39	0.0803	0.9089	0.055
F-3	0.4154	31.49	0.1579	0.8286	0.042
F-4	0.5148	50.20	0.1956	0.6707	0.033
F-5	0.1845	56.91	0.0701	0.4750	0.027
F-6	0.3206	68.56	0.1218	0.4049	0.023
F-7	0.2472	77.54	0.0940	0.2831	0.018
F-8	0.4975	95.63	0.1891	0.1891	0.012

^a w_x is the weight fraction of each fraction; W_x the cumulative weight fraction.

^b Values for \bar{M}_w have been interpolated from the integral distribution curve.

The results shown in Table V for the molecular weight and radius of gyration show the same trend as the Styron 683K. The extent of degradation, however, seems to be greater for the polystyrene. The results on ultracentrifuged fractions show that the molecular weights obtained from the distorted plots are somewhat high.

In Table IV are shown the various ratios calculated from the results in Table III. For these results the correction for polydispersity was not made since the polymer had been fractionated. If the correction had been made the values of ϕ for the unoxidized polystyrene would be fairly close to the theoretical 2.5×10^{21} . Fraction E-1 is, however, out of line. Similar results were obtained by the dissymmetry method for unoxidized fractions. The results for ultracentrifuged fractions should be considered the most reliable. Although the oxidized fractions generally show the same values for $A_2 \bar{M}_w / [\eta]$, the ratio \bar{M}_w / \bar{r}_w^2 has increased over the unoxidized value. Although the latter can reflect branching, this branching effect may be obscured by the decrease in polydispersity which will be shown to have occurred. In the case of fraction F-2, a sizeable increase in ϕ , \bar{M}_w / \bar{r}_w^2 , and $A_2 \bar{M}_w^2 / (\bar{s}_w^2)^{3/2}$ has occurred, which indicates that the oxidized polystyrene is branched.

In Figure 5 is shown the integral distribution curves for unoxidized and oxidized polystyrene and in Figure 6 the differential distribution curves.

These curves, which are approximations, show a narrowing of the molecular weight distribution with chain scission as predicted by theory for random chain scission.² The curves were drawn from the data shown in Table V. The 96% loss of the oxidized polystyrene represents normal loss

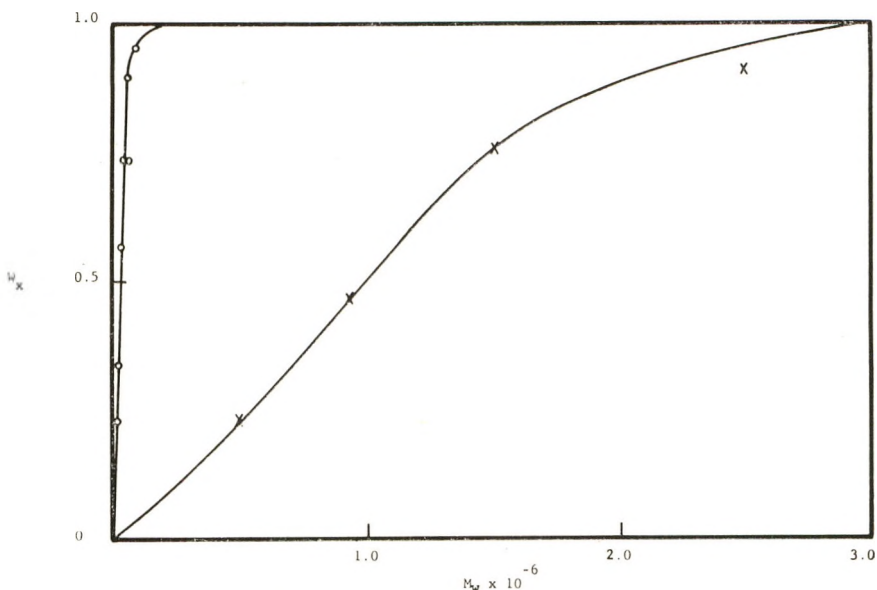


Fig. 5. The integral molecular weight distribution curve for polystyrene: (X) unoxidized; (O) oxidized.

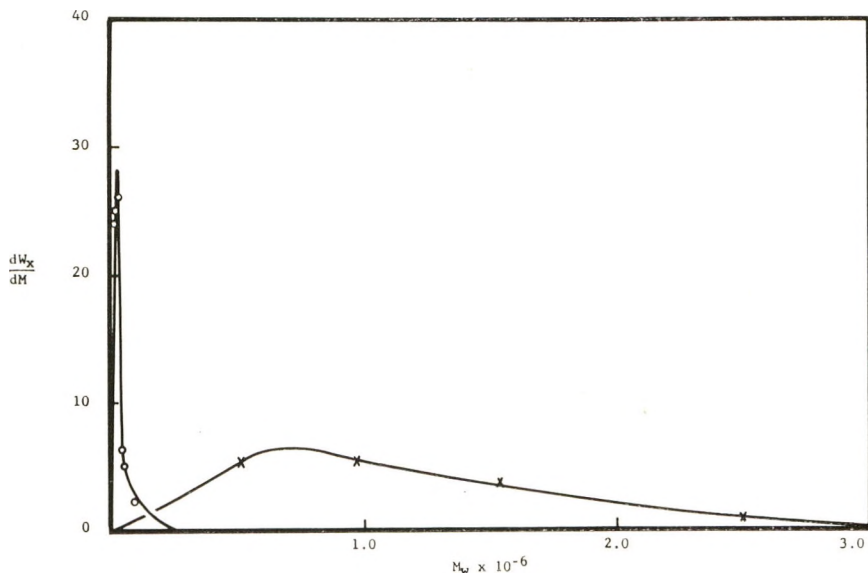


Fig. 6. The differential molecular weight distribution curve for polystyrene: (X) unoxidized (ordinate $\times 10^7$); (O) oxidized (ordinate $\times 10^6$).

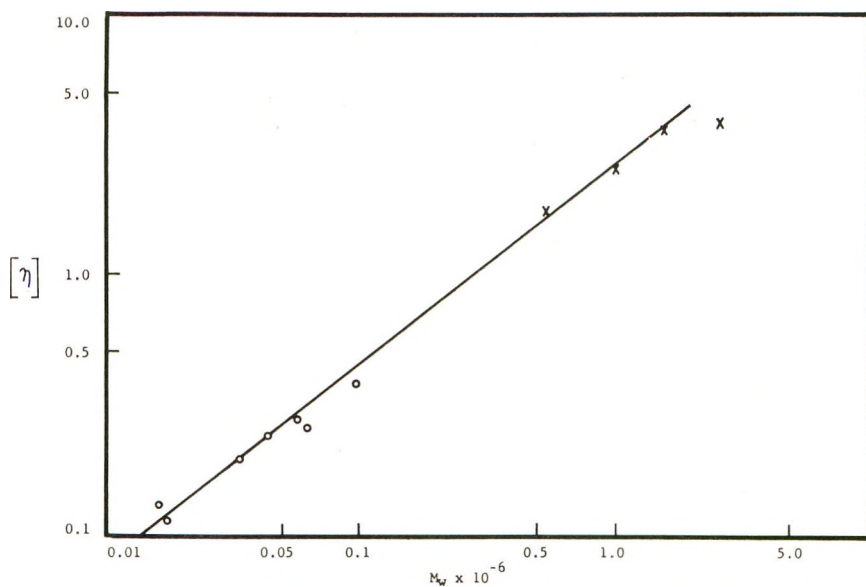


Fig. 7. Viscosity-molecular relationship for fractionated polystyrene: (X) unoxidized; (O) oxidized.

from fractionation showing that losses from depolymerization to styrene are negligible.

The above distribution represents the nonmicrogel portion of the polystyrene. Concentration decreases after the removal of microgel ranged from 0 to 25% for the various fractions after allowance for the 5-6% loss which normally occurred after filtration. The highest loss was for fraction F-2 and the lowest for F-7. It is estimated then that 7% of the oxidized whole polystyrene was microgel.

Although the formation of crosslinked polymer may lead to increased polydispersity, this is not the case here. Further, since for monodispersed linear polymer chains the value of ϕ reaches a maximum of 2.5×10^{21} , values of ϕ higher than this would indicate branched polymer. Inasmuch as ϕ exceeds this maximum in only one case, the occurrence of branched polystyrene in the clarified fraction cannot be clearly demonstrated. This is probably a result of the difficulty of measuring the radius of gyration on the low molecular weight oxidized fractions obtained.

In Figure 7 is shown the viscosity-molecular weight relationship obtained for polystyrene. A straight line through the best three points for the unoxidized polymer and through the four points of the oxidized polymer gives $[\eta] = 9.6 \times 10^{-5} \bar{M}_w^{0.77}$, which agrees well with the relations $[\eta] = 2.1 \times 10^{-3} \bar{M}_w^{0.70}$ calculated from the data of Manson and Cragg¹⁵ and $[\eta] = 2.16 \times 10^{-5} \bar{M}_w^{0.85}$ of Bueche.⁸ Whether any fundamental difference in polymer structure has occurred other than chain scission is not revealed. Therefore, the nature of any branched polymer must be short chain branches since no appreciable change in slope has occurred. This seems

reasonable since any long branches which occur would probably be scissioned after a short period of time.

Nemphos,²¹ in his infrared study of a similar polystyrene, indicates that a small amount of carbonyl group is present after 4 hr. at 200°C. Since the major part of the carbonyl formation occurs after 4 hr., further degradation may represent a rather complex reaction. Unfortunately the molecular weight may be too low to obtain further information by the method used in the present study.

Infrared spectrum on a film of unoxidized fraction E-8 gave a typical polystyrene spectrum. The spectrum for oxidized fraction F-8 showed a moderate carbonyl formation. A differential analysis of the films showed that when the aromatic C-H stretching and bending absorptions were approximately balanced, so that a slight absorption occurred for the oxidized polymer (thus assumed to be of an approximately equal thickness), moderate absorption bands for aliphatic C-H stretching and bending appeared in the unoxidized and a moderate carbonyl absorption band in the oxidized. On fivefold expansion these absorptions were off-scale. Although the two fractions were not of equivalent molecular weight, the fact that the concentration of C-H bonds was reduced in the oxidized polymer can only lead to the conclusion that the scission occurs in the aliphatic part of the chain.

In conclusion, the major structural change which occurs during the initial part of the bulk oxidation of polystyrene is a random chain scission. The only clear evidence for branching is the formation of microgel. Since, when microgel forms, crosslinking reactions have occurred, it must be assumed that crosslinked and branched structures occur in the scissioned molecules from similar reactions.

We are indebted to Professor Stig Claesson for many helpful discussions. One of us (JCS) is further indebted to the National Lead Company for its research fellowship.

References

1. Mesrobian, R. B., and A. V. Tobolsky, *J. Am. Chem. Soc.*, **67**, 785 (1945).
2. Jellinek, H. H. G., *J. Polymer Sci.*, **4**, 1 (1949).
3. Light Scattering Photometer Operation Manual OM-1000, Phoenix Precision Instrument Co., Philadelphia, Pa., 1955.
4. Witnauer, L., H. J. Scherr, *Rev. Sci. Instr.*, **23**, 99 (1952).
5. Carlson, D. W., Ph.D. Thesis, Univ. of Delaware, 1959.
6. Halwer, M., *J. Am. Chem. Soc.*, **70**, 3985 (1948).
7. Frank, H. P., and H. Mark, *J. Polymer Sci.*, **10**, 129 (1953).
8. Bueche, A. M., *J. Am. Chem. Soc.*, **71**, 1452 (1949).
9. Sorenson, W. R., and T. W. Campbell, *Preparative Methods of Polymer Chemistry*, Interscience, New York, 1961.
10. Allen, P. W., *Techniques of Polymer Characterization*, Butterworth, London, 1959.
11. Zimm, B. H., *J. Chem. Phys.*, **16**, 1099 (1948).
12. Beattie, W. H., and C. Booth, *J. Polymer Sci.*, **44**, 81 (1960).
13. Cleverdon, D., D. Laker, and P. G. Smith, *J. Polymer Sci.*, **17**, 133 (1955).
14. Shultz, A. R., *J. Am. Chem. Soc.*, **76**, 3422 (1954).
15. Manson, J. A., and L. H. Cragg, *J. Polymer Sci.*, **33**, 193 (1958).

16. Frisch, H. L., and J. L. Lundberg, *J. Polymer Sci.*, **37**, 123 (1959).
17. Boundy, R. H., and R. F. Boyer, *Styrene, Its Polymers, Copolymer and Derivatives*, Reinhold, New York, 1952.
18. Peebles, L. H., *J. Am. Chem. Soc.*, **80**, 5603 (1958).
19. Muus, L. T., and F. W. Billmeyer, Jr., *J. Am. Chem. Soc.*, **79**, 5079 (1957).
20. Heyn, A. N. J., *J. Polymer Sci.*, **41**, 23 (1959).
21. Nemphos, S. P., Ph.D. Thesis, Univ. of Delaware, 1957.

Résumé

On a effectué une recherche par diffusion lumineuse et par viscosimétrie sur la nature des changements structurels et moléculaires, qui se passent lors de l'oxydation en masse du polystyrène. On a effectué les oxydations sur des films dans un four à air pendant 0, 2, 4 et 5 heures à 200°C. Les films oxydés ont été dissous et on a déterminé les différents paramètres de ces solutions. Le fractionnement du polystyrène, polymérisé thermiquement, montre un rétrécissement de la distribution du poids moléculaire par suite de l'oxydation. Le poids moléculaire moyen en poids diminuait de 1.090.000 à 33.000. Un polystyrène commercial nonfractionné, styron 683K, diminuait de 281.000 à 16.000. Ces résultats montrent que la scission au hasard du polymère oxydé se passe toujours avec la formation de groupement carbonyles, donnant des molécules de polymère avec une longueur de chaîne plus courte, dont la plupart conserve la structure initiale linéaire en pelote statistique. Outre la scission de la chaîne, on constate une distorsion des graphiques de Zimm par microgel, ce qui indique des ramifications et du pontage moléculaire.

Zusammenfassung

Eine Untersuchung der Natur der strukturellen und molekularen Veränderungen während der Oxydation von Polystyrol in Substanz wurde mittels Lichtstreuung und viskosimetrischer Methoden durchgeführt. Filme wurden in einem Luftofen durch 0, 2, 4, und 5 Stunden bei 200° oxydiert. Die oxydierten Filme wurden gelöst und verschiedene Parameter an den Lösungen erhalten. Fraktionierung des nichtoxydierten und des oxydierten thermisch polymerisierten Polystyrols zeigte eine Verengung der Molekulargewichtsverteilung während der Oxydation. Das Gewichtsmittel des Molekulargewichts fiel von 1090000 auf 33000. Ein unfraktioniertes technisches Polystyrol, Styron 683K, fiel von 281000 auf 16000 ab. Diese Ergebnisse zeigen, dass statistische Kettenspaltung des oxydierten Polymeren zugleich mit der Bildung von Carbonylgruppen auftritt, wobei Polymermoleküle von kürzerer Kettenlänge meistens wahrscheinlich unter Beibehaltung der Ausgangsstruktur eines linearen statistischen Knäuels entstehen. Neben der Kettenspaltung weist die Störung des Zimm-Diagramms durch Mikrogel auch auf Verzweigung und Vernetzung hin.

Received October 29, 1962

Clay-Catalyzed Reactions of Olefins. I. Polymerization of Styrene*

JAMES A. BITTLES, A. K. CHAUDHURI,[†] and SIDNEY W. BENSON,
*Department of Chemistry, University of Southern California, University Park,
Los Angeles, California*

Synopsis

Qualitative observations are reported on the polymerization of styrene with acid clay cracking catalysts. Molecular weights were 500-2000, depending on solvent, catalyst quantity, monomer concentration, and temperature, monomer conversions approached 100%. The reaction rate is rapid at 0°C. and at ambient temperatures and is severely inhibited by water and other proton acceptors. The polymer was structurally the same as polystyrene and contained saturated endgroups formed by solvent termination and by a competitive cyclization reaction. The chain termination products and polymer endgroups were identified.

INTRODUCTION

The cationic polymerization of vinyl monomers has been investigated extensively by Plesch,¹ Dainton,² Evans,³ Pepper,⁴⁻⁶ Overberger,⁷ Heiligmann,⁸ and others.⁹ The catalysts boron trifluoride, aluminum chloride, stannic chloride, titanium tetrachloride, and other electrophilic reagents have been employed in an investigation of the kinetics and mechanism of the polymerization. The effects of a cocatalyst were the subject of detailed study¹⁻⁴ and were a source of error in the interpretation of data. It was established in 1947 by Evans³ that a cocatalyst such as water was required for the polymerization of isobutylene with boron trifluoride. Other acid producing electrophilic polymerization catalysts were also found to require trace quantities of proton producing cocatalysts.

Stanley¹⁰ and Salt¹¹ have indicated that styrene and α -methylstyrene can be polymerized to low molecular weight liquids with solid acid catalysts. Work in this laboratory¹² showed that styrene was converted to solid polymer with acid clay cracking catalysts. The polymerization of styrene with acid clays to solid polymers has not been previously reported, although acid silica-alumina catalysts have been used in making polymer gasoline at high temperature and pressure.¹³ The polymerization of α -methylstyrene

* This work has been supported by grants from the Goodyear Tire and Rubber Company, Akron, Ohio.

[†] Present address: Indian Association for the Advancement of Science, Calcutta, India.

to liquids has been the subject of a patent.¹⁴ The method employed for acid clay polymerization resulted in solid products of molecular weights up to 2000 in the solvents used and monomer conversions up to 100%.

DISCUSSION OF RESULTS

The polymerization of styrene monomer with the use of commercial Filtrol clay as a catalyst has been done in toluene and 1,2-dichloroethane at temperatures from -70 to 60°C . Monomer concentrations of 0.1 to $1.0M$ were employed. The polymerization also proceeded readily in the bulk monomer where the maximum concentration of about $8.63M$ was obtained, and in the gas phase. The polymerization is believed to be surface-promoted; however, this will be discussed in another paper.

Molecular weights of polymer have been as high as 2000 and as low as 440 (4 units) at $0.1M$ in toluene. The polymerization has been found to be inhibited by trace amounts of moisture and other proton acceptors and is even inhibited by small quantities of α -methylstyrene.

Polymer Structure and Endgroups

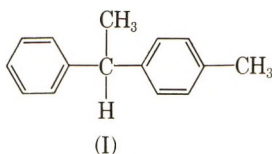
Polymer prepared by the clay-catalyzed polymerization of styrene in toluene and 1,2-dichloroethane solvents has a backbone structure similar to that of radical-produced polystyrene, which is mainly head-to-tail polymerization. This is shown by the infrared spectra, physical properties, and solubilities. The structural difference in the polymers occurs in the endgroups which are apparent in the infrared spectra, in the endgroup analysis, and in the structure of the liquid products. The endgroups of the polymer are saturated hydrocarbon groups for the most part. A maximum of 2.26% of olefin ends was indicated by the bromination, and a maximum of 10% of hydroxyl ends was indicated by chemical analysis.

The saturated hydrocarbon endgroups of the polymer prepared in toluene were a mixture of *p*-methylphenyl and methylphenylindane endgroups. These were formed by the reactions with solvent toluene and by cyclization. Chemical analysis of polymer supports the contention that a major fraction of the saturated ends are methylphenyl formed by condensation with solvent toluene.

The polymer prepared in 1,2-dichloroethane contained practically no solvent endgroups, was saturated, and is, therefore, terminated by a methylphenylindane group. The infrared spectra and chemical analysis support this contention. The possibility of a small quantity of solvent endgroups was indicated since the polymer contained 0.017% Cl by analysis. This calculated out to 0.58% of $\text{ClCH}_2\text{CH}_2-$ ends for a polymer of molecular weight 1200 (11 units plus 1 end).

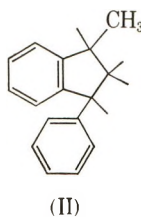
Structure of Dimer and Liquid Products

The most volatile liquid product isolated from polymerization in dilute toluene solution was established by chemical analysis, NMR spectra, and



infrared spectra. This product was 1-phenyl-1-*p*-methylphenylethane (I). This structure constitutes the main argument for solvent endgroup in higher polymer as well.

The liquid product from polymerization in 1,2-dichloroethane was 1-methyl-3-phenylindane (II).



The evidence for this was the MNR spectra and to a lesser extent the infrared spectra. This material was not as easily purified as 1-phenyl-1-*p*-methylphenylethane because of the small quantity and high boiling point, but the evidence is considered conclusive for this product. The structure of this product combined with the infrared spectra of polymer from 1,2-dichloroethane constitutes the inference of methylphenyl indane endgroups in the polymer obtained from the same reaction mixture.

EXPERIMENTAL

The polymerization was studied by measuring rates of monomer consumption with time, by measuring yields of polymers, and by determinations of polymer molecular weights. The polymerizations were conducted in a 500-cc., three-necked, round-bottomed flask. Yields were determined by precipitation and weighing of dried polymer. The molecular weights were determined by freezing point depression of their benzene solutions.

Catalyst Preparation

The catalyst employed was fluid catalytic cracking catalyst prepared commercially from natural clays by acid washing and calcining (commercial grade 13 SV7494 made by Filtrol Corporation).

The catalyst was prepared for polymerization by heating 10 g. in a glass vessel *in vacuo*. The vessel of 50-ml. capacity was evacuated to 10^{-5} mm. of Hg pressure at ambient temperature for 2 hr. This procedure served to remove adsorbed moisture and was detected by its cooling effect. The catalyst was then gradually heated to 280°C. *in vacuo* and heating continued at this temperature for 2 hr.

Storage of the catalyst in a closed vessel in a dry box resulted in deactivation due to moisture adsorption, but activity was restored by reheating *in vacuo* at 280°C. (oil bath temperature.)

Purification of Solvents

The solvents were reagent grade chemicals and were purified by distillation through a 3-ft. fractionating column packed with glass beads. Toluene and 1,2-dichloroethane were purified by this method, and the center cuts were used in the polymerization. The boiling point of 1,2-dichloroethane solvent purified in this manner was 83.3–83.5°C. at 760 Hg pressure (Lit.: b.p. of 1,2-dichloroethane is 83.7°C./760 mm.¹⁰). The boiling point of toluene solvent obtained from the fractionating column was 110–110.5°C. (Lit.: b.p. of toluene is 110.8°C./760 mm.¹⁵). The distilled solvents were dried for 48 hr. over freshly activated silica gel and were stored in a dry box until ready for use.

Styrene monomer was commercial grade containing 0.1% *tert*-butylcatechol. The crude monomer was dried over silica gel and then fractionally distilled on a 4-ft. Podbielniak column *in vacuo*. The center cut of this material, b.p. 46.5°C./22.5 mm., was used for polymerization. The purified monomer was stored over silica gel under refrigeration at –20°C. and finally distilled *in vacuo* immediately prior to use.

Polymer Preparation

General. The polystyrene was prepared in a 500-cc. three-necked flask fitted with nitrogen inlet tube, stirrer, and tube for removal of samples. Prior to addition of catalyst the flask was flamed while passing dry nitrogen through the vessel. The nitrogen was dried by passing through silica gel and activated charcoal at liquid nitrogen temperature. Catalyst was then added to the flask in a dry box followed by 265 cc. of dried solvent. The flask was sealed tight in the dry box and removed to a polymerization setup. Freshly dried and distilled monomer was added to the flask through a rubber stopper by means of a hypodermic syringe. Monomer was not exposed to the atmosphere during the transfer process.

Stirring of the flask was done by a magnetic stirrer when run at ambient temperature and by a pressure-tight Teflon ASCO stirrer at 0°C. in a thermostat.

Polymer Precipitation and Purification. The reaction mixture was worked up as follows. Clay catalyst was filtered from the mixture and washed with benzene. The solvent was removed from the filtrate by distillation *in vacuo*, leaving a residue of about 50 cc. Polymer was precipitated from the benzene solution by addition of about 200 cc. of methanol. The methanol was decanted after allowing the polymer to settle. Polymer was redissolved in benzene and reprecipitated with methanol. A colorless product was obtained, and this was dried in a vacuum oven at 65°C. The weight of solid product was 28.60 g. in the case of 1,2-dichloroethane sol-

vent (94.10% yield). The liquid product was recovered by distillation of the methanol solution, and 2.19 g. was obtained (7.2% yield). The overall yield was, therefore, 101.3%, representing complete recovery of product. The overall yield of product obtained from solvent toluene was 95–100%.

Elemental Analysis of Polymer

The elemental analysis of polymer prepared in 1,2-dichloroethane indicated a structure very close to polystyrene, although the possibility of a trace amount of chlorine-containing endgroups cannot be ruled out.

ANAL. Calcd. for $(C_8H_8)_n$ (polystyrene): C, 92.26%; H, 7.74%. Found: C, 92.31%; H, 7.69%; Cl, 0.017%.

The analytical results of solid polymer prepared in toluene indicated a structure other than $(C_8H_8)_n$ polystyrene. Indications were that solvent toluene had participated in the termination of chains.

ANAL. Calcd. for $(C_8H_8)_n$ (polystyrene): C, 92.26%; H, 7.74%. Found: C, 91.37%; H, 7.85%.

Preparation and Identification of 1-*p*-Methylphenyl-1-phenylethane (Solvent Termination Product)

The methanol washings from polymerization of 1M monomer in toluene were employed for isolation of solvent termination products. There was obtained from a run about 10 cc. of a viscous liquid which was fractionated under vacuum on a 6-in. Vigreux column. The cuts obtained are listed in Table I.

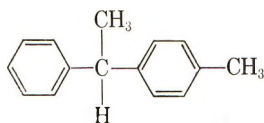
TABLE I

Fraction	Boiling range, °C.	pressure, mm.	Wt., g.	Identity
1	120–128	7.5	0.5904	Monoadduct
2 ^a	120–128	7.5		
3 ^a	135–154	7.5	0.6182	Monoadduct and diadduct
4	159–	3.5	1.1371	Impure diadduct

^a ANAL. Calcd. for $C_{15}H_{16}$: C, 91.84%; H, 8.16%. Found: C, 91.90%; H, 8.10%.

The proton resonance spectrum of the solvent termination product was determined on an A-60 high resolution spectrometer. The sample employed was obtained by redistillation of the combined fractions 1, 2, and 3. There was obtained 0.2566 g. of product boiling at 115.5°C./7 mm. Hg pressure. This product was substantially pure 1-*p*-methylphenyl-1-phenylethane.

The NMR spectra substantiated the structure as



There were obtained spin resonances for the H on the carbon between the benzene rings and spin interactions between this proton and the methyl group attached to the same carbon. There was also obtained the resonance of the methyl group attached to the benzene ring. The latter structure was also obtained in the infrared spectrum.

Isolation of Distyryl Toluene Adduct

A higher boiling material, b.p. range 120–135°C./7.5 mm. was obtained after separation of 1-*p*-methylphenyl-1-phenylethane by distillation. This material was presumed to be mainly the distyryl toluene condensation product. C and H analysis indicated a mixture of products. The material was not the cyclization product, since the boiling point was lower.

1-Methyl-3-Phenylindane (Cyclic Dimer Preparation)

The cyclic dimer was prepared and isolated from a 0.1*M* run of monomer in 1,2-dichloroethane solvent. The liquid by-product obtained after removal of polymer was distilled *in vacuo*. There was obtained 3.0645 g. of distillate, boiling range 95–106°C./2 mm., which on redistillation gave 0.5 g. of constant boiling liquid, b.p. 86–88°C./1 mm. Hg pressure.

ANAL. Calcd. for C₁₆H₁₆: C, 92.26%; H, 7.74%; Found: C, 92.08%; H, 7.60%.

The NMR spectrum of the constant-boiling liquid was consistent with the cyclic structure of 1-methyl-3-phenylindane. There were also signals indicating the isomeric 1-methyl-2-phenylindane, which product could arise by the attack of a secondary carbonium ion on the α -carbon of another styrene monomer. The presence of other structures as impurities was definitely indicated.

Endgroup Analysis

Polymer of molecular weight 1500 was subjected to a chemical analysis of olefin endgroups by the following procedure.

A standard solution of polymer was prepared by dissolving 2.3205 g. in 50 ml. of benzene. Three 10-ml. aliquots were treated with exactly 10 cc. of standard bromine in acetic acid for periods of 10 min., 1 hr., and 18 hr. at 0°C. A control sample was run with each sample as a blank. Bromination by substitution was minimized by conducting the brominations in blackened flasks. The results obtained are given in Table II.

Since the polymer molecular weight was 1500, there was 0.31 mmole of polymer or 0.31 meq. of olefin ends, assuming one olefin endgroup per mole.

TABLE II

Time, hr.	Volume 0.1007 <i>N</i> Thiosulfate, ml.		
	Control, ^a	Polymer solution ^b	Olefin, meq.
1/6	8.88 ± 0.02	8.83 ± 0.02	0.005
1	8.95 ± 0.02	8.83 ± 0.02	0.012
18	8.88 ± 0.02	8.84 ± 0.02	0.005
Avg.			0.007

^a Unreacted bromine was determined by titration of iodine liberated from excess KI solution. This value is milliliters of 0.1007*N* thiosulfate solution.

^b Polymer solution was 0.4641 g./10 cc. or 0.31 millimoles.

These results show approximately 0.007 meq. of olefin or an average of 2.26% of olefin ends.

Polymer of molecular weight 1500 was analyzed for hydroxyl ends by the procedure of Griehl and Neue¹⁶ as described by Price.¹⁷ Duplicate analyses were made on 0.4942 and 0.4810 g. of polymer in benzene. The bromide ion was estimated chemically with standard AgNO₃ solution, and the average was 0.013 meq. of bromide ion. Since the value for the polymer (including bromoacetyl ends) was 0.13 meq., the average fraction of hydroxyl ends could be 0.013/0.13 or 10%.

Infrared Spectra of Products

The infrared spectra from 4000 to 670 cm.⁻¹ of polymer prepared in toluene and in 1,2-dichloroethane were determined. The spectra of the liquid products, 1-*p*-methylphenyl-1-phenylethane, 1-methyl-3-phenylindane, and the unidentified liquid products were also determined. The instrument was a double-beam Perkin-Elmer Infra cord, Model 137.

Solid polymer (m.p. 80°C.) was melted on NaCl windows between a 0.1 mm. aluminum spacer and pressed by another NaCl window to approximate 0.1 mm. thickness. The liquid products were also pressed between a pair of NaCl windows with a 0.1 mm. spacer between. A comparison was made of these spectra with those of commercial polystyrene and indane.¹⁸ These results are discussed under polymer and dimer structure.

Nuclear Magnetic Resonance Spectra of Products

NMR spectra of the liquid products 1-methyl-3-phenylindane and 1-*p*-methylphenyl-1-phenylethane were taken on a high resolution A-60 Varian spectrometer in CCl₄. The final identification of the liquid products was based upon these spectra.

Molecular Weight Determination

The molecular weights of polymer and liquid products were determined by freezing point measurements in benzene. Molecular weights of selected polymer were also determined by viscosity measurements in benzene solu-

TABLE III
 Polymer Molecular Weights

Monomer concn., mole/l.	Catalyst concn., mmole/c. ^a	Temp., °C.	Solvent	Polymer molecular weight	Polymer yield, %
1.0	2.68	0	Toluene	986	50
1.0	2.68	0	Toluene	500	60
1.0	2.68	0	Toluene	737	79
1.0	2.01	0	Toluene	907	—
1.0	2.68	-62	Toluene	752	—
1.0	2.68	-70	Toluene	600	—
0.7	2.68	-70	Toluene	1240	—
0.5	2.68	0	Toluene	748	—
0.1	2.01	0	Toluene	442	—
0.1	2.68	0	Toluene	289 ^b	—
0.1	0.86	32	Toluene	287 ^b	—
1.0	2.68	0	Ethylene chloride	1130	—
1.0	2.68	0	Ethylene chloride	1445	94
1.0	1.34	0	Ethylene chloride	1735	49.5
0.5	1.34	0	Ethylene chloride	2320 ^c	41
0.1	2.68	0	Ethylene chloride	1019	—

^a This is based on the assumption that there is 0.1 meq. H⁺/g. catalyst.

^b Liquid polymer was obtained by solvent evaporation.

^c The polymer was fractionated by precipitation with methanol.

tion and compared with values obtained by the method of depression of freezing point. The molecular weights of polymer are shown in Table III.

The freezing point depressions were done in a standard Beckmann freezing point apparatus¹⁹ immersed in an iced Dewar flask maintained at 0°C. The freezing points of pure dry benzene and the benzene solutions of polymer were determined with a Beckmann thermometer. The precision of the thermometer was 0.001°C.

In most determinations approximately 1 g. of polymer was dissolved in 15 cc. of benzene ($d_4^{25} = 0.8683$) giving freezing point depressions of about 0.230°C. for a molecular weight of 1800. Since the precision of the measurements is limited by the temperature depression, the precision was 0.4%. Reproducibility from run to run was about 1%.

Polymer solutions were ideal over a range of 8.25 to 2.25%; therefore, the higher concentrations were employed in order to obtain the greater precision. The ideal nature of these solutions is shown in Figure 1 for polymer of molecular weight 1480 ± 14 .

The molecular weight of a selected polymer was determined by a viscosity measurement in benzene at 25°C. The calculation was made using

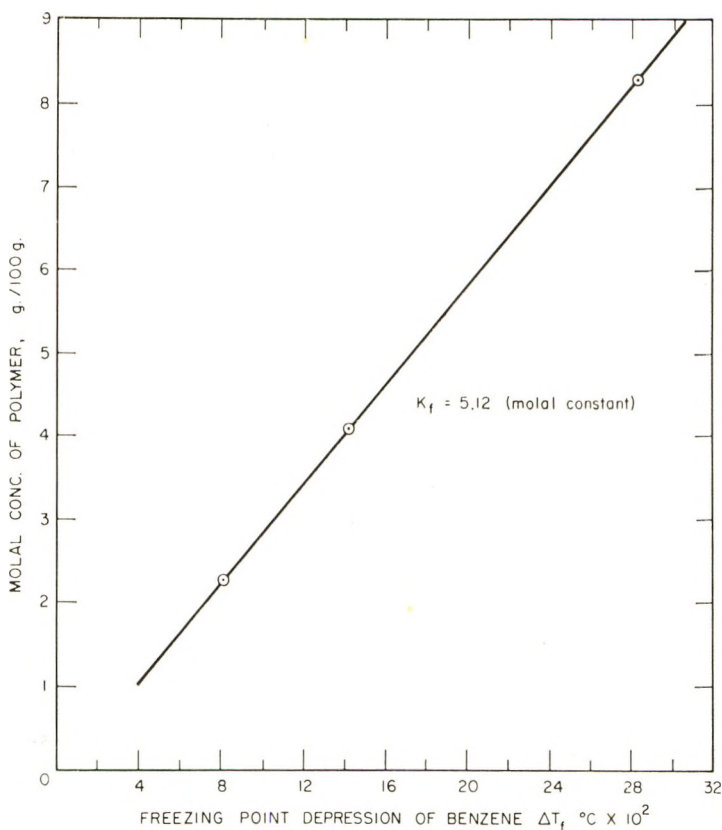


Fig. 1. Freezing points of polystyrene solutions (M.W. = 1480 ± 14 ; solvent benzene).

Staudinger's equation, where M is polymer molecular weight, and $K = 2.7 \times 10^{-4}$, $a = 0.66$ (according to Pepper⁵). (More recent values of K and a are 2.27×10^{-4} and 0.72 , respectively.⁶) The molecular weight obtained by viscosity was 2000 for the polymer having a molecular weight of 1850 as determined by freezing point depression. Because of this lesser precision and the uncertainty of the constants K and a , viscosity measurements were discarded in favor of the freezing point method.

Discussion of Polymer Infrared Spectra

The infrared spectra of polymer prepared in toluene and in 1,2-dichloroethane were identical, with minor differences, to that of commercial polystyrene of molecular weight 200,000. The minor differences in the spectra are attributable to the type of endgroups found in polymer prepared in the two solvents. A difference in spectra structure occurs at 1225 cm.^{-1} for polymer made in toluene and in 1,2-dichloroethane. A distinct absorption peak occurs at 820 cm.^{-1} in the spectra of polymer made in toluene. This absorption maximum does not occur in commercial polystyrene nor in polymer prepared in 1,2-dichloroethane.

The definite absorption maximum at 820 cm.^{-1} is the frequency of deformation of adjacent C—H's attached to a benzene ring²⁰ and has been observed by Plesch.¹ This shows the presence of a *p*-methylphenyl group in the polymer and, because of the relative weakness of the absorption, a *p*-methylphenyl endgroup. Evidence for the methylphenyl endgroup was inferred from the structure of the dimer.

The spectra in the region of 1225 cm.^{-1} show two small absorption maxima which are not present in commercial polystyrene. The maximum at 1225 cm.^{-1} is also found in the indane spectrum and is attributable to phenylindane endgroups. Other distinct features of the indane spectrum are masked by features of the polystyrene spectrum.

Spectra of Dimer and Liquid Products

The infrared spectra of the distillable liquid products from toluene and 1,2-dichloroethane solvent show distinct differences. These spectra are also distinctly different from the polymer spectra. The liquid toluene-styrene condensation product has a strong maximum at 820 cm.^{-1} due to the *p*-methylphenyl group.

NMR Spectra of Liquid Products

The proton resonance spectrum of the toluene styrene adduct confirms the structure of this material to be 1-*p*-methylphenyl-1-phenylethane. A group of resonance lines at 230–250 cycles/sec. was obtained which arises from protons on carbon atoms attached to two benzene rings. A single sharp resonance line was obtained at 130 cycles/sec. due to a methyl group attached directly to a benzene ring. A doublet was obtained at 85 and at 100 cycles/sec. due to a methyl group on carbon between two benzene rings also bearing a proton. The doublet is due to spin coupling of the methyl group with the proton.

The nuclear magnetic resonance spectrum of the liquid from polymerization in 1,2-dichloroethane showed a complex signal at 110–130 cycles/sec. which was possibly due to protons of the structure of 1-methyl-3-phenylindane. In addition to these signals there was obtained proton resonance due to a proton attached to a carbon adjacent to a benzene ring and to a methyl group attached to this same carbon. Such signals are consistent with the proposed 1-methyl-3-phenylindane. Due to the complicated spectrum obtained, further purification of this product is necessary to establish a firm spectrum for the product in question.

References

1. Plesch, P. H., *Cationic Polymerization and Related Complexes*, Academic Press, New York, 1953.
2. Dainton, F. S., and R. H. Tomlinson, *J. Chem. Soc.*, **1953**, 151.
3. Evans, A. G., and G. W. Meadows, *Trans. Faraday Soc.*, **46**, 327 (1950).
4. Pepper, D. C., *Trans. Faraday Soc.*, **45**, 397 (1949).
5. Pepper, D. C., *Trans. Faraday Soc.*, **45**, 404 (1949).

6. Pepper, D. C., and M. J. Hayes, *Proc. Chem. Soc.*, **1958**, 228.
7. Endres, G. F., and C. G. Overberger, *J. Am. Chem. Soc.*, **77**, 2201 (1955).
8. Heiligmann, R. G., *J. Polymer Sci.*, **6**, 155 (1951).
9. Jordan, D. O., and A. R. Mathieson, *J. Chem. Soc.*, **1952**, 611.
10. Stanley, H. M., *Chem. Ind. (London)*, **17**, 1082 (1939).
11. Salt, F. E., *Clay Minerals Bull.*, No. 2, 55 (Aug. 1948).
12. Kessar, I., and R. Gobran, unpublished results.
13. Emmett, P. H., *Catalysis*, **6**, 341 (1958).
14. Stanley, H. M., and F. E. Salt (to Distillers Co., Ltd.), Brit. Pat. 524, 156 (1940).
15. Lange's *Handbook of Chemistry*, 9th ed., Handbook Publishers, Inc., Sandusky, Ohio, 1956.
16. Griehl, W., and S. Neue, *Faserforsch. Textiltech.*, **5**, 423 (1954).
17. Price, G. F., in *Techniques of Polymer Characterization*, P. W. Allen, Ed., Butterworth London, 1959, p. 226.
18. American Petroleum Institute Research Project, *Infrared Spectra of Petroleum Hydrocarbons*, Carnegie Institute of Technology, Pittsburgh, Pa., Ser. No. 1147, April 30, 1955.
19. Daniels, F., J. H. Mathews, J. W. Williams, P. Bender, and R. A. Alberty, *Experimental Physical Chemistry*, McGraw-Hill, New York, 1956, pp. 68-70.
20. Bellamy, L. J., *Infrared Spectra of Complex Molecules*, Methuen London, 1954, pp. 8, 55, 67.

Résumé

On rapporte des observations qualitatives a sujet de la polymérisation du styrène avec des catalyseurs de cracking à base d'argile acide. Les poids moléculaires variaient de 500 à 2.000, selon le solvant, la quantité de catalyseur, la concentration en monomère et la température; les degrés de conversion du monomère s'approchaient de 100%. La vitesse de la réaction est grande à 0°C et à des températures ambiantes, et elle est fortement inhibée par l'eau et par les autres accepteurs de protons. Le polymère avait la même structure que le polystyrène et il contenait des groupements terminaux insaturés, formés par une réaction de terminaison avec le solvant et par une réaction compétitive de cyclisation. Les produits formés par la terminaison des chaînes et les groupements terminaux ont été identifiés.

Zusammenfassung

Qualitative Beobachtungen über die Styrolpolymerisation mit sauren Tonerdecrackkatalysatoren werden mitgeteilt. Die Molekulargewichte lagen je nach Lösungsmittel, Katalysatormenge, Monomerkonzentration und Temperatur zwischen 500 und 2000; der Monomerumsatz näherte sich 100%. Die Reaktionsgeschwindigkeit ist bei 0°C und bei Raumtemperatur gross und Wasser und andere Protonenakzeptoren sind starke Inhibitoren. Das Polymere war strukturell dem Polystyrol gleich und enthielt gesättigte, durch Lösungsmittelabbruch und eine kompetitive Cyklisierungsreaktion gebildete Endgruppen. Die Kettenabbruchprodukte und Polymerendgruppen wurden identifiziert.

Received December 26, 1962

Revised February 11, 1963

Free Radical Homopolymerization and Copolymerization of Vinyl Phosphines, Oxides, and Sulfides*

ROBERT RABINOWITZ, RUTH MARCUS, and JOSEPH PELLON,
*Chemical Research Department, Central Research Division, American
Cyanamid Company, Stamford, Connecticut*

Synopsis

A variety of free radical catalysts failed to homopolymerize diphenylvinylphosphine and diisobutylvinylphosphine oxide. Oligomeric products were obtained with diphenylvinylphosphine oxide and sulfide. It was shown that in the homopolymerization of the oxide at 100 and 130°C., the molecular weight is independent of catalyst concentration. Further a minimum kinetic chain length for the 0.10 mole-% di-*tert*-butyl peroxide-initiated bulk polymerization at 130°C. was calculated to be 500 units. Reactivity ratios with styrene and methyl methacrylate (MMA) were obtained from copolymerization data (phosphorus monomer is M_2). The following r_1 values were obtained (all r_2 values were close to zero): with diphenylvinylphosphine sulfide: styrene (2.1 ± 0.3), MMA (13 ± 3); with diphenylvinylphosphine oxide: styrene (5 ± 1), MMA (11 ± 4); with diisobutylvinylphosphine: styrene (7 ± 1), MMA (5.1 ± 0.2); with diisobutylvinylphosphine oxide: styrene (17 ± 5), MMA (30 ± 10). It was concluded that the phosphorus groups do not exert strong conjugative stabilization of an adjacent carbon radical but can be considered as mildly activating on the basis of a comparison of the relative reactivities of these monomers and a series of common monomers toward a styryl radical.

INTRODUCTION

Many unsaturated compounds in which the olefinic group is directly bonded to phosphorus are known.¹⁻⁸ These are almost exclusively phosphonic acid esters and have shown little tendency to homopolymerize or copolymerize under free radical conditions. Very little information exists in the literature concerning vinyl phosphines and their derivatives.⁹ Furthermore, aside from a few scattered reports, no systematic study of the free radical polymerization behavior of this class of compounds had been carried out. In this work, such a study has been made. Free radical homopolymerizations were run under a variety of conditions. Copolymerizations with styrene and methyl methacrylate were carried out and the reactivity ratios determined.

* The homopolymerization studies reported herein were presented at the 140th American Chemical Society Meeting, Chicago, September 1961. See R. Rabinowitz and J. Pellon, *Abstracts of Papers*, p. 43Q.

EXPERIMENTAL

The preparative procedures for the monomers, diphenylvinylphosphine, diphenylvinylphosphine oxide, diphenylvinylphosphine sulfide, and dibutylvinylphosphine oxide have been described in our recent publication.⁹

Polymerization Studies

All polymerizations were carried out by adding the components to heavy-walled, constricted test tubes, degassing three times at $-78^{\circ}\text{C}.$, and sealing. The tube contents were allowed to thaw and then were heated at the desired temperature.

Homopolymerization of Diphenylvinylphosphine Oxide

The homopolymerizations were carried out on 1.0 g. samples of monomer. At the end of the heating period the tubes were opened, diluted with benzene and precipitated into hexane. The data are summarized in Table I.

TABLE I
Homopolymerization of Diphenylvinylphosphine Oxide

Initiator ^a	Amt. initiator, mole-%	Benzene, ml.	Temp., $^{\circ}\text{C}.$	Time, hr.	Yield, %	Melting range, $^{\circ}\text{C}.$ ^b	Mol. wt. ^c	Recovered monomer, %
AIBN	2.0	3.0	70	96	15	100–140	—	—
Bz ₂ O ₂	1.0	2.0	80	24	34	100–130	1270	60
<i>t</i> -BPB	1.2	2.0	100	24	92	75–125	902 ^d	—
<i>t</i> -BPB	0.12	2.0	100	46.5	48	—	1020	53
DTBP	1.0	0.20	130	24	100	125–155	1370	—
DTBP	0.10	0.20	130	24	96	65–145	1380	—
DTBP	0.010	0.20	130	24	11	100–140	1430	88

^a Di-*tert*-butyl peroxide (DTBP); azobisisobutyronitrile (AIBN); benzoyl peroxide (Bz₂O₂); *tert*-butyl perbenzoate (*t*-BPB).

^b Melting ranges were determined using a Fisher-Jones apparatus.

^c Molecular weights determined by a vapor pressure lowering technique.

^d $[\eta]$ at $30^{\circ}\text{C}.$ in benzene is 0.027 dl./g.

Attempted Homopolymerization of Diphenylvinylphosphine

The reactions were carried out in bulk with approximately 1.0 g. samples of freshly distilled monomer. In every case where initiator was present the polymerization mixture discolored rapidly. However, in the absence of initiator, the monomer remained colorless, even at $150^{\circ}\text{C}.$ A summary of the data appears in Table II. No viscosity increases were noted in these polymerizations. The infrared spectra of the final polymerization

solutions showed little to no aliphatic C—H leading to the conclusion that little or no polymer was present. Finally a series of completed reaction mixtures was combined (6.15 g.) and distilled. A total of 5.52 g. (90%) of diphenylvinylphosphine was recovered. The pot residue, 0.54 g. was a

TABLE II
Attempted Free Radical Polymerization of Diphenylvinylphosphine

Initiator (1.0 mole-%)	Temperature, °C.	Time, hr.
Azobisisobutyronitrile	70	48
Azobisisobutyronitrile	80	48
Azobisisobutyronitrile	90	48
Azobiscyclohexanenitrile	95	27
None	90–150	48

brown, viscous, almost solid material, showing strong P(O) and O—H bands in the infrared. The only identifiable material isolated from it was diphenylvinylphosphine oxide.

Attempted Homopolymerization of Diisobutylvinylphosphine Oxide

A mixture of 1.0 g. diisobutylvinylphosphine oxide, 7.0 mg. AIBN, and 0.50 ml. benzene was heated for 10 days at 60°C. No increase in viscosity was noted, and infrared examination of the final mixture indicated considerable monomer present.

Homopolymerization of Diphenylvinylphosphine Sulfide

A solution of 1.00 g. of the monomer and 10.1 mg. AIBN (1.4 mole-%) in 2.0 ml. of benzene was heated at 60°C. for 43 hr. The solution was precipitated into methanol, and 10 mg. of polymer was obtained. A total of 0.61 g. of monomer was recovered from the filtrate.

A solution of 9.9 mg. azobiscyclohexanenitrile (1 mole-%) in 1.00 g. of the monomer was heated at 90°C. for 43 hr. The resultant polymer was dissolved in benzene and precipitated into hexane. This purification process was repeated, and a 39% recovery of polymer was obtained. A total of 0.46 g. of monomer was recovered. The polymer had an intrinsic viscosity of 0.040 dl./g. at 30°C. in chloroform and a molecular weight of 4470 in benzene using the vapor pressure technique. Its melting range was 60–130°C. Thermal gravimetric analysis at a heating rate of 10°C./min. revealed that the initial weight loss (T_i) in air or nitrogen occurred at 300°C. The temperature for 10% weight loss (T_{10}) was 343°C. in air and 330°C. in nitrogen.

Reactivity Ratio Determinations

Monomer mixtures weighing between 2.5 and 4.5 g. were prepared. The diphenylvinylphosphine and diisobutylvinylphosphine oxide copoly-

merizations were carried out in bulk. The others contained 2-5 ml. of benzene, enough to allow complete homogeneity. Approximately 0.3 wt.-% of AIBN was also present. All copolymerizations were carried out to relatively low conversion, the mixtures then diluted with toluene, and

TABLE III
Copolymerization Studies on Vinyl Phosphorus Compounds at 60°C.

Monomers	Molar feed ratio, m_1/m_2^a	Polymerization, %	Phosphorus, % ^b	Molar polymer ratio, m_1/m_2
Methyl methacrylate,	4.225	26.6	1.20	23.72
CH ₂ =CHP(C ₆ H ₅) ₂	8.130	17.0	0.71	41.57
	15.130	21.3	0.39	77.22
Styrene,	4.141	19.0	0.80	35.16
CH ₂ =CHP(C ₆ H ₅) ₂	8.441	33	0.47	61.12
	8.180	15.4	0.46	62.42
	16.000	26.0	0.32	91.17
Methyl methacrylate,	1.835	12.4	0.40	75.58
CH ₂ =CHP(O)(<i>i</i> -C ₄ H ₉) ₂	5.275	16.7	0.06	516.1
	10.706	11.5	0.13	236.6
Styrene,	1.846	5.95	0.67	42.6
CH ₂ =CHP(O)(<i>i</i> -C ₄ H ₉) ₂	5.708	9.0	0.28	104.4
	11.078	11.4	0.22	133.4
Methyl methacrylate,	1.549	4.57	1.09	26.0
CH ₂ =CHP(S)(C ₆ H ₅) ₂	7.647	7.1	0.33	91.0
	14.684	11.3	0.22	138.5
Styrene,	2.312	3.0	3.02	7.51
CH ₂ =CHP(S)(C ₆ H ₅) ₂	11.78	5.3	1.23	21.84
	19.28	7.8	0.78	35.75
Methyl methacrylate,	1.487	11.47	1.24	22.72
CH ₂ =CHP(O)(C ₆ H ₅) ₂	7.071	13.94	0.50	59.80
	13.694	17.90	0.34	89.46
Styrene,	2.857	5.2	1.45	18.33
CH ₂ =CHP(O)(C ₆ H ₅) ₂	8.746	8.8	0.71	39.91
	17.912	6.8	0.36	80.60

^a Subscript 1 refers to styrene or methyl methacrylate. Feeds containing smaller m_1/m_2 ratios than those reported below would have been desirable in evaluating the reactivity ratios. However decreasing the m_1/m_2 ratios much below those actually used results in poor yields of low molecular weight polymers. These would necessarily contain foreign fragments from the initiator and transfer reactions which can only be ignored in high molecular weight copolymers.

^b The percentages are the averages of close independent duplicate gravimetric procedures. Although the possibility exists that traces of the phosphorus monomers were carried through in the polymer purification procedure, this is deemed relatively unimportant in affecting the semiquantitative results in Table IV.

precipitated into methanol. The resultant polymers were then redissolved in toluene and reprecipitated into low boiling petroleum ether. They were dried overnight at 56°C./0.1 mm. and analyzed. The data and results are presented in Table III.

RESULTS AND DISCUSSION

Homopolymerization

No high polymers were obtained with the nonester, vinyl-phosphorus monomers of this paper. However, oligomeric products were obtained with diphenylvinylphosphine oxide and sulfide.

Attempts were made under a variety of free radical conditions to homopolymerize diphenylvinylphosphine (see Experimental). No polymer was obtained in any case. Paisley and Marvel,¹⁰ who recently reported success with ionic initiation, also failed using a free radical initiator, benzoyl peroxide. However, as they imply, benzoyl peroxide is reduced by phosphines and undoubtedly disappears by a nonradical path.

Diphenylvinylphosphine oxide did homopolymerize under a variety of conditions (see Table I). The molecular weights of these polymers were quite low as was that of the polymer reported by Berlin and Butler.¹¹ A study of the effect of the variation of the initiator concentration on the molecular weight of polydiphenylvinylphosphine oxide was made. The results also appear in Table I. It is evident from these data that the molecular weight is independent of initiator concentration. This point is particularly clear in the DTBP study, where varying the initiator concentration over 100-fold range produced no change in molecular weight. Also noteworthy is that the kinetic chain lengths are quite long. For example, use of 0.10 mole-% of DTBP at 130°C. gave almost complete polymerization and hence a kinetic chain length of at least 500 units. Thus from this data it can be concluded that the low molecular weight polymers are a result of a nondegradative chain transfer process. No attempt is made to specify the exact nature of this process.

A recent report¹² describes the homopolymerization of diphenylvinylphosphine oxide and diethylvinylphosphine oxide at 130 and 70°C., respectively, by using x-ray radiation. Soluble polymers having molecular weights in the region of 30,000 were obtained. Neither the mechanism nor the chemical structure of these polymers were described and these details are necessary before one can consider this as an example of free radical vinyl polymerization.

A brief study of the homopolymerization of diphenylvinylphosphine sulfide was carried out. Berlin¹³ had obtained no polymer using the following free radical initiators: azobisisobutyronitrile (80°C.), di-*tert*-butyl peroxide (100°C.), and radiation. We found very little homopolymerization of the sulfide occurring at 60°C. using AIBN. However, at 90°C., in the presence of 1.0 mole-% azobiscyclohexanenitrile, a polymer was obtained having a molecular weight of 4470. Aside from the Tsetlin work,¹² this is the highest molecular weight free radical vinylphosphorus homopolymer reported to date.

To obtain a more quantitative picture of the reactivity of vinyl phosphorus compounds in polymerization it was decided to measure the reac-

TABLE IV
Copolymerization of Vinyl Phosphorus Compounds with Styrene and Methyl Methacrylate at 60°C.

Phosphorus monomer	Reactivity ratios ^a	
	Styrene (r_1) ^b	Methyl methacrylate (r_1) ^b
$\text{CH}_2=\text{CHP}(\text{S})(\text{C}_6\text{H}_5)_2$	2.1 ± 0.3	13 ± 3
$\text{CH}_2=\text{CHP}(\text{O})(\text{C}_6\text{H}_5)_2$	5 ± 1	11 ± 4
$\text{CH}_2=\text{CHP}(\text{C}_6\text{H}_5)_2$	7 ± 1	5.1 ± 0.2
$\text{CH}_2=\text{CHP}(\text{O})(i\text{-C}_4\text{H}_9)_2$	17 ± 5	30 ± 10

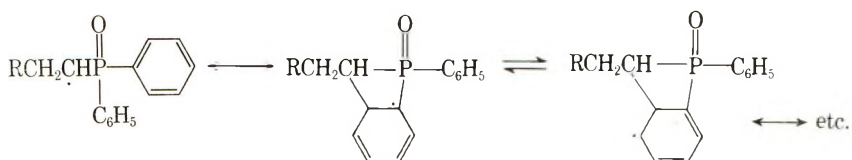
^a M_1 is styrene or methyl methacrylate.

^b r_1 values calculated by using the Fineman-Ross equation.¹⁴ All r_2 were about zero.

tivity ratios of these materials with two reference monomers, styrene and methyl methacrylate. Table IV is a summary.

These data demonstrate that, except for diphenylvinylphosphine sulfide, these monomers compete poorly with styrene for a styryl radical. It is worthwhile noting that the oxides and sulfides (acceptor-type monomers) are more reactive towards styrene (donor-type monomer) than they are towards methyl methacrylate (acceptor type). This order of reactivity is reversed in the case of diphenylvinylphosphine (a donor type) as was anticipated from a prior conclusion concerning polar effects in free radical copolymerization.

Diisobutylvinylphosphine oxide was, by a factor of at least two, the least reactive of the four monomers investigated. Steric considerations may account for this lower order of reactivity. However, models are of little help since all the monomers are sterically hindered. Another possible explanation is the participation of the phenyls of the other monomers in the following manner:



The above resonance forms might be expected to contribute slightly toward the stabilization of the radical.

CONCLUSION

The results given indicate that the phosphorus groups studied do not exert strong conjugative stabilization of an adjacent carbon radical. Arcus and Matthews¹ reached the same conclusion concerning the $-\text{P}(\text{O})(\text{OC}_2\text{H}_5)_2$ group. However these phosphorus moieties are capable of mildly activating a double bond toward radical addition. This is evidenced by comparison of the relative reactivities of the phosphorus monomers and several other common monomers toward a common radical, styryl. Table

TABLE V
Relative Reactivities of Various Monomers With a Styryl Radical^a

Monomer	Relative reactivity
Methyl methacrylate	1.9 ^a
Methyl acrylate	1.3 ^a
CH ₂ =CHP(S)(C ₆ H ₅) ₂	0.5 ^b
CH ₂ =CHP(O)(OC ₂ H ₅) ₂	0.3 ^c
CH ₂ =CHP(O)(C ₆ H ₅) ₂	0.2 ^b
CH ₂ =CHP(C ₆ H ₅) ₂	0.1 ^b
Vinyl chloride	0.05 ^a
Vinyl acetate	0.02 ^a

^a Data reported by Flory.¹⁵

^b This work.

^c Data of Arcus and Matthews.²

V lists these relative reactivities which are merely the $1/r_1$ values when M_1 is styrene.

On this basis the phosphorus monomers are seen to be intermediate in reactivity. The following paper¹⁶ discusses results of a copolymerization study on *p*-styryl analogs of the monomers of this paper. This was carried out in order to further define phosphorus reactivity effects.

The authors wish to express their thanks to Mr. R. Polistina who carried out many of the copolymerizations.

References

1. Arcus, C. L., and R. J. S. Matthews, *J. Chem. Soc.*, **1956**, 4607.
2. Arcus, C. L., and R. J. S. Matthews, *Chem. Ind. (London)*, **1958**, No. 28, 890.
3. Pike, R. M., and R. A. Cohen, *J. Polymer Sci.*, **44**, 531 (1960).
4. Marvel, C. S., and J. C. Wright, *J. Polymer Sci.*, **8**, 255 (1952).
5. Kosolapoff, G. M., U. S. Pat. 2,486,657, to Monsanto (1949).
6. Kosolapoff, G. M., U. S. Pat. 2,389,576, to Monsanto (1945).
7. Pudovik, A. N., N. P. Denisova, *Sbornik Statei Obshchei Khim. Akad. Nauk. SSSR*, **1**, 388 (1953).
8. Abramov, V. S., and G. A. Karp, *Zh. Obshchei Khim.*, **24**, 1823 (1954).
9. A compilation of these references through mid-1961 can be found in a recent publication from this laboratory: R. Rabinowitz and J. Pellon, *J. Org. Chem.*, **26**, 4623 (1961).
10. Paisley, D. M., and C. S. Marvel, *J. Polymer Sci.*, **56**, 533 (1962).
11. Berlin, K. D., and G. B. Butler, *J. Org. Chem.*, **26**, 2537 (1961).
12. Tseltin, B. L., T. Ya. Medved, Yu. G. Chikishev, Yu. M. Polykarpov, S. R. Rafikov, and M. I. Kabachnik, *Vysokomol. Soedin.*, **3**, 1117 (1961).
13. Berlin, K. D., *Chem. Ind. (London)*, **1962**, 139.
14. Fineman, M., and S. D. Ross, *J. Polymer Sci.*, **5**, 259 (1950).
15. Flory, P. J., *Principles of Polymer Chemistry*, Cornell Univ. Press, Ithaca, N. Y., 1953, p. 188.
16. Rabinowitz, R., R. Marcus, and J. Pellon, *J. Polymer Sci.*, **A2**, 1241 (1964).

Résumé

Un certain nombre de catalyseurs à radicaux libres ne permettent pas l'homopolymérisation de la diphenylvinylphosphine et de l'oxyde de diisobutylvinylphosphine.

Des oligomères sont obtenus au départ d'oxyde et de sulfure de diphénylvinylphosphine. On montre que lors de l'homopolymérisation de l'oxyde à 100°C et 130°C le poids moléculaire est indépendant de la concentration en catalyseurs. De plus, la longueur de chaîne cinétique à 0.10 mole % en di-*t*-butyl peroxyde lors d'une polymérisation en bloc à 130°C est évaluée à 500 unités. On obtient des rapports de réactivités du styrène et du méthacrylate de méthyle (MMA) des données de copolymérisation (le monomère phosphoré étant M₂). On obtient des valeurs r_1 (toutes les valeurs r_2 étant considérées comme nulles). Sulfure de diphénylvinylphosphine: styrène (2.1 ± 0.3), MMA (13 ± 3); oxyde de diphénylvinylphosphine: styrène (5 ± 1), MMA (11 ± 4); diphénylvinylphosphine: styrène (7 ± 1) MMA (5.1 ± 0.2); oxyde de diisobutylvinylphosphine: styrène (17 ± 5), MMA (30 ± 10). On en conclut que le groupe phosphoré n'exerce pas une forte stabilisation de conjugaison sur le radical carboné adjacent mais peut être considéré comme un faible activant si on se base par comparaison sur les réactivités relatives de ces monomères et celles d'une série de monomères ordinaires à l'égard d'un radical styryle.

Zusammenfassung

Es gelang nicht Diphenylvinylphosphin und Diisobutylvinylphosphinoxid mit einer Reihe von radikalischen Katalysatoren zur Homopolymerisation zu bringen. Mit Diphenylvinylphosphinoxid und -sulfid wurden oligomere Produkte erhalten. Bei der Homopolymerisation des Oxyds bei 100° und 130°C ist das Molekulargewicht von der Katalysatorkonzentration unabhängig. Weiters wurde für die durch 0,10 Mol-prozent Di-*t*-butylperoxyd gestartete Polymerisation in Substanz eine kinetische Mindestkettenlänge von 500 berechnet. Reaktivitätsverhältnisse mit Styrol und Methylmethacrylat (MMA) wurden aus Copolymerisationsdaten erhalten (das phosphorhaltige Monomere ist M₂). Folgende r_1 -Werte wurden bestimmt (alle r_2 -Werte liegen nahe bei Null). Diphenylvinylphosphinsulfid:Styrol (2,1 ± 0,3, MMA (13 ± 3); Diphenylvinylphosphinoxid:Styrol (5 ± 1), MMA (11 ± 4); Diphenylvinylphosphin:-Styrol (7 ± 1), MMA (5,1 ± 0,2); Diisobutylvinylphosphinoxid:Styrol (17 ± 5), MMA (30 ± 10). Man kommt zu dem Schluss, dass die Phosphorgruppe keine starke konjugative Stabilisierung eines benachbarten Kohlenstoffradikals bewirkt, sondern, auf Grund eines Vergleiches der relativen Reaktivität dieser Monomeren gegen ein Styrylradikal mit der einer Reihe von üblichen Monomeren, als schwach aktivierend betrachtet werden kann.

Received December 7, 1962

Revised February 18, 1963

Synthesis, Polymerization, and Copolymerization of Diphenyl-*p*-Styrylphosphine, Phosphine Oxide, and Phosphine Sulfide

ROBERT RABINOWITZ, RUTH MARCUS, and JOSEPH PELLON,
Chemical Research Department, Central Research Division, American Cyanamid Company, Stamford, Connecticut

Synopsis

Diphenyl-*p*-styrylphosphine (I), prepared by the reaction of diphenylchlorophosphine with *p*-styrylmagnesium chloride, was converted to the corresponding oxide (II) and sulfide (III) by treatment with *tert*-butyl hydroperoxide and sulfur, respectively. These substituted styrenes polymerize readily with thermal or free radical initiation to high molecular weight polymers. These polymers are somewhat more thermally stable than polystyrene. Thus their T_i 's in air were in the range 320–365°C. and in nitrogen, 375–395°C. Their T_{10} 's were in the 390–415°C. range in air and 425–435°C. in nitrogen. Polystyrene in air has a T_i of 263°C. and a T_{10} of 340°C. The monomers copolymerize readily with styrene and methyl methacrylate, the low conversion polymers always containing more phosphorus than the monomer mixtures. Reactivity ratios were determined, from which Q and e values were calculated. These values for the following monomer pairs are (phosphorus monomer M_2): styrene-I, r_1 0.52, r_2 1.43, Q_2 1.34, e_2 -0.30; styrene-II, r_1 0.42, r_2 1.40, Q_2 1.34, e_2 -0.07; styrene-III, r_1 0.43, r_2 1.49, Q_2 1.37, e_2 -0.13; MMA-I, r_1 0.32, r_2 0.91, Q_2 1.58, e_2 0.80; MMA-II, r_1 0.38, r_2 1.46, Q_2 1.42, e_2 -0.35; MMA-III, r_1 0.29, r_2 1.22, Q_2 1.58, e_2 -0.62. Analysis of these data indicates that these phosphorus moieties are activating through strong electronegative effects. The extent of activation is intermediate in intensity between mildly activating groups (e.g. Cl) and strongly activating groups (e.g. C≡N or NO₂). The behavior of diphenyl-*p*-styrylphosphine is of particular interest in this respect, since its electronegativity points to strong electron delocalization.

INTRODUCTION

In an earlier study^{1,2} of the homopolymerization and copolymerization of vinyl phosphines, oxides, and sulfides, it was revealed that while a phosphorus moiety did not exhibit strong conjugative stabilization of an adjacent carbon radical, limited activation was in evidence. In order to obtain a better insight into activating effects by these phosphorus groups it was necessary to study the vinylphosphorus system in the absence of steric complications. Copolymerization study on phosphorus-substituted *p*-styrenes is well suited for this objective.

EXPERIMENTAL

Synthesis of Monomers

Diphenyl-*p*-Styrylphosphine. The synthesis of this monomer in this laboratory has been described in the literature.³

Diphenyl-*p*-Styrylphosphine Oxide. To a solution of 40.4 g. (0.14 mole) of diphenyl-*p*-styrylphosphine in 150 ml. of low boiling petroleum ether and 250 ml. of heptane was slowly added a solution of 17.7 g. of 75% *tert*-butyl hydroperoxide (0.198 mole) in 20 ml. heptane. External cooling maintained the temperature below 10°C. The further addition of 0.5 ml. of the hydroperoxide produced no heat, indicating an excess was present. An oil separated during the oxidation, and this crystallized during a 10 min. vigorous stirring period following the completion of the addition. A white solid was obtained, 24.6 g., m.p. 68–72°C. An additional 12.33 g., m.p. 94–100°C. and 2.38 g., m.p. 70–75°C. were obtained by reduction of the volume of the filtrate. The dehydration of these solids was accomplished as follows using solvents that had been previously dried over alumina. A solution of 26.6 g. of the above low melting oxide was dissolved in chloroform and 8.8 g. of alumina was added. After being agitated for 5 min., the solution was filtered and the chloroform removed at room temperature by using an aspirator. The viscous residue was dissolved in benzene (this must be carried out immediately since upon standing, even at 0°C., the residue converts to an insoluble gel). Hexane was added until the solution became cloudy, whereupon an oil separated. The oil began to crystallize and after standing overnight at 0°C., the crystalline product was collected, 19.05 g., m.p. 98–101.5°C. Thus a total of 31.4 g. (73%) of dehydrated oxide resulted from the oxidation.

ANAL. Calcd. for $C_{20}H_{17}PO$: C, 78.93%; H, 5.63%; P, 10.18%. Found: C, 78.75%; H, 5.38%; P, 10.64%.

Preparation of Diphenyl-*p*-Styrylphosphine Sulfide. To a solution of 75 g. (0.26 mole) of diphenyl-*p*-styrylphosphine in 110 ml. of benzene was slowly added a mixture of 8.5 g. (0.265 mole) of sulfur in 150 ml. of benzene. The exothermic reaction was maintained at 40°C. using external cooling. When the addition was complete, the solution was allowed to cool to room temperature. An additional 0.5 g. of sulfur was added to insure that an excess was present. The solution was filtered and the filtrate devolatilized under reduced pressure at room temperature. The resulting white solid was taken up in low boiling petroleum ether and collected, 76.1 g. (91%), m.p. 100.5–106.5°C. It was recrystallized by dissolving 64 g. in 770 ml. of boiling heptane. Upon cooling 49.3 g. of white crystalline solid, m.p. 105–107°C. was obtained.

ANAL. Calcd. for $C_{20}H_{17}PS$: C, 74.34%; H, 5.14%; P, 9.73%; S, 10.65%. Found: C, 74.98%; H, 5.35%; P, 9.67%; S, 10.01%.

Homopolymerizations

Free radical homopolymerizations were carried out in a sealed, heavy-walled glass tubes in benzene solution with azobisisobutyronitrile (AIBN) as a catalyst. The mixtures were degassed at least three times at -78°C . prior to sealing.

Tables I, II, and III summarize the homopolymerization results.

TABLE I
Homopolymerization of Diphenyl-*p*-Styrylphosphine Oxide

AIBN, g./g. monomer	Time, hr.	Temp., $^{\circ}\text{C}$.	Yield, %	$[\eta]$ (30°C ., CHCl_3), dl./g.
No catalyst	23	60	63	2.0
No catalyst	23	100	93	0.48
0.005	23	60	94	0.59
0.005	20	60	96	0.89
0.0005	23	60	83	1.3

TABLE II
Homopolymerization of Diphenyl-*p*-Styrylphosphine

AIBN, g./g. monomer	Time, hr.	Temp., $^{\circ}\text{C}$.	Yield, %	$[\eta]$ (30°C ., Toluene), dl./g.
No catalyst	208	60	24	0.84
No catalyst	65	100	65	0.50
0.005	41	60	86	0.22
0.0057	50	60	97	0.28
0.0005	41	60	79	0.14
0.0002	51	60	86	0.26

TABLE III
Homopolymerization of Diphenyl-*p*-Styrylphosphine Sulfide

AIBN, g./g. monomer	Time, hr.	Temp., $^{\circ}\text{C}$.	Yield, %	$[\eta]$ (30°C ., CHCl_3), dl./g.
No catalyst	832	60	67	0.68
No catalyst	64	100	65	0.33
0.005	40	60	96	0.31
0.0046	50	60	97	0.59
0.0005	40	60	77	0.77
0.0002	51	60	95	1.3

Copolymerization

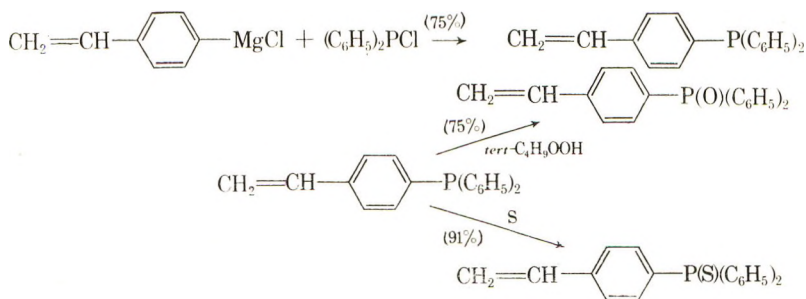
The monomers, AIBN (0.2 wt.-%), and benzene solvent were placed in constricted, heavy-walled glass tubes which were degassed three times at -78°C . and sealed. These tubes were heated at 60°C . until they showed

signs of small viscosity increases. They were then opened, the contents diluted with an appropriate solvent, and these solutions added to nonsolvents to precipitate the copolymers. The appropriate dilution solvent was toluene in the case of the phosphine copolymers and chloroform for the others. The nonsolvent used was generally hexane; however, a number of precipitations of the copolymers of the sulfide were carried out in methanol. These were redissolved and reprecipitated at least one further time to insure purity. They were then dried at $56^{\circ}\text{C}/0.1\text{ mm.}$ and analyzed for phosphorus content. The copolymer compositions ranged from 3.5 to 9.5% phosphorus.

RESULTS AND DISCUSSION

Monomer Synthesis

Diphenyl-*p*-styrylphosphine was prepared by the direct reaction of diphenylchlorophosphine with *p*-styrylmagnesium chloride.³ The preparation of diphenyl-*p*-styrylphosphine sulfide was accomplished in high yield (91%) by treating the phosphine with sulfur. Diphenyl-*p*-styrylphosphine oxide was prepared in 75% yield by oxidation of the phosphine with *tert*-butyl hydroperoxide followed by dehydrating the resultant hydrated product with alumina. (Hydrated triphenylphosphine oxide has been previously reported.⁴)

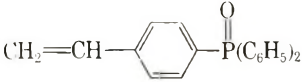
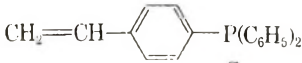
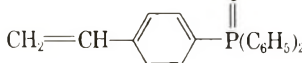
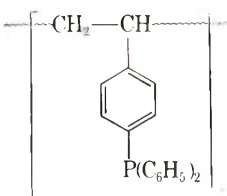


Ultraviolet Spectra of the Monomers

In an effort to discover if any resonance interaction between the phosphorus moieties and the aromatic ring and the vinyl group was occurring, a study of the ultraviolet spectra of these monomers was made. The data are presented in Table IV.

The absorption pattern of diphenyl-*p*-styrylphosphine is very similar to that of triphenylphosphine and no special conjugation can be noted between the phosphorus and the vinyl group. A similar conclusion follows from the patterns of the oxide and sulfide; the absorption is very similar to that observed for any *para*-substituted styrene.

TABLE IV
 Ultraviolet Spectra of Substituted Styrenes

Substance	λ_{max} , m μ	Molar extinction coefficient
	297	1,249
	285 (sh)	2,955
	271 (sh)	19,600
	262	25,500
	258 (sh)	24,050
	285 (sh)	15,460
	263 (sh)	18,240
	257	18,390
	298 (sh)	4,000
	260	24,400
	271 (sh)	10,850
	265	10,550

Homopolymerization Studies

Homopolymerization experiments were carried out on the phosphine, oxide, and sulfide. As expected, these substituted styrenes polymerized readily with thermal or free radical initiation to high molecular weight polymers. The details are tabulated in the Experimental Section.

Thermogravimetric analysis revealed that these homopolymers were more thermally stable than polystyrene. Table V summarizes the results.

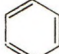
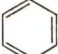
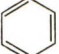
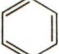
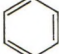
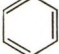
 TABLE V
 Thermogravimetric Analysis on *p*-Phosphorus-Containing Styrene Homopolymers

	T_i , °C. ^a		T_{10} , °C. ^a	
	In air	In N ₂	In air	In N ₂
p -(C ₆ H ₅) ₂ P(C ₆ H ₄)CH=CH ₂	325	375	396	425
p -(C ₆ H ₅) ₂ P(O)(C ₆ H ₄)CH=CH ₂	320	395	390	435
p -(C ₆ H ₅) ₂ P(S)(C ₆ H ₄)CH=CH ₂	365	395	415	430
Polystyrene	263		341	

^a The T_i and T_{10} are the temperatures at which initial and 10% weight loss were observed, respectively, when the sample was heated at a rate of 10°C./min.

Although the softening points of these polymers were between 110 and 210°C., no glass transition was observed above room temperature when the polymers were examined by differential thermal analysis.

TABLE VI
Relative Reactivities of *p*-Phosphorus-Containing Styrenes with Styrene and Methyl Methacrylate at 60°C.

M ₁	M ₂	r ₁	r ₂	Q ₂ ^a	e ₂ ^a
Styrene	$\text{CH}_2=\text{CH}-$  $-\text{P}(\text{C}_6\text{H}_5)_2$	0.52 ± 0.05 ± 0.23	1.43 ± 0.25 ± 1.1	1.25	-0.30
Styrene	$\text{CH}_2=\text{CH}-$  $-\text{P}(\text{S})(\text{C}_6\text{H}_5)_2$	0.43 ± 0.05 ± 0.15	1.49 ± 0.33 ± 1.4	1.37	-0.13
Styrene	$\text{CH}_2=\text{CH}-$  $-\text{PO}(\text{C}_6\text{H}_5)_2$	0.42 ± 0.02 ± 0.07	1.40 ± 0.15 ± 0.41	1.34	-0.07
MMA	$\text{CH}_2=\text{CH}-$  $-\text{P}(\text{C}_6\text{H}_5)_2$	0.32 ± 0.02 ± 0.06	0.91 ± 0.12 ± 0.33	1.58	-0.80
MMA	$\text{CH}_2=\text{CH}-$  $-\text{P}(\text{S})(\text{C}_6\text{H}_5)_2$	0.29 ± 0.01 ± 0.04	1.22 ± 0.34 ± 1.08	1.58	-0.62
MMA	$\text{CH}_2=\text{CH}-$  $-\text{PO}(\text{C}_6\text{H}_5)_2$	0.38 ± 0.02 ± 0.04	1.46 ± 0.10 ± 0.27	1.42	-0.35

^a The *Q* and *e* for styrene that were used are 1.00 and -0.80, respectively; for methyl methacrylate *Q* = 0.74 and *e* = 0.4 were used.

Copolymerizations

As mentioned earlier, these *p*-substituted styrenes, through copolymerization studies, presented a convenient means to weigh the resonance and polar stabilization effects of the substituents on a carbon radical. Methyl methacrylate and styrene were chosen as representative comonomers. Six series of six copolymerizations each were run at 60°C. It was found that the phosphorus substituted styrenes in each case were more reactive than styrene or methyl methacrylate. The reactivity results appear in Table VI.

The r_1 and r_2 values were the least-squares best estimates as calculated on a Burroughs 205 Computer using a program based on the copolymerization equation.⁵ The Q and e values were calculated from these reactivity ratios by using the Price-Alfrey⁶ equation. The upper \pm values are standard errors. The lower \pm values were calculated by a statistical technique. They are, approximately, the limits of an elliptical region in which the probability is 0.95 that the true values of r_1 and r_2 lie. This ellipse is conveniently called a confidence region. Alfrey, Bohrer, and Mark⁷ call this method "an objective scheme for calculating r_1 and r_2 and the probable errors thereof."

A convenient way to compare substituent effects in the *p*-substituted styrene series is in terms of the relative reactivity of the *p*-substituted styrene and styrene toward the styryl and methyl methacrylate radicals. Walling and co-workers have plotted the logs of these relative reactivities versus the Hammett σ values for the substituents and have obtained linear correlations. Table VII lists the calculated relative reactivities of the monomers of this report and the corresponding σ values as read from the Walling graphs.⁸

TABLE VII
Relative Reactivities of Substituted Styrenes Towards Indicated Radicals and Derived Hammett σ Values

Substituent	Styrene radical		MMA radical	
	Relative reactivity	Derived σ	Relative reactivity	Derived σ
Hydrogen	1.0		1.0	
(C ₆ H ₅) ₂ P	1.92	0.5	1.44	0.3
(C ₆ H ₅) ₂ P(O)—	2.3	0.65	1.20	0.0
(C ₆ H ₅) ₂ P(S)—	2.3	0.65	1.60	0.45

Except for the oxide, the corresponding σ values obtained from the styryl and from the methyl methacrylate radicals are in good agreement. Most noteworthy is that these σ values place these moieties in the class of strong electron-withdrawing groups. [Some σ values for electron-withdrawing *p*-substituents are; COOH(0.27), I(0.28), C(O)CH₃(0.52), CF₃(0.55), CN(0.63), NO₂(0.78).] This is in agreement with the e values for the

p-phosphorus-substituted styrenes which in most cases also indicate considerable electron withdrawal. Electronegative effects were anticipated with the oxide and sulfide but are quite unexpected for the electron pair containing $(C_6H_5)_2P$ moiety and indicate major delocalization of the electron pair on phosphorus.

To sum up, this work has shown these phosphorus moieties [$(C_6H_5)_2P-$, $(C_6H_5)_2P(O)$, $(C_6H_5)_2P(S)$] to be mildly activating and to exhibit strong electronegative influence in a radical addition process. Major conjugative effects are not indicated. These findings are consistent with the indications of intermediate activation by the phosphorus groups in the analogous vinyl compounds.² Since the phosphorus groups appear to exert an activating effect in copolymerization reactions where steric effects are minimized or absent, the failure of the vinyl phosphorus monomers to homopolymerize to high molecular weight points to significant steric effects in the propagation reaction. The reduction of the rate of the propagation step by steric interference would make the termination and chain transfer processes correspondingly more important and would account for the low molecular weight polymers observed.²

The authors wish to thank Dr. R. G. Schmitt for his interpretations of the ultraviolet spectra of the monomers and Dr. D. W. Behnken and Mr. K. F. Kolb for analyzing the data mathematically.

References

1. Rabinowitz, R. and J. Pellon, paper presented at 140th Meeting, American Chemical Society, Chicago, Ill., Sept. 1961; *Abstracts*, p. 43Q.
2. Rabinowitz, R., R. Marcus, and J. Pellon, *J. Polymer Sci.*, **A2**, 1233 (1964).
3. Rabinowitz, R., and R. Marcus, *J. Org. Chem.*, **26**, 4157 (1961).
4. Halmann, M., and S. Pinchas, *J. Chem. Soc.*, **1958**, 3264.
5. Mayo, F. R., and F. M. Lewis, *J. Am. Chem. Soc.*, **66**, 1594 (1944).
6. Alfrey, T., Jr., and C. C. Price, *J. Polymer Sci.*, **2**, 101 (1947).
7. Alfrey, T., Jr., J. J. Bohrer, and H. Mark, *Copolymerization*, Interscience, New York, 1952, p. 23.
8. Walling, C., E. R. Briggs, K. B. Wolfstirn, and F. R. Mayo, *J. Am. Chem. Soc.*, **70**, 1537 (1948).

Résumé

La diphényl *p*-styrylphosphine, préparée par la réaction de la diphénylchlorophosphine avec le chlorure de *p*-styrylmagnésium, a été transformée en oxyde et sulfure correspondants par traitement avec le peroxyde de tétrabutyle ou avec le soufre. Les styrènes substitués polymérisent facilement par initiation thermique ou radicalaire, en polymères de haut poids moléculaire. Ces polymères sont un peu plus stables thermiquement que le polystyrène. Ainsi leurs T_i à l'air se situent de 320–365°C, sous azote entre 375–395°C. Leut T_{10} se situent entre 390–415°C sous air et 425–435°C sous azote. Le polystyrène à l'air a un T_i de 263°C et T_{10} de 340°C. Les monomères copolymérisent facilement avec le styrène et le méthacrylate de méthyle; les polymères obtenus avec des taux de conversion peu élevés contiennent toujours plus de phosphore que les mélanges de monomères. Les rapports de réactivité ont été déterminés et les valeurs de Q et e calculées. Ces valeurs sont: (monomère phosphoré M_2): styrène-I, r_1 0.52, r_2 1.43, Q_2 1.34, e_2 -0.30; styrène-II, r_1 0.42, r_2 1.4, Q_2 1.34, e_2 -0.07; styrène-

III, r_1 0.43, r_2 1.49, Q_2 1.37, e_2 -0.13; MMA-I, r_1 0.32, r_2 0.91, Q_2 1.58, e_2 0.80; MMA-II, r_1 0.38, r_2 1.46, Q_2 1.42, e_2 -0.35; MMA-III, r_1 0.29, r_2 1.22, Q_2 1.58, e_2 -0.62. L'analyse de ces données indique que ces résidus phosphoriques sont activateurs à cause de leur effet électronégatif élevé. L'effet est intermédiaire en intensité entre celui exercé par les groupes peu activateurs (p.ex. Cl) et les groupes fortement activateurs (p.ex. CN ou NO₂). Le comportement de la diphenyl-*p*-styrylphosphine est d'un intérêt particulier à ce point de vue puisque sa forte électro-négativité indique une forte délocalisation électronique.

Zusammenfassung

Diphenyl-*p*-styrylphosphin, das durch Reaktion von Diphenylchlorphosphin mit *p*-Styrylmagnesiumchlorid dargestellt worden war, wurde durch Behandlung mit *t*-Butylhydroperoxyd bzw. Schwefel in das entsprechende Oxyd bzw. Sulfid umgewandelt: Diese substituierten Styrole polymerisieren bei thermischer oder radikalischer Anregung leicht zu hochmolekularen Polymeren. Die Polymeren sind thermisch etwas stabiler als Polystyrol. Ihr T_i in Luft lag zwischen 320 und 365°C und in Stickstoff zwischen 375 und 395°. Ihr T_{10} lag in Luft zwischen 390 und 416°C und in Stickstoff zwischen 425 und 435°C. Polystyrol besitzt in Luft ein T_i von 263°C und ein T_{10} von 340°C. Die Monomeren bilden leicht Copolymere mit Styrol und Methylmethacrylat, wobei die Polymeren bei niedrigem Umsatz immer mehr Phosphor enthalten als die Monomerenmischung. Reaktivitätsverhältnisse wurden bestimmt und daraus Q - und e -Werte berechnet. Die Werte für die folgenden Monomerenpaare (phosphorhaltiges Monomeres ist M_2) sind: Styrol-I, r_1 0,52, r_2 1,43, Q_2 1,35, e_2 -0,30; Styrol-II, r_1 0,42, r_2 1,40, Q_2 1,34, e_2 -0,07; Styrol-III, r_1 0,43, r_2 1,49, Q_2 1,37, e_2 -0,13; MMA-I, r_1 0,32, r_2 0,91, Q_2 1,58, e_2 0,80; MMA-II, r_1 0,38, r_2 1,46, Q_2 1,42, e_2 -0,35; MMA-III, r_1 0,29, r_2 1,22, Q_2 1,58, e_2 -0,62. Eine Analyse dieser Daten zeigt, dass die phosphorhaltigen Gruppen durch starke elektronegative Effekte aktivierend wirken. Das Ausmass der Aktivierung liegt zwischen dem von schwach aktivierenden Gruppen (z.B. Cl) und stark aktivierenden Gruppen (z.B. C≡N oder NO₂). Das Verhalten von Diphenyl-*p*-styrylphosphin ist in dieser Hinsicht von besonderem Interesse, da seine Elektronegativität für eine starke Elektronendelokalisierung spricht.

Received December 7, 1962

Revised February 18, 1963

Polysulfones of Norbornene and Derivatives

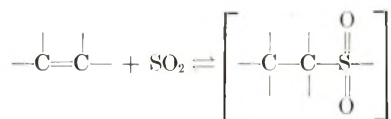
EDWARD H. HILL and JOHN R. CALDWELL, *Research Laboratories, Tennessee Eastman Company, Division of Eastman Kodak Company, Kingsport, Tennessee*

Synopsis

Norbornene and some of its monosubstituted and disubstituted derivatives reacted with sulfur dioxide to give polysulfones. These polysulfones are very stable thermally, compared to those of 1-butene and cyclohexene. Their stability can be further improved by using tin(II) oxide or thioacetamide as stabilizers. The polysulfones of norbornene and its derivatives have very high polymer melt temperatures.

Introduction

The reaction of sulfur dioxide with an olefin or other double-bond-containing compound to produce a polysulfone is well known and may be represented by the following equation:



A large number of monomers have been investigated.¹⁻³ Most of the polysulfones made from these monomers have the common defect of poor thermal stability; that is, the polymer when heated reverts rapidly to the monomer and sulfur dioxide. We have found that polysulfones prepared from norbornene and some of its derivatives are very stable thermally⁴ and that this stability can be further improved by the use of stabilizers.

Experimental

The polysulfones of norbornene and its derivatives are easily prepared, although the purity of the monomers and the reaction solvents are of great importance in obtaining high molecular weights. The polymers discussed here were prepared in 16-oz. pressure bottles under a nitrogen atmosphere, *tert*-butyl hydroperoxide being used as the catalyst. Either methanol or methylene chloride was the reaction solvent. The polymers precipitated in the former, but were soluble in the latter, and a viscous dope was obtained. A typical recipe using methyl 5-norbornene-2-carboxylate as the monomer and either methanol or methylene chloride as solvent is as follows: 15.2 g. (0.1 mole) methyl 5-norbornene-2-carboxylate,

12.8 g. (0.2 mole) sulfur dioxide, 100 ml. solvent, 0.1 g. *tert*-butyl hydroperoxide; allow to stand at -20°C . for 8 hr. The polymers prepared in methanol were filtered, washed several times with isopropyl alcohol, and dried at 60°C . The viscous solutions obtained in methylene chloride were poured into methanol with vigorous stirring and the precipitated polymer was treated as above. The yields were 98% or better.

The norbornene monomers were purified by distillation and had the physical constants shown in Table I.

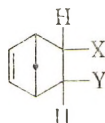
TABLE I
Physical Constants of Norbornene and Some of Its Derivatives Used in Preparing Polysulfones

Compound	B.p., $^{\circ}\text{C}/$ (pressure, mm.)	n_D^{20}
5-Norbornene	94.5/733.4	Solid
5-Norbornene-2-carbonitrile	65/6	1.4856
5-Norbornene-2-carboxylic acid, methyl ester	82/14.5	1.4743
5-Norbornene-2-carboxylic acid, octyl ester	138/12	1.4452
3-Methyl-5-norbornene-2-carboxylic acid, methyl ester	93.5/19.5	1.4698
5-Norbornene-2-yl acetate	68/8	—
5-Norbornene-2,3-dicarboxylic acid, diisobutyl ester	140/1.4	1.4570
5-Norbornene-2,3-dicarboxylic acid, bis(2-ethylhexyl) ester	100/2 μ	1.4708
<i>N</i> -(2-Ethylhexyl)-5-norbornene-2,3- dicarboximide	83/70 μ	1.5009
<i>N</i> -Butyl-5-norbornene-2,3-dicarbox- imide	108/110/0.5	Solid

Methanol and methylene chloride were distilled and had the following physical constants: methanol, b.p. $64^{\circ}\text{C}/732$ mm., n_D^{20} 1.3284; methylene chloride, b.p. $39.5^{\circ}\text{C}/729.8$ mm., n_D^{20} 1.4240. The sulfur dioxide was distilled into the chilled reaction vessel at room temperature.

Results and Discussion

Norbornene and its derivatives have the following general structure:



Polysulfones were prepared from norbornene; from the derivatives where Y is hydrogen and X is $-\text{CN}$, $-\text{OC}(\text{O})\text{CH}_3$, $-\text{C}(\text{O})\text{OCH}_3$, and $-\text{C}(\text{O})-\text{OC}_8\text{H}_{17}$; and from the derivative in which Y is a methyl group and X

is $-\text{C}(\text{O})\text{OCH}_3$. Polymers could not be made from those derivatives in which both X and Y were $-\text{C}(\text{O})\text{OCH}_2\text{CH}(\text{CH}_3)_2$ or both were $-\text{C}(\text{O})\text{OCH}_2(\text{CH}_2)_3\text{CH}(\text{CH}_3)\text{C}_2\text{H}_5$. Efforts to polymerize the imides were also unsuccessful. It was thought possible that -20°C . was above the ceiling temperature for the polymerization of the diesters and imides, but no polymer was obtained even when the reaction temperature was lowered to -70°C .

The thermal stabilities of polysulfones prepared from norbornene derivatives are shown in Table II, along with those of the polysulfones of 1-butene and cyclohexene. The stabilities were determined by heating a weighed sample of the polymer in a test tube at 190°C . and determining the weight loss due to the breakdown of the polymer into monomer and sulfur dioxide at intervals of 0.5, 1, and 3 hr.

TABLE II
Comparison of the Stability of the Polysulfones of 1-Butene, Cyclohexene, and Norbornene Derivatives

Polysulfone	Weight loss at 190°C ., %		
	0.5 Hr.	1 Hr.	3 Hr.
Cyclohexene	4.1	6.8	16.1
1-Butene	12.8	18.3	30.5
5-Norbornene-2-carbonitrile	2.2	3.8	5.4
5-Norbornene-2-carboxylic acid, methyl ester	1.9	5.7	9.5
5-Norbornene-2-yl acetate	3.3	5.8	8.9

These inherent stabilities can be improved further by the addition of stabilizers which have been shown to be effective for other polysulfones.⁵ The stabilized polysulfones of the norbornene derivatives show an im-

TABLE III
Comparison of the Stabilities of the Polysulfones of 1-Butene, Cyclohexene, and Norbornene Derivatives Stabilized With Tin(II) Oxide

Polysulfone ^a	Weight loss at 190°C ., %		
	0.5 Hr.	1 Hr.	3 Hr.
1-Butene	0	0	0.8
Cyclohexene	0	0.2	1.3
5-Norbornene-2-yl acetate	0	0	0.95
5-Norbornene-2-carboxylic acid, methyl ester	0	0.25	0.67
5-Norbornene-2-carboxylic acid, octyl ester	0	0.12	0.74
3-Methyl-5-norbornene-2-carboxylic acid, methyl ester	0	0.31	1.04

^a Tin(II) oxide, 1 wt.-%, added.

TABLE IV
Comparison of the Stabilities of the Polysulfones of 1-Butene, Cyclohexene, and Norbornene Derivatives Stabilized With Thioacetamide

Polysulfone ^a	Weight loss at 190°C., %		
	0.5 Hr.	1 Hr.	3 Hr.
1-Butene	0.9	1.5	3.8
Cyclohexene	1.2	1.7	3.5
5-Norbornen-2-yl acetate	0	0.01	1.34
5-Norbornene-2-carboxylic acid, methyl ester	0	0.5	1.98
5-Norbornene-2-carboxylic acid, octyl ester	0.06	0.34	1.91
3-Methyl-5-norbornene-2-carboxylic acid, methyl ester	0.21	0.56	1.71

^a Thioacetamide, 1 wt.-%, added.

proved stability, although not so striking as the polysulfones of 1-butene and cyclohexene, as shown in Tables III and IV.

The decomposition products of the thermal breakdown were identified by gas chromatography as sulfur dioxide and the norbornene derivative monomer. This is in accordance with other polysulfones and there would seem to be no difference in the mechanism of breakdown between the norbornene polysulfones and other, less stable sulfones.

All of the polysulfones of norbornene and its derivatives have very high polymer melt temperatures, as shown in Table V. Polymer melt temperature is defined as the temperature at which the polymer melts and leaves a trail of polymer when moved across a hot metal bar.⁶

TABLE V
Comparison of Polymer Melt Temperatures of the Polysulfones of Cyclohexene, 1-Butene, and Norbornene

Polysulfone	Polymer melt temp., °C.
5-Norbornene-2-yl acetate	240-245
3-Methyl-5-norbornene-2-carboxylic acid, methyl ester	245-248
5-Norbornene-2-carboxylic acid, octyl ester	240-248
5-Norbornene-2-carbonitrile	275-280
5-Norbornene	280-290
Cyclohexene	200-205
1-Butene	160

Thus, it would appear that the polysulfones of norbornene and its derivatives are not only very stable thermally, but also have higher polymer melt temperatures than most other polysulfones.

References

1. Snow, R. D. (to Phillips Petroleum Co.), U. S. Pat. 2,136,932 (1938).
2. Frey, F. E., L. H. Fitch, Jr., and R. D. Snow (to Phillips Petroleum Co.), U. S. Pat. 2,114,292 (1938).
3. Brubaker, M. M., and J. Harmon (to E. I. du Pont de Nemours and Co.), U. S. Pat. 2,241,900 (1941).
4. Caldwell, J. R., and E. H. Hill (to Eastman Kodak Co.), U. S. Pat. 2,899,412 (1959).
5. Crouch, W. W., and J. E. Wicklatz, *Ind. Eng. Chem.*, **47**, 160 (1955).
6. Sorenson, W. R., and T. W. Campbell, *Preparative Methods of Polymer Chemistry*, Interscience, New York-London, 1960, p. 49.

Résumé

Le norbornène et certains de ses dérivés mono- et disubstitués réagissent avec l'anhydride sulfureux pour former des polysulfones. Ces polysulfones sont très stables thermiquement, comparés à celles du butène-1 et du cyclohexène. Leur stabilité peut être accrue par l'emploi d'oxyde d'étain bivalent ou de thioacétamide comme stabilisants. Les polysulfones du norbornène et de ses dérivés possèdent de très hautes températures de fusion.

Zusammenfassung

Norbornen und einige seiner mono- und disubstituierten Derivate reagierten mit Schwefeldioxyd unter Bildung von Polysulfonen. Diese Polysulfone sind in Vergleich zu denjenigen von 1-Buten und Cyclohexen thermisch sehr stabil. Ihre Stabilität kann durch Verwendung von Zinn-II-oxyd oder Thioacetamid als Stabilisator noch verbessert werden. Die Polysulfone aus Norbornen und seinen Derivaten besitzen sehr hohe Schmelzpunkte.

Received January 28, 1963

Molecular Weight Dependence of the Second Virial Coefficient. Solutions of Styrene Dimers up to High Polymers and Other Systems

H. SOTOBAYASHI* and K. UEBERREITER, *Fritz-Haber-Institut der Max-Planck-Gesellschaft, Berlin-Dahlem, Germany*

Synopsis

The second virial coefficient B or A_2 has been calculated from cryoscopic measurements in naphthalene of polymers of styrene from dimers up to high polymers. The B -degree of polymerization curve has a maximum in the range of the tetramer. The portion of the curve showing the increase to a maximum is explained as a "macromolecule effect" of rigid rods according to the theory of Flory and Huggins. The A_2 - P (or B - P) curves investigated so far are described by the equation, $A_2 = (a/M^{1/2}) + b$. It is assumed that the shape of a macromolecular coil in solution depends upon the fact whether the main chain skeleton and its sidegroups have the same or opposite affinity to the solvent. In the case of polystyrene in naphthalene it is assumed that the C-C chain behaves as a lyophobic and the benzene groups as a lyophil. This leads to an increased density of the benzene sidegroups in the surface of the macromolecular coil. The interaction potential between the coils as a whole is therefore different from that in the interior. This effect is realized by splitting the excluded volume into two parts and leads to the reciprocal square root dependence of A_2 . This equation has been tested for many endothermal and exothermal systems. The constants a and b are zero at the θ -temperature and can be determined therefrom.

I. GENERAL CONSIDERATION OF THE B VALUE

The second virial coefficient A_2 is defined by the virial expansion of the osmotic pressure:

$$\pi = RT [(c/M) + A_2 c^2 + \dots] \quad (1)$$

M is the molecular weight and c the concentration. Sometimes the equivalent expansion

$$\pi = (RT/M) c + Bc^2 + \dots \quad (2)$$

is used and therefore $B = RTA_2$.

The value of B measures the deviation of the osmotic pressure of a solution from vant'Hoff's law. In order to analyze the solution properties of a macromolecular substance it is customary to regard B as resulting from the superposition of an entropy and an enthalpy factor:

$$B = B_S + B_H \quad (3)$$

* Permanent address: Institute for High Polymers, Kyoto University, Japan.

The entropy coefficient B_S is mainly a "conformational" factor. It describes implicitly the conformation of a macromolecule, which depends on its size and shape and is determined by the free or hindered rotation of its chain segments. The enthalpy coefficient B_H , on the other hand, depends upon the differential heat of dilution Δh_1 of the solvent which expresses the interaction of the solvent with the solute. The enthalpy coefficient therefore is an "interaction" factor which is zero in an athermal solution.

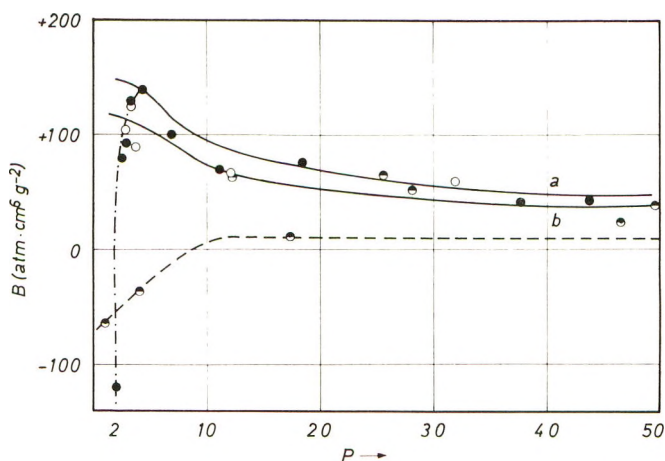


Fig. 1. Dependence of the second virial coefficient B and the enthalpy coefficient B_H on the degree of polymerization P of polystyrenes in naphthalene and benzene solution (cryoscopic measurements): (O) data of Kemp and Peters⁵ (in benzene); (●) data of Schulz and Marzolph⁶ and Horbach¹ (in benzene); (●) our values⁴ (in naphthalene); (-a-) B from eq. (16) (naphthalene); (-b-) B from eq. (16) (benzene); (- -) B_H .

We have investigated the B values of very low polymers of styrene in naphthalene and shall consider the conformational and interaction factors of these solutions including values obtained by other investigators for benzene and toluene solutions of short and long chain polystyrene (low and high polymers, respectively).

II. B_H COEFFICIENT OF POLYSTYRENE-BENZENE SOLUTIONS

Figure 1 shows among others the B_H - P curve of polystyrene-benzene solutions determined by Schulz.¹ The B_H values* of the monomer and tetramer deviate very much from those of the longer polystyrene chains; the sign of their heat of dilution is opposite to those of the higher homologs.

Schulz¹ proposed an explanation which has proved to be useful in con-

* B_H is expressed in atm. cm. g.⁻² for comparison with osmotic measurements. The change of units is given by the relation 1 cal. cm.³ g.⁻² = 41.2 atm. cm.⁶ g.⁻² = 4.19 joule cm.³ g.⁻².

sidering glass transitions² and melting points, the division of the macromolecules into endgroups and middle groups.

The task of developing a formula for the B value of long chain polystyrene solutions had led us to a different view point. The properties of an endgroup which have the same chemical constitution as the middle group² do not seem different enough from those of a middle group if the macromolecule is suspended in a dilute solution. We therefore regard polystyrene macromolecules as built of paraffin chains with benzene side groups. Each constituent differs in its interaction with the solvent, in our case benzene or naphthalene. While benzene rings, of course, though attached to a carbon chain mix readily with benzene molecules, this is not so much the case with paraffins. Paraffin-benzene solutions are endothermal and so are solutions of short chain polystyrenes in benzene where full contact of all the constituents with solvent molecules is unavoidable. The coiling up of longer chains enables the macromolecule to reduce the points of contact of its paraffin chain with the solvent molecules relative to those of the benzene side groups. Thereby the heat of dilution of the macromolecule as a whole is changed by the suppression of the paraffin character of the polystyrene backbone chain.

III. DETERMINATION OF B VALUES OF POLYSTYRENE-NAPHTHALENE SOLUTIONS

a. Experimental Values

We have measured the depression of the freezing points of short chain polystyrenes in naphthalene solution with a semimicrocryoscopic apparatus described in a previous paper.³ The osmotic pressure can be calculated from cryoscopic data with the help of known thermodynamic relations.* The B values were determined by plotting π and π/c versus c . The results are shown in Figure 1.⁴ The values determined by Kemp and Peters⁵ and Schulz and Marzolph⁶ with benzene solutions are also given.

The plot of the second virial coefficient B versus the degree of polymerization P , increases from negative values, has a maximum at $P = 4$, and decreases with increasing chain length. This is a surprising and so far unknown behavior.

b. Calculation of the Excess Entropy Coefficient B_s^E

The chemical potential of the solvent in a solution is proportional to the logarithm of its molar fraction; its expansion in a power series of the volume fraction agrees with vant' Hoff's law if we use only the linear term⁷ and

* From equation $\pi = [L/(V_1 T_0)]\Delta T$ we obtain the equation $\pi = 4.00 \cdot \Delta T$ (atm) for the case of naphthalene with a heat of melting $L = 4.49$ kcal. mole⁻¹ = 18.55×10^4 cm.³ atm. mole⁻¹, the partial molar volume $V_1 \cong$ molar volume of pure naphthalene = $V_{01} = 131.04$ cm.³ mole⁻¹ and the freezing point of naphthalene $T_0 = 80^\circ\text{C}$.

shows an ideal entropy coefficient B_S^{id} as a parameter of the quadratic term. The B_S^{id} value is of the form

$$B_S^{\text{id}} = (RTV_1/2M_0^2P) [2 - (1/P)] \quad (4)$$

where V_1 is the partial molar volume of the solvent, P the degree of polymerization and M_0 the molecular weight of a segment. We therefore have to realize that the entropy coefficient B_S is in fact composed of an ideal entropy coefficient B_S^{id} and the excess entropy coefficient B_S^{E} :

$$B_S = B_S^{\text{id}} + B_S^{\text{E}} \quad (5)$$

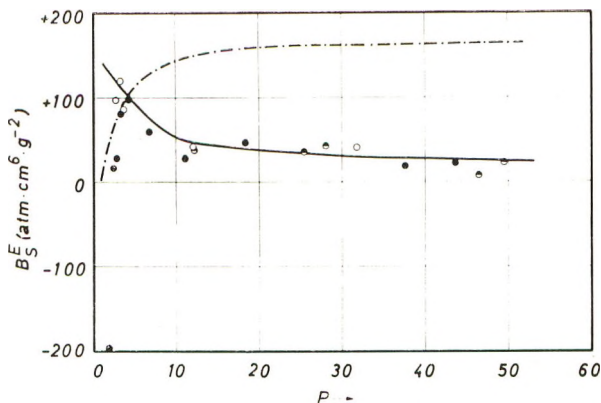


Fig. 2. Dependence of the excess entropy coefficient B_S^{E} on the degree of polymerization P of polystyrenes in naphthalene and benzene solution: (—) from eq. (17) for naphthalene; (---) from eq. (10) for naphthalene. Other symbols as in Figure 1.

The excess entropy coefficient depends only upon the size and shape of the solute macromolecule, as it describes the deviation of the properties of a solution from an ideal one. Equations (3) and (5) can be used to determine it:

$$B_S^{\text{E}} = B - B_H - B_S^{\text{id}} \quad (6)$$

We have used eq. (4) to calculate the B_S^{id} values, the B_H - P curve in Figure 1 for the B_H values, and our experimental B values of short chain polystyrenes in naphthalene solution to calculate their B_S^{E} coefficient. These values are shown in Figure 2 as a function of the degree of polymerization. Again the surprising result is obtained that the B_S^{E} - P curve, too, has a maximum which is in the neighborhood of $P = 4$, while the B_S^{E} value of the dimer is approximately zero.

IV. $B_{S_{\text{ath}}}^{\text{E}}$ VALUES OF RIGID RODLIKE MOLECULES ACCORDING TO FLORY-HUGGINS

The B_S^{E} - P curve shown in Figure 2 can be compared with a theoretical curve if we assume that the subtraction of B_H was sufficient to eliminate the influence of the interaction expressed by the heat of dilution.

Flory⁸ and Huggins⁹ themselves indicate that their model is mainly suited for homogeneously entangled or rodlike stretched macromolecules.¹⁰ Meyerhoff,¹¹ furthermore concludes from solution viscosity measurements that short chains are more or less stretched, a fact that seems plausible as they are not yet long enough to build a coil. The model of Flory and Huggins therefore seems very adequate to describe the B_s^E values of very short chains of a homologous series, i.e., the increasing portion of the B_s^E - P curve up to its maximum. We therefore shall use their theory for the description of this part of the B_s^E - P curve.¹²

Flory-Huggins' equation for the differential entropy of dilution ΔS_1 of an athermal system of N_1 solvent molecules and N_2 macromolecules of the degree of polymerization P is in terms of volume fractions φ_i of the form

$$S_1 = -R \left[\ln \varphi_1 + \left(1 - \frac{1}{P} \right) \varphi_2 \right] \quad (7)$$

The differential excess entropy of dilution S_1^E can be calculated from its definition with the help of eq. (7):

$$S_1^E = -R \left[\ln \frac{1 - \varphi_2}{1 - x_2} + \left(1 - \frac{1}{P} \right) \varphi_2 \right] \quad (8)$$

If we express the molar fraction x_2 by the volume fraction φ_2 and develop the logarithm up to the second term we obtain

$$S_1^E = \frac{R}{2} \left(1 - \frac{1}{P} \right) \varphi_2^2 \quad (9)$$

With the approximation for dilute solutions

$$c = \frac{M_0}{V_0} \varphi_2 \cong \frac{M_0}{V_1} \varphi_2$$

and the definition of the second excess entropy coefficient

$$B_s^E = \frac{TS_1^E}{V_1 c^2}$$

we obtain finally from eq. (9) an expression for the excess entropy coefficient B_{sath}^E

$$B_{sath}^E = \frac{RTV_1}{2M_0^2} \left(1 - \frac{1}{P} \right)^2 \quad (10)$$

This curve which we have calculated from Flory-Huggins' theory is plotted according to eq. (10) in Figure 2 for naphthalene as solvent. The B_{sath}^E values for rodlike short chains increase very sharply with increasing length of the rod and soon approach a limiting value. They are therefore independent of the degree of polymerization in the range of high polymers.

Equation (10) holds for rodlike rigid molecules. One can therefore say that it describes the "macromolecular effect," i.e., the increase of the en-

tropy of dilution with chain length. Dimers and trimers must be regarded as rigid rods, as their length does not permit a large number of configurations. The B_s^E - P curve therefore follows the course of eq. (10) up to the maximum at $P = 4$.

V. A_2 -VALUES FOR POLYMER COILS WITH INTERACTION

A solution with no interaction between solvent molecules and solute is athermal ($B_H = 0$), and a solute macromolecule is coiled up in a manner which can be described by the random flight theory. In an endo- or exothermal solution ($B_H = 0$) the interaction between polymer and solvent molecules influences the conformation of the former.

We therefore would like to propose the consideration of a possible opposite tendency of the atoms of the main chain of a polymer and its side groups to influence the configuration of the polymer coils. This influence will probably be mostly pronounced if the behavior of the solvent molecule is lyophobic with respect to the main chain and lyophilic with respect to the side groups or vice versa. In this case—lyophobic main chain—we propose that the chain tries to coil up in a manner which minimizes its contacts with the solvent molecules. The part of the polymer coil where the effect of this tendency will be readily visible is its surface. In the case of benzene or naphthalene solutions of polystyrenes, the side groups of which should be lyophilic to the solvent in opposition to the paraffin main chain, we therefore should assume a coil surface which is preferentially built of benzene rings from the polystyrene chain, which have turned their rings toward the pure solvent outside of the coil.

This effect leads us to the hypothesis that we should take an interaction potential for the chain segments within a polymer coil different from that between the coils as a whole.

In order to express this difference we have used the free volume model of a liquid, as, among others, it was used by Flory.¹³ He calculates for the second virial coefficient $A_2 (= B/RT)$ the relation

$$A_2 = N_L u / 2M^2 \quad (11)$$

We shall use the eq. (11), but divide the excluded volume into two parts: the intra- or micro-excluded volume u_{micro} which is caused by chain segment interactions within a coil and the inter- or macro-excluded volume u_{macro} which is an effect of the interactions of the polymer coils as a whole. We assume that u_{macro} is proportional to the volume of the coil in its expanded form and u_{micro} to the volume difference between an expanded and an undisturbed coil. These assumptions lead to the expression for the total excluded volume⁴

$$u = (k_1 + k_2) \frac{4}{3} \pi r_\theta^3 \alpha^3 - k_2 \frac{4}{3} \pi r_\theta^3 \quad (12)$$

Equation (12) still contains α , the expansion coefficient¹² of the polymer coil. It can be eliminated with the help of a theoretical expression devel-

oped by Zimm and collaborators.¹⁴ Using their formula for α and eqs. (11) and (12) we finally obtain

$$A_2 = (a/M^{0.5}) + b \quad (13)$$

with

$$a = 2\pi N_L b_0^3 k_1 / 3(6M_0)^{3/2} \quad (14)$$

and

$$b = N_L (k_1 + k_2) k \beta / 8\pi^{1/2} M_0^2 \quad (15)$$

a and b are constants which are dependent of the molecular weight. The factor k has been given a value of 134/105 by Zimm¹⁴ and Yamakawa,¹⁵ b_0 is the effective segment length at the θ -temperature, and β its excluded volume.

Equation (13) of course includes Zimm's theory for the expansion factor α expressed as a series which is used to the term describing single contact-interactions only. It therefore has its obvious limitation, and we can only expect that it holds for the description of experiments with a congruent accuracy.

Equation (13) with $B = RTA_2$ gives an expression for the second virial coefficient

$$B = RT \{ [a/(M_0P)^{0.5}] \} + b \quad (16)$$

which we have used for a description of that part of the B - P curve in Figure 1 which is at the right side of the maximum. It is now possible to calculate the excess entropy coefficient B_S^E from eqs. (6) and (16):

$$B_S^E = RT \{ [a/(M_0P)^{0.5}] + b \} - B_H - B_S^{id} \quad (17)$$

The values for B_H can be taken from the B_H - P curve in Figure 1 and those for B_S^{id} can be calculated from eq. (4) with naphthalene as solvent. Figure 2 shows the resulting curve which demonstrates that the function is capable of describing the dependence of the B_S^E values on the degree of polymerization P up to high molecular weights.

VI. TEST OF EQUATION (13)

We have already tested eq. (13) with various systems:⁴ (a) exothermal: polystyrene in benzene,^{5,6} polystyrene in naphthalene,⁴ polystyrene in toluene,¹⁶⁻¹⁸ polystyrene in butanone,¹⁹ and nitrocellulose in acetone;^{20,21} (b) endothermal: polymethyl methacrylate in acetone,²²⁻²⁴ polymethyl methacrylate in dioxane,²⁴ polymethyl methacrylate in butyl acetate,²⁴ and polymethyl methacrylate in butyl chloride.²⁵

In this paper we shall continue this test series with systems which have been investigated by different authors.

1. Polyacrylonitrile in Dimethylformamide

The second virial coefficient A_2 was calculated from the diffusion measurements of Kobayashi.²⁶ Figure 3 shows a plot of these A_2 values versus $M_D^{-0.5}$. The A_2 function is of the form

$$A_2 = (0.258/M_D^{0.5}) + 8.6 \times 10^{-4}$$

where $M = 28,000$ – $575,000$.

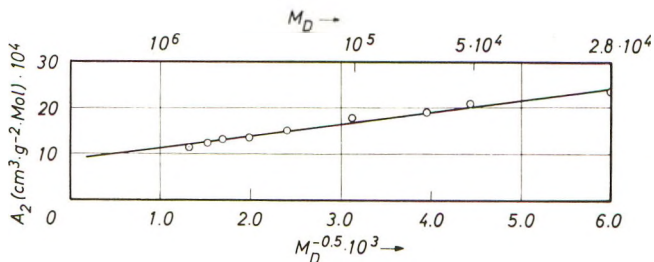


Fig. 3. Dependence of the second virial coefficient A_2 on the molecular weight M_D of polyacrylonitrile in dimethylformamide (diffusion). Data of Kobayashi.²⁶

2. Atactic Polypropylene in Benzene

This system has been well investigated by Kinsinger and Hughes²⁷ applying the osmotic method. We calculated the A_2 values; they again obey the function in Figure 4:

$$A_2 = (0.048/M_n^{0.5}) + 1.5 \times 10^{-4}$$

for $M = 14,000$ – $308,000$.

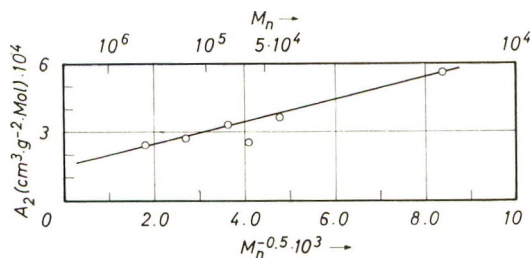


Fig. 4. Dependence of the second virial coefficient A_2 on the molecular weight M_n of atactic polypropylene in benzene (osmosis). Data of Kinsinger and Hughes.²⁷

3. Isotactic Polypropylene in Tetralin

This system has been investigated by Parrini, Sebastiano, and Messina²⁸ with the osmotic method. The A_2 function in Figure 5 is of the form

$$A_2 = (0.08/M_n^{0.5}) + 8.7 \times 10^{-4}$$

where $M = 43,000$ – $541,000$.

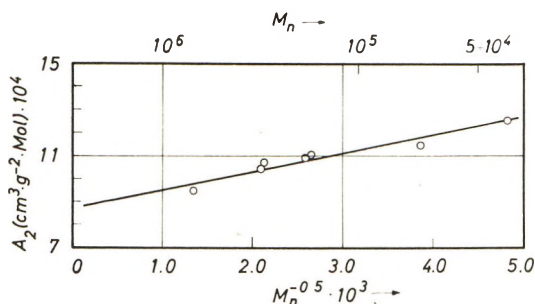


Fig. 5. Dependence of the second virial coefficient A_2 on the molecular weight M_n of isotactic polypropylene in tetralin (osmosis). Data of Parrini, Sebastiano, and Messina.²⁸

4. Isotactic Polypropylene in α -Chloronaphthalene

Parrini, Sebastiano, and Messina²⁸ have investigated this system with the light-scattering method. Figure 6 proves that their values can be described by a function

$$A_2 = (0.07/M_w^{0.5}) + 3.6 \times 10^{-4}$$

for $M = 85,600$ – $631,600$.

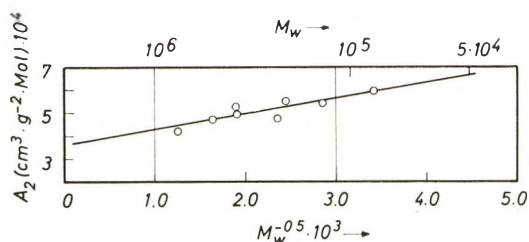


Fig. 6. Dependence of the second virial coefficient A_2 on the molecular weight M_w of isotactic polypropylene in chloronaphthalene (light scattering). Data of Parrini, Sebastiano, and Messina.²⁸

5. Polycarbonate in Tetrahydrofuran

We have taken the results of diffusion and sedimentation measurements from Schulz and Horbach.²⁹ Figure 7 shows that their A_2 values can be approximated by the function

$$A_2 = (0.12/M_{s.D.}^{0.5}) + 4.2 \times 10^{-4}$$

for $M = 8,500$ – $266,000$.

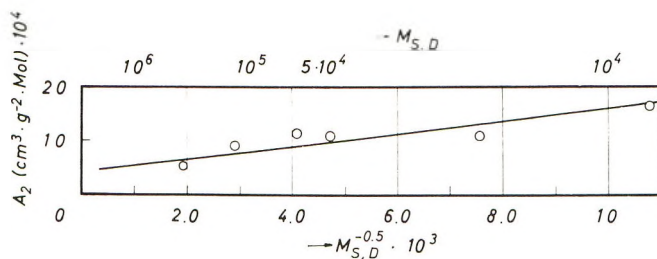


Fig. 7. Dependence of the second virial coefficient A_2 on the molecular weight $M_{S,D}$ of polycarbonate in tetrahydrofuran (Diffusion and sedimentation). Data of Schulz and Horbach.²⁹

6. Polycarbonate in Methylene Chloride

Osmotic measurements of Schulz and Horbach²⁹ permit calculation of A_2 . Figure 8 proves the validity of the equation

$$A_2 = (0.11/M_n^{0.5}) + 8.7 \times 10^{-4}$$

for $M = 23,600$ – $182,000$.

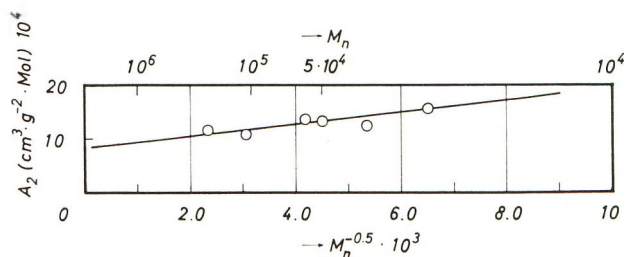


Fig. 8. Dependence of the second virial coefficient A_2 on the molecular weight M of polycarbonate in methylene chloride (osmosis). Data of Schulz and Horbach.²⁹

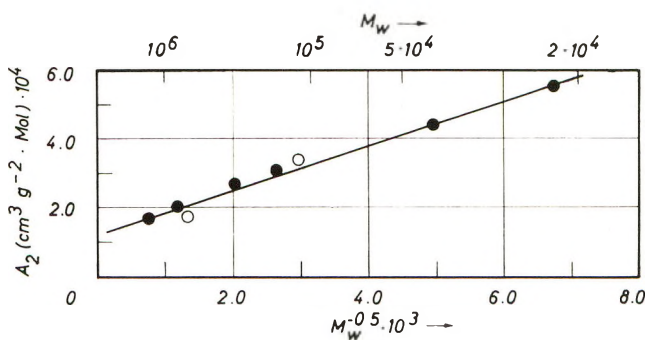


Fig. 9. Dependence of the second virial coefficient A_2 on the molecular weight M_w of polymethyl methacrylate in nitroethane (light scattering): (O) fractionated; (●) unfractionated. Data of Casassa and Stockmayer.³⁰

7. Polymethyl Methacrylate in Nitroethane and Butanone

Figures 9 and 10 show the results of light-scattering measurements of fractionated and unfractionated polymethyl methacrylate in nitroethane and butanone which have been made by Casassa and Stockmayer.³⁰ The A_2 functions are of the form

$$A_2 = (0.0646/M_w^{0.5}) + 1.2 \times 10^{-4}$$

for nitroethane, $M = 22,000$ – $1,700,000$, and

$$A_2 = (0.0567/M_w^{0.5}) + 0.95 \times 10^{-4}$$

for butanone, $M = 41,000$ – $2,760,000$.

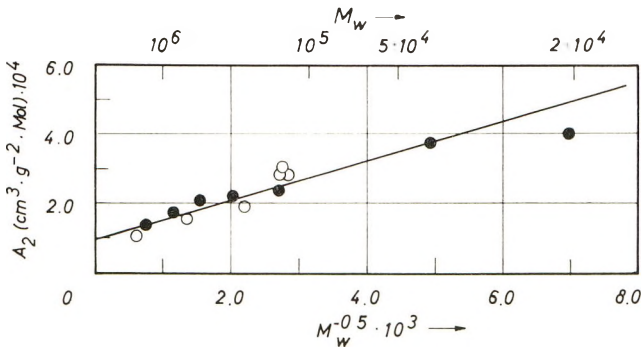


Fig. 10. Dependence of the second virial coefficient A_2 on the molecular weight M_w of polymethyl methacrylate in butanone (light scattering): (○) fractionated; (●) unfractionated. Data of Casassa and Stockmayer.³⁰

8. Polyisobutylene in Cyclohexane

This system has been well investigated by Krigbaum and Flory¹⁷ with the osmotic method. The function of A_2 in Figure 11 is in this case

$$A_2 = (0.062/M_n^{0.5}) + 5.0 \times 10^{-4}$$

for $M = 38,000$ – $710,000$.

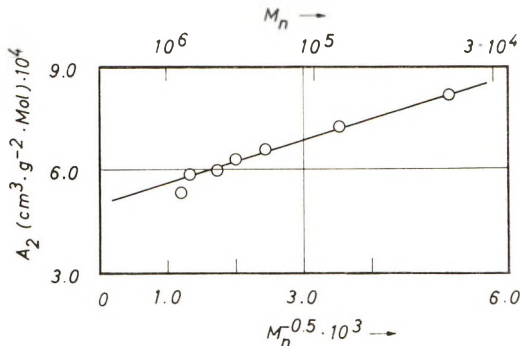


Fig. 11. Dependence of the second virial coefficient A_2 on the molecular weight M_n of polyisobutylene in cyclohexane (osmosis). Data of Krigbaum and Flory.¹⁷

9. Polyvinyl Acetate in Methyl Ethyl Ketone

Matsumoto and Ohyanagi³¹ and Schulz³² have investigated this system with light-scattering measurements. Figure 12 shows the validity of the function

$$A_2 = (0.0946/M_w^{0.5}) + 2.22 \times 10^{-4}$$

for $M = 40,000$ – $3,460,000$.

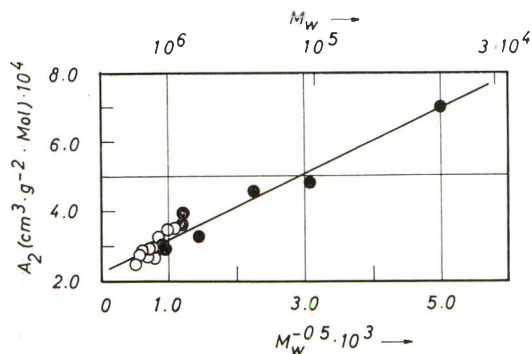


Fig. 12. Dependence of the second virial coefficient A_2 on the molecular weight M_w of polyvinyl acetate in methyl ethyl ketone (light scattering): (●) data of Matsumoto and Ohyanagi;³¹ (○) data of Schulz.³²

10. Polyvinyl Acetate in Acetone

Light-scattering data of Matsumoto and Ohyanagi³¹ have been used to calculate the A_2 values in Figure 13, which follow the relation

$$A_2 = (0.102/M_w^{0.5}) + 2.6 \times 10^{-4}$$

for $M = 27,000$ – $286,000$.

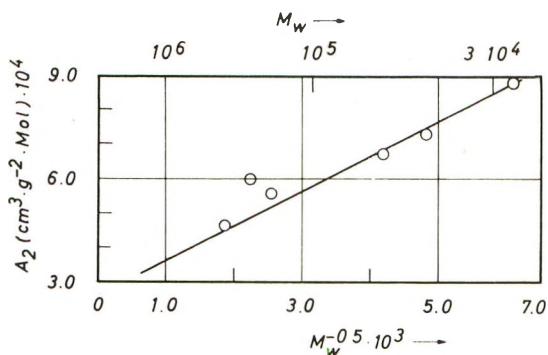


Fig. 13. Dependence of the second virial coefficient A_2 on the molecular weight M_w of polyvinyl acetate in acetone (light scattering). Data of Matsumoto and Ohyanagi.³¹

11. Polyisobutylene in Benzene

Krigbaum and Flory³³ investigated this system with the osmotic method in the neighborhood of the θ -temperature. Figure 14 shows the A_2 values from their data, where the fact of a change of the θ -temperature with the molecular weight has been neglected. The functions are:

At 313°K.

$$A_2 = (0.021/M_n^{0.5}) + 1.26 \times 10^{-4}$$

At 303°K.

$$A_2 = (0.0065/M_n^{0.5}) + 0.625 \times 10^{-4}$$

At 293°K.

$$A_2 = (-0.001/M_n^{0.5}) - 0.69 \times 10^{-4}$$

for $M = 101,000$ – $710,000$.

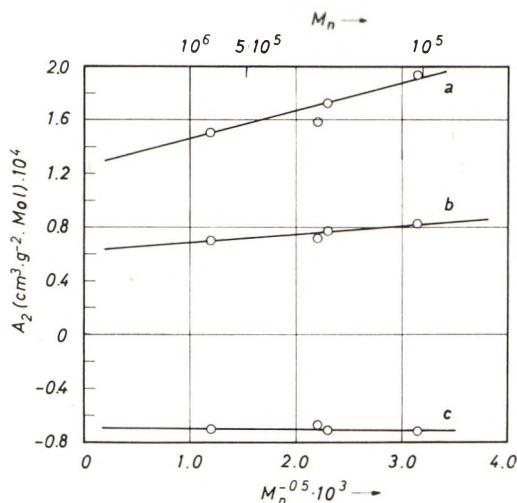


Fig. 14. Dependence of the second virial coefficient A_2 on the molecular weight M_n of polyisobutylene in benzene (osmosis): (a) 313°K.; (b) 303°K.; (c) 293°K. Data of Krigbaum and Flory.³³

12. Polystyrene in Cyclohexane

Krigbaum³⁴ investigated this system with the osmotic method in the range of the θ -temperature. Figure 15 shows the capability of eq. (13) to describe the values of A_2 . The functions are:

At 323°K.

$$A_2 = (0.0128/M_n^{0.5}) + 0.78 \times 10^{-4}$$

At 313°K.

$$A_2 = (0.00476/M_n^{0.5}) + 0.46 \times 10^{-4}$$

At 303°K.

$$A_2 = (-0.00316/M_n^{0.5}) - 0.14 \times 10^{-4}$$

for $M = 50,500$ – $566,000$.

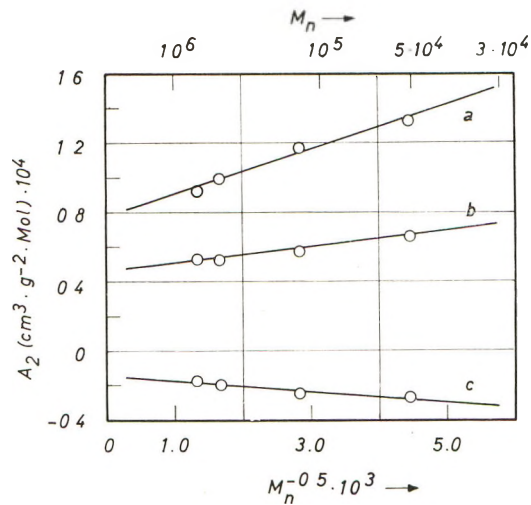


Fig. 15. Dependence of the second virial coefficient A_2 on the molecular weight M_n of polystyrene in cyclohexane (osmosis): (a) 323°K.; (b) 313°K.; (c) 303°K. Data of Krigbaum.³⁴

We hope that these examples are sufficient to prove the validity of eq. (13). It should be noted that the equation (13) is well suited for both endothermal and exothermal systems. Its accuracy is limited by the fact that we have used Zimm's description for the expansion coefficient α in form of a series which has been terminated after the linear term.

VII. CONSTANTS a AND b IN EQUATION (13) AT THE θ -TEMPERATURE

The macro-excluded volume is proportional to the expanded volume of a polymer coil which is zero at the θ -temperature. Our proportionality constant k_1 therefore should also be zero at this critical point as well as the constant a of eq. (13) which contains k_1 . The constant b in eq. (13) should be zero at the θ -temperature also, as b contains the excluded volume β of a segment as factor which is zero at the θ -temperature.

Three more examples shall serve as a test for these demands.

1. Polymethyl Methacrylate in Butyl Chloride

This system has been investigated by Kirste and Schulz²⁵ with the light-scattering method in the neighborhood of the θ -temperature. In a previous paper⁴ it was demonstrated that this system can be described with

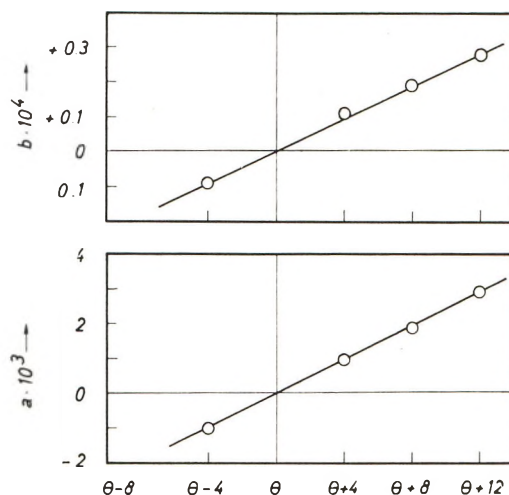


Fig. 16. Dependence of the constants a and b on the temperature of polymethyl methacrylate in butyl chloride (light scattering). Data of Kirste and Schulz.²⁵

sufficient accuracy by eq. (13) in the molecular weight range 30,000–4,600,000. The constants a and b have been calculated at $\theta + 12$, $\theta + 8$, $\theta + 4$, and $\theta - 4$. These values have been plotted in Figure 16 versus the temperature. It can be seen from this figure that a and b are in fact zero at the θ -temperature.

2. Polyisobutylene in Benzene and Polystyrene in Cyclohexane

The $A_2-M^{-0.5}$ functions of these systems have already been shown in Figures 14 and 15. The temperature dependence of the constants a and b of these functions is shown in Figures 17 and 18. Krigbaum determined the θ -temperature of these systems by the relation between A_2 and the temperature. We are now able to determine θ -temperatures independently as zero points of the a or b vs. temperature curves. Values taken from the intercept of these curves in Figures 17 and 18 with the temperature scale are contained in Table I together with Krigbaum's data. Values calculated by both methods agree very satisfactorily.

This we take as a further proof that eq. (13) is a good basis for a description of the A_2 values of polymer solutions when the accuracy of A_2 is limited in such a way that single contact interactions only need to be taken into account.

TABLE I

System	θ -temperature, °K.		
	by Krigbaum	From a	From b
Polyisobutylene–benzene	297.5	298	298
Polystyrene–cyclohexane	305.6	307	305

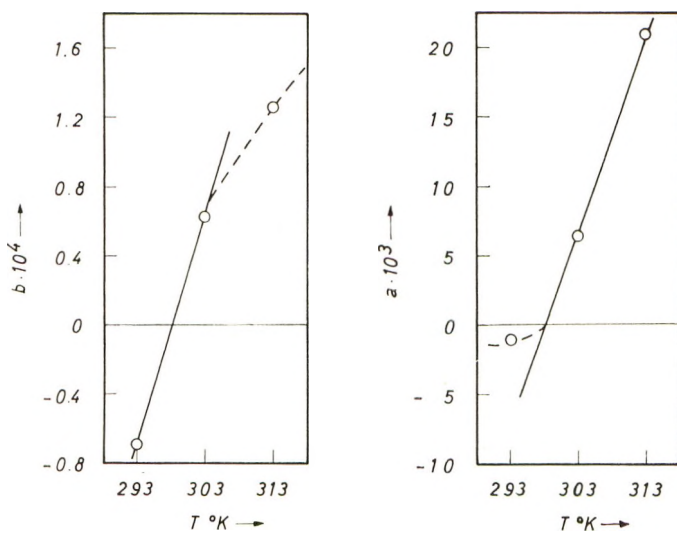


Fig. 17. Dependence of the constants a and b on the temperature of polyisobutylene in benzene (osmosis). Data of Krigbaum and Flory.³³

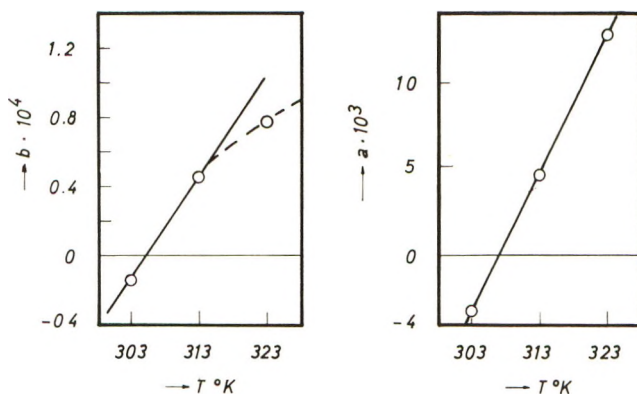


Fig. 18. Dependence of the constants a and b on the temperature of polystyrene in cyclohexane (osmosis). Data of Krigbaum.³⁴

VIII. CONCLUSION

In our view the experimental fact that the functional dependence of the second virial coefficient on the degree of polymerization shows a maximum in the range of very short polystyrene chains in naphthalene solution is very interesting. We have tried to explain the maximum as the result of a change in chain configuration: the transition from rodlike short chains to balllike coils of long ones. We have contented ourselves with this qualitative explanation of the B - P curve as this maximum is the only one known so far and more measurements in the short chain region are necessary to draw final conclusions.

A second result was an A_2 - M function which can describe exothermal as well as endothermal solutions and the constants of which have the value zero at the θ -temperature. We are now measuring other systems to investigate whether these findings are of a general nature or not.

References

1. Schulz, G. V., and A. Horbach, *Z. Physik. Chem. (Frankfurt)*, **22**, 377 (1959).
2. Ueberreiter, K., and U. Rhode-Liebenau, *Makromol. Chem.*, **49**, 164 (1961).
3. Ueberreiter, K., and H. Sotobayashi, *Makromol. Chem.*, **59**, 71 (1963).
4. Sotobayashi, H., and K. Ueberreiter, *Z. Elektrochem.*, **66**, 838 (1962).
5. Kemp, A., and H. Peters, *Ind. Eng. Chem.*, **34**, 1097 (1942).
6. Schulz, G. V., and H. Marzolph, *Z. Elektrochem.*, **58**, 211 (1954).
7. Cantow, H. J., *Z. Physik. Chem. (Frankfurt)*, **7**, 58 (1956).
8. Flory, P. J., *J. Chem. Phys.*, **9**, 660 (1941); *ibid.*, **10**, 51 (1942).
9. Huggins, M. L., *J. Chem. Phys.*, **9**, 440 (1941); *J. Phys. Chem.*, **46**, 151 (1942); *Ann. N. Y. Acad. Sci.*, **43**, 1 (1942).
10. Münster, A., in *Die Physik der Hochpolymeren*, Vol. II, H. A. Stuart, Ed., Springer-Verlag, Berlin, 1953, p. 81.
11. Meyerhoff, G., *Z. Physik. Chem. (Frankfurt)*, **4**, 346 (1955).
12. Sotobayashi, H., and K. Ueberreiter, *Z. Elektrochem.*, **67**, 178 (1963).
13. Flory, P. J., *Principles of Polymer Chemistry*, Cornell Univ. Press, Ithaca, N. Y., 1953.
14. Zimm, B. H., W. Stockmayer, and M. Fixman, *J. Chem. Phys.*, **21**, 1715 (1953).
15. Yamakawa, H., and M. Kurata, *J. Phys. Soc. Japan*, **13**, 78 (1958).
16. Bawn, C. H., R. F. J. Freeman, and A. R. Kamaliddin, *Trans. Faraday Soc.*, **46**, 862 (1950).
17. Krigbaum, W. R., and P. J. Flory, *J. Am. Chem. Soc.*, **75**, 1778 (1953).
18. Schulz, G. V., and H. Hellfritz, *Z. Elektrochem.*, **57**, 835 (1953).
19. Outer, P., C. Carr, and B. Zimm, *J. Chem. Phys.*, **18**, 830 (1950).
20. Münster, A., *Z. Physik. Chem. (Leipzig)*, **197**, 17 (1950).
21. Münster, A., *J. Polymer Sci.*, **8**, 633 (1952).
22. Schulz, G. V., and G. Meyerhoff, *Z. Elektrochem.*, **56**, 545 (1952).
23. Cantow, H. J., and G. V. Schulz, *Z. Physik. Chem. (Frankfurt)*, **2**, 117 (1954).
24. Schulz, G. V., and H. Craubner, *Z. Elektrochem.*, **63**, 301 (1959).
25. Kirste, R., and G. V. Schulz, *Z. Physik. Chem. (Frankfurt)*, **27**, 301 (1961).
26. Kobayashi, H., *J. Polymer Sci.*, **39**, 369 (1959).
27. Kinsinger, J. B., and R. E. Hughes, *J. Phys. Chem.*, **63**, 2002 (1959).
28. Parrini, P., F. Sebastiano, and G. Messina, *Makromol. Chem.*, **38**, 27 (1960).
29. Schulz, G. V., and A. Horbach, *Makromol. Chem.*, **29**, 93 (1959).
30. Casassa, E. F., and W. H. Stockmayer, *J. Polymer Sci.*, **3**, 53 (1962).
31. Matsumoto, M., and Y. Ohyanagi, *J. Polymer Sci.*, **46**, 441 (1960).
32. Schulz, A. R., *J. Am. Chem. Soc.*, **76**, 3422 (1954).
33. Krigbaum, W. R., and P. J. Flory, *J. Am. Chem. Soc.*, **75**, 5254 (1953).
34. Krigbaum, W. R., *J. Am. Chem. Soc.*, **76**, 3760 (1954).

Résumé

Le second coefficient du viriel B ou A_2 a été calculé à partir de mesures cryoscopiques effectuées dans la naphthalène depuis les dimères du styrène jusqu'aux polystyrènes. La courbe B -degré de polymérisation, présente un maximum pour le tétramère. La partie croissante du maximum s'explique par un "effet macromoléculaire" des bâtonnets rigides suivant la théorie de Flory et Huggins. La courbe A_2 - P (ou B - P) qui est la seule à avoir été étudiée d'une façon aussi approfondie est décrite par une formule $A_2 = a/\sqrt{M} + b$. On admet que la forme de pelote macromoléculaire en solution dépend du

fait que le squelette de la chaîne principale et ses groupements latéraux ont la même affinité ou une affinité contraire vis-à-vis du solvant. Dans le cas du polystyrène dans le naphthalène, on admet que la chaîne carbonée C-C est lyophobic et que les groupements benzéniques sont lyophiles. Cela conduit à une distance accrue de groupements latéraux benzéniques à la surface de la pelote macromoléculaire. Le potentiel d'interaction entre les pelotes est par conséquent différent de celui qui règne à l'intérieur de la pelote. Cet effet est réalisé par la division du volume exclu en deux parties et conduit à une dépendance inverse de la racine de A_2 . Cette équation a été essayée avec plusieurs systèmes endo- et exothermiques. Les constantes a et b sont nulles à la température- θ et peuvent être déterminées de cette façon.

Zusammenfassung

Aus kryoskopischen Messungen von Styroldimeren bis zu Polystyrolen in Naphthalin wird der zweite Virialkoeffizient B oder A_2 berechnet. Die B -Polymerisationsgrad-Kurve hat ein Maximum im Gebiet des Tetrameren. Der ansteigende Ast des Maximums wird als "Makromoleküleffekt" gestreckter Stäbchen nach Flory und Huggins gedeutet. Für den absteigenden Ast, den bislang nur untersuchten Teil der A_2 - P (oder B - P)-Kurve, wird eine Formel $A_2 = (a/M^{1/2}) + b$ entwickelt. Es wird angenommen, dass die Form des Makromoleküls in Lösung davon abhängt, ob seine Hauptkette und seine Seitengruppen sich gleich- oder verschiedenartig zum Lösungsmittel verhalten. Im Falle des Polystyrols in Naphthalin wird lyophiles Verhalten der Seitengruppen und lyophobes der C-C-Kette angenommen. Das führt zu einem Drängen der Seitengruppen an die Oberfläche des Knäuels. Die Wechselwirkung der Knäuel gegeneinander wird dadurch verschieden von derjenigen der Segmente im Innern. Dieser Effekt wird durch eine Aufteilung des ausgeschlossenen Volumens berücksichtigt und führt zur reziproken Wurzelabhängigkeit von A_2 . Die Formel wird an zahlreichen endo- und exothermen Systemen bestätigt gefunden. Die Konstanten a und b sind an der θ -Temperatur Null, woraus man sie bestimmen kann.

Received February 5, 1963

Electron Spin Resonance Studies of Irradiated Polypropylene

LLOYD J. FORRESTAL and WILLIAM G. HODGSON, *Central Research
Division, American Cyanamid Company, Stamford, Connecticut*

Synopsis

Polypropylene has been irradiated at -196°C . and its electron spin resonance spectra studied at temperatures between -196°C . and room temperature. The intensity of the eight-line spectrum observed at -196°C . corresponded to a G for radical production of 3.3. The spectrum could be reconstructed from theoretical curves assuming equal concentrations of radicals with four- and eight-line spectra. On warming to room temperature the radical concentration was reduced to 30% of the initial concentration. In experiments in which the sample was warmed to -100°C . no change in radical concentration was observed. Annealing experiments at temperatures between -100°C . and the glass transition temperature showed that at each temperature there was a rapid decay of radicals after which no further change in radical concentration took place. Above the glass transition temperature a continuous decay occurred. The onset of decay above -100°C . may be associated with the onset of segmental motion in the amorphous regions of the polymer. The rapid decay of the radicals suggests that they are formed near each other as the results of hot hydrogen atom reactions.

INTRODUCTION

The effect of ionizing radiation on polypropylene has been examined by several workers.¹⁻⁴ The major results of the irradiation are the evolution of hydrogen and the formation of double bonds. The pertinent 100 e.v. yields (G values) are listed in Table I.

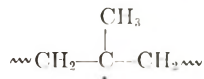
TABLE I

	Dole ⁴	Black and Lyons ²
G (H_2)	2.55	
G (CH_4)	0.058	
G (vinylidene)	~2	
G (scission)	0.34	4.95
G (crosslink)	0.23	4.95

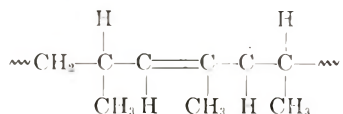
The value for chain scission obtained by Black and Lyons is from initial viscosity changes whereas that reported by Dole is from gel data obtained at higher doses. The equivalence of vinylidene unsaturation and scission yields was interpreted by Black and Lyons for a mechanism whereby vinylidene unsaturation is formed as a result of chain scission. Dole,

on the other hand, favors the view that vinylidene unsaturation is formed as a result of C-H scission. The latter interpretation is more consistent with the results of this investigation.

Investigations of the electron spin resonance (ESR) spectrum for polypropylene, irradiated and observed over a range of temperatures, have been reported. Tsvetkov, Molin, and Voevodskii⁵ observed an eight-line symmetrical spectrum at -150°C . which they attributed to the radical



in which the electron interacts with seven equivalent protons. Ayscough, Ivins, and O'Donnell⁶ confirmed this result at -196°C . and attributed it to the same species. Ohnishi et al.⁷ attempted to analyze the spectrum at room temperature and concluded that there were four different species with some stability at room temperature. Characteristic of these species were eight-, seven-, six-, and one-line spectra. The spectra were not assigned to specific radicals. Fischer and Hellwege⁸ reported experiments on oriented samples of polypropylene. They also assigned the low temperature spectrum to the tertiary radical and found that the spectrum was independent of orientation. At room temperature the use of oriented samples gave additional information so that there was good evidence for assigning the room temperature spectrum to an allyl radical with resonance possibilities:



Most analyses of spectra of radiation damaged polymers have been based on the so-called α - β -hypothesis in which it is assumed that the α - and β -protons of aliphatic radicals are magnetically equivalent. Deviations from the predictions of the hypothesis have been reported,⁹ but it has nevertheless proved to be a useful working hypothesis and was used in our considerations. It is encouraging that the three multiline components of the room temperature pattern as analyzed by Ohnishi et al.⁷ have very similar hyperfine splitting intervals.

EXPERIMENTAL

The polypropylene used in this investigation was in the form of a 100 mesh powder. Ultraviolet emission analysis indicated that the major metallic impurities, titanium and aluminum, were at concentrations less than 0.01%. The degree of crystallinity of the polymer as determined by infrared and x-ray diffraction measurements was between 50 and 60%.

Samples were irradiated at -196°C ., in vacuum by 3 M.e.v. peak x-rays from a Van de Graaff generator. Irradiation cells consisted of

20 mm. Pyrex glass tubulations with side arm extensions which fitted into a Dewar flask in the cavity of the ESR spectrometer. The polymer was irradiated in the 20 mm. tubulation and then transferred under liquid nitrogen, to the side arm which was previously annealed to remove unpaired spin centers formed in the glass during irradiation.

The rate of energy absorption, 2.91×10^{18} e.v./g. min., was determined by conventional ferrous sulfate dosimetry. Appropriate corrections were made to account for the electron density of the polymer powder. The total dose in each experiment was 3.50×10^{20} e.v./g.

The ESR measurements were made with a Varian V4500 spectrometer using a modulation frequency of 400 cycles/sec. Standard Varian accessories were used in making observations at -196°C . and at temperatures between -196°C . and room temperature. The microwave power was kept below 1 mw. to minimize errors due to saturation of the resonance.

The concentration of unpaired spins was determined by measuring the area under the absorption curve and comparing it with the area under a resonance curve from a spectrophotometrically calibrated solution of α, α -diphenyl- β -picryl hydrazyl (DPPH) in benzene. Corrections were made for variations in the Q factor of the cavity by monitoring the $g = 4$ glass resonance.

Lack of a suitable standard for use at -196°C . required the use of a roundabout method for the estimation of spin concentration of the total radicals formed at -196°C . which includes a species unstable at room temperature. The initial spectrum was measured at -196°C ., the sample warmed to room temperature, the spectrum recorded and the sample quickly cooled to -196°C . where the spectrum was again recorded. The room temperature spectrum was estimated quantitatively by comparison with DPPH solution. By making the reasonable assumption that the number of radicals contributing to the room temperature resonance was the same as that contributing after cooling it was possible to estimate the initial radical concentration by comparison of areas of the low temperature spectra. Reproducibility of initial radical concentrations was within $\pm 3\%$.

RESULTS AND DISCUSSION

Nature of the Radicals

The spectrum observed at -196°C . after irradiation at -196°C . is shown by the solid line in Figure 1. It is obviously the same eight line spectrum recorded by others^{5,6,8} and attributed by them to the tertiary radical. Attempts were made to fit this spectrum with a synthetic curve generated by a computer programmed with the assumption that the seven interacting protons were equivalent (this is reasonable since all are β protons⁸). In attempting to fit the spectrum the ratio of hyperfine splitting to width ratio was varied systematically. No success was achieved in producing an approximate fit. It was concluded that the low temperature

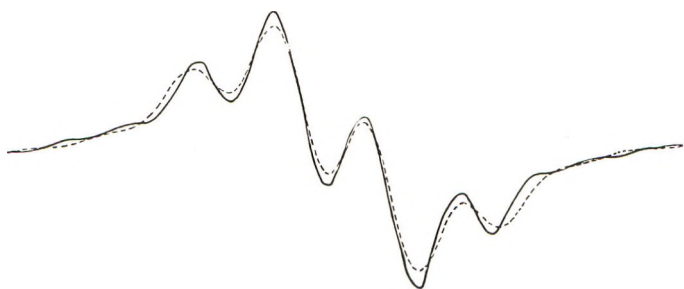
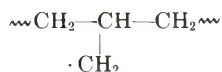
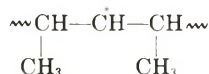


Fig. 1. ESR spectrum of polypropylene observed at -196°C . after irradiation at -196°C . (—) and a curve computed with the assumption that there are equal concentrations of radicals with four- and eight-line spectra (- - -).

spectrum was composite. The curve shown by the dotted line in Figure 1 is the synthesis of the spectrum which would be given by a mixture of 50% of a radical with an eight line spectrum and 50% of a radical with a four-line spectrum. The eight-line spectrum would correspond to the tertiary radical and the four-line spectrum would correspond to equal interaction with three equivalent protons as in



and



On warming to room temperature, the eight-line spectrum immediately decayed to the odd-numbered line spectrum reported by others. These labile radical species are apparently formed in proximity of each other, perhaps as the results of hot hydrogen atom reactions within the spurs of the electron tracks.

Investigation of the room temperature spectrum produced little new information which would alter the interpretation of Fischer and Hellwege.⁸ It was, however, observed in our experiments that during the first two hours at room temperature 40% of the spectrum assigned to the allyl radical decayed while a sharp singlet grew into the center of the spectrum reaching a maximum after 2 hr. After this time the spectrum of the allyl radical decayed much more slowly and the singlet decayed at a parallel rate.

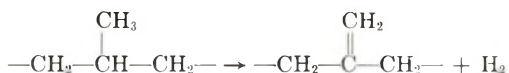
Efficiency of Radical Production

The G value for radical production at -196°C . in polypropylene determined in three separate experiments was 3.3 ± 0.1 . A higher value $G = 6.2$ has been reported by Ohnishi.¹⁰

The absence of a significant contribution of six-line structure by the radical $-\text{CH}_2-\dot{\text{C}}\text{H}-\text{CH}_2-$, resulting from methyl cleavage, is confirmed by the fact that $G(\text{CH}_3) = 0.058^4$ is some fiftyfold lower than our observed radical yield.

If chain scission contributed significantly to the radical spectrum at -196°C . one would expect to see some evidence of a spectrum with an odd number of lines from the structure $-\text{CH}_2-\dot{\text{C}}\text{H}-\text{CH}_3$. The predominance at -196°C . of spectra with an even number of lines tends to confirm the low value of $G(\text{scission}) = 0.34$.⁴ The earlier value² of $G(\text{scission})$ is too high to be consistent with the radical yield observed in this work.

The assumption that the entire yield of hydrogen $G = 2.55$ ⁴ results from a process with a radical intermediate which is stable at -196°C . requires a radical yield of at least 5.1. The lower yield observed in these experiments suggest the possibility of some hydrogen being formed by molecular detachment. Evidence for such a process has been observed in the radiation chemistry of cyclohexane.¹¹ The formation of vinylidene unsaturation could be due, in part, to a process leading to the reaction



Effect of Temperature

An experiment was performed in which a sample was warmed to successively higher temperatures and the decay of radicals followed at these temperatures. When it was required to compare the concentration with the initial concentration the sample was cooled to -196°C . and the spectrum thus measured compared with that obtained initially. When the sample was warmed from -196° to -100°C . there was no change in radical concentration. Warming to -50°C . resulted, within 2-3 min., in a decrease in radical concentration to 84% of the original value. This concentration persisted for a period of 3 hr. On warming to -25°C . a similar rapid decrease in radical concentration and subsequent stabilization at 68% of its original value was observed. When the polymer was warmed to $+10^{\circ}\text{C}$., i.e., above its glass transition temperature, a further rapid decrease in radical concentration to 30% of its original value occurred, but a stable concentration was not observed in contrast to the behavior at lower temperatures. In experiments in which the sample was warmed directly from -196°C . to room temperature and then cooled to -196°C . again it was found that the concentration of radicals was 30% of its initial value.

Nuclear magnetic resonance studies¹² indicate that in the temperature region of initial radical decay, -100 to -50°C ., there is relatively little motion in the crystalline regions of polypropylene. On the other hand, dynamic mechanical measurements¹³ in this region show the onset of a secondary transition associated with the motion of short segments of the polymer chain in the amorphous region. In the absence of any alternative it seems likely that the onset of radical decay in the irradiated polymer is associated with this transition. This requires that the labile radical species be located in the amorphous regions of the polymer.

We are indebted to Dr. J. E. Lehnsen for his efforts in developing the computer program and to Dr. R. F. Stamm and Mr. C. Spiers for their assistance in carrying out the irradiations.

References

1. Miller, A. A., E. J. Lawton, and J. S. Balwit, *J. Polymer Sci.*, **14**, 503 (1954).
2. Black, R. M., and B. J. Lyons, *Proc. Roy. Soc. (London)*, **A253**, 322 (1959).
3. Black, R. M., and B. J. Lyons, *Nature*, **180**, 1346 (1957).
4. Dole, M., *Trans. Am. Nuclear Soc.*, **3**, 356 (1960).
5. Tsvetkov, Yu. D., Yu. N. Molin, and V. V. Voevodskii, *Vysokomol. Soedin.*, **1**, 1805 (1959).
6. Ayscough, P. B., K. J. Ivin, and J. H. O'Donnell, *Proc. Chem. Soc.*, **1961**, 71.
7. Ohmishi, S., Y. Ikeda, M. Kashiwagi, and I. Nitta, *Polymer*, **2**, 119 (1961).
8. Fischer, H., and K. H. Hellwege, *J. Polymer Sci.*, **56**, 33 (1962).
9. Ayscough, P. B., A. P. McCann, C. Thomson, and D. C. Walker, *Trans. Faraday Soc.*, **57**, 1487 (1961).
10. Ohmishi, S., *Bull. Chem. Soc. Japan*, **35**, 254 (1962).
11. Forrestal, L. J., and W. H. Hamill, *J. Am. Chem. Soc.*, **83**, 1535 (1961).
12. Slichter, W. P., and E. R. Mandell, *J. Appl. Phys.*, **29**, 1438 (1958).
13. Sauer, J. A., R. A. Wall, N. Fuschillo, and A. E. Woodward, *J. Appl. Phys.*, **29**, 1385 (1958).

Résumé

On a irradié du polypropylène à -196°C et son spectre de résonance de spin électronique a été étudié entre -196°C et la température de chambre. L'intensité des huit raies spectrales observées à -196°C correspond à un G de production radicalaire égal à 3.3. On peut rétablir le spectre au départ des courbes théoriques en supposant des concentrations radicalaires égales avec quatre et huit raies spectrales. En chauffant jusqu'à température ordinaire, la concentration en radicaux est réduite à 30% de sa concentration initiale. Au cours des expériences où l'échantillon est chauffé à -100°C on n'observe aucune variation de la concentration radicalaire. Les expériences de recuit à des températures situées entre -100°C et la température de transition vitreuse, montrent qu'à chaque température, il y a une rapide décroissance en radicaux après quoi, aucune variation de concentration radicalaire n'a lieu. Au-dessus de la température de transition vitreuse on assiste à une décroissance continue. Le démarrage de cette décroissance au-dessus de -100°C peut être associé au démarrage de mouvements segmentaires dans les régions amorphes du polymère. La décroissance rapide de la teneur en radicaux suggère qu'ils sont formés les uns près des autres suite à des réactions d'atomes d'hydrogènes "chauds."

Zusammenfassung

Polypropylen wurde bei -196°C bestrahlt und sein Elektronenspinresonanzspektrum bei Temperaturen zwischen -196°C und Raumtemperatur untersucht. Die Intensität des bei -196°C beobachteten Acht-Linien-Spektrums entsprach einem G-Wert für die Radikalbildung von 3,3. Das Spektrum konnte unter der Annahme gleicher Konzentration von Radikalen mit Vier- und Acht-Linien-Spektren aus theoretischen Kurven aufgebaut werden. Beim Erwärmen auf Raumtemperatur wurde die Radikalkonzentration auf 30% des Anfangswertes herabgesetzt. Bei Versuchen, bei denen die Probe auf -100°C erwärmt wurde, trat keine Änderung der Radikalkonzentration auf. Temperungsversuche bei Temperaturen zwischen -100°C und der Glasumwandlungstemperatur zeigten, dass bei jeder Temperatur ein rasches Abklingen der Radikale und nachher keine weitere Änderung der Radikalkonzentration stattfand. Oberhalb der Glasumwandlungstemperatur war ein kontinuierliches Abklingen vorhanden. Der Eintritt des Abklingens oberhalb -100°C ist wahrscheinlich mit dem Einsetzen der Segmentbewegung in den amorphen Bereichen des Polymeren verknüpft. Das rasche Abklingen der Radikale spricht dafür, dass sie nahe nebeneinander durch Reaktionen heisser Wasserstoffatome gebildet werden.

Received February 5, 1963

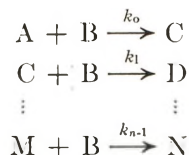
Product Distribution of Consecutive Competitive Second-Order Reactions

HENRI J. R. MAGET, *Fuel Cell Laboratory, General Electric Company,
West Lynn, Massachusetts*

Synopsis

Product distribution of consecutive competitive second-order reactions can be calculated from a general distribution equation independently of the number of reaction steps.

The reactions considered are of the type:



and the number of reaction steps can vary from two to n .

Much work has been done to establish correlations predicting the concentration of the different components as a function of time. This paper is mainly concerned with the prediction of product distribution as a function of the actual concentration of the starting material A, and with applications of a general distribution equation to various types of reactions.

The following symbols will be adopted: distribution constants are $K_i = k_i/k_0$, where $1 \leq i \leq n - 1$; actual concentrations of components C, D, . . . , N are y_1, y_2, \dots, y_n ; initial and actual concentrations of A are, respectively, a and $(a - x)$; the relative concentration $(a - x)/a$ will be represented by X ; initial and actual concentrations of B are, respectively, b and $(b - Y)$.

From considerations of the reaction rates for the different reaction steps, the following general differential equation can be obtained:

$$\frac{dy_i}{dX} = -K_{i-1} \frac{y_{i-1}}{X} + K_i \frac{y_i}{X} \quad (1)$$

The concentration of the i th component becomes:

$$y_i = K_{i-1} X^{K_i} \int_X^1 y_{i-1} X^{-K_i-1} dX \quad (2)$$

The solution of eq. (2) depends on the values of the distribution constants K_{i-1} . In the particular case where $y_{i-1} X^{-K_{i-1}} = CX^{-1}$, a logarithmic term will appear in the general equation describing the product distribution. The general solution of eq. (2), obtained by Martin and Fuchs¹ in an attempt to predict the product distribution of the stepwise chlorination of methane, can be written in a slightly different form:

$$\frac{y_i}{a} = (-1)^i \prod_{j=0}^{i-1} K_j \sum_{j=0}^i \frac{X^{K_i}}{\prod_{\substack{k=0 \\ k \neq j}}^i (K_j - K_k)} \quad (3)$$

This equation is not applicable if any two reaction rate constants are identical, but can be applied to the reaction step where the distribution constants become identical. The distribution constants can be calculated from eq. (3) if the product distribution is known. To obtain the reaction rate constants it will be necessary to determine one value of k_i , i.e., k_0 . This can be done by studying the first reaction step in very dilute solutions, to avoid formation of higher members of the series. Product distribution can be expressed as a function of the concentration of the reactive component B or as a function of time, if the following reactions are considered:

$$x = \sum_{i=1}^n y_i \quad (4)$$

$$Y = \sum_{i=1}^n iy_i \quad (5)$$

as well as the reaction rate of each individual step.

Martin and Fuchs,¹ assuming that the reaction probability is directly related to the reaction rate constants and that it depends only on the number of free reactive groups, obtained the following sequence of rate constants:

$$k_0:k_1:k_2:\dots:k_n = m:(m-1):(m-2):\dots:1$$

The general solution for the product distribution then becomes:

$$\frac{y_i}{a} = \binom{m}{i} X \left[\left(\frac{1}{X} \right)^{1/m} - 1 \right]^i \quad (6)$$

TABLE I
Saponification of Ethyl Succinate

X	y_1/a		y_2/a	
	Exptl.	Calc.	Exptl.	Calc.
0.704	0.287	0.288	0.009	0.009
0.604	0.377	0.380	0.019	0.016
0.526	0.443	0.450	0.030	0.024

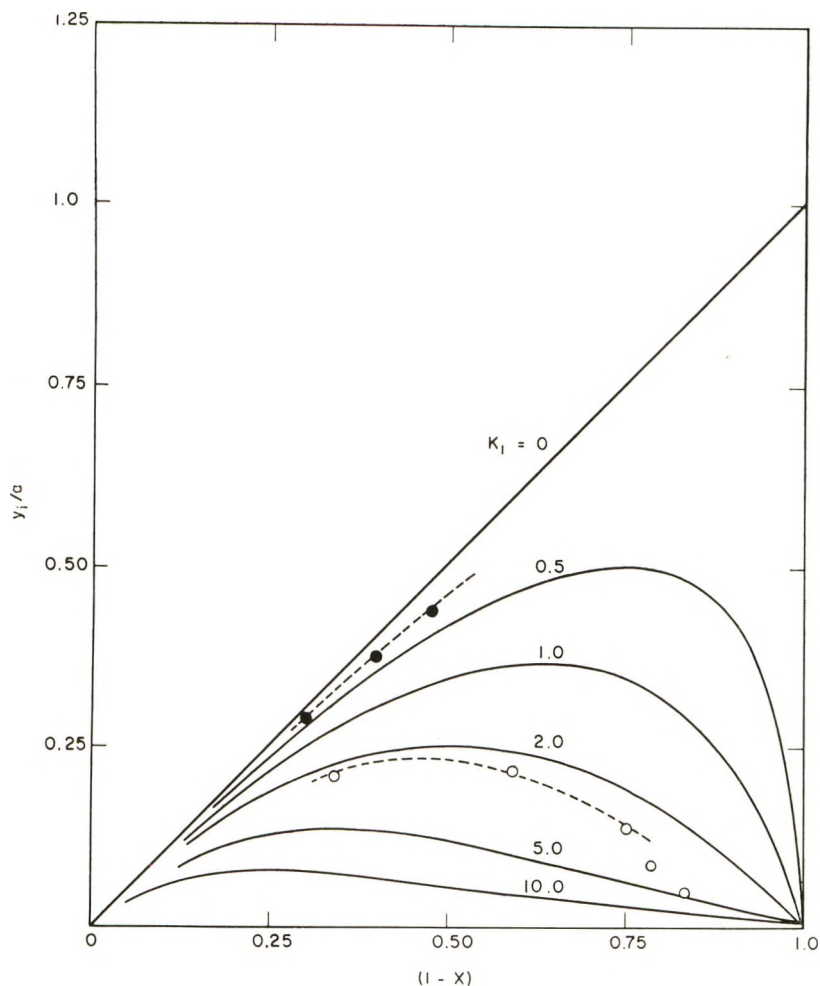


Fig. 1. Concentration of the first reaction product as a function of $(1 - X)$: (○) chlorination of methane; (●) saponification of a diester.

However, such a result was not obtained for the chlorination of methane, and in some cases the reaction rate constants increase from the first to the n -th reaction step.

Applications of eq. (3) to reactions involving 2, 3, 4, and n reaction steps will be discussed.

1. TWO REACTION STEPS

In this case $K_2 = 0$, and eq. (3) yields the values of y_1 and y_2 :

$$\frac{y_1}{a} = \frac{1}{K_1 - 1} \left[X - X^{K_1} \right] \quad (7)$$

$$\frac{y_2}{a} = 1 + \frac{X^{K_1}}{K_1 - 1} - X \frac{K_1}{K_1 - 1} \quad (8)$$

These equations are applicable for all values of K_1 but $K_1 = 1$. This special case will be discussed later. The concentration of y_1 will always be expressed by eq. (7) independently of the number of steps and independently of the values of the distribution constants. Equations (7) and (8) were obtained respectively by McMillan² and Wells.³

In Figure 1, y_1/a is represented as a function of $(1 - X)$, with K_1 as parameter. Values of y_2/a can be obtained readily from eq. (4). Single values of y_1/a and X , or y_2/a and X will, in principle, yield the complete distribution of all components. Trial-and-error calculations can be avoided by using Figure 1.

Some of the experimental results obtained by Ritchie,⁴ for the saponification of ethyl succinate and reproduced in Figure 1, as well as the first reaction step in the chlorination of methane. Results obtained for $K_1 = 0.147$ are reproduced in Table I and compared with experimental results obtained by Ritchie.

If $k_1 \ll k_0$, ($K_1 \cong 0$) the first reaction step proceeds exclusively, and y_2 is formed after total disappearance of y_1 . Such a result was observed by Patat, Cremer, and Bobleter⁵ for the reaction between propylene oxide and phenol. A similar case was reported by Pecorini and Banchero⁶ for the reaction of propylene oxide with methanol catalyzed by NaOH. These authors obtained values of K_1 varying from 0.148 to 0.0729 for temperatures between 35 and 100°C., and consequently observed the formation of small amounts of methoxydipropylene glycol, for values of X of 0.8.

Distribution constants are temperature-dependent. Data obtained by Lay and Banchero⁷ show that for the NaOH-catalyzed reaction of propylene oxide with methoxydipropylene and methoxytripropylene glycols the distribution constant varies from 0.58 to 1.24 for temperatures ranging from 35 to 100°C.

2. THREE REACTION STEPS

In this case $K_3 = 0$. The relative concentration y_1/a is given by eq. (7). The following product distributions were obtained from eq. (3):

$$\frac{y_2}{a} = K_1 \left[\frac{X}{(1 - K_1)(1 - K_2)} + \frac{X^{K_1}}{(K_1 - 1)(K_1 - K_2)} + \frac{X^{K_2}}{(K_2 - 1)(K_2 - K_1)} \right] \quad (9)$$

and

$$\frac{y_3}{a} = 1 - \frac{K_1 K_2 X}{(K_1 - 1)(K_2 - 1)} + \frac{K_2 X^{K_1}}{(K_1 - 1)(K_2 - K_1)} - \frac{K_1 X^{K_2}}{(K_2 - 1)(K_2 - K_1)} \quad (10)$$

y_3 can also be readily obtained from eq. (4).

If $K_2 \ll K_1$, then $y_3/a = 0$, and y_2/a is given by eq. (8). If K_1 is negligible compared to K_2 , then $y_2/a = 0$, and y_3/a is given by eq. 8. Applications of these equations were discussed by Potter and McDonald⁸ and applied by Natta and Mantica⁹ to reactions of NH_3 with ethanol and isopropanol, and by Abel¹⁰ to the progressive saponification of glycerides.

3. FOUR REACTION STEPS

In this case $K_4 = 0$. The concentrations y_1/a and y_2/a are given by eqs. (7) and (9), respectively,

$$\frac{y_3}{a} = -K_1K_2 \left[\frac{X}{(1-K_1)(1-K_2)(1-K_3)} + \frac{X^{K_1}}{(K_1-1)(K_1-K_2)(K_1-K_3)} + \frac{X^{K_2}}{(K_2-1)(K_2-K_1)(K_2-K_3)} + \frac{X^{K_3}}{(K_3-1)(K_3-K_1)(K_3-K_2)} \right] \quad (11)$$

$$\frac{y_4}{a} = 1 + \frac{K_1K_2K_3X}{(1-K_1)(1-K_2)(1-K_3)} + \frac{K_2K_3X^{K_1}}{(K_1-1)(K_1-K_2)(K_1-K_3)} + \frac{K_1K_3X^{K_2}}{(K_2-1)(K_2-K_1)(K_2-K_3)} + \frac{K_1K_3X^{K_3}}{(K_3-1)(K_3-K_1)(K_3-K_2)} \quad (12)$$

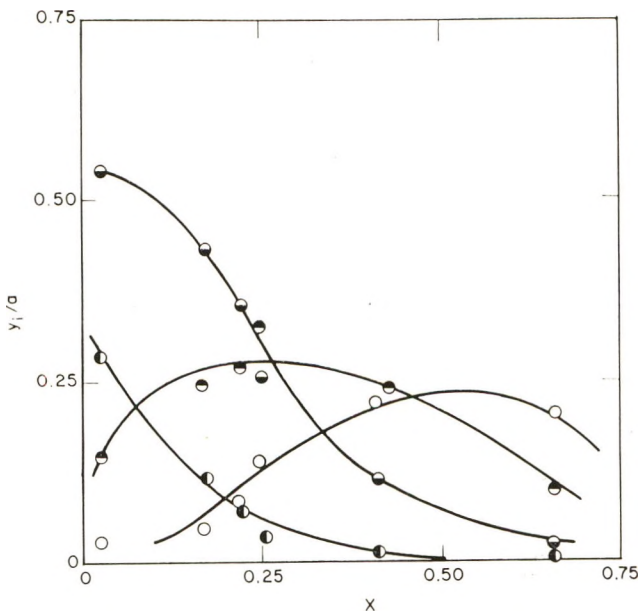


Fig. 2. Product distribution for the stepwise chlorination of methane: (○) mono-chloromethane; (●) di-chloromethane; (◐) tri-chloromethane; (◑) tetra-chloromethane.

These results were also obtained by Fuoss.¹¹ This author considered special cases of interest, i.e., decreasing reaction rate constants, $k_0 = 4$, $k_1 = 3$, $k_2 = 2$, $k_3 = 1$ [see the general solution, eq. (6)] and identical reaction rate constants for all reaction steps, $K_1 = K_2 = K_n = 1$. The product distribution obtained for the chlorination of methane by McBee et al.¹² was discussed by Natta⁹ and represented as a function of the concentration of the reactive component B. Figure 2 reproduces the same results as a function of X . Trial-and-error calculations can be avoided in the determination of the distribution constants if the maxima of the distribution are known. From eq. (1), $dy_i/dX = 0$ for

$$\frac{(y_i)_{\max.}}{y_{i-1}} = \frac{K_{i-1}}{K_i} \quad (13)$$

For the particular case where $i = 1$,

$$K_i = \frac{X}{(y_i/a)} \quad (14)$$

The following values were obtained from Figure 2: $(y_1/a)_{\max.} = 0.237$, $X = 0.55$, $K_1 = 2.32$; $(y_2/a)_{\max.} = 0.27$, $(y_1/a) = 0.16$, $K_2 = 1.38$. Values of K_1 and K_2 compare well with the results obtained by Natta, i.e., 2.3 and 1.4, respectively.

4. N REACTION STEPS

If all reactions proceed with different rate constants, the integration of eq. (2) leads to the product distribution represented by eq. (3).

However, some cases are known, where the reactivities of the first terms of the series are different, whereas all subsequent reaction steps proceed with identical velocities. This type of reaction is encountered when the molecular structure has some influence on rate constants, that is, when reactive groups in small molecular chains can interact and affect the rate constants, whereas the higher members of the series are not influenced by the reactive groups. A general distribution equation can be derived for this type of reaction.

If the sequence of distribution constants is such that

$$K_1 \neq K_2 \dots \neq K_m = K_{m+1} = \dots = K_n$$

eq. (3) can be applied up to the $(m - 1)$ first terms of the series. A logarithmic term will appear in the general equation for y_i , when distribution constants K_m are introduced in integral eq. (2). The series can be terminated by writing that $K_n = 0$. Integration of eq. (2) leads to the following equation:

$$\frac{y_i}{a} = (-1)^i K_m^{i-m} \prod_{j=0}^{m-1} K_j \sum_{j=0}^{m-1} \frac{X^{K_j} - X^{K_m} \sum_{l=0}^{i-m} [(K_j - K_m) \ln X]^l / l!}{(K_j - K_m) \prod_{\substack{k=0 \\ k \neq j}}^m (K_j - K_k)} \quad (15)$$

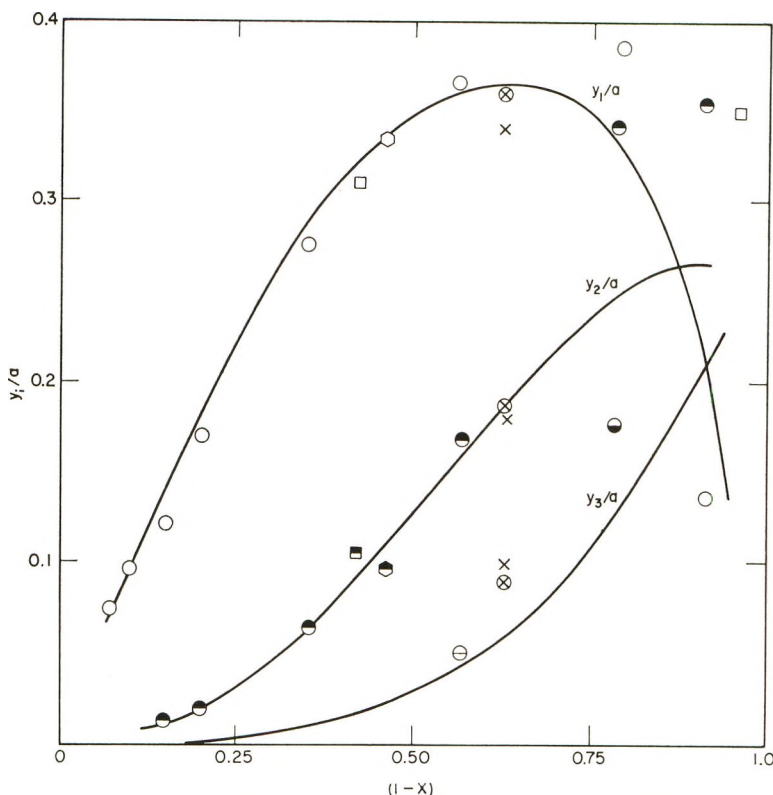


Fig. 3. Product distribution for identical reactivities of all steps: (⊗) ethylene glycol monoethyl ether-ethylene oxide; (×) ethylene glycol-ethylene oxide; (○, ●, ◐) diethylene glycol-ethylene oxide; (□, ◑) monopropylene glycol-propylene oxide; (◒, ◓) tripropylene glycol-propylene oxide.

and since

$$X^{K_j} - X^{K_m} \sum_{l=0}^{n-m} [(K_j - K_m) \ln X]^l / l! \equiv X^{K_m} \sum_{l=n-m+1}^{\infty} [(K_j - K_m) \ln X]^l / l! \tag{16}$$

eq. (15) becomes:

$$\frac{y_i}{a} = (-1)^i K_m^{i-m} \prod_{j=0}^{m-1} K_j \sum_{j=0}^{m-1} \sum_{l=i-m+1}^{\infty} \frac{[(K_j - K_m) \ln X]^l / l!}{(K_j - K_m)^{i-m} \sum_{\substack{k=0 \\ k \neq j}}^m (K_j - K_k)} X^{K_m} \tag{17}$$

Product distribution will be obtained from eq. (3) for $i < m$ and from eq. (17) for $i \geq m$. Special cases, reported in the literature, for which $m = 0, 1, 2$ can be derived from eq. (17). These cases are: (a) $K_1 = K_2 = \dots =$

$K_n = 1$; (b) $K_1 = K_2 = \dots = K_n = K$; (c) $K_1 \neq K_2 = K_3 = K_n = K$; (d) all distribution constants are different.

$$\text{a. } K_1 = K_2 = \dots = K_n = 1$$

The general solution obtained from eq. (17) becomes:

$$\frac{y_i}{a} = X(-\ln X)^i / i! \quad (18)$$

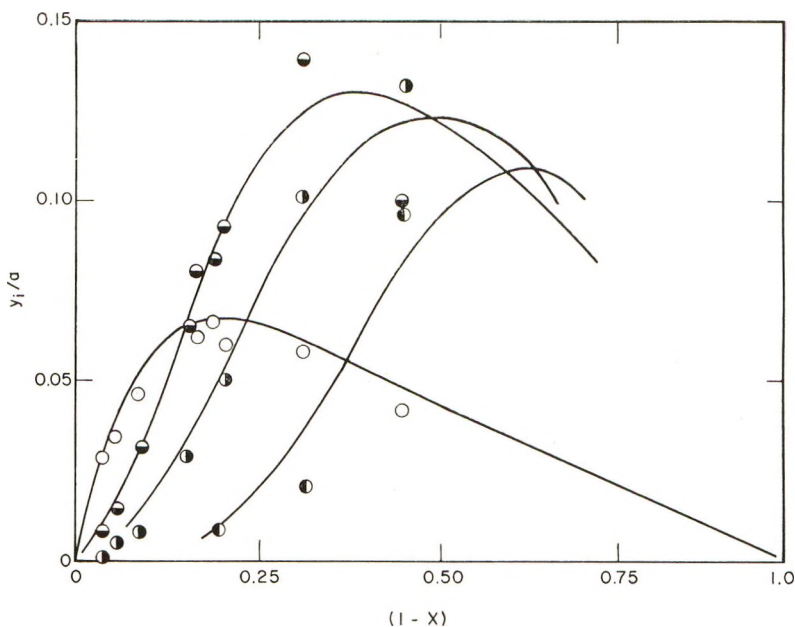


Fig. 4. Product distribution for the reaction propylene oxide-water: (O) monopropylene glycol; (◐) dipropylene glycol; (◑) tripropylene glycol; (●) tetrapropylene glycol.

Flory¹³ has already obtained such a result present in the following form:

$$\frac{y_i}{a} = \frac{e^{-v} v^i}{i!} \quad (19)$$

where $v = Y/a$. The identity of eqs. (18) and (19) can readily be shown by combining eqs. (5) and (18) if the summation goes from 1 to infinity. Equation (19) has been applied by Flory to the reaction of water with ethylene oxide. This application is justified if the starting material (water) has the same reactivity as the ethylene glycols formed. Weibull and Nycander¹⁴ have shown that the distribution constant is greater than 1. However, Flory's equation has been applied successfully for values of $(1 - X)$ up to 0.6 to the following reactions: ethylene glycol monoethyl ether-ethylene oxide (Weibull and Nycander¹⁴); ethylene glycol-ethylene

oxide (Weibull and Nycander¹⁴); diethylene glycol-ethylene oxide (Ishiguro and Kato¹⁵); monopropylene glycol-propylene oxide (this author); tripropylene glycol-propylene oxide (this author). Results are reproduced in Figure 3. The curves represent the calculated values of eq. (18).

$$\text{b. } K_1 = K_2 = \dots = K_n = K$$

Here, all distribution constants are identical, but different from 1. The product distribution can be obtained by integration of eq. (2) starting from the value of y_1/a given by eq. (3). A logarithmic term will appear for $i > 1$.

The general equation for the product distribution [derived from eq. (17)]

$$\frac{y_i}{a} = \frac{(-1)^i K^{i-1}}{(1-K)^i} \left[X - X^K \sum_{l=0}^{i-1} [(1-K) \ln X]^l / l! \right] \quad (20)$$

was obtained by Weibull and Nycander¹⁴ and by Gold¹⁶ and applied to the reactions of ethylene oxide with water and ethanol. The same authors have applied eq. (20) successfully to data obtained by Matignon, Moureu, and Dode¹⁷ for the hydration of ethylene oxide catalyzed by H_2SO_4 . The same equation can be applied to data obtained by Kurata¹⁸ for the non-catalyzed ethylene oxide-water reaction. Experimental values can be well represented by $K = 2$. However, if data obtained by the same author for the NaOH-catalyzed reaction are treated by eq. (20), an effect of catalyst concentration can be observed. The distribution constant varies from 7 to 11 for catalyst concentration varying from 0.01 to 0.1%.

$$\text{c. } K_1 \neq K_2 = K_3 = K_n = K$$

In this case, the first three reaction steps have different reactivities. Equation (3) can be applied to the first two reaction steps. A logarithmic term will appear for $i > 2$.

The following general equation has been obtained by this author:¹⁹

$$\frac{y_i}{a} = \frac{(-1)^i K^{i-2} K_1}{(1-K_1)} \times \left[\frac{X - X^K \sum_{l=0}^{i-2} [(1-K) \ln X]^l / l!}{(1-K)^{i-1}} - \frac{X^{K_1} - X \sum_{l=0}^{i-2} [(K_1-K) \ln X]^l / l!}{(K_1-K)^{i-1}} \right] \quad (21)$$

and applied to the NaOH-catalyzed reaction of propylene oxide with water. Figure 4 represents experimental results and the calculated values of y_i/a (for i up to 4) for $K_1 = 12$ and $K_2 = 5$.

From eq. (13) and for $i > 2$, $(y_i)_{\max} = y_{i-1}$, and the intersection of y_1 and y_{i-1} will happen at the maximum of y_i .

d. All Distribution Constants Are Different

The general solution for the product distribution is represented by eq. (3). This equation has been discussed in detail by Natta²⁰ for the reaction of ethylene oxide with methanol.

The author is indebted to Professor J. T. Banchemo for valuable advice and criticism concerning this problem.

References

1. Martin, F., and O. Fuchs, *Z. Elektrochem.*, **27**, 150 (1921).
2. McMillan, W. G., *J. Am. Chem. Soc.*, **79**, 4838 (1957).
3. Wells, P. R., *J. Phys. Chem.*, **63**, 1979 (1959).
4. Ritchie, M., *J. Chem. Soc.*, **1931**, 3112.
5. Patat, F., E. Cremer, and O. Bobleter, *Monatsh.*, **83**, 322 (1952).
6. Pecorini, H. A., and J. T. Banchemo, *Ind. Eng. Chem.*, **48**, 1287 (1956).
7. Lay, M. D., and J. T. Banchemo, unpublished data.
8. Potter, C., and W. C. McDonald, *Can. J. Res.*, **25B**, 415 (1947).
9. Natta, G., and E. Mantica, *J. Am. Chem. Soc.*, **74**, 3152 (1952).
10. Abel, E., *Z. Physik. Chem.*, **56**, 558 (1906).
11. Fuoss, R. M., *J. Am. Chem. Soc.*, **65**, 2406 (1943).
12. McBee et al., *Ind. Eng. Chem.*, **34**, 296 (1942).
13. Flory, P., *J. Am. Chem. Soc.*, **62**, 1561 (1940).
14. Weibull, B., and B. Nycander, *Acta Chem. Scand.*, **8**, 847 (1954).
15. Ishiguro, T., and S. Kato, *J. Pharm. Soc. Japan*, **64**, 294 (1944).
16. Gold, L., *J. Chem. Phys.*, **28**, 91 (1958).
17. Matignon, C., H. Moureu, and M. Dode, *Bull. Soc. Chem.* [5], **1**, 1308 (1934).
18. Kurata, F., P. C. Davis, and C. E. Von Waaden, *Chem. Eng. Progr. Symp. Series*, **48**, No. 4, 91 (1952).
19. Maget, H. J. R., *J. Polymer Sci.*, **55**, 773 (1962).
20. Natta, G., *Rend. Ist. Lombardo Sci.*, **78**, No. 1, 307 (1945).

Résumé

Une distribution de produit de réactions compétitives consécutives de second ordre, peut être calculée à partir d'une équation générale de distribution indépendamment du nombre d'étapes de réaction.

Zusammenfassung

Die Verteilung der Reaktionsprodukte bei kompetitiven Folgereaktionen zweiter Ordnung kann aus einer allgemeinen Verteilungsgleichung unabhängig von der Zahl der Reaktionsschritte berechnet werden.

Received February 5, 1963

Die sekundäre Keimbildung bei Polyäthylen-Sphärolithen*

I. HEBER, *Deutsches Kunststoff-Institut, Darmstadt, Germany*

Synopsis

The growth of two dimensional polyethylene spherulites has been followed in the range of 115° to 125°C. The radial growth velocity v_r has been assumed to be determined by the rate of formation of secondary nuclei on the spherulite border. Thus the nucleation theory gives the expression

$$v_r = v_{r0} e^{-Q/kT} e^{\Delta F^*/kT}$$

The critical free energy ΔF^* has been calculated for rectangular nuclei $\Delta F^* = x(4\sigma_e\sigma_s/\Delta f)$. This nucleus according to the calculation consists of a single layer of attached chain segments. Specific surface tensions σ_e/σ_s of the critical nucleus derived from the radial growth rate on the base of the theory agree with the values obtained for polyethylene single crystals with folded chains. On the base of the known folding length in polyethylene the secondary nucleus consists of three closely arranged folded chain segments 100 Å. in length. The satisfactory agreement between the values derived from growth rates of two-dimensional spherulites and the results obtained on polyethylene single crystals confirms the assumption that the growth velocity of spherulites is determined by the rate of formation of secondary nuclei on their surface.

Aus der Schmelze erstarrtes Polyäthylen zeigt im Polarisationsmikroskop Sphärolithe. In der vorliegenden Arbeit wird die radiale Wachstumsgeschwindigkeit zweidimensionaler Sphärolithe auf die Keimbildungsrate sekundärer Keime¹ an ihrer Peripherie zurückgeführt.

1. Experimentelles

Untersucht wurde das Polyäthylen Marlex Typ 9 der Rheinischen Olefinwerke. Die Substanz wurde in einer 10–30 μ dicken Schicht auf ein verspiegeltes Kupferplättchen aufgeschmolzen, das sich längs eines Kofler'schen Heiztisches verschieben liess. Die angegebene Kristallisationstemperatur wurde in der Kupferunterlage des Polyäthylens gemessen. Zur Geschwindigkeitsbestimmung wurden mit einer elektrisch registrierenden Stoppuhr die Zeiten gemessen, zu denen das Bild des wachsenden Sphärolithen die Teilstriche eines Okularmikrometers passierte, Beobachtet wurde im Polarisationsmikroskop für auflicht.

Mit der gewählten Anordnung konnten beim Polyäthylen Wachstumsgeschwindigkeiten bis herauf zu 5 μ /sec gemessen werden.

* Vorgetragen auf der Physiker-Tagung 1962, Stuttgart.

2. Messergebnisse

An mehreren zweidimensionalen Präparaten aus Marlex Typ 9 wurde die radiale Wachstumsgeschwindigkeit v_r als Funktion der Temperatur gemessen; sie nimmt von $0,01 \mu/\text{sec}$ bei 125°C auf etwa $5 \mu/\text{sec}$ bei 115°C zu* (Abb. 1). Da meist eine heterogene Keimbildung vorlag, konnte man erreichen, dass die kurzzeitig aufgeschmolzenen Sphärolithe an der gleichen Stelle des Präparates wieder wuchsen. Die einzelnen Messkurven in Abbildung 1 sind daher so aufgenommen, dass man einen Sphärolithen nach wiederholtem Aufschmelzen am gleichen Ort bei verschiedenen Temperaturen wachsen liess.

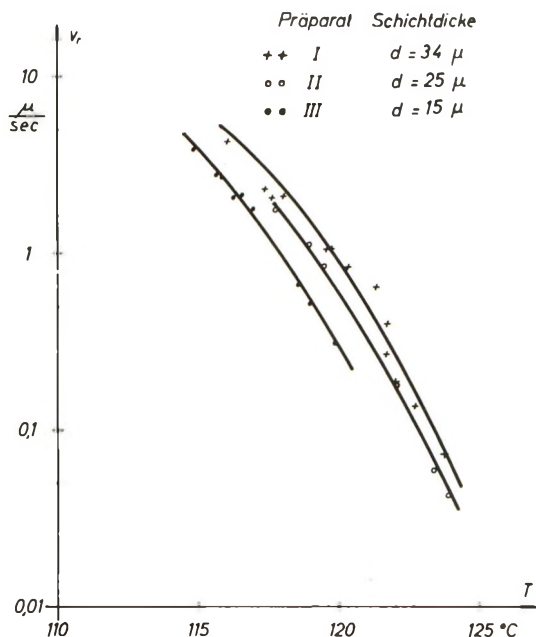


Abb. 1. Abhängigkeit der radialen Wachstumsgeschwindigkeit v_r von der Temperatur T bei zweidimensionalen Präparaten verschiedener Dicke.

Die kleinen Temperaturverschiebungen bei den einzelnen Messkurven der Abbildung 1 werden durch die unterschiedliche Schichtdicke der Präparate verursacht, und zwar ist bei gleicher Kristallisationstemperatur die Wachstumsgeschwindigkeit um so kleiner, je dünner das Präparat ist.

Die voll ausgebildeten Polyäthylen-Sphärolithe zeigen unter dem Polarisationsmikroskop neben dem charakteristischen Auslöschungskreuz ein konzentrisches Ringsystem, das auf eine Drehung der Indikatrix längs des Radius zurückzuführen ist.³ Hervorgerufen wird diese Drehung der Indikatrix durch ein schraubenförmiges Wachsen der Strukturele-

* Im Rahmen der Messgenauigkeiten passen auch einige von F. P. Price² angegebene Werte in unsere Kurven.

mente der Sphärolithe. Nach unseren Messungen gilt für jedes einzelne Präparat die folgende Beziehung zwischen der Ringbreite b und der Wachstumsgeschwindigkeit v_r :

$$bv_r^\kappa = \text{const.} \quad (1)$$

Der Exponent κ variiert jedoch von Präparat zu Präparat in den Grenzen 0,4 bis 1,0; ebenso hat die Konstante der Gleichung (1) bei den verschiedenen Präparaten verschiedene Werte.

Es scheint, dass bei gleicher Wachstumsgeschwindigkeit die Ringbreite um so grösser ist, je dünner das Präparat ist. Wir vermuten, dass bei den kleinen Schichtdicken das schraubenförmige Wachsen der Strukturelemente des Sphärolithen durch die räumlichen Begrenzungen behindert wird. Diese Behinderung verursacht wahrscheinlich auch die oben beschriebene Verringerung der radialen Wachstumsgeschwindigkeit bei den dünneren Präparaten.

3. Diskussion der Messwerte

Für einige Hochpolymere wurde schon von anderen Autoren die Temperaturabhängigkeit der radialen Sphärolith-Wachstumsgeschwindigkeit gemessen, z.B. für Polyamid 66,¹ Nylon 610 und Polyamid 66,⁴ Polyäthylenoxyd⁵ und Polyoxymethylen.⁶ Die Wachstumsgeschwindigkeit durchläuft unterhalb der Schmelztemperatur ein Maximum und wird bei genügend tiefer Temperatur wieder sehr klein. Beim Polyäthylen kann man prinzipiell die Wachstumsgeschwindigkeit nicht für den gesamten Kristallisationsbereich messen. Es ist nämlich die maximale Wachstumsgeschwindigkeit so gross, dass man eine Probe nicht auf eine Temperatur unterhalb der Maximumtemperatur abkühlen kann, ohne dass die Substanz schon bei einer höheren Temperatur kristallisiert ist.

Da die Wachstumsgeschwindigkeit unabhängig vom Radius r des Sphärolithen ist, folgt nach Burnett und McDevit,¹ dass eine sekundäre Keimbildung an der Peripherie der Sphärolithe die Wachstumsgeschwindigkeit bestimmt. Deshalb lässt sich die von Becker und Döring⁷ entwickelte Theorie für die Keimbildungsgeschwindigkeit auf die Sphärolith-Wachstumsgeschwindigkeit anwenden:

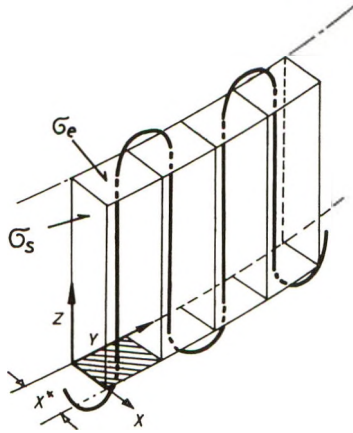
$$v_r = v_{r_0} e^{-Q/kT} e^{-\Delta F^*/kT} \quad (2)$$

Hierbei ist v_{r_0} eine (schwach temperaturabhängige) "Konstante" und Q die zum Heranbringen eines Kristallbauelementes an die Phasengrenze notwendige Arbeit. ΔF^* ist die Freie Energie, die zur Bildung eines Keimes kritischer Grösse aufgebracht werden muss. Bei der jetzt folgenden Berechnung der kritischen Freien Energie ΔF^* geht wesentlich die geometrische Form des sekundären Keimes ein. Aus früheren Untersuchungen¹ ist bekannt, dass die Molekelketten vorwiegend senkrecht zum Sphärolith-Radius stehen. Ferner weiss man aus elektronenmikroskopischen Untersuchungen, dass die Molekelketten sowohl im Einkristall als auch beim aus der Schmelze gewachsenen Sphärolithen gefaltet sind.⁸

Man darf daher annehmen, dass auch die sekundären Keime aus gefalteten Kettensegmenten aufgebaut werden (Abb. 2). Für die Freie Energie eines solchen Keimes gilt dann:

$$\Delta F = 2xy\sigma_e + 2xz\sigma_s - xyz\Delta f \quad (3)$$

Dabei ist σ_s die spezifische Oberflächenspannung der Seitenflächen, σ_e die spezifische Oberflächenspannung der Deckflächen und Δf die spezifische Freie Energie des Keims.



$$\Delta F = 2xy\sigma_e + 2xz\sigma_s - xyz\Delta f$$

Abb. 2. Schematische Darstellung des sekundären Keimes.

Zur Bildung eines Keimes wird zunächst Energie benötigt. Erst von der sogenannten kritischen Keimgröße an wird beim weiteren Wachstum Energie gewonnen. Die kritische Freie Energie ist daher als Sattelpunkt in der Energiefläche (ΔF aufgetragen als Funktion der Koordinaten) zu bestimmen. Da ΔF proportional zu x ist, ergibt sich notwendigerweise, dass für x der kleinst mögliche Wert zu nehmen ist, sich also nach Abbildung 2 nur eine Schicht von Kettensegmenten als sekundärer Keim anlagert; damit ist x^* festgelegt. Die kritischen Koordinaten y^* und z^* erhält man nach Differentiation zu:

$$\begin{aligned} y^* &= 2\sigma_s/\Delta f \\ z^* &= 2\sigma_e/\Delta f \end{aligned} \quad (4)$$

Durch Einsetzen der kritischen Längen in die Gleichung (3) erhält man für die Freie Energie des kritischen Keimes:

$$\Delta F^* = x^*4\sigma_e\sigma_s/\Delta f \quad (5)$$

Nach Hoffman¹⁰ kann man die Temperaturabhängigkeit der spezifischen Freien Energie beschreiben durch:

$$\Delta f = \Delta h_s [(T_s - T)/T_s] (T/T_s) \quad (6)$$

mit Δh_s = spezifische Schmelzenthalpie und T_s = Schmelztemperatur.

Fasst man die Gleichungen (2), (5) und (6) zusammen, so ergibt sich für die Temperaturabhängigkeit der radialen Wachstumsgeschwindigkeit v_r :

$$\ln \frac{v_r}{v_{r_0}} = -\frac{Q}{kT} + B [T_s^2/T^2(T_s - T)] \quad (7)$$

mit

$$B = -4x^* \sigma_e \sigma_s / k \Delta h_s$$

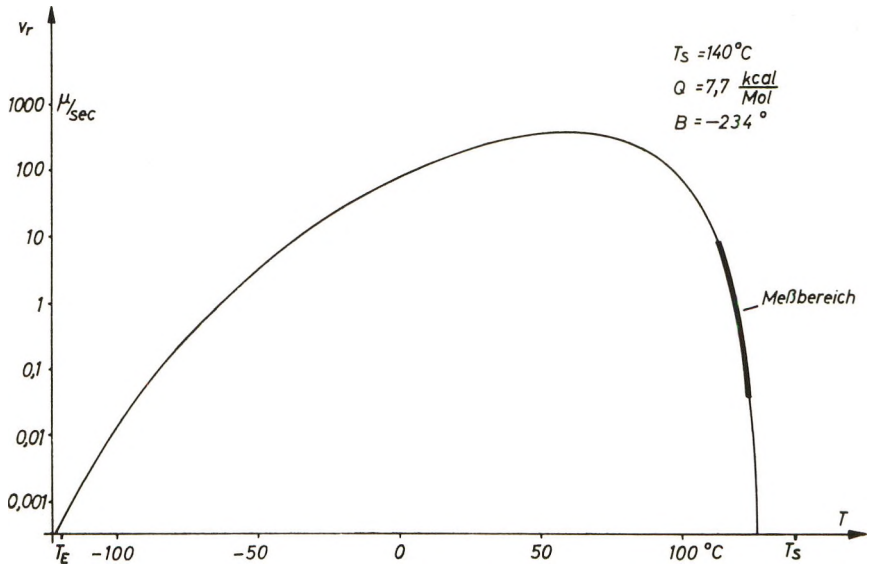


Abb. 3. Darstellung der Gleichung (6) für den gesamten Kristallisationsbereich mit den oben angegebenen Parametern. Es ergibt sich eine maximale Sphärolith-Wachstumsgeschwindigkeit des Polyäthylens von 380 μ /sec bei der Temperatur von 62°C.

Kennt man die Wachstumsgeschwindigkeit v_r für vier verschiedene Temperaturen, so kann man an Hand der Gleichung (7) die Parameter Q , B und T_s berechnen. Wir haben zunächst aus einer über die verschiedenen Präparate gemittelten Messkurve jeweils vier Werte für $v_r(T)$ entnommen und Q , B und T_s errechnet. Bei dieser Auswertung ist notwendigerweise die Grösse Q mit dem grössten Fehler behaftet, da der Faktor $e^{-Q/kT}$ in der Gleichung (7) die Wachstumsgeschwindigkeit in dem Temperaturbereich bestimmt, für den prinzipiell keine Messungen möglich sind.

Deshalb haben wir zur genaueren Bestimmung von Q nachträglich noch folgende Tatsache beachtet:

Das γ -Dispersionsgebiet des Elastizitätsmoduls liegt für Niederdruck-Polyäthylen bei -105°C .¹¹ Diese Dispersion wird dem Einfrieren der Segmentbeweglichkeit zugeordnet.

Mit der oben geschilderten Annahme über die Bildung des sekundären Keimes muss mit dem Einfrieren der Segmentbeweglichkeit auch die Kristallisationsgeschwindigkeit, d.h. in unserem Fall die Wachstumsgeschwindigkeit der Sphärolithe sehr klein werden. Dies wurde wie folgt benutzt:

Mit den aus unseren Messwerten bestimmten Parametern Q , B und T_s haben wir nach der Gleichung (7) die Wachstumsgeschwindigkeit v_r als Funktion der Temperatur für den gesamten Kristallisationsbereich dargestellt. Dann haben wir den Wert für Q und die Grössen B und T_s durch ein iteratives Verfahren so weit korrigiert, dass bei -105°C die radiale Wachstumsgeschwindigkeit unter einen grössenordnungsmässig abgeschätzten Wert von $0,01 \mu/\text{sec}$ abgenommen hat (Abb. 3) und dass sich ausserdem die gemittelten Messwerte durch die Gleichung (7) darstellen lassen. Hierdurch wurde der Wert für Q etwa um den Faktor 10 verringert, der Parameter B wurde etwa um den Faktor 2 kleiner, und die Schmelztemperatur T_s wurde um etwa 5 Grad herabgesetzt.

Auf die erläuterte Weise erhielten wir nach der Korrektur die folgenden Werte für die Parameter:

$$Q = 7,7 \text{ kcal/Mol}$$

$$T_s = 140^\circ\text{C}$$

$$B = -4x^* \sigma_e \cdot \sigma_s / k \cdot \Delta h_s = -234 \text{ Grad}$$

Mit diesen Werten beschreibt die Gleichung (7) die gemittelten Messwerte, wie in der speziellen Darstellung der Abbildung 4 noch einmal gezeigt ist.

Im Folgenden möchten wir die Grösse B näher diskutieren: Aus Arbeiten von Dole und Mitarbeitern¹² übernehmen wir für die spezifische Schmelzenthalpie des Polyäthylens den Wert $\Delta h_s = 66,3 \text{ cal/g}$. Die Elementarzelle der Polyäthylen-Einkristalle ist orthorhombisch und es wird angenommen, dass die Faltungsebene eine 110-Ebene ist.¹³ Für die Dicke x^* einer Faltungsebene (Abb. 2) haben wir deshalb den Abstand der 110-Ebenen mit $4,1 \text{ \AA}$ eingeführt.¹⁴ Damit können wir das Produkt der spezifischen Oberflächenspannungen $\sigma_e \sigma_s$ bestimmen:

$$\sigma_e \sigma_s = 570 \text{ erg}^2/\text{cm}^4$$

In der Literatur existieren bisher nur folgende Richtwerte für die spezifischen Oberflächenspannungen σ_e und σ_s .¹⁵ Die Grösse σ_e wurde aus theoretischen Berechnungen über die Dicke der Polyäthylen-Einkristalle abgeschätzt zu $\sigma_e = 13\text{--}75 \text{ erg/cm}^2$, während σ_s aus Messungen an Paraffinen zu $\sigma_s = 5\text{--}25 \text{ erg/cm}^2$ bestimmt wurde. Unser Ergebnis bestätigt,

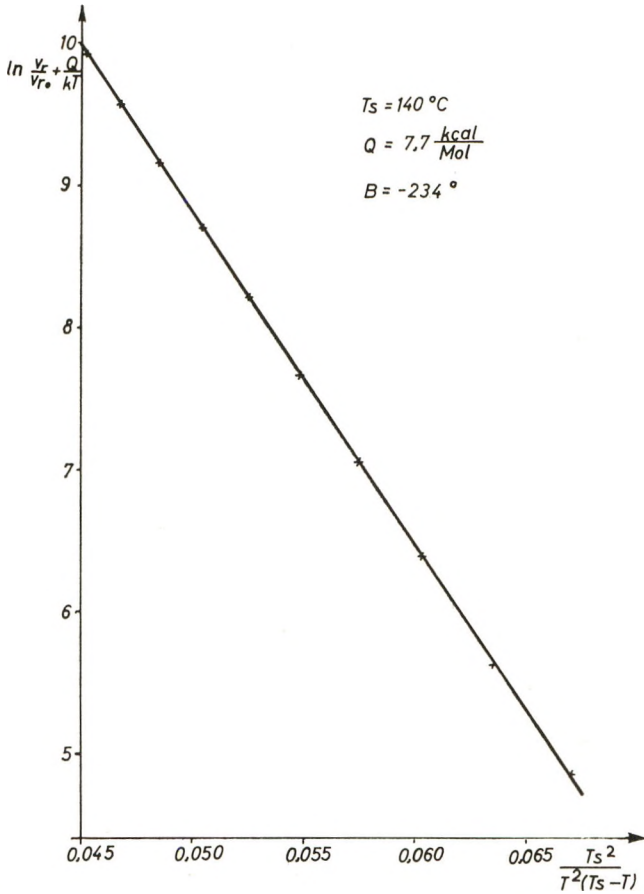


Abb. 4. Spezielle Darstellung: $\ln(v/v_0) + (Q/kT) = f[T_s^2/T^2(T_s - T)]$ der über die verschiedenen Präparate gemittelten Messkurve.

dass sich als sekundärer Keim tatsächlich vorwiegend gefaltete Ketten-segmente anlagern, da nur durch die relativ grosse Oberflächenspannung der Deckebene, in der die Falten liegen, das von uns ermittelte Produkt der Oberflächenspannungen erklärt werden kann.

Die Faltungslänge des Polyäthylens, die bei unserem Modell des sekundären Keimes mit der kritischen Länge z^* identisch ist (Abb. 2), liegt in der Grössenordnung von $z^* \approx 100 \text{ \AA}$. Nach den Gleichungen (4) und (6) galt:

$$z^* = 2\sigma_e/\Delta f = (2\sigma_e/\Delta h_s)[T_s^2/T(T_s - T)]$$

Bei einer Unterkühlung von 20 Grad ($T = 120^\circ\text{C}$; $T_s = 140^\circ\text{C}$) er-rechnen wir daher mit $\Delta h_s = 66,3 \text{ cal/g}$ eine spezifische Oberflächenspannung σ_e :

$$\sigma_e = 67 \text{ erg/cm}^2$$

die in dem angegebenen Bereich liegt.

Aus dem von uns bestimmten Produkt der Oberflächenspannungen $\sigma_e \sigma_s$ folgt dann für die spezifische Oberflächenspannung der Seitenflächen:

$$\sigma_s = 8,6 \text{ erg/cm}^2$$

Mit diesem Wert können wir die kritische Länge $y^* = 2\sigma_s/\Delta f$ ebenfalls bei einer Unterkühlung von 20 Grad errechnen. Es ist:

$$y^* \approx 13 \text{ \AA}$$

Für unser Modell des sekundären Keims und mit den bekannten Abmessungen der Elementarzelle des Polyäthylens¹⁴ bedeutet dieser Wert anschaulich, dass sich bei 120°C sekundäre Keime bilden, die im Durchschnitt aus drei Kettensegmenten aufgebaut sind.

Ich danke Herrn Professor Dr. K.-H. Hellwege für die Anregung zu dieser Arbeit, Herrn Dr. U. Johnsen für viele fördernde Diskussionen.

Literatur

1. Burnett, B. B., und W. F. McDevit, *J. Appl. Phys.*, **28**, 1101 (1957).
2. Price, F. P., *J. Phys. Chem.*, **64**, 169 (1960).
3. Hellwege, K.-H., und G. Hoff, *Kolloid-Z.*, **170**, 144 (1960).
4. Lindegren, C. R., *J. Polymer Sci.*, **50**, 181 (1961).
5. Barnes, W. J., W. G. Luetzel, und F. P. Price, *J. Phys. Chem.*, **65**, 1742 (1961).
6. Inoue, M., und T. Takayanagi, *J. Polymer Sci.*, **47**, 498 (1960).
7. Becker, R., und W. Döring, *Ann. Physik*, **5**, 719 (1935).
8. Keller, A., *Nature*, **171**, 170 (1953).
9. Fischer, E. W., *Z. Naturforschung*, **12a**, 753 (1957).
10. Hoffman, J. D., *J. Chem. Phys.*, **29**, 1192 (1958).
11. Wolf, K. A., *Z. Elektrochem.*, **65**, 604 (1961).
12. Dole, M., W. P. Hettinger, Jr., N. Larson, und J. A. Wethington, Jr., *J. Chem. Phys.*, **20**, 781 (1952).
13. Reneker, D. H., und P. H. Geil, *J. Appl. Phys.*, **31**, 1916 (1960).
14. Bunn, C. W., *Trans. Faraday Soc.*, **35**, 491 (1939).
15. Lauritzen, J. I., Jr., und J. D. Hoffman, *J. Res. Natl. Bur. Std.*, **64A**, 73 (1960).

Zusammenfassung

Das Wachstum zweidimensionaler Polyäthylen-Sphärolithe wurde in dem Temperaturbereich von 115°C bis 125°C verfolgt. Für die Auswertung wurde vorausgesetzt, dass die radiale Wachstumsgeschwindigkeit v_r durch die Bildungsrate sekundärer Keime an der Peripherie der Sphärolithe bestimmt wird. Dann gilt nach der Keimbildungstheorie:

$$v_r = v_{r0} e^{-Q/kT} e^{-\Delta F^*/kT}$$

Die kritische Freie Energie ΔF^* wurde für quaderförmige Keime zu $\Delta F^* = x^*(4\sigma_e \sigma_s/\Delta f)$ berechnet. Dieser Keim besteht nach der Rechnung aus einer einzigen Schicht von angelagerten Kettensegmenten. Die nach dieser Theorie aus der radialen Wachstumsgeschwindigkeit abgeleiteten spezifischen Oberflächenspannungen $\sigma_e \sigma_s$ des kritischen Keimes stimmen mit den Werten überein, die für Polyäthylen-Einkristalle aus gefalteten Ketten gelten. Mit der für Polyäthylen bekannten Faltungslänge besteht der sekundäre Keim aus drei nebeneinander liegenden, gefalteten Kettensegmenten von etwa 100 Å Länge. Die gute Übereinstimmung der aus der Wachstumsgeschwindigkeit zweidimensionaler Sphärolithe hergeleiteten Werte mit den Ergebnissen an Polyäthylen-

Einkristallen bestätigt die Annahme: Die Wachstumsgeschwindigkeit der Sphärolithe wird durch die Bildungsrate sekundärer Keime an ihrer Oberfläche bestimmt.

Résumé

L'accroissement d'un sphérolithe de polyéthylène bidimensionnel a été suivi dans un domaine de température allant de 115 à 125°C. Pour l'interprétation on est parti de la supposition que la vitesse d'accroissement radiale V_2 était déterminée par les taux de formation de germes secondaires à la périphérie du sphérolithe. On a alors d'après la théorie de la formation des germes:

$$v_r = v_{r0} e^{-Q/kT} e^{-\Delta F^*/kT}$$

L'énergie libre critique ΔF^* a été estimée pour des germes de forme carrée à $\Delta F^* = \pi^* (4\sigma_e \sigma_s / \Delta f)$. Ce germe consiste d'après le calcul en une seule courbe de segments de chaîne accolés les uns aux autres. Les tensions superficielles spécifiques $\sigma_e \sigma_s$ du germe critique déduite d'après cette théorie de la vitesse d'accroissement radiale correspondent aux valeurs des tensions chez les monocristaux de polyéthylène à chaînes plissées. Chez le polyéthylène le germe secondaire pour une longueur de plissement connue consiste en 3 segments croisés adjacents d'environ cent Å de longueur. La parfaite coïncidence des valeurs obtenues à partir de la vitesse d'accroissement de sphérolithes bidimensionnels avec les résultats correspondant chez les monocristaux de polyéthylène confirme l'hypothèse: la vitesse d'accroissement des sphérolithes est déterminée par les taux de formation de germes secondaires à la surface de ces sphérolithes.

Received February 5, 1963

Density of Polyethylene*

GEORGE A. MORTIMER and WILLIAM F. HAMNER,
*Research Department, Plastics Division, Monsanto Chemical Company,
Texas City, Texas*

Synopsis

The density of polyethylene produced by free-radical-initiated batch polymerization at elevated pressures and temperatures was found to be determined by the amount of short-chain branching and the molecular weight. The short-chain branching was shown to depend solely upon the pressure and temperature of polymerization. This branching increased as the pressure was reduced or as the temperature was increased. The molecular weight was shown to have an important influence on the density at much higher molecular weight levels than previously reported (up to 50,000 \bar{M}_n). The density increased as molecular weight decreased. At a constant polymerization pressure and temperature, the type and amount of initiator and chain-transfer agent had no effect on short-chain branching. Inasmuch as the type and amount of these substances do have an effect on molecular weight, they did affect density indirectly through the molecular weight. An equation relating the density, molecular weight, and polymerization pressure and temperature is given.

INTRODUCTION

Density is an important property of polyethylene, inasmuch as it is related to such other properties as stiffness, melting point, vapor transmission, sorption of reagents, etc.¹ It is perhaps the most sensitive and most easily determined of the properties which are dependent on the degree of crystallinity of the sample.²

Considerable study has been devoted to the elucidation of the factors which influence density and crystallinity. It was recognized early that polyethylene molecules prepared by the normal high pressure reaction were branched.³ That these branches interrupted crystallization⁴ and reduced density³ was soon established. Recognition of two kinds of branching, long and short,⁵ and the identification of the short branches as the major cause of interruption of crystallinity followed.^{1,2}

Two other factors have also been shown to influence density. At very low molecular weight levels (below 20,000), molecular weight was found to have some influence, although none was found above $\bar{M}_n = 20,000$.² The thermal treatment of the polymer also has been shown to influence density and crystallinity.^{1,5}

* Presented at the Southwest Regional Meeting of the American Chemical Society Dallas, Texas, Dec. 7, 1962.

Although the effects of molecular structure on bulk density have been thoroughly studied, there is a paucity of published information relating these molecular structural parameters to the polyethylene synthesis conditions. It was the purpose of this study to uncover and define the effects of the polymerization variables on the density-controlling molecular parameters.

The effect of thermal treatment will not be considered in the present paper inasmuch as such treatment does not alter the molecular characteristics of the polymer but only the degree to which these characteristics manifest themselves. The densities reported in this paper are for annealed samples.^{1,6} It has been possible to show in this laboratory that even though a variety of thermal treatments was carried out on polyethylene samples, the original annealed density was always obtained when the sample was reannealed. Thus, in this study, the effect of thermal history has been eliminated.

EXPERIMENTAL

The ethylene used in this work was 99.5% pure or better, containing approximately 0.3% ethane and 0.2% methane. Oxygen concentration was less than 0.0002%. All initiators were obtained from commercial sources. Solvents were redistilled in an argon atmosphere and stored under argon or nitrogen.

First Polymerization Procedure

A 120-cc. steel high pressure vessel was thoroughly cleaned, evacuated, and purged three times with ethylene. The initiator and solvents in benzene solution were introduced in such a way as to avoid introduction of oxygen. Ethylene was then added until the desired pressure had been reached. The reaction vessel was heated to the desired temperature, the pressure being kept constant by venting excess ethylene. Normally, 10–15 min. was required for the reaction charge to reach the predetermined temperature. The vessel was kept at constant pressure by adding more ethylene as necessary. The reaction charge was not agitated during polymerization. The pressure was sensed by a Baldwin-Lima-Hamilton SR-4 strain gauge. The temperature was measured by a thermocouple, which extended into the reaction mixture. To end polymerization, which generally ran 60–90 min., the pressure was released. Any polymer which was carried out with the ethylene was collected in a trap. The polyethylene remaining in the vessel was dissolved in hot xylene, precipitated with cold methanol, filtered, washed, and dried in a vacuum oven at 80°C. The data from these experiments are summarized in Table I.

Second Polymerization Procedure

A 240-cc. steel high pressure vessel containing an internal agitator and otherwise fitted as in the first procedure was thoroughly cleaned, evacu-

TABLE I
Unagitated Polymerizations

Avg. pressure, psi	Avg. temperature, °C.	No. of runs	Avg. density, g./cc.	Initiator ^a
10,000	88	5	0.935 ± 0.003	DTBP, TBPA, LP
20,000	88	4	0.934 ± 0.002	LP
30,000	87	2	0.939 ± 0.001	LP
10,000	128	3	0.927 ± 0.001	DTBP, TBPA
20,000	127	6	0.929 ± 0.001	DTBP, TBPB
25,000	127	3	0.932 ± 0.002	TBPB
30,000	127	4	0.937 ± 0.002	TBPB
10,000	152	13	0.922 ± 0.001	DTBP
15,000	151	5	0.924 ± 0.002	DTBP
20,000	152	7	0.926 ± 0.001	DTBP
25,000	152	4	0.931 ± 0.001	DTBP
30,000	152	4	0.933 ± 0.001	DTBP, O ₂
35,000	151	3	0.934 ± 0.001	DTBP
40,000	151	4	0.936 ± 0.003	DTBP
20,000	175	4	0.922 ± 0.001	EN
25,000	174	3	0.925 ± 0.001	EN
30,000	174	3	0.926 ± 0.002	EN
35,000	174	3	0.926 ± 0.001	EN

^a DTBP = di-*tert*-butyl peroxide; TBPA = *tert*-butyl peracetate; LP = dilauroyl peroxide; TBPB = *tert*-butyl perbenzoate; EN = ethyl nitrate.

TABLE II
Agitated Polymerizations

Pressure, psi	Temperature, °C.	Density, g./cc.	\bar{M}_n	Initiator ^a
20,000	130	0.931	52,000	DTBP
20,000	129	0.931	49,300	"
20,000	129.5	0.938	34,700	"
20,000	200	0.930	33,800	AO
20,000	200	0.928	44,900	"
20,000	200	0.930	31,300	"
29,750	132	0.940	35,800	DTBP
30,000	130	0.940	34,900	"
30,000	131	0.945	25,000	"
29,750	200	0.931	37,100	AO
30,000	199.5	0.929	43,900	"
30,000	200	0.937	24,500	"
25,000	149.5	0.938	32,300	DTBP
25,000	150.5	0.941	28,600	"
25,000	150	0.943	21,400	"
25,000	150	0.943	22,100	"
25,000	162	0.930	50,500	EN
25,000	163	0.938	24,600	"

^a DTBP = di-*tert*-butyl peroxide; AO = acetone oxime; EN = ethyl nitrate.

ated, and purged three times with ethylene. The vessel was heated to the predetermined temperature and part of the ethylene was introduced. With agitation, the initiator, chain-transfer agents, and solvents were pressured into the vessel with the remaining ethylene necessary to give the final desired pressure. Normally, 2-4 min. was required to bring the pressure to the desired level after the initiator had been introduced. After both pressure and temperature were held constant for 45-60 min., the polymerization was terminated by releasing the pressure. Both the polymer which blew out with the ethylene and the polymer in the vessel were dissolved in hot xylene and worked up as in the first procedure. The data from these runs are summarized in Table II.

Evaluation Procedures

The density samples were melted, pressed into slabs of 20-60 mil thickness of weight 0.5-1.5 g., cooled, annealed 30-60 min. in boiling water, and cooled slowly. The densities were determined using a water displacement method. Duplicate determinations were made for each polymerization. The density determination itself had a standard deviation of about ± 0.0002 g./cc. However, the densities obtained for duplicate polymerizations varied by about ± 0.002 g./cc. for the first polymerization procedure and slightly less than ± 0.001 g./cc. for the second, so the densities are reported to only three significant figures. Different annealing procedures were found to give slightly different density values. However, this observation is of no importance as long as relative densities only are being considered and a constant annealing procedure is maintained.⁶

Number-average molecular weights were determined osmotically⁷ unless otherwise noted.

The $\text{CH}_3/100\text{C}$ values given in this paper were obtained by an early infrared method⁸ that had good precision but which did not give accurate absolute values. Absolute data, obtained later, will appear elsewhere.¹¹

DISCUSSION

From Figure 1, which presents graphically the data from Table I, it is easily seen that both the temperature and pressure of synthesis have a marked effect on the polymer density. The change in density, at least for 0.92 density polymers, corresponded well for most samples with the change in short-chain branching as measured by infrared analysis.¹¹ The equation of Sperati, Franta, and Starkweather¹ giving density in terms of $\text{CH}_3/100\text{C}$ values was obeyed quite well for $\text{CH}_3/100\text{C}$ values greater than 1. Because of this correlation, it was felt that most, if not all, of the change in density could be ascribed to changes in short-chain branching.

However, at $\text{CH}_3/100\text{C}$ values near or below unity, serious deviations from Sperati, Franta, and Starkweather's equation arose. The reasons for this behavior are probably twofold. First, the $7.25\ \mu$ band is a composite of overlapping CH_3- and $-\text{CH}_2-$ bands. For low methyl con-

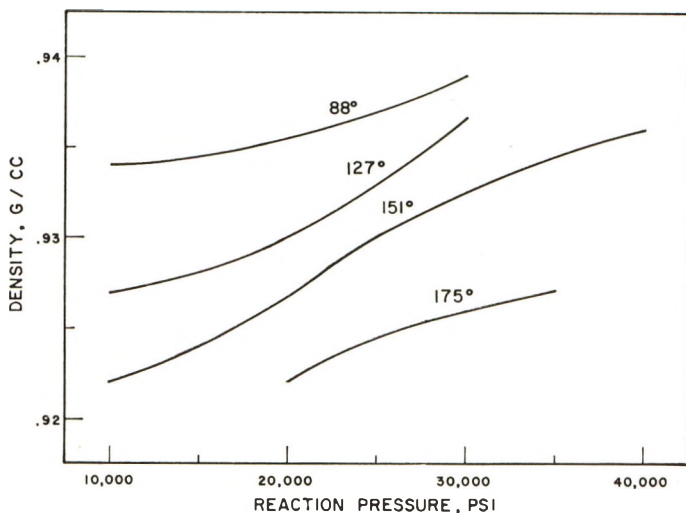


Fig. 1. Density as a function of pressure and temperature.

tents, the methyl peak occurs only as a partial shoulder on the methylene band, making accurate measurement of the methyl content difficult.

A second reason for some of the deviation was that the effect of molecular weight on density was assumed to be negligible, as claimed.^{1,2,9} As will be shown later, this was a false assumption. Those samples which had $\text{CH}_3/100\text{C}$ values near 1.0 were of extremely high molecular weight because of the synthesis conditions,¹⁰ and hence the lack of correction for molecular weight effects was serious. Even with these inaccuracies, the results of the experiments of Table I are very valuable.

It is clear from Figure 1 that as the synthesis pressure rises, the polymer density increases also. The decrease in branching with an increase in synthesis pressure is consistent with current theory,¹²⁻¹⁴ although it has not always been observed.¹⁵ Both an increase in pressure *per se* and the fact that an increase in ethylene pressure cause an increase in monomer concentration lead to the prediction that the propagation rate would be increased by increasing the pressure.¹⁶ However, the short-chain branching reaction, which is described in an intramolecular chain-transfer step,⁵ should be only slightly affected by pressure. Hence, the relative amount of short-chain branching is decreased.

That the effect of increasing the synthesis temperature is to decrease the polymer density is also clearly apparent from Figure 1. The change in density again correlates with an observed increase in $\text{CH}_3/100\text{C}$ ¹¹ which is of sufficient magnitude to be completely responsible for the change in density. This conclusion is also consistent with present theory. A chain-transfer reaction,⁵ having a higher activation energy than the propagation reaction, would become relatively more frequent as the temperature is raised. The effect of temperature on density is well documented.¹³⁻¹⁵

The combination of low temperature and high pressure has been used to prepare polyethylene of densities in the range 0.95–0.97 g./cc.¹⁷

In order to assess the effect of molecular weight on density, the runs in Table II were made in which varying amounts of chain-transfer agents were added to intentionally vary \bar{M}_n . It can be seen that polyethylene samples prepared at the same pressure and temperature had quite different densities when the number-average molecular weights were different. Tables III and IV show additional data at common synthesis pressures and temperatures where the type and amount of chain-transfer agent has been varied. These tables show that the $\text{CH}_3/100\text{C}$ values obtained, at constant temperature and pressure, are constant within experimental error. Therefore, these changes in density cannot be ascribed to changes in short-chain branching, but must be ascribed to changes in molecular weight. The molecular weight effect is believed to be a manifestation of the greater ease of orientation of shorter polymer chains into crystalline lattices.¹⁸ Clearly, molecular weight has an important effect on density up to at least 50,000 \bar{M}_n . This effect has been overlooked in previous work,¹⁵ except at much lower molecular weight levels.² However, it has been noted by others that the density was greater when polymerization was conducted in the presence of ethanol (a chain-transfer agent) than in the presence of water.¹³

The possibility was considered that the effect of \bar{M}_n on density might be a result faster and therefore more thorough annealing of lower \bar{M}_n materials than of higher \bar{M}_n polymers. However, various annealing procedures were tried, from fast cooling to a 16-hr. slow cooling. The maximum

TABLE III
Effect of Molecular Weight at 20,000 psi, 130°C.

Chain-transfer agent	\bar{M}_n	$\text{CH}_3/100\text{C}$	Density, g./cc.
Acetone	62,200	0.3	0.932
"	56,600	0.2	0.931
"	52,000	0.2	0.931
Propane	48,700 ^a	0.2	0.932
"	35,900 ^a	0.2	0.933
Acetone	34,700	0.2	0.938
Propane	33,000 ^a	0.2	0.936
"	31,900 ^a	0.3	0.938

^a Determined by a correlation between melt flow and \bar{M}_n .¹⁹

TABLE IV
Effect of Molecular Weight at 10,000 psi, 150°C.

Chain-transfer agent	\bar{M}_n	$\text{CH}_3/100\text{C}$	Density, g./cc.
None	84,000	2.2	0.922
"	65,000	2.4	0.921
"	62,500	2.5	0.923
<i>p</i> -Xylene	23,300	2.3	0.930
"	21,000	2.5	0.931

variation in density due to these annealing differences was less than the differences between samples of widely different \bar{M}_n . Furthermore, the relative difference between such samples was always maintained, regardless of the density level set by the annealing procedure. These findings are corroborated by the more complete annealing study of Everett⁶ and lead to the conclusion that the density differences reported here are real.

When the data of Table II were subjected to a Forward-Doolittle regression analysis, the equation

$$d = 0.963 + 2.4 \times 10^{-7}P - 1.18 \times 10^{-4}T - 4.0 \times 10^{-7}\bar{M}_n \pm 0.001$$

was obtained, where d is density (in g./cc.), P is polymerization pressure (in psi), T is polymerization temperature (in °C.), and \bar{M}_n is the number-average molecular weight of the polymer.

Although the equation satisfactorily fits the data at hand, it should not be inferred that it represents a correct, extrapolatable, mathematical model of the density-pressure-temperature- \bar{M}_n relationship over a wide range of conditions. Indeed, limited attempts to extrapolate the equation, especially to higher molecular weights, have indicated quite the opposite. Also, the particular annealing process used in the density determination will affect the coefficients in the equation. The point to be emphasized here is that, within the range covered in Table II (20,000–30,000 psi, 130–200°C., 25,000–50,000 \bar{M}_n , the density and \bar{M}_n of the polymer can be described, within experimental error, in terms of each other and the pressure and temperature of polymerization.

During these studies, a wide variety of chain-transfer agents were used, a few of which are specifically included as examples in the tables. In all instances, no effect on density was observed which was not completely explained by the \bar{M}_n change. Substances which have little or no chain-transfer activity (such as benzene and methane) had no detectible effect on the polymer density. The only exception to these statements arose when highly halogenated substances were used in such an amount that the resulting polymer contained more than 1% halogen by weight. In such instances, an additional incremental increase in density was noted, which presumably was due to the incorporation of the high density endgroups in detectible amounts.

The patent literature contains numerous claims of increased polyethylene density as a result of using specific initiators. During the present studies, many initiators were used. Some of them are listed in Tables I and II. In no instance was any effect on density observed which was not completely describable in terms of the polymerization pressure and temperature and the polymer molecular weight. As is implied in Table I, the same densities were obtained from a variety of initiators when polymerization pressure and temperature were the same. Apparently, the only function of the patented initiators is to generate free radicals at an acceptable rate at low temperature where short-chain branching is minimized.

The authors wish to acknowledge the help of Dr. H. J. L. Schuurmans who determined the number-average molecular weights, assisted in preparing the data for computer calculation, and provided encouragement and helpful suggestions. Appreciation is also expressed for the laboratory assistance of Mr. L. C. Arnold.

References

1. Sperati, C. A., W. A. Franta, and H. W. Starkweather, Jr., *J. Am. Chem. Soc.*, **75**, 6127 (1953).
2. Richards, R. B., *J. Appl. Chem. (London)*, **1**, 370 (1951).
3. Fox, J. J., and A. E. Martin, *Proc. Roy. Soc. (London)*, **A175**, 208 (1940).
4. Bryant, W. M. D., *J. Polymer Sci.*, **2**, 547 (1947).
5. Roedel, M. J., *J. Am. Chem. Soc.*, **75**, 6110 (1953).
6. Everett, H. W., *Mater. Res. Std.*, **2**, 278 (1962).
7. Mendelson, R. A., *J. Polymer Sci.*, **46**, 493 (1960).
8. Bryant, W. M. D., and R. C. Voter, *J. Am. Chem. Soc.*, **75**, 6113 (1953).
9. Raff, R. A. V., and J. B. Allison, *Polyethylene*, High Polymers XI, Interscience, New York, 1956, p. 228.
10. Franta, W. A., U. S. Patent 2,586,322 (1952).
11. Woodbrey, J. C., and P. Ehrlich, *J. Am. Chem. Soc.*, **85**, 1580 (1963).
12. Renfrew, A., and P. Morgan, *Polythene*, 2nd Ed., Iliffe, London, 1960, pp. 58-63.
13. Kodama, S., et al., *J. Polymer Sci.*, **55**, 285 (1961).
14. Grimsby, F. N., Thesis, Department of Chemical Engineering, Massachusetts Institute of Technology, 1953.
15. Kodama, S., et al., *J. Polymer Sci.*, **41**, 83 (1959).
16. Symcox, R. O., and P. Ehrlich, *J. Am. Chem. Soc.*, **84**, 531 (1962).
17. Larcher, A. W., and D. C. Pease, U. S. Pat. 2,816,883 (1957).
18. Willbourn, A. H., *J. Polymer Sci.*, **34**, 569 (1959).
19. Mortimer, G. A., G. W. Daues, and W. F. Hamner, *J. Appl. Polymer Sci.*, in press.

Résumé

On a trouvé que la densité du polyéthylène, produit par initiation radicalaire dans une série de polymérisation à pressions et températures élevées, était déterminée par la quantité de ramifications à chaînes courtes et par le poids moléculaire. On a montré que la ramification à chaînes courtes dépendait uniquement de la pression et de la température de polymérisation. Cette ramification croît avec une diminution de pression et une augmentation de température. On a montré que le poids moléculaire avait une influence importante sur la densité en ce qui concerne les plus hauts poids moléculaires, comme il a été reporté auparavant (au-dessus de M_n 50.000). La densité augmente avec une diminution du poids moléculaire à température et pression constantes de polymérisation; la nature et la quantité d'initiateur et d'agent de transfert de chaîne n'ont pas d'effet sur les ramifications à courtes chaînes. Dans la mesure où le type et la quantité de ces substances doivent avoir un effet sur le poids moléculaire, ils doivent affecter indirectement la densité par l'intermédiaire du P.M. Une équation reliant la densité, le poids moléculaire et la pression et température de polymérisation est donnée.

Zusammenfassung

Es wurde gefunden, dass die Dichte von Polyäthylen, welches durch radikalisch gestartete "Batch"-Polymerisation bei erhöhten Drucken und Temperaturen hergestellt wurde, durch das Ausmass der Kurzkettenverzweigung und durch das Molekulargewicht bestimmt wird. Dass Ausmass der Kurzkettenverzweigung hängt nur von Druck und Temperatur während der Polymerisation ab. Diese Verzweigung nahm mit sinkendem Druck und mit steigender Temperatur zu. Es wurde gezeigt, dass der Einfluss des Molekulargewichtes auf die Dichte bis zu weitaus höheren Molekulargewichtsbereichen

(M_n bis 50000) von Bedeutung ist als früher angenommen wurde. Die Dichte steigt mit sinkendem Molekulargewicht. Bei gleichbleibender Grösse von Polymerisationsdruck und -temperatur, hatten Art und Menge von Starter und Kettenüberträger keinen Einfluss auf die Kurzkettenverzweigung. Insofern als Art und Menge dieser Substanzen einen Einfluss auf das Molekulargewicht haben, beeinflussen sie die Dichte indirekt über das Molekulargewicht. Es wird eine Gleichung angegeben, die Dichte, Molekulargewicht sowie Polymerisationsdruck und -temperatur in Beziehung zueinander setzt.

Received February 18, 1963

An Elementary Theory of Nonlinear Viscoelasticity*

JULIAN L. DAVIS, *Polymer Research Section, Picatinny Arsenal,
Dover, New Jersey*

Synopsis

A first-order, nonlinear, one-dimensional theory of viscoelasticity is constructed by use of an elementary perturbation technique. It is based on applying some simple hypotheses of nonlinearity to single nonlinear Maxwell and Voigt models. The response of the Maxwell model to a sinusoidally applied strain is governed by a nonlinear complex modulus whose nonlinear part is given as a function of applied strain and strain rate as well as external frequency and internal or model parameters. This is a nonlinear relaxation effect. A nonlinear creep effect is obtained by describing the nonlinear response of the Voigt model to a sinusoidally applied stress in terms of a nonlinear complex compliance.

Introduction

There has been built up a vast body of literature¹ on the subject of linear viscoelasticity, wherein the stress developed in a viscoelastic element (as a result of an externally applied stress or strain) is assumed to be a linear function of strain and strain rate.^{1,2} This is a first approximation which accounts for the response of a material to an external load, the material being neither an elastic solid nor a viscous fluid, but having the properties of both. Mechanical models consisting of springs and dashpots (arranged in series or parallel) have been constructed from which simplified linear viscoelastic theories have been developed. Two well-known models are those of Maxwell (spring and dashpot in series) and Voigt (spring and dashpot in parallel). More complex models are constructed by connecting Maxwell elements in parallel or Voigt elements in series or by combining both.

The basic hypothesis in the classical models of linear viscoelasticity is (as mentioned above) that the stress is a linear function of strain and strain rate. This means that the elastic and viscous coefficients—parameters representing the spring and dashpot, respectively—are independent of the strain and strain rate. In this article we shall relax this requirement by assuming that the elastic coefficient has added to it a small term depending on the elastic strain to the first order and the viscous coefficient has added to it a term depending on the strain rate to the first order. This will be described in detail below.

* Based on a paper presented at a meeting of the American Chemical Society, Polymer Chemistry Group, New York, January 1963.

Nonlinear Hypothesis

The basic assumption of nonlinearity, expressed by eqs. (2) and (3) below, is used to construct an elementary nonlinear theory and is common to the nonlinear Maxwell and Voigt models. Each of these models, which will be used to illustrate the theory, involves both a nonlinear viscous (dashpot) and elastic element (spring). Each model, then, is governed by a set of two parameters (E, η) which describe its physical properties. The nonlinear elastic coefficient E , describing the nonlinear spring, is assumed to be a prescribed function of strain on the elastic element ϵ_E ; the nonlinear viscosity coefficient η , describing the nonlinear dashpot, is assumed to be a prescribed function of strain on the viscous element $\dot{\epsilon}_\eta$. A condition on (E, η) must be that they reduce to the respective linear coefficients (E_0, η_0) for the classical linear models.

In general E can be approximated by a polynomial in ϵ_E whose leading term is E_0 , and η by a polynomial in $\dot{\epsilon}_\eta$ whose leading term is η_0 . Specifically:

$$\begin{aligned} E &= E_0 + \sum_{n=1}^{\infty} a_n \gamma_E^n \epsilon_E^n \\ \eta &= \eta_0 + \sum_{n=1}^{\infty} b_n \gamma_\eta^n \dot{\epsilon}_\eta^n \end{aligned} \quad (1)$$

where (γ_E, γ_η) are dimensionless parameters measuring the nonlinearity in the (spring, dashpot) and $\{a_n, b_n\}$ are constants depending on (E_0, η_0) . For small nonlinearities the second and higher order terms in $\gamma_E \epsilon_E$ and $\gamma_\eta \dot{\epsilon}_\eta$ are neglected, giving

$$\begin{aligned} E &\simeq E_0 + \gamma_E E_0 \epsilon_E \\ \eta &\simeq \eta_0 + \gamma_\eta \tau^2 E_0 \dot{\epsilon}_\eta \\ \tau &= \eta_0 / E_0 \end{aligned} \quad (2)$$

where τ is the relaxation time for the linear system, and (γ_E, γ_η) are so chosen that

$$\begin{aligned} |\gamma_E \epsilon_E| &\ll 1 \\ \tau |\gamma_\eta \dot{\epsilon}_\eta| &\ll 1 \end{aligned} \quad (3)$$

We take condition (3) to mean that second and higher order terms in $\gamma_E \epsilon_E$ and $\gamma_\eta \dot{\epsilon}_\eta$ are to be neglected, and we shall call (3) the condition of first-order nonlinearity.

Maxwell Model

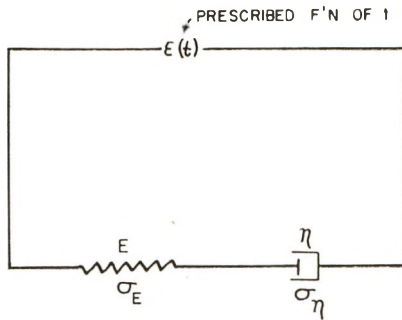
Consider a single Maxwell model (as shown in Fig. 1) with a nonlinear elastic and viscous element governed by the conditions described by eqs. (2) and (3) and subject to a prescribed time-varying external strain. The Maxwell model is defined by

$$\sigma_E = \sigma_\eta = \sigma \quad (4)$$

where σ_E, σ_η are the stresses on the elastic and viscous elements, respectively, and

$$\epsilon_E + \epsilon_\eta = \epsilon(t) \tag{5}$$

where $\epsilon(t)$ is the applied time-varying strain. In fact the actual mechanical model was used by Maxwell merely as a "psychological crutch" upon which to derive the differential equation of motion for the system. It would be equally valid to replace the concept of the mechanical model by eqs. (4) and (5) as the defining properties of a model that couples an elastic and viscous element in series.



$$\begin{aligned} \sigma &= E \epsilon_E = \eta \dot{\epsilon}_\eta \\ E &\sim E_0 + \gamma_E E_0 \epsilon_E \\ \eta &\sim \eta_0 + \gamma_\eta \tau^2 E_0 \dot{\epsilon}_\eta \end{aligned}$$

Fig. 1. Single nonlinear Maxwell model.

The simple constitutive equations for the nonlinear elastic and viscous elements are independent of the model, i.e., independent of their coupling. They are

$$\begin{aligned} \sigma_E &= E \epsilon_E \\ \sigma_\eta &= \eta \dot{\epsilon}_\eta \end{aligned} \tag{6}$$

where (E, η) are given by eq. (2). The application of eqs. (6) to the Maxwell model is obtained by using eqs. (4), (5), and the hypothesis of nonlinearity (2). Thus

$$\begin{aligned} \sigma &= E_0 \epsilon_E + \gamma_E E_0 \epsilon_E^2 \\ \sigma &= \eta_0 \dot{\epsilon}_\eta + \gamma_\eta \tau^2 E_0 \dot{\epsilon}_\eta^2 \end{aligned} \tag{7}$$

We may, of course, solve these quadratics for ϵ_E and $\dot{\epsilon}_\eta$ in closed form. However, it is instructive to expand ϵ_E and $\dot{\epsilon}_\eta$ in power series in σ of the form

$$\begin{aligned} \epsilon_E &= \sigma/E_0 + \sum_{n=1}^{\infty} \gamma_E^n c_n \sigma^{n+1} \\ \dot{\epsilon}_\eta &= \sigma/\eta_0 + \sum_{n=1}^{\infty} \gamma_\eta^n d_n \sigma^{n+1} \end{aligned} \tag{8}$$

where $\{c_n, d_n\}$ are constants depending on E_0, η_0 . Putting eqs. (8) into the system of eqs. (7) and keeping only terms of order (γ_E, γ_η) [to satisfy condition (3)] we get

$$\begin{aligned} \epsilon_E &\simeq \frac{\sigma}{E_0} - \frac{\gamma_E}{E_0^2} \sigma^2 \\ \dot{\epsilon}_\eta &\simeq \frac{\sigma}{\eta_0} - \frac{\gamma_\eta}{E_0 \eta_0} \sigma^2 \end{aligned} \tag{9}$$

It is clear that eqs. (9) reduce to the classical linear Maxwell model for $\gamma_E = \gamma_\eta = 0$. Thus the σ^2 terms are the nonlinear terms in the approximate constitutive eqs. (9). Differentiating eqs. (5) with respect to t and using eqs. (9) we get the following approximate nonlinear differential equation:

$$\begin{aligned} \dot{\sigma} + \lambda \sigma - \frac{2\gamma_E \sigma \dot{\sigma}}{E_0} - \frac{\gamma_\eta \sigma^2}{\eta_0} &= E_0 \dot{\epsilon} \\ \lambda &= \frac{E_0}{\eta_0} = \frac{1}{\tau} \end{aligned} \tag{10}$$

where $\dot{\epsilon}$ is a prescribed function of t . It is clear that eq. (10) now describes our nonlinear Maxwell model within the condition of first-order non-linearity.

Now consider the following perturbation method for solving eq. (10). We seek an expansion for σ in powers of γ_E and γ_η , the coefficients being functions of t to be determined. The expansion is to have the property of reducing to the well-known solution of eq. (10) for σ in the linear case where $\gamma_E = \gamma_\eta = 0$. We therefore set

$$\sigma = \sigma_0 + \sum_{n=1}^{\infty} \gamma_E^n \sigma_n + \sum_{n=1}^{\infty} \gamma_\eta^n s_n \tag{11}$$

where $\sigma_0, \sigma_1, \sigma_2, \dots, s_1, s_2, \dots$ are unknown functions of t . In general the procedure would be to put eq. (11) into eq. (10), set the coefficients of each power of γ_E and γ_η separately equal to zero, since γ_E and γ_η are parameters that vary independently, and thereby arrive at a set of easily solvable nested linear first-order nonhomogeneous differential equations for the functions $\{\sigma_{n-1}\}, \{s_n\}, n = 1, 2, 3, \dots$, the nonhomogeneous terms being functions of the solutions to the preceding equations. The form is

$$\dot{\sigma}_0 + \lambda \sigma_0 = E_0 \dot{\epsilon} \tag{12}$$

$$\begin{aligned} \dot{\sigma}_i + \lambda \sigma_i &= F_i(\sigma_0, \sigma_1, \sigma_2, \dots, \sigma_{i-1}) \\ \dot{s}_i + \lambda s_i &= G_i(\sigma_0, \sigma_1, \sigma_2, \dots, s_1, s_2, s_2, \dots, s_{i-1}) \quad i = 1, 2, \dots \end{aligned} \tag{13}$$

where the forcing functions F_i, G_i are known functions of their respective arguments. The system (13) is an infinite set of equations since the series in eq. (11) are infinite. In practice, of course, a finite number of equations in the system (13) would be used: $i = 1, 2, \dots, N$, where N is the number of terms in each series in eq. (11). N depends on the rapidity of the convergence of these series which in turn depend on the magnitude of the parameters γ_E, γ_η . Note that eq. (12) is the linear differential equation obtained from eq. (10) by setting $\gamma_E = \gamma_\eta = 0$. Equation (12) governs the behavior of the classical linear Maxwell model.

Using the condition of first-order nonlinearity, eq. (11) becomes approximately

$$\begin{aligned} \sigma &= \sigma_0 + \gamma_E \sigma_1 + \gamma_\eta s_1 \\ \sigma_n &= s_n = 0 \quad n = 2, 3, \dots \end{aligned} \tag{14}$$

and eqs. (13) reduce to two linear differential equations. We then get the system of linear differential equations:

$$\dot{\sigma}_0 + \lambda \sigma_0 = E_0 \dot{\epsilon} \tag{12}$$

$$\dot{\sigma}_1 + \lambda \sigma_1 = 2\dot{\sigma}_0 \sigma_0 / E_0 \tag{15a}$$

$$\dot{s}_1 + \lambda s_1 = \sigma_0^2 / \eta_0 \tag{15b}$$

Case of Applied Sinusoidal Strain

Let us now solve the system of eqs. (12) and (15) for the case of a pure sinusoidal strain $\epsilon(t)$ applied to our Maxwell model. ϵ can then be given in complex notation by

$$\epsilon = \bar{\epsilon} e^{i\omega t} \tag{16}$$

where $\bar{\epsilon}$ and ω are two prescribed positive numbers, $\bar{\epsilon}$ being the amplitude and ω the frequency. Then eq. (12) becomes

$$\dot{\sigma}_0 + \lambda \sigma_0 = i\omega E_0 \bar{\epsilon} e^{i\omega t} \tag{17}$$

whose steady-state solution is (we neglect the transient part of the solution)

$$\sigma_0 = E_0^* \epsilon \tag{18}$$

where

$$\begin{aligned} E_0^* &= \frac{iE_0}{\mu + i} = u_0 + iv_0 \\ u_0 &= E_0 / (1 + \mu^2) \\ v_0 &= \mu E_0 / (1 + \mu^2) \\ \mu &= \lambda / \omega = 1 / \omega \tau \end{aligned} \tag{19}$$

We shall call E_0^* the linear complex modulus. The expression for L_0^* given by eq. (19) can easily be shown to have, for example, the same form as that given in Bland.¹ In Bland's notation

$$\frac{F^\circ(\omega)}{a^\circ(\omega)} = \left(\frac{1}{E} + \frac{1}{i\omega\eta} \right)^{-1}$$

and the correspondence (\leftrightarrow) between Bland's notation and ours is: $L^\circ(\omega)/a^\circ(\omega) \leftrightarrow E_0^*$, $E \leftrightarrow E_0$, $\eta \leftrightarrow \eta_0$, and $E/\eta \leftrightarrow \lambda$. E_0^* is the ratio of the stress to strain for the classical case, and E_0^*/E_0 is a complex-valued function of the dimensionless parameter μ . u_0 , v_0 are the real and imaginary parts, respectively, of E_0^* .

To solve for σ_1 , eq. (15a) becomes

$$\dot{\sigma}_1 + \lambda\sigma_1 = 2\sigma_0\dot{\sigma}_0/E_0 = 2i\omega L_0^{*2}\epsilon^2/E_0 \quad (20)$$

by using eqs. (16) and (18). Setting

$$\sigma_1 = \sigma_1^* e^{2i\omega t} = \sigma_1^* \epsilon^2 / \bar{\epsilon}^2 \quad (21)$$

we can solve for σ_1^* by putting eq. (21) into eq. (20). Thus

$$\sigma_1^* = 2iE_0^{*2}\epsilon^2/E_0(\mu + 2i) \quad (22)$$

Recalling that E_0^* is given by eq. (19) we see that σ_1 is a sinusoidal function of t involving the second harmonic, whose amplitude σ_1^* is a complex-valued function of ω (or more specifically the dimensionless μ).

We solve for s_1 in eq. (15b) in the same manner. Equation (15b) becomes

$$\dot{s}_1 + \lambda s_1 = \sigma_0^2/\eta_0 = E_0^{*2}\epsilon^2/\eta_0 = E_0^*\bar{\epsilon}^2 e^{2i\omega t}/\eta_0 \quad (23)$$

Setting

$$s_1 = s_1^* e^{2i\omega t} = s_1^* \bar{\epsilon}^2 / \epsilon^2 \quad (24)$$

and putting this into eq. (23) we get

$$s_1^* = \mu E_0^{*2}\bar{\epsilon}^2/E_0(\mu + 2i) = -i\mu\sigma_1^*/2 \quad (25)$$

Gathering the above results the approximate solution of eq. (10) for σ , given by eq. (14), becomes

$$\sigma = E_0^*\epsilon + (\gamma_E\sigma_2^*/\bar{\epsilon}^2)\bar{\epsilon}^2 - (\gamma_{\eta\mu}\sigma_2^*/2\omega\bar{\epsilon}^2)\epsilon\dot{\epsilon} \quad (26)$$

We now introduce the concept of a nonlinear complex modulus E^* defined by

$$E^* = \sigma/\epsilon$$

as an extension of the classical definition of E_0^* such that

$$E_0^* = \sigma/\epsilon$$

We then get

$$E^* = E_0^* + (\gamma_E\sigma_2^*/\bar{\epsilon}^2)\epsilon - (\gamma_{\eta\mu}\sigma_2^*/2\omega\bar{\epsilon}^2)\dot{\epsilon} = E' + iE'' \quad (27)$$

where the real and imaginary parts of E^* are given by

$$\begin{aligned} E' &= u_0 + u_1 \epsilon \\ E'' &= v_0 + v_1 \epsilon \end{aligned} \tag{28}$$

where u_0 and v_0 are given by eq. (19) and

$$\begin{aligned} u_1 &= [4\gamma_E(1 - 2\mu^2) + \gamma_\eta\mu^2(5 - \mu^2)]/D \\ v_1 &= [4\gamma_E\mu(5 - \mu^2) - 2\gamma_\eta(1 - 2\mu^2)]/D \end{aligned} \tag{29}$$

and

$$D = [(4 + \mu^2)(1 + \mu^2)]/E_0$$

Equation (27) shows that the nonlinear complex modulus E^* is a linear function of ϵ and $\dot{\epsilon}$ arising from the nonlinear terms in the constitutive equations for the spring and dashpot, respectively ($\gamma_E E_0 \epsilon E^2$, $\gamma_\eta \tau^2 E_0 \dot{\epsilon} \eta^2$). The terms $\gamma_E \sigma_2^* \epsilon / \bar{\epsilon}^2$ and $\gamma_\eta \mu \sigma_2^* \dot{\epsilon} / 2\omega \bar{\epsilon}^2$ in eq. (27) are those terms in E^* that take care of first-order nonlinearities in the spring and dashpot, respectively. The coefficient of ϵ and $\dot{\epsilon}$ in these terms are known functions of μ from eq. (29). Obviously for the linear case $\gamma_E = \gamma_\eta = 0$ and $E^* = E_0^*$, a known function of μ from eq. (19).

Voigt Model

We now apply the same mathematical technique to the single Voigt model (as shown in Fig. 2) with a nonlinear elastic and viscous element coupled in parallel and governed by the conditions described by eqs. (2)

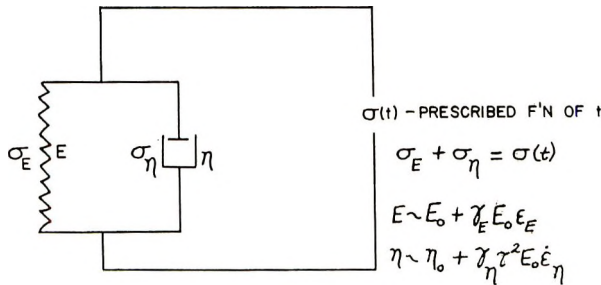


Fig. 2. Single nonlinear Voigt model.

and (3), and subject to a prescribed time varying external stress. The defining conditions for the Voigt model are

$$\epsilon_E = \epsilon_\eta = \epsilon \tag{30}$$

$$\sigma_E + \sigma_\eta = \sigma(t) = \bar{\sigma} e^{i\omega t} \tag{31}$$

for the case of a sinusoidally applied stress. The positive constants $(\bar{\sigma}, \omega)$ are the amplitude and frequency, respectively, of the applied time-varying stress $\sigma(t)$. The constitutive equations for the elastic and viscous

elements are given by eq. (6) where B and η are defined by eq. (2). (The same notation is applied to both the Maxwell and Voigt models; there is no ambiguity.) Using eqs. (2), (6), and (31), and the hypothesis of first-order nonlinearity, the approximate nonlinear differential equation that governs our Voigt model becomes

$$\dot{\epsilon} + \lambda\epsilon + \gamma_B\lambda\epsilon^2 + (\gamma_\eta/\lambda)\dot{\epsilon}^2 = (\bar{\sigma}/\eta_0)e^{i\omega t} \tag{32}$$

(Note the reciprocal relation with eq. (10), the analogous differential equation for the Maxwell model for the case $\epsilon = \bar{\epsilon}e^{i\omega t}$.) We now attempt to solve eq. (32) approximately for ϵ by a perturbation method. To this end we set

$$\epsilon = \epsilon_0 + \sum_{n=1}^{\infty} \gamma_E \epsilon_n + \sum_{n=1}^{\infty} \gamma_\eta^n e_n \tag{33}$$

where $\epsilon_0, \epsilon_1, \epsilon_2, \dots, e_1, e_2, \dots$ are unknown functions of t . In the same manner as for the Maxwell model we would get the following system of nested linear first-order nonhomogeneous differential equations of the form

$$\begin{aligned} \dot{\epsilon}_0 + \lambda\epsilon_0 &= \bar{\sigma}e^{i\omega t}/\eta_0 \\ \dot{\epsilon}_i + \lambda\epsilon_i &= F_i(\epsilon_0, \epsilon_1, \dots, \epsilon_{i-1}) \\ \dot{e}_i + \lambda e_i &= G_i(\epsilon_0, \epsilon_1, \dots, e_1, \dots, e_{i-1}) \end{aligned} \tag{34}$$

$i = 1, 2, \dots$

On using the approximation of first-order nonlinearity, eq. (33) reduces to

$$\epsilon = \epsilon_0 + \gamma_E \epsilon_1 + \gamma_\eta e_1 \tag{35}$$

and the system of eqs. (34) reduces to the system

$$\dot{\epsilon}_0 + \lambda\epsilon_0 = \bar{\sigma}e^{i\omega t}/\eta_0 \tag{36}$$

$$\dot{\epsilon}_1 + \lambda\epsilon_1 = -\lambda\epsilon_0^2 \tag{37}$$

$$\dot{e}_1 + \lambda e_1 = -\dot{\epsilon}_0^2/\lambda \tag{38}$$

The steady-state solution for ϵ_0 is

$$\epsilon_0 = J_0^* \sigma \tag{39}$$

where the linear complex compliance J_0^* is given as an explicit function of dimensionless frequency μ by

$$\begin{aligned} J_0^* &= \frac{\mu}{E_0(\mu + i)} = \frac{\mu^2}{E_0(1 + \mu^2)} - \frac{i\mu}{E_0(1 + \mu^2)} = J_0' + iJ_0'' \\ \mu &= \lambda/\omega \end{aligned} \tag{40}$$

which is classical, see Bland,¹ for example. Then eq. (37) becomes

$$\dot{\epsilon}_1 + \lambda\epsilon_1 = -\lambda J_0^{*2} \bar{\sigma}^2 e^{2i\omega t} \tag{41}$$

whose steady-state solution is

$$\epsilon_1 = \epsilon_1^* e^{2i\omega t} \tag{42}$$

where

$$\epsilon_1^* = -J_0^{*2} \bar{\sigma}^2 \mu / (\mu + 2i) \tag{43}$$

The steady-state solution of eq. (38) for e_1 [from eq. (39)] is

$$e_1 = e_1^* e^{2i\omega t} \tag{44}$$

where

$$e_1^* = J_0^{*2} \bar{\sigma}^2 / \mu (\mu + 2i) = -\epsilon_1^* / \mu^2 \tag{45}$$

We now introduce the nonlinear complex compliance J^* such that

$$\epsilon = J^* \sigma \tag{46}$$

Putting the above expressions for ϵ_0 , ϵ_1 , and e_1 into eq. (35) we solve for J^* in the following form:

$$\begin{aligned} J^* &= J' + iJ'' \\ J' &= J_0 + [\gamma_E - (\gamma_\eta / \mu^2)] J_1' \\ J'' &= J_0'' + [\gamma_E - (\gamma_\eta / \mu^2)] J_1'' \\ J_0' &= \mu^2 / [E_0(1 + \mu^2)] \\ J_0'' &= -\mu / [E_0(1 + \mu^2)] \\ J_1' &= u\bar{\sigma} \cos \omega t - v\bar{\sigma} \sin \omega t \\ J_1'' &= v\bar{\sigma} \cos \omega t + u\bar{\sigma} \sin \omega t \\ u &= \mu(5 - \mu^2) / [(\mu^2 + 4)(\mu^2 + 1)^2] \\ v &= -2\mu^3(1 - 2\mu^2) / [(\mu^2 + 4)(\mu^2 + 1)^2] \end{aligned} \tag{47}$$

For the linear Voigt model $\gamma_E = \gamma_\eta = 0$, and J^* reduces to the linear complex compliance $J_0^* = J_0' + iJ_0''$. The terms J_1' and J_1'' express first-order nonlinearity in the real and imaginary parts (respectively) of J^* . Note the form of J_1' and J_1'' ; they are given as explicit functions of t [depending on $\sigma(t)$] as well as μ .

We have constructed a first-order, nonlinear, one-dimensional theory of viscoelasticity based on an elementary perturbation scheme. The condition of first-order nonlinearity was applied to the nonlinear Maxwell and Voigt models. The response of these models to a sinusoidally applied load was expressed in terms of the nonlinear complex modulus for the Maxwell model (showing a nonlinear relaxation effect) and the nonlinear complex compliance for the Voigt model (showing a nonlinear creep effect).

References

1. Bland, D. R., *The Theory of Linear Viscoelasticity*, Pergamon Press, New York, 1960, p. 13.
2. For some other selected works on linear viscoelasticity the reader is referred to: T. Alfrey, *Mechanical Behavior of High Polymers*, Interscience, New York, 1948; W. N. Findley, *Creep and Relaxation of Plastics*, N. J. Hoff, Ed., reprinted from *High Temperature Effects in Aircraft Structures*, Pergamon Press, London, 1958; J. C. Jaeger, *Elasticity, Fracture and Flow*, Methuen, London, 1956; J. T. Bergen, Ed., *Viscosity, Phenomenological Aspects*, Academic Press, New York, 1960; H. Kolsky, *Stress Waves in Solids*, Oxford Univ. Press, Oxford 1953, Chaps. V and VI; B. Gross, *Mathematical Structure of the Theories of Viscoelasticity*, reprinted (in English) from *Rheologie*, No. 1190 Publications de l'Institut National de Technologie Bresil, 1953; E. H. Lee, *Quart. Appl. Math.*, **13**, 183 (1955); E. H. Lee and J. R. M. Radok, *Proc. 9th Intern. Congr. Appl. Mech.*, **5**, 321 (1957); D. R. Bland and E. H. Lee, *J. Appl. Phys.*, **26**, 1497 (1955); D. R. Bland and E. H. Lee, *J. Appl. Mech.*, **23**, 416 (1956); J. D. Ferry, *Viscoelastic Properties of Polymers*, Wiley, New York, 1961.

Résumé

On a établi une théorie du premier ordre, non-linéaire et unidimensionnelle pour la visco-élasticité, au moyen d'une technique de perturbation élémentaire. Elle est basée sur l'application de quelques hypothèses simples de la non-linéarité à des modèles non-linéaires de Maxwell et Voigt. La réponse du modèle de Maxwell à une tension sinusoïdale est régie par "un module complexe non-linéaire" dont la partie linéaire est une fonction de la tension appliquée et de la vitesse de tension, de même que de la fréquence externe et des paramètres internes ou du module. Ceci est un effet de relaxation non-linéaire. On obtient un effet de rétrécissement non-linéaire en décrivant la réponse non-linéaire du modèle de Voigt à une tension sinusoïdale appliquée dans des termes d'une concordance complexe non-linéaire.

Zusammenfassung

Unter Verwendung einer elementaren Störungsmethode wird eine nichtlineare ein-dimensionale Viskoelastizitätstheorie erster Ordnung entwickelt. Sie beruht auf der Anwendung gewisser einfacher Nichtlinearitätshypothesen auf einzelne nichtlineare Maxwell- und Voigt-Modelle. Das Verhalten des Maxwell-Modelles bei sinusförmig angelegter Spannung gehorcht einem "nichtlinearen komplexen Modul," dessen nicht-linearer Teil als Funktion sowohl von angewandeter Beanspruchung und Beanspruchungsgeschwindigkeit als auch von äusserer Frequenz und inneren oder Modell-Parametern gegeben ist. Das ist ein nichtlinearer Relaxationseffekt. Einen nichtlinearen Kriecheffekt erhält man, wenn man das nichtlineare Verhalten des Voigt-Modells bei sinusförmig angelegter Spannung in Form einer "nichtlinearen komplexen Nachgiebigkeit" beschreibt.

Received February 28, 1963

Nature of the Price-Alfrey q and ϵ Parameters

MARVIN CHARTON and ANTHONY J. CAPATO, *Department of Chemistry, Pratt Institute, Brooklyn, New York*

Synopsis

The equation, $\epsilon_X = m\sigma_X + c$, has been derived from the Price-Alfrey and Hammett equations. The σ_p constants give the best correlation. With multiple substituted monomers, the equation $\epsilon_{X,Z} = m(\sigma_X + \sigma_Z) + c$ has been found to be applicable. Thus the ϵ parameter is found to be a function of both inductive and resonance effects. The equation $q_X = n\sigma_X + d$ has been derived from the Price-Alfrey and Hammett equations. Correlations of q_X have been attempted with a number of substituent constants. The correlation, though generally best with σ_p and related constants, remains poor, even in series in which steric effects should be constant.

The Price-Alfrey equation¹⁻⁴ has been of great interest in the correlation of copolymerization reactivity ratios. The equation has recently been reexamined by Schwan and Price,⁵ and in its present form is written:

$$r_1 = \exp \left\{ -(q_1 - q_2)/RT \right\} \exp \left\{ -7.23 \times 10^{20} \epsilon_1(\epsilon_1 - \epsilon_2)/RT \right\} \quad (1)$$

$$r_2 = \exp \left\{ -(q_2 - q_1)/RT \right\} \exp \left\{ -7.23 \times 10^{20} \epsilon_2(\epsilon_2 - \epsilon_1)/RT \right\} \quad (2)$$

$$r_1 r_2 = \exp \left\{ -7.23 \times 10^{20} (\epsilon_1 - \epsilon_2)^2 / RT \right\} \quad (3)$$

These equations may be rewritten.

$$\log r_1 = - \frac{(q_1 - q_2)}{RT} - \frac{7.23 \times 10^{20}}{RT} \epsilon_1(\epsilon_1 - \epsilon_2) \quad (4)$$

$$= \log (k_{11}/k_{12})$$

$$\log r_2 = - \frac{(q_2 - q_1)}{RT} - \frac{7.23 \times 10^{20}}{RT} \epsilon_2(\epsilon_2 - \epsilon_1) \quad (5)$$

$$= \log (k_{22}/k_{21})$$

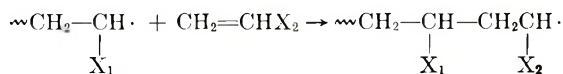
$$\log r_1 + \log r_2 = - \frac{7.23 \times 10^{20}}{RT} (\epsilon_1 - \epsilon_2)^2 \quad (6)$$

$$= \log (k_{11}/k_{12}) + \log (k_{22}/k_{21})$$

From transition state theory it is apparent that they are linear free energy relationships. They are related to the Hammett equation:⁶⁻⁸

$$Q_X = \rho\sigma_X + Q_H \quad (7)$$

Schwan and Price⁵ consider q to represent the "relative resonance stabilization conferred on the new radical" by some attached group, X_2 , and ϵ as the charge induced by X_1 or X_2 on either of the carbons forming the new carbon-carbon covalent bond in the transition state for the propagation step:



or



The Price-Alfrey ϵ Values

We have attempted to investigate the composition of the ϵ and q factors by attempting correlations with the various Hammett substituent constants by means of eq. (8):

$$\epsilon_X = m\sigma_X + c \quad (8)$$

Taft and Lewis⁹ have proposed σ_I constants which may be taken as a measure of purely permanent electrostatic effects, and σ_R constants which are considered to be a measure of resonance effects. They have proposed that the σ_m and σ_p constants are given by

$$\sigma_m = \sigma_I + (\sigma_R/3) \quad (9)$$

$$\sigma_p = \sigma_I + \sigma_R \quad (10)$$

We have correlated the ϵ values of Schwan and Price with σ_m , σ_p , and σ_I for $\text{XCH}=\text{CH}_2$ (1) and for $\text{XMeCH}=\text{CH}_2$ (2a, b). The ϵ values used in each series correlated are given in Table I. All correlations were made by the method of Jaffé.⁷ The σ_m and σ_p constants were taken from McDaniel and Brown,¹⁰ and from Jaffé when available. In some cases, they were estimated by a method which will be described elsewhere.²¹ The σ_I and σ_R values are those reported by Taft and Lewis^{9,11} when available. In some cases σ_I values were calculated from $\sigma_I = \sigma^*/6.23$ or from $\sigma_I = (3\sigma_m - \sigma_p)/2$,⁹ σ_R^+ and σ_R^- values were obtained from $\sigma_R^+ = \sigma^+ - \sigma_I$, $\sigma_R^+ = \sigma^- - \sigma_I$. σ_R^\pm values are equal to σ_R^+ values for electron-donor substituents by resonance and to σ_R^- values for substituents which are electron acceptors by resonance. The results of the correlations are given in Table II. For $\text{XMeCH}=\text{CH}_2$, correlations were made which included (2a) and excluded (2b) the value of ϵ for $\text{X} = \text{OAc}$. In both cases, best correlation was obtained with the σ_p values, as is shown by the values of the correlation coefficients (r) and the standard deviations (s). In the case of the $\text{CH}_2=\text{CHX}$, the best correlation was also with the σ_p values. While Schwan and Price had found that ϵ values for 3- and 4-substituted styrenes were linearly related to the Hammett substituent constants, the groups so situated were of course not directly attached to the double bond undergoing reaction, or to the radical carbon atom (the carbon atom bearing the unpaired electron)

TABLE I
Values of ϵ Used in Correlations

Series no.	ViX	Series ^a							
		X = OEt $\epsilon = -0.50$ X = Cl $\epsilon = -0.04$ X = CN $\epsilon = 0.34$	SMe -0.43 Br 0.03 CO ₂ H 0.28	Bu -0.4 CO ₂ Me 0.18	Ph -0.24 Ac 0.19	OAc -0.11 MeSO 0.28	CO ₂ - -0.06 MeSO ₂ 0.33		
2a	1-MeVnX	X = Me $\epsilon = -0.42$ X = CN $\epsilon = 0.23$	Ph -0.37 OAc -0.22	CHO -0.10	Ac -0.08	CO ₂ Me 0.07	CO ₂ H 0.22		
2b	1-MeVnX	X = Me $\epsilon = -0.42$	Ph -0.37	CHO -0.10	Ac -0.08	CO ₂ Me 0.07	CO ₂ H 0.22		
3	cis-2-XVnY	X, Y = Ph, Ph $\epsilon = -0.14$	Cl, Cl 0.32	CO ₂ Et, CO ₂ Et 0.40	CO ₂ Me, CO ₂ Me 0.42	CO ₂ Me 0.48	CO ₂ H 0.48		
4	trans-2-XVnY	X, Y = Ph, Ph $\epsilon = -0.27$ X, Y = CO ₂ Et, CO ₂ Et $\epsilon = 0.41$	OEt, CO ₂ Et 0.10 CO ₂ Et, CO ₂ H 0.45	Br, OEt 0.11	Me, CO ₂ H 0.3	Cl, Cl 0.35	CN, CN 0.54		
5	1-XVnY	X ₁ Y = Ph, Ph $\epsilon = -0.6$	Me, Me -0.42	Cl, Cl 0.11	CO ₂ Me, Cl 0.38	Ph, OAc -0.20	CN, CN 0.76		

^a Vi = vinyl, 1-Vn = vinylidene, 2-Vn = vinylene.

TABLE II
 Results of Correlation of q with σ

Series no. ^a	Slopes ^b			Correlation coefficient r	Standard deviation s	Intercept c	No. points in correlation n	
	m_m	m_p	m_I					
1	1.00			0.784	0.189	-0.303	14	
			0.915		0.943	0.101		-0.237
				0.769	0.569	0.251		-0.248
2a	0.948			0.817	0.154	-0.373	8	
			0.787		0.883	0.126		-0.339
2b	1.02			0.731	0.182	-0.353	7	
			0.784	0.937	0.887	0.132		-0.362
3	0.887			0.901	0.124	-0.320	5	
				1.12	0.857	0.147		-0.364
4	0.647			0.934	0.103	-0.222	9	
			0.592	0.664	0.952	0.0882		-0.0700
5	0.981			0.695	0.208	-0.0945	6	
			0.460	0.513	0.813	0.157		-0.122
				0.858	0.139	0.0205		
				0.609	0.214	-0.503		
				0.931	0.208	-0.501		
				0.943	0.190	-0.328		
				0.892	0.259	-0.560		

^a Numbers refer to Table I.

^b Slopes m_m , m_p , m_I for correlation with σ_m , σ_p , σ_I , respectively.

but rather to a benzene ring which remained intact throughout the course of the reaction. Furukawa and Tsuruta¹² have plotted the Price-Alfrey ϵ values against σ constants and find a linear relationship. From eq. (8) it is apparent that ϵ is a function of both resonance and electrostatic effects. The results obtained are not entirely unexpected. It has been shown¹³⁻¹⁶ that the reactions of *trans*-1,2-vinylene reaction series, where X is some substituent and Y a reaction site, are correlated with the Hammett equation by means of the σ_p constants. In the propagation step, reaction of the monomer is occurring at the C₁, the atom which bears the Y group in the *trans*-vinylene reaction series. Bamford and co-workers¹⁷ have proposed a parameter which describes the polarity of radicals. This parameter has been shown to be linearly related to the σ_p values. These results justify the assumption of Price and Alfrey that the effect of a group on monomer reactivity is equal to its effect on radical reactivity.

To determine whether the relation between ϵ and σ was additive for disubstituted compounds, correlations with eq. (11) were made.

$$\epsilon_{X,Y} = m\Sigma \sigma + c = m(\sigma_X + \sigma_Y) + c \quad (11)$$

The data used and results obtained are again given in Tables I and II, respectively. The series studied were the *cis*-vinylene (3), *trans*-vinylene (4), and vinylidene, $\text{XYC} = \text{CH}_2$ (5). While in all three series best correlation was obtained with the σ_p values, the correlation obtained with σ_m

was significantly better than before. Each carbon atom of the double bond in the vinylene series is vinylidene with respect to one of the substituents and vinylene with respect to the other. It has been reported that vinylidene reaction series are best correlated by the σ_m values.¹⁸ Thus the improvement in correlation with σ_m might be expected for the vinylene series (3) and (4). The improved correlation with σ_m in the vinylidene series is unexpected.

The results suggest that the equation,

$$\epsilon_{X,Y} = m_m \sigma_{mX} + m_p \sigma_{pY} + c \quad (12)$$

would give improved results for reaction of the monomer at the carbon atom to which X is attached. The uncertainties in the available ϵ values suggested that the use of eq. (12) would be premature at the present time.

To rationalize our results, we have derived an equation analogous to eq. (6) from the Hammett equation. From eq. (7), where Q is $\log k$,

$$\log k_{11} = \rho_1 \sigma_1 + \log k_{10} \quad (13)$$

where k_{10} represents the rate of reaction of $\sim \cdot$ with the monomer for which X = H. Thus,

$$\log k_{12} = \rho_1 \sigma_2 + \log k_{10} \quad (14)$$

and

$$\log (k_{11}/k_{12}) = \rho_1 (\sigma_1 - \sigma_2) \quad (15)$$

Similarly,

$$\log (k_{22}/k_{21}) = \rho_2 (\sigma_2 - \sigma_1) = -\rho_2 (\sigma_1 - \sigma_2) \quad (16)$$

Then

$$\log (k_{11}/k_{12}) + \log (k_{22}/k_{21}) = (\rho_1 - \rho_2) (\sigma_1 - \sigma_2) \quad (17)$$

We assume

$$\rho_n = \alpha \sigma_n + \beta \quad (18)$$

Then

$$(\rho_1 - \rho_2) = \alpha (\sigma_1 - \sigma_2) \quad (19)$$

and

$$\log (k_{11}/k_{12}) + \log (k_{22}/k_{21}) = \alpha (\sigma_1 - \sigma_2)^2 \quad (20)$$

which is analogous to eq. (6). Combining eqs. (6) and (20) gives;

$$-\frac{7.23 \times 10^{20}}{RT} (\epsilon_1 - \epsilon_2)^2 = \alpha (\sigma_1 - \sigma_2)^2 \quad (21)$$

or

$$(\epsilon_1 - \epsilon_2)^2 = \gamma^2 (\sigma_1 - \sigma_2)^2 \quad (22)$$

TABLE III
Values of q Used in Correlations

Series No.	Series	Series															
		X = Ph	Ac	CN	CO ₂ -Na ⁺	CO ₂ Me	CO ₂ H	MeS	MeSO	MeSO ₂	Cl	OAc	Bu	Br	OEt		
1a	ViN	$q = -3.10$	-2.8	-2.7	-2.7	-2.5	-2.5	-2.5	-1.6	-1.2	-1.1	-0.72	-0.4	-0.3	-0.1		
1b		X = Ph	CN	CO ₂ -Na ⁺	CO ₂ Me	CO ₂ H	MeS	Cl	Br								
2a	1-MeVnX	$q = -3.10$	-2.7	-2.7	-2.5	-2.5	-2.5	-1.1	-0.3								
2b		X = Me	CHO	CO ₂ H	Ac	CN	Ph	CO ₂ Me	OAc								
3	3-XC ₆ H ₄ Vi	$q = -0.6$	-3.6	-3	-3.20	-3	Ph	CO ₂ Me									
4	4-XC ₆ H ₄ Vi	$q = -3.0$	-3.6	-3	-3.0	-2.9	H										
		X = Me	Cl	Br	NO ₂												
		X = Me ₂ N	MeO	Me	I	Cl	Br	CN	NO ₂	H							
		$q = -3.3$	-3.3	-3.1	-3.1	-2.9	-3.1	-3.4	-3.5	-3.10							

TABLE IV
Results of Correlation of q with σ

Series No. ^a	Series	Slopes ^b				Correlation coefficient r	Standard deviation s	Intercept d	No. points in series n
		n_p	n_l	n_R	n_{R+}				
1a		-1.02	1.05	-3.28		0.290	1.07	-1.47	14
1b		0.123				0.216	1.09	-2.06	
						0.644	0.851	-1.91	
						0.032	1.03	-2.21	8

Then taking the square root, we have

$$(\epsilon_1 - \epsilon_2) = \gamma(\sigma_1 - \sigma_2) \quad (23)$$

or

$$\Delta\epsilon = \gamma\Delta\sigma \quad (24)$$

Choosing H as the standard substituent, we have

$$\epsilon_X = \gamma\sigma_X + \epsilon_H - \gamma\sigma_H \quad (25)$$

and as $\sigma_H = 0$, by definition,

$$\epsilon_X = \gamma\sigma_X + \epsilon_H \quad (26)$$

which is equivalent to eq. (8).

The Price-Alfrey q Values

We have also considered the nature of the q factor. Values of q reported by Schwan and Price⁵ were correlated with σ_p , σ_I , and σ_R , and in some series with σ_R^+ , σ_R^- , and σ_R^\pm by means of the equation,

$$q_X = n\sigma_X + d \quad (27)$$

The q values used are given in Table III; the results of the correlations are given in Table IV. The results did not show any definite clear-cut correlation with σ_I , σ_R , or σ_p . There may be a rather ill-defined relationship with σ_R in the $\text{CH}_2=\text{CHX}$ (1a) and $\text{CH}_2=\text{CMeX}$ series. In the short series of $\text{CH}_2=\text{CHX}$ (1b), where a comparison of all of the above σ constants is possible, best correlation was obtained with σ_R , σ_R^- , and σ_R^\pm , but in all three cases correlation was very poor. To determine the possible significance of steric effects on q , the q values for 3- and 4-substituted styrenes were correlated with σ_m for the 3- and σ_p for the 4-substituted series (3) and (4) respectively, and with σ_R , σ_R^+ , σ_R^- , and σ_R^\pm for both series. As in the 3- or 4-substituted styrenes, the substituent is far removed from the reaction site; thus, the only possible steric effect, that due to the benzene ring, will be constant throughout the styrene series. While best correlation is still obtained with σ_R , it is so poor as to be essentially meaningless. It should be noted, however, that after this work was completed, Kanabata, Tsuruta, and Furukawa¹⁹ reported that a plot of $\log Q$ values for 3- and 4-substituted styrenes against the approximate σ values was linear. Thus the significance of the q parameter in terms of electrostatic and resonance effects is obscure.

In an attempt to relate the q parameter to the Hammett ρ and σ parameters, we may obtain from eqs. (15) and (18):

$$\log(k_{11}/k_{12}) = (\alpha\sigma_1 + \beta)(\sigma_1 - \sigma_2) \quad (28)$$

Equating eqs. (28) and (4) results in

$$-\frac{(q_2 - q_1)}{RT} - \frac{7.23 \times 10^{20}}{RT} \epsilon_1(\epsilon_1 - \epsilon_2) = \alpha\sigma_1(\sigma_1 - \sigma_2) + \beta(\sigma_1 - \sigma_2) \quad (29)$$

Substituting eq. (23) in eq. (29) gives

$$-\frac{(q_2 - q_1)}{RT} - \frac{7.23 \times 10^{20}}{RT} \epsilon_1\gamma(\sigma_1 - \sigma_2) = \alpha\sigma_1(\sigma_1 - \sigma_2) + \beta(\sigma_1 - \sigma_2) \quad (30)$$

Writing eq. (26) for ϵ_1 and substituting in eq. (30) gives

$$-\frac{(q_1 - q_2)}{RT} - \frac{7.23 \times 10^{20}}{RT} (\gamma\sigma_1 + \epsilon_H)\gamma(\sigma_1 - \sigma_2) = \alpha\sigma_1(\sigma_1 - \sigma_2) + \beta(\sigma_1 - \sigma_2) \quad (31)$$

Then

$$-\frac{(q_1 - q_2)}{RT} = \frac{7.23 \times 10^{20}}{RT} \gamma^2\sigma_1(\sigma_1 - \sigma_2) + \gamma\epsilon_H(\sigma_1 - \sigma_2) + \alpha\sigma_1(\sigma_1 - \sigma_2) + \beta(\sigma_1 - \sigma_2) \quad (32)$$

$$\gamma^2 = \alpha RT / -7.23 \times 10^{20} \quad (33)$$

Then,

$$-(q_1 - q_2)/RT = -\alpha\sigma_1(\sigma_1 - \sigma_2) + \alpha\sigma_1(\sigma_1 - \sigma_2) + (\beta + \gamma\epsilon_H)(\sigma_1 - \sigma_2) \quad (34)$$

Which simplifies to

$$(q_1 - q_2) = (\beta + \gamma\epsilon_H)(-RT)(\sigma_1 - \sigma_2) \quad (35)$$

or

$$\Delta q = \delta\Delta\sigma \quad (36)$$

Choosing, as before, H as the standard substituent, gives

$$q_X = \delta\sigma_X + q_H \quad (37)$$

This equation, which is equivalent to eq. (22), does not appear to correlate the q values at all well.

In the derivation of eqs. (26) and (36), eq. (18) was assumed valid. We have been able to show empirically that eq. (18) is applicable to ρ values for the ionization in water of substituted benzoic acids bearing a constant 3- or 4-substituent and also of substituted acetic acids bearing a constant substituent. Equation (18) was also derived from the relationship

$$Q_X = \rho_1\sigma_X + \rho_2\sigma_Z + \rho_{12}\sigma_X\sigma_Z \quad (38)$$

proposed by Miller²⁰ for the treatment of unsymmetrically disubstituted reaction series. The demonstration of the validity of eq. (18) will be reported in detail elsewhere.²¹

References

1. Alfrey, T., and C. C. Price, *J. Polymer Sci.*, **2**, 101 (1947).
2. Price, C. C., *J. Polymer Sci.*, **3**, 752 (1948).
3. Alfrey, T., J. J. Bohrer, and H. Mark, *Copolymerization*, Interscience, New York, 1952, p. 116.
4. Mayo, F. R., and C. Walling, *Chem. Revs.*, **46**, 191 (1950).
5. Schwan, T. C., and C. C. Price, *J. Polymer Sci.*, **40**, 457 (1959).
6. Hammett, L. P., *Physical Organic Chemistry*, McGraw-Hill, New York, 1940.
7. Jaffé, H. H., *Chem. Revs.*, **53**, 191 (1953).
8. Taft, R. W., Jr., in *Steric Effects in Organic Chemistry*, M. S. Newman, Ed., Wiley, New York, 1956.
9. Taft, R. W., Jr., and I. C. Lewis, *J. Am. Chem. Soc.*, **80**, 2436 (1958).
10. McDaniel, D. H., and H. C. Brown, *J. Org. Chem.*, **23**, 420 (1958).
11. Taft, R. W., Jr., *J. Phys. Chem.*, **64**, 1805 (1960).
12. Furukawa, J., and T. Tsuruta, *J. Polymer Sci.*, **36**, 275 (1959).
13. Charton, M., and H. Meislich, *J. Am. Chem. Soc.*, **80**, 5940 (1958).
14. Hine, J., and W. C. Bailey, *J. Am. Chem. Soc.*, **81**, 2075 (1959).
15. Hine, J., and W. C. Bailey, *J. Org. Chem.*, **26**, 2098 (1961).
16. de la Mare, P. B. D., *J. Chem. Soc.*, **1960**, 3823.
17. Bamford, C. H., A. D. Jenkins, and R. Johnston, *Trans. Faraday Soc.*, **55**, 418 (1959).
18. Charton, M., paper presented at 140th Meeting American Chemical Society, Chicago, September 1961; *Abstracts*, p. 91Q.
19. Kawabata, N., T. Tsuruta, and J. Furukawa, *Makromol. Chem.*, **51**, 70 (1962).
20. Miller, S. I., *J. Am. Chem. Soc.*, **81**, 161 (1959).
21. Charton, M., unpublished results.

Zusammenfassung

Die Gleichung $\epsilon_X = m\sigma_X + c$ wurde aus der Price-Alfrey- und der Hammett-Gleichung abgeleitet. Die σ_p -Konstanten liefern die beste Korrelation. Es wurde gefunden, dass auf mehrfach substituierte Monomere die Gleichung $\epsilon_{X,Z} = m(\sigma_X + \sigma_Z) + c$ anwendbar ist, dass also ϵ eine Funktion sowohl von induktiven als auch von Resonanzeffekten ist. Die Gleichung $q_X = n\sigma_X + d$ wurde aus der Price-Alfrey- und der Hammett-Gleichung abgeleitet. Eine Korrelation von q_X mit einer Anzahl von Substituentenkonstanten wurde versucht. Obwohl die Korrelation im allgemeinen mit den σ_p -Werten und verwandten Grössen am besten ist, lässt sie sogar in Reihen mit konstanten sterischen Effekten sehr zu wünschen übrig.

Résumé

L'équation $\epsilon_X = m\sigma_X + c$ a été tirée des équations de Price-Alfrey et de Hammett. Les constantes σ_p donnent la meilleure corrélation. Avec de nombreux monomères substitués on a trouvé que $\epsilon_{X,Z} = m(\sigma_X + \sigma_Z) + c$ était applicable. On trouve donc que le paramètre ϵ est une fonction des 2 effets: inductif et de résonance. L'équation $q_X = n\sigma_X + d$ a été tirée des équations de Price-Alfrey et de Hammett. Des corrélations de q_X ont été essayées avec un nombre de substituants constants. La meilleure corrélation, cependant générale entre σ_p et les constantes citées, reste déficiente même dans les séries dans lesquelles les effets stériques seraient constants.

Received February 11, 1963

Rapid Characterization of Ion-Exchange Resins by NMR

J. P. de VILLIERS and J. R. PARRISH, *National Chemical Research Laboratory, South African Council for Scientific and Industrial Research, Pretoria, South Africa*

Synopsis

The proton magnetic resonance spectrum of an ion-exchange resin is often characteristic of that type of resin. It has been shown that the internal molality of a strongly acidic or strongly basic polystyrene resin can be determined from its NMR spectrum.

The use of ion-exchange resins for various separations and analytical procedures requires that the resins be fully characterized with respect to swelling and capacity if such work is to be reproducible. Usually only the nominal percentage of divinylbenzene in the styrene-divinylbenzene copolymers is reported. Because this is an approximate figure, different batches of resin of the same nominal crosslinking may differ in swelling and hence in selectivity and reaction rate. Kressman and Millar¹ have recommended that crosslinked polystyrene resins should no longer be characterized by their nominal, but by their true divinylbenzene content, obtained from the specific water regains of the final resins. While this suggestion would lead to improved precision, its value is limited by the fact that the graphs published by these authors for the conversion of regains to true divinylbenzene contents are not applicable to all polystyrene resins. Mikes² has shown that resins with the same divinylbenzene content can be prepared with various degrees of swelling if controlled amounts of inert solvents are added to the original mixture of monomers used in the polymerization. Variations of this procedure have been patented and are used for the production of macroporous resins in which the divinylbenzene content cannot be related directly to the swelling.

In order to avoid confusion and to include a wider range of resins, we recommend that an ion-exchange resin should be characterized not by its divinylbenzene content, but by its ion exchange capacity (expressed as milliequivalents/gram of dry resin) and water regain (grams water/gram dry resin). The molality of the internal solution, or the reciprocally related specific water regain, can be calculated from these two quantities which are determined by the usual methods. Conversely, the capacity and water regain can be calculated from the molality and the percentage of

water in the resin, and for some resins these values can be obtained from the NMR spectra.

Sulfonated Polystyrene Resins

Gordon³ has shown that aqueous suspensions of sulfonated polystyrene resins in the hydrogen form give particularly well defined proton magnetic resonance spectra, and that the observed shift of the internal water peak may be used to calculate the molality of the internal solution. Unfortunately the values he obtained in this way were compared with values obtained by conventional methods on different batches of resin with the same nominal divinylbenzene content, and the agreement was only approximate.

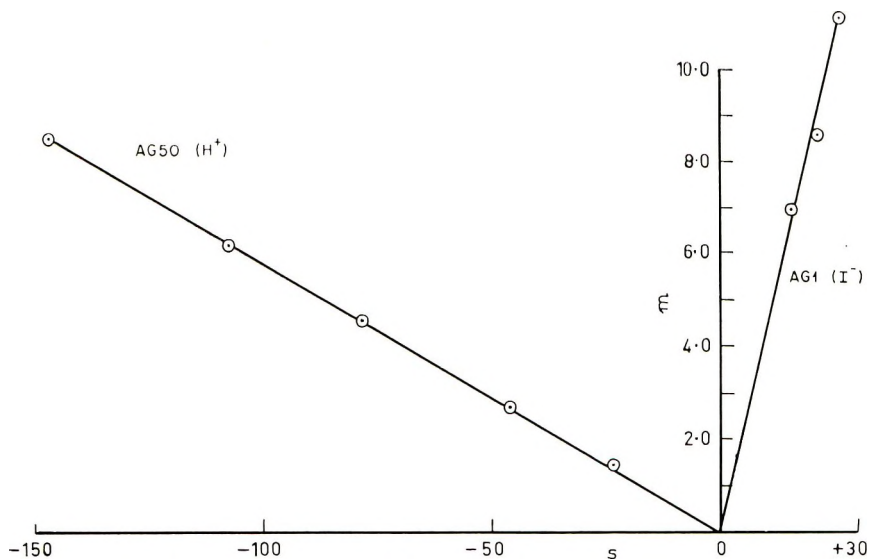


Fig. 1. Chemical shifts s (in cycles/sec.) plotted against internal molalities, m , for resins AG50 (H^+) and AG1 (I^-).

In this laboratory the molalities obtained by conventional methods were plotted against the chemical shifts of the same samples of resin (Fig. 1). The points fell on a straight line, and accurate molalities can be obtained from measured chemical shifts by means of this graph. It is interesting to note that the plot of shift against the quantity p , which has been used previously⁴ to evaluate the NMR spectra of strong acids, gave a slight curve instead of a straight line. In our opinion the use of p , the fraction of protons present in hydronium ions, is fundamentally incorrect since the hydronium ions influence the structure of the surrounding water, and the shift due to the protons in the water is not constant. The molalities of the hydrogen counterions reported by Gordon³ were apparently obtained from a relation involving p , and therefore they are probably not exact.

The water content of sulfonated polystyrene resins can also be obtained from the NMR spectra. With the use of the Varian A60 NMR spectrometer, the procedure is as follows. The resin is allowed to settle to a height of about 5 cm. in the NMR sample tube, previously filled with water. After the spectrum has been recorded the same tube is filled with approximately $10^{-4}M$ $MnSO_4$ solution (to give a water peak of comparable height at the same instrument settings), and the water peak is recorded on the same paper. The areas under the three peaks are found by integration, and the packing density of the resin in the tube is given by

$$1 - \text{external water/water only}$$

The volume percentage, P , of water in the resin is given by

$$P = \frac{\text{internal water} \times 100}{\text{water only} \times \text{packing density}}$$

If the densities of the wet resins are known, these figures can be converted to water regains, and the resins can thus be characterized rapidly. Table I shows that the percentage of water by weight obtained in this way is generally within 2% of the value obtained by centrifuging⁵ and drying. The greatest source of error in this method appears to be in the measurement of the areas under the peaks, and the error is largest for the most swollen resin where the distance between the internal and external water peaks is the smallest. If part of the internal water were tightly bound to the sulfonic groups of the resin matrix and consequently gave no signal, the water content obtained from the NMR spectrum would be less than the true water content, and the observed difference could be used to calculate the number of molecules of bound water per sulfonic group. The differences actually found are probably due to experimental errors, but the figures indicate that not more than one molecule of water could be bound to a sulfonic group in this way. For purposes of characterization, it is unnecessary to allow for bound water or for the extra protons present in the sulfonic acid groups.

The required densities of the wet resins can be measured quickly by a flotation method,⁶ using kerosene and dibromoethane. The values obtained were in close agreement with those obtained by the usual method employing S. G. bottles (Table II). However, in the case of sulfonated

TABLE I

Resin	Water content from NMR, %	Water content by drying, %
AG50 × 2	74.0	78.3
AG50 × 4	64.6	66.5
AG50 × 8	54.0	53.0
AG50 × 12	44.2	45.6
AG50 × 16	36.0	37.0

polystyrene resins in the hydrogen form, the measurement is unnecessary because densities can be calculated from the values of P , the percentage of water by volume. The relation established⁵ between the swollen volume V , and the weight of water absorbed, W , by 1 g. of the dry hydrogen form of the resin may be written

$$V = W + 0.63 \quad (1)$$

Since the density, D , of the swollen hydrogen form is given by $D = (W + 1)/V$, and since $P = 100W/V$, from eq. (1):

$$D = 1.59 - 0.0059P \quad (2)$$

Densities calculated from eq. (2) using the values of P obtained from the NMR spectra are compared with measured densities in Table II. The use of calculated densities does not appreciably alter the values obtained in Table I.

TABLE II

Resin	Calculated density, g./cc.	Density by S.G. bottle, g./cc.	Density by flotation, g./cc.
AG50 \times 2	1.12	1.09	1.09
AG50 \times 4	1.16	1.15	1.15
AG50 \times 8	1.20	1.21	1.21
AG50 \times 12	1.27	1.25	1.26
AG50 \times 16	1.32	1.30	1.34

Other Cation-Exchange Resins

Sulfonated polystyrene resins of the macroporous type had NMR spectra indistinguishable from those of the ordinary type. The commercial resin Amberlite 200 exhibited a broad internal water peak (16 cycles/sec. at half height), but a macroporous resin made according to a published method⁷ had a sharp internal water peak (Fig. 2). The water content of these

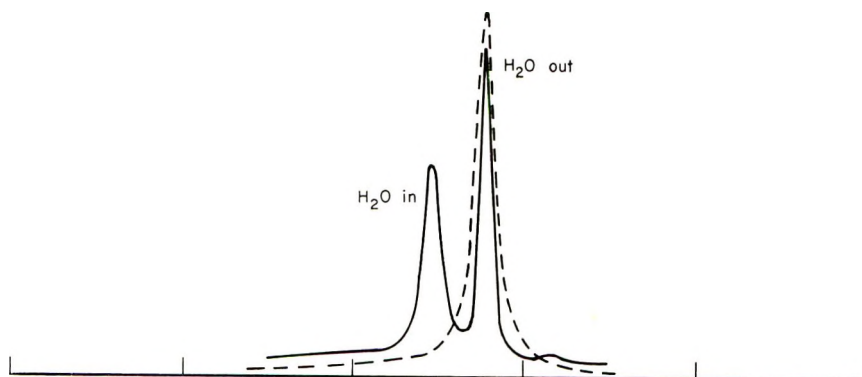


Fig. 2. Proton magnetic resonance spectra of (—) macroporous sulfonated polystyrene resin (H^+) in water; (---) water only.

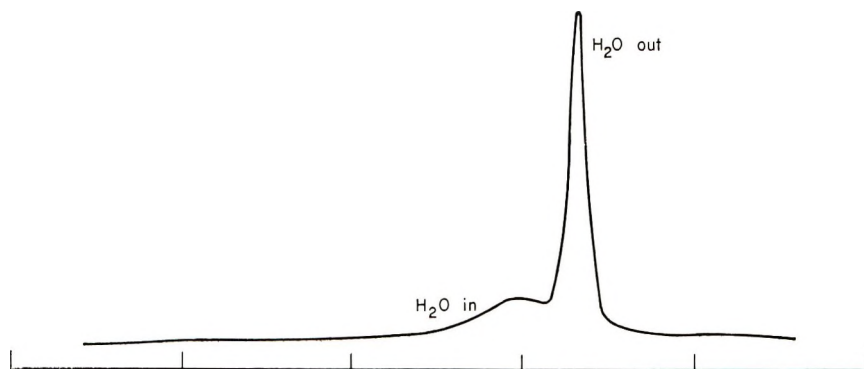


Fig. 3. Proton magnetic resonance spectrum of phenolsulfonic acid resin (H^+).

resins obtained from their NMR spectra was in agreement with the true water content, which proved that even the water in large pores was recorded as internal water.

Although, under our experimental conditions, the matrix of a resin gave no signal and no peaks at all were shown by resins in deuterium oxide, it was still possible to distinguish sulfonic acid resins made by a phenol-aldehyde condensation from those made from crosslinked polystyrene. The spectra of resins of the phenol-aldehyde type had far broader and lower internal water peaks. The extreme case was the spectrum of Amberlite IR-100H, which showed only one peak, that due to external water. The internal band had apparently been broadened to the point of disappearance. Gordon³ has suggested that unusually broad internal bands may be caused by the presence of paramagnetic counterions, but in this case washing the resin with dilute hydrochloric acid did not alter the spectrum. However, spectrographic examination of the ash revealed the presence of iron and manganese which could not be detected in the polystyrene resins. Quantitative chemical analysis showed 95 ppm of iron and a trace of manganese in the washed, dried resin. These quantities appeared too low to account for the disappearance of the internal peak, and to verify this, three phenolic resins were made in the laboratory from iron-free chemicals. The first resin was prepared by an alkaline condensation of potassium *p*-phenolsulfonate, resorcinol, and formaldehyde, and its NMR spectrum showed only a broad shoulder instead of an internal band. The second resin was made with sulfonic groups in the side chain,⁸ and a very similar spectrum was obtained. The third resin, which was expected to have the most regular structure of the three, was made by the acid condensation of *p*-phenolsulfonic acid with formaldehyde.⁹ Its spectrum (Fig. 3) showed the least broadened internal band. Thus the extreme broadening of the internal water band in the case of phenolic resins was apparently caused by inhomogeneity within the resin particles.

In general, the shape of the particles did not affect the width of the internal band and did not alter the chemical shift. This was shown by crushing

large beads of the polystyrene resin IR-120H until no spherical particles remained. The spectrum was unaltered save for the broadening of the external water peak as the particles became smaller. The magnetic susceptibility of the swollen phenolic resins was not appreciably different from that of water for there was virtually no shift of the external water peak due to the presence of the resin.

Polystyrene resins containing phosphonous and phosphonic acid groups (Bio-rex 62 and 63) showed very broad bands for both internal and external water, but here the shift of the external water band due to the presence of the resins was 11 cycles/sec.

Weakly acidic resins, such as crosslinked poly(methacrylic acid), would not be expected to show an internal water peak when they are in the hydrogen form because the degree of dissociation is very small. This has been confirmed³ for Amberlite IRC-50. However, the spectra of the sodium and potassium forms of this resin showed unresolved broadening due to slight hydrolysis of the salts, whereas the tetramethylammonium form showed a separate internal peak. This peak at lower field was caused by the presence of an appreciable concentration of hydroxyl ions in the internal solution and this can be explained by the fact that tetramethylammonium hydroxide is a stronger base than either sodium or potassium hydroxide. A very similar spectrum was given by the ion-retardation resin AG11A8 in the zwitterion form. This resin contains a polymeric acrylic acid neutralized by a crosslinked polymeric benzyltrimethylammonium hydroxide, and the salt hydrolyzes to produce hydroxyl ions in the internal solution.

Anion-Exchange Resins

Weakly basic resins did not show an internal band even when they were in the salt form, and the same applied to chelating resins such as Dowex A-1. This behavior was probably caused by incomplete dissociation and hydrogen bonding.

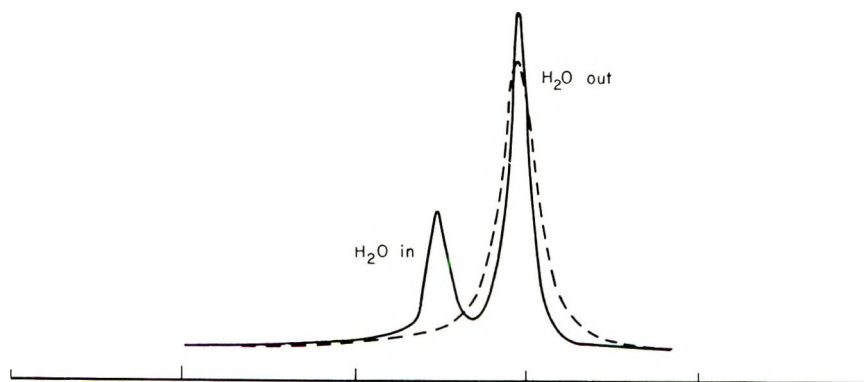


Fig. 4. Proton magnetic resonance spectra of (—) IRA-400 (OH⁻) resin in water; (--) water only.

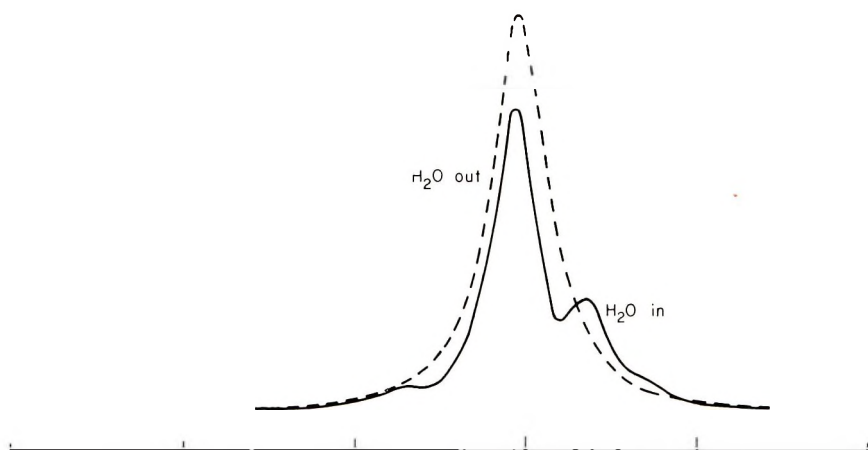


Fig. 5. Proton magnetic resonance spectra of (—) IRA-400 (I⁻) resin in water; (--) water only.

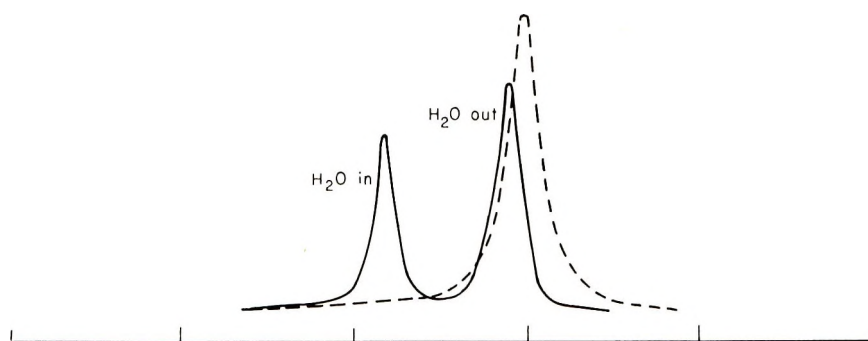


Fig. 6. Proton magnetic resonance spectra of (—) AG2 × 8 (OH⁻) resin in water; (--) water only.

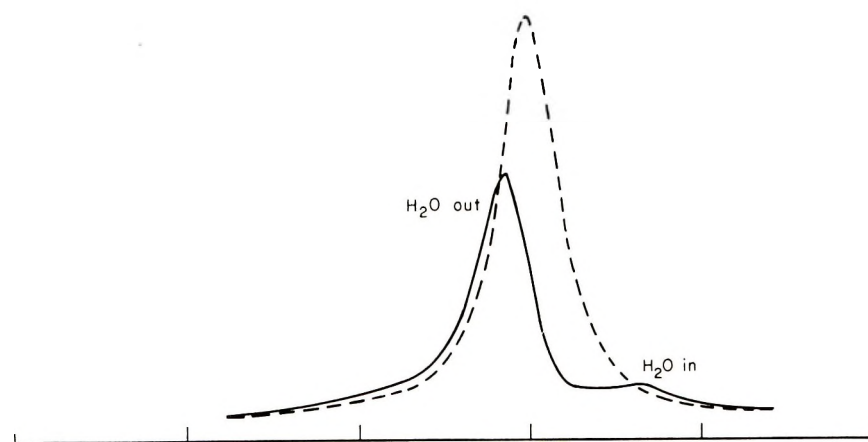


Fig. 7. Proton magnetic resonance spectra at (—) AG2 × 8 (I⁻) resin in water; (--) water only.

The spectra of the hydroxide and iodide forms of the strongly basic resin IRA-400 and of the slightly less strongly basic resin AG2X8 are reproduced in Figures 4-7. Resin IRA-400 contains polymeric trimethylbenzylammonium ions, whereas AG2X8 contains polymeric hydroxyethyl-dimethylbenzylammonium ions. For the hydroxide forms (Figs. 4 and 6) there is little difference between the internal water peaks of the two resins, but for the iodide forms (Figs. 5 and 7) resin AG2X8 shows a much broader internal band. Since the hydroxide form of AG2X8 shows a sharp internal peak, the presence of hydroxyl groups in the phenolsulfonic acid resins could not have been responsible for the extreme broadening of their internal bands.

The swelling and capacity of a strongly basic resin is usually measured on the chloride form, but the chemical shift caused by the chloride ion is small and no resolution of the water peaks is possible when the resin is in this form. The hydroxide form shows the greatest chemical shift, but strongly basic resins are unstable in this form, and they blacken when dried even at room temperature. The hydroxide form can also absorb carbon dioxide from the air, and it therefore seems undesirable to express swelling and capacity on this form of the resins. The fluoride form showed a peak due to internal water at lower field, whereas the iodide form showed a peak at higher field. It was found that for a given resin the shift was greater for the iodide form, and the shifts for the iodide form have therefore been plotted against the internal molalities (Fig. 1). The water content of these resins can also be obtained from their NMR spectra, but the wet densities have to be found experimentally. The matrix is not as constant in these resins as in the sulfonated polystyrene resins, because chloromethylation may produce additional crosslinking, and the extent of the reaction is more difficult to control than in the case of sulfonation. Thus the sulfonated resins studied in this work had very similar weight capacities (5.0-5.3 meq./g.). However, resin AG1X10 had a capacity of 2.40 meq./g. instead of 3.0-3.2 meq./g. which was found for the iodide forms of the other anion-exchange resins. Although the weight capacity of the X10 resin was lower than that of the X8, and in spite of the difference in nominal divinylbenzene content, the two resins had the same water content (Table III).

The chemical shift of the X10 resin corresponded to a molality of 9.3 on the graph in Figure 1, but the measured molality was 8.34. This dis-

TABLE III

Resin	Water content from NMR, %	True water content, %
×2	33.0	31.4
AG1 × 8	23.6	21.6
AG1 × 10	22.9	22.4
IRA-400	27.1	26.2

crepancy could be explained by the fact that the magnetic susceptibility of the X10 resin was out of line with that of the other resins in the series. In the spectrum of this resin the shift of the external water peak, due to the presence of the resin, differed by -2 cycles/sec. from the corresponding shifts for the X8 and the IRA-400 resins. When a correction was made for this difference, a molality of 8.4 was obtained from the graph.

When the iodide forms of anion-exchange resins were used, the points for the X8 and the X2 resins were not widely separated on the graph (Fig. 1), and the accuracy of the NMR method for determining molalities was limited. The greater shifts and sharper peaks produced by the hydroxide forms could be used by plotting these shifts against the molalities of the resins in the chloride form. The graph was linear and it could be used to characterize resins from the NMR spectra, but the X10 resin gave an incorrect result, and in this case no correction could be applied. The water content of resins in the chloride form had to be obtained by drying.

Other Applications

In aqueous solutions of electrolytes the shift of the water peak increases with the charge and the reciprocal of the radius of the cation, and is also affected by the anion.¹⁰ The effects of anion and cation are difficult to separate, but it should be possible to use suitable ion-exchange resins to determine the absolute values of the shifts caused by the counterions, as the fixed ions are unlikely to affect the shift appreciably.

Conclusions

Although the NMR spectra of many ion-exchange resins cannot be used for quantitative measurements, valuable information can be obtained about the nature of the resins. In the case of sulfonated polystyrene resins in the hydrogen form, capacities and water regains can be determined very rapidly from the spectra. Similar measurements can be made on the iodide or hydroxide forms of strongly basic anion-exchange resins, but with diminished accuracy.

The authors thank Mr. H. Schutte for the spectrographic analysis.

References

1. Kressman, T. R. E., and J. R. Millar, *Chem. Ind. (London)*, **1961**, 1833.
2. Mikes, J. A., *J. Polymer Sci.*, **30**, 615 (1958).
3. Gordon, J. E., *J. Phys. Chem.*, **66**, 1150 (1962); *Chem. Ind. (London)*, **1962**, 267.
4. Gutowsky, H. S., and A. Saika, *J. Chem. Phys.*, **21**, 1688 (1953).
5. Pepper, K. W., D. Reichenberg, and D. K. Hale, *J. Chem. Soc.*, **1952**, 3129.
6. Moore, W. R., and R. P. Sheldon, *Polymer*, **2**, 315 (1961).
7. Kressman, T. R. E., and J. R. Millar, S. Afr. Pat. 59/2589 (1959).
8. Wassenegger, H., Ger. Pat. 968,543 (1958).
9. Jakubovic, A. O., *J. Chem. Soc.*, **1960**, 4820.
10. Shcherbakov, V. A., *Zh. Struktur. Khim.* **2**, 484 (1961); *J. Structural Chem.*, **2**, 452 (1961).

Résumé

Le spectre de résonance magnétique protonique d'une résine échangeuse d'ions est souvent particulier à celle-ci. On a démontré la possibilité d'évaluer la molalité intérieure d'une résine polystyrénique très acide ou très alcaline d'après son spectre RMN.

Zusammenfassung

Das Protonenresonanzspektrum eines Ionenaustauscher-Harzes ist oft charakteristisch für den Typ des Harzes. Es wird gezeigt, dass die Molalität im Innern eines stark sauren oder stark basischen Polystyrol-Harzes aus dem KMR-Spektrum bestimmt werden kann.

Received February 11, 1963

Random Degradation of Chain Polymers Accompanied by Partial Dissolution of the Degraded Material*

D. MEJZLER, *Institute for Fibres and Forest Products Research, State of Israel, Ministry of Commerce and Industry, Jerusalem, Israel*

Synopsis

Some processes of random degradation of chain polymers in suspension are accompanied by the dissolution of the part of the degraded material having the shortest chain lengths. The molecular weight determinations are then usually made not on the total degraded material, but only on its undissolved part. It is shown that if any two of the following three experimentally determinable values are known: (1) weight fraction of undissolved degraded material, (2) number-average DP of undissolved degraded material, (3) weight-average DP of undissolved degraded material, the following parameters may be calculated: (1) the third experimental value; (2) the extent of degradation of the total degraded material and, therefore, the true values of the number-average and weight-average DP of the total material; (3) the maximum chain length of the degraded material in solution; (4) the number-average and the weight-average DP of the dissolved part of the degraded material; (5) the respective number fractions of the dissolved and undissolved chains in the degraded material. The calculations are carried out for the two conventional models of random degradation, that of Kuhn and that of Montroll-Simha. For the former model, simple approximate formulas are also given, which yield solutions with a satisfactory accuracy.

Introduction

Cases are known in polymer chemistry, where random degradation of a chain polymer is accompanied by partial dissolution of the degraded material, fragments of the lowest molecular weight passing into solution. Oxidative and acid degradation of cellulose, starch, and starch components may serve as an example.

In such cases, as a rule, certain parameters, including the distribution of molecular weights, can be determined on the undissolved part of the degraded material, such determinations cannot be carried out on the dissolved fractions, owing to great experimental difficulties.

It is the purpose of this paper to show that, as far as chain polymers are concerned, full information on the state of the dissolved fraction may be obtained from the experimental data available for the undissolved part alone; the assumptions on which the demonstration is based have been accepted in polymer chemistry for a long time.

* This work forms part of the research being carried out at this Institute under grant number FG-IS-101-58 issued by the Agricultural Research Service, United States Department of Agriculture.

The fundamental assumption is that the dissolved fraction consists of the shortest chains present. In other words, we shall assume that if the dissolved part of the material contains molecules of chain length n , the undissolved part will not contain molecules of a chain length shorter than n .

The degraded chain polymer may be regarded as a system $\{n_k\}$ composed of n_1 monomeric, n_2 dimeric, . . . , n_k k -meric, . . . molecules.

Let n be the degree of polymerization (DP) of the longest molecules still in solution. If p is the weight fraction of the undissolved material (calculated on the total amount of material), then

$$p = \left(\sum_{k=n+1}^{\infty} kn_k \right) / \sum_{k=1}^{\infty} kn_k \quad (1)$$

and the weight fraction of the dissolved material q will be

$$q = 1 - p = \left(\sum_{k=1}^n kn_k \right) / \sum_{k=1}^{\infty} kn_k \quad (2)$$

We also assume a perfectly random degradation from the initial DP distribution $\{n_k^0\}$ to the final distribution $\{n_k\}$. The latter is then known to be fully determined by the initial state $\{n_k^0\}$ and by the extent of degradation α defined by

$$\alpha = \frac{\text{number of bonds broken}}{\text{total number of bonds}}$$

or

$$\alpha = 1 - \left[\sum_{k=1}^{\infty} (k-1)n_k \right] / \sum_{k=1}^{\infty} (k-1)n_k^0 \quad (3)$$

We shall discuss here two mathematical models of random degradation: (1) that of W. Kuhn,¹ where the starting, undegraded, material consists of one single infinitely long molecule; (2) that of Montroll and Sinha,² where the undegraded starting material consists of an infinitely large number of chains, all having the same DP equal to N_0 (For a discussion of these models see also Mejzler et al.³)

The extent of degradation α may be calculated from the experimentally determined average DP of the degraded product. This may be either the number-average DP N , defined as

$$N = \left(\sum_{k=1}^{\infty} kn_k \right) / \sum_{k=1}^{\infty} n_k \quad (4)$$

or the weight-average DP N_w defined as

$$N_w = \left(\sum_{k=1}^{\infty} k^2 n_k \right) / \sum_{k=1}^{\infty} kn_k \quad (5)$$

(Other average DP's, such as Z -average or viscosity-average DP, will not be considered here.)

When a part of the degraded material has passed into solution, the number-average and/or weight-average DP is determined on the undissolved part only and not on the entire material. That is, the experimentally determined values M and M_w are

$$M = \left(\sum_{k=n+1}^{\infty} kn_k \right) / \sum_{k=n+1}^{\infty} n_k$$

and

$$M_w = \left(\sum_{k=n+1}^{\infty} k^2 n_k \right) / \sum_{k=n+1}^{\infty} kn_k \quad (6)$$

Obviously, if the proportion of the material dissolved is considerable, M and M_w will differ from N and N_w , respectively. In that case, if M and M_w are used in the formulas commonly employed instead of N and N_w , considerable errors are to be expected.

The values of p , M , and M_w may be determined by experiment. Our purpose is to show that if any two of these three parameters are known, the following may be calculated: (a) the third of these three parameters; (b) the extent of degradation α , and hence the average DP's N and N_w ; (c) the degree of polymerization n of the longest molecules still in solution; (d) the number-average DP, m , and the weight-average DP, m_w , of the dissolved material. These magnitudes are defined by the formulas

$$m = \left(\sum_{k=1}^n kn_k \right) / \sum_{k=1}^n n_k$$

and

$$m_w = \left(\sum_{k=1}^n k^2 n_k \right) / \sum_{k=1}^n kn_k \quad (7)$$

(e) the number fraction of the undissolved chains A and the number fraction of the dissolved chains a , defined as

$$A = \left(\sum_{k=n+1}^{\infty} n_k \right) / \sum_{k=1}^{\infty} n_k$$

and

$$a = 1 - A = \left(\sum_{k=1}^n n_k \right) / \sum_{k=1}^{\infty} n_k \quad (8)$$

It is easily seen that the parameters determined above are connected by following relations:

$$M = pN/A \quad (9)$$

$$m = qN/a \quad (10)$$

$$pM_w + qm_w = N_w \quad (11)$$

In the considerations which follow, we shall use the following well known elementary identities, which are valid for any real value of x and any positive integer n :

$$(1 - x) \sum_{k=1}^{\infty} x^{k-1} = 1 - x^n \tag{12}$$

$$(1 - x)^2 \sum_{k=1}^n kx^{k-1} = 1 - (n + 1)x^n + nx^{n+1} \tag{13}$$

$$(1 - x)^3 \sum_{k=1}^n k^2x^{k-1} = 1 + x - (n + 1)^2x^n + (2n^2 + 2n - 1)x^{n+1} - n^2x^{n+2} \tag{14}$$

$$(1 - x)^4 \sum_{k=1}^n k^3x^{k-1} = 1 + 4x + x^2 - (n + 1)^3x^n + (3n^2 + 6n^2 - 4)x^{n+1} - (3n^3 + 3n^2 - 3n + 1)x^{n+2} + n^3x^{n+3} \tag{15}$$

Kuhn's Model

According to Kuhn's model, the following equalities are valid:^{1,3}

$$n_k / \sum_{k=1}^{\infty} n_k = \alpha(1 - \alpha)^{k-1} \tag{16}$$

$$kn_k / \sum_{k=1}^{\infty} kn_k = k\alpha^2(1 - \alpha)^{k-1} \tag{17}$$

It is also known⁴ that

$$N = 1/\alpha \tag{18}$$

$$N_w = (2 - \alpha)/\alpha = 2N - 1 \tag{19}$$

We shall immediately see that $p, q, M, M_w, n, m_w, A,$ and a may be expressed as functions of α and n only. According to eqs. (2) and (17),

$$q = \alpha^2 \sum_{k=1}^n k(1 - \alpha)^{k-1} \tag{20}$$

Using the identity (13) and substituting $x = 1 - \alpha$ we obtain

$$q = 1 - (1 - \alpha)^n(1 + n\alpha) \tag{21}$$

hence

$$p = (1 - \alpha)^n(1 + n\alpha) \tag{22}$$

In view of eqs. (8) and (16), we get

$$a = \alpha \sum_{k=1}^{\infty} (1 - \alpha)^{k-1} \tag{23}$$

Hence, in view of the identity (12)

$$a = 1 - (1 - \alpha)^n \tag{24}$$

and therefore

$$A = (1 - \alpha)^n \quad (25)$$

In view of the relations (9) and (10), the parameters M and m may be expressed by using eqs. (18) and (21)–(25). In particular, we obtain

$$M = 1/\alpha + n \quad (26)$$

In view of eq. (2) the parameter m_w defined as in eq. (7), may be written as

$$m_w = (1/q) \left(\sum_{k=1}^n k^2 n_k \right) / \sum_{k=1}^{\infty} k n_k \quad (27)$$

From eq. (17) we get

$$m_w = (\alpha^2/q) \sum_{k=1}^{\infty} k^2 (1 - \alpha)^{k-1} \quad (28)$$

Hence, using the identity (14) and equality (21) we obtain

$$m_w = \frac{2 - \alpha - (1 - \alpha)^n [(1 + \alpha n)^2 + 1 - \alpha]}{\alpha [1 - (1 - \alpha)^n (1 + \alpha n)]} \quad (29)$$

and therefore, from eqs. (11), (19), (21) and (22) we get

$$M_w = \frac{(1 + \alpha n)^2 + 1 - \alpha}{\alpha(1 + \alpha n)} \quad (30)$$

If any two of the three parameters p , M , and M_w are known, two suitable equations from eqs. (22), (26), and (30) may be chosen, which, on being simultaneously solved, will yield the values of α and n . The latter values will permit us to find the remaining parameters.

We may distinguish between three cases, depending on which two parameters have been experimentally determined.

Case I. Let us first consider the mathematically simplest case, when the values of M and M_w are known. By eliminating n from eqs. (26) and (30), we obtain the following equation for α

$$\alpha^2(M_w M - M^2) + \alpha - 1 = 0 \quad (31)$$

Hence, since $M_w > M$ we get

$$\alpha = (\sqrt{1 + 4M(M_w - M)} - 1) / 2M(M_w - M) \quad (32)$$

and, in view of eq. (26), we get

$$n = M - 1/\alpha \quad (33)$$

It follows from the definition of M and N that $M > N$. Hence, in view of eq. (18),

$$\alpha > 1/M \quad (34)$$

Since M and M_w are large numbers, we may obtain from eq. (32) an approximate expression for α :

$$\alpha \doteq 1/\sqrt{M(M_w - M)} \quad (35)$$

The value of p may now be calculated from eq. (22) by using eqs. (32) and (33). Since p is easy to determine experimentally, the agreement between the experimental and calculated value of p may be used to check the validity of the fundamental assumptions.

Case II. Let us now consider the second case, when the values of p and M are determined experimentally. Let us take eqs. (22) and (26). By eliminating n we obtain for α the equation

$$p = \alpha M (1 - \alpha)^{M-1/\alpha} \quad (36)$$

By applying suitable approximations, the value of α may be calculated with any desired accuracy, and n may then be calculated by using eq. (33).

However, eq. (36) is quite complex, since α cannot be explicitly expressed. We shall now show that in view of the fact that the value of α is in practice always a small number, eq. (36) may be replaced by another equation, which is only approximate but which is much simpler. It is known that

$$\lim_{\alpha \rightarrow 0} (1 - \alpha)^{1/\alpha} = e^{-1} \quad (37)$$

where e is the base of natural logarithms. Equation (36) may be written in the form

$$p = \alpha M [(1 - \alpha)^{1/\alpha}]^{M\alpha - 1} \quad (38)$$

Using eq. (37), if α is sufficiently small, we obtain the approximate equation

$$p = \bar{\alpha} M \exp \{1 - \bar{\alpha} M\} \quad (39)$$

Let us denote $\bar{\alpha} M = t$. Equation (39) may then be written as

$$p = t \exp \{1 - t\} \quad (40)$$

This equation for an unknown t is much simpler than eq. (36) for an unknown α . From the known value of p we may calculate t , and therefore α by

$$\alpha \doteq \bar{\alpha} = t/M \quad (41)$$

Owing to the fact that eq. (40) contains p as the single parameter, a table such as Table I may be constructed, giving the values of t as function of p .

Example 1. Let $p = 0.75$, $M = 100$; eq. (36) now becomes

$$0.75 = 100\alpha(1 - \alpha)^{100-1/\alpha} \quad (42)$$

A rather elaborate calculation gives the solution $\alpha = 0.01942$. As against that, we obtain from Table I that $t = 1.961$ for $p = 0.075$. Hence we obtain the approximate solution $\bar{\alpha} = 0.01961$. We shall prove in what follows that $\bar{\alpha}$ is always greater than α . The relative error

$$\delta = (\bar{\alpha} - \alpha)/\alpha = \Delta\alpha/\alpha \quad (43)$$

TABLE I

p	t
1.000	1.000
0.999	1.045
0.998	1.065
0.997	1.080
0.996	1.092
0.995	1.103
0.990	1.149
0.980	1.215
0.970	1.268
0.960	1.314
0.950	1.355
0.940	1.394
0.930	1.431
0.920	1.466
0.910	1.499
0.900	1.532
0.890	1.563
0.880	1.594
0.870	1.624
0.860	1.654
0.850	1.683
0.840	1.712
0.830	1.741
0.820	1.769
0.810	1.797
0.800	1.824
0.790	1.852
0.780	1.879
0.770	1.907
0.760	1.934
0.750	1.961
0.700	2.097
0.650	2.235

caused by using eq. (39) instead of the exact eq. [eq. (36)] is $\delta = 0.00019/0.01942 < 1\%$. A rigorous proof is given in the Appendix that this relative error is bounded from above by $\bar{\alpha}/2$ and does not exceed 1% , when the experimental values of the parameters p and M satisfy the inequalities $p \geq 0.75$, $M \geq 100$.

Case III. Let us now consider the last case, when p and M_w are the values found experimentally. We use eqs. (22) and (30). Equation (30) may be written as

$$\alpha^2 n^2 + \alpha n(2 - \alpha M_w) + (2 - \alpha - \alpha M_w) = 0 \quad (44)$$

it is obvious that $M_w > N_w$; hence, in view of eq. (19),

$$M_w > (2 - \alpha)/\alpha$$

We therefore obtain from eq. (44)

$$n = (\alpha M_w - 2 + \sqrt{\alpha^2 M_w^2 - 4 + 4\alpha})/2\alpha \quad (45)$$

If this expression is substituted in eq. (22), an equation is obtained with α as the sole unknown, which is, however, too complex to be directly used. We shall show that the method previously employed is also applicable to the present case.

In view of eq. (26), eq. (30) may be written as

$$M_w = [(M\alpha)^2 + 1 - \alpha]/\alpha(M\alpha) \quad (46)$$

But, as has been seen, the product $(M\alpha)$ is determined with a good approximation solely by the value of p . This means that the equality (41) is valid to a good approximation. Therefore, the following equation is also valid to a good approximation

$$M_w \doteq (t^2 + 1 - \alpha)/(\alpha t) \quad (47)$$

hence

$$\alpha \doteq (t^2 + 1)/(tM_w + 1) \quad (48)$$

If the value of α is known, n may be calculated by

$$n \doteq (t - 1)\alpha \quad (49)$$

This formula follows from eqs. (33) and (41).

Example 2. Let $p = 0.87$, $M_w = 110$. We obtain from Table I that $t = 1.624$ for $p = 0.87$. Hence, by eq. (48), we obtain the approximate solution $\alpha = 0.0202$ and, by eq. (49), $n = 30.9$. The remaining parameters can now be calculated from the equations developed above.

We shall prove in the Appendix that in the present case, too, the relative error in the value of α , caused by using the approximate equation, eq. (48), does not exceed 1% when the values of p and M_w satisfy the inequalities $p \geq 0.75$, $M_w \geq 100$.

The Model of Montroll and Simha

For the Montroll and Simha model the following equalities are valid:^{2,3}

$$\frac{n_k}{\sum_{k=1}^{N_0} n_k} = \begin{cases} \frac{\alpha(1-\alpha)^{k-1}}{1+\alpha(N_0-1)} [2 + \alpha(N_0-1) - \alpha k] & \text{if } 1 \leq k \leq N_0 - 1 \\ \frac{(1-\alpha)^{N_0-1}}{1+\alpha(N_0-1)} & \text{if } k = N_0 \end{cases} \quad (50)$$

$$\frac{k n_k}{\sum_{k=1}^{N_0} k n_k} = \begin{cases} \frac{k}{N_0} \alpha(1-\alpha)^{k-1} [1 + \alpha(N_0-1) - \alpha k] & \text{if } 1 \leq k \leq N_0 - 1 \\ (1-\alpha)^{N_0-1} & \text{if } k = N_0 \end{cases} \quad (51)$$

where N_0 denotes the initial chain length, which is considered to be known (e.g., in cellulose).

It is known that^{2,5}

$$N = N_0/[1 + \alpha(N_0 - 1)] \quad (52)$$

$$N_w = \frac{\alpha^2 N_0 + 2(1-\alpha)[(1-\alpha)^{N_0} + \alpha N_0 - 1]}{\alpha^2 N_0} \quad (53)$$

Using the formulas (50) and (51) and the identities (12)–(15), all the parameters defined in the introduction may be expressed in terms of α and n only, as has been done for Kuhn's model. According to eqs. (2) and (51)

$$q = \frac{\alpha}{N_0} [2 + \alpha(N_0 - 1)] \sum_{k=1}^n k(1-\alpha)^{k-1} - \frac{\alpha^2}{N_0} \sum_{k=1}^n k^2(1-\alpha)^{k-1} \quad (54)$$

and hence, by using eqs. (13) and (14),

$$q = 1 - (1-\alpha)^n [1 + \alpha n - \alpha n(n+1)/N_0] \quad (55)$$

also

$$p = (1-\alpha)^n [1 + \alpha n - \alpha n(n+1)/N_0] \quad (56)$$

According to eqs. (8) and (50)

$$a = \frac{\alpha[2 + \alpha(N_0 - 1)]}{1 + \alpha(N_0 - 1)} \sum_{k=1}^n (1-\alpha)^{k-1} - \frac{\alpha^2}{1 + \alpha(N_0 - 1)} \sum_{k=1}^n k(1-\alpha)^{k-1} \quad (57)$$

and hence, by using eqs. (12) and (13),

$$a = 1 - (1-\alpha)^n [1 - \alpha n/(\alpha N_0 + 1 - \alpha)] \quad (58)$$

also

$$A = (1-\alpha)^n [1 - \alpha n/(\alpha N_0 + 1 - \alpha)] \quad (59)$$

Using the relation (9) and the expressions developed above, we obtain

$$M = [N_0 + \alpha n(N_0 - n - 1)]/[1 + \alpha(N_0 - n - 1)] \tag{60}$$

The expression for m may be obtained from eq. (10). From eqs. (27) and (51) we obtain

$$m_w = \frac{\alpha}{q \cdot N_0} \left\{ [2 + \alpha(N_0 - 1)] \sum_{k=1}^n k^2(1 - \alpha)^{k-1} - \alpha \sum_{k=1}^n k^3(1 - \alpha)^{k-1} \right\} \tag{61}$$

Using the identities (14) and (15), we obtain an expression for m_w as a function of α and n only, which is, however, complicated and will not be written here; from that expression and relation (11) we obtain

$$M_w = \frac{2(1 - \alpha)^{N_0+1}}{\alpha^2 N_0 p} + \frac{(\alpha N_0 - 1)(2 - \alpha + 2n\alpha + \alpha^2 n^2) + \alpha + \alpha^2 n - \alpha^3 n^3 - \alpha^3 n^2}{\alpha^2 [N_0(1 + \alpha n) - \alpha n(n + 1)]} \tag{62}$$

m_w may be now calculated from eqs. (11) and (62).

Just as for the previous model, three separate cases may be distinguished and α and n calculated by solving a suitable pair of simultaneous equations. These equations are much more complex, and no simplified method of calculation seems available, as was the case for the previous model. However, in any particular instance, the expressions can be simplified by neglecting certain terms. Since, for large values of N_0 , the two models are practically identical, the formulas developed for Kuhn's model may also be used for the present model in such cases.

It has been assumed in the above considerations, that the value of N_0 is known. If all three values, viz., p , M , and M_w have been experimentally determined, the value of N_0 may be calculated by using the three simultaneous eqs. (56), (60), and (62).

Appendix

We shall now estimate the relative error in the value of α involved by using the approximate formulas (41) and (48).

We shall first deal with the case when the value of α is calculated from the experimental values of p and M . It is known⁶ that for any positive integer n the following inequalities exist:

$$(1 + 1/n)^n < e < (1 + 1/n)^{n+1} \tag{63}$$

where e is the basis of natural logarithms. Hence it may be deduced that

$$1 < \frac{M\alpha \exp \{-M\alpha + 1\}}{M\alpha(1 - \alpha)^{M-1/\alpha}} < [1/(1 - \alpha)]^{M\alpha-1} \tag{64}$$

for every $\alpha(0 < \alpha < 1)$ and $M(M > 0)$.

Let α be the root of the exact eq. (36). According to the above inequality

$$M\alpha \exp \{-M\alpha + 1\} = p + \Delta p \quad (65)$$

where $\Delta p > 0$ and

$$1 < 1 + \Delta p/p < [1/(1 - \alpha)]^{M\alpha - 1} \quad (66)$$

The function $f(t) = t \exp \{1 - t\}$ is a monotonic decreasing function in the interval $(1, \infty)$, since its derivative is negative for $t > 1$. It follows that if $\bar{\alpha}$ is the root of the approximate eq. (39), $\bar{\alpha}$ is always greater than α . Let us denote $\bar{\alpha} = \alpha + \Delta\alpha$; then $\Delta\alpha > 0$ and

$$p = M(\alpha + \Delta\alpha) \exp \{1 - M\alpha - M\Delta\alpha\} \quad (67)$$

In view of eq. (65) we obtain

$$\frac{\exp \{M\Delta\alpha\}}{1 + \Delta\alpha/\alpha} = 1 + \Delta p/p \quad (68)$$

Hence, in view of inequality eq. (66) and of the inequality

$$\exp \{M\Delta\alpha\} > 1 + M\Delta\alpha \quad (69)$$

we obtain

$$\delta(M\alpha - E) < E - 1 \quad (70)$$

where δ is the relative error [eq. (43)] and E denotes the expression

$$E = [1/(1 - \alpha)]^{M\alpha - 1} = [1 + \alpha/(1 - \alpha)]^{M\alpha - 1} \quad (71)$$

Let us now estimate the value of E . To do this we have to lay down certain limitations as to the intervals within which p and M may vary. Let us first assume that

$$0.75 \leq p < 1 \quad (72)$$

This range is sufficiently wide for most practical purposes. It has been proved that $\bar{\alpha} > \alpha$ and hence also $\alpha M < \bar{\alpha} M = t$. But, as may be seen from Table I,

$$1 < t \leq 1.961 < 2 \quad (73)$$

in the entire interval (72). Therefore, in view of the inequality (34), if p satisfies (72), then

$$1 < M\alpha < 2 \quad (74)$$

whatever the value of M . Let us now assume that

$$M > 4 \quad (75)$$

then

$$0 < \alpha < 0.5$$

and

$$0 < \alpha/(1 - \alpha) < 1 \tag{76}$$

It is therefore legitimate to develop the expression (71) in a power series of $\alpha/(1 - \alpha)$:

$$E - 1 = \left[\frac{(M\alpha - 1)}{1} \right] \left(\frac{\alpha}{1 - \alpha} \right) + \left[\frac{(M\alpha - 1)(M\alpha - 2)}{1 \cdot 2} \right] \left(\frac{\alpha}{1 - \alpha} \right)^2 + \left[\frac{(M\alpha - 1)(M\alpha - 2)(M\alpha - 3)}{1 \cdot 2 \cdot 3} \right] \left(\frac{\alpha}{1 - \alpha} \right)^3 + \dots \tag{77}$$

By the inequality (74) the following inequality is valid for any positive integer n :

$$|(M\alpha - n)/n| < 1 \tag{78}$$

Because of (74) and (76), it follows that this series is an alternating series, the general term of which monotonically tends to zero. It follows that $(E - 1)$ is smaller than the sum of the three terms written above. These considerations bring us to the following estimate:

$$E < 1 + [\alpha(M\alpha - 1)]/[2(1 - \alpha)] \tag{79}$$

Hence, in view of inequality (76), *a fortiori* $E < M\alpha$. We may now deduce from the expression (70) that $\delta < (E - 1)/(M\alpha - E)$ and hence, by relation (79)

$$\delta < \alpha/(2 - 3\alpha) \tag{80}$$

since $\bar{\alpha} > \alpha$, also $\delta < \bar{\alpha}/(2 - 3\bar{\alpha})$. Since $2 \gg 3\bar{\alpha}$, we may deduce that the value of the relative error δ is bounded from above by $\bar{\alpha}/2$. This is true if the limitations (72) and (75) are accepted. But, in view of eqs. (41) and (73), $\bar{\alpha}/2 = t/(2M) < 1/M$. It follows that for any p and M which satisfy the conditions $0.75 \leq p < 1$, $M \geq 100$, the value of δ will not exceed 1%.

It follows from the numerical example that this estimate cannot be further improved to any significant extent.

Let us now consider the case where α is determined from the experimental values of p and M_w .

Denote

$$\bar{\alpha} = (t^2 + 1)/(tM_w + 1) \tag{81}$$

Let α be the root of the accurate equations. Then, in view of eq. (46),

$$\alpha = [(M\alpha)^2 + 1]/[(M\alpha)M_w + 1] \tag{82}$$

Hence, since $M\alpha < t$, $\bar{\alpha} > \alpha$. Let

$$\delta_w = (\bar{\alpha} - \alpha)/\alpha \tag{83}$$

It may be deduced from eqs. (81) and (82) that

$$\delta_w = \delta \frac{(M\alpha)^2}{(M\alpha)^2 + 1} \left\{ 1 - \frac{M_w - t}{M_w + 1} \right\} \quad (84)$$

where δ is determined by eq. (43).

However, if the condition (72) is satisfied, the relation (74) is valid and hence $(M\alpha)^2/[(M\alpha)^2 + 1] < 0.8$ and, in view of eq. (84), $\delta_w < 0.8\delta$.

Because of relation (80) and since $\bar{\alpha} > \alpha$,

$$\delta_w < (0.8\bar{\alpha})/(2 - 3\bar{\alpha}) \quad (85)$$

If, in addition to (72), we also require $M_w \geq 100$, then it follows from eq. (81) that $\bar{\alpha} < 0.0246$ and $\bar{\alpha}/(2 - 3\bar{\alpha}) < 0.0125$. From relation (85) we may deduce that for any p and M_w which satisfy the conditions $0.75 \leq p < 1$, $M_w \geq 100$, the relative error δ_w does not exceed 1%.

It may be pointed out in conclusion that the error introduced in the calculated values of the other parameters through the use of $\bar{\alpha}$ and/or $\bar{\alpha}$ will also be negligible, except for the value of m_w : it may be seen from eq. (11) that a small error in the value of α may cause a considerable error in the value of m_w , if q is very small.

The author is grateful to Dr. M. Lewin, Director of this Institute, for his valuable advice and continuing interest in this work.

References

1. Kuhn, W., *Ber.*, **63**, 1503 (1930).
2. Montroll, E. W., and R. Simha, *J. Chem. Phys.*, **8**, 721 (1940).
3. Mejzler, D., J. Schmorak, and M. Lewin, *J. Polymer Sci.*, **46**, 289 (1960).
4. Flory, P. J., *Principles of Polymer Chemistry*, Cornell Univ. Press, Ithaca, N. Y., 1953, p. 325.
5. Grassie, N., *Chemistry of High Polymer Degradation Processes*, Butterworths, London, 1956, p. 128.
6. Pólya, G., and G. Szegő, *Aufgaben und Lehrsätze aus der Analysis*, Part I, Springer, Berlin, 1925, p. 31.

Résumé

Certains processus de dégradation statistique de chaînes polymériques en suspension sont accompagnés par une dissolution de la partie du polymère possédant la chaîne la plus courte. Alors on préfère ne plus faire de déterminations de poids moléculaires sur le total du matériel dégradé, mais seulement sur la partie restée indissoute. On a trouvé que, si on connaît deux des valeurs expérimentales suivantes: (1) la fraction en poids du matériel dégradé *non-dissous* (2) poids moléculaire moyen en poids du matériel dégradé *non-dissous*, (3) poids moléculaire en nombre du matériel dégradé *non-dissous*, on peut dès lors calculer: (1) la troisième valeur expérimentale, (2) le degré de dégradation du matériel dégradé global, et par la suite les valeurs réelles des poids moléculaires moyens en nombre et en poids du matériel total, (3) la longueur maximum de la chaîne du matériel dégradé en solution, (4) le poids moléculaire moyen en nombre et en poids de la partie dissoute du matériel dégradé, (5) les fractions respectives en nombres des chaînes dissoutes et non-dissoutes, dans le matériel dégradé. On a fait des calculs sur les deux modèles conventionnels de dégradation statistique, c.à.d. celui de Kuhn et celui de Montroll-Simha. Pour le premier modèle on a trouvé des formules approximatives qui donnent des résultats avec que précision suffisante.

Zusammenfassung

Bei gewissen statistischen Abbauprozessen an Kettenpolymeren in Suspension geht ein Teil des abgebauten Materials, nämlich jener mit der geringsten Kettenlänge, in Lösung. Die Molekulargewichtsbestimmungen werden dann gewöhnlich nicht am gesamten abgebauten Material, sondern nur an dessen ungelösten Anteil ausgeführt. Es wird gezeigt, dass bei Kenntnis von zweien der folgenden drei experimentell bestimm- baren Grössen, nämlich: (1) Gewichtsbruch des ungelösten abgebauten Materials, (2) Zahlenmittel des Polymerisationsgrades (DP) des ungelösten abgebauten Materials und (3) Gewichtsmittel des Polymerisationsgrades (DP) des ungelösten abgebauten Materials, folgende Grössen berechnet werden können: (1) Die dritte experimentell bestimm- bare Grösse; (2) das Ausmass des Abbaues des gesamten abgebauten Materials und somit die wahren Werte des Zahlen- und des Gewichtsmittels von DP des gesamten Materials; (3) die maximale Kettenlänge des gelösten abgebauten Materials; (4) Zahlen- und Gewichtsmittel von DP des gelösten Anteils des abgebauten Materials; (5) Die Molenbrüche der gelösten bzw. ungelösten Ketten im abgebauten Material.—Die Berechnungen werden für die beiden üblichen Modelle des statistischen Abbaues, nämlich das von Kuhn und das von Montroll-Simha, ausgeführt. Für das erstere werden auch einfache Näherungsformeln angegeben, die Resultate von befriedigender Genauigkeit liefern.

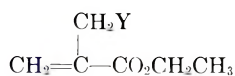
Received February 11, 1963

Polymerization Studies on Allylic Compounds. Part II*

SAMUEL F. REED and M. G. BALDWIN, *Rohm & Haas Company, Redstone Arsenal Research Division, Huntsville, Alabama*

Synopsis

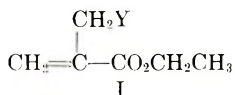
The free radical polymerization of a series of compounds having the general formula



in which Y was F, Cl, Br, I, NO₂, and CN has been studied. The compounds were found to vary markedly in polymerizability. An explanation is advanced in which it is postulated that chain transfer involving a substituent in the allylic position of the monomers is the controlling factor in determining their polymerization behavior.

INTRODUCTION

It has been demonstrated that certain allylic compounds, by which is meant compounds having the general formula CH₂=CX-CH₂Y, undergo rapid free radical polymerization while others do not polymerize. A number of workers have reported on the polymerization kinetics of allylic compounds in which X in the above general formula is hydrogen.¹⁻⁴ An earlier paper⁵ discussed the behavior of compounds having the general formula I where Y was OH, OCH₂CH₃, OCOCH₃, COOCH₂CH₃, and H.



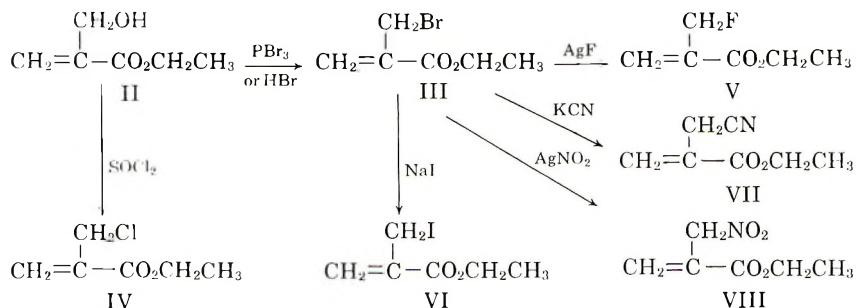
It was shown that the polymerizability of the allylic double bond is greatly enhanced by the X group (CO₂CH₂CH₃) but that the Y group among those studied has only secondary effects on the polymerizability.

It is the purpose of this paper to describe the polymerization behavior of a class of compounds which have the general formula I but in which Y is F, Cl, Br, I, NO₂, and CN. In this later series of compounds the Y group has a pronounced effect on the polymerizability.

* This work was performed under the sponsorship of the U. S. Army under Contract No. DA-01-021 ORD-11878.

MONOMER PREPARATION

The compounds employed in this study were prepared by the reactions of scheme (1). Both ethyl α -(bromomethyl)acrylate (III) and ethyl



α -(chloromethyl)acrylate (IV) have previously been prepared by the action of the appropriate halogen acid on diethyl bis(hydroxymethyl) malonate.⁶ It was found that bromination of ethyl α -(hydroxymethyl)acrylate (II) with phosphorus tribromide or dry gaseous hydrogen bromide gave III in yields of 68 and 85%, respectively. No tendency for the addition of hydrogen bromide to the double bond was observed even though attempts to effect addition were made. Ethyl α -(chloromethyl)acrylate (IV) was prepared in a yield of 91% by treating II with thionyl chloride.

The remaining α -(substituted methyl)acrylates were prepared from compound III. Ethyl α -(fluoromethyl)acrylate (V) was obtained by a metathetical reaction of III with silver fluoride in acetonitrile. The relatively low yield (45%) was due to the loss of V by its facile polymerization during distillation. This acrylate has been prepared^{7,8} previously and was found to polymerize readily.

The reaction of III with sodium iodide in acetone gave ethyl α -(iodomethyl)acrylate (VI) in a 80% yield. Welch⁹ prepared α -(iodomethyl)acrylic acid which was subsequently found to decompose readily to liberate free iodine. The ester (VI) showed little, if any, tendency towards decomposition at ambient temperature, but could not be successfully distilled without some decomposition occurring. Gas chromatography showed the crude product as obtained from the reaction to be at least 95% pure and it was used without further purification.

Ethyl α -(cyanomethyl)acrylate (VII) and α -(nitromethyl)acrylate (VIII) were prepared from reaction of ethyl α -(bromomethyl)acrylate (III) with potassium cyanide and silver nitrite, respectively. These two compounds had previously been prepared by Ferris.¹⁰

RESULTS

Ethyl α -(fluoromethyl)acrylate (V) polymerizes quite readily with AIBN initiation at 60°C. in ethyl acetate solution. Polymerization rate and intrinsic viscosity data are shown in Table I.

TABLE I
 Polymerization Data for Ethyl α -(Fluoromethyl)acrylate in Ethyl Acetate at 60°C.

[M], moles/l.	[AIBN], moles/l. $\times 10^3$	Initial polymerization rate $R_p \times 10^4$, moles/l./sec.	$R_p/[M][I]^{1/2}$ $\times 10^4$	$[\eta]$
3.87	6.16	2.58	8.49	0.83
3.92	3.13	1.85	8.45	1.00
3.88	0.632	0.743	7.64	1.36
3.88	0.333	0.615	8.71	1.63

The quantity of $R_p/[M][I]^{1/2}$, which is predicted by simple kinetic theory to be a characteristic constant for a monomer at a given temperature and for a given initiator, affords a means of comparison of monomers polymerized under identical conditions. From the data of Part I⁵ it is seen that (V) polymerizes more than twice as fast as methyl methacrylate ($R_p/[M][I]^{1/2} = 3.2 \times 10^{-4}$) and is only slightly slower than the corresponding hydroxy monomer (II), ($R_p/[M][I]^{1/2} = 10.94 \times 10^{-4}$), which was the fastest of the monomers studied. The above observations together with the fact that high viscosity polymer was obtained from V, indicate that neither normal chain transfer nor degradative chain transfer is important in its polymerization.

Polymerization of ethyl α -(chloromethyl)acrylate (IV) and ethyl α -(cyanomethyl)acrylate (VII) under the conditions described in Table I was too slow for accurate study, so bulk polymerization at 60°C. was observed dilatometrically. The data are shown in Table II.

TABLE II
 Polymerization Data for Ethyl α -(Chloromethyl)acrylate (IV) and
 α -(Cyanomethyl)acrylate (VII) at 60°C.

Monomer	[M], moles/l.	[AIBN], moles/l.	$R_p/[M][I]^{1/2}$ $\times 10^5$	η_{sp}/C
IV	7.30	0.031	4.93	0.13
VII	7.31	0.028	1.22	0.10

Heating the bromo, iodo, and nitro derivatives (III, VI, and VIII, respectively) with 1% AIBN at 70°C. for 24 hr. failed to cause a detectable viscosity increase, and dilatometric runs such as that described above for the chloro compound indicated no polymerization. Rather, there was observed an apparent reaction between the monomers and the mercury used as the confining fluid in the dilatometer. A precipitate formed at the interface of the monomer and mercury.

Copolymerization with Methyl Methacrylate

The effect of several of the monomers on the polymerization of methyl methacrylate was investigated with respect to polymerization rate and

polymer viscosity. In the cases of the fluoromethyl and chloromethyl monomers, the polymers were isolated after 10% conversion and analyzed for halogen content. There were found 31% of the fluoro monomer and 18% of the chloro monomer, respectively, in the copolymers. In each of the copolymerization experiments benzene was the solvent and the monomer and initiator concentrations were: methyl methacrylate, 4.7 moles/l.; α -(substituted methyl)acrylate, 1.0 moles/l.; and AIBN, 1.0×10^{-3} moles/l. The approximate copolymerization rate was calculated from dilatometric data on the assumption that each of the comonomers shrinks the same amount as methyl methacrylate during polymerization. Any error introduced by this assumption is small.⁵ The data are shown in Table III.

TABLE III
Copolymerization of α -(Substituted Methyl) Acrylates with Methyl Methacrylate at 60°C.

Comonomer number	Y substituent in comonomer	Approximate polymerization rate, %/min.	η_{sp}/C
		0.126 ^a	1.45 ^a
V	F	0.209	1.52
IV	Cl	0.115	0.31
VII	CN	0.126	0.51
III	Br	0.118	0.023
VIII	NO ₂	0.011	Very low

^a Homopolymerization of methyl methacrylate under the above conditions.

From Table III it is seen that the fluoro derivative increases both the overall rate of the polymerization and the molecular weight of the polymer produced, whereas, the chloro, cyano, and bromo derivatives have little effect on the rate but decrease the molecular weight markedly. The nitro derivative on the other hand greatly reduces both the polymerization rate and polymer viscosity.

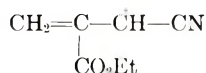
DISCUSSION

The marked differences in free radical polymerization behavior of the compounds studied in this work can be explained in terms of chain transfer with monomer and the stability of the radicals produced in the chain transfer. The frequency of occurrence of chain transfer for a given monomer depends on the energy required to remove the atom or group of atoms involved in the transfer. From a consideration of the bond energies of the compounds in question it is likely that transfer involves the allylic Y groups in all cases except the fluoro and cyano derivatives. In these, allylic hydrogen abstraction should be the dominating transfer mechanism.

Bond energies are not available for the compounds studied in this work, but the appropriate values for propene and the simple allyl halides, except

the fluoride, are known. These are listed in Table IV together with the C—Y bond energies for each of the CH₃—Y compounds. The latter data provide a means of ranking the C—Y bond strengths in a given series of compounds.

It appears from the data in Table IV that Cl, Br, I, and NO₂ would be removed in chain transfer in preference to H, but that F and CN would not be so removed. In the case of the fluoro derivative, appreciable chain transfer was not observed, which is in accordance with the behavior of the methacrylate monomers. The sluggish polymerization of the cyano compound must be due to resonance stabilization of the radical



by the cyano group.

TABLE IV
Bond Dissociation Energies for C—Y Bonds^a

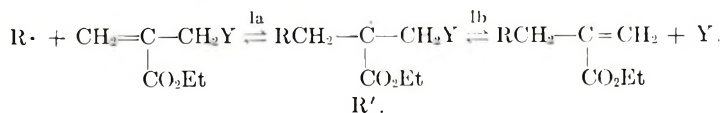
Compound	Y	D, kcal./mole
CH ₃ =CH—CH ₂ —Y	H	77 ^b
	Cl	60
	Br	46
	I	36
CH ₃ —Y	H	101
	F	107
	Cl	80
	Br	67
	I	53
	NO ₂	54
	CN	103

^a Data of Cottrell.¹¹ All data except that for propene were obtained from this reference.

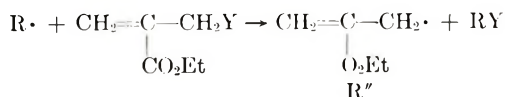
^b Data of Sebron and Swarc.¹²

There are two paths by which the chain transfer reactions might occur. These are:

(1) Allylic radical displacement:



(2) Radical abstraction:



The allylic displacement reaction (1) should depend strongly on the nature of the R· and Y· radicals involved. If R· is Br and Y· is Cl, for example,

displacement would be very unlikely, but the reverse reaction would be favored. The frequency of allylic displacement (i.e., loss of either $Y\cdot$ or $R\cdot$ by $R'\cdot$) would also depend on the lifetime of the intermediate radical $R'\cdot$ and would thus be affected by the presence of monomers such as methyl methacrylate.

It seems reasonable that the initial step in the displacement process, addition of a given $R\cdot$ to monomer to form $R'\cdot$, should be relatively independent on the nature of the Y group. Radical abstraction, reaction (2), on the other hand would be affected by the Y group, since steric considerations would be important and it is unlikely that abstraction of a polyatomic Y substituent would occur. Radical displacement, reaction (1), of large substituent groups has been postulated in other allylic systems.³

Both transfer mechanisms lead to the same overall polymerization kinetics provided that the radicals formed in the transfer ($Y\cdot$ or $R''\cdot$) rapidly initiate new polymer chains. It is thus not possible to determine the exact mechanism from the data presented in this paper. But from the energies of the bonds involved it seems likely that no displacement occurs in the fluoro and cyano derivatives, both displacement and abstraction occur in the chloro and bromo derivatives, and only displacement occurs in the nitro derivative. Whatever the path taken, the radicals formed in chain transfer with all of the compounds except the nitro (and presumably the iodo) readily initiate the polymerization of methyl methacrylate.

EXPERIMENTAL*

Ethyl α -(hydroxymethyl)acrylate (I) was purchased from Koppers Company, Inc. and employed without further purification. Each of the monomers with the exception of VI was doubly distilled through an 18-in. semimicro spinning band column and checked for purity by vapor phase chromatography (an Aerograph gas chromatographic instrument, Model A-100-C with a Silicone Dow 11 on Fluoropak column at 100°C. was used). These compounds were considered to be at least 99.5% pure.

Preparation of Ethyl α -(Bromomethyl)acrylate (III)

To a flask containing 28.0 (0.215 mole) ethyl α -(hydroxymethyl)-acrylate cooled externally with an ice-water bath to 0–5°C. was added 21.6 g. (0.08 mole) phosphorus tribromide at such a rate that the temperature did not exceed 10°C. After standing for a period of 3 hr. with stirring, 100 ml. of ether was added and the solution washed with 5% sodium carbonate, then with water and the ether solution dried over anhydrous magnesium sulfate. The ether was removed at reduced pressure and the residue distilled through an 18-in. spinning band column to give 28.5 g.

* All boiling points are uncorrected.

(68%) ethyl α -(bromomethyl)-acrylate, b.p. 51–52°C./1 mm., n_D^{20} 1.4778 [Lit.:¹ b.p. 44–45°C./1.7 mm., n_D^{20} 1.4787).

ANAL. Calcd. for $C_6H_9BrO_2$: C, 37.31%; H, 4.66%; Br, 41.45%. Found: C, 37.38%; H, 4.75%; Br, 41.02%.

The α -(bromomethyl)acrylate was prepared in 85% yield by passing gaseous hydrogen bromide into a solution of the α -(hydroxymethyl)-acrylate in carbon tetrafluoride maintained at a temperature below 25°C. by the use of an externally placed ice-water bath. The product was isolated as above.

Preparation of Ethyl α -(Chloromethyl)acrylate (IV)

To a three-necked flask fitted with magnetic stirrer, condenser, thermometer, and dropping funnel (all outlets covered with Drierite drying tubes) was introduced 20.0 g. (0.223 mole) of ethyl α -(hydroxymethyl)acrylate and 100 ml. of anhydrous ether. After cooling to 0–5°C. in an external ice-water bath, 40.5 g. (0.3 mole) thionyl chloride was added slowly to maintain the temperature below 10°C. The reaction was continued for six hours after the addition was complete. The excess thionyl chloride and ether were removed at reduced pressure. The residue redissolved in ether and washed with 5% sodium bicarbonate and water followed by drying over anhydrous magnesium sulfate. The ether was removed at reduced pressure and the residue distilled through an 18-in. Holtzman column to give 30.23 g. (91%) of ethyl α -(chloromethyl)acrylate, b.p. 40°C./1 mm., n_D^{20} 1.4485.

ANAL. Calcd. for $C_6H_9ClO_2$: C, 48.50%; H, 6.11%; Cl, 23.86%. Found: C, 48.77, 48.61%; H, 6.32, 6.38%; Cl, 23.9, 23.7%.

Preparation of Ethyl α -(Fluoromethyl)acrylate (V)

A mixture of 22.6 g. (0.117 mole) ethyl α -(bromomethyl)acrylate and 35 g. (0.275 mole) silver fluoride in 100 ml. dry acetonitrile was rapidly stirred for a period of 20 hr. A gas chromatogram made at this time indicated complete reaction based on the disappearance of the peak attributed to ethyl α -(bromomethyl)acrylate. The reaction was continued by adding 0.5 g. methylene anthrone and heating to 65°C. for a period of 1 hr. On cooling the solid material was removed by filtration and the major part of the solvent removed by evaporation at reduced pressure. The residue was distilled through an 18-in. spinning band column to give (a) acetonitrile, b.p. 29–31°C./92 mm., identified by its infrared spectrum and (b) 6.94 g. (45%) ethyl α -(fluoromethyl)acrylate, b.p. 53–55°C./54 mm. Fraction b was redistilled to give 2.2 g., b.p. 59–60°C./58 mm., n_D^{20} 1.4084. (lit.:³ b.p. 47–48°C./41 mm., n_D^{20} 1.4094).

A white solid material form in the distillation assembly during distillation was identified as polyethyl α -(fluoromethyl)acrylate.

ANAL. Calcd. for $C_6H_9FO_2$: C, 54.55%; H, 6.82%; F, 14.39%. Found: C, 54.36%; H, 6.91%; F, 14.31%.

Ethyl α -(Iodomethyl)acrylate (VI)

A mixture of 21.0 g. (0.109 mole) ethyl α -(bromomethyl) acrylate, 30.0 g. (0.2 mole) sodium iodide, and 150 ml. acetone was introduced into a round-bottomed flask fitted with magnetic stirrer and condenser. The mixture was allowed to stand at ambient temperature for a period of two days with stirring. The acetone was then stripped off at reduced pressure and the residue taken up in ether. The ether insoluble portion was filtered off and the ether solution washed thoroughly with water. After drying over anhydrous magnesium sulfate the ether was removed at reduced pressure to give 21.0 g. (80%) of ethyl α -(iodomethyl)acrylate found to be of 95% purity by vapor-phase chromatography. Attempts to purify the iodo ester by distillation were not successful, resulting in partial decomposition with liberation of iodine. The ester appeared to be stable indefinitely at ambient temperature.

Preparation of Ethyl α -(Cyanomethyl)acrylate (VII)

A mixture of 29.0 (0.15 mole) ethyl α -(bromomethyl) acrylate, 19.5 g. (0.3 mole) potassium cyanide and 150 ml. dry acetonitrile contained in a 200-ml. round-bottomed flask fitted with magnetic stirrer and condenser was stirred at ambient temperature for a period of three days. The reaction mixture was poured into 500 ml. of water and the organic phase extracted with ether. The ether extracts were combined, washed thoroughly with water, dried over anhydrous magnesium sulfate, and finally the ether removed by evaporation at reduced pressure. The liquid residue was distilled twice through an 18-in. spinning band column to give 10.23 g. (49%) of ethyl α -(cyanomethyl)acrylate, b.p. 55°C./0.6 mm., n_D^{20} 1.4403.

ANAL. Calcd. for $C_7H_9NO_2$: C, 60.43%; H, 6.47%; N, 10.07%. Found: C, 60.65%; H, 6.43%; N, 10.20%.

Preparation of Ethyl α -(Nitromethyl)acrylate (VIII)

A solution of 20.0 g. (0.13 mole) silver nitrite in 100 ml. dry acetonitrile was treated with 19.3 g. (0.1 mole) ethyl α -(bromomethyl)acrylate in 25 ml. acetonitrile. After 20 hr. at ambient temperature the mixture was examined by gas chromatography which indicated the presence of three components. The mixture was dissolved in 500 ml. of water and the organic layer extracted with ether. The ether extracts were combined, washed with water, dried over anhydrous magnesium sulfate and the ether removed at reduced pressure. The reddish-colored residue which remained was distilled through an 18-in. spinning band column to give three fractions: (a) 2.53 g. ethyl α -(bromomethyl)acrylate, b.p. 52°C./1 mm.; (b) 3.62 g. of an unidentified component, b.p. 62–64°C.; and (c) 8.93 g. (56%) of ethyl α -(nitromethyl)acrylate, b.p. 72°C./1 mm., $n_D^{21.5}$ 1.4515.

ANAL. Calcd. for $C_6H_9NO_4$: C, 45.28%; H, 5.66%; N, 8.86%. Found: C, 45.20%; H, 5.87%; N, 8.66%.

Polymerization Studies

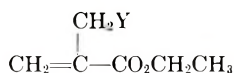
The dilatometric and viscometric techniques used in this study have been described previously.⁵

References

1. Bartlett, P. D., and R. Altschul, *J. Am. Chem. Soc.*, **67**, 812 (1945).
2. Gaylord, N. G., and F. R. Eirich, *J. Am. Chem. Soc.*, **74**, 334 (1952).
3. Gaylord, N. G., *J. Polymer Sci.*, **22**, 71 (1956).
4. Gaylord, N. G., and F. M. Kujawa, *J. Polymer Sci.*, **41**, 495 (1959).
5. Baldwin, M. G., and S. F. Reed, *J. Polymer Sci.*, **A1**, 1919 (1963).
6. Ferris, A. F., *J. Org. Chem.*, **20**, 780 (1955).
7. Yakubovich, A. Ya., N. A. Bogoslovskii, E. P. Pravova, and S. M. Pozenshinet,, *Z. Obshchei Khim*, **28**, 2288 (1950).
8. Voong, S.-T., and T.-C. Chiang, *Hua Hsueh Hsueh Pao*, **24**, 155 (1958).
9. Welch, K. N., *J. Chem. Soc.*, **1930**, 257.
10. Ferris, A. F., unpublished results.
11. Cottrell, T. L., *The Strength of Chemical Bonds*, 2nd Ed., Butterworths, London, 1958.
12. Sebron, A. H., and M. Swarc, *Proc. Roy. Soc. (London)*, **A202**, 263 (1950).

Résumé

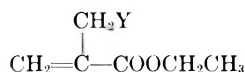
On a étudié la polymérisation avec des radicaux libres d'une série de composés qui ont la formule générale



dans laquelle Y était F, Cl, Br, I, NO₂, et CN. On a trouvé que la possibilité de polymérisation change d'une manière remarquable. Une explication a été avancée dans laquelle on a postulé que le facteur qui détermine leur manière de polymériser est le transfert de chaîne, impliquant un substituent dans la position allylique des monomères.

Zusammenfassung

Die radikalische Polymerisation einer Reihe von Verbindungen der allgemeinen Formel



(Y = F, Cl, Br, J, NO₂ und CN) wurde untersucht. Diese Verbindungen unterscheiden sich merklich in ihrer Polymerisationsfähigkeit. Zur Erklärung wird angenommen, dass der für das Polymerisationsverhalten bestimmende Faktor in einer Kettenübertragung mit einem Substituenten in der Allylstellung des Monomeren besteht.

Received February 14, 1963

Determination of Halogen in Copolymers by Dye-Partition Technique and Calculation of r_1 Therefrom

MIHIR KUMAR SAHA, PREMAMOY GHOSH, and SANTI R. PALIT,
Indian Association for the Cultivation of Science, Calcutta, India

Synopsis

Halogen-bearing polymers have been prepared by copolymerization of monomers (M_1) such as styrene, methyl methacrylate, methyl acrylate, and vinyl acetate with traces of chlorine-bearing monomers (M_2) such as allyl chloride and tetrachloroethylene at varying $M_1:M_2$ ratios in the 100:1 composition range. The halogen atoms in the copolymers were transformed to quaternary pyridinium halide groups by quaternization with pyridine. The copolymer compositions and the monomer reactivity ratio r_1 were determined by the estimation of the quaternary halide groups in the copolymers by the dye-partition technique, with aqueous disulfine blue VN150 in 0.01M hydrochloric acid as the dye reagent.

Functional groups can be well incorporated in polymers by copolymerization with monomers bearing the specific groups. Estimation of the specific groups thus introduced in the copolymers provides an easy and simple determination of copolymer composition and monomer reactivity ratio. This has been done for carboxyl-bearing monomers¹ by using a dye-interaction method of estimation of carboxyl groups in copolymers.

Recently, a dye-partition method,² described herein in detail, has been developed for the determination of halogen atoms in polymers. Copolymers at low conversions from monomers (M_1) such as styrene, methyl methacrylate, methyl acrylate, or vinyl acetate with a chlorine-bearing monomer (M_2) such as allyl chloride and tetrachloroethylene at varying $M_1:M_2$ ratios in the 100:1 composition range have been prepared, and the copolymer composition determined by the dye-partition method. The monomer reactivity ratio, i.e., the r_1 value for each copolymer is obtained with the help of the following simplified equation,¹

$$\lim_{(M_2/M_1)_f \rightarrow 0} \frac{(M_2/M_1)_f}{(M_2/M_1)_p} = r_1 \quad (1)$$

where $(M_2/M_1)_f$ and $(M_2/M_1)_p$ represent the molar ratio of the component monomers M_2 and M_1 in the feed and the copolymer, respectively.

EXPERIMENTAL

Materials

Monomers. Styrene, methyl methacrylate, and methyl acrylate were purified as usual by washing with 5% caustic soda solution until free of inhibitors, subsequently washed with distilled water, dried over fused calcium chloride for 24 hr., and finally purified by vacuum fractional distillation. Allyl chloride and tetrachloroethylene were purified by vacuum fractional distillation. Vinyl acetate was also purified by the usual procedure.³ The purified vinyl monomers were stored in a refrigerator.

Other Reagents. Chloroform (E. Merck) was used as the solvent for the copolymers. Pure pyridine (E. Merck) was used to quaternize halogen atoms in polymers to quaternary pyridinium halide groups. Analytical grade benzoyl peroxide (Eastman Kodak) was used as initiator of all copolymerization reactions. Disulfine blue VN150 was the dye used for the dye-partition test.

Preparation of Copolymers

For the preparation of polymers, known quantities of the required monomers were mixed together in clean Pyrex sealing tubes containing weighed amounts of benzoyl peroxide. The tubes were then flushed with nitrogen, frozen in liquid oxygen, and finally sealed under vacuum. Copolymerizations were carried out at a temperature of $60 \pm 0.1^\circ\text{C}$. to low conversions.

Quaternization of the Halogen Atoms in Polymers to Quaternary Pyridinium Halide Groups

The copolymers obtained were then quaternized with pyridine. About 0.2–0.3 g. of a copolymer was dissolved in about 2–5 ml. of pyridine in a clean Pyrex sealing tube. The solution was then frozen in liquid oxygen, and the tube was sealed under vacuum. The sealed tubes containing the halogen-bearing polymers in pyridine solution were then placed in a thermostated bath maintained at $90 \pm 1^\circ\text{C}$., and the quaternization was allowed to continue for 90 hr.

Purification of the Quaternized Copolymers

The quaternized copolymers were then precipitated with petroleum ether or alcohol. The precipitated polymers were further purified by repeated precipitation from their benzene solutions with a mixture of alcohol and petroleum ether as the nonsolvent. The process was repeated 5 to 6 times to ensure complete removal of all impurities. The finally precipitated polymers were then washed with petroleum ether and dried in air.

Dye-Partition Method for the Determination of Quaternary Halide Groups

The test for quaternary halide groups in polymers was carried out with an aqueous disulfine blue reagent prepared by dissolving 80 mg. of the

disulfine blue VN150 dye in one liter of 0.01*M* hydrochloric acid. A 10-ml. portion of the purified quaternized copolymer solution of known concentration in chloroform in a well-stoppered centrifuge tube was then well shaken with an equal volume of the aqueous disulfine blue reagent for a period of 1–2 hr. The two-phase system was then allowed to stand for about 2 hours. A distinct blue color in the chloroform layer indicates the presence of quaternary halide groups in the polymer. This dye-partition test is specific only for quaternary halide endgroups (ammonium or pyridinium chloride, bromide, or iodide).

The chloroform layer was then separated from the aqueous layer and then centrifuged, if necessary, to get a clear solution, and the color developed was measured in a Hilger spectrophotometer at 630 $m\mu$ with the use of stoppered 1 cm. cells. The quantity of quaternary halide endgroup present in a polymer was obtained by comparing the experimental optical density values with a calibration curve of laurylpyridinium chloride (LPC) or laurylpyridinium bromide (LPB), obtained by following a similar procedure. Complications sometimes arise, particularly with methyl methacrylate polymers of high molecular weight owing to the tendency for

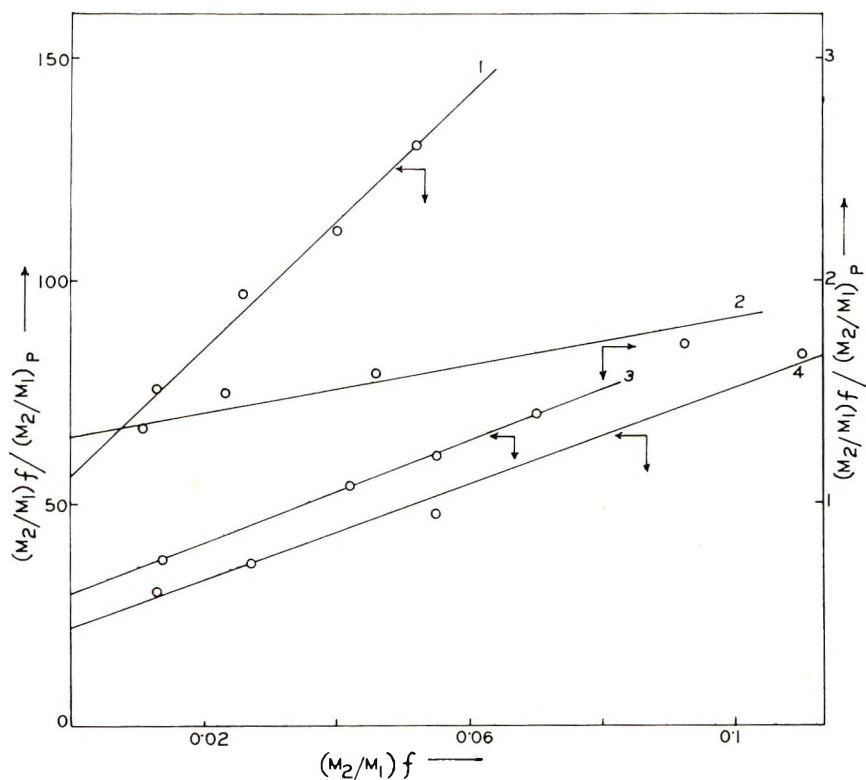


Fig. 1. Plot of $(M_2/M_1)_f / (M_2/M_1)_p$ vs. $(M_2/M_1)_f$ for copolymers: (1) methyl methacrylate-allyl chloride; (2) vinyl acetate-allyl chloride; (3) styrene-allyl chloride; (4) methyl acrylate-allyl chloride.

TABL.
 Copolymer Composition and Monomer Reactivity

Copolymer	$(M_2/M_1)_f$	Conditions of polymerization	Conversion, %	Polymer solution (quaternized), %
Styrene (M_1)- allyl chloride (M_2)	0.070	60°C.,	6.5	0.15
	0.055	0.1 mole-	4.6	0.15
	0.042	% Bz_2O_2 ,	4.4	0.15
	0.014	bulk	2.5	0.15
Styrene (M_1)- tetrachloro- ethylene (M_2)	0.113	60°C.,	5.8	0.2
	0.091	0.15 mole-	6.1	0.2
	0.056	% Bz_2O_2 ,	6.1	0.2
	0.022	bulk	7.0	0.2
Methyl methacrylate (M_1)- allyl chloride (M_2)	0.052	60°C.,	4.5	0.2
	0.040	0.2 mole-%	2.5	0.2
	0.026	Bz_2O_2 ,	2.2	0.2
	0.013	bulk	2.1	0.2
Methyl methacrylate (M_1)- tetrachloro- ethylene (M_2)	0.052	60°C.,	3.2	0.5
	0.042	0.1 mole-	2.8	0.5
	0.021	% Bz_2O_2 ,	2.5	0.5
	0.011	bulk	2.5	0.5
Methyl acrylate (M_1)- allyl chloride (M_2)	0.110	60°C.,	12.0	0.05
	0.055	0.4 mole-	2.1	0.05
	0.027	% Bz_2O_2 ,	5.0	0.05
	0.013	bulk	2.2	0.05
Vinyl acetate (M_1)- allyl chloride (M_2)	0.092	60°C.,	11.2	0.0014
	0.046	0.4 mole-	10.8	0.0018
	0.023	% Bz_2O_2 ,	12.6	0.0068
	0.011	bulk	12.9	0.0068

formation of emulsions in the organic phase. The complications may however, be greatly overcome on long standing and centrifugation. For polystyrene and polyvinyl acetate and for relatively low molecular weight polyacrylates and methacrylates, no such complications generally arise.

RESULTS AND DISCUSSION

The results of copolymerization are shown in Table I. The monomer reactivity ratio r_1 was obtained with the help of eq. (1). For each copolymer, $(M_2/M_1)_f/(M_2/M_1)_p$ values were plotted against $(M_2/M_1)_f$ values. The plots follow a straight line. The intercept, obtained by extrapolating the straight line to zero $(M_2/M_1)_f$ value, gives the r_1 value for the copolymer (Figs. 1 and 2). The copolymer composition $(M_2/M_1)_p$ was obtained by

I
 Ratio as Determined by Dye-Partition Method

O.D. at 630 $m\mu$ using disulfine blue reagent	Corre- sponding LPC concn., $10^{-4}N$	$(M_2/M_1)_p$ $\times 10^{-3}$	$(M_2/M_1)_f$ $(M_2/M_1)_p$	r_1	
				Experi- mental	Litera- ture
1.4	13.9	1.0	70		
1.29	12.9	0.91	60.1	30	31.2 ± 4
1.14	11.5	0.78	53.6		
0.54	5.36	0.37	37.8		
0.24	2.36	0.062	1800		
0.23	2.29	0.058	1520	200 ± 20	$185 \pm 20,$
0.20	1.98	0.052	1080		20S
0.17	1.7	0.043	528		
0.78	7.8	0.39	130		
0.70	7.0	0.35	111	56	42
0.53	5.3	0.27	97		
0.34	3.42	0.17	76		
0.30	3.0	0.030	1733		
0.32	3.2	0.032	1313	240 ± 20	—
0.26	2.62	0.026	808		
0.20	1.99	0.020	550		
0.78	7.78	1.34	83.2		
0.675	6.8	1.18	47.4	22 ± 4	—
0.43	4.3	0.74	36.1		
0.25	2.5	0.433	30.0		
0.85	8.5	53.8	1.70		
0.58	5.8	29.1	1.58	1.30	0.7
1.20	12.0	15.4	1.50		
0.64	6.4	8.17	1.34		

the application of dye partition test, taking laurylpyridinium chloride (or bromide) as the basis of comparison.

An important step in the present method of determination of specific quaternary groups in a polymer is the process of quaternization, which is generally slow and sluggish.^{4,5} In our present method of quaternization we used the quaternizing agent (pyridine) as the solvent to dissolve the substrates to be quaternized. Fairly high temperature (90°C.) and sufficiently long hours of heating (90 hr.) were allowed to ensure that the quaternization be complete as far as practicable. It is known that in a long chain polymer the quaternization with pyridine is highly dependent on steric factors. When allyl chloride was used as a component monomer in copolymerization, this steric factor is negligible and all the chlorine atoms

in the copolymer are presumably quaternizable. But when tetrachloroethylene bearing two chlorine atoms on each of the two carbon atoms, is used as a component monomer in copolymerization, the steric factor probably plays a great part in the quaternization process. The bulky quaternary pyridinium groups formed when one chlorine atom from each of the two carbon atoms of a tetrachloroethylene segment of a copolymer is quaternized shield the other two chlorine atoms of the same tetrachloroethylene segment from being quaternized, and we assume that two chlorine

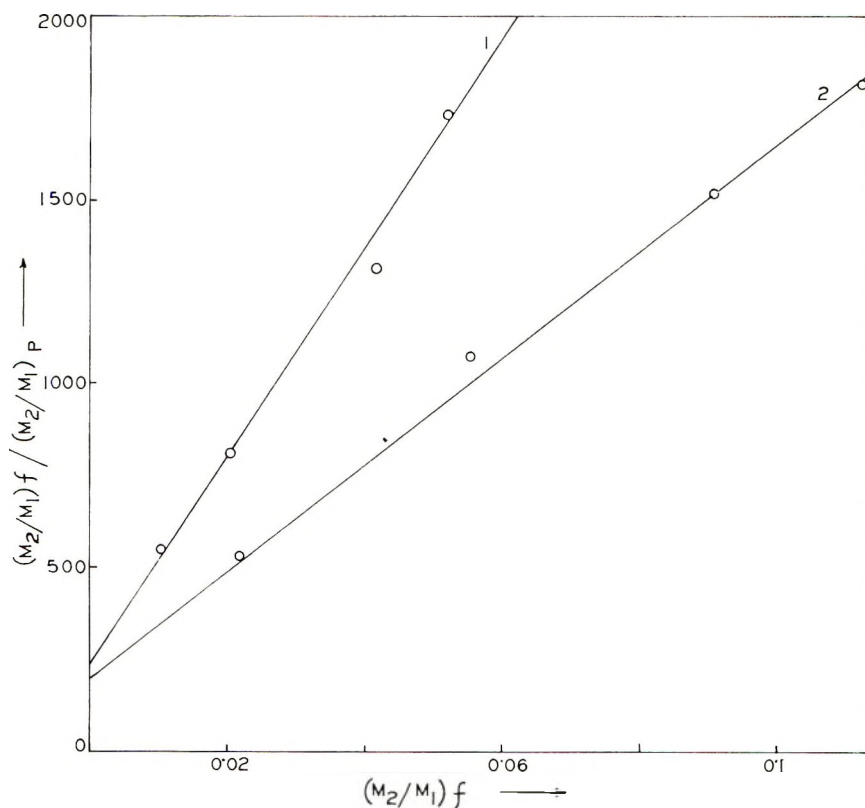


Fig. 2. Plot of $(M_2/M_1)_f / (M_2/M_1)_p$ vs. $(M_2/M_1)_f$ for copolymers: (1) methyl methacrylate-tetrachloroethylene; (2) styrene-tetrachloroethylene.

atoms, on the average, of each tetrachloroethylene segment of a copolymer are quaternized. The results (r_1 values) presented in Table I are obtained on the basis of these assumptions and are found to compare well with some values given in the literature.^{6,7} Some of our experimental r_1 values, e.g., those for methyl methacrylate-allyl chloride and vinyl acetate-allyl chloride do not agree closely with the literature values,^{9,10} but nevertheless our experimental values are of the same order as those given in the literature.

There may be some uncertainty in the quantitative aspects of the present method because the r_1 values for the copolymers have been obtained by empirical comparison with a long chain pyridinium chloride (LPC), and it is difficult to make an independent check at the present stage. Allowing for this uncertainty, it may be seen from Table I that the experimental r_1 values for styrene allyl chloride⁶ and styrene-tetrachloroethylene^{7,8} copolymers are in close agreement with the literature values, while those for MMA-allyl chloride⁹ and vinyl acetate-allyl chloride¹⁰ are higher than the values given in the literature. The r_1 values for the other two copolymers could not be checked from the literature.

Quaternization of polyvinylpyridine with butyl bromide has been extensively studied by Fuoss,^{4,5,11} and it has been shown that the extent of quaternization in this system is not always complete and varies from about 70 to 100%. In our present method for the determination of copolymer composition, it is apparent that incomplete quaternization will always lead to a higher r_1 value. From the fair agreement of the experimental r_1 values with the existing literature values, it may be concluded that the dye-partition method gives a fairly reasonable estimate of halogen content in copolymers.

Thanks are due to the Council of Scientific and Industrial Research (Government of India) for research fellowships (to M. K. S. and P. G.).

References

1. Palit, S. R., and P. Ghosh, *J. Polymer Sci.*, **58**, 1225 (1962).
2. Palit, S. R., *Makromol. Chem.*, **36**, 89 (1959); *ibid.*, **38**, 96 (1960).
3. Das, S., and S. R. Palit, *Proc. Roy. Soc. (London)*, **A226**, 82 (1954).
4. Fuoss, R. M., and V. P. Strauss, *J. Polymer Sci.*, **3**, 246 (1948).
5. Fuoss, R. M., M. Watanabe, and B. D. Coleman, *J. Polymer Sci.*, **48**, 5 (1960).
6. Alfrey, T., Jr., and J. G. Harrison, Jr., *J. Am. Chem. Soc.*, **68**, 299 (1946).
7. Doak, K. W., *J. Am. Chem. Soc.*, **70**, 1525 (1948).
8. Breitenbach, J. W., A. Schindler, and C. Pflug, *Monatsh. Chem.*, **81**, 21 (1950).
9. Mayo, F. R., F. M. Lewis, and C. Walling, *J. Am. Chem. Soc.*, **70**, 1529 (1948).
10. Agron, P., T. Alfrey, Jr., J. Bohrer, H. Haas, and H. Wechsler, *J. Polymer Sci.*, **3**, 157 (1948).
11. Fuoss, R. M., and G. I. Cathers, *J. Polymer Sci.*, **4**, 97, 121 (1949).

Résumé

Des polymères porteurs d'halogènes ont été préparés par copolymérisation de monomères (M_1) tels que le styrène, le méthacrylate de méthyle, l'acrylate de méthyle et l'acétate de vinyle avec des traces de monomères (M_2) porteurs de chlore tels que le chlorure d'allyle et le tétrachloroéthylène en variant les rapports $M_1:M_2$ dans le rapport et composition de 100:1. Les atomes d'halogènes dans les copolymères ont été transformés en groupement halogénure de pyridine quaternée en recourant à la quaternation avec la pyridine. Les compositions du copolymère et de là, le rapport de réactivité du monomère (r_1) ont été déterminés par estimation des groupes quaternaires halogénés dans les copolymères au moyen de la technique de partition de couleurs en employant une solution aqueuse de bleu de disulfine VN150 dans 0.01M d'acide chlorhydrique comme réactif coloré.

Zusammenfassung

Durch Copolymerisation von Monomeren (M_1) wie Styrol, Methylmethacrylat, Methacrylat und Vinylacetat mit Spuren von halogenhaltigen Monomeren (M_2) wie Allylchlorid und Tetrachloräthylen bei wechselndem Verhältnis $M_1:M_2$ im Bereich von etwa 1 Molprozent M_2 wurden halogenhaltige Polymere hergestellt. Die Halogenatome in den Copolymeren wurden durch Quaternisierung mit Pyridin in quaternäre Pyridiniumhalogenid-Gruppen übergeführt. Die Zusammensetzung des Copolymeren und damit das Monomerreaktivitätsverhältnis r_1 wurde durch Bestimmung der quaternären Halogenid-Gruppen mittels einer Anfärbemethode mit wässrigem Disulfinsblau VN150 in 0,01M HCl als Farbagens ermittelt.

Received February 14, 1963

Critical Analysis of Molecular Weight Distributions Derived from Fractionation Data.

I. Column Elution*

A. M. KOTLIAR, *Esso Research and Engineering Company, Enjay
Laboratories Division, Linden, New Jersey*

Synopsis

The evaluation of broad molecular weight distributions, based on the fractionation data obtained by column elution techniques and the Schulz-Dinglinger approximation, is critically analyzed employing an electronic computer and a solubility function based on the Flory-Huggins theory. The results, based on Schulz and Wesslau type distributions, show that although some characteristic features may be established, the determined values of the distribution parameters may be greatly in error.

Introduction

The evaluation of the molecular weight distribution of polymers is of basic importance to the understanding of the associated rheological behavior, mechanical properties, polymerization mechanisms, and random chain degradation and crosslinking processes. Recent developments in fractionation techniques have led many workers into the belief that accurate molecular weight distribution information can be obtained easily from simple viscometric determinations on the fractions eluted from polymeric material deposited on a support in a column or from the conventional precipitation methods, and by using the Schulz-Dinglinger¹ method of treating polymer fractionation data.

The Schulz-Dinglinger¹ method attempts to account for the polydispersity and the overlapping of molecular distributions of fractions by assuming that the weight distribution within a fraction is symmetrical; i.e., 50 wt.-% of the fraction has molecular weights above the average and 50 wt.-% below, but with an overlapping of adjacent fractions. The resulting cumulative weight of the fractions is given by

$$I(P)_j = W_j/2 + \sum_{i=1}^{j-1} W_i$$

where W_j is the weight of the j th fraction and W_i the weight of each fraction having a mean molecular weight less than the j th fraction.

* Presented at the American Chemical Society Meeting, New York Metropolitan Regional Meeting, Jan. 28, 1963, at the Hotel Robert Trent, Newark, New Jersey.

The validity of the approach has been questioned by a number of workers,²⁻⁴ in that the polydispersity and the overlap of molecular weights of fractions are more severe than that taken into account by the Schulz-Dinglinger method and that any success of the method depends on the optimum compensation of the many overlaps. However, this "internal" compensation is not generally valid for all distributions, and, as shown below, is generally poor when $\bar{M}_w/\bar{M}_n > 4$.

Theory

The theory of polymer fractionation yields a solubility function⁵⁻¹² for two phases in equilibrium, of the form

$$f(p) = \frac{1}{1 + Re^{\sigma P}} \quad (1)$$

and

$$f'(p) = \frac{Re^{\sigma P}}{(1 + Re^{\sigma P})^2} \quad (2)$$

for the dilute (eluted) and concentrated (precipitated or deposited) phases, respectively. Here, P is the size of the molecule, R the ratio of the volume of the concentrated phase to the volume of the dilute phase, and σ is a parameter describing the partitioning of every component species between the two phases. An extremely important consequence of the theory is that every component species is more soluble in the concentrated phase since the basis for separation is the exponential σP term, inefficient though it be, with most of the smaller species being retained in the more dilute phase merely as a consequence of its larger volume. It is also important to note that the presence of low molecular weight material in the dilute phase increases the solubility of larger species in this phase. Therefore, fractionation of measurable amounts of polymeric material on a solubility basis will always yield a broad distribution in that all species present in the original polymer will also be present in each fraction. The sharpness of each fraction, as measured by the ratio of measurable molecular weight-averages, i.e., number-, weight-, and z -averages, is then a measure of the extent we have partially separated the various molecular species, and is governed by the parameters R and σ in eqs. (1) and (2). The above is true for any finite concentration and number of equilibrium fractionation steps. In column elution experiments, equilibrium is generally not achieved, and poorer separations may be obtained than indicated by eqs. (1) and (2). In addition, if specific adsorption occurs the major effect will be the partial loss of the high molecular weight material, since the precipitated phase is generally too concentrated with respect to the number of adsorption sites to effect the fractionation, except near the conclusion of the experiment, where the distribution of residual deposited material has already become rather sharp as a result of the repeated extraction process.

Computation Procedure

A given distribution is initially stored on a 7090 computer in the form $W(P)$, the weight fraction of size P , in 500 intervals with a ΔP equal to one and \bar{P}_w set equal to 55. A value for σ [see eqs. (1) and (2)] is chosen so that the dilute phase in column elution, or concentrated phase in precipitation separation will contain a small fraction of the polymer of the order of 10 wt.-% with a R value of 10^{-3} . The weight distribution eluted (dilute phase) is given by eq. (1) times the initial or residual weight distribution function, and similarly the weight distribution remaining on the column or the precipitated phase is given by eq. (2) multiplied by the weight per cent distribution fraction. The distribution of the fraction and the remaining bulk material is stored and the process continued N times yielding $N + 1$ fractions. This method has been used by Schulz,¹³ Booth and Beason,¹⁴ and Tung¹⁵ to fractionate relatively narrow distributions.

The sharpness of each fraction, for a given distribution, is governed by the parameters R and σ of eqs. (1) and (2). It was assumed for convenience in the calculations, that R was constant for all fractions and had a value of 10^{-3} , which is perhaps unusually favorable. Increasing this value to 10^{-2} will yield somewhat broader fractions and larger overlap errors, while decreasing it to a value of 10^{-4} will not change the results significantly for the same weight fraction of material removed. The values for σ can be arbitrarily chosen and result, for a given distribution of molecular species and R value, in fractions having different weights and distributions. The computed distribution for the whole polymer will, nevertheless, be the same provided each fraction is completely described. However, if we assume a particular method for computing the overlap between fractions which is not exact, the resulting computed distributions will be somewhat different depending on how broad or narrow the distributions of the fractions become. The values for σ chosen in the calculations generally yielded \bar{M}_w/\bar{M}_n values of less than 1.10, except for the first fraction, which in some cases gave values as large as 1.2. These values indicate that the fractions obtained were somewhat less disperse than reported experimental values. To effect any significant change in these values, greatly different values for σ must be chosen which will result in either extremely small or rather large weight per cent fractions. Hence, the particular values of σ used are representative of a range of values and yield fraction sizes generally encountered or aimed at experimentally; e.g., 10 wt.-%.

The computations on the computer were generally normalized to a \bar{P}_w value of 55. To compare the computed results with experimental data, ideally one merely normalizes the values of the respective averages by the factor \bar{P}_w (experimental)/ \bar{P}_w (computer) with no loss of generality. However, there are two unavoidable errors in the computer calculations in the range $P = 0$ to 1 and $P > 500$, the largest size stored. The $P = 0$ to 1 range produces an error in the overall \bar{P}_n value of the distribution which fortunately affects the \bar{P}_n of each fraction insignificantly compared to the

error involved in the experimental evaluation of this quantity. The cutoff at $P = 500$ is of no consequence to the \bar{P}_n values but can, however, affect the \bar{P}_w and \bar{P}_z values computed. This error is again quite small in all fractions other than the last. The net effect is that although the fractionation data are essentially correct, normalization to experimental values becomes problematic with a wide Wesslau distribution in that we have two possible \bar{P}_w averages, the theoretical value of 55 or the computed value with the arbitrary cutoff at 500. The choice of values depends on whether or not we can expect a polymer with a \bar{M}_w of 300,000 to have molecular species greater than 3 million. However, since the fractions are generally unaffected by the cutoff value, normalization can be made at the 50% cumulative weight. It is important to bear in mind that neither this above procedure, nor the errors described, significantly affect the conclusions of the calculations, but rather emphasize the inability of rather simple two parameter distribution functions, normalized in the interval 0 to ∞ , to adequately describe a real polymer distribution, in particular a Wesslau distribution with a realistic cutoff value. The significance of the computations rests on whether eqs. (1) and (2) describe correctly the solubility function of real polymer solvent systems, particularly if there is a substantial heat of mixing, and provides a correlation of a nonequilibrium experimental method with equilibrium calculations. The form of eqs. (1) and (2) may be derived from the free energy change involved in transferring a molecule of a particular size from one phase to another and therefore the form of eqs. (1) and (2) is in general correct, although the significance attached to the value of σ is difficult to interpret.¹⁶ The equilibrium calculations should therefore correspond to an infinitely slow extraction process. Since the computer fractionation data yields fractions generally having \bar{M}_w/\bar{M}_n ratios smaller than the reported experimental values, it is reasonable to conclude that the computations can yield instructive information on the value of the method used to evaluate the experimental results with a reasonable degree of confidence. The recent work of Tung¹⁵ supports this conclusion.

Two general distribution functions were used in the computer studies, the Schulz¹⁷ (generalized exponential) and Wesslau¹⁸ (logarithmic normal). The respective analytical functions are:

$$W(P) = \frac{y^{a+1}}{\Gamma(a+1)} p^a \exp \{-yP\} \quad (\text{Schulz}) \quad (3)$$

where

$$y = a/\bar{P}_n = (a+1)/\bar{P}_w = (a+2)/\bar{P}_z$$

and

$$W(P) = \frac{1}{\beta P \pi^{1/2}} \exp \left\{ -\frac{1}{\beta^2} \ln^2 P/P_0 \right\} \quad (\text{Wesslau}) \quad (4)$$

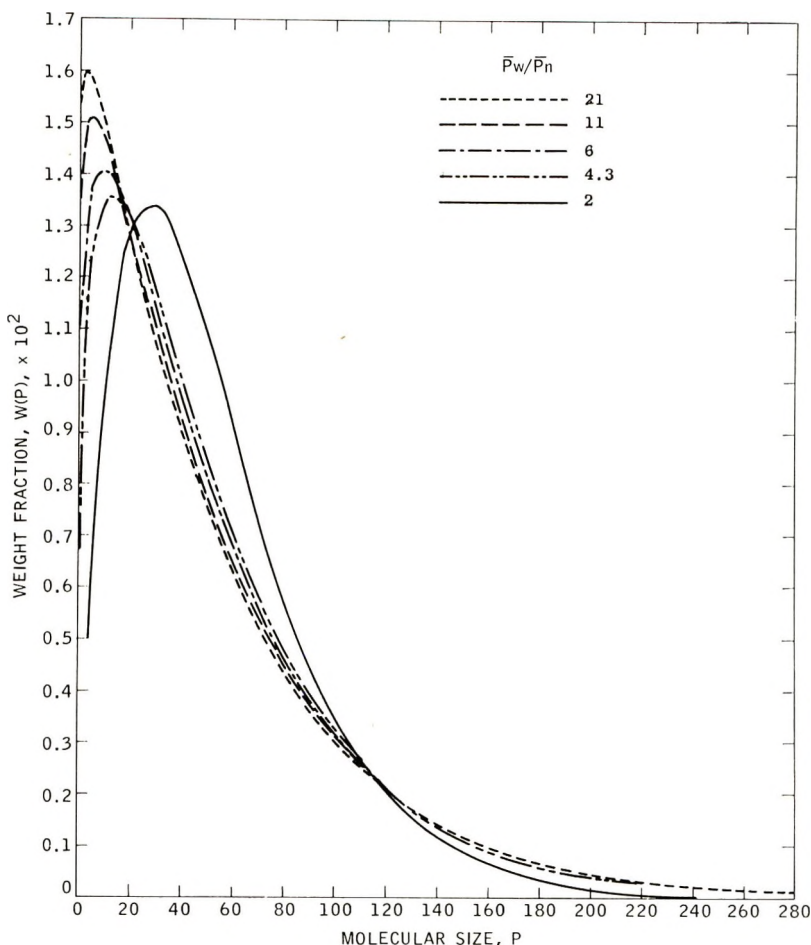


Fig. 1. Differential distribution curves for wide Schultz distributions, $\bar{P}_w = 55$.

where

$$\bar{P}_n = P_0 e^{-\beta^2/4}$$

$$\bar{P}_w = P_0 e^{\beta^2/4}$$

$$\bar{P}_z = P_0 e^{3\beta^2/4}$$

These distributions are shown in Figures 1 and 2 for several values of \bar{P}_w/\bar{P}_n . Although a two-parameter simple type distribution will generally not completely describe the results of a polymerization process, the chosen functions represent single peaked distributions at either end of a spectrum of distribution types differing in the width of the peak and relative amounts of polymeric material in the high molecular end of the distribution. Of particular interest is the rather sharp distribution of the low molecular weight species for wide Wesslau distributions. This sharpness means that

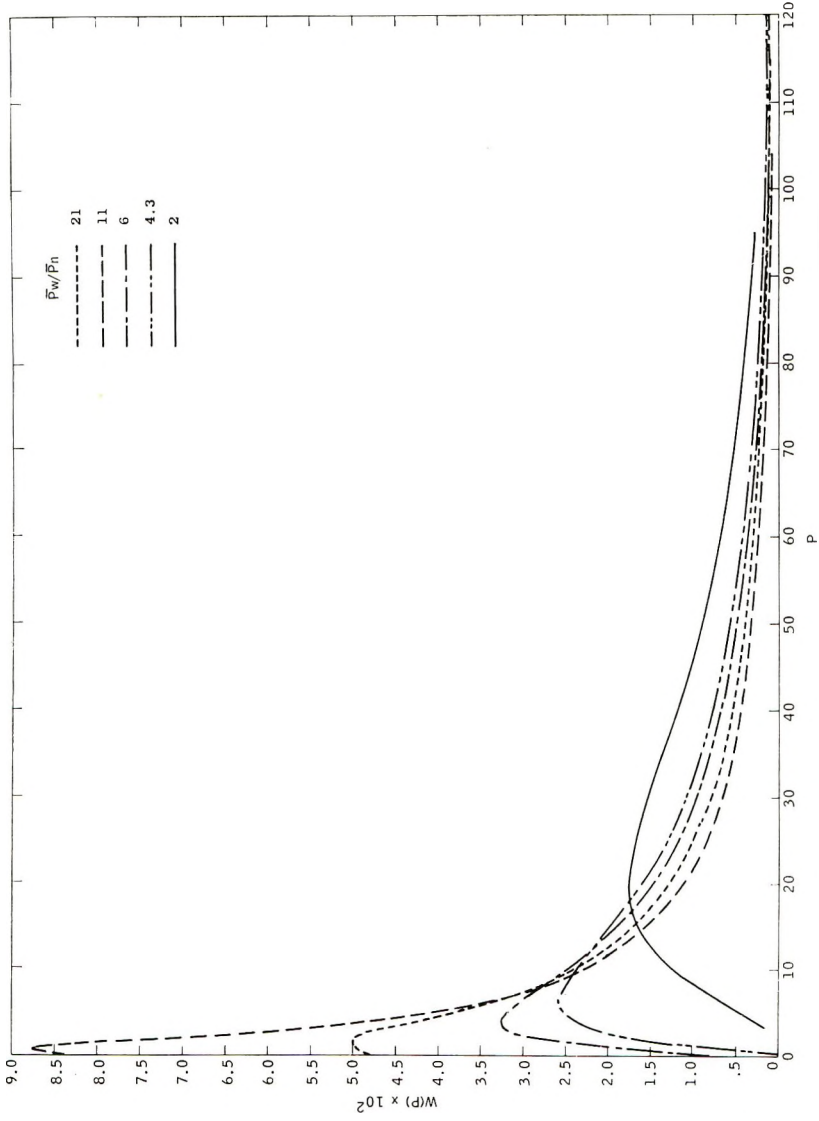


Fig. 2. Differential distribution curves for wide Wesslau distributions, $P_w = 55$.

very important features of the distribution will be found in the first eluted fraction and emphasizes the necessity of including it in the evaluation of the parameters of the distribution.

Results and Discussion

The two general distribution types used in the computations, i.e., Schulz and Wesslau, are shown in Figures 1 and 2. It is quite apparent that differentiation between broad Schulz distributions, as measured by $\bar{M}_w/\bar{M}_n > 4$, is not possible with current experimental techniques. This

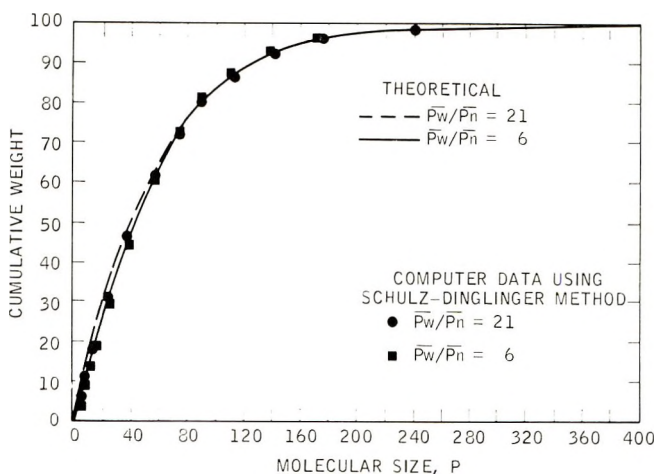


Fig. 3. Comparison of computer fractionation data with theoretical values of a Schulz distribution, $\bar{P}_w = 55$.

conclusion is borne out by the cumulative plots in Figures 3 and 4. However, as the distribution becomes less disperse, differentiation does become possible with accurate evaluation of the distribution parameters possible when $\bar{M}_w/\bar{M}_n < 2$. This is shown in Figure 5, where agreement of the theoretical and computer data at the point of steepest ascent, the number-average molecular weight for a Schulz distribution, is very good. However, the computed fractionation data of a distribution composed of two narrow molecular weight distributions do not yield true values of the distribution, as shown in Figure 6. This important observation is supported by the experimental data of Krigbaum and Kurz and stresses the fact that the partitioning exponential σP term is rather inefficient. The differences between the experimental and computed values are most likely due to errors in the experimental molecular weight determinations, the fit of the two components to a Schulz distribution, and the true cutoff in the high molecular tail for a real polymer.

The relatively larger differences in the low and high molecular weight ends of broad Wesslau distributions, Figure 2, do indicate that some dis-

crimination between distributions having different \bar{M}_w/\bar{M}_n ratios is possible with the major differences being found in the first few fractions. The computer fractionation using the Schulz-Dinglinger method and the theoretical curves are shown in Figure 7. The figure shows that in the

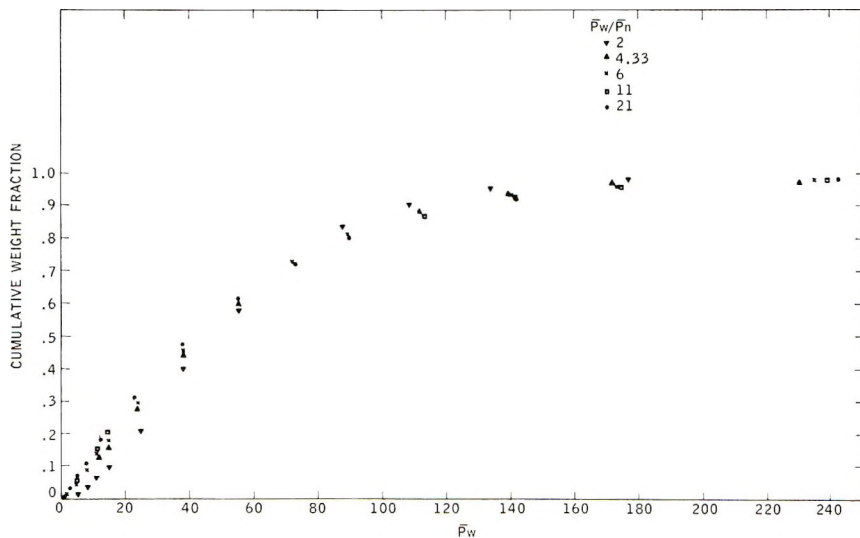


Fig. 4. Integral distribution curves for Schulz distributions from computer fractionation data, $\bar{P}_w = 55$.

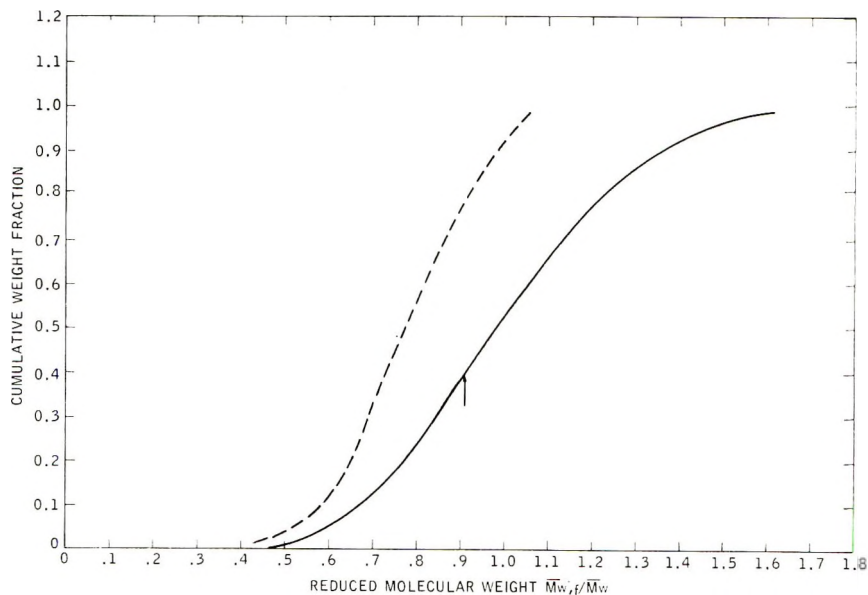


Fig. 5. Integral distribution curve from fractionation data of a Schulz distribution, $M_w/M_n = 1.1$: (—) computer data; (---) data of Krigbaum and Kurz. Arrow indicates theoretical point of steepest ascent.

region of cumulative weight of the order of 85–95%, the highest values generally encountered in column elution experiments, there is a general convergence of the theoretical lines, the differences being of the order of generally encountered experimental errors, and therefore stresses the importance of the correlation of P_0 and β obtained from the Wesslau plot with molecular weight measurements on the whole polymer. The second feature is the poor agreement of the cumulative weight and theoretical lines, par-

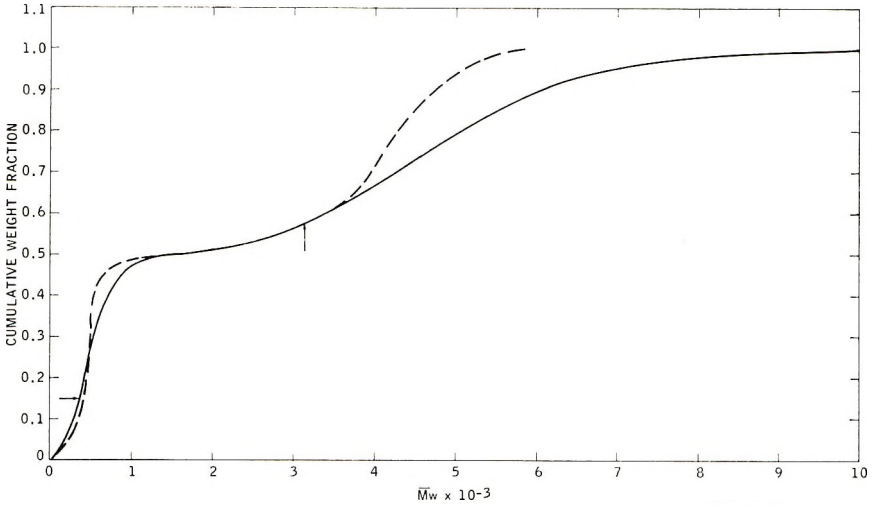


Fig. 6. Integral distribution curve from a 50–50 mixed Schulz distribution $\bar{M}_{w1} = 50,280$, $\bar{M}_{w1}/M_{n1} = 1.4$, $\bar{M}_{w2} = 473,000$, $\bar{M}_{w2}/\bar{M}_{n2} = 1.15$: (—) computer data; (---) experimental data of Krigbaum and Kurz. Arrows indicate theoretical points of steepest ascent.

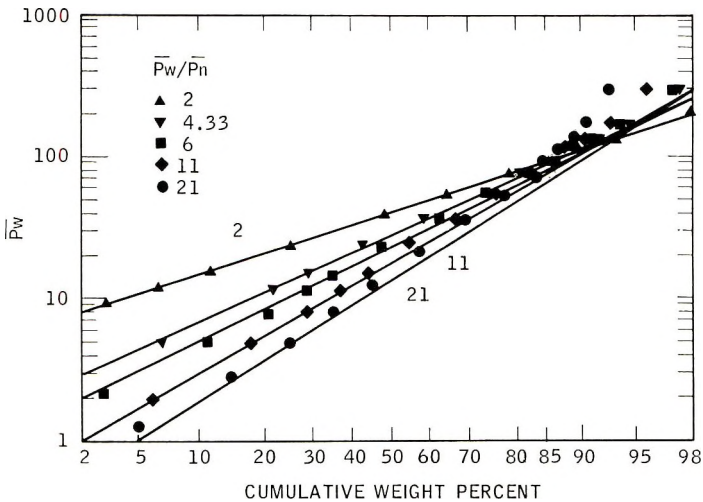


Fig. 7. Comparison of computer fractionation data (points) with theoretical values (lines), Wesslau distributions, $\bar{P}_w = 5$.

ticularly at the low and high ends. It is particularly interesting to observe the correlation of the cumulative weight of the first few fractions using the Schulz-Dinglinger method, the shape of the distribution curve, and the theoretical value. There seems to be a fortuitous agreement up to a cumulative weight of about 40% for the distribution having a $\bar{P}_w/\bar{P}_n = 11$. In all cases, when $\bar{P}_w/\bar{P}_n > 2$, the computer data is above the theoretical line at higher cumulative weights due to overlapping of fractions, and the moment of the distribution used to characterize the fractions. Typical computer fractionation data for Schulz and Wesslau distributions are shown in Tables I and II.

Tables III and IV list the computer storage characteristics and

TABLE I
Schulz Distribution $\bar{P}_w/\bar{P}_n = 11$; $\bar{P}_w = 55$

Fraction	Wt.-%	Cumulative wt. fraction	\bar{P}_w	\bar{P}_w/\bar{P}_n	\bar{P}_z/\bar{P}_w
1	3.615	0.0181	1.917	1.237	1.213
2	4.572	0.0590	4.793	1.112	1.097
3	4.724	0.1055	7.937	1.075	1.069
4	4.754	0.1529	11.20	1.057	1.056
5	4.689	0.2001	14.55	1.048	1.048
6	17.20	0.3095	23.87	1.082	1.081
7	14.87	0.4699	38.07	1.074	1.068
8	13.54	0.6120	55.12	1.060	1.057
9	9.080	0.7251	72.43	1.049	1.048
10	6.434	0.8027	89.77	1.041	1.040
11	6.653	0.8681	112.8	1.040	1.040
12	4.681	0.9248	141.4	1.042	1.041
13	2.450	0.9606	174.5	1.040	1.039
14	2.124	0.9834	239.4	1.059	1.062

TABLE II
Wesslau Distribution $\bar{P}_w/\bar{P}_n = 11$; $\bar{P}_w = 55$

Fraction	Wt.-%	Cumulative wt. fraction	\bar{P}_w	\bar{P}_w/\bar{P}_n	\bar{P}_z/\bar{P}_w
1	12.30	0.0615	1.863	1.229	1.211
2	12.00	0.1830	4.584	1.115	1.098
3	9.415	0.2901	7.604	1.078	1.070
4	7.524	0.3748	10.78	1.058	1.056
5	6.122	0.4430	14.05	1.048	1.047
6	15.75	0.5523	22.49	1.082	1.082
7	9.614	0.6791	36.27	1.080	1.074
8	6.929	0.7618	53.55	1.065	1.061
9	4.140	0.8172	71.55	1.053	1.051
10	2.831	0.8520	89.85	1.043	1.043
11	3.056	0.8814	114.8	1.044	1.044
12	2.496	0.9092	147.2	1.046	1.046
13	1.705	0.9302	186.0	1.004	1.044
14	3.662	0.9570	302.6	1.086	1.081

TABLE III
Comparison of Initial Stored Schulz Distributions, $1 \leq P \leq 500$, with Mathematical Model, $0 \leq P \leq \infty$

	\bar{P}_n	\bar{P}_w	\bar{P}_z	\bar{P}_w/\bar{P}_n	$\Sigma W(p)$
Theory	2.619	55.00	107.4	21.00	1.000
Computer	14.41	54.97	107.0		0.993
Theory	5.000	55.00	105.0	11.00	1.000
Computer	15.14	54.97	104.7		0.994
Theory	9.167	55.00	100.8	6.00	1.000
Computer	16.64	54.98	100.7		0.996
Theory	12.69	55.00	97.31	4.33	1.000
Computer	18.17	55.02	97.29		0.997
Theory	27.50	55.00	82.50	2.00	1.000
Computer	28.00	55.00	82.50		0.999
Theory	118.2	130.0	141.8	1.091	1.000
Computer	118.2	130.0	141.8		1.000

TABLE IV
Comparison of Initially Stored Wesslau Distributions, $1 \leq P \leq 500$, Mathematical Model, $0 \leq P \leq \alpha$, and Wesslau Plot of Fractions Using Schulz-Dinglinger Method, (W.P.S.D.)

	\bar{P}_n	\bar{P}_w	\bar{P}_z	\bar{P}_0	\bar{P}_w/\bar{P}_n	$\Sigma W(p)$
Theory	2.619	55.0	1150.0	12.01	21.00	1.000
Computer	5.209	35.90	156.1			0.949
W.P.S.D.	3.000	77.66	2011.0	15.25	25.89	
Theory	5.00	55.00	605.0	16.58	11.00	1.000
Computer	5.209	40.85	150.6			0.975
W.P.S.D.	4.221	80.65	1541.0	18.45	19.11	
Theory	9.167	55.00	330.0	22.46	6.00	1.000
Computer	9.817	46.01	142.1			0.989
W.P.S.D.	11.04	52.77	252.2	24.13	4.78	
Theory	12.69	55.00	238.3	26.42	4.33	1.000
Computer	12.90	48.86	134.9			0.992
W.P.S.D.	15.11	53.21	187.4	28.36	3.52	
Theory	27.50	55.00	110.0	38.89	2.00	1.000
Computer	27.50	54.30	102.5			0.999
W.P.S.D.	28.54	56.69	112.6	40.23	1.99	

distribution parameter. The values for β from the computer fraction data are unfortunately somewhat arbitrary because of curvature of the results on a Wesslau plot. Nevertheless, the results definitely show that the Schulz-Dinglinger approximation is rather poor for broad distributions and introduces considerable error in the evaluated distribution parameters. The lack of agreement between the measured molecular

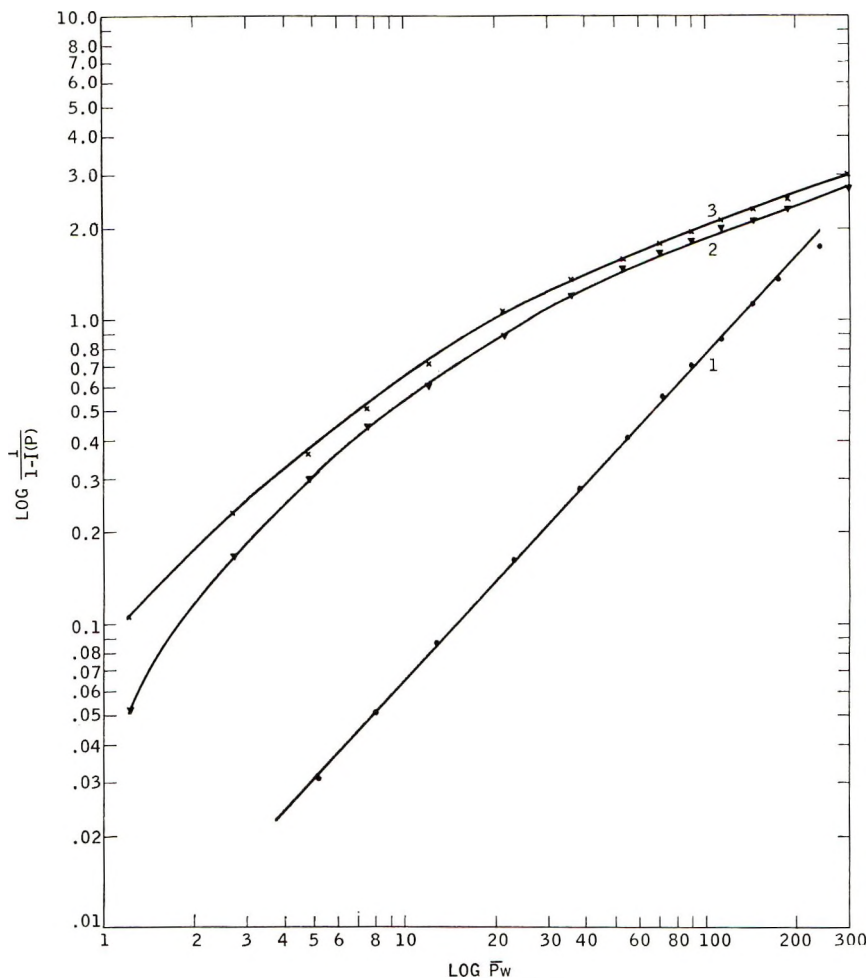


Fig. 8. Tung plots for (1) Schulz distribution, $\bar{P}_w/\bar{P}_n = 21$, Schulz-Dinglinger method; (2) Wesslau distribution, $\bar{P}_w/\bar{P}_n = 21$, Schulz-Dinglinger method; (3) Wesslau distribution, $\bar{P}_w/\bar{P}_n = 21$, Mark-Roth method.

weight and the value determined from the fractionation data removes the uniqueness of the identification of an unknown distribution with a distribution type. This is dramatically shown when a Schulz type distribution is plotted on a Tung plot in Figure 8. Here one would conclude that the distribution had a $\bar{M}_w/\bar{M}_n = 1.7$, when it is, in fact, 21. Additional data of the cumulative weight at the low and high ends (not shown), of course, would indicate a rather poor fit. Hence the importance of precise data at either end of the broad distributions cannot be over-stressed. Also shown is the fractionation data of a Wesslau distribution having a $\bar{P}_w/\bar{P}_n = 21$ by the Mark-Roth and Schulz-Dinglinger methods. The fact that one observes curvature on a particular distribution type plot does not necessarily mean one has a bimodal distribution. It simply means that the distribu-

tion under investigation just does not fit the particular plot or the method of arriving at a cumulative weight is in error.

Aside from the limitation of the approximate manner by which the data are analyzed, is the question of sensitivity of the fractionation data to irregularities in the distribution type, which can have pronounced effects on the properties of the material. The blending of Schulz distributions, Figure 9, and the Wesslau distributions, Figure 10, show that the evaluation of the fractionation data, by the Schulz-Dinglinger method, offers

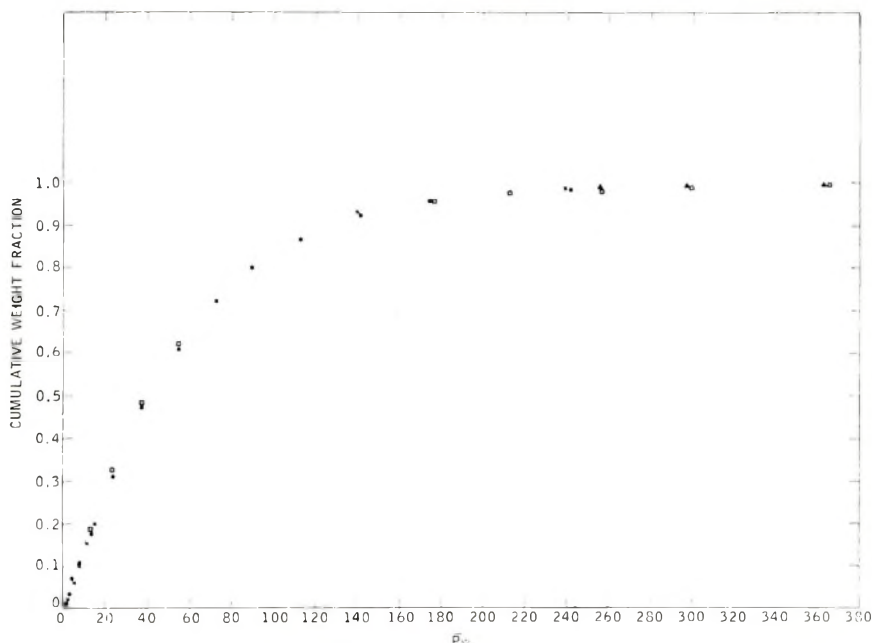


Fig. 9. Integral distribution curves from fractionation data of 50-50 blends: (□) $\bar{P}_w = 55$ $P_{w_1} = 1.59$ P_{w_2} , $P_{w_1}/P_{n_1} = P_{w_2}/P_{n_2} = 21$; (▲) 50-50 blend, $\bar{P}_w = 55$, $\bar{P}_{w_1} = 1.59$ \bar{P}_{w_2} , $\bar{P}_{w_1}/\bar{P}_{n_1} = \bar{P}_{w_2}/\bar{P}_{n_2} = 11$; (●) single component distribution $\bar{P}_w/\bar{P}_n = 21$, $\bar{P}_w = 55$; (X) single component distribution, $\bar{P}_w/\bar{P}_n = 11$, $\bar{P}_w = 55$. Schulz distributions.

little or no discrimination between the blend and single-component system within generally encountered experimental errors. The lack of sensitivity for blends of distributions is also true for the recent method, as suggested by Tung,¹⁵ for evaluating \bar{M}_w/\bar{M}_n from the relationships

$$\bar{M}_w = \sum W_i M_{w_i} \tag{5}$$

and

$$M_n = \frac{1}{\frac{W_1}{M_{n_1}} + \sum_{i=2}^N \frac{W_i}{M_{w_i}}} \tag{6}$$

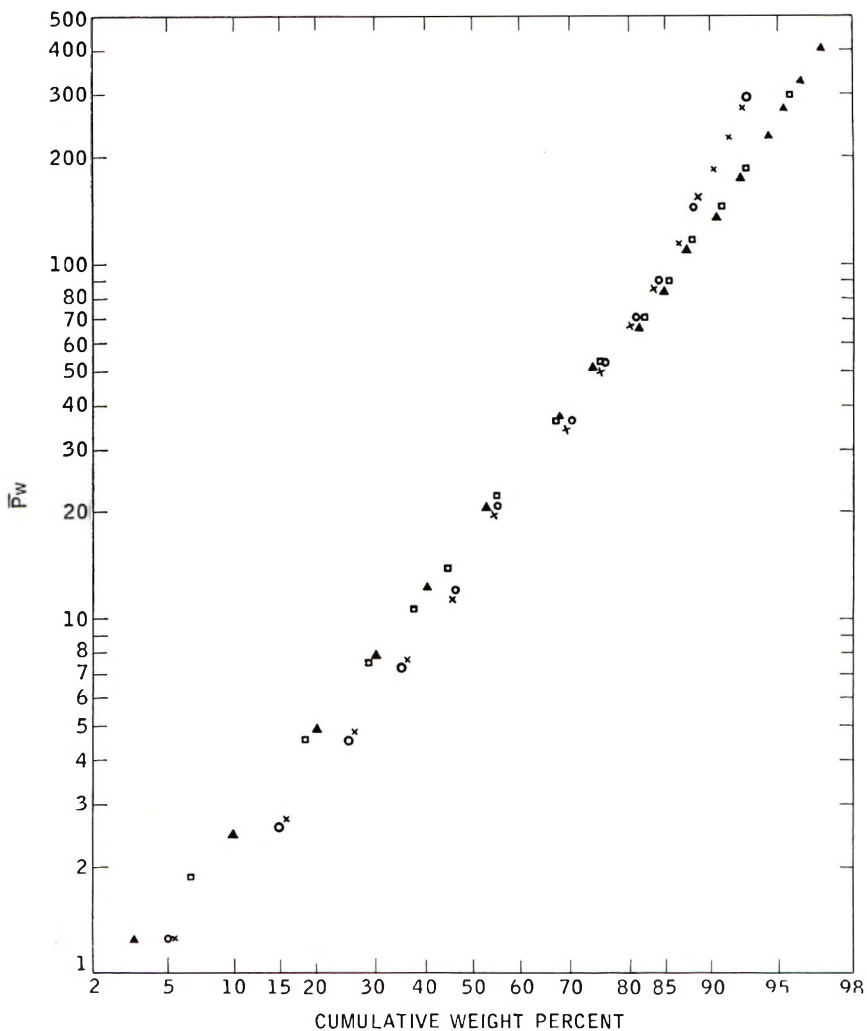


Fig. 10. Integral distribution curves from fractionation data of 50-50 blends: (x) $\bar{P}_w = 55$, $\bar{P}_{w_1} = 1.59 \bar{P}_{w_2}$, $\bar{P}_{w_1}/\bar{P}_{n_1} = \bar{P}_{w_2}/\bar{P}_{n_2} = 21$; (Δ) 50-50 blend, $\bar{P}_w = 55$, $\bar{P}_{w_1} = 1.59 \bar{P}_{w_2}$, $\bar{P}_{w_1}/\bar{P}_{n_1} = \bar{P}_{w_2}/\bar{P}_{n_2} = 11$; (O) single component distribution, $\bar{P}_w/\bar{P}_n = 21$, $\bar{P}_w = 55$; (\square) single component distribution, $\bar{P}_w/\bar{P}_n = 11$, $\bar{P}_w = 55$. Wesslau distributions.

since some of the distinguishing differences will be lost in assuming $M_{w_i} = M_{n_i}$ for all fractions other than the first. In addition, the lack of specific information about the \bar{M}_z/\bar{M}_w ratio of broad distribution severely limits the usefulness of the method.

Comparison of Experimental and Computer Results

In Figure 11 and experimental data on polypropylene reported by Davis and Tobias¹⁹ are compared with the theoretical calculations. The best

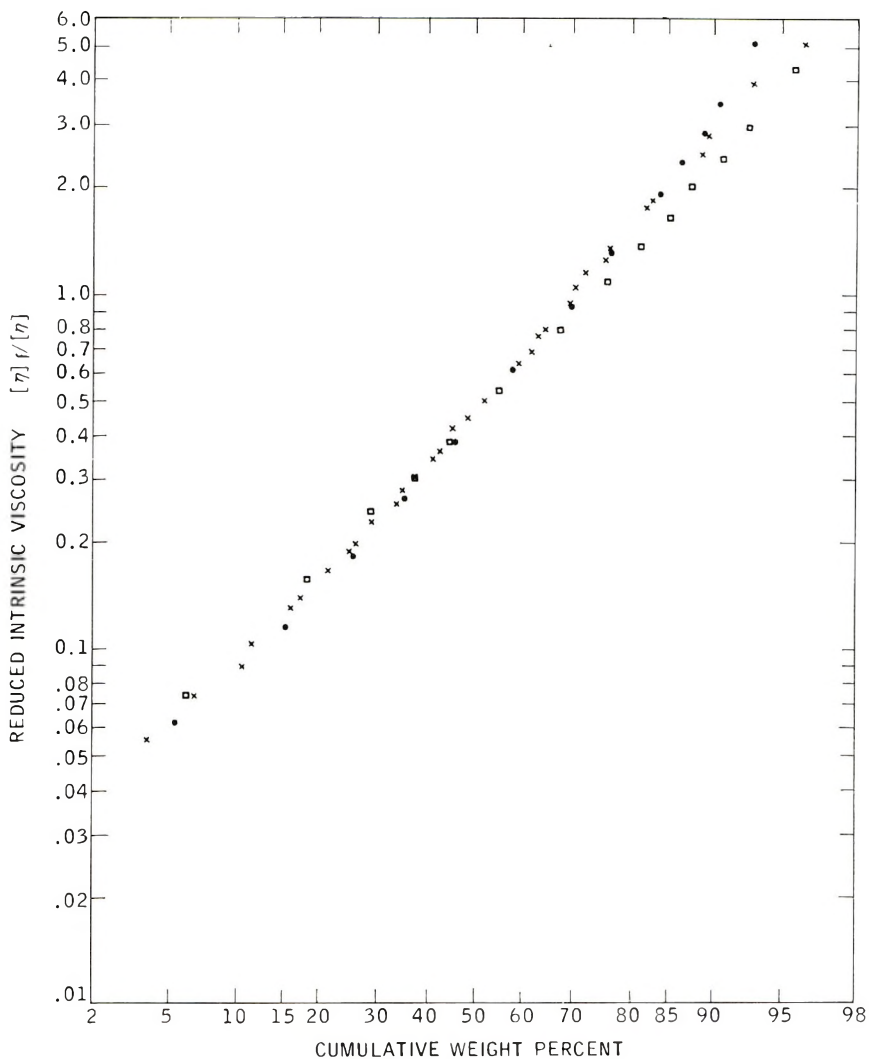


Fig. 11. Integral distribution curve from fractionation data of Wesslau distributions: (●) computer data; (□) $\bar{P}_w/\bar{P}_n = 21$; (x) experimental data of Tobias and Davis.

correlation appears to be with a Wesslau distribution having a \bar{M}_w/\bar{M}_n ratio of 21 although they report a value of 9.8 from numerical integration of the distribution data, and 11.7 from the slope of the Wesslau plot. Comparison of the normalization methods at cumulative weight of 50% and the theoretical \bar{M}_w value of the distribution are in excellent agreement (Table V) confirming the conclusion that the cutoff at $P = 500$ introduces negligible error in all fractions other than the last. This does not mean that it is unimportant, as is shown by the differences in the values of \bar{M}_w/\bar{M}_n . This is due primarily to the significance attributed to the single fraction at 96% cumulative weight relative to the other 36 fractions. This supports

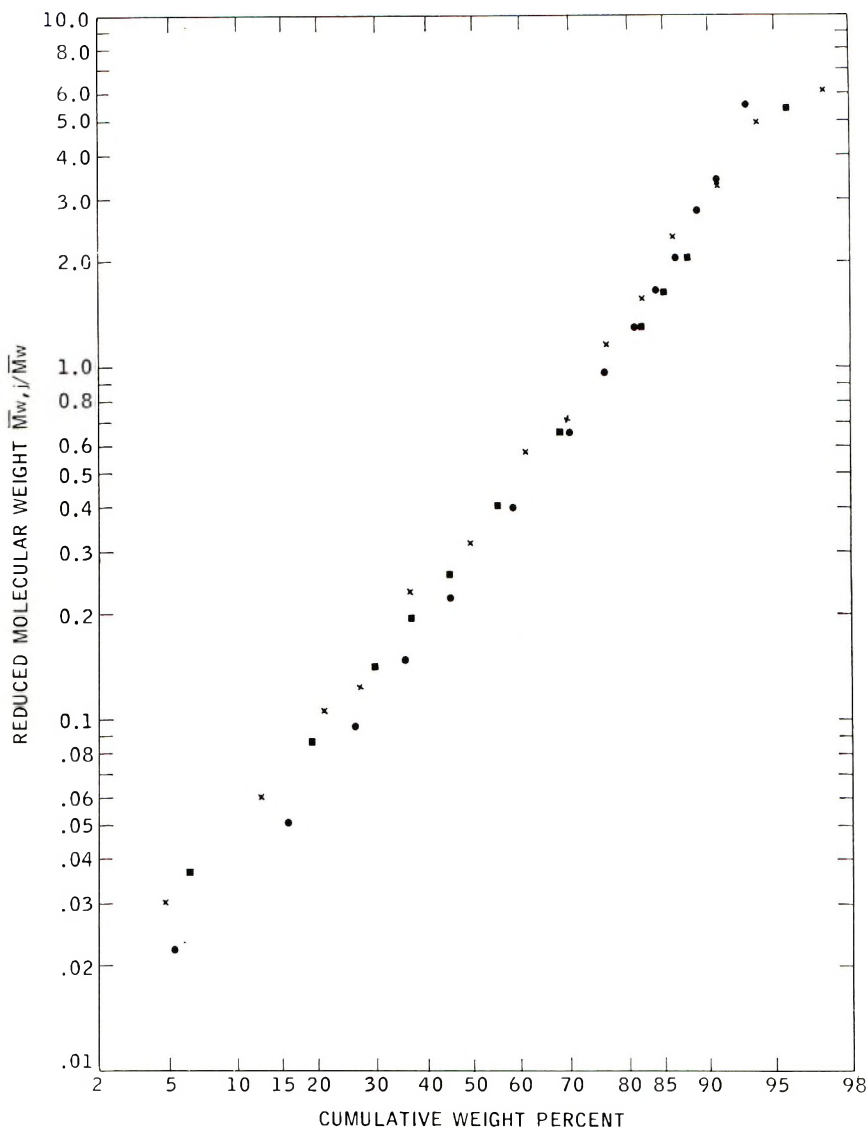


Fig. 12. Integral distribution curve from fractionation data of a Wesslau distribution: (●) $\bar{P}_w/\bar{P}_n = 21$; (■) $\bar{P}_w/\bar{P}_n = 11$; (X) experimental data of Henry, sample A.

the contention made in the theoretical part that the characterization of a distribution type by the \bar{M}_w/\bar{M}_n value may be extremely misleading, particularly with the Schulz-Dinglinger method of obtaining the cumulative sum.

In Figure 12, the experimental data on polyethylene reported by Henry²⁰ are compared with the theoretical calculations. The best fit is a Wesslau type distribution with a \bar{M}_w/\bar{M}_n value of 11, which is in agreement with Henry's evaluation of 10.8. However, the evaluation of the \bar{M}_w from the

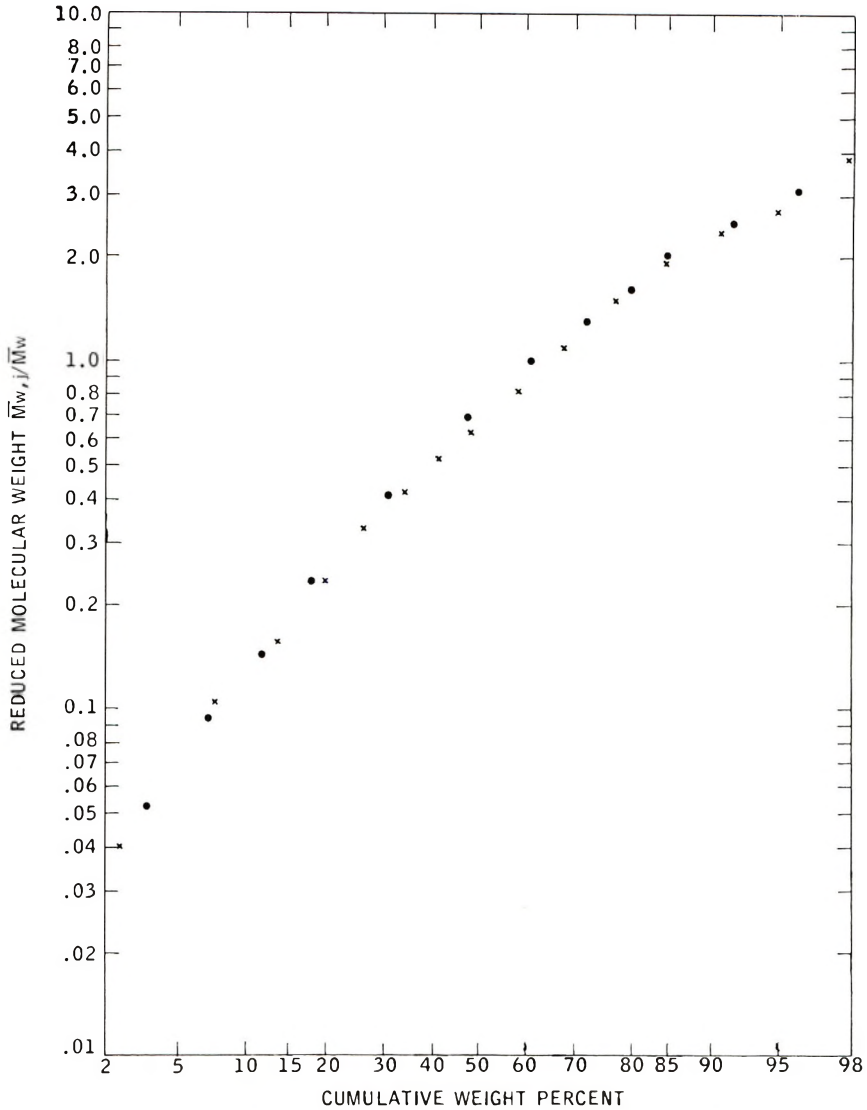


Fig. 13. Integral distribution curve from fractionation data of a Schulz distribution: (●) computer data, $\bar{P}_w/\bar{P}_n = 21$; (X) experimental data of Henry, sample B.

parameters of the distribution yields a value of 1.37×10^5 as compared with 1.06×10^5 obtained by light-scattering measurements. This poor agreement is quite serious and reflects the considerable uncertainty of the value of the parameters and distribution type.

Figure 13 shows the comparison of the computed experimental data of another polyethylene sample reported by Henry.²⁰ Although the reported value for \bar{M}_w/\bar{M}_n is 3.3, the results for a Schulz distribution in the range $\bar{M}_w/\bar{M}_n = 2-21$ show little or no differences, so that any value for \bar{M}_w/\bar{M}_n in this range is equally likely within experimental error.

Figures 5 and 6 show the fractionation data of Krigbaum and Kurz²¹ on previously fractionated and characterized polystyrene; i.e., the number-average and weight-average molecular weight were determined. Since the point of steepest ascent is the number-average molecular weight for a Schulz distribution, there is good correlation of the computer results for the single peak of distribution and rather poor correlation for the bimodal (blend) distribution due to the poor separation of molecular sizes on a solubility basis. Krigbaum interprets the rather poor correlation of the experimental results with theory particularly at the high ends, on the basis of a poor distribution model. However, recent results by Cooper et al.²² attribute

TABLE V
Fractionation Data for Wesslau Distribution $\bar{P}_w/\bar{P}_n = 21$ Normalized to Results of Davis and Tobias

Cumulative wt. fraction	Reduced $[\eta]^a$	Reduced $[\eta]^b$
0.0508	0.0602	0.0615
0.1550	0.1143	0.1168
0.2593	0.1815	0.1855
0.3552	0.2601	0.2658
.4569	0.3765	0.3847
0.5862	0.6000	0.6132
0.6991	0.9054	0.9249
0.7675	1.242	1.269
0.8130	1.570	1.605
0.8417	1.886	1.927
0.8663	2.296	2.346
0.8900	2.804	2.865
0.9079	3.383	3.457
0.9324	5.008	5.118

^a Computed from the calculated $[\eta]$ of the fraction and the theoretical value of $[\eta]$ of the whole polymer.

^b Normalized to the experimental value at 50% cumulative weight.

the rather sharp cutoff in the molecular weight at the high end as back-diffusion of the lower molecular weight species caused by too rapid a change in solvent power along the column. Such a process can cause the differences between the experimental and computer results noted in Figures 9 and 10.

In addition, this new finding casts additional uncertainty on the meaning of all previously published results. The fact that several determinations, refractionation and ultracentrifuge measurements, on middle fractions indicate narrow distributions and that no regression is observed, i.e., the molecular weight of the fractions does not suddenly decrease and then increase with elution, does not necessarily mean that this process is not occurring and skewing the distribution in some unknown way.

Conclusions

The evaluation of the characteristics of molecular weight distributions having an \bar{M}_w/\bar{M}_n ratio greater than about four is at best an extremely uncertain process when the Schulz-Dinglinger cumulative weight approximation is used. In addition, the lack of sensitivity of the fractionation technique to irregularities in the distribution, e.g., due to blending of polymers with different molecular weights, means the experimental results will generally add little or no quantitative information to the understanding of the observed physical measurements.

The best procedure is to fractionate the material into several fractions so that the square root of the second moment about the mean is sufficiently small to allow good characterization of the fraction by the \bar{M}_w/\bar{M}_n ratio and a distribution model, such as a Schulz type. The original distribution may then be obtained by a linear superposition of distributions of the fraction properly weighted by their respective weight fractions. The suggested modification by Tung¹⁶ is a good improvement on the Schulz-Dinglinger method.

The author gratefully acknowledges the very stimulating discussions with Drs. J. Rehner, Jr. and D. Poller and the helpful assistance of Mr. H. Oakley and Miss D. Mahon in the computations.

References

1. Schulz, G. V., and A. Dinglinger, *Z. Physik. Chem.*, **B43**, 47 (1939).
2. Koningsveld, R., and C. A. F. Tuijman, *J. Polymer Sci.*, **39**, 445 (1959).
3. Channen, E. W., *Rev. Pure Appl. Chem.*, **9**, 225 (1959).
4. Guzman, G. M., *J. Polymer Sci.*, **19**, 519 (1956).
5. Flory, P. J., *J. Chem. Phys.*, **12**, 425 (1944).
6. Scott, R. L., and M. Magat, *J. Chem. Phys.*, **13**, 172 (1945).
7. Guggenheim, E. A., *Proc. Roy. Soc. (London)*, **A183**, 203, 213 (1944).
8. Scott, R. L., *J. Chem. Phys.*, **13**, 178 (1945).
9. Sayre, E. V., *J. Polymer Sci.*, **10**, 175 (1953).
10. Broda, A., *J. Polymer Sci.*, **25**, 117 (1957).
11. Broda, A., B. Gawronska, T. Newenska, and S. Potowinski, *J. Polymer Sci.*, **29**, 183 (1958).
12. Broda, A., and M. B. Chodkowska, *J. Polymer Sci.*, **30**, 639 (1958).
13. Schulz, G. V., *Z. Physik. Chem.*, **B47**, 155 (1940).
14. Booth, C., and L. R. Beason, *J. Polymer Sci.*, **42**, 81 (1960).
15. Tung, I. H., *J. Polymer Sci.*, **61**, 449 (1962).
16. Tompa, H., *Polymer Solutions*, Academic Press, New York, 1956, Chap. 7.
17. Schulz, G. V., *Z. Physik. Chem.*, **B43**, 25 (1939); B. H. Zimm, *J. Chem. Phys.*, **16**, 1099 (1948).
18. Wesslau, H., *Makromol. Chem.*, **20**, 111 (1950).
19. Davis, T. E., and R. L. Tobias, *J. Polymer Sci.*, **50**, 227 (1961).
20. Henry, P. M., *J. Polymer Sci.*, **36**, 3 (1959).
21. Krigbaum, W. R., and J. E. Kurz, *J. Polymer Sci.*, **41**, 275 (1959).
22. Cooper, W., G. Vaughan, and J. Yardley, *J. Polymer Sci.*, **59**, 53 (1962).

Résumé

L'estimation de larges distributions de poids moléculaires, basée sur des résultats de fractionnements au moyen des techniques d'élution sur colonne et de l'approximation de Schulz-Dinglinger, est analysée de façon critique au moyen d'un ordinateur électronique et une fonction de solubilité basée sur la théorie de Flory-Huggins. Les résultats, basés sur des distributions du type de Schulz et Wesslau, montrent que, malgré l'établissement possible de certains traits caractéristiques, les valeurs déterminées pour les paramètres de distribution peuvent être fort erronées.

Zusammenfassung

Der Ermittlung breiter Molekulargewichtsverteilungen auf der Basis der durch Säulenelementmethoden und der Schulz-Dinglinger-Näherung erhaltenen Fraktionierungsdaten wird unter Verwendung einer elektronischen Rechenmaschine und einer auf der Flory-Huggins-Theorie basierenden Löslichkeitsfunktion kritisch analysiert. Auf der Grundlage von Verteilungen vom Schulz- und Wesslau-Typ können zwar gewisse charakteristische Züge festgelegt werden, die hieraus bestimmten Werte der Verteilungsparameter können jedoch gross Fehler aufweisen.

Received February 15, 1963

Branching in High Conversion Poly(methyl Methacrylate)*

SONJA KRAUSE and ELIZABETH COHN-GINSBERG, *Research Division, Rohm & Haas Company, Bristol, Pennsylvania*

Synopsis

The dilute solution properties (intrinsic viscosity, weight-average molecular weight, and mean square radius of gyration) of fractions of high conversion, free-radically initiated poly(methyl methacrylate) samples indicate a slight amount of branching in these samples, consistent with the chain transfer constant with polymer (exclusive of endgroups), $C_p = 2.2 \pm 0.7 \times 10^{-5}$, found by Schulz and co-workers. The dilute solution properties of these fractions are compared with those of fractions of low conversion poly(methyl methacrylate) of comparable molecular weight and with the dilute solution properties of fractions of deliberately branched sample, also of comparable molecular weight. Some evidence was obtained which indicated that impurities in the monomer used for polymerization can lead to additional branching sites in the polymer chains.

Introduction

In the free-radically initiated polymerization of pure methyl methacrylate, chain branching can occur only by means of chain transfer with polymer. Since there is no obvious site on the poly(methyl methacrylate) molecule for chain transfer to occur, the chain transfer constant with polymer is expected to be very small and most samples of the polymer are expected to contain only unbranched (linear) molecules. In spite of this expectation, Schulz and co-workers¹ found rather large values for the chain transfer constant of growing methyl methacrylate radicals with preformed poly(methyl methacrylate) in their first experiments. Since these values depended on the molecular weight of the preformed polymer, Schulz and co-workers were able to determine that their measured values for this chain transfer constant were really the sums of two chain transfer constants with the polymer, one with an endgroup and one with the rest of the polymer chain. Only the second of these, which will be referred to as C_p , is concerned with branching of the molecules.

Schulz and co-workers,¹ in their first paper on this subject, had found a value of 1.5×10^{-4} for C_p at 50°C. In a later paper,² however, they found a lower value, $2.2 \pm 0.7 \times 10^{-5}$. They attributed the larger value, found previously, to impurities in the benzene in which their preformed polymer

* Presented, in part, at the 135th Meeting of the American Chemical Society, Boston, Mass., April 1959.

had been polymerized. They assumed that these impurities had polymerized with the monomer and had been present in the polymer chains as sites having a greater tendency toward chain transfer than the polymer chains alone. Morton and Piirma³ found values for C_p of 2.10×10^{-4} at 60°C. and 2.48×10^{-4} at 80°C. In the light of the work done by Schulz' group, these values can probably be attributed, in part, to impurities in the polymer chains.

It is possible to calculate the extent of branching to be expected for poly-(methyl methacrylate) depending upon the extent of conversion at which the polymerization is stopped. Assuming a bulk polymerization, i.e., no solvent present, the average degree of polymerization per branch in the polymer chain, γ , can be calculated from:⁴

$$1/\gamma = -C_p[1 + (1/\theta) \ln(1 - \theta)] \quad (1)$$

where θ is the conversion at which the polymerization is stopped.

Table I shows calculated values of γ , at various degrees of conversion of monomer to polymer, for two of the experimental values of C_p . Calculations were not made beyond fractional conversions above 0.90, since Schulz and Harborth⁵ found that polymerization ended at about this conversion at 50°C. in the bulk polymerization of methyl methacrylate. In order to obtain conversions greater than 0.90, the sample must generally be heated to reduce the viscosity. It will be seen below that samples that have been subjected to this extra heating step, usually called curing, do not appear to be more branched than those which have not been cured.

TABLE I
Calculated Degree of Polymerization per Branch for Two Values of C_p

Conversion θ	Value of γ	
	$C_p = 2.2 \times 10^{-5a}$	$C_p = 2.1 \times 10^{-4b}$
0.05	1.75×10^6	1.83×10^5
0.10	8.40×10^5	8.85×10^4
0.25	3.01×10^5	3.16×10^4
0.50	1.17×10^5	1.23×10^4
0.90	2.92×10^4	3.06×10^3

^a Data of Schultz et al.²

^b Data of Morton and Piirma.³

It can be seen from Table I that virtually no branching is to be expected at conversions less than 0.10, whether the higher or the lower value of the chain transfer constant is the correct one. If the lower value of C_p is the correct one, branching should only be observed in very high molecular weight samples at very high conversions of monomer to polymer. For this reason, the samples in which we attempted to observe branching all had weight-average molecular weights above 2×10^6 .

Branching in polymers can be studied by a combination of dilute solution data from intrinsic viscosity and light-scattering measurements. In

general, it is necessary to compare data obtained with narrow fractions of the linear polymer with data obtained with the best achievable fractions from the polymer which is suspected of being branched. Data on fractions of equal molecular weight and of the narrowest possible molecular weight distribution must be compared because most theoretical calculations of the effect of branching on dilute solution properties have been made for monodisperse samples. Polydispersity affects the same dilute solution properties that are affected by branching, although not necessarily in the same way.

The particular dilute solution properties studied in this work are the root mean square radius of gyration as obtained from light-scattering measurements, and the intrinsic viscosity. Zimm and Stockmayer⁶ first calculated the reduction to be expected in the mean square radius of gyration of polymer molecules which contained different numbers and types of branches. They included the case of trifunctional branch points with a random distribution of chain lengths in the branches; this case is the one to be expected when branching occurs during polymerization by means of chain transfer with polymer. In this treatment, the degree of branching is identified with a factor, g , which is equal to 1.0 for an unbranched polymer and decreases with increased branching and which is defined as:

$$g = (\bar{s}^2)_{br}/(\bar{s}^2)_{st} \quad (2)$$

where $(\bar{s}^2)_{br}$ and $(\bar{s}^2)_{st}$ refer to the mean square radius of gyration of the branched polymer and of the straight-chain polymer of equal molecular weight, respectively.

There have been a number of attempts in the literature to relate the factor, g , to the intrinsic viscosities of the polymers. For a number of years, the equation of Thurmond and Zimm⁷ was used:

$$g = ([\eta]_{br}/[\eta]_{st})^{2/3} \quad (3a)$$

but this has recently been supplanted by:

$$g = ([\eta]_{br}/[\eta]_{st})^2 \quad (3b)$$

as derived by Zimm and Kilb.⁸ In all cases, the factor g is related back to the actual degree of branching in the samples through the calculations of Zimm and Stockmayer.⁶

In a study on branch formation in polyacrylamide, Gleason, Miller, and Sheats⁹ demonstrated the validity of the Zimm-Stockmayer treatment in connection with eq. (2), while Cantow, Meyerhoff, and Schulz¹⁰ and Morton and co-workers¹¹ demonstrated the validity of eq. (3b). Stockmayer and Fixman¹² have shown that eq. (3a) does not fit the available experimental data. In the present work, eqs. (2) and (3b) were used in conjunction with the Zimm-Stockmayer calculations in order to obtain the extent of branching in fractions of high conversion poly(methyl methacrylate).

EXPERIMENTAL

Samples

Two samples of high molecular weight, low conversion poly(methyl methacrylate) were studied in this work. One of these, LI, was polymerized from Rohm and Haas plant grade uninhibited monomer in bulk at 60°C., azobisisobutyronitrile (AIBN) being used as initiator. The mixture was taken to 8.9% conversion; the polymer was recovered by precipitating from Skellysolve B (*n*-hexane) and then freeze-drying from benzene. The second low conversion sample, LII, was polymerized in a 50 wt.-% distilled benzene solution at 60°C. with AIBN as initiator. The monomer for this sample was distilled before use in a spinning band column at reduced pressure. Polymerization was taken to 13.6% conversion, and the polymer was recovered in the same way as sample LI.

Four samples of high conversion poly(methyl methacrylate) were studied in this work. One of these, HI, was polymerized in bulk at 60°C. overnight with AIBN as initiator. The monomer was purified in the same way as that used for sample LII. The resulting polymer was dissolved in chloroform and was then recovered in the same way as sample LI. Samples HII and HIII were high conversion, suspension-polymerized poly(methyl methacrylates). Both were polymerized for about 6 hr. at 60°C. under nitrogen with AIBN as initiator; sample HII was then "cured" at 120–125°C. for 5 hr. under vacuum, while sample HIII was not cured. Sample HIV was a sheet of commercial Plexiglas (trademark of Rohm & Haas Co.), cast poly(methyl methacrylate).

One sample of deliberately branched poly(methyl methacrylate), sample BI, was studied in this work. This sample was made by using a very small amount of ethylene dimethacrylate (0.0014 g./59.94 g. methyl methacrylate) as comonomer. The sample was suspension polymerized at 60–65°C., and was cured at 120–125°C. Ethylene dimethacrylate has been used by Smets and Schmets¹³ to prepare branched poly(methyl methacrylate).

Fractionation

All the samples were fractionated from benzene solution at 30.0°C. with Skellysolve B as nonsolvent. The main fractionations were generally from 0.5% solution, and the subfractionations of some of the fractions were from 0.1% solution.

Intrinsic Viscosities

The intrinsic viscosity measurements were obtained in Cannon-Ubbelohde No. 75 semimicro viscometers in which the solvent flow times exceeded 90 seconds so that no kinetic energy corrections were necessary. Reagent grade acetone and benzene were used for almost all viscosity determinations. In a few cases which will be noted under Results, dis-

tilled acetone was used in order to make sure that impurities in the reagent grade solvents had no great effect on the intrinsic viscosities. At least three concentrations of each sample were run in order to extrapolate to the intrinsic viscosity in each case.¹⁴

Light Scattering

Distilled reagent grade acetone was used for all light-scattering measurements. The refractive index increment, dn/dc , of poly(methyl methacrylate) in acetone at 25°C. was previously measured in this laboratory,¹⁵ 0.136 and 0.134 ml./g. at 436 m μ and 546 m μ , respectively. Light-scattering measurements were made at 436 m μ and at 546 m μ in a Brice-Phoenix light-scattering photometer at scattering angles from 30 or 45 to 135°, depending on the sample. At least five concentrations were run for each sample. The method used in this laboratory for obtaining the instrument calibration constant and for calculating the weight-average molecular weight and the radius of gyration from the experimental data have been described previously.¹⁶

RESULTS

The dilute solution data for fractions of sample LII were used as the reference data, $[\eta]_{st}$ and $(\bar{s}^2)_{st}$, in eqs. (2) and (3b) since this was the purest sample of free-radically initiated, low conversion, high molecular weight poly(methyl methacrylate) available. The data used to calculate reference $[\eta]-M$ and $(\bar{s}^2)^{1/2}-M$ relationships for high molecular weight poly(methyl methacrylate) are shown in Table II.

TABLE II
Dilute Solution Properties of the Fractions of the Reference Sample, LII

Fraction No.	$[\eta]$ (30° C., acetone), dl./g.	$\bar{M}_w \times 10^{-6}$		$(\bar{s}^2)^{1/2}$, A.	
		436 m μ	546 m μ	436 m μ	546 m μ
1A1	5.74	11.6	11.0	1590	1570
1B	3.63	6.51	5.91	1050	1030
2A	4.62	8.06	7.74	1260	1130
3	2.88	4.67	4.50	890	850
4	2.64	3.57	3.66	740	760
5	2.15	2.79	2.70	630	610
9	1.51	1.61	1.45	440	420
11, 12	1.09	1.01	0.96 _s	350	320

The data presented in Table II, together with $[\eta]-\bar{M}_w$ data obtained by Fox et al.¹⁷ for low conversion poly(methyl methacrylate) fractions whose weight-average molecular weights exceeded 2×10^6 were used to derive:

$$[\eta] = 1.40 \times 10^{-4} M^{0.654} \quad (4)$$

and

$$(\bar{s}^2)^{1/2} = 4.65 \times 10^{-2} M^{0.641} \quad (5)$$

Equation (4) is quite different from the relationship:

$$[\eta] = 7.7 \times 10^{-5} M^{0.70} \quad (6)$$

obtained in acetone by Fox and co-workers¹⁷ for all their fractions, whose molecular weights varied from 9×10^4 to 3×10^6 . Four of the fractions used to determine eqs. (4) and (6) were the same. The large discrepancy probably could be traced back to the shear dependence of the intrinsic viscosity which often becomes evident when the intrinsic viscosity exceeds 2 dl./g. The measured intrinsic viscosities for the highest molecular weight fractions were probably much lower than those which would have been obtained at negligible shearing stress. Cantow and co-workers¹⁸ showed that the measured intrinsic viscosity in acetone of a poly(methyl methacrylate) fraction whose \bar{M}_w was 5.83×10^6 changed from 3.6 dl./g. at a shear rate of 5000 sec.⁻¹ to 3.8 dl./g. at a shear rate of 0.25 sec.⁻¹. The Cannon-Ubbelohde semimicro No. 75 viscometers used to obtain the intrinsic viscosities shown in Table II probably result in a shear rate somewhat below 5000 sec.⁻¹.

The proper equation relating intrinsic viscosity and molecular weight for poly(methyl methacrylate) in acetone in cases in which no shear dependence on viscosity is expected (molecular weights below 3×10^6) should be eq. (6). Equation (4) is strictly a utilitarian equation, valid when using a Cannon-Ubbelohde No. 75 semimicro viscometer, i.e., eq. (4) should have no theoretical significance as it stands.

The alternation of numbers and letters in the fraction number designations in Table II and in subsequent tables indicates various stages of fractionation and subfractionation. For example, the designation 1A1 in Table II indicates the first subfraction of fraction 1A, which, in turn, was the first subfraction of fraction 1 of the sample. In some of the subsequent tables, data on some fractions *and* on their subfractions will be shown. In

TABLE III
Dilute Solution Properties of Low Conversion Sample LI

Fraction No.	[η] (30° C., acetone), dl./g.	$\bar{M}_r \times 10^{-6}$ [eq. (4)]	$\bar{M}_w \times 10^{-6}$		$(\bar{s}^2)^{1/2}$, A. (436 m μ)
			436 m μ	546 m μ	
1A	5.17	9.2	11.7	13.5	1500
1B	4.26	6.9	7.67	9.86	1150
2A	4.02	6.4	7.48	9.42	1140
2B1	3.68	5.55	6.17	5.99	1000
	3.60 ^a	5.4			
2B1A	3.94	6.2	10.6	10.7	1340
2B1B	3.24	4.6	6.68	7.71	1050
3	2.94	3.95	4.95	5.70	920
	3.05 ^a	4.2			
4B	2.01	2.22	3.07	3.65	670
	2.16 ^a	2.47			

^a Intrinsic viscosity taken in the distilled solvent used for light scattering.

TABLE IV
 Dilute Solution Data of High Conversion Samples

Sample	Fraction No.	[η] (30° C., acetone), $M_v \times 10^{-6}$		$\bar{M}_w \times 10^{-6}$		$(\bar{s}^2)^{1/2}$, A. (436 m μ)
		dl./g.	[eq. (4)]	436 m μ	546 m μ	
HI	1B	4.42	7.4	8.9 ₆	7.9 ₀	1260
	1C	3.58	5.35	6.34	5.80	1020
	2	2.27	2.65	3.71	3.48	670
HII	1	4.04	6.5	9.3	11.8	1390
	2	2.83	3.75	4.33	4.84	860
	4	1.56	1.53	1.92	2.14	—
HIII	1A	4.06	6.45	10.9	13.6	1420
	1B	4.00	6.35	8.64	10.2	1170
HIV	1F1	4.22	6.9	9.1	10.9	1400
	1F2	3.46	5.1	6.04	6.48	1010
	1F3	2.91	3.90	4.58	4.54	850
	1F4	—	—	3.68	3.61	680
	1F5	2.20	2.55	3.09	4.13	650
	2F1	3.98	6.3	7.71	9.38	1160
	2F1A	4.56	7.7	9.91	11.6	1320
	2F1A1A	4.60	7.9	18.7	19.8	1710
	2F1A2A	3.98	6.3	7.2	8.34	990

this way, the effects of subfractionation, which should make the fractions more homogeneous, can be observed.

Table III contains the dilute solution data obtained on sample LI, the low conversion sample which was prepared from monomer which was not purified as carefully as the monomer from which sample LII was prepared.

Table IV contains the dilute solution data of fractions of the various high conversion poly(methyl methacrylate) samples studied.

The fraction numbers under sample HIV which start with 1F and with 2F refer to fractions from two different fractionations of this sample. The molecular weights of fraction 2F1 are less than those of fraction 1F1

 TABLE V
 Dilute Solution Data on Deliberately Branched Poly(methyl Methacrylate), B1

Fraction No.	[η] (30° C., acetone), $\bar{M}_v \times 10^{-6}$		$\bar{M}_w \times 10^{-6}$		$(\bar{s}^2)^{1/2}$, A. (436 m μ)
	dl./g.	[eq. (4)]	436 m μ	546 m μ	
1	2.66	3.40	9.91	11.1 ₉	1330
1A	3.46	5.1	15.3	16.5	1530
	3.45 ^a	5.1			
1B	1.54	1.55	3.16	3.68	790
2	2.16	2.50	4.18	4.52	810
2A	2.50	3.12	6.8	—	900
2B	1.84	1.95	3.43	3.75	680
4	1.78	1.84	2.65	3.05	600

^a Intrinsic viscosity was run in distilled solvent used for light scattering.

because fraction 2F1 represented a much greater percentage of the total sample.

Table V contains the dilute solution data obtained on fractions of the deliberately branched sample, B1.

DISCUSSION

The calculated viscosity-average molecular weights of sample LI, HI through HIV, and B1 fractions all fall appreciably below the weight-average molecular weights of those fractions. In the absence of other data, this could be ascribed to molecular weight polydispersity in the fractions instead of branching. It will be observed that the same in-

TABLE VI
Branching Parameters, g , for Poly(methyl Methacrylate) Fractions

Sample	Fraction No.	$(\bar{s}^2)_{br}^{1/2}$, A.	$(\bar{s}^2)_{st}^{1/2}$, A [eq. (5)]	g [eq. (2)]	$[\eta]_{br}$, dl./g.	$[\eta]_{st}$, [eq. (4)], dl./g.	g [eq. (3b)]
LI	1A	1500	1620	0.86	5.17	6.00	0.74
	1B	1150	1280	0.81	4.26	4.73	0.81
	2A	1140	1250	0.83	4.02	4.61	0.76
	2B1	1000	1050	0.91	3.68	3.73	0.97
	2B1A	1340	1440	0.87	3.94	5.31	0.55
	2B1B	1050	1120	0.88	3.24	4.18	0.60
	3	920	930	0.98	2.94	3.42	0.74
HI	4B	670	690	0.94	2.01	2.55	0.62
	1B	1260	1250	"	4.42	4.61	0.92
HII	1C	1020	1010	"	3.58	3.72	0.92
	2	670	720	0.87	2.27	2.68	0.72
	1	1390	1440	0.93	4.04	5.31	0.58
HIII	2	860	840	"	2.83	3.11	0.83
	4	—	—	—	1.56	1.85	0.71
	1A	1420	1580	0.81	4.06	5.82	0.49
HIV	1B	1170	1340	0.76	4.00	4.96	0.65
	1F1	1400	1400	"	4.22	5.30	0.63
	1F2	1010	1030	0.96	3.46	3.81	0.82
	1F3	850	840	"	2.91	3.11	0.88
	1F4	680	730	0.87	—	—	—
	1F5	650	730	0.79	2.20	2.68	0.67
	2F1	1160	1250	0.86	3.98	4.62	0.74
	2F1A	1320	1450	0.83	4.56	5.35	0.44
	2F1A1A	1710	2110	0.66	4.60	7.80	0.32
	2F1A2A	990	1180	0.70	3.98	4.35	0.84
B1	1	1330	1440	0.85	2.66	5.31	0.25
	1A	1530	1880	0.66	3.46	6.80	0.26
	1B	790	700	"	1.54	2.60	0.35
	2	810	810	"	2.16	3.02	0.51
	2A	900	1080	0.69	2.50	4.01	0.39
	2B	680	720	0.89	1.84	2.66	0.48
	4	600	620	0.94	1.78	2.30	0.60

* Calculation of branching parameter would be meaningless when $(\bar{s}^2)_{br}^{1/2} \geq (\bar{s}^2)_{st}^{1/2}$.

formation in Table VI which is used to calculate the branching parameter, g , from eqs. (2) and (3b) indicates that in most cases polydispersity of molecular weight in the fractions cannot be used to explain the data.

In Table VI, $(\bar{S}^2)_{st}^{1/2}$ and $[\eta]_{st}$ were calculated for each fraction from eqs. (4) and (5) by using the average weight-average molecular weight of that fraction.

The branching parameter calculated from the root mean square radii of gyration by means of eq. (2) is expected, in general, to underestimate the extent of branching in the polymer, i.e., it is expected to be too high. Molecular weight polydispersity in a fraction increases the value of the root mean square radius of gyration as obtained from light-scattering measurements above the value to be expected for a monodisperse fraction of the same weight-average molecular weight since the radius of gyration as determined by light scattering depends on a higher average of the molecular weight than the weight-average. On the other hand, the branching parameter calculated from the intrinsic viscosities by means of eq. (3b) can be expected to overestimate the extent of branching in the polymer, i.e., it is expected to be too low. Molecular weight polydispersity decreases the value of the intrinsic viscosity below that expected for a monodisperse fraction of the same molecular weight. In other words, both branching and polydispersity decrease the intrinsic viscosity. The branching parameter calculated for a sample from eq. (5) should be higher than that calculated for the same sample from eq. (3b). The true branching parameter for that sample should be somewhere between those two values. There are only two fractions in Table VI, sample LI fraction 2B1, and sample HIV fraction 2F1A2A, for which the branching parameter calculated from intrinsic viscosity is greater than that calculated from the root mean square radius of gyration. This can probably be ascribed to experimental error in one of the measurements. There are seven fractions in Table VI for which the branching parameter would have been equal to or greater than one if calculated from the radii of gyration. This might be ascribed to experimental error in the case of fractions 1B

TABLE VII
Average Number of Branches per Molecule as a Function of g

g	Avg. No. branches
0.976	0.250
0.953	0.500
0.912	1.000
0.840	2.000
0.784	3.000
0.73	4.00
0.69	5.00
0.58	10.0
0.50	15.0
0.32	50.0

TABLE VIII
Molecular Weight per Branch in Poly(methyl Methacrylate) Fractions

Sample	Fraction No.	No. of branches per molecule			$\bar{M}_w \times 10^{-6}$	Degree of polymerization per branch $\gamma \times 10^{-4}$
		From $[\eta]$	From $(\bar{s}^2)^{1/2}$			
LI	1A	3.8	1.8	12.6	3.3-7.0	
	1B	2.6	2.6	8.76	3.4	
	2A	3.4	2.2	8.45	2.5-3.8	
	2B1	0.3	1.0	6.08	6.1-20	
	2B1A	11.5	1.6	10.6	0.9-6.6	
	2B1B	8.8	1.4	7.20	0.8-5.1	
	3	3.8	0.2	5.32	1.4-10.6	
	4B	7.8	0.6	3.36	0.4-5.6	
HI	1B	1.0	0	8.43	8.4-∞	
	1C	1.0	0	6.07	6.1-∞	
	2	4.3	1.6	3.60	0.8-2.2	
HII	1	9.8	0.8	10.6	1.1-13	
	2	2.2	0	4.58	2.1-∞	
	4	4.6	—	2.03	0.4	
HIII	1A	15.7	2.5	12.2	0.8-4.9	
	1B	6.5	3.5	9.42	1.4-2.7	
HIV	1F1	7.4	0	10.0	1.4-∞	
	1F2	2.4	0.4	6.27	2.6-15.7	
	1F3	1.4	0	4.56	3.3-∞	
	1F4	—	1.6	3.64	2.3	
	1F5	5.8	2.9	3.61	0.6-1.2	
	2F1	3.8	1.6	8.54	2.2-5.3	
	2F1A	20.7	2.2	10.7	0.5-4.9	
	2F1A1A	50	6.1	19.2	0.4-3.1	
	2F1A2A	2.0	4.8	7.7	1.6-3.8	
B1	1	>50	1.9	10.6	<0.5-5.6	
	1A	>50	6.1	15.9	<0.3-2.6	
	1B	38	0	3.42	0.1-∞	
	2	14.2	0	4.35	0.3-∞	
	2A	28	5.1	6.8	0.2-1.3	
	2B	16.5	1.3	3.59	0.2-2.8	
	4	8.8	0.6	2.85	0.3-4.8	

and 1C from sample HI and in the case of fraction 1F3 from sample HIV since, in those cases, the branching parameter calculated from intrinsic viscosity is 0.9, i.e., it indicates little branching. In the other cases, however, polydispersity in the fractions has canceled out the effect, if any, of branching in lowering the root mean square radius of gyration.

Table VII shows the total number of branches per molecule as a function of g as calculated for trifunctional branch units with branches of random length by Zimm and Stockmayer.⁶

Table VIII shows the number of branches per molecule calculated from both values of g obtained for each fraction. The table also shows the weight-average degree of polymerization per branch as calculated from

these values and from the average weight-average molecular weight of each fraction.

Because of the molecular weight heterogeneity in the fractions, the number of branches per molecule calculated from intrinsic viscosities is quite different, sometimes by an order of magnitude, from the number of branches calculated from radii of gyration. For this reason, it would probably not be advisable to try to calculate values of the chain transfer constant with polymer from the data in Table VIII. However, these calculations can be compared with the calculations in Table I to show the order of magnitude of the chain transfer constant with polymer necessary to give the observed amount of branching.

Since the deliberately branched sample, B1, was prepared by a method other than chain transfer with polymer, its dilute solution properties should not be used to obtain such a chain transfer constant. The data on this sample have been calculated up to this point in order to show that the dilute solution data of fractions of a deliberately branched sample show the same trends as those of the samples in which branching was only surmised.

Of the four high conversion samples of poly(methyl methacrylate) investigated, only sample HI was prepared from purified monomer. The degree of polymerization per branch found for this sample seems to be somewhat higher than the values found for fractions of HII, HIII, and HIV. It is possible that impurities in the monomer contributed somewhat to the branching sites in the polymer in the manner discussed by Schulz et al.² Assuming 90% conversion for sample HI, as discussed in the introduction, the expected degree of polymerization per branch would be 3×10^4 , using the lowest experimentally determined value of C_p for which calculations were made in Table I. The calculations for sample HI in Table VIII indicate that except for fraction 2, the degree of polymerization per branch may be even higher than this expected value. Although this could be taken to indicate that the chain transfer constant with polymer is even lower than the lowest value found by Schulz et al.,² it may simply indicate that the degree of conversion in the polymerization was not quite 90%. Possibly, the fractionation separated the sample into more branched and less branched fractions. At any rate, the observed values of γ are much too high to be consistent with the chain transfer constant found by Morton and Piirma.³ Samples HII and HIV, which were taken to 100% conversion by a high temperature "curing" step, do not seem to be very much more branched than the noncured samples, HI and HIII.

It was disturbing to note that one low conversion sample of poly(methyl methacrylate), sample LI, exhibited about the same amount of branching, i.e., had about the same degree of polymerization per branch, as the high conversion samples. Since this sample was taken to only 9% conversion in its polymerization, the degree of polymerization per branch, using Schulz's lowest experimental value of C_p , should have been greater than 8×10^5 . Even for Morton and Piirma's much greater value of C_p , $2.1 \times$

10^{-4} , the expected degree of polymerization per branch is greater than 9×10^4 according to Table I. The data in Table VIII are consistent with a chain transfer constant with polymer of the order of magnitude of 10^{-4} . When Schulz and co-workers¹ found such a chain transfer constant with polymer in their first set of experiments, they were forced to attribute it to impurities which had polymerized with the monomer and had then acted as sites in the polymer chain having a greater chain transfer constant than the monomer units in the polymer chains. The same hypothesis will have to be used here to explain the data on sample LI. The impurities which are to blame for the branching in sample LI can apparently be removed by distillation of the uninhibited monomer, since sample LII did not show this branching.

CONCLUSIONS

The two main conclusions from this work are: (1) the degree of branching observed in fractions of high conversion free-radically initiated poly-(methyl methacrylate) is consistent with the chain transfer constant with polymer, $C_p = 2.2 \times 10^{-5}$ found by Schulz and co-workers,² and (2) impurities in the polymerization mixture may lead to extra branching sites in the polymer chains; the impurities in uninhibited monomer are removable by means of careful distillation.

Thanks are due to Dr. J. C. H. Hwa, Mr. L. Miller, and Mr. J. Gormley for providing some of the polymer samples used in this work and to Mr. C. F. Ryan for aid in preparing the samples made from distilled monomer, to Miss I. L. Scogna and Mrs. E. Cherry, who fractionated most of the samples, to Mr. V. McFadden, Mr. W. Buggy, Mr. J. Begley, and Mrs. R. Collis who obtained the intrinsic viscosities of the samples, and to Dr. S. Gratch for some helpful discussions.

References

1. Schulz, G. V., G. Henrici, and S. Olivé, *J. Polymer Sci.*, **17**, 45 (1955).
2. Henrici-Olivé, G., S. Olivé, and G. V. Schulz, *Makromol. Chem.*, **23**, 207 (1957).
3. Morton, M., and I. Piirma, *J. Am. Chem. Soc.*, **80**, 5596 (1958).
4. Flory, P. J., *J. Am. Chem. Soc.*, **69**, 2893 (1947).
5. Schulz, G. V., and G. Harborth, *Makromol. Chem.*, **1**, 106 (1947).
6. Zimm, B. H., and W. H. Stockmayer, *J. Chem. Phys.*, **17**, 1301 (1949).
7. Thurmond, C. D., and B. H. Zimm, *J. Polymer Sci.*, **5**, 477 (1952).
8. Zimm, B. H., and R. W. Kilb, *J. Polymer Sci.*, **37**, 19 (1959).
9. Gleason, E. H., M. L. Miller, and G. F. Sheats, *J. Polymer Sci.*, **38**, 133 (1959).
10. Cantow, M., G. Meyerhoff, and G. V. Schulz, *Makromol. Chem.*, **49**, 1 (1961).
11. Morton, M., T. E. Helminiak, S. D. Gadkary, and F. Bueche, *J. Polymer Sci.*, **57**, 471 (1962).
12. Stockmayer, W. H., and M. Fixman, *Ann. N. Y. Acad. Sci.*, **57**, 334 (1953).
13. Smets, G., and J. Schmets, *Bull. Soc. Chim. Belges*, **62**, 358 (1953).
14. Fox, T. G., J. B. Kinsinger, H. F. Mason, E. M. Schuele, *Polymer*, **3**, 71 (1962).
15. Cohn, E. S., and E. M. Schuele, *J. Polymer Sci.*, **14**, 309 (1954).
16. Krause, S., and E. Cohn-Ginsberg, *Polymer*, **3**, 565 (1962).
17. Cohn-Ginsberg, E., T. G. Fox, and H. F. Mason, *Polymer*, **3**, 97 (1962).
18. Cantow, H. J., J. Pouget, and C. Wippler, *Makromol. Chem.*, **14**, 110 (1954).

Résumé

Les propriétés de solutions dilués (viscosité intrinsèque, poids moléculaire moyen en poids et rayon de gyration quadratique moyen) d'échantillons de polyméthacrylate de méthyle initiés par les radicaux libres et obtenus à taux de conversion élevés présentent une faible quantité de ramifications en accord avec la constante de transfert sur polymère (à l'exclusion des groupes terminaux), $C_p = 2.2 \pm 0.7 \times 10^{-3}$, trouvée par Schulz et ses collaborateurs. Des propriétés des solutions diluées de ces fractions sont comparées à celles de fractions de polyméthacrylate de méthyle obtenu à faible conversion et de poids moléculaire semblable, de même qu'avec les propriétés de solution diluée de fractions d'un échantillon intentionnellement ramifié, également de poids moléculaire comparable. On montre que les impuretés présentes dans le monomère utilisé pour la polymérisation peut produire de sites de ramification supplémentaires dans les chaînes polymériques.

Zusammenfassung

Die Eigenschaften von Fraktionen von radikalisch bei hohem Umsatz erhaltenen Polymethylmethacrylatproben in verdünnter Lösung (Viskositätszahl, Gewichtsmittel des Molekulargewichts und mittleres Gyrationradiusquadrat) lassen bei diesen Proben eine geringe Verzweigung erkennen, die der von Schulz und Mitarbeitern bestimmten Übertragungskonstanten des Polymeren (ausschliesslich der Endgruppen), $C_p = (2,2 \pm 0,7) \times 10^{-3}$, entspricht. Die Eigenschaften dieser Fraktionen in verdünnter Lösung werden mit denjenigen von Fraktionen von bei niedrigem Umsatz erhaltenen Polymethylmethacrylat von vergleichbarem Molekulargewicht sowie mit den Eigenschaften von Fraktionen einer absichtlich verzweigten Probe, ebenfalls von vergleichbarem Molekulargewicht, in verdünnter Lösung verglichen. Gewisse Hinweise darauf, dass Verunreinigungen in dem zur Polymerisation verwendeten Monomeren zu zusätzlichen Verzweigungstellen in der Polymerkette führen können, wurden erhalten.

Received February 21, 1963

Vinyl Polymerization. LXXIII. Polymerization and Copolymerization of Bornyl or Isobornyl Methacrylate

MINORU IMOTO, TAKAYUKI OTSU, KAZUICHI TSUDA, and
TOSHIO ITO, *Faculty of Engineering, Osaka City University,
Minamiogimachi, Kita-ku, Osaka, Japan*

Synopsis

A study of the radical polymerization and copolymerization of bornyl (endo-bornyl) methacrylate (BMA) or isobornyl (exo-bornyl) methacrylate (IBMA) with styrene has been made at 50–70°C. BMA polymerized faster than IBMA, and the polymer obtained from BMA (PBMA) was higher in molecular weight than that from IBMA (PIBMA). From the results of the detailed kinetic investigation, it was found that the values of activation energy, activation entropy, and Q and e for BMA were nearly the same as those for methyl methacrylate (MMA), but those for IBMA differed somewhat in activation entropy and Q value from those for MMA. It was also found that PIBMA could be easily acetolyzed to give an atactic polymethacrylic acid, while PBMA was stable to acetolysis as well as PMMA. Accordingly, it might be concluded that endo-bornyl group in BMA showed the same electric and steric effects on the rate and the reactivity for radical polymerization to methyl group in MMA, while the exo-bornyl group showed a somewhat increased steric effect.

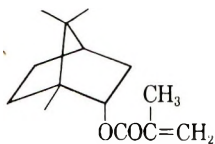
INTRODUCTION

It is well known that 1,2-disubstituted ethylene monomers have little tendency for homo- or copolymerization. For this reason, it was considered that the steric effect of the substituent in these monomers might be significant in the polymerization. Recently, it was reported by several workers¹ that some vinyl monomers having a bulky substituent polymerized through radical mechanism at rather high temperatures to yield a stereoregular polymer. However, few detailed studies on the steric effect in radical polymerization of vinyl monomers are found in the literature.^{2,3}

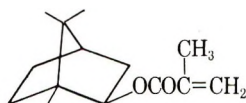
It was deemed very interesting to investigate the steric effect of the substituent in vinyl monomer on the rate and the reactivity in radical polymerization and on the stereoregularity of the resulting polymer. In a previous paper,⁴ we reported on the radical polymerization of endo- or exo-vinyl bicyclo[2.2.1]heptane 2-carboxylate (VBHC) and found that the exo-VBHC polymerized faster than the endo-VBHC and that bicyclo[2.2.1]heptane group in VBHC behaved like the methyl group in vinyl acetate.

In order to further clarify the steric effect, we have synthesized endo-bornyl methacrylate (bornyl methacrylate, BMA) and exo-bornyl methacrylate (isobornyl methacrylate, IBMA), which are shown in the following

structures; we investigated kinetically the effect of the endo-or exo-bornyl group on radical polymerization and copolymerization of these monomers.



BMA



IBMA

EXPERIMENTAL

1. Synthesis of Bornyl Methacrylate (BMA)

BMA was synthesized by the alcoholysis of methyl methacrylate (MMA) with borneol in the presence of *p*-toluenesulfonic acid. The commercial grade borneol was purified with 20% sulfuric acid in methanol solution and then recrystallized from ligroin.

A mixture of 1 mole of pure borneol, 2.5 moles of MMA, 7.7 g. of *p*-toluenesulfonic acid, 1 ml. of sulfuric acid, 4 g. of hydroquinone, and 4 g. of picric acid was heated in a stream of nitrogen at about 100°C. During the reaction, the forming methanol was distilled together with MMA and the reaction temperature was gradually increased to 130°C. After completion of the reaction (6 hr.), the mixture was washed with dilute sodium bicarbonate aqueous solution and then water. The oily layer was separated and dried on anhydrous sodium sulfate. The crude BMA was obtained in 64.1% yield by the vacuum distillation in nitrogen atmosphere. BMA was then purified by the distillation several times in the stream of nitrogen under reduced pressure, b.p. 70.0–70.5°C./2mm. Hg, n_D^{25} 1.4745, d_4^{30} 0.9760.

ANAL. Calcd.: C, 75.62%; H, 9.98%. Found: C, 75.64%; H, 9.90%.

2. Synthesis of Isobornyl Methacrylate (IBMA)

IBMA was synthesized by the ester-interchange reaction of isobornyl acetate with MMA. Isobornyl acetate was prepared by heating a mixture of camphene and glacial acetic acid in the presence of sulfuric acid at 50°C. for 5 hr.

The ester-interchange reaction was carried out in the same manner described for BMA. A mixture of 1 mole of MMA, 200 ml. of benzene, 0.54 g. of sodium methoxide, and 5 g. of phenyl- β -naphthylamine was heated at 80–85°C. for 4 hr. in nitrogen atmosphere. Aftertreatment and purification of IBMA was performed according to the method described in the case of BMA. The yield was 67.4%, b.p. 73.0–74.0°C./2 mm. Hg, n_D^{25} 1.4750, d_4^{25} 0.9798.

ANAL. Calcd.: C, 75.62%; H, 9.98%. Found: C, 75.52%; H, 10.04%.

3. Purification of Reagents

Styrene used in copolymerization was purified by usual method and distilled under reduced pressure in the stream of nitrogen before use. α, α' -Azobisisobutyronitrile (AIBN) was purified by recrystallization twice from ethanol. Benzene and other reagents were purified by the usual method.

4. Polymerization and Copolymerization Procedures

Polymerizations of BMA and IBMA were carried out in benzene at 50–70°C. The required amount of the monomer and benzene containing AIBN was charged into the polymerization tube, and it was then degassed under vacuum by the usual freezing and thawing technique and the tube sealed off. Polymerization was performed on shaking the tube in a thermostat. After a given time, the tube was opened and its contents were poured into a large amount of methanol to precipitate the polymer. Conversion was calculated from the weight of the dry polymer obtained.

Copolymerizations of BMA or IBMA with styrene were carried out in the polymerization tube in bulk by shaking at 60°C. Most reactions were carried out to 15% conversion. The resulting copolymer was purified by reprecipitating from the benzene solution into a large amount of methanol. The composition of the resulting copolymer was determined by carbon analysis.

5. Acetolysis and Alkaline Hydrolysis of the Polymer

A mixture of 0.5 g. of the resulting polymer, 50 g. of glacial acetic acid, and 1 g. of concentrated sulfuric acid was heated at 125°C. for 5 hr.

Polysisobornyl methacrylate (PIBMA) was acetolyzed to give methanol-soluble polymer. The polymer was then purified by reprecipitating from methanol solution into benzene. This purified polymer was confirmed to be polymethacrylic acid by elementary analysis and infrared spectra. Polybornyl methacrylate (PBMA) did not change during the above treatment.

Alkaline hydrolysis of both polymers was carried out in a sealed tube by heating a mixture of 0.5 g. of the polymer, 9.3 g. of isopropyl alcohol, and 0.5 ml. of 50% NaOH aqueous solution at 85°C. for 12 hr.

6. Molecular Weight and Intrinsic Viscosity Determination of the Polymer

Number-average molecular weights of PBMA and PIBMA were determined by osmotic pressure measurement on benzene solution at $30 \pm 0.005^\circ\text{C}$. A Gee-type osmometer and collodion membranes were used in this work.

Intrinsic viscosities of both polymers were determined in benzene with a Ubbelohde viscometer at 30°C. The intrinsic viscosity of acetolyzed PIBMA was determined in methanol at 30°C. and its number-average molecular weight was calculated by the following equation for polymethacrylic acid:⁵

$$[\eta] = 2.42 \times 10^{-3} \bar{M}_n^{0.51} \quad (1)$$

RESULTS

1. Homopolymerizations of BMA and IBMA

The time-conversion relations are shown in Figure 1 for the polymerization of BMA and IBMA initiated by AIBN at 50, 55, 60, 65, and 70°C. in benzene. The rates of polymerization R_p were computed from the slopes of these straight lines. The results are shown in Table I, in which the overall polymerization constants k and the number-average degree of polymerization \bar{P}_n are also tabulated.

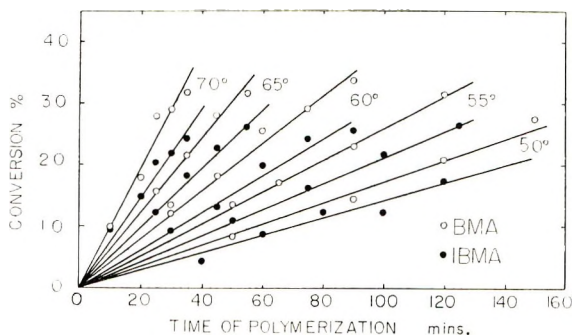


Fig. 1. Time-conversion relations for the polymerization of BMA or IBMA initiated by AIBN in benzene at 50-70°C.; $[AIBN] = 5.5 \times 10^{-3}$ mole/l.; $[M] = 1.76$ mole/l.

TABLE I
Results of Polymerization of BMA and IBMA at $[AIBN] = 5.5 \times 10^{-3}$ mole/l., $[M] = 1.76$ mole/l. in Benzene

Monomer	Temp., °C.	$R_p \times 10^5$, mole/l. sec.	$k \times 10^4$, l./mole sec. ^a	\bar{P}_n ^b
BMA	50	5.01	3.63	1650
	55	7.92	5.73	1100
	60	12.03	8.71	790
	65	18.51	13.40	530
	70	28.87	20.90	350
IBMA	50	4.04	2.92	1100
	55	6.32	4.57	670
	60	9.16	6.63	520
	65	14.77	10.69	450
	70	23.02	16.67	230

^a k values were calculated from the observed rate equation: $k = R_p/[AIBN]^{0.5}[M]^{1.1} = k_p(k_d f/k_t)^{1/2}$.

^b Number-average degrees of polymerization were calculated from results of intrinsic viscosity measurements in benzene by use of eq. (4).

As can be seen from Figure 1 and Table I, the endo-monomer (BMA) polymerized faster than the exo-monomer (IBMA), and \bar{P}_n of the resulting PBMA was higher than that of PIBMA.

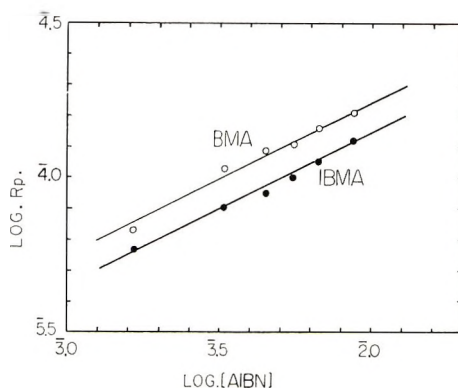


Fig. 2. Relationship between R_p and $[AIBN]$ at 60°C .; $[M] = 1.76$ mole/l.

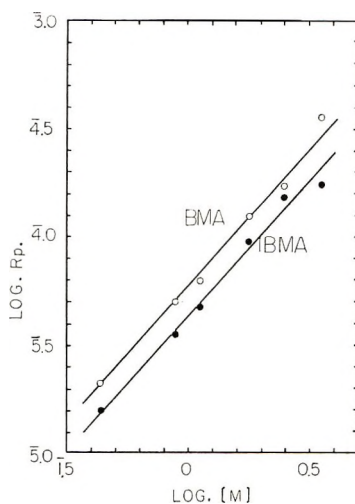


Fig. 3. Relationship between R_p and $[M]$ at 60°C .; $[AIBN] = 5.5 \times 10^{-3}$ mole/l.

The dependence of R_p on the concentrations of monomer and initiator was also investigated at 60°C . The results are shown in Figures 2 and 3. These results indicated that R_p was found to be proportional to the 0.5 power of AIBN initiator concentration and to the 1.1 power of monomer concentration for both BMA and IBMA monomers:

$$R_p = k[AIBN]^{0.5} [M]^{1.1} \quad (2)$$

According to the Arrhenius equation, $\log k$ calculated from equation (2) was plotted against $1/T$ as shown in Figure 4. From these straight lines obtained, the overall activation energies and frequency factors were calculated for both monomers. The results are shown in Table II, in which the corresponding values for MMA are also tabulated. The activation entropies are calculated according to the transition state theory.

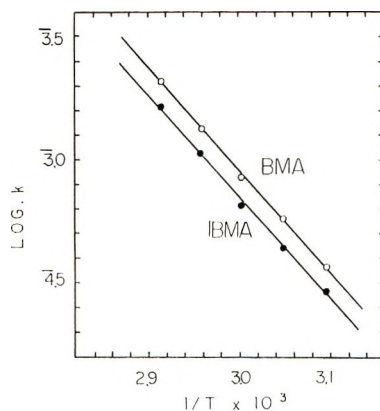


Fig. 4. Relationship between polymerization constant k and $1/T$; $[AIBN] = 5.5 \times 10^{-3}$ mole/l.; $[M] = 1.76$ mole/l.

As can be seen from Table II, the activation energies for BMA and IBMA were the same within experimental error, but the frequency factors and activation entropies for both monomers differed. It was noticeable that these figures for BMA were in good agreement with those of MMA, indicating that the endo-bornyl group shows the same effect for radical polymerization as the methyl group in alkyl methacrylate.

Figure 5 shows the relationship between $1/\bar{P}_n$ of the resulting polymers and R_p for both BMA and IBMA. The linear relationships were drawn and found to follow eq. (3):

$$\frac{1}{\bar{P}_n} = C_m + C_s \frac{[S]}{[M]} + \frac{k_t R_p}{k_p^2 [M]^2} \quad (3)$$

where C_m and C_s are the chain transfer constants to monomer (M) and to benzene (S), and k_t and k_p the rate constants for termination and propagation, respectively.

From the slopes and the intercepts of the straight lines obtained as shown in Figure 5, the values of k_t/k_p^2 and of the apparent transfer constant ($C_m + C_s[S]/[M]$) were calculated. If the chain transfer constants to benzene at 60°C. for both BMA and IBMA are nearly the same as for MMA ($C_s = 4 \times 10^{-6}$),⁷ the chain transfer constants to monomer (k_{trm}/k_p)

TABLE II
Kinetic Constants for BMA and IBMA: $k = A \exp \{-E/RT\}$

Monomer	E , kcal./mole	$A \times 10^{-3}$, mole/l. sec.	S^\ddagger (60°C.), e.u.
BMA	19.1	3.3	-15.3
IBMA	19.0	2.1	-16.1
MMA*	19.9	3.7	-15.0

* Data of Tobolsky and Mesrobian.⁶

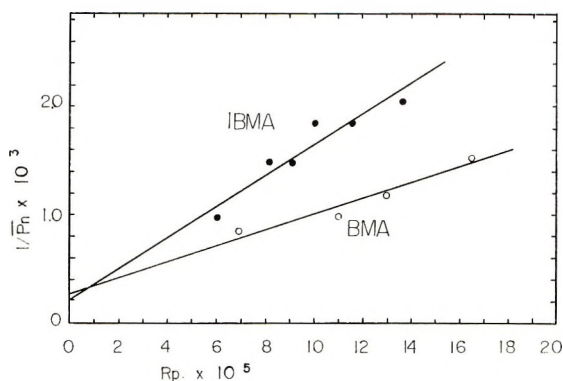


Fig. 5. Relationship between $1/\bar{P}_n$ and R_p at 60°C.

for both monomers can approximately be computed. The results are shown in Table III, in which the values of $k_p/k_t^{1/2}$ calculated from k in eq. (2) are also tabulated.

TABLE III
Rate Constants for Polymerization of BMA and IBMA at 60°C.

Monomer	$k_p/k_t^{1/2}$ ^a	k_t/k_p^2	$C_m (= k_{trm}/k_p) \times 10^4$
BMA	0.286	23.1	2.85
IBMA	0.217	46.3	1.85
MMA	0.103 (0.120) ^b	87.6 ^b	0.07–0.1 ^c

^a Calculated from k values by assuming that $k_d = 1.33 \times 10^{-5}$ sec.⁻¹ and $f = 0.7$.

^b Data of Matheson et al.⁸

^c Data of Baysal and Tobolsky.⁹

As can be seen from Table III, the values of $k_p/k_t^{1/2}$ decreased in the order: BMA > IBMA > MMA, and k_t/k_p^2 increased in the reverse order. This fact indicated that either k_p decreased or k_t increased. The transfer constant to BMA and IBMA was larger (20–30 times) than that of MMA.

2. Copolymerizations of BMA or IBMA with Styrene

The results of the bulk copolymerization of BMA or IBMA with styrene (St) initiated by AIBN at 60°C. are shown in Table IV.

From the results of Table IV, the monomer–copolymer composition curves for both copolymerization systems were plotted as shown in Figure 6, in which the corresponding curve for MMA is also plotted by using the values of r_1 and r_2 as indicated in Table V. The curve drawn experimentally for BMA–St copolymerization was identical with that for MMA–St copolymerization, but that for IBMA–St system differed.

According to the method of Fineman and Ross, the monomer reactivity ratios (r_1 and r_2) were calculated for both copolymerization systems. The results are shown in Table V, where M_1 stands for BMA or IBMA and M_2

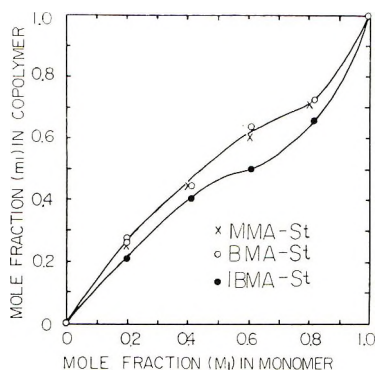


Fig. 6. Monomer-polymer composition curves for the copolymerization of BMA or IBMA with styrene at 60°C.

TABLE IV
Copolymerizations of BMA and IBMA with St at 60°C.

Expt. no.	Monomer composition, mole-%		Copolymer. conditions		Copolymer composition mole-%	
	BMA or IBMA	St	Time, hr.	Yield, %	BMA or IBMA	St
BMA-St, [AIBN] = 3.11×10^{-3} mole/l.						
1.1	100	0	1.0	20.67	100	0
1.2	82.05	17.95	2.5	12.89	72.92	27.08
1.3	61.63	38.37	2.5	9.03	64.00	36.00
1.4	40.20	59.80	2.5	6.88	43.62	56.38
1.5A	19.98	80.02	2.5	5.94	26.65	73.35
1.5B	19.98	80.02	2.5	8.23	27.66	72.34
1.6	0	100	2.5	6.04	0	100
IBMA-St, [AIBN] = 2.56×10^{-3} mole/l.						
2.1	100	0	3.5	4.66	100	0
2.2	82.08	17.92	3.0	7.44	65.43	34.57
2.3	61.71	38.29	3.0	7.82	49.91	50.09
2.4	40.28	59.72	3.0	7.36	41.16	58.84
2.5	20.05	79.95	3.0	7.20	21.50	78.50
2.6	0	100	3.0	6.62	0	100

for St. In Table V, the values of r_1 and r_2 obtained through the copolymerizations of BMA and IBMA with vinyl chloride (VC) at 60°C. are also tabulated.¹¹

From the values of r_1 and r_2 indicated in Table V, Q and e values for BMA and IBMA monomers were calculated by assuming $Q = 1.0$, $e = -0.8$ for St. The results are shown in Table VI.

As can be seen from Table VI, e values for both BMA and IBMA monomers were the same as for MMA. However, while the Q value for BMA was the same as that for MMA, that for IBMA differed. It is clear that

TABLE V
Values of r_1 and r_2 for the Copolymerizations of BMA or
IBMA (M_1) with St(M_2) and with VC(M_2) at 60°C.

M_1	M_2	r_1	r_2
BMA	St	0.44	0.49
IBMA	St	0.32	0.70
MMA ^a	St	0.46	0.52
BMA	VC ^b	12.5	0.06
IBMA	VC ^b	10.0	0.12
MMA ^a	VC	12.5	0

^a Data of Alfrey et al.²

^b Data Imoto et al.¹¹

TABLE VI
 Q and e values for BMA and IBMA Monomers

Monomer	Q	e
BMA	0.79	0.46
IBMA	0.54	0.42
MMA ^a	0.74	0.4

^a Data of Alfrey et al.²

the endo-bornyl group in BMA shows nearly the same electric and steric effects in radical polymerization as the methyl group in MMA.

3. Acetolysis and Alkaline Hydrolysis of the Resulting Polymer

Both PBMA and PIBMA were colorless powders like polymethyl methacrylate (PMMA); their infrared spectra are shown in Figure 7. PBMA

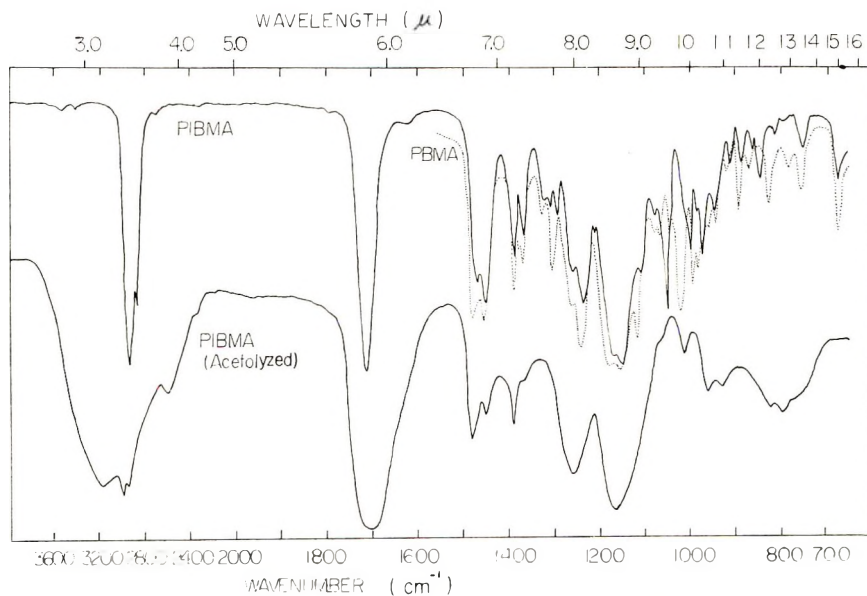


Fig. 7. Infrared spectra of PBMA, PIBMA, and acetolyzed PIBMA.

TABLE VII
 Acetolysis and Alkaline Hydrolysis of PBMA and PIBMA

Original polymer		Resulting polymer				
Polymer	[η] in benzene	Soluble in C ₆ H ₆ , %	Soluble in CH ₃ OH, %	Analysis ^a		[η] in benzene
				C, %	H, %	
Acetolysis at 125°C., 5 hr.						
PBMA	3.10	99.5	—	75.69	9.99	3.60
PBMA	1.04	85.5	—	75.76	9.96	1.10
PBMA	0.82	92.5	—	75.39	9.94	0.78
PBMA	0.74	81.5 ^b	—	75.16	9.80	0.65
PIBMA	2.90	—	100.0	54.80	7.50	3.60 (7500) ^c
PIBMA	0.96	—	92.8	46.80	7.29	1.35 (1100) ^c
PIBMA	0.65	—	100.0	53.52	7.46	1.05 (670) ^c
PIBMA	0.62	—	100.0 ^d	48.23	6.75	0.78 (370) ^c
Alkaline hydrolysis at 85°C., 12 hr.						
PBMA	0.82	93.0	—	74.98	9.68	—
PIBMA	0.65	96.5	—	75.18	9.86	—

^a Calculated values for PBMA and PIBMA: C, 75.62%; H, 9.98%; for polymethacrylic acid: C, 55.81%; H, 6.98%.

^b Acetolyzed for 15 hr.

^c Methanol was used as solvent; values in parenthesis are \bar{P}_n from eq. (1) as polymethacrylic acid.

^d Acetolyzed for 3 hr.

and PIBMA obtained by the bulk polymerization softened at 225–235 and 230–239°C., respectively.

The results of acetolysis and alkaline hydrolysis of both polymers are summarized in Table VII.

As clearly indicated in Table VII, PBMA was not changed by acetolysis, but PIBMA could easily be converted to polymethacrylic acid. PMMA was known to be stable to acetolysis,¹⁰ and this fact was also the same as that observed for PBMA. However, both polymers were stable to alkaline hydrolysis. Figure 7 shows the changes in the infrared spectrum of PIBMA during the acetolysis. PBMA shows no change in its infrared spectrum, however.

Polymethacrylic acid obtained by the acetolysis of PIBMA was found to be atactic by comparison of results of the infrared spectral studies and those of Greber and Egle.¹

4. Determination of Intrinsic Viscosity–Molecular Weight Relationship for PBMA and PIBMA

The number-average molecular weight (\bar{M}_n) determined by osmotic pressure and intrinsic viscosity of PBMA and PIBMA in benzene at 30°C. were plotted on a log-log scale. The results are shown in Figure 8, which

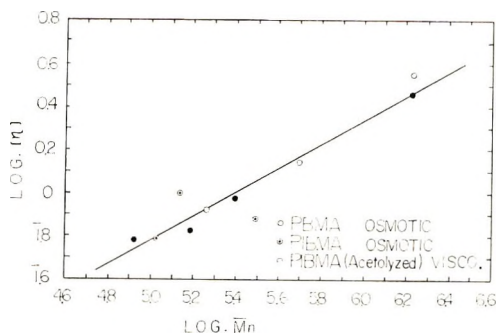


Fig. 8. Relationship between \bar{M}_n and $[\eta]$ of PBMA and PIBMA in benzene at 30°C.

also shows the results for PIBMA calculated from $[\eta]$ measurement of polymethacrylic acid obtained after acetolysis. For both PBMA and PIBMA, the same straight line was obtained within experimental error. Accordingly, the following eq. (4) was obtained as the \bar{M}_n - $[\eta]$ relationship for PBMA and PIBMA in benzene at 30°C.:

$$[\eta] = 9.95 \times 10^{-4} \bar{M}_n^{0.556} \quad (4)$$

DISCUSSION

Recently, Greber and Egle¹ found that 2,4,6-triphenylbenzyl methacrylate which contained a bulky alkyl group could be polymerized by a radical initiator to yield a syndiotactic polymer. As can be seen from the results of elementary analysis and of infrared spectra for acetolyzed PIBMA, however, it was proved that the polymers obtained by radical polymerization at 50–70°C. showed no stereoregularity.

The molecular weights of PBMA and PIBMA obtained by radical polymerization were rather small, as shown in Table I. This result could be easily understood from the fact that the transfer constants to BMA and IBMA were 20–30 times that for MMA as indicated in Table III. Since bornyl group contains a number of active hydrogen atoms, it is clear that effective chain transfer to monomer is very important in radical polymerization of these monomers. This fact is characteristic of radical polymerization of monomers possessing the bicycloheptane group.

Considering the effect of endo-bornyl (bornyl) and exo-bornyl (isobornyl) groups in these monomers on the rate and the reactivity in radical polymerization, the results obtained are as follows.

(1) BMA polymerizes faster than IBMA, and the molecular weight of the resulting PBMA is higher than that of PIBMA (Table I).

(2) Activation energies for the polymerization of BMA and IBMA are the same as those for MMA, but the activation entropy for IBMA differs somewhat from that for BMA and also for MMA (Table II).

(3) The values of Q and e for BMA are the same to those for MMA, while these for IBMA differs in Q value only from those for MMA (Table VI).

(4) PIBMA is easily acetolyzed to give polymethacrylic acid, while PBMA is stable to acetolysis as well as PMMA (Table VII).

From the above results, it might be concluded that the endo-bornyl group in BMA showed the same electric and steric effects on the rate and the reactivity in radical polymerization as the methyl group in MMA, while the exo-bornyl group showed somewhat increased steric effect.

As shown in Table III, $k_p/k_t^{1/2}$ for BMA is larger than that for IBMA and k_i/k_p^2 for BMA is smaller than that for IBMA. These results indicate that either k_p in BMA is larger than that in IBMA or k_t in BMA is smaller than that in IBMA. Since the monomer reactivity ratio and Q value of IBMA for the copolymerizations differed from those of BMA and also MMA as shown in Tables V and VI, a decrease in k_p of IBMA may be considered to be important. Accordingly, the fact that BMA polymerizes faster than IBMA may be concluded to be appeared from a decrease in k_p on the basis of the steric effect of exo-bornyl group.

When the molecular model for IBMA was set up, the dimethyl group on the 7-position in bornyl group was near the vinyl group; then the configuration and bornyl group in these monomers becomes significant for radical polymerization.

References

1. Greber, G., and G. Egle, *Makromol. Chem.*, **40**, 1 (1960).
2. Alfrey, T., Jr., J. J. Bohrer, and H. Mark, *Copolymerization*, Interscience, New York, 1952.
3. Bevington, J. C., *Radical Polymerization*, Academic Press, New York, 1961.
4. Imoto, M., T. Otsu, and W. Fukuda, *J. Polymer Sci.*, **B1**, 225 (1963).
5. Wiederhorn, N., and A. Brown, *J. Polymer Sci.*, **8**, 651 (1952).
6. Tobolsky, A. V., and R. B. Mesrobian, *Organic Peroxide*, Interscience, New York, 1954, p. 137.
7. Chadha, R. N., J. S. Shukla, and G. S. Misra, *Trans. Faraday Soc.*, **53**, 240 (1957).
8. Matheson, M. S., E. B. Bevilacqua, E. E. Auer, and E. J. Hart, *J. Am. Chem. Soc.*, **71**, 497 (1949).
9. Baysal, B., and A. V. Tobolsky, *J. Polymer Sci.*, **8**, 534 (1952).
10. Glavis, F. J., *J. Polymer Sci.*, **36**, 547 (1959).
11. Imoto, M., T. Otsu, and K. Tsuda, *Kogyo Kagaku Zasshi*, **66**, 988 (1963).

Résumé

Une étude a été faite de la polymérisation et copolymérisation radicalaire de méthacrylate de bornyle (endo-bornyle) (BMA) ou de méthacrylate d'isobornyle (exo-bornyle) (IBMA) et de styrène à 50–70°C. Le BMA polymérise plus vite que l'IBMA et le polymère obtenu à partir du BMA était de poids moléculaire plus élevé de celui qu'on obtient avec l'IBMA. Aux dépens des résultats de l'étude cinétique détaillée, il résulte que les valeurs de l'énergie d'activation, de l'entropie d'activation, de Q et de e pour le BMA sont pratiquement identiques à celles du méthacrylate de méthyle (MMA), mais celles de l'IBMA diffèrent quelque peu par l'entropie d'activation et la valeur de Q du MMA. On trouva également que le PIBMA peut aisément être acétylé donnant ainsi de l'acide polyméthacrylique atactique, tandis que le PBMA résiste à l'acétylé de même que le MMA. On peut donc en conclure que le groupe endobornyle dans le BMA exerce les mêmes effets électriques et stériques sur la vitesse et la réactivité dans la

polymérisation radicalaire que le groupe méthyle du MMA, tandis que le groupe exobornyle exerce un effet stérique quelque peu accru.

Zusammenfassung

Eine Untersuchung der radikalischen Polymerisation und Copolymerisation mit Styrol von Bornyl-(Endobornyl)-methacrylat (BMA) und Isobornyl-(Exobornyl)-methacrylat (IBMA) wurde bei 50–70°C durchgeführt. BMA polymerisierte rascher als IBMA und das Polymere aus BMA war höhermolekular als das aus IBMA. Die kinetische Untersuchung lieferte für BMA Werte der Aktivierungsenergie, Aktivierungsentropie und von Q und e , die mit denjenigen von Methylmethacrylat (MMA) nahezu übereinstimmten; IBMA unterschied sich in der Aktivierungsentropie und dem Q -Wert etwas von MMA. Weiters wurde gefunden, dass PIBMA leicht unter Bildung ataktischer Polymethacrylsäure acetolysiert werden konnte, während PBMA ebenso wie PMMA gegen Acetolyse stabil war. Es kann daher geschlossen werden, dass die Endobornylgruppe in BMA den gleichen elektrischen und sterischen Einfluss auf die Geschwindigkeit und Reaktivität bei der radikalischen Polymerisation hat wie die Methylgruppe in MMA, während die Exobornylgruppe einen etwas grösseren sterischen Effekt zeigt.

Received February 25, 1963

Diffusion and Viscosity of Polyvinyl Acetate-Diluent Systems

AKIRA KISHIMOTO,* *Physical Chemistry Laboratory, Department of
Fisheries, University of Kyoto, Maizuru, Japan*

Synopsis

The diffusion coefficient of methanol in polyvinyl acetate (PVAc) and the steady flow viscosity of the PVAc-diethyl phthalate (DEP) system have been studied. In diffusion studies the sorption and permeation of methanol vapor in the polymer were measured over a temperature range above and below T_g of the pure polymer. The mutual diffusion coefficient, D , was estimated from the rates of absorption and desorption from and back to nonzero initial and final concentration, and also from the steady state permeability. The D derived by different methods agreed within experimental error. By using the equation of Frisch, the time lag for permeation was calculated as a function of penetrant concentration from the D data. The calculated values were larger than the observed ones at temperatures slightly above and below T_g , but when the temperature was well above T_g both values agreed with each other. At temperatures below T_g anomalous permeation curves which could not be fully explained at the present stage appeared. In viscosity studies measurements were made over the complete range of DEP composition at temperatures from 10 to 100°C. by using four different experimental techniques. The plot for the logarithm of the viscosity against weight fraction of polymer at a fixed temperature was convex upward at low concentration and then became concave upward at high concentration. In the intermediate region an inflection point appeared. Experimental data for the thermodynamic diffusion coefficient of methanol in PVAc and the isothermal viscosity data for the system PVAc-DEP have been analyzed in terms of the free volume theory presented previously. It was found that experimental data were well represented by the theory.

INTRODUCTION

In previous papers¹⁻⁶ Fujita and Kishimoto have developed a free volume theory to account for concentration dependence of the diffusion coefficient and the steady flow viscosity at high polymer concentrations for systems of amorphous polymer and organic diluent. The diffusion and viscosity data for several typical polymer and diluent systems were found to be well described in terms of the theory presented. Available data at high concentrations, however, have been limited to few systems.⁷⁻⁹ Especially at temperatures slightly above and below the glass transition, T_g , no systematic data^{10,11} for the variation of mutual diffusion coefficient, D , with concentration have been reported. The first purpose of the present paper is

* Present address: The Composite Research & Development Center, Toyo Seikan and Toyo Kohan Companies, Okazawa, Hodogaya, Yokohama, Japan.

to find out features of the D versus concentration relation for amorphous polymer-solvent systems in the temperature range encompassing T_g . The systems chosen for this purpose was the polyvinyl acetate (PVAc)-methanol pair.

Recently, Fujita and Maekawa¹² reported extensive data of viscosity for the system polymethyl acrylate (PMA)-diethyl phthalate (DEP) over the complete range of composition at temperatures from 20 to 110°C., and discussed the applicability as well as limitation of the free volume equation. We made a similar viscosity study with the system PVAc-DEP, and the results are presented below.

EXPERIMENTAL

Materials

The PVAc used in the present study was furnished from Kurashiki Rayon Co. Ltd. through the courtesy of Dr. Y. Ohyanagi. The polymer was used without further purification. Its intrinsic viscosity in a mixture of methanol (60 vol.-%) and ethanol (40 vol.-%) at 26.5°C. was 0.285 dl./g., which corresponds to a viscosity-average molecular weight of 9.9×10^4 , according to the equation given by Naito.¹³

In diffusion studies, films 3.75×10^{-3} to 1.20×10^{-2} cm. thick were prepared by casting acetone solutions onto a mercury surface. The method of film preparation and thickness determination has been described elsewhere.⁴ The methanol used as penetrant was purified by fractional distillation from reagent grade product after the removal of acetone by caustic potash and of water by anhydrous carbonate.

DEP of reagent grade was used as diluent in viscosity studies. Its density at 20°C. was 1.120 g./cc., and its specific volume-temperature coefficient was 6.75×10^{-4} . Concentrations of 0, 5, 10, 20, 30, 40, 50, 60, 70, 80, 85, 90, 95, and 100% by polymer weight were studied. Highly plasticized samples of concentrations up to 50% were prepared by sealing the polymer and DEP in a glass flask which was then heated and agitated at elevated temperatures. The more concentrated samples were prepared in a sheet form by casting solutions of PVAc and DEP in acetone on a mercury surface.

For the computation of the densities of plasticized polymers at various temperatures it is necessary to know the densities of the diluent and the polymer as functions of temperature. The density of PVAc was obtained from literature data:¹⁴

$$1/d_2 = 0.843 + 5.98 \times 10^{-4}(\theta - 29) \quad (\theta \geq 29^\circ\text{C.})$$

$$1/d_2 = 0.843 - 2.07 \times 10^{-4}(29 - \theta) \quad (\theta \leq 29^\circ\text{C.})$$

where d_2 is the density of PVAc and θ the temperature. By assuming no volume change on mixing, the densities at given concentrations were calculated as functions of temperature.

Apparatus and Procedure

The sorption and permeation apparatuses described previously^{2,4} were used throughout this study. Integral absorption from and integral desorption back to nonzero pressure were measured for several external pressures of methanol vapor at temperatures in the range 15 to 35°C. At temperatures in the range 45–65°C., integral sorptions from and back to zero pressure were studied. The permeation measurements were carried out at temperatures in the range 15–45°C. In sorption and permeation experiments the temperature of the system was controlled to within $\pm 0.1^\circ\text{C}$.

Measurements of steady flow viscosity of the system PVAc–DEP were performed by using four kinds of experimental apparatus; Ostwald viscometer, falling ball viscometer, coaxial falling cylinder viscometer, and tensile creep instrument. The Ostwald viscometer, coaxial falling cylinder viscometer, and tensile creep instrument were the same as those described by Fujita and Maekawa,¹² and were employed to measure the viscosity of the order of 10^{-2} –1 poise, 10^5 – 10^{10} poises, and above 10^{10} poises, respectively.

To measure viscosities in the range of 1– 10^5 poises we employed the falling ball method, using steel bearing balls in glass tubes. The ball diameter and tube diameter were varied respectively in the range from 6×10^{-2} to 2×10^{-1} cm. and from 1 to 2 cm., depending upon the magnitude of viscosity of a given solution. The solution depth in the glass tube ranged from 10 to 20 cm. The falling velocity was measured by means of a travelling microscope, and the viscosity was calculated with the Faxen correction for the effect of the tube radius. The density of the ball was obtained from weighing several balls and calculating the volume from the specified diameter. No correction for rate of shear effects was made, since it was found that the flow could be regarded as Newtonian under the conditions of our experiments. In these experiments the temperature was controlled to within $\pm 0.1^\circ\text{C}$.

RESULTS AND DISCUSSION

Diffusion

It was found that the equilibrium absorption isotherm of methanol in PVAc becomes less steep with increase of temperature at low temperatures, but above 35°C. it remained almost independent of temperature. Formal application of the Flory-Huggins thermodynamic equation of polymer solutions, assuming no volume change on mixing, showed that at 15 and 25°C. the interaction parameter χ_1 decreased with increasing equilibrium concentration C_0 , giving 1.07 and 1.10, respectively, as average values. Above 35°C., it was nearly independent of C_0 and was 1.19.

Preliminary experiments have shown that integral absorption and desorption of methanol by PVAc from and back to zero pressure were nonFickian

type at 15 and 25°C., and that the successive differential absorption curves at these temperatures changed in type according to the scheme: two-stage type \rightarrow pseudo-Fickian type \rightarrow Fickian type. These are the features expected from the previous generalization¹⁵ of sorption behavior in glassy polymers. It has been shown that the transition from pseudo-Fickian to Fickian absorption occurred when the penetrant concentration passed the point at which the polymer-penetrant mixture underwent glass transition at the temperature of the experiment.¹⁵⁻¹⁷ From the data for the previous system, we may estimate a critical concentration to be 0.022 g. methanol/dry PVAc at 15°C. and 0.005 g. at 25°C. Recent measurements^{18,19} have shown that even when a polymer-penetrant mixture or a polymer solid is in the rubbery state at the start of the absorption experiment the absorption does not strictly follow the normal Fickian process; the sorption curves with films of different thicknesses cannot be reduced to a single curve.

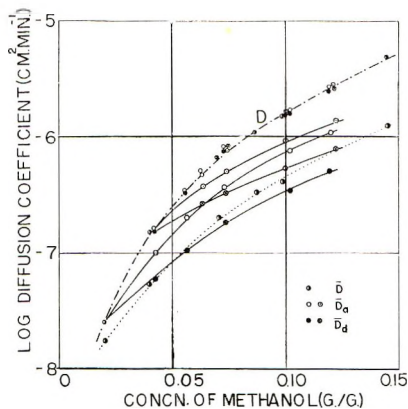


Fig. 1. Plots of various diffusion coefficients against penetrant concentration for the system PVAc-methanol at 25°C.

With this experimental finding in mind, the present integral sorption measurements were started not from respective critical concentrations at 15 and 25°C., but from certain concentrations above the critical concentrations.

For all the external pressures and temperatures studied, the absorption and desorption plots had shapes expected from the normal Fick diffusion mechanism.^{2,3} From the initial slopes of the reduced absorption and desorption curves two apparent diffusion coefficients, \bar{D}_a and \bar{D}_d , were determined. The values of \bar{D}_a and \bar{D}_d obtained from two fixed initial concentrations $C_0^i = 0.021$ g./g. and 0.041 g./g. at 25°C. are plotted semilogarithmically against final methanol concentration C_0^f in Figure 1. It is seen that at fixed initial concentration C_0^i both \bar{D}_a and \bar{D}_d increase with C_0^f and the difference between them becomes larger as C_0^f increases, and that the concentration dependence of \bar{D}_a and \bar{D}_d becomes noticeable as C_0^i decreases. Similar data were obtained at other temperatures studied.

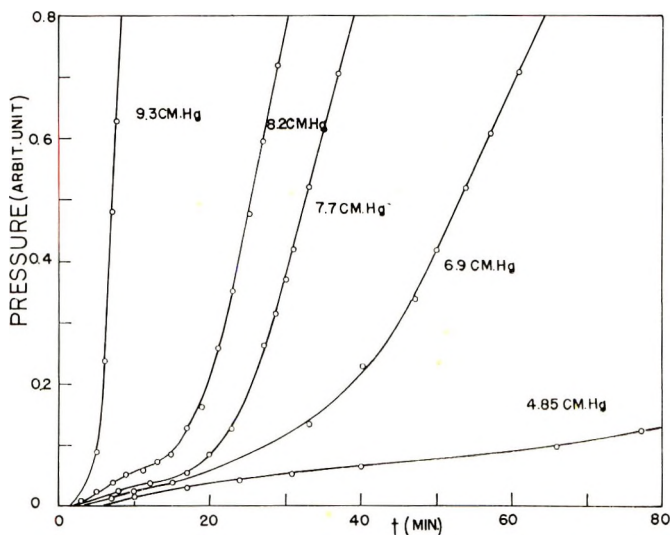


Fig. 2. Permeation curves of methanol for PVAc at 25°C. as a function of ingoing pressure. The film thicknesses are approximately 5×10^{-3} cm.

Evaluation of mutual diffusion coefficient $D(C)$ from experimentally determined values of \bar{D}_o and \bar{D}_d in terms of Crank's approximation method²⁰ was carried out as described in a previous paper.² Figure 1 includes D values so obtained. It is seen that the D values derived from absorption and desorption data agree quite well, irrespective of the values of C_0^i . Such agreements have also been observed at other temperatures. These results suggest that all the absorption and desorption processes were truly Fickian within the range of temperatures and concentrations measured.

Figure 2 gives results of permeation of methanol through PVAc films having almost equal thickness 5×10^{-3} cm. at 25°C. for different ingoing pressures p_0 ; here the ordinate is the pressure of the vapor issuing from the lower pressure side of the film. It is seen from the figure that at low and medium external pressures there are two time-dependent processes taking place. At these pressures the permeation rate increases initially, passes through a maximum, again increases, and eventually approaches a steady-state level. It is noted that the position of the inflection point in the initial stage of permeation shifts toward the short time region with increasing ingoing pressure. With further increase of pressure the inflection point in the first stage disappears, and the permeation apparently turns out to be normal in the sense that it is convex toward the time axis and approaches asymptotically a steady state. Similar anomalous permeation curves were found at 15 and 35°C. At 45°C. all the permeation curves had shapes expected from the normal Fick diffusion mechanism.²

The general feature shown in Figure 2 resembles that of the permeation curves of allyl chloride in PVAc at 40°C. found by Meares.²¹ He interpreted his anomalous curves in terms of the stress effect induced by an

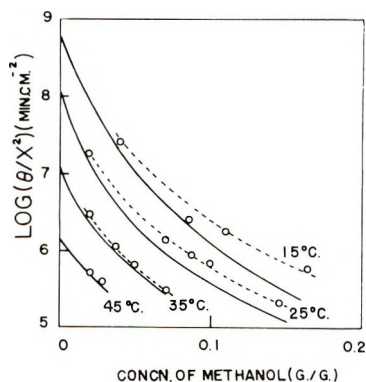


Fig. 3. Reduced time lags for methanol diffusing through PVAc at various temperatures as functions of methanol concentration: (O) experimental data; (—) calculated curve.

appreciable concentration gradient between the surfaces of the film under conditions of usual permeation experiments. Prior to Meares, Park,¹¹ studying the permeation of methylene chloride through polystyrene membrane at 25°C., had observed a similar behavior, in which a high initial permeation rate gradually decreased to the final steady value. He suggested the phenomenon was due to rapid permeation through cracks in the dry polymer which sealed up as the polymer absorbs vapor. This observation was concerned with a polymer far below the glass transition temperature. At temperatures above T_g , PVAc has the structure of equilibrium liquid and could not have an internal capillary system. Since the anomalous permeation curves were found at temperatures both below and above T_g of PVAc, Park's explanation may no longer be generally valid. Recently, Long and Richman²² showed that anomalous absorption curves of vapors by glassy polymers can be derived from the Fick diffusion equation subject to the boundary condition in which the surface concentration gradually approaches an equilibrium value. Mathematical analysis with this boundary condition shows, however, that permeation is convex toward the time axis and approaches a straight line as time increases.

The time lag θ , the intercept of the steady-state portion of a permeation curve extrapolated to the time axis, is plotted against C_0 in Figure 3. It is seen that the reduced time lag θ/X^2 decreases with increase of concentration. Prediction of θ from the $D(C)$ data derived from steady-state measurements by using Frisch's equation²³ gives the solid line shown in Figure 3. The time lag values so calculated are smaller than those determined experimentally, but the difference between them becomes smaller with increase of temperature, and eventually at 45°C. both curves agree with each other. A similar agreement has been found for the PMA-benzene system at 30°C.² and the polyethylene-benzene system at 0°C.²⁴ The divergence of the observed time lags and the theoretical ones at lower temperatures may be interpreted as due to slow relaxation of polymer

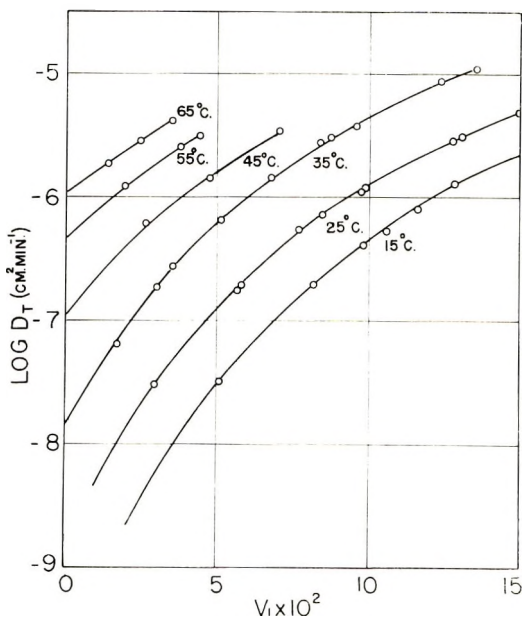


Fig. 4. Thermodynamic diffusion coefficient D_T for the system PVAc-methanol at different temperatures.

chain.²⁵ The steady-state measurement refers to the polymer in which all stresses have decayed out, whereas the nonsteady-state measurement is influenced by residual elastic stress. When the temperature is well above T_g , the relaxation process may become so rapid that the two methods give equal values for θ .

Combination of steady-state permeability with equilibrium absorption isotherms enables us to calculate the integral diffusion coefficient D as a function of methanol concentration, which in turn allows ready determination of $D(C)$. Plots of $\log \bar{D}$ and $\log D$ versus methanol concentration at 25°C. are shown in Figure 1. It is seen that the D values determined from the steady-state permeation rates agree with those deduced from sorption rates. Similar agreements of the three sets of D values have also been observed at other temperatures studied.

We have calculated the thermodynamic diffusion coefficient² of methanol, D_T , from the data for $D(C)$ assuming no volume change on mixing. The values of D_T so computed are plotted against the volume fraction of methanol, v_1 , in Figure 4. It is seen that $\log D_T$ versus v_1 relations are similar to those^{1,2,26} observed for other amorphous polymer-solvent systems at temperatures above T_g , though the present experiments were conducted at temperatures both above and below T_g of PVAc.

Extrapolation of $\log D_T$ to zero penetrant concentration gives the value of D_0 . Because of the lack of experimental data at lower concentrations, it is increasingly difficult to obtain D_0 at temperatures near T_g . Assuming

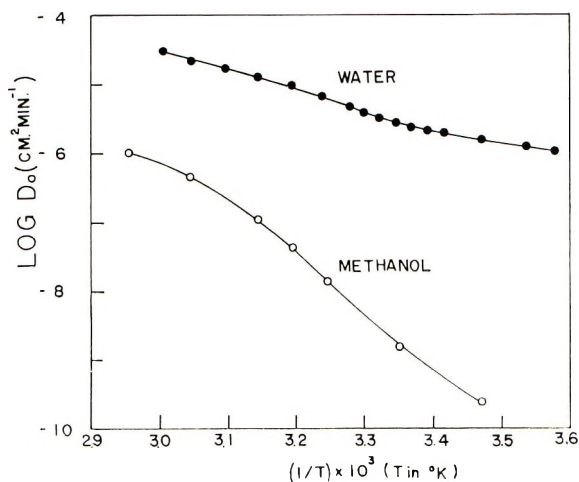


Fig. 5. Mutual diffusion coefficient at zero penetrant concentration as a function of reciprocal absolute temperature.

that the free volume theory discussed later holds in the region of low concentration below the minimum concentration studied, we may estimate the value of D_0 . In Figure 5 the values of D_0 thus estimated are semilogarithmically plotted against the reciprocal of absolute temperature T . In the figure the value of D_0 at 40°C. was taken from previous studies.⁴ For comparison the data²⁷ for the system PVAc-water previously reported are included. It is seen that an inflection point appears on the plot for methanol at a temperature near T_g just as on the plot for water. The apparent activation energy for diffusion of methanol in PVAc calculated from Figure 5 increases as the temperature is lowered toward T_g , reaches a maximum at a temperature near T_g , and then decreases with further decrease of temperature.

Viscosity

Observed viscosity values in the falling cylinder viscometer were independent of applied load, when they were smaller than 10^9 poises. For higher viscosities, of the order of 10^{10} poises the apparent viscosity at zero load was obtained by linear extrapolation according to the procedure proposed by Fox and Flory.²⁸

Tensile creep data for a given concentration at various temperatures were plotted in the form of $\log D(t)$ against the logarithm of time, where $D(t)$ is the tensile creep compliance. It was found that the curves so obtained can be superposed to form a single composite curve by shifting them horizontally along the log time axis. The desired viscosity was estimated from this composite curve by using the extrapolation method of Nino-miya.²⁹ Under the assumption that Poisson's ratio of the sample was equal to $1/2$, the tensile viscosity η_1 thus obtained was transformed to the

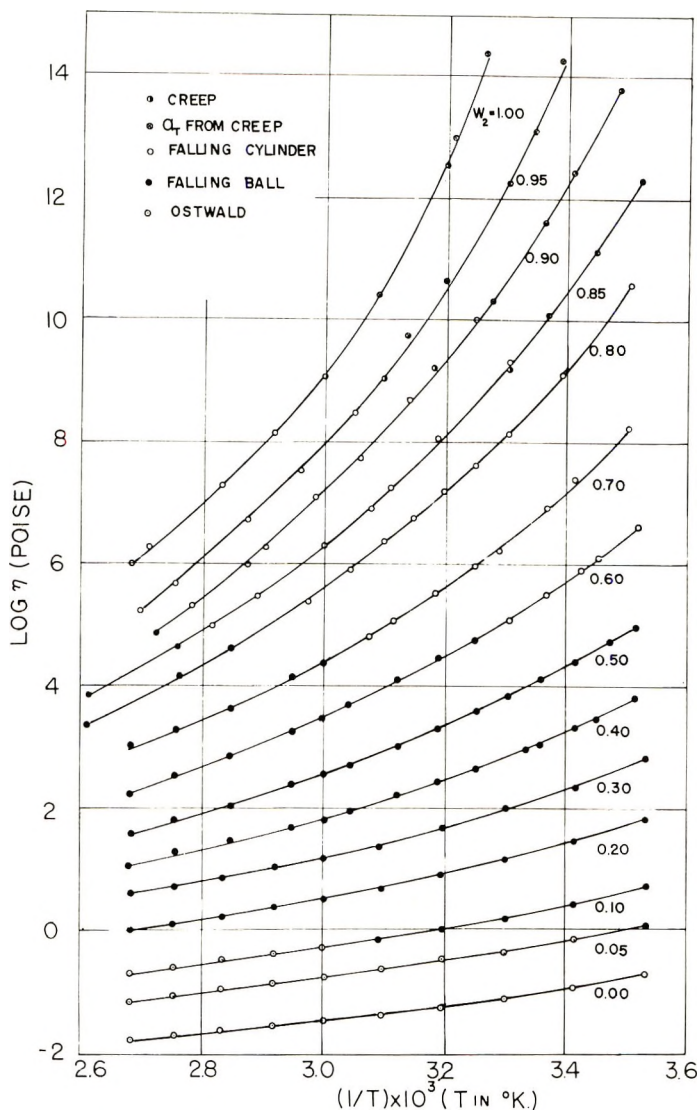


Fig. 6. Steady flow viscosities for the system PVAc-DEP at different concentrations.

shear viscosity η by the relation $\eta_1 = 3\eta$. The viscosity values at temperatures other than the temperature chosen as the reference in the above superposition process was indirectly estimated from shift factors.

In Figure 6 is plotted the logarithm of the viscosity, $\log \eta$, against $1/T$ as a function of the weight fraction of polymer, w_2 . It is seen that the curves are almost linear at low polymer concentrations but show considerable curvature as the polymer concentration is increased. The general trend of this family of curves is similar to those for the systems polystyrene-dibenzyl ether⁷ and polymethyl acrylate-DEP.¹² The tempera-

TABLE I
Variation of $\log \eta$ for Polyvinyl Acetate as a Function of Temperature and DEP Concentration

w_1^a	v_1^b	$\log \eta^c$									
		10°C.	20°C.	30°C.	40°C.	50°C.	60°C.	70°C.	80°C.	90°C.	100°C.
0	0			15.50	12.55	10.60	9.10	8.20	7.35	6.64	6.02
0.05	0.053		14.80	12.34	10.65	9.15	8.00	7.17	6.43	5.80	5.20
0.10	0.106	14.70	12.50	10.80	9.40	8.20	7.12	6.35	5.70	5.19	4.65
0.15	0.158	12.60	10.75	9.32	8.14	7.20	6.35	5.70	5.12	4.67	4.10
0.20	0.210	11.00	9.45	8.18	7.20	6.40	5.62	5.05	4.55	4.15	3.75
0.30	0.314	8.65	7.35	6.38	5.62	5.00	4.55	4.00	3.60	3.30	3.00
0.40	0.415	6.75	5.82	5.10	4.50	3.98	3.52	3.13	2.80	2.52	2.26
0.50	0.516	5.15	4.45	3.86	3.35	2.95	2.57	2.28	2.02	1.80	1.60
0.60	0.615	3.92	3.35	2.88	2.52	2.20	1.85	1.62	1.42	1.27	1.12
0.70	0.714	2.86	2.395	2.04	1.73	1.44	1.24	1.06	0.90	0.76	0.63
0.80	0.811	1.86	1.687	1.37	0.96	0.75	0.54	0.45	0.25	0.14	0.02
0.90	0.906	0.75	0.482	0.24	0.06	-0.11	-0.23	-0.35	-0.45	-0.55	-0.66
0.95	0.953	0.13	-0.117	-0.31	-0.48	-0.62	-0.75	-0.84	-0.94	-1.04	-1.12
1.00	1.000	-0.69	-0.891	-1.08	-1.22	-1.34	-1.45	-1.52	-1.61	-1.69	-1.76

^a Weight fraction of DEP.

^b Volume fraction of DEP.

^c η is the shear viscosity in poises.

ture dependence of steady flow viscosity in amorphous polymers is well represented by the equation of Williams, Landel, and Ferry.³⁰ Fits of this equation with the present data for higher polymer concentrations were quite satisfactory, in which the reference temperatures T'_s were 75, 65, 57, 48, 40, and 24.5°C. for $w_2 = 1.00, 0.95, 0.90, 0.85, 0.80,$ and $0.70,$ respectively. The initial portion of the relation between T'_s and w_2 is represented by

$$T'_s = T'_g - 180 w_1 \quad (1)$$

where T'_g is the reference temperature for pure polymer and w_1 is the weight fraction of diluent. If the difference ($T'_s - T'_g$) is assumed to be the same for all the compositions studied, eq. (1) gives

$$T_g = T'_g - 180 w_1 \quad (2)$$

in which T'_g is the glass transition temperature of pure PVAc. This equation stands in good agreement in form with that proposed by Jenckel and Heusch.³¹

Ninomiya and Fujita³² have derived the molecular weight dependence of the steady flow viscosity of PVAc in tension at 75°C.,

$$\eta_1 = 10^{-8.05 \bar{M}_v^{3.4}} \quad (3)$$

where \bar{M}_v is the viscosity-average molecular weight. In evaluating \bar{M}_v from intrinsic viscosities in acetone at 30°C. they used the equation of Sakurada and Chiba.³³ In order to estimate the molecular weight of the present sample in terms of Sakurada-Chiba's equation, the intrinsic viscosity in acetone at 30°C. was measured and the value of 0.42 dl./g. was obtained, which gives 6×10^4 for \bar{M}_v of the sample. Introduction of this value into eq. (3) and conversion of the steady flow viscosity in tension to that in shear gives 7.75 for $\log \eta$ at 75°C., which may be favorably compared with the value of 7.70 determined experimentally.

The viscosities read from the smooth curves drawn in Figure 6 are listed in Table I. Figure 7 shows viscosities at various temperatures plotted as a function of polymer concentration. It is seen that the curves are convex upward at low polymer concentrations and become concave upward at high polymer concentrations; in the intermediate region there appears an inflection point. The position of inflection shifts toward higher concentration as the temperature is increased.

The general character of this family of curves is similar to those obtained for the systems polystyrene-dihethylbenzene,⁹ polystyrene-dibenzyl ether,⁷ polymethyl methacrylate (PMMA)-DEP,⁸ and PMA-DEP.¹² However, there are some important differences among these previous studies. For comparison with the present data, it is convenient to use the data for PMMA-DEP and PMA-DEP, since these three systems refer to the same diluent and the molecular weights of the respective polymers are in the neighborhood of 1×10^5 . The most striking difference is in the absolute magnitude of the viscosities compared at the same temperature. For

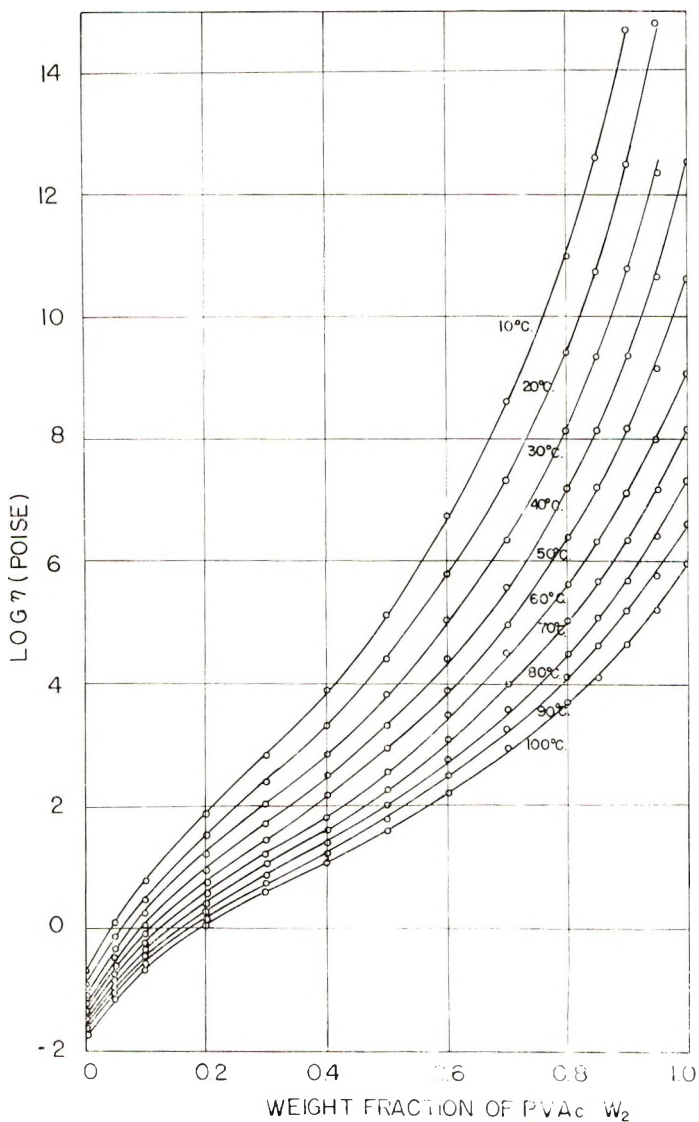


Fig. 7. Steady flow viscosities for the system PVAc-DEP at different temperatures.

instance, at 60°C. pure PMMA has η more than 10^{15} times larger than those for PMA and PVAc. This difference may be attributed to the difference in the glass transition temperatures of these polymers. The second point of interest is the position of the inflection point appearing in the region of medium concentration. At 60°C. the inflection point for PMA and PVAc appear at w_2 of about 0.5 and 0.3, respectively, while for PMMA no inflection point can be seen. These facts suggest that the position of inflection shifts toward higher polymer concentration as the glass transition temperature is lowered. In fact, unpublished data³⁴ for a sample of poly-

isobutylene in decalin show plots for $\log \eta$ versus concentration which are concave toward the concentration axis at low concentrations and are almost linear at high concentrations.

Application of Free Volume Theory

According to the free volume theory of Fujita and Kishimoto,^{3,5} the dependence on concentration of the diffusion coefficient and the viscosity in concentrated polymer solution at a fixed temperature is represented by the equations:

$$\frac{1}{\log [D_T(v_1, T)/D_T(v_1^*, T)]} = 2.303 \frac{f(v_1^*, T)}{B_d} + \frac{[f(v_1^*, T)]^2}{B_d \beta(T)} \frac{1}{(v_1 - v_1^*)} \quad (4)$$

$$\frac{1}{\log a_c} = 2.303 f(v_1^*, T) + 2.303 \frac{[f(v_1^*, T)]}{\beta(T)} \frac{1}{(v_1 - v_1^*)} \quad (5)$$

in which a_c is defined by

$$a_c = \frac{\eta(v_1^*, T)(1 - v_1)}{\eta(v_1, T)(1 - v_1^*)} \quad (6)$$

Here $\eta(v_1, T)$ is the viscosity of the solution at a concentration v_1 and a temperature T , v_1^* is the value of v_1 chosen as a reference, $D_T(v_1, T)$ is the thermodynamic diffusion coefficient of the penetrant at a concentration v_1 and a temperature T , B_d is a constant characteristic of the system, and $f(v_1^*, T)$ is the average fractional free volume of the solution at v_1^* and T and is given by

$$f(v_1^*, T) = f(0, T) + \beta(T)v_1^* \quad (7)$$

where $\beta(T)$ stands for

$$\beta(T) = \gamma(T) - f(0, T) \quad (8)$$

The quantity $f(0, T)$ represents the average fractional free volume in the pure polymer, and $\gamma(T)$ is a constant depending on temperature.

Theory³ shows that the parameter B_d in eq. (4) may be determined by means of the following relation:

$$\ln (D_0/RT) = K - B_d \ln \eta(0, T), \quad (9)$$

where R is the gas constant, K is a constant independent of T , and $\eta(0, T)$ is the steady flow viscosity of the pure polymer at a fixed temperature T . Use of eq. (9) requires accurate data for D_0 as a function of temperature. As can be seen from Figure 4, the extrapolation of D_T to zero penetrant concentration is quite difficult especially at low temperature. Therefore, we are forced to estimate D_0 by means of the following calculation. Equation (4) determines the values of $f(v_1^*, T)/B_d$ and $[f(v_1^*, T)]^2/B_d$ for a given value of v_1^* . Assuming that eq. (4) holds down to zero penetrant concentration, combining eq. (4) with eq. (7), and using the values of $f(v_1^*, T)/B_d$ and $[f(v_1^*, T)]^2/B_d$ obtained, we can determine the value of D_0 .

Application of eq. (4) to the diffusion data at 15, 25, and 35°C. with a nonzero reference concentration yields a good straight line. Following the above procedure D_0 values were determined for respective reference values of v_1^* . An average value of D_0 has already been shown in Figure 5 as a

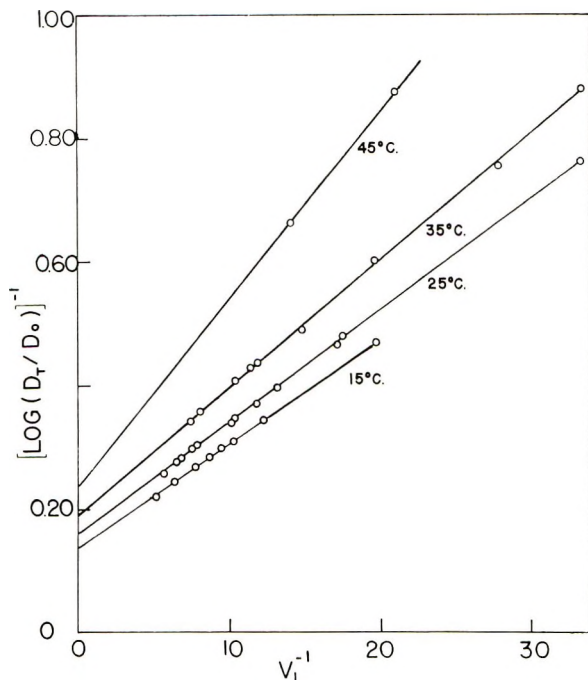


Fig. 8. $[\log (D_T/D_0)]^{-1}$ as a function of reciprocal volume fraction of methanol in PVAc.

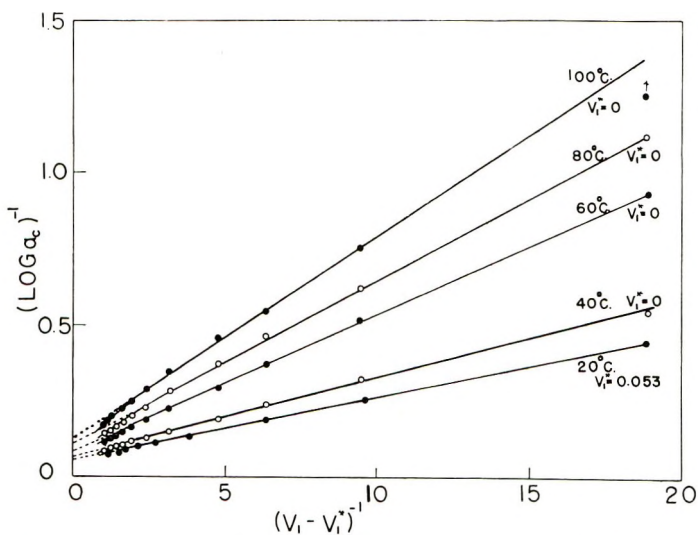


Fig. 9. $(\log a_c)^{-1}$ as a function of reciprocal volume fraction of DEP in PVAc.

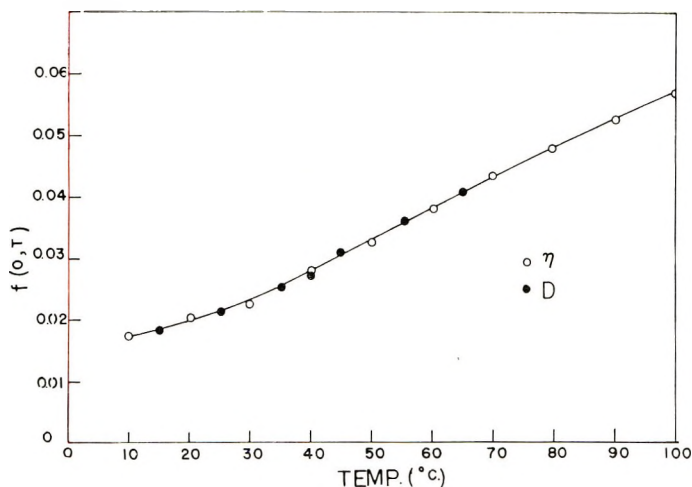


Fig. 10. Values of $f(0, T)$ for the systems PVAc-methanol and PVAc-DEP.

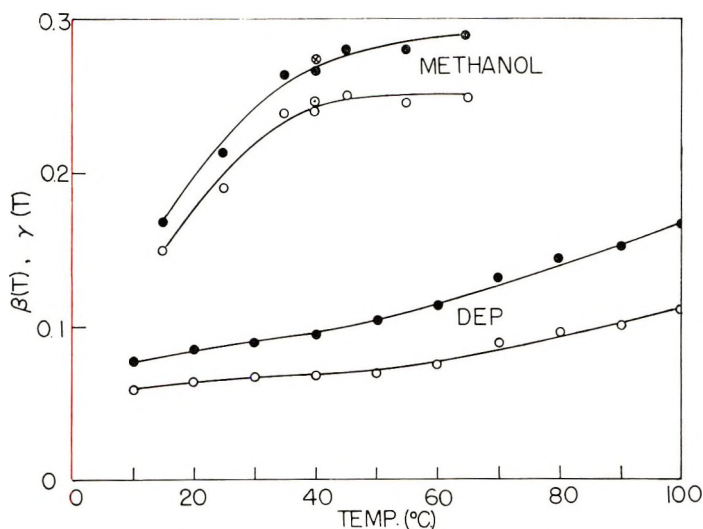


Fig. 11. Values of $\beta(T)$ and $\gamma(T)$ for the systems PVAc-methanol and PVAc-DEP: (O) $\beta(T)$; (●) $\gamma(T)$; (○, ⊗) $\beta(T)$, $\gamma(T)$ from stress relaxation study.

function of temperature. Further application of eq. (4) to the present data is shown in Figure 8, in which v_1^* is taken as zero. It is seen that the data at each temperature are represented well by a straight line.

The plots for $\ln(D_0/RT)$ against $\ln \eta(0, T)$ were found to be linear over the range of temperature, giving $B_d = 0.31$. With this B_d value the values of $f(0, T)$ (closed circles), $\beta(T)$, and also $\gamma(T)$ have been calculated as functions of temperature from the intercepts and slopes of the plots shown in Figure 8, and are shown in Figures 10 and 11.

Fits of eq. (5) to the isothermal viscosity data of concentrated solutions

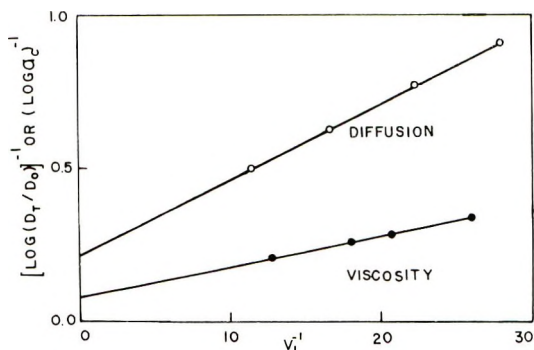


Fig. 12. $[\log(D_T/D_0)]^{-1}$ and $(\log a_c)^{-1}$ as functions of reciprocal volume fraction of methanol in PVAc at 40°C.

of PVAc in DEP are illustrated in Figure 9. The value of v_1^* chosen as a reference at each temperature is indicated in the graph. It is seen that for all the cases examined the plots are linear, although the plots show some downward deviation from linearity in the region of small values of $(v_1 - v_1^*)^{-1}$. A similar failure of the theory has been observed for the system PMA-DEP.¹² The values of $f(0, T)$, $\beta(T)$, and $\gamma(T)$ determined are plotted in Figures 10 and 11.

According to the definition of $f(0, T)$,⁵ this function must be independent of the kinds of penetrant, and characteristic of the polymer species concerned. The results shown in Figure 10 indicate that the $f(0, T)$ data from both diffusion and viscosity studies fall on a single curve. This behavior of the $f(0, T)$ curve for PVAc is similar to those for polystyrene and PMMA reported previously.⁵ The curve in the range from 30 to 90°C. is approximately fitted by the equation

$$f(0, T) = 0.0235 + 5.0 \times 10^{-4}(T - 30)$$

Below T_g of the polymer (about 30°C.³⁵), the $f(0, T)$ decreases slightly with decrease of temperature.

General trends of the $\beta(T)$ and $\gamma(T)$ curves deduced from the methanol study are similar to those for systems PMMA-DEP,⁸ polystyrene-dibenzyl ether,⁷ polystyrene-diethylbenzene,⁹ PMA-benzene, and polyethyl acrylate-benzene.² It is of interest to compare the value of $\gamma(T)$ for the PVAc-DEP system in Figure 11 with that for the PMA-DEP system. An average value of $\gamma(T)$ at temperatures above 30°C. for PVAc is 0.125, which is in good agreement with the value of 0.112 for PMA. Fujita and Kishimoto⁶ have shown that the values of $\gamma(T_g)$ are 0.068 for the PMMA-DEP system and 0.073 for poly-*n*-butyl methacrylate-DEP system, respectively, when comparison is made at T_g of respective polymers. These values are not very different from the value of 0.088 for PVAc at 30°C.

Data of D_T and η as functions of v_1 for the same polymer-diluent pair are available only for the system PVAc-methanol at 40°C.⁴ Figure 12 shows plots of $[\log(D_T/D_0)]^{-1}$ and $(\log a_c)^{-1}$ against v_1^{-1} calculated from those

data. It is seen that eqs. (4) and (5) hold well for this system. From the intercept and the slope of the straight line for the viscosity plot the value of $f(0, T)$, $\beta(T)$, and $\gamma(T)$ are found to be 0.0326, 0.240, and 0.273, respectively. Similar analysis of the diffusion coefficient data gives for these three parameters the values 0.0281, 0.237 and 0.265, when a value of 0.31 is used for B_d , which has been derived above from the variations of D_0 and $\eta(0, T)$ with temperature. These values derived from both diffusion and viscosity studies are included in Figures 10 and 11, and fall on the respective curves.

By combining eqs. (4) and (5) and then choosing a v_1^* common to both equations, one can obtain the relation:

$$\log [D_T(v_1, T)/D_T(v_1^*, T)] = B_d \log a_c \quad (10)$$

This equation provides another means for estimating B_d , when the data for the diffusion coefficient and the viscosity are available as functions of diluent concentration at a given temperature. It can be shown that this equation gives for B_d a value of 0.38, in agreement with the value deduced above.

The author wishes to express his hearty thanks to Professor Hiroshi Fujita, Department of Polymer Science, Osaka University, Osaka, for his continued interest and his helpful advice during the course of this work. Thanks are also due Miss Yoshiko Miki for her aid in making various experiments. Part of this work was supported by a grant-in-aid of research from the Ministry of Education.

References

1. Fujita, H., A. Kishimoto, and K. Matsumoto, *Trans. Faraday Soc.*, **56**, 424 (1960).
2. Kishimoto, A., and Y. Enda, *J. Polymer Sci.*, **A1**, 1799 (1963).
3. Fujita, H., *Fortschr. Hochpolymer. Forsch.*, **3**, 1 (1961).
4. Fujita, H., and A. Kishimoto, *J. Polymer Sci.*, **28**, 547 (1958).
5. Fujita, H., and A. Kishimoto, *J. Chem. Phys.*, **34**, 393 (1961).
6. Fujita, H., and A. Kishimoto, *Bull. Chem. Soc. Japan*, **33**, 274 (1960).
7. Fox, T. G., S. Gratch, and S. Loshaek, in *Rheology*, F. R. Eirich, Ed., Academic Press, New York, 1956, Vol. I, Chap. 12.
8. Bueche, F., *J. Appl. Phys.*, **26**, 738 (1955).
9. Bueche, F., *J. Appl. Phys.*, **24**, 423 (1953).
10. Meares, P., *J. Polymer Sci.*, **27**, 391 (1958).
11. Park, G. S., *Trans. Faraday Soc.*, **48**, 11 (1952).
12. Fujita, H., and E. Maekawa, *J. Phys. Chem.*, **66**, 1053 (1962).
13. Naito, R., *Kobunshi Kagaku*, **16**, 7 (1959).
14. Wiley, R. H., and G. M. Brauer, *J. Polymer Sci.*, **4**, 351 (1949).
15. Kishimoto, A., H. Fujita, H. Odani, M. Kurata, and M. Tamura, *J. Phys. Chem.*, **64**, 594 (1960).
16. Kokes, R. J., F. A. Long, and J. L. Hoard, *J. Chem. Phys.*, **20**, 1711 (1953).
17. Long, F. A., and R. J. Kokes, *J. Am. Chem. Soc.*, **75**, 2232 (1953).
18. Odani, H., S. Kida, M. Kurata, and M. Tamura, *Bull. Chem. Soc. Japan*, **34**, 571 (1961).
19. Kishimoto, A., and K. Matsumoto, *J. Polymer Sci.*, **A2**, 679 (1964).
20. Crank, J., *Trans. Faraday Soc.*, **51**, 1632 (1955).
21. Meares, P., *J. Polymer Sci.*, **27**, 405 (1958).
22. Long, F. A., and D. Richman, *J. Am. Chem. Soc.*, **82**, 513 (1960).

23. Frisch, H. L., *J. Phys. Chem.*, **61**, 93 (1957).
24. Rogers, C. E., V. Stannett, and M. Szwarc, *J. Polymer Sci.*, **45**, 61 (1960).
25. Kishimoto, A., and K. Matsumoto, *J. Phys. Chem.*, **63**, 1529 (1959).
26. Hayes, M. J., and G. S. Park, *Trans. Faraday Soc.*, **51**, 1134 (1955).
27. Kishimoto, A., E. Maekawa, and H. Fujita, *Bull. Chem. Soc. Japan*, **33**, 988 (1960).
28. Fox, T. G., and P. J. Flory, *J. Am. Chem. Soc.*, **70**, 2384 (1948).
29. Ninomiya, K., Thesis, Kyoto University, 1961.
30. Williams, M. L., R. F. Landel, and J. D. Ferry, *J. Am. Chem. Soc.*, **77**, 3701 (1955).
31. Jenckel, E., and R. Heusch, *Kolloid-Z.*, **130**, 89 (1953).
32. Ninomiya, K., and H. Fujita, *J. Colloid Sci.*, **12**, 204 (1957).
33. Sakurada, I., and T. Chiba, *Kogyo Kagaku Zasshi*, **47**, 135 (1944).
34. Kishimoto, A., unpublished data.
35. Kovacs, A., *J. Polymer Sci.*, **30**, 131 (1958).

Résumé

Le coefficient de diffusion du méthanol dans l'acétate de polyvinyle (PVAc) et la viscosité moyenne d'écoulement du système PVAc-phtalate de diéyle (DEP) ont été étudiés. Au cours d'études de diffusion, la sorption et la pénétration de la vapeur de méthanol ont été mesurées dans un domaine de températures au-dessus et en-dessous de T_g du polymère pur. On a évalué le coefficient de diffusion mutuelle D à partir des vitesses d'absorption et de désorption partant et retournant à une concentration initiale et terminale différente de zéro, et également à partir de la perméabilité de l'état stationnaire. Les valeurs de D déterminées par différentes méthodes sont équivalentes à l'erreur expérimentale près. On calcule le retard de pénétration comme une fonction de la concentration en agent pénétrant à partir des valeurs de D , en faisant usage de l'équation de Frisch. Les valeurs calculées sont plus élevées que celles trouvées à des températures légèrement au-dessus et en-dessous de T_g , mais quand la température était nettement au-dessus de T_g , les deux valeurs s'accordent. À des températures en-dessous de T_g , des courbes de pénétration anormales apparaissent, qui ne peuvent être entièrement expliquées en ce moment. Dans les études de viscosité les mesures ont été faites dans le domaine complet des composition du DEP à des températures de 10 à 100°C. en faisant appel à quatre techniques expérimentales différentes. Le graphique du logarithme de la viscosité en fonction de la fraction en poids du polymère à des températures déterminées, est convexe vers le haut aux basses concentrations et devient concave aux concentrations élevées. Dans la région intermédiaire apparaît un point d'inflexion. On a analysé d'après la théorie du volume libre, présentée précédemment, les données expérimentales du coefficient de diffusion thermodynamique du méthanol dans le PVAc et les données de la viscosité isothermique, du système PVAc-DEP. Les données expérimentales ont été trouvées en bon accord avec la théorie.

Zusammenfassung

Der Diffusionskoeffizient von Methanol in Polyvinylacetat (PVAc) sowie die Viskosität des PVAc-Diäthylphthalat-(DEP)-Systems bei stationärem Fließen wurden untersucht. Bei den Diffusionsversuchen wurde die Sorption und Permeation von Methanoldampf im Polymeren in einem Temperaturbereich oberhalb und unterhalb von T_g des reinen Polymeren gemessen. Der Diffusionskoeffizient D wurde aus der Absorptions- und Desorptionsgeschwindigkeit von und zur nicht verschwindenden Ausgangs- und Endkonzentration und auch aus der Permeabilität im stationären Zustand bestimmt. Die nach verschiedenen Methoden erhaltenen D -Werte stimmten innerhalb der Versuchsfehler überein. Mit der Gleichung von Frisch wurde die Permeationsdurchbruchzeit als Funktion der Konzentration des penetrierenden Stoffes aus den D -Daten

berechnet. Bei Temperaturen schwach oberhalb und unterhalb T_g waren die berechneten Werte höher als die beobachteten, bei Temperaturen hinreichend oberhalb T_g stimmten aber die beiden Werte überein. Bei Temperaturen unterhalb T_g traten anomale Permeationskurven auf, die gegenwärtig dem Verständnis noch Schwierigkeiten bereiten. Bei den Viskositätsuntersuchungen wurden Messungen nach vier verschiedenen Methoden über den gesamten Zusammensetzungsbereich bei Temperaturen von 10 bis 100°C. ausgeführt. Im Diagramm Logarithmus der Viskosität gegen Gewichtsbruch des Monomeren bei gegebener Temperatur trat bei niedriger Konzentration eine gegen oben konvexe Krümmung und bei hoher Konzentration eine konkave auf. Im Mittelbereich befand sich ein Wendepunkt. Die Versuchsergebnisse für den thermodynamischen Diffusionskoeffizienten von Methanol in PVAc und die isothermen Viskositätsdaten für das System PVAc-DEP wurden anhand der früher mitgeteilten Freien-Volums-Theorie einer Analyse unterzogen. Es zeigte sich, dass eine adäquate Darstellung der Versuchsergebnisse durch die Theorie möglich ist.

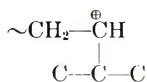
Received February 25, 1963

Intramolecular Hydride Shift Polymerization by Cationic Mechanism. I. Introduction and Structure Analysis of Poly-3-Methylbutene-1

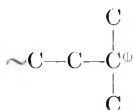
J. P. KENNEDY, L. S. MINCKLER, JR., G. G. WANLESS, and R. M. THOMAS, *Esso Research and Engineering Company, Linden, New Jersey*

Synopsis

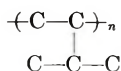
The low temperature cationic polymerization of 3-methylbutene-1 proceeds by intramolecular hydride shift mechanism. The secondary carbonium ion



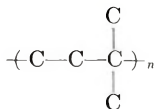
rearranges to a tertiary one



prior to propagation. Thus the repeat unit of cationically obtained poly-3-methylbutene-1 is not the expected



or 1,2 structure but an α, α' -dimethylpropane-type 1,3 unit, e.g.,



Detailed structure analyses involved vacuum pyrolysis and depolymerization studies. Fragmentation products of various poly-3-methylbutene-1 samples, e.g., cationic 1,3 polymers (I) and conventional 1,2 polymers (II), were analyzed by gas chromatography and by infrared and by mass spectrometric techniques. The gaseous fraction of I yielded ~ 22 mole-% C_3 fraction whereas II gave ~ 70 mole-% (pendant isopropyl groups); on the other hand, I yielded 26.3 mole-% isobutene, while II gave only ~ 6.8 mole-%. Cationic pyrolyzates show distinct $\text{CH}_2=\text{CH}-$ bonds but weak $-\text{CH}=\text{CH}-$ and $\text{CH}_2=\text{C}-$ bonds, whereas conventional II pyrolyzates show predominantly

$\text{CH}_2=\text{C}-$ and some $-\text{CH}=\text{CH}-$ bonds. Both, the gas chromatographic and infrared

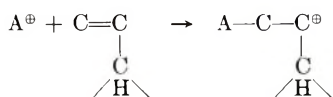
analyses indicate independently that cationic poly-3-methylbutene-1 is a mixture of about 30% conventional 1,2 head-to-tail enchainment and 70% 1,3 polymer. The mass

spectrum of depolymerized I and II samples gave different and characteristic fragmentation patterns. These were analyzed and explained. The latter findings also substantiate fundamental structural differences between I and II.

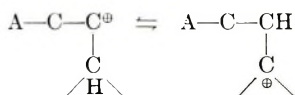
I. INTRODUCTION

This paper concerns an unusual polymerization mechanism which we call intramolecular hydride shift polymerization. The principle of the mechanism is as follows: the carbonium ion which is formed by direct interaction between monomer and cationic catalyst (initiation) rearranges itself to an energetically more favored carbonium ion before it reacts with the next monomer unit (propagation):

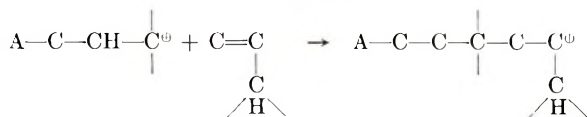
Initiation:



Hydride shift:



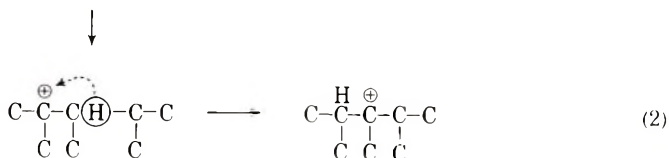
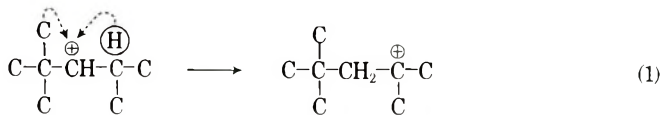
Propagation.



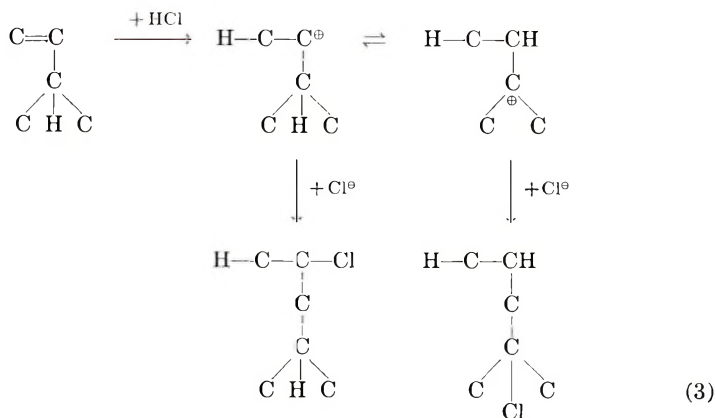
Termination and Chain Breaking are by conventional cationic mechanisms.

Intramolecular hydride shifts are not uncommon in the chemistry of small organic molecules. They have been proposed many times to explain the experimental results of isomerizations, cracking, and alkylations, but few direct experiments have been carried out to prove the actual existence of intramolecular hydride shifts.

A comprehensive analysis of the dehydration products of *tert*-butyl-isopropyl carbinol gives conclusive evidence that energetically favored intramolecular hydride shifts do occur:¹



Significantly, an intramolecular hydride shift occurs during the hydrochlorination of 3-methylbutene-1.²

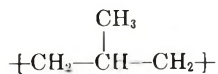


At room temperature, an equimolar mixture of the two chlorides formed. It was shown conclusively that the *sec*-chloride did not isomerize to the tertiary chloride but that hydride shift occurred prior to the reaction with the chloride ion. In further work, Whitmore and Johnston³ showed that secondary alkyl halides with branching on the cation adjacent to the carbon carrying the halogen cannot be prepared from corresponding alcohols. Rearrangement occurs to give the *tert.* halide. Friedman and Morris⁴ found that when benzene was alkylated with 3-methylbutene-1 in the presence of aluminum chloride catalyst at 21°C., 2-methyl-3-phenylbutane formed; however, at -40°C. 2-methyl-2-phenylbutane was obtained exclusively. Apparently, hydride shift occurred prior to alkylation. Various other intramolecular hydride shifts have been described.⁵⁻⁷ More recently, intramolecular hydride shifts have been invoked to explain certain infrared data for cationically polymerized propylene.⁸

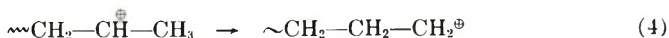
Intermolecular hydride migrations are quite common and well authenticated. A large number of such reactions are known and have been summarized.^{9,10} Well established cases of intermolecular hydrogen migration polymerization have been surveyed.¹¹ Discussion of intermolecular hydrogen migration falls outside the scope of this paper.

The concept of intramolecular hydrogen migration polymerization is by no means new. Staudinger¹² in 1935 proposed that so called 1,3-polymerization takes place during the contacting of propenylbenzene and its *p*-alkoxy derivatives with Lewis acid catalysts. Peculiarities in the viscosity of the product and pyrolysis data were brought up as evidence. Somewhat later, Hungarian chemists showed¹³ that the mechanism proposed was incorrect and that polymerization proceeded by conventional 1,2 head-to-tail mechanism. Similar conclusions were reached on the basis of spectroscopic studies in our laboratories.¹⁴

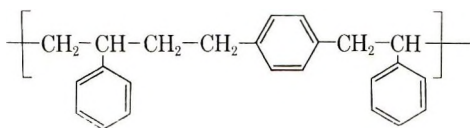
A similar hydride shift mechanism has been claimed by Russian authors to occur during certain isobutene polymerizations, and 2-methylpropane-type repeat units were proposed,¹⁵ i.e.,



Although this work has not been followed up, the experimental results are unsupported and strongly in doubt. More recently, it was reported that with the use of Ziegler-Natta type catalysts propylene was polymerized but instead of polypropylene, pure polyethylene was obtained.¹⁶ These findings were explained by assuming that intramolecular hydride shifts occur before propagation can take place e.g.,



Such a mechanism is highly unlikely, the energetics being unfavorable by at least 11 kcal./mole.¹⁷ It has also been claimed that by the judicious choice of the catalyst, ethylene-propylene copolymers can be obtained by polymerizing propylene alone. The same source states that styrene can be polymerized to give products containing 1,6-polymerized styrene units in the chain:



Unfortunately, no references are given, and none of these statements has been substantiated.¹⁶

For the first time, it is now possible to present convincing evidence for intramolecular hydride shift polymerization in the case of cationically initiated low temperature polymerization of 3-methylbutene-1. In the first paper of this series we describe and discuss heat degradation and depolymerization studies. In a subsequent paper we will discuss our spectroscopic findings.

II. EXPERIMENTAL

General experimental technique, apparatus, manipulations, and handling of materials have been described.¹⁸ The purity and source of chemicals as well as polymer synthesis have also been described.¹⁹ In this investigation, rubbery, amorphous cationically obtained poly-3-methylbutene-1 samples were analyzed.

High vacuum pyrolysis of various poly-3-methylbutene-1 samples was carried out at two levels of cracking severity, in all-glass equipment, using 1.0 g. and 0.5 g. samples. The apparatus for both procedures is shown in Figure 1.

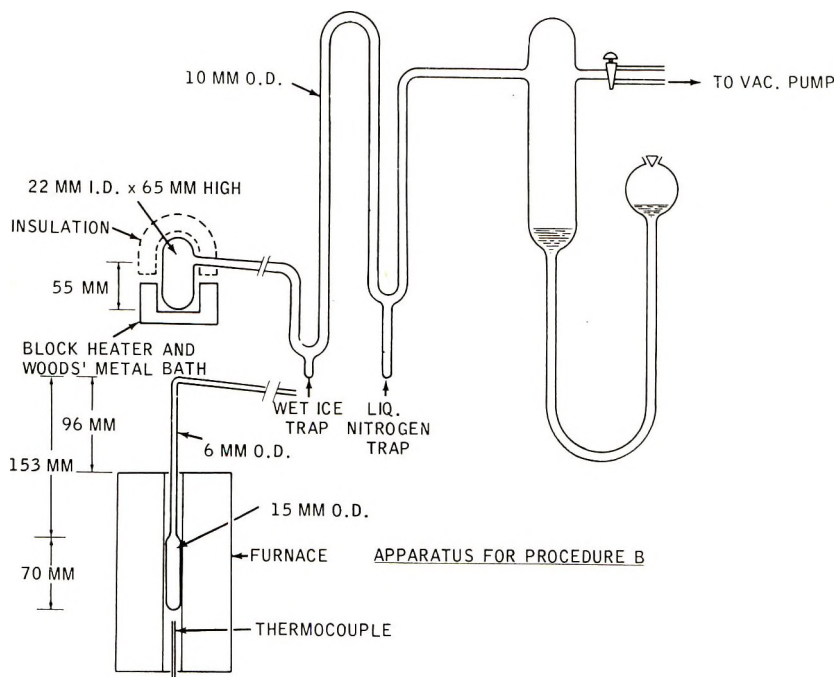


Fig. 1. Polymer depolymerization apparatus.

The samples are melted ($\sim 230^\circ\text{C}$.) and degassed under vacuum, the system sealed off, and the cooling traps (wet ice and liquid nitrogen consecutively) are put in place; then one of two heating cycles are imposed: procedure I: 50 min. to 490°C ., 10 min. at 490°C .; procedure II: 6 min. to 410°C ., 20 min. at $420\text{--}440^\circ\text{C}$., 10 min. at 480°C ., 10 min. at 505°C .

At the end of the run, the still pot is isolated, the heavier sample in the wet ice trap is degassed at 100°C ., and the light oil sample in the nitrogen trap is degassed at 25°C .

The heavy oil fraction from procedure I ranges from about C_{10} to C_{60} . In procedure II the sample refluxes in the long neck of the still, and the heavy oil distilled ranges from about C_{10} to C_{20} (dimers, trimers, tetramers).

The products from these studies are: (a) $\text{C}_1\text{--}\text{C}_5$ gases, representing 4.4–16.5% of charge, which are assayed by gas chromatography with a hexane-2,5-dione column; (b) $\text{C}_5\text{--}\text{C}_{10}$ light oil, representing about 20% of charge; (c) C_{10} + heavy oil fractions, representing about 40% of charge. The two oil fractions are analyzed by infrared and by mass spectrometric techniques.

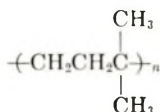
III. RESULTS AND DISCUSSION

Poly-3-methylbutene-1 was first polymerized cationically in 1927 by Norris and Joubert, who thought that they obtained dimers and higher

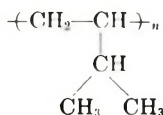
polymers with sulfuric acid catalyst.²⁰ Seven years later, Leendertse et al.²¹ treated the monomer with aluminum chloride at -80°C ., but only oily products formed, presumably because reaction conditions were unfavorable (solid AlCl_3 in bulk). Only one patent appeared in the literature which concerned the polymerization of the monomer in recent years.²² This patent described the preparation of poly-3-methylbutene-1 with Lewis acid-type catalysts in alkyl chloride diluent at low temperatures (-78°C .). The product obtained was a colorless, amorphous, tough semisolid having a rather low molecular weight. However, none of the earlier investigators studied the structure of the material.

3-Methylbutene-1 can be polymerized readily with alkyl metal coordination catalysts (Ziegler-Natta type) at ambient temperatures.²³⁻²⁵ The product obtained by this process is a highly crystalline isotactic polymer and has a conventional 1,2 head-to-tail structure.

Recently, in the course of fundamental studies on cationic polymerization, aluminum chloride, alkyl halide at low temperatures were used in the study of 3-methylbutene-1 polymerizations. Preliminary NMR studies indicated that the product of the early investigators consisted of α, α' -dimethylpropane repeating units, i.e.,



and did not have the expected structure:^{26, 27}

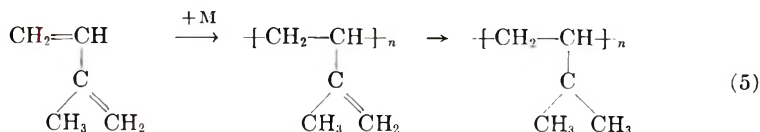


When 3-methylbutene-1 is polymerized with strong Lewis acid catalyst at -130°C ., a crystalline polymer is obtained. This crystalline product is not isotactic.²⁶ It was recognized immediately that the x-ray diffraction pattern of the low temperature product is different from that of the isotactic Ziegler-Natta type product. Detailed structure analyses carried out in these laboratories revealed that cationically initiated low temperature polymerization of 3-methyl butene-1 has an unexpected structure and that it consists predominantly of α, α' -dimethylpropane repeating units.

One way of establishing unknown structures is that of comparison with well-defined compounds. Unfortunately, no material existed which could be used as a model compound for the 1,3 polymer structure in this investigation.

Isotactic poly-3-methylbutene-1 having a *bona fide* 1,2 structure could not be used as model compound in our spectroscopic studies because this polymer is insoluble in common solvents. However, it can be made soluble by depolymerization. To obtain a model compound, isoprene was

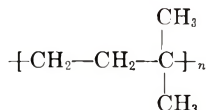
polymerized selectively through its 3,4 double bonds²⁸ and the polymer hydrogenated, i.e.,



This material, which is structurally equivalent to a 1,2 polymer of 3-methylbutene-1, was used as prototype polymer in some phases of our structure studies.

A. Pyrolysis and Fragment Analysis

Depolymerization by pyrolysis is a useful tool in structure analysis. Careful evaluation of polymer fragments can yield important clues as to the original structure. Conventional 1,2 polymerization of 3-methylbutene-1 would yield a $\text{---CH}_2\text{---CH---}$ backbone with pendant isopropyl groups and it was theorized that careful pyrolysis would yield large amounts of propane or propene in the gaseous fraction. On the other hand, fewer C_3 fragments were expected from the structure:



Using the high vacuum apparatus described in the experimental part, three types of poly-3-methylbutene-1 samples were pyrolyzed, e.g., low temperature cationic type, alkyl metal-coordination catalyst (Ziegler-Natta) type, and hydrogenated 3,4-polyisoprene. Our technique yielded three fractions of each of the polymers analyzed, i.e., a gaseous, a light oil, and a heavy oil fraction.

B. Analysis of the Gaseous Fraction

Table I shows the composition of the gaseous fractions obtained by vacuum pyrolysis of the three types of polymers at two cracking severities. Pyrolysis of two Ziegler-Natta type polymers and one hydrogenated polyisoprene sample (conventional 1,2 structures) yielded a total of 79.6, 65.4, and 66.7 mole-% C_3 fragments (propane + propene), respectively. In contrast, three low temperature, cationically polymerized poly-3-methylbutene-1 samples gave a total of 27.0, 18.5, and 20.7 mole-% C_3 fragments.

Equally impressive differences were obtained in the C_4 fraction, particularly in the isobutene (olefin) fraction. Whereas the Ziegler-Natta samples and the hydrogenated 3,4-polyisoprene yielded 4.4, 9.1, and 5.3 mole-% isobutene, the cationic samples gave 26.5, 22.3, and 30.0 mole-%.

Other differences are found in comparing the total yields of gaseous C_4 and C_6 olefins. Thus, the conventional 1,2 polymers yielded 8.6, 20.6, and

TABLE I
Composition of the Gaseous Fractions of Vacuum Pyrolyzed Poly-3-Methylbutene-1
Samples

	Content, mole-%					Hydrogenated polyisoprene
	Low temperature cationic polymer			Ziegler-Natta polymer		
	I ^a	I ^a	II ^a	I ^a	II ^a	
Ethane	3.4	12.8	1.6	1.3	0.62	2.8
Ethylene	15.7	18.0	6.0	5.4	2.4	2.2
Propane	13.3	9.0	10.9	68.8	54.8	59.0
Propylene	13.7	9.5	9.8	10.8	10.6	7.7
Isobutane	7.9	1.0	8.7	1.8	2.2	1.7
<i>n</i> -Butane	1.1	0.57	1.0	0.13	1.5	3.7
Butene-1	0.59	0.42	0.87	0.18		0.68
Isobutylene	26.5	22.3	30.0	4.4	9.1	5.3
Isopentane or <i>trans</i> -butene-2						
	5.9	0.52	11.5	3.8	11.5	6.3
<i>cis</i> -Butene-2	0.24	7.6	0.38	0.18		
3-Methylbutene-1	8.8	11.4	14.7	2.8	7.2	3.9
Butadiene-1,3	0.69	0.56	0.65			0.68
Pentenes-1,		0.33				0.05
2-Methylbutene-1	0.29	9.9	1.6	0.13		0.82
<i>trans</i> -Pentene-2	0.58	0.66	2.2	0.18		1.2
<i>cis</i> -pentene-2	0.59			0.04		0.29
2-Methylbutene-2	0.34	3.3				3.4
C ₆ and higher						
Total	99.63	99.86	99.90	99.94	99.92	99.96
Wt. % of gas yield	14.2	12.9	11.0	9.4	4.4	5.7
Total olefins	73.9	76.5	77.7	27.9	40.8	32.7
Total saturates	25.7	23.4	22.2	72.0	59.2	67.2
Total C ₄ olefins	33.2	30.8	42.8	8.6	20.6	12.6
Total C ₅ olefins	11.3	15.2	19.2	3.2	7.2	10.5

* Cracking severity (refers to procedures I and II; see experimental section).

12.5 mole-% total C₄ olefins, whereas the cationic polymers yielded 33.2, 30.8, and 42.8 mole-% of total C₄ olefins.

Total C₅ olefins for the Ziegler-Natta and hydrogenated polyisoprene polymers are 3.2, 7.2, and 10.5 mole-%, while for the cationic polymers they are 11.3, 15.2, and 19.2 mole-%.

These differences are summarized in Table II.

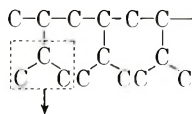
Although only a small number of runs has been made, the reproducibility of the technique is fairly satisfactory. (Compare columns I and II of Table I.) The effect of the two levels of cracking severity can be observed also, in Table I. However, these differences do not alter the conclusions which are drawn from the work.

These findings can be explained readily by assuming fragmentation of the following types; the fragments marked off were identified by gas chromatography.

TABLE II
Differences in Gas Composition from Vacuum Pyrolysis of Polymers
(Summarized from Table I)

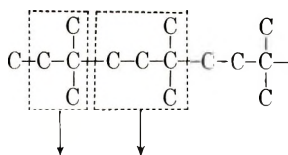
Gas components	Content, mole-%			Estimated maximum % 1-2 polymer content in cationic polymers
	Cationic polymers (avg. of 3)	Ziegler polymers (avg. of 2)	Hydrogenated polyisoprene	
Propane	11.1	61.8	59.0	18.0
Propene	11.0	10.7	7.7	
Total saturates	23.8	65.6	67.2	35.4
Total olefins	75.4	34.4	32.1	
Total C ₄ olefins	35.6	14.6	12.5	
Isobutane	5.9	2.0	1.7	
Isobutene	26.3	6.8	5.3	
Total C ₅ olefins	15.6	5.2	9.7	
				26.7

Conventional 1-2 type polymer:



Propane, Propene

Cationic 1-3 type polymer:



Isobutane, 3-Methyl
isobutylene 1-butene
and other
C₅ olefins

It is conceivable that the low temperature cationic polymerization of 3-methylbutene-1 does not result in an exclusively 1,3 type enchainment and that some 1,2 enchainment occurs in the backbone. Data in Table I are helpful in estimating the amount of 1,2 contribution in the cationic polymer. Assuming that the Ziegler-Natta type polymer represents a 100% 1,2 polymer, the estimated amount of 1,2 enchainment in the cationic polymer is in the average 26.7%. Similarly, when the hydrogenated 3,4-polyisoprene is used as a basis for 100% 1,2 polymer, the estimated 1,2 enchainment in the cationic polymer is 27.1%. (See Table II and compare with similar estimates made below from infrared data.)

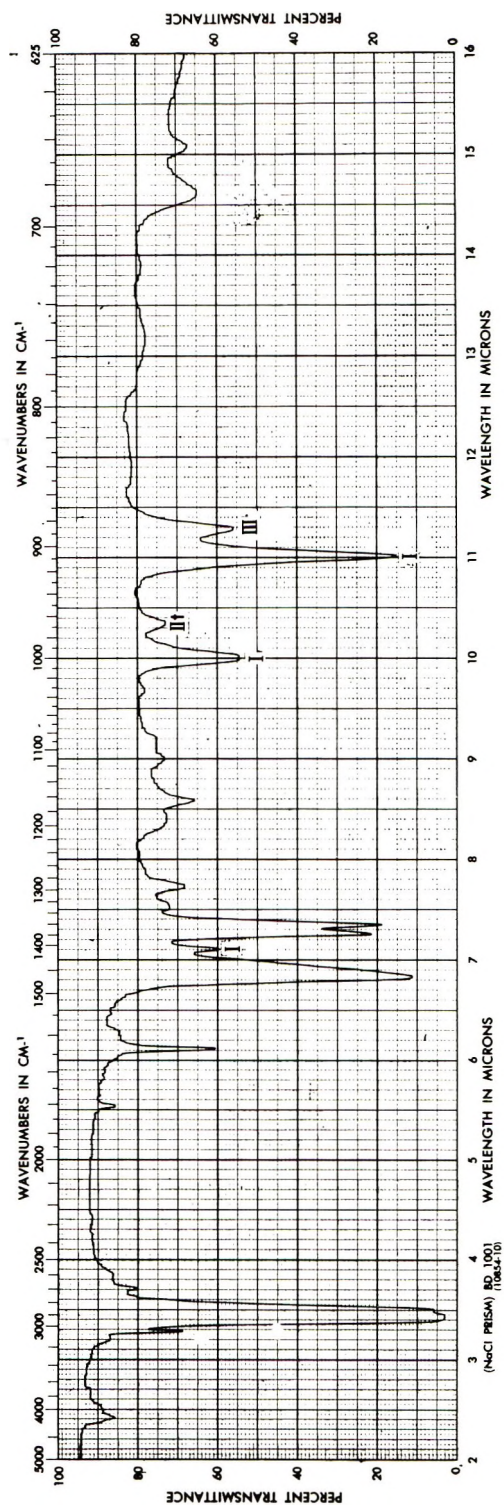


Fig. 2. Infrared spectrum of cationic poly-3-methylbutene-1. Light oil depolymerizate.

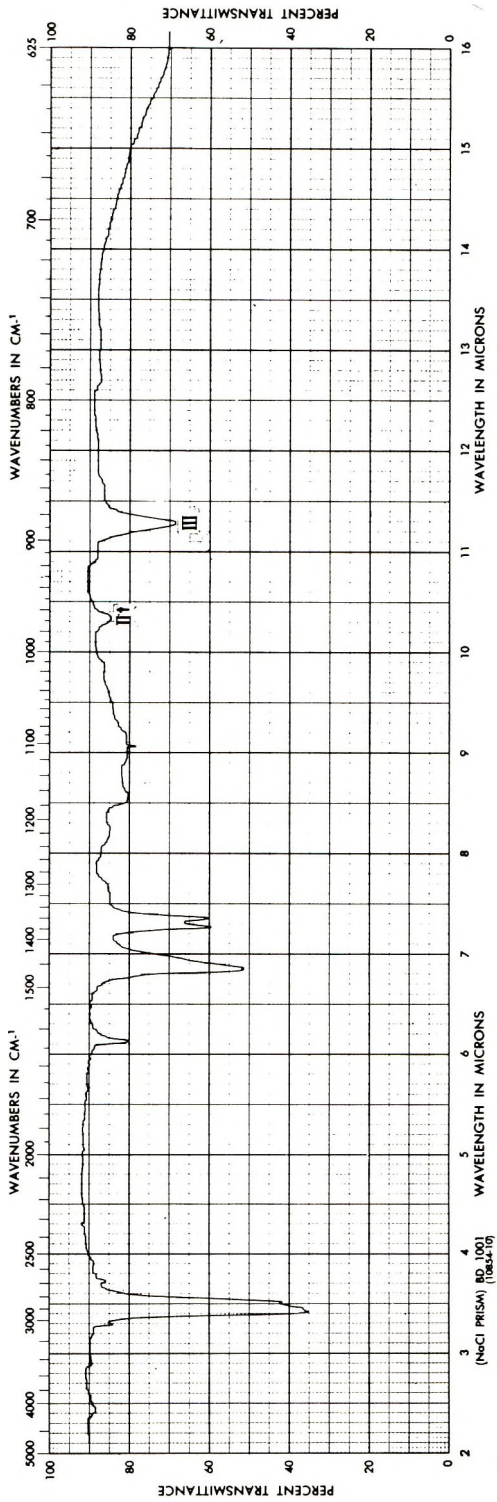


Fig. 3. Infrared spectrum of isotactic, Ziegler-Natta poly-3-methyl-butene-1. Light oil depolymerizate.

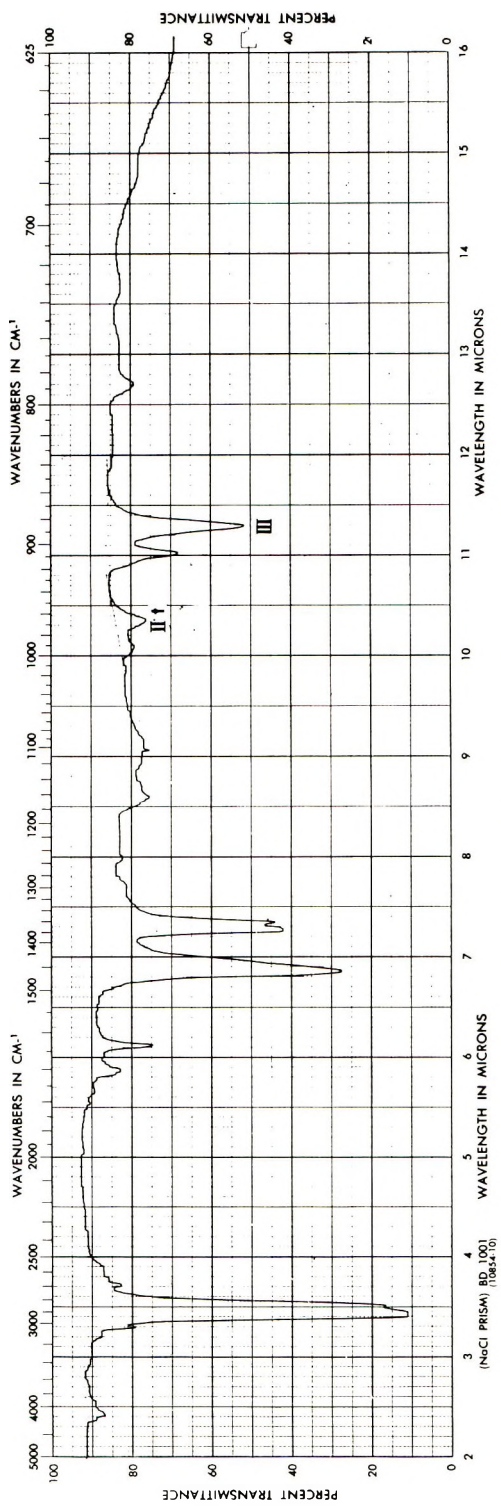


Fig. 4. Infrared spectrum of hydrogenated 3,4-polyisoprene. Light oil depolymerizate.

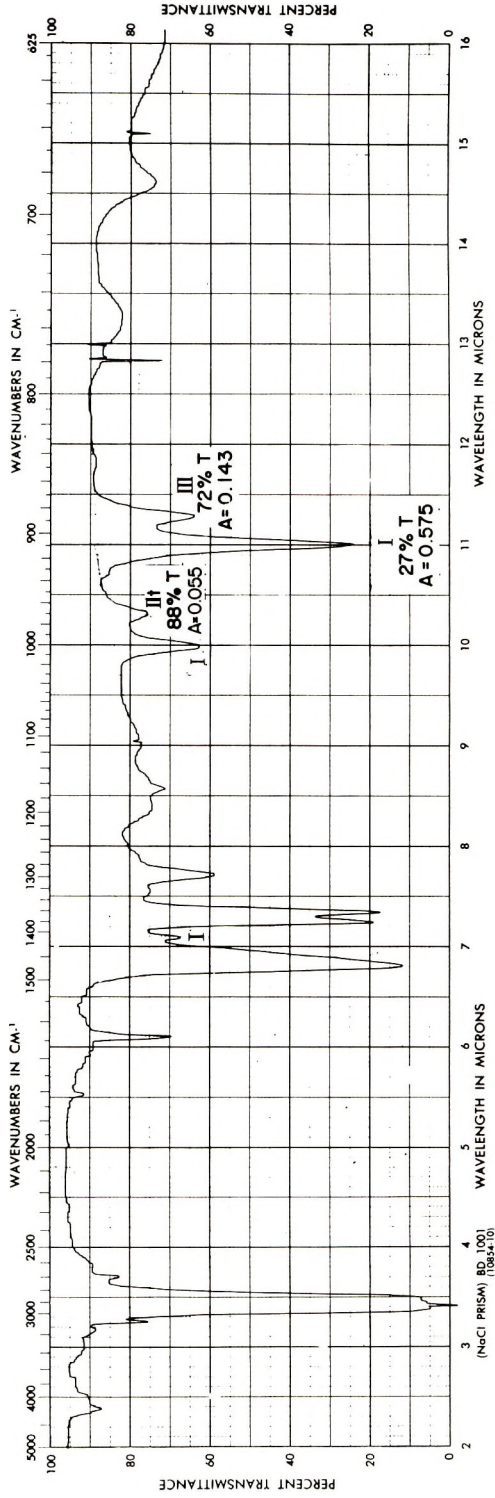


Fig. 5. Infrared spectrum of cationic poly-3-methylbutene-1. Heavy oil depolymerizate.

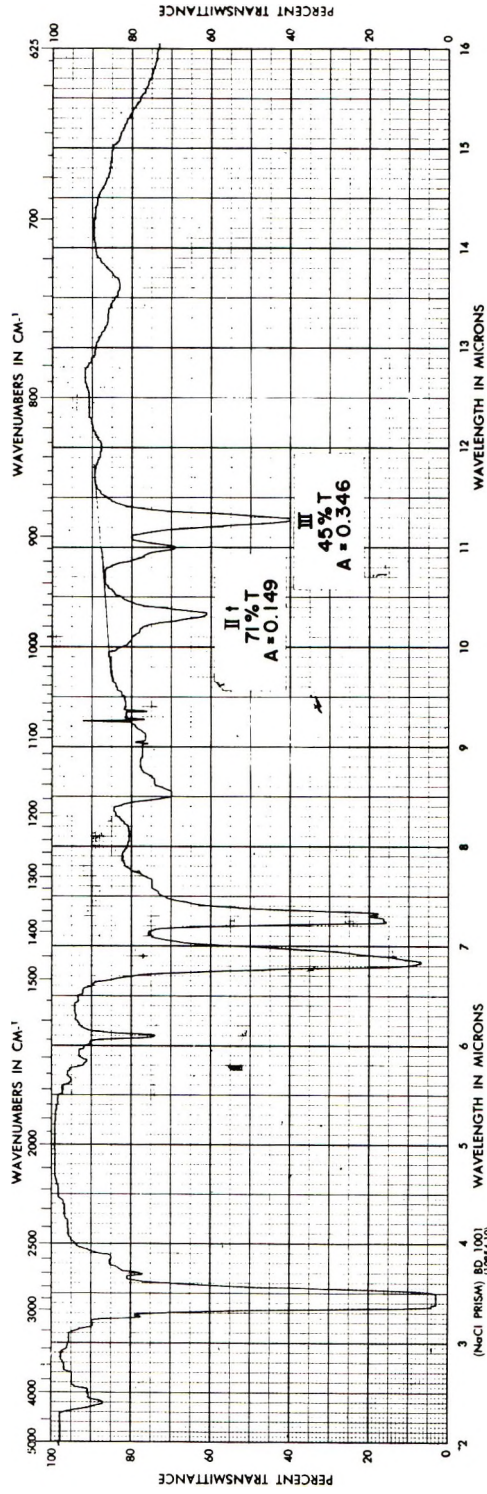


Fig. 6 Infrared spectrum of isotactic, Ziegler-Natta poly-3-methylbutene-1. Heavy oil depolymerizate.

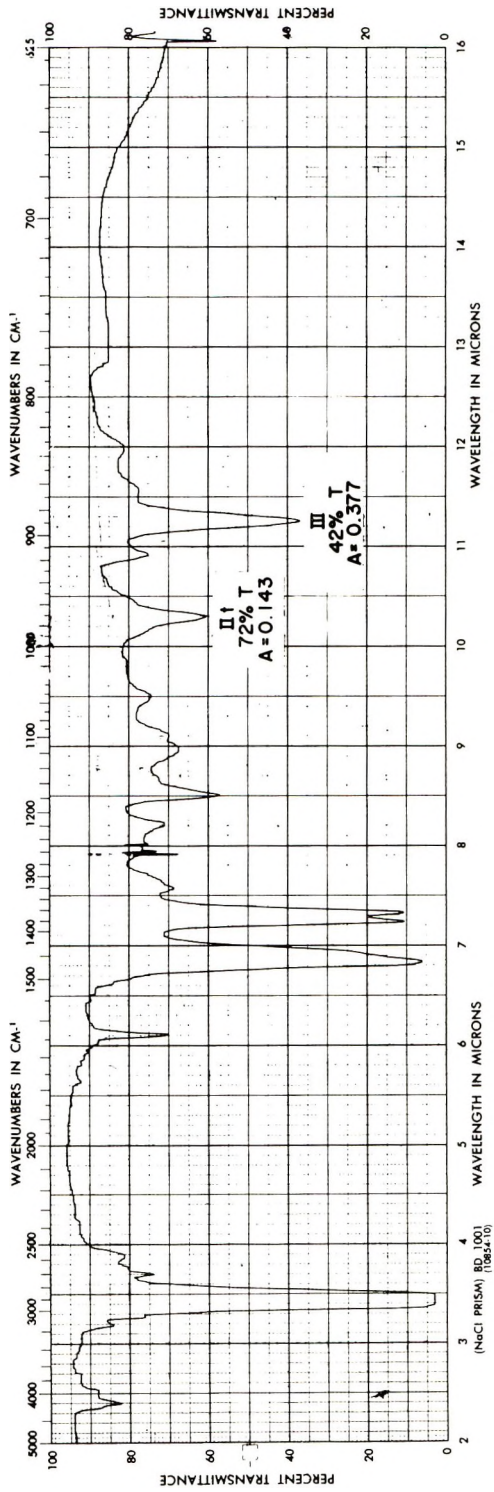
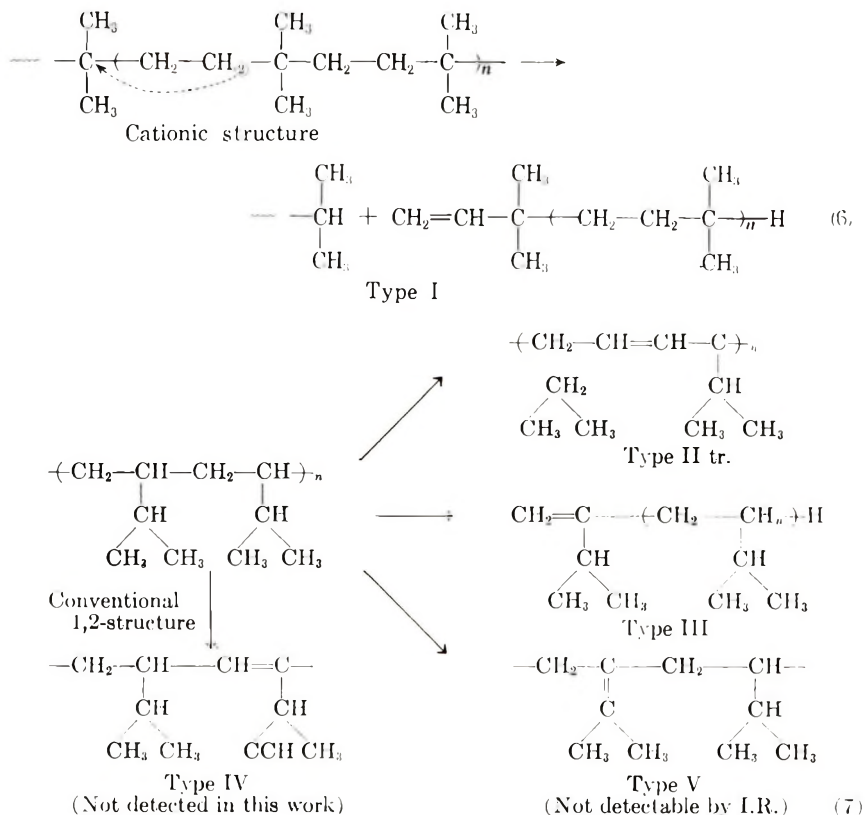


Fig. 7. Infrared spectrum of hydrogenated 3,4-polyisoprene. Heavy oil depolymerizate.

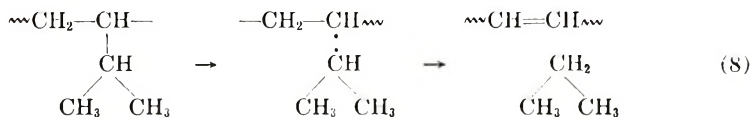
C. Infrared Analyses of the Oil Fractions

Light oil and heavy oil fractions obtained in the wet ice and the liquid nitrogen traps, respectively, were analyzed by infrared spectroscopy. Figures 2-7 show the spectra of these two fractions obtained by depolymerizing cationic, Ziegler-Natta, and hydrogenated 3,4-isoprene samples. Significantly, the cationic pyrolyzates show distinct Type I olefin (vinyl) bands at 3.28, 7.1, 10.0, and 11.05 μ but a weak Type II tr olefin ($-\text{CH}=\text{CH}-$) band at 10.35 μ , and a medium or weak Type III olefin ($\text{CH}_2=\text{C}-$) band at 11.25 μ . The situation is just the reverse with the Ziegler-Natta and hydrogenated 3,4-polyisoprene samples. These spectra show exclusively Type III and II tr. bands, and practically no Type I bands are present. These results can readily be explained by considering the eqs. (6) and (7).



Significantly, no type I double bonds (vinyl groups) can form from a 1,2 type polymer unless some unlikely major rearrangement precedes bond scission. In contrast, the formation of vinyl groups is quite probable from the cationic structure: Cleavage between the quaternary and secondary carbon atoms with simultaneous β -hydrogen migration is a well-known

process and it readily accounts for the findings. In a similar vein, the simplest mechanism (Accam's razor) explains the formation of type II tr. and III double bonds from the 1,2 polymers. Backbone scission between the tertiary and secondary carbon coupled with β -hydrogen migration is a well-known process and accounts for the strong Type III band. A probable source of Type II tr. double bonds is the splitting off of the isopropyl group. The isopropyl radical stabilizes itself by hydrogen abstraction and the polymer radical by hydrogen ejection. Large amounts of propane found in the gaseous fraction substantiate this hypothesis:



We obtained no evidence for simple backbone dehydrogenation occurring between adjacent tertiary and secondary carbon atoms which would yield type IV ($-\text{CH}=\text{C}-$) olefin bonds.

Semiquantitative evaluation of the infrared spectra was helpful in estimating the contribution of 1,2 type enchainment in the cationic polymer. Assuming that the isotactic Ziegler-Natta polymer is 100% 1,2 type polymer the per cent 1,2 structure in the cationic poly-3-methylbutene-1 can be estimated from the peak height ratios of the Type III and Type II tr. olefin bonds. Thus by comparing the Type III bands at 11.25μ we calculated (two independent samples) 41.5 and 39.9%, and from the Type II tr. bands at 10.35μ were obtained 25.2 and 27.6% 1,2 contributions in the polymer backbone of the cationic polymer. Very similar figures were obtained when the hydrogenated 3,4-polyisoprene was used as a basis for 100% 1,2 enchainment.

These infrared results are in agreement with those obtained from a study of the composition of the gases and both indicate independently that the low temperature cationic poly-3-methylbutene-1 is a mixture of about 30% conventional 1,2 head-to-tail polymer and 70% 1,3 type polymer. The exact nature of the mixture (i.e., block copolymer, physical mixture, etc.) is unknown.

D. Mass Spectra of Heavy Oils from Depolymerization Experiments

The mass spectra of heavy oils obtained by depolymerization of Ziegler-Natta type and low temperature cationic polymers have been investigated (depolymerization by procedure I, see Experimental section). Figure 8 shows the mass patterns of the olefinic series (C_nH_{2n}) in the range C_4-C_{45} . It is evident that the patterns obtained are different and characteristic for the two types of polymers. The cracking patterns are consistent with the structures which we propose for these two kinds of poly-3-methylbutene-1.

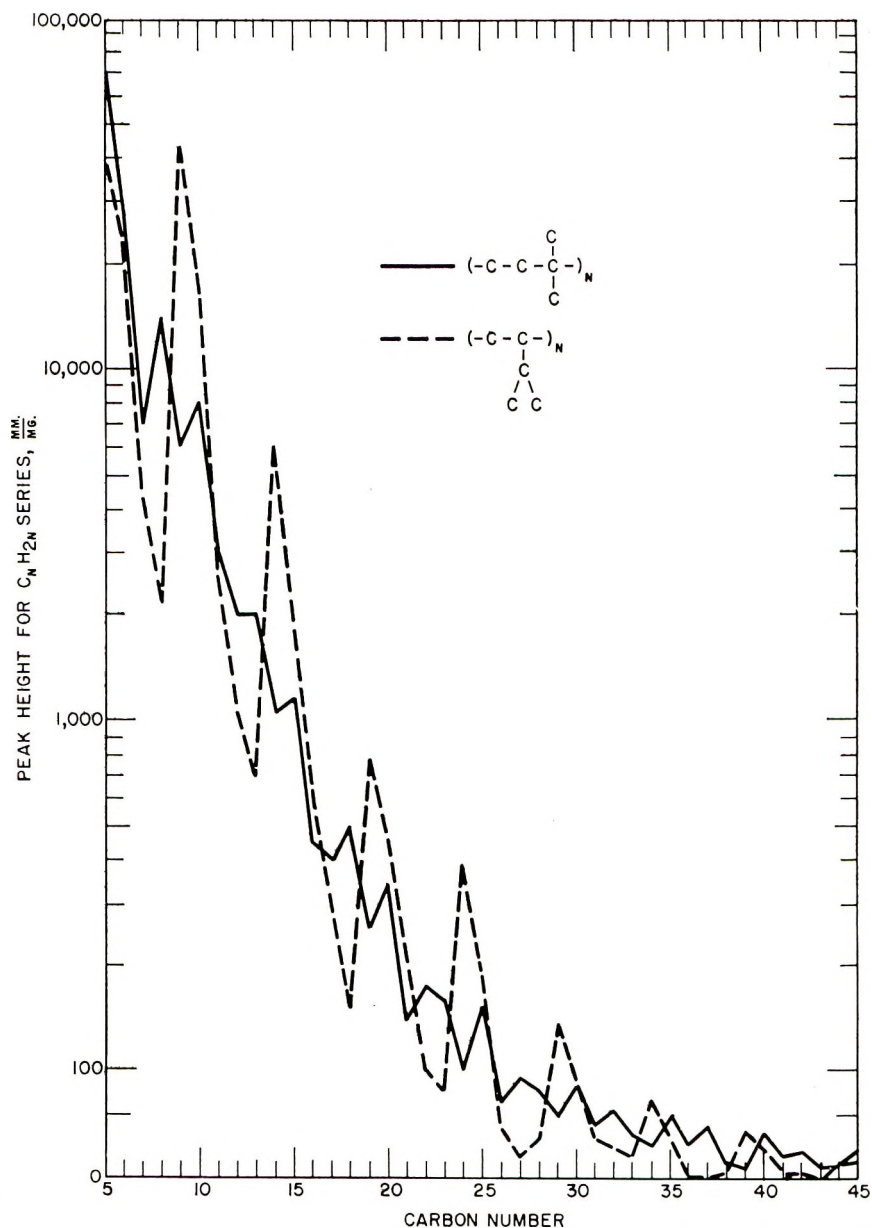
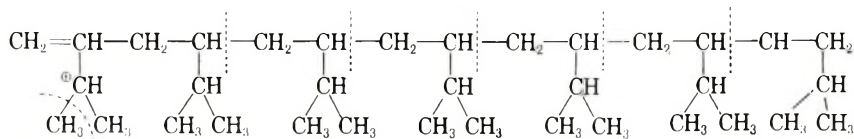
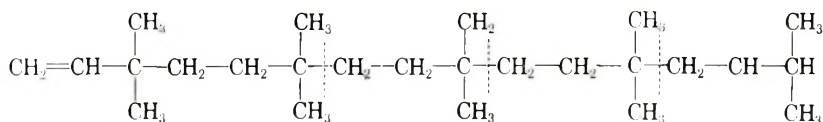


Fig. 8. Mass spectra of oils from poly-3-methylbutene-1 pyrolysis (isotope corrected and normalized).

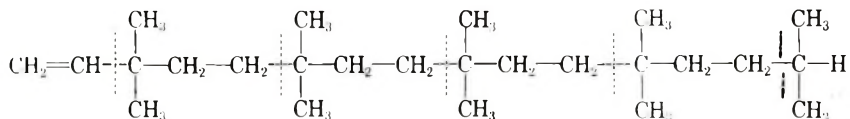
The Ziegler-Natta or 1,2 type polymer shows a predominant series which is maximized at carbon number 9, 14, 19, 24, 29, 34, 39, and etc. This series is considered to be due²⁹ to the loss of a branched methyl group (on electron bombardment) and subsequent fragmentation after consecutive C_6 units, for example, for C_{34}



The pattern of the low temperature cationic polymer is somewhat more complex. Basically, three different series (i.e., processes) can be distinguished. The predominant series is represented by peaks at carbon atoms 10, 15, 20, 25, 30, 35, 40, etc. This simple, even fragmentation can be explained by a dimer to octamer distribution, for example, pentamer C₂₅:



The other two series appear at carbon atoms 8, 13, 18, 23, 28, etc., and at 22, 27, 32, 37, 42, etc., respectively. Both processes can be explained simultaneously by one dominant type of cleavage:



Consider the fragments on the right-hand side of the cleavage lines counting from right to left. These fragments will account for the olefins whose carbon numbers are 8, 13, 18, 23, 28, etc. The remaining (left-hand) portions of the polymer chain will deliver the third sequence. This series

TABLE III
Pyrolyzate Fragment Pattern of Cationic Polymer

Number of monomer units in polymer chain	Total no. of carbons	Fragment series
<i>n</i> = 6	30	<i>22</i> and 8
<i>n</i> = 7	35	<i>22</i> and 13; or <i>27</i> and 8
<i>n</i> = 8	40	<i>22</i> and 18; or <i>27</i> and 13; or <i>32</i> and 8, etc.

becomes dominant only at C₂₂, e.g., 22, 27, 32, 37, 42, and etc. The pattern of appearance of the latter two series is shown in Table III (fragments which belong to the last sequence are italicized).

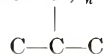
The authors are indebted to Dr. H. F. Strohmayer for the synthesis of hydrogenated poly-3,4-isoprene, and to Dr. B. E. Hudson, Jr. for helpful NMR discussions. George A. Glock, Jr. prepared the depolymerizates and examined them by mass spectroscopy.

References

1. Dixon, J. A., N. C. Cook, and F. C. Whitmore, *J. Am. Chem. Soc.*, **70**, 3361 (1948).
2. Whitmore, F. C., and F. Johnston, *J. Am. Chem. Soc.*, **55**, 5020 (1933).
3. Whitmore, F. C., and F. Johnston, *J. Am. Chem. Soc.*, **60**, 2265 (1938).
4. Friedman, B. S., and F. L. Morritz, *J. Am. Chem. Soc.*, **78**, 2000 (1956).
5. Michael, A., and F. Zeidler, *Ann.*, **393**, 81 (1912).
6. Zinke, T. H., and K. Zahn, *Ber.*, **43**, 849 (1910).
7. Ipatieff, V., and V. Leonovitch, *J. Russ. Phys. Chem. Soc.*, **35**, 606 (1903).
8. Ketley, A. D., and M. C. Harvey, *J. Org. Chem.*, **26**, 4649 (1961).
9. Pines, H., in *The Chemistry of Petroleum Hydrocarbons*, B. T. Brooks, C. E. Brood, S. T. Kurtz, and L. Schmerling, Eds., Reinhold, New York, 1955, Chap. 39; B. T. Brooks, *ibid.*, Chap. 44; L. Schmerling, *ibid.*, Chap. 54.
10. Deno, N. C., H. J. Peterson, and G. S. Saines, *Chem. Revs.*, **60**, 7 (1960).
11. Schildknecht, C. E., *Ind. Eng. Chem.*, **50**, 107 (1958).
12. Staudinger, H., and E. Dreher, *Ann.*, **517**, 73 (1935).
13. Müller, A., L. Toldy, and Z. van Rácz, *Ber.*, **77**, 777 (1944).
14. Kennedy, J. P., and A. W. Langer, *Adv. Polymer Sci.*, in press.
15. Topchiev, A. V., B. A. Krentsel, N. F. Bogomolova, and Y. Y. Goldfarb, *Dokl. Akad. Nauk SSSR*, **111**, 121 (1956).
16. Hagen, H., and H. Domininghaus, *Polyäthylen und Andere Polyolefine*, Brunke Garrels, 2nd ed., Verlag, Hamburg, 1961, p. 127.
17. Evans, A. G., *The Reactions of Organic Halides in Solution*, The Manchester Univ. Press, Manchester, England, 1946, p. 15.
18. Kennedy, J. P., and R. M. Thomas, in *Polymerization and Polycondensation Processes*, Advances in Chemistry Series, No. 34, American Chemical Society, Washington, D. C., 1962, Chap. 7.
19. Kennedy, J. P., L. S. Minckler, Jr., and R. M. Thomas, *J. Polymer Sci.*, **A2**, 367 (1964).
20. Norris, R. G. W., and J. P. Joubert, *J. Am. Chem. Soc.*, **49**, 873 (1927).
21. Leendertse, J. J., A. J. Tulleners, and H. I. Waterman, *Rec. Trav. Chim.*, **53**, 715 (1934).
22. Thomas, R. M., and H. C. Reynolds (to Standard Oil Development Company), U. S. Pat. 2,387,784 (1945).
23. Natta, G., *Angew. Chem.*, **68**, 393 (1956).
24. Kvanova, T. N., B. A. Krentsel, N. A. Pokatilo, and A. V. Topchiev, *Dokl. Akad. Nauk SSSR*, **129**, 999 (1957).
25. Campbell, T. W., and A. C. Haven, *J. Appl. Polymer Sci.*, **1**, 73 (1959).
26. Kennedy, J. P., and R. M. Thomas, *Makromol. Chem.*, **53**, 28 (1962).
27. Edwards, W. R., and N. F. Chamberlain, paper presented at 142nd Meeting, American Chemical Society, Atlantic City, N. J., September 1962.
28. Wilke, G., *Angew. Chem.*, **68**, 306 (1956).
29. American Petroleum Institute, Project No. 44, Mass spectra numbers 114, 146, 148, 149, and 164.

Résumé

La polymérisation cationique à basse température du 3-méthylbutène-1 procède par glissement d'hydrure intramoléculaire. L'ion carbonium secondaire se réarrange en ion tertiaire avant l'étape de propagation. Ainsi l'unité répétée dans le poly(3-méthylbutène-1) préparé cationiquement n'est pas la structure 1,2 attendue -(C-C)_n mais



une unité 1,3 du type α, α' -diméthylpropane (v. le résumé anglais). Les analyses détaillées de la structure ont été faites par des études de pyrolyse sous vide et de dépolymérisation. On a analysé les produits de fragmentation de divers échantillons de poly-

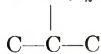
(3-méthylbutène-1) (p.ex. polymères cationiques 1,3, I, et polymères conventionnels 1,2 II) par chromatographie gazeuse, par spectrométrie infrarouge et spectrométrie de masse. La fraction gazeuse de I produit 22 mole % de fraction C₃ tandis que II fournit 70 mole % (groupes isopropyles latéraux); d'autre part, I fournit 26,3 mole % d'isobutène, tandis que II fournit seulement 6,8 mole %. Les pyrolysats cationiques révèlent nettement la présence de liaisons CH₂=CH— mais peu de —CH=CH— et de CH₂=C— tandis que dans les pyrolysats de II il y a essentiellement des groupes

CH₂=C— et quelques —CH=CH—. Aussi la chromatographie gazeuse et les analyses

par infrarouge indiquent que le poly(3-méthylbutène-1) cationique est un mélange d'environ 30% d'enchaînement conventionnel, 1,2 tête-queue et 70% de polymère 1,3. Les spectres de masse d'échantillons de I et II dépolymérisés donnent des diagrammes de fragmentation différents mais caractéristiques. Ils ont été analysés et expliqués. Ces derniers résultats confirment également les différences fondamentales de structure entre I et II.

Zusammenfassung

Die kationische Tieftemperaturpolymerisation von 3-Methylbuten-1 verläuft über einen intramolekularen Hydridverschiebungsmechanismus. Das sekundäre Carbeniumion lagert sich vor dem Wachstumsschritt in ein tertiäres um. Der Kettenbaustein des kationisch erhaltenen Poly(3-methylbuten-1) besitzt daher nicht die erwartete $-(C-C)-_n$ oder 1,2-Struktur sondern ist vom α, α' -Dimethylpropanotyp, besitzt also



1,3-Struktur siehe englische Zusammenfassung. Die genaue Strukturanalyse erfolgte durch Vakuumpyrolyse und Depolymerisationsuntersuchungen. Die Fragmentierungsprodukte verschiedener Poly-(3-methylbuten-1)-proben (nämlich kationische 1,3-Polymere, I, und konventionelle 1,2-Polymere, II) wurden gaschromatographisch und infrarot- und massenspektrometrisch analysiert. Die Gasfraktion von I lieferte 22 Mol% einer C₃-Fraktion, während II 70 Mol% (Isopropylseitengruppen) ergab; andererseits lieferte I 26,3 Mol% Isobuten und II nur 6,8 Mol%. Kationische Pyrolysate zeigen gut ausgeprägte CH₂=CH-Bindungen aber nur schwache —CH=CH— und CH₂=C-Bindungen, während Pyrolysate von konventionellem II vorwiegend CH₂=C—

und etwas —CH=CH-Bindungen aufweisen. Gaschromatographie und Infrarotanalyse zeigen unabhängig, dass kationisches Poly(3-methylbuten-1) ein Gemisch aus etwa 30% konventionellem 1,2-Kopf-Schwanzpolymerem und 70% 1,3-Polymerem ist. Das Massenspektrum depolymerisierten I- und II-Proben zeigte verschiedene und charakteristische Fragmentierungsprodukte. Die Analyse bestätigte auch hier das Vorhandensein fundamentaler Strukturunterschiede zwischen I und II.

Received February 13, 1963

Temperature Dependence of Birefringence in Irradiated Polyethylene*

E. KENEALLY,† J. GARD,‡ and G. ADLER, *Brookhaven National Laboratory, Upton, Long Island, New York*

Synopsis

The birefringence of irradiated polyethylene was observed as a function of temperature. The data are consistent with a mechanism in which crosslinking limits the growth and annealing of crystallites. Crosslinks formed in material which was oriented at the time the crosslinks were formed, results in an oriented gel. This effect explains the birefringence and the persistence of nucleation sites at high temperatures.

In the past, this laboratory has studied the graft copolymerization of styrene to polyethylene initiated by radiation.¹ Part of this work has involved microscopic examination of the grafts.^{1,2} As an aid to understanding the observed phenomena, a preliminary investigation of the temperature dependence of birefringence in irradiated polyethylene was undertaken.

Experimental

The polyethylene film used here had a density of 0.92 g./cc., a thickness of 0.13 mm., and it was lightly oriented due to processing. It was equivalent to the low density polymer used in our previous investigation, and like it, was not annealed prior to use.

The film was irradiated to the required dose at the rate of 0.51 Mrad/hr. in a Co⁶⁰ source. Dose rate was determined by the Fricke technique.

The irradiation was performed in air at 25°C. to conform to the 2b grafting condition of reference 1 and the type II grafting condition of reference 2. The specimen was placed in a Köffler hot stage on a Leitz CMU polarizing microscope and heated at the rate of 0.75°C./min. Optical retardance was measured as a function of temperature using an elliptical compensator and a sodium vapor lamp as the light source. The melting point was taken as the temperature at which the birefringence disappeared (retardance = zero).

* This work performed under the auspices of the U. S. Atomic Energy Commission.

† Present address: Chemistry Department, John Adams High School, South Ozone Park, New York.

‡ Present address: United States Army.

Results and Discussion

Figure 1 shows the retardance plotted as a function of temperature for an unirradiated specimen. The retardance at first increases slowly then drops. At 106°C. there is a sharp rise to a peak at about 110°C. and then a precipitous drop to zero at 113°C. This retardance "spike" was reproducible in all unirradiated specimens but it was completely absent in specimens given a radiation dose of 25 Mrad.

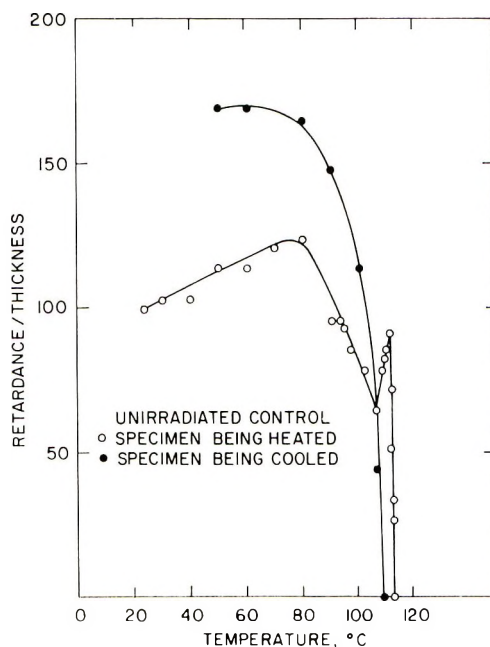


Figure 1.

On cooling down from the melting point, the specimen recrystallized in its previous orientation, the retardance becoming greater than before. This showed that the nucleation sites were not completely destroyed at the melting point. On reheating, the spike almost completely disappeared, showing that it was due to annealing and recrystallization. If the specimen were heated considerably above the melting point (200°C.) and cooled, it recrystallized in random fashion, retaining no trace of its previous orientation.

Figure 2 shows the data for a specimen having a dose of 200 Mrad. The annealing spike has disappeared. The melting point is now 105°C. On cooling from the melting point it recrystallizes, but this time with the retardance less than before. On heating to 230°C., however, it recrystallizes, but this time the specimen seems to retain a trace of its previous orientation. This can also be seen in the specimen given a dose of 150 Mrad.

Figure 3 shows a specimen given a dose of 500 Mrad. Here a new phenomenon becomes apparent. The birefringence does not drop precipitously to zero. Instead it drops sharply to a low value then decreases very slowly as a function temperature. The high temperature birefringence is not due to the presence of crystallites,³ since the temperatures involved

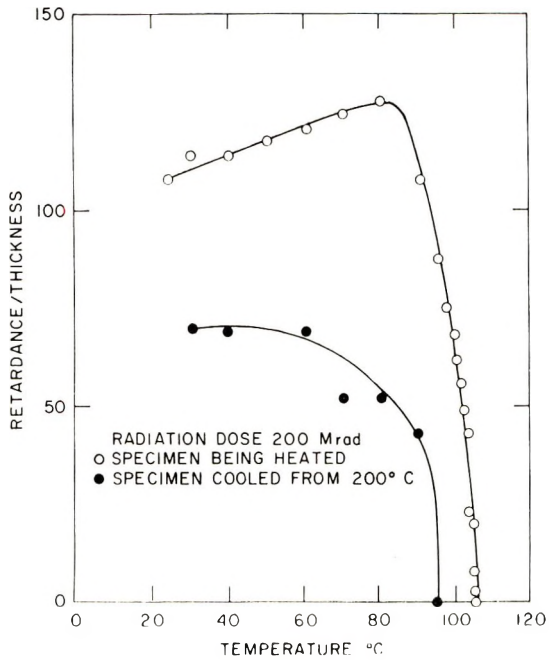


Figure 2.

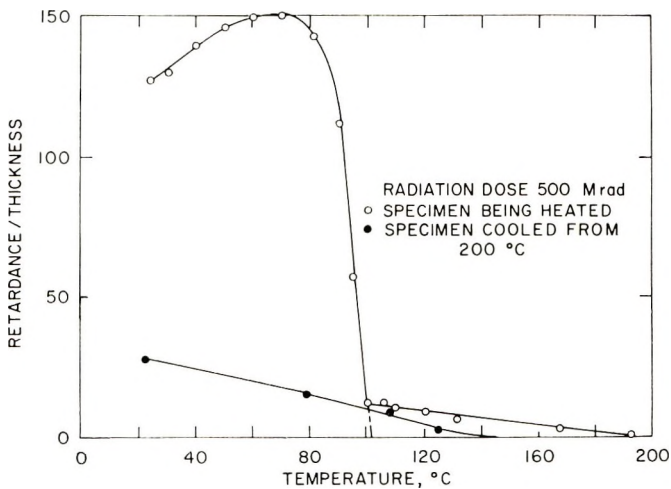


Figure 3.

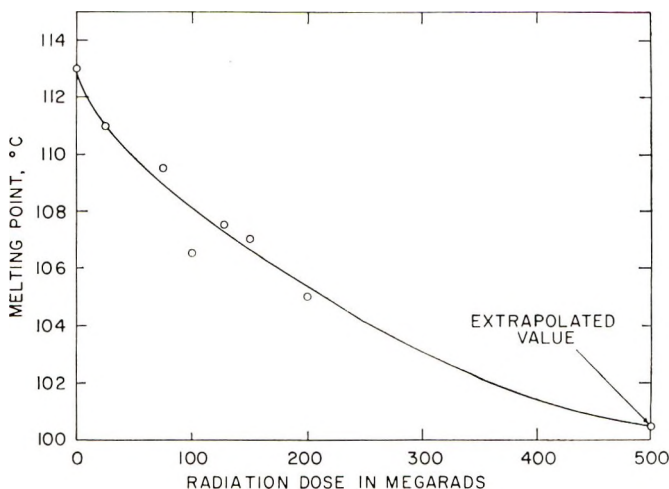


Fig. 4. Melting point of irradiated polyethylene.

are considerably above the normal crystalline melting point. If the sharp drop in retardance is extrapolated to zero for this specimen, a melting point is obtained which is consistent with the other observed data. The retention of birefringence above the normal melting point in irradiated polyethylene has been noted by others.^{3,4}

It may be assumed that, in all cases except the 500 Mrad specimen, the disappearance of birefringence correlates with the crystalline melting point. Figure 4 shows that the melting point decreases in a uniform manner with radiation dose, agreeing with the results of Dole and Howard⁵ and others.^{3,6} In addition, it is seen that the steepness of the retardance-temperature curve near the melting point decreases with dose.

These effects can be explained by a simple picture. The crystallites in polyethylene may be expected to vary in size and perfection. The smaller, more defective ones will have a lower melting point than the larger ones. As the unirradiated material is slowly heated below the melting point, the smaller crystallites melt while the larger ones grow at their expense. Those defects that can be annealed out. The effect is similar to that of aging a precipitate. As a result of this the melting point appears higher and sharper. This explains the annealing spike seen on the unirradiated and unannealed samples.

One of the results of irradiation is crosslinking. Even when irradiated in air, this is true, especially if the specimen is subsequently heated. A crosslink may be looked on as an unannealable defect which cannot be incorporated in the crystallite lattice without causing a great deal of distortion.⁷ The crosslinking however, can take place freely in the amorphous regions. The crosslink will prevent the material immediately surrounding it from being incorporated into a crystallite. This would interfere with the recrystallization and annealing and the observable effect would be a

decrease in the slope of the melting curve and a disappearance of the annealing spike. Both these effects were observed.

Due to the restraints imposed by the lattice, the formation of crosslinks within the crystallites themselves are extremely improbable compared to the amorphous region.⁷ However, active species such as radicals can form and be stored within them. When the crystallites melt, these are free to form crosslinks. On cooling down from the melting point, the specimen then can no longer crystallize to the same extent as before. This explains why the retardance in recrystallized irradiated polyethylene is less

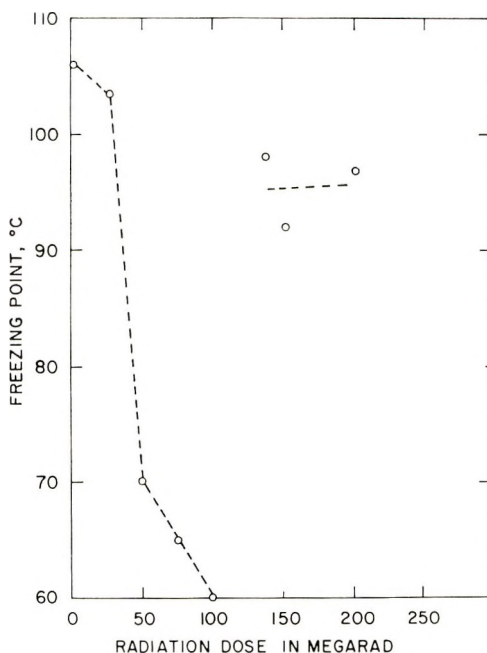


Fig. 5. Freezing point in irradiated polyethylene.

than the initial retardance while the reverse is true for the unirradiated material.

If polyethylene is heated considerably above the melting point, the nucleation sites are destroyed. On cooling, recrystallization may be expected to occur in random fashion. In irradiated specimens a new phenomenon can occur. As the crystallites approach their melting point, crosslinking occurs while the molecules are still oriented relatively parallel to each other. The result is an oriented, crosslinked gel that takes considerably more energy to disorient than in the unirradiated material. Whenever this material is cooled down, a trace of its former orientation is retained as was seen in specimens given a radiation dose of 125 Mrad or more.

If the sample is given a high radiation dose, more than one crosslink can be expected to form between molecules originally adjacent to each other in the crystallite. The chain length between crosslinks is then the same for both molecules, and they are forced to remain in each others vicinity and more or less parallel. If the crosslinks are not too close together, the result is an oriented nucleation site which persists to very high temperatures in spite of the fact that the overall melting point is lower. This would help explain the observed high temperature birefringence.

If this were true there should be another observable effect. The polyethylene when cooled from the melt crystallizes at a somewhat lower temperature than it melts. Due to the interference of crosslinks with nucleation, the freezing point should decrease with radiation dose. However, if nucleation sites persist at high temperature due to crosslinking of originally crystallized material, then the freezing point should start to increase with high doses. In Figure 5 the temperature at which measurable retardance first appears is plotted. This temperature first decreases, then increases as expected. The first specimen to show this increase is the first one to show retained orientation on cooling from above the melting point. This is consistent with the presence of oriented nucleation sites formed from crystallites. The freezing point determination shows poor reproducibility due to its extreme sensitivity to such factors as the rate of cooling, etc. However, qualitatively at least, the effect shown in Figure 5 is unmistakable.

The points in Figure 5 with radiation dose of 128 Mrad or above are for specimens cooled from 200°C. or above. Those for doses less than 128 Mrad are for specimens cooled from the melting temperature. This had to be done because retardance could not be measured for the specimens if cooled from 200°C. This in no way affects the argument.

References

1. Ballantine, D., A. Glines, G. Adler, and D. J. Metz, *J. Polymer Sci.*, **34**, 419 (1959).
2. Ballantine, D., D. J. Metz, J. Gard, and G. Adler, *J. Appl. Polymer Sci.*, **2**, 371 (1959).
3. Mandelkern, L., D. E. Roberts, J. C. Halpin, and F. P. Price, *J. Am. Chem. Soc.*, **82**, 46 (1960).
4. Hammer, C. F., W. W. Brandt, and W. L. Peticolas, *J. Polymer Sci.*, **24**, 291 (1957).
5. Dole, M., and W. H. Howard, *J. Phys. Chem.*, **61**, 137 (1957).
6. Marker, L., R. Early, and S. L. Aggarwal, *J. Polymer Sci.*, **38**, 369 (1959).
7. de Zarauz, Y., private communication.

Résumé

La biréfringence de polyéthylène irradié fut étudiée en fonction de la température. Les données s'accordent avec un mécanisme où le pontage limite la croissance et les réorientations des cristallites. Les pontages formés dans la matière déjà orientée, donnent un gel orienté. Cet effet explique la biréfringence et la stabilité des centres de nucléation aux températures élevées.

Zusammenfassung

Die Doppelbrechung von bestrahltem Polyäthylen wurde in Abhängigkeit von der Temperatur untersucht. Die Daten lassen sich durch einen Mechanismus mit Einschränkung des Wachstums und der Ausheilung der Kristallite durch Vernetzung erklären. Vernetzungen, die in einem zur Zeit der Vernetzungsbildung orientierten Material entstehen, führen zu einem orientierten Gel. Dieser Effekt erklärt die Doppelbrechung und die Persistenz der Keimbildungsstellen bei hoher Temperatur.

Received February 15, 1963

Role of Organic Diluents in a Sol-Phase Polymerization

T. GUHA, M. BISWAS, R. S. KONAR, and S. R. PALIT, *Indian Association for the Cultivation of Science, Jadavpur, Calcutta, India*

Synopsis

The effect of organic solvents on the rate of heterogeneous aqueous polymerization initiated by the $K_2S_2O_8$ - $Na_2S_2O_4$ redox pair has been studied. The separating polymer phase remains in colloidal dispersion, the stability of which is partly due to charge and partly due to hydration. Both the water-miscible and water-immiscible organic liquids decrease the rate of polymerization, the limiting conversion, and the molecular weight of the polymers. It has been suggested that the water-miscible organic liquids preferentially solvate the latex particles and thereby decrease the hydration stability and monomer concentration in the latex particles, whereas the water-immiscible organic liquids decrease the monomer concentration in the latex particles due to the partition of the monomer between the aqueous and the nonaqueous phases. Thus the fall in the rate and molecular weight of the polymers may be ascribed to the increase in the termination rate by the faster coagulation of the latex particles and dilution of monomer concentration at the reaction site.

INTRODUCTION

In a heterogeneous vinyl polymerization where the polymer separates as a coarse, insoluble precipitate, some of the propagating free radicals become occluded in the solid phase with the consequent partition of the polymerization locus between the liquid phase and the solid phase of the system. At the latter the termination of the macroradicals is diffusion-controlled, and this leads to a gradual build-up of long-lived radicals in the medium, giving rise to a typical gel effect.¹ When an organic diluent which has solvent power for the insoluble polymer is added to the medium, it swells and partly dissolves the insoluble phase. This attenuates the strength of the physical protection offered by the solid polymer phase to the propagating radicals. The termination reaction tends to become as rapid as that in a homogeneous process and thus the result of adding a polymer solvent as diluent to a heterophase polymerization is depression of the overall rate and polymer molecular weight.² Similarly, a build-up of relatively high radical concentration takes place in heterogeneous polymerizations, where the polymer separates in the form of a stabilized dispersion of fine particles in the medium. The protection of radicals from rapid termination is effected in such a loose phase by a strong interface surrounding each suspended particle to which the polymerization locus

overwhelmingly shifts from the liquid phase subsequent to phase separation.³ Reports on the effect of organic diluents on the heterogeneous polymerization in such emulsion-type systems are very few in the literature.^{4,5} During a study of heterogeneous vinyl polymerizations in aqueous solution, an investigation has been made of the role of organic diluents in those processes where the water-insoluble polymer particles have been maintained as a stable dispersion in the medium. The results of the investigation are reported here, together with a tentative mechanism of the role of organic additives in such systems.

EXPERIMENTAL

Materials

Monomers. Vinyl monomers, such as acrylonitrile, methyl acrylate, and vinyl acetate, which had some solubility in water at 35°C. were used for the study. They were freed from inhibitors and purified before polymerization by the conventional methods reported earlier.^{6,7}

Initiators. The initiating system was a redox pair, $K_2S_2O_8$ - $Na_2S_2O_4$. The reagents were all analytical reagent quality samples supplied by E. Merck and B. D. H.

Organic Diluents. The diluents selected had least transfer capacity in polymerization under the heterogeneous condition. They were of two types: water-miscible and water-immiscible. Dioxane, *tert*-butanol, ethanol, ethylene glycol, acetone, dimethylformamide (DMF) and hexamethyl phosphoramide (HMP) belonged to the water-soluble type, whereas benzene, toluene, and chloroform were typical water-insoluble diluents. Not all of the diluents were used for each of the monomers mentioned above. For each monomer the diluents were selected on the basis of graded affinity for the corresponding polymer. Thus, for acrylonitrile, as a typical example, the diluents investigated were dioxane (polymer nonsolvent), DMF (a moderate polymer solvent), and hexamethyl phosphoramide (a good polymer solvent).

The solvents used were of analytical reagent quality and distilled before use. Benzene and toluene were made free from sulfur impurities by repeated washing with concentrated H_2SO_4 followed by distillation.

Procedure

The apparatus and polymerization procedure have been described earlier.⁸ Measured volumes of the liquid additives together with the monomer were injected into the system just at the start of the experiments. The agitation of the system by mechanical stirring was stopped just after the onset of polymerization as signalled by the appearance of a haze in the medium. The polymerization was carried out at 35°C. In typical experiments, the concentration of the redox initiators was so maintained that the insoluble polymer phase remained colloidal during the polymerization. The extent of polymerization was measured gravimetrically by

estimating the yield of polymer in the reaction. The intrinsic viscosity of the polymer was used as an indication of the polymer molecular weight; this was measured for polyacrylonitrile in DMF, polymethyl acrylate in acetone, polymethyl methacrylate in benzene and polyvinyl acetate in acetone. The coagulation value of the latex formed in the polymerization was used as an indication of the dispersion stability of the insoluble polymer in the aqueous medium. This was measured in terms of the liminal strength of a suitable electrolyte solution ($MgSO_4$ for polymethacrylate sol and $NaCl$ for polyacrylonitrile sol) by the conventional procedure followed for an aquosol. The effective solvent power, i.e., the dissolving power of an organic liquid for the polymer sol in presence of water as diluent, of the water-soluble organic diluents for the polymer formed in the polymerization was measured in the following way: to 1 cc. of the polymer latex of known solid content, the organic liquid was added dropwise by a microburet with constant stirring of the latex. There was a visible precipitation of the polymers on the addition of the water-soluble diluent, and the precipitate was dissolved on further addition of the solvent. The point of almost complete dissolution of the coagulum in the water-diluent mixture was regarded as the endpoint of such titration. Diluents having no solvent power for the polymer did not cause any physical change in the latex and simply diluted the polymer dispersion. Water-insoluble solvents, such as benzene or chloroform, could not dissolve the polymer in presence of water. They simply converted the latex to a coacervate.

RESULTS AND DISCUSSION

Table I reports the effective solvent power of the diluents for the polymers. Figures 1-3 present graphically the effect of the diluents on the

TABLE I
Effective Solvent Power of Water-Soluble Organic Diluents for Vinyl Polymers

Diluent	Polymer latex (1 ml.)	Solid content of the latex, g./cc.	Volume of diluent for incipient flocculation, cc.	Volume of diluent for polymer dissolution, cc.
Ethanol	Polyvinyl acetate	0.011	0.2	5.0
Acetone	"	"	0.2	2.5
Dioxane	"	"	1.0	4.5
Ethanol	Polymethyl acrylate	0.007	0.5	10
Acetone	"	"	0.2	6
Dioxane	"	"	0.5	10
Ethanol	Polyacrylonitrile	0.007	No flocculation	—
Acetone	"	"	No flocculation	—
Dioxane	"	"	No flocculation	—
DMF	"	"	0.3	10

rate of aqueous polymerization of the monomers, acrylonitrile, vinyl acetate, and methyl acrylate, respectively. Table II reports the effect of the diluents on the dispersion stability of the latex in the typical polymerization of methyl acrylate and acrylonitrile. Table III reports the intrinsic viscosity data for the polymers with and without the additives.

It appears that the diluents retard the overall rate as well as the molecular weight (Table III). It should be noted that for the diluents soluble

TABLE II
Effect of Diluents on the Dispersion Stability of the Latex

Polymer latex	Redox-pair concentration, moles/l.		Organic diluent	Coagulation value, mmole/l.
	K ₂ S ₂ O ₈	Na ₂ S ₂ O ₄		
Polymethyl acrylate	3.7×10^{-4}	5.7×10^{-4}	—	15 (MgSO ₄)
	"	"	Dioxane (5% v/v)	10
	"	"	Ethanol(")	11
	"	"	Acetone(")	8
Polyacrylonitrile	2.6×10^{-3}	5.7×10^{-4}	—	10(NaCl)
	"	"	Dimethylformamide (2% v/v)	6 "

TABLE III
Effect of Diluents on the Polymer Molecular Weight

Monomer	Redox pair concentration, moles/l.		Organic diluent	[η], ml./g.
	K ₂ S ₂ O ₈	Na ₂ S ₂ O ₄		
Methyl acrylate (0.1 mole/l.)	3.7×10^{-4}	5.7×10^{-4}	—	1.95
	"	"	Dioxane (5% v/v)	1.6
	"	"	<i>tert</i> -Butanol "	1.7
	"	"	Acetone "	1.4
	"	"	Benzene "	0.95
Acrylonitrile (0.25 mole/l.)	2.6×10^{-3}	5.7×10^{-4}	—	1.25
	"	"	Dioxane (1.6% v/v)	1.1
	"	"	DMF (")	1.08

in water, the rate-depressing action is apparently related to their flocculating power on the polymer aqueous solution and their dissolving power on the insoluble polymer, as shown in Table I. Thus in the case of acrylonitrile polymerization (Fig. 1) dimethylformamide depressed the rate and molecular weight much more than dioxane and alcohol. Dimethylformamide flocculates the aqueous solution of polyacrylonitrile as well as dissolving the insoluble polymer (Table I), whereas dioxane, ethanol, acetone, etc. do not affect the polyacrylonitrile solution. In the case of methyl acrylate (Fig. 3),

dioxane and alcohol are relatively poorer rate-depressants than acetone, which is a better flocculant for the polymethyl acrylate sol as well as a solvent for the insoluble polymer than dioxane and alcohol (Table I). In the case of vinyl acetate, a more or less similar trend is observed; acetone and ethanol depress the rate better than dioxane, which has less flocculating power on the polyvinyl acetate aqueous sol and poorer solvent power for the polymer.

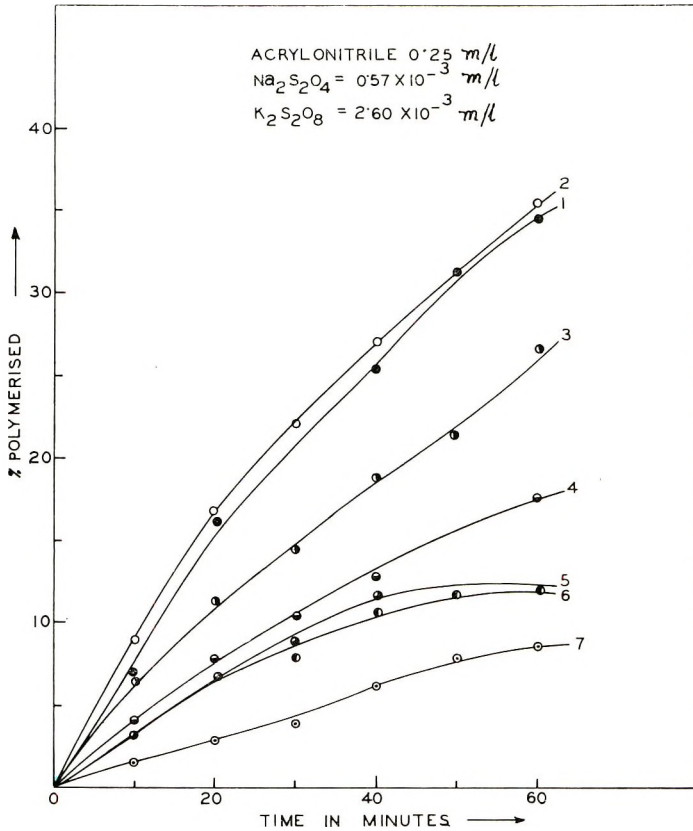


Fig. 1. Effect of organic liquids on the rate of aqueous polymerization of acrylonitrile initiated by $K_2S_2O_8$ - $Na_2S_2O_4$ at $35^\circ C$.: (1) control; (2) dioxane, 1.6% (v/v); (3) *tert*-butyl alcohol, 1.6% (v/v); (4) DMF, 1.6% (v/v); (5) DMF, 3.3% (v/v); (6) DMF, 5.0% (v/v); (7) hexamethyl phosphoramide, 1.6% (v/v).

When water-soluble diluents are added to the latex, the primary effect is to upset the dispersion stability of the insoluble polymer particles. The latter are colloidal, stabilized partly by charge and partly by hydration.⁵ The degree of charge stabilization is determined by the critical balance between the ionic strength in the medium and the particle size, while the hydration stabilization depends on the hydrophilic loading on the polymer chains. Water-soluble organic diluents tend to displace the hydration

layer from the polymer particles, and this dehydration capacity may be correlated with the better polymer affinity of the diluents than water. The dehydrated polymer particles become unstable as colloid in the aqueous medium, as shown in Table II by the reduction of the coagulation value of the polymer sol on the addition of the water miscible diluents. The reduction of the dispersion stability of the latex would be accompanied with the fall in fine particle concentration in the medium and increased rate of chain

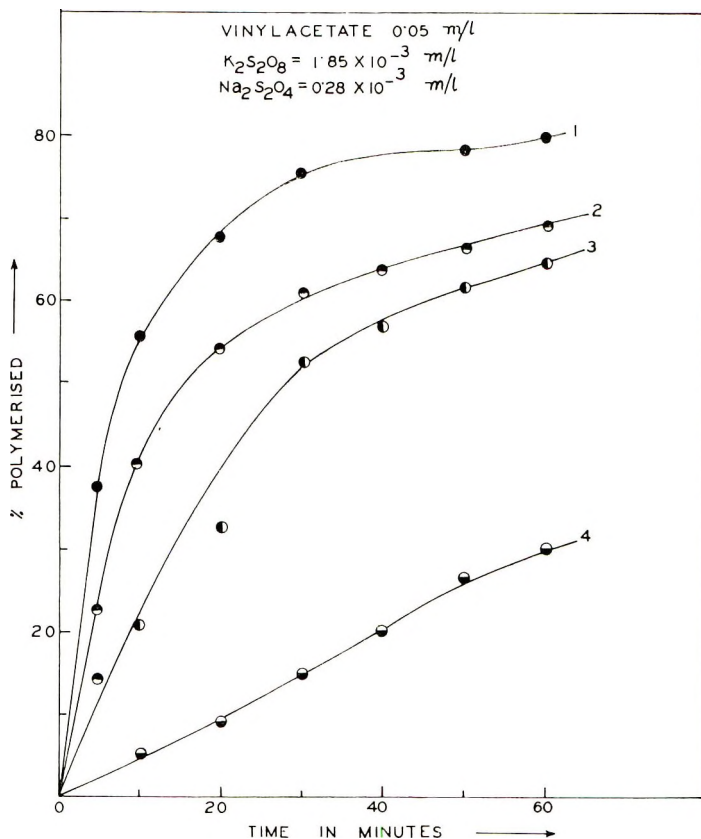


Fig. 2. Effect of organic liquids on the rate of aqueous polymerization of vinyl acetate initiated by $K_2S_2O_8$ - $Na_2S_2O_4$ at $35^\circ C$.: (1) control; (2) dioxane, 1.6% (v/v); (3) ethyl alcohol, 1.6% (v/v); (4) acetone, 1.6% (v/v).

termination, leading to the fall in rate and molecular weight. In the case of acrylonitrile polymerization, it is noteworthy that water-soluble alcoholic and ketonic solvents cannot "wet" the polyacrylonitrile particles dispersed in aqueous medium. Presumably the hydration layer is quite strongly adherent to the polyacrylonitrile particles, and this is possibly due to the relatively strong hydrogen bond established between the nitrogen atom of the CN group and the hydrogen atom of a water molecule. Dimethylformamide, however, can displace the hydration layer from the acrylonitrile

particle; this is possibly due to its greater solvent power than water and by virtue of this property it can overcome the dipolar interaction between water and polyacrylonitrile.

Apart from reducing the dispersion stability of the latex, the diluents having solvent power for the polymer, would be transported from the aqueous phase to the insoluble polymer phase similar to the monomer. The

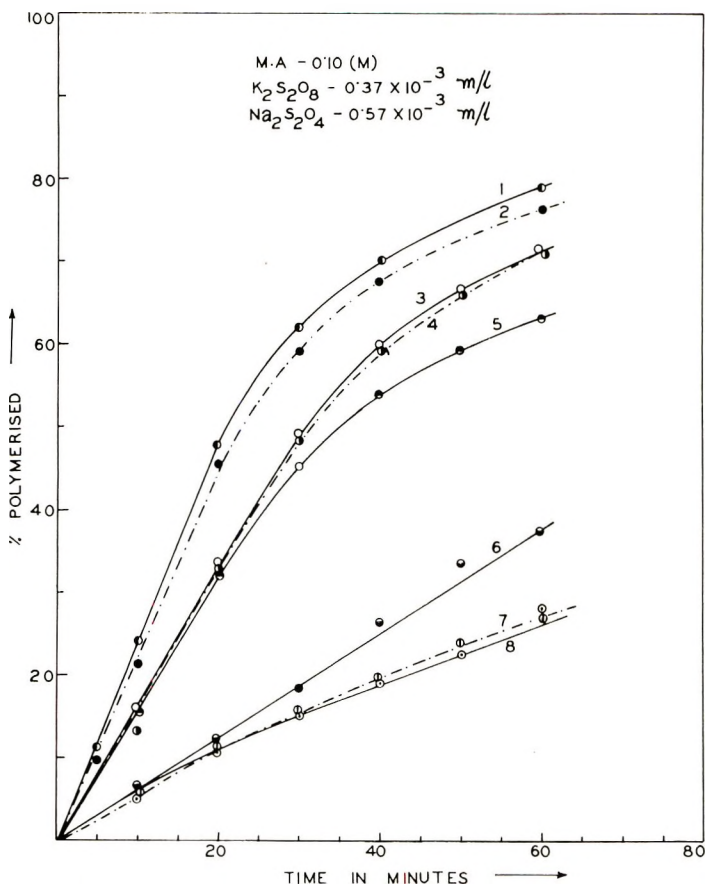


Fig. 3. Effect of organic liquids on the rate of aqueous polymerization of methacrylate initiated by $K_2S_2O_8$ - $Na_2S_2O_4$ at $35^\circ C$.: (1) control; (2) dioxane, 5.0% (v/v); (3) acetone, 2.0% (v/v); (4) dioxane, 10.0% (v/v); (5) *tert*-butyl alcohol 10.0% (v/v); (6) acetone, 4.0% (v/v); (7) chloroform, 1.0% (v/v); (8) benzene, 2.0% (v/v).

latter at the insoluble phase becomes diluted by the solvents,⁹ and hence the lowering of rate of polymerization occurs predominantly at the insoluble phase.

Water-insoluble diluents, such as benzene or chloroform, also retard the rate and polymer molecular weight. These diluents, however, affect the latex physically, only slightly, possibly because of their poor dielectric

strength and hence their inability to displace the hydration layer from the polymer particles. It is supposed that in the presence of water-immiscible diluents the monomer is distributed between the aqueous and nonaqueous phase; and as a result, the concentration of monomer in the aqueous phase decreases considerably leading to the observed fall in the rate of polymerization, yield, and degree of polymerization. To test this idea, the partition of a monomer (methyl methacrylate), between water and chloroform was determined and at 25°C., $K = C_{\text{CHCl}_3}/C_{\text{H}_2\text{O}}$ for the vinyl monomer was found to be nearly 140. Thus the water-insoluble organic diluent extracts the monomer out of the aqueous phase in which the water-soluble redox pair is dissolved; the initial rate of polymerization then undergoes a marked depression compared with that of the reaction in absence of the diluent.

References

1. Bamford, C. H., A. D. Jenkins, W. G. Barb, and P. F. Onyon, *Kinetics of Vinyl Polymerization*, Butterworths, London, 1958.
2. Bamford, C. H., and A. D. Jenkins, *Proc. Roy. Soc. (London)*, **A228**, 220 (1955).
3. Smith, W. V., and R. H. Ewart, *J. Chem. Phys.*, **16**, 592 (1948).
4. Whitby, G. S., M. D. Gross, J. R. Miller, and A. J. Costanza, *J. Polymer Sci.*, **16**, 549 (1955).
5. Thomas, W. M., E. H. Gleason, and G. Mino, *J. Polymer Sci.*, **24**, 43 (1957).
6. Palit, S. R., and T. Guha, *J. Polymer Sci.*, **34**, 243 (1959).
7. Palit, S. R., and R. S. Konar, *J. Polymer Sci.*, **57**, 609 (1962).
8. Biswas, M., and S. R. Palit, *J. Sci. Ind. Res. (India)*, **20B**, 160 (1961).
9. Peaker, F. W., *J. Polymer Sci.*, **34**, 195 (1959) (discussion).

Résumé

On a étudié l'effet de solvants organiques sur la vitesse de la polymérisation hétérogène aqueuse initiée par la paire redox $\text{K}_2\text{S}_2\text{O}_8\text{-Na}_2\text{S}_2\text{O}_4$. La phase de polymère en séparation reste en dispersion colloïdale, la stabilité de celle-ci est due partiellement à la charge et partiellement à l'hydratation. Aussi bien les liquides organiques miscibles à l'eau et immiscibles à l'eau diminuent la vitesse de polymérisation, la conversion limite et le poids moléculaire des polymères. On suggère que les liquides organiques miscibles à l'eau dissolvent préférentiellement les particules de latex et par conséquent diminuent la stabilité d'hydratation et la concentration en monomère dans les particules de latex tandis que les liquides organiques immiscibles à l'eau diminuent la concentration en monomère dans les particules de latex, due au partage du monomère entre la phase aqueuse et non aqueuse. On attribue donc la chute de la vitesse et du poids moléculaire des polymères à l'augmentation de la vitesse de terminaison par coagulation plus rapide des particules de latex et la dilution de la concentration en monomères au sein du milieu réactionnel.

Zusammenfassung

Der Einfluss organischer Lösungsmittel auf die Geschwindigkeit der heterogenen wässrigen, durch das Redoxpaar $\text{K}_2\text{S}_2\text{O}_8\text{-Na}_2\text{S}_2\text{O}_4$ gestarteten Polymerisation wurde untersucht. Die sich abscheidende Polymerphase bildet eine kolloide Dispersion, deren Stabilität teils durch Aufladung, teils durch Hydratation bedingt ist. Sowohl mit Wasser mischbare als auch mit Wasser nicht mischbare organische Flüssigkeiten erniedrigen die Polymerisationsgeschwindigkeit, den erreichbaren Umsatz und das Molekulargewicht

des Polymeren. Es wird angenommen, dass die mit Wasser mischbaren organischen Flüssigkeiten in erster Linie die Latexteilchen solvatisieren und dadurch die Hydrationsstabilität sowie die Monomerkonzentration in den Latexteilchen erniedrigen, während die mit Wasser nicht mischbaren organischen Flüssigkeiten die Monomerkonzentration in den Latexteilchen durch die Verteilung des Monomeren zwischen wässriger und nichtwässriger Phase vermindern. Somit kann der Abfall der Geschwindigkeit und des Molekulargewichtes der Polymeren der durch schnellere Koagulation der Latexteilchen erhöhten Abbruchgeschwindigkeit und der Erniedrigung der Monomerkonzentration am Reaktionsort zugeschrieben werden.

Received February 18, 1963

Role of Organic Diluents in a Precipitative Aqueous Polymerization

R. S. KONAR, T. GUHA, and S. R. PALIT, *Indian Association for the Cultivation of Science, Jadavpur, Calcutta, India*

Synopsis

The effect of organic liquids on the rate of heterogeneous aqueous polymerization initiated by the $\text{KMnO}_4\text{-H}_2\text{C}_2\text{O}_4$ redox pair has been studied. The separating polymer phase is a precipitate under experimental conditions. The rate of polymerization, the limiting yield, and the molecular weight of the polymers were found to decrease in presence of organic liquids. This behavior has been ascribed to (1) the increase in the termination rate due to the swelling of the precipitated polymer particles containing trapped radicals and (2) the fall in the monomer concentration at the reaction site.

INTRODUCTION

In the previous part of this study¹ results were reported for aqueous polymerizations carried out under conditions when the water-insoluble polymer phase remained as a stable dispersion of fine particles. Polymerization of some monomers was also carried out in aqueous solution under conditions in which the insoluble polymer always remained as a coarse coagulum in the medium right from the onset of polymerization. The redox pair used for such precipitative aqueous polymerizations was $\text{KMnO}_4\text{-H}_2\text{C}_2\text{O}_4$; the role of this system as a redox initiator has been reported earlier.² The monomers selected were methyl methacrylate (MMA), a typical vinyl monomer which is water-soluble but has strong affinity for its polymer, and acrylonitrile (AN), a vinyl monomer which has much more solubility in water than in its polymer. The present paper reports the observations made of the effect on the rate of adding of both water-miscible and water-immiscible organic diluents to the precipitative aqueous polymerization of these monomers.

EXPERIMENTAL

The monomers, methyl methacrylate and acrylonitrile, obtained from Eastman Kodak, were purified from the inhibitors by the usual methods reported earlier.² They were freshly distilled before use. The redox pair, potassium permanganate and oxalic acid, were of analytic reagent grade supplied by E. Merck. The organic additives added as diluents to the system were: acetone, *tert*-butanol, ethanol, dioxane, and DMF as

water-soluble diluents, and benzene and toluene water-insoluble additives. They were all freshly distilled before use.

The experimental procedure for the polymerizations in presence of the diluents was the same as that reported previously.³ Blank experiments were carried out in absence of the monomer in aqueous solution of the diluents to check the effect of the redox pair on the organic diluents present in the system during the reaction. Excepting ethanol, the diluents were inert to the redox pair. Partial oxidation of alcohols was found to be possible.

RESULTS

Figures 1-3 show the effect of the organic diluents on the overall rate of polymerization of methyl methacrylate and acrylonitrile. Tables I and II report the same on the polymer molecular weight for the two monomers. The salient features which follow from the Figures 1-3 and Tables I and II are the following.

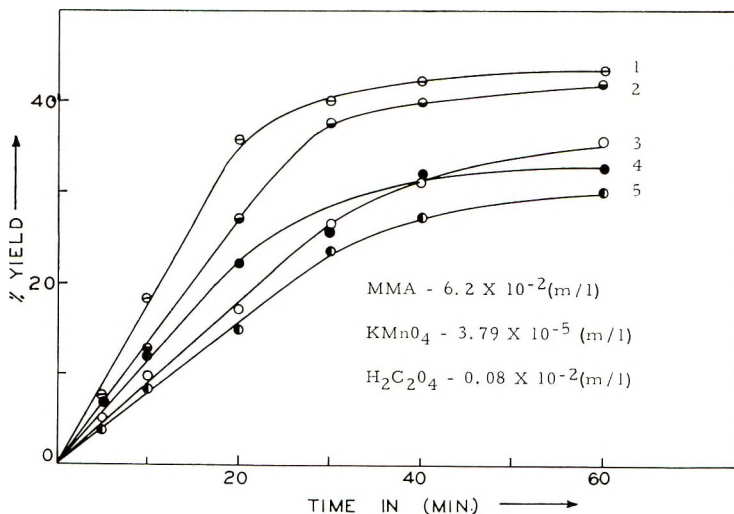


Fig. 1. Effect of organic liquids on the rate of aqueous polymerization of methyl methacrylate initiated by KMnO_4 - $\text{H}_2\text{C}_2\text{O}_4$ redox system at 32°C .: (1) control; (2) acetone, 5.0% (v/v); (3) acetone, 10.0% (v/v); (4) *tert*-butyl alcohol, 10.0% (v/v); (5) toluene, 1.0% (v/v).

The water-miscible solvents depress the overall rate as well as the final yield; the rate-depressing effect increases with the increase in the concentration of the diluent in the medium.

The water-immiscible solvents are better rate depressants than the water-miscible ones.

Among the water-miscible diluents, there is an apparent relationship between the solvent power or affinity of the diluents and the polymers of the corresponding monomers. Thus in the polymerization of methyl

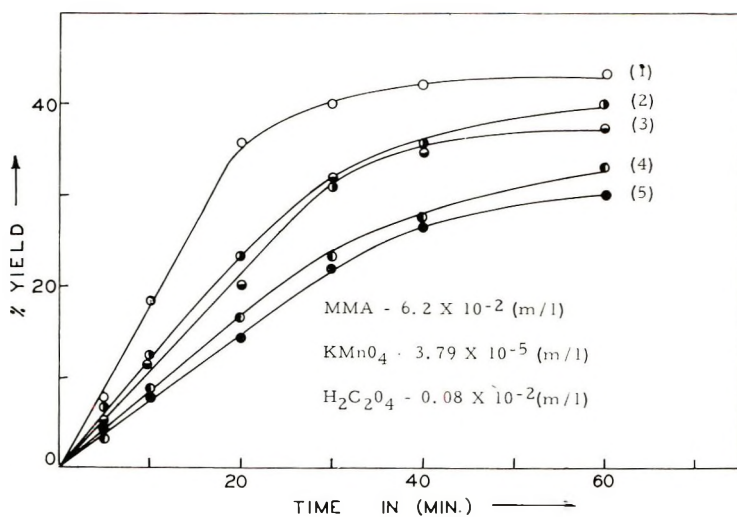


Fig. 2. Effect of organic liquids on the rate of aqueous polymerization of methyl methacrylate initiated by KMnO_4 - $\text{H}_2\text{C}_2\text{O}_4$ redox system at 32°C : (1) control; (2) ethyl alcohol, 10.0% (v/v); (3) dioxane, 5.0% (v/v); (4) dioxane, 10.0% (v/v); (5) benzene, 1.0% (v/v).

methacrylate (Figs. 1 and 2), acetone, a typical solvent for the insoluble polymer, is a more powerful rate depressant than dioxane and alcohols.

In these precipitated phase polymerizations, in contrast to the "sol-phase" ones, the characteristic feature is the increase in polymer degree of polymerization as measured by η with polymerization time (Tables I and II). The addition of the organic diluents has no effect except that the degree of polymerization always remains at a lower level at the corresponding time.

In these precipitated-phase heterogeneous aqueous polymerizations, the locus of polymerization is distributed between the coagulated phase and

TABLE I
Effect of Solvents on the Degree of Polymerization in MMA Polymerization^a

Time, min.	η				
	Control	10% <i>tert</i> -butyl alcohol	10% acetone	10% dioxane	1% toluene
5	0.4	0.4	0.2	0.3	0.32
10	0.6	0.5	0.42	0.38	0.4
20	0.9	0.65	0.63	0.65	0.47
30	1.05	0.8	0.8	0.8	0.6
40	1.1	0.85	0.95	0.9	0.7
10	1.2	1.05	0.95	1.0	0.75

^a $[\text{MMA}] = 6.2 \times 10^{-2}$ mole/l.; $[\text{KMnO}_4] = 4 \times 10^{-3}$ mole/l.; $[\text{H}_2\text{C}_2\text{O}_4] = 1.1 \times 10^{-3}$ mole/l.; temperature: $32 \pm 0.2^\circ\text{C}$.

TABLE II
Effect of Solvents on the Degree of Polymerization in AN polymerization^a

Time, min.	η			
	Control	2% DMF	10% acetone	10% dioxane
5	0.7	—	—	—
10	1.2	0.92	0.85	—
20	1.8	1.7	1.5	—
30	2.1	1.9	—	1.3
40	2.2	1.97	2.0	—
60	2.2	2.0	2.1	1.8

^a [AN] = 0.3 mole/l.; [KMnO₄] = 1.3×10^{-4} mole/l.; [H₂C₂O₄] = 1.1×10^{-3} mole/l.

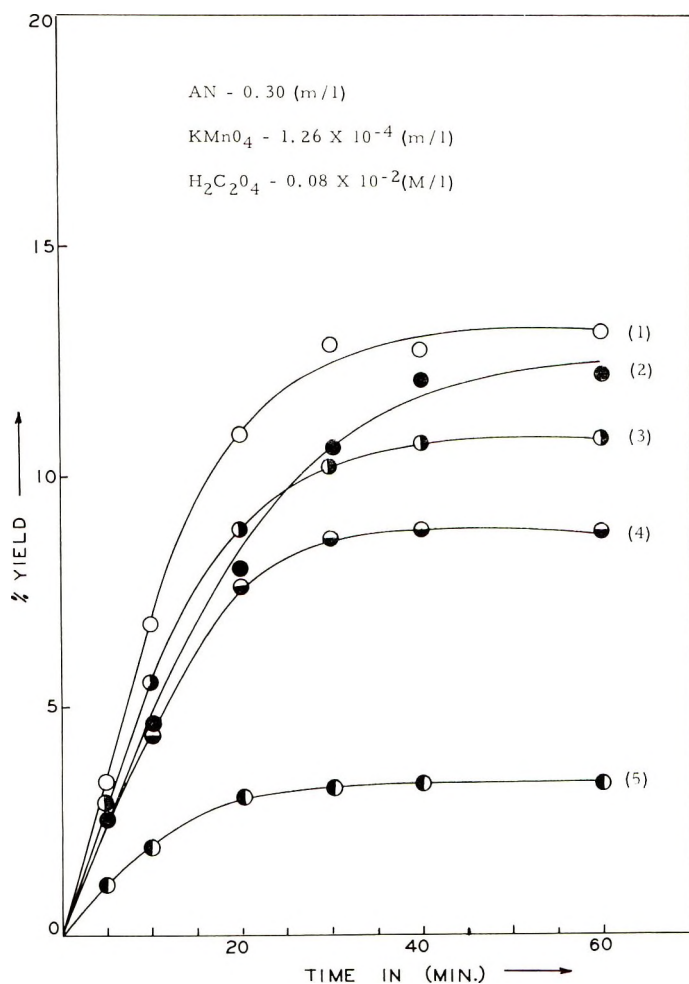


Fig. 3. Effect of organic liquids on the rate of aqueous polymerization of acrylonitrile initiated by KMnO₄-H₂C₂O₄ redox system at 32°C.: (1) control; (2) acetone, 10.0% (v/v); (3) DMF, 2.0% (v/v); (4) dioxane, 10.0% (v/v); (5) DMF, 10.0% (v/v).

the aqueous phase. The polymerization in the solid phase should follow apparently non steady-state "explosive" kinetics due to a build-up in the concentration of trapped radicals with the progressive accumulation of the insoluble precipitate, whereas the polymerization of the dissolved monomer in the aqueous phase is more or less similar to a homogeneous solution polymerization. This is partly evidenced by the increase in degree of polymerization with polymerization time (Table I). The ratio between the solid phase and the aqueous phase polymerizations in these systems should determine the overall rate features. Thus, in the polymerization of methyl methacrylate (MMA), the polymerization in the solid phase should be more significant, evidently due to the greater solubility of the monomer in its polymer, whereas for acrylonitrile (AN), which has more affinity for water than for its polymer, the locus of polymerization will be relatively more localized in the aqueous phase. In such heterogeneous processes, the mechanism by which organic diluents may lower the rate as well as the molecular weight is either to reduce the rate of the solid-phase polymerization of the polymer-dissolved monomer by the long-lived radicals or the liquid-phase polymerization of the water-dissolved monomer or both. It should be noted that the diluents added to the system were too small in amount to dissolve the insoluble polymer in the presence of a large amount of water in the medium. It is supposed that similar to the monomer compatible with its polymer, an organic diluent having good solvent power for the polymer, will be distributed between the insoluble polymer and the aqueous phase.¹ The diluent present in the solid phase should lower the concentration of the monomer at the reactive sites⁴ and consequently lower the rate. This may also be due to the swelling and consequent loosening effect of the diluents (which have solvent power for the polymer) on the compact coagulum, as a result of which the termination of the occluded radicals becomes facilitated. However, this does not lead to a complete elimination of the trapped radicals. This is borne out by the fact that the molecular weight of the polymer increased with time as well as the progress of polymerization, even in presence of the diluent (Tables I and II). However, the molecular weight in presence of the additives remained everywhere less than that in their absence, and this is possibly due to the dilution of the monomer in the solid phase by the organic liquids.

The rate-depressing effect of the water-immiscible diluents such as benzene and chloroform is possibly due to the extraction of the monomer from the aqueous phase to the water-immiscible diluent phase. The radicals generated in the aqueous phase frequently cannot enter into the latter, and hence a good fraction of the monomer becomes unavailable for polymerization, and the overall rate consequently falls.

Thanks are due to the Council of Scientific and Industrial Research (Government of India) for fellowship to one of us (R. S. K.).

References

1. Guha, T., M. Biswas, R. S. Konar, and S. R. Palit, *J. Polymer Sci.*, **A2**, 1471 (1964).
2. Palit, S. R., and R. S. Konar, *J. Polymer Sci.*, **57**, 609 (1962).
3. Palit, S. R., and R. S. Konar, *J. Polymer Sci.*, **58**, 85 (1962).
4. Peaker, F. W., *J. Polymer Sci.*, **34**, 195 (1959) (discussion).

Résumé

On a étudié l'effet de liquides organiques sur la vitesse de polymérisation hétérogène aqueuse initiée par la paire redox $\text{KMnO}_4\text{-H}_2\text{C}_2\text{O}_4$. La phase de polymère en séparation est un précipité dans les conditions expérimentales. La vitesse de polymérisation, le rendement limite et le poids moléculaire des polymères diminuent en présence de liquides organiques. On attribue ceci à (1) l'augmentation de la vitesse de terminaison due au gonflement des particules de polymère précipité contenant des radicaux trappés et (2) à la chute de la concentration en monomère dans le milieu réactionnel.

Zusammenfassung

Der Einfluss organischer Flüssigkeiten auf die Geschwindigkeit der heterogenen wässrigen, durch das Redoxpaar $\text{KMnO}_4\text{-H}_2\text{C}_2\text{O}_4$ gestarteten Polymerisation wurde untersucht. Unter den gegebenen experimentellen Bedingungen scheidet sich die Polymerphase als Niederschlag ab. Es wurde gefunden, dass die Polymerisationsgeschwindigkeit, der erreichbare Umsatz und das Molekulargewicht der Polymeren in Gegenwart organischer Flüssigkeiten abnehmen. Es werden dafür zwei Ursachen angegeben: (1) Erhöhung der Abbruchgeschwindigkeit durch Quellung der ausgefällten Polymerpartikel, in denen Radikale eingeschlossen sind; (2) Erniedrigung der Monomerkonzentration am Reaktionsort.

Received February 18, 1963

A Novel Diels-Alder Polymerization

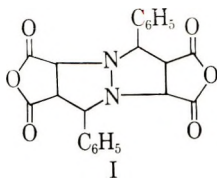
J. K. STILLE and T. ANYOS, *Chemistry Department,
State University of Iowa, Iowa City, Iowa*

Synopsis

The double dienophiles *N,N'*-hexamethylene-bismaleimide and the *o*-, *m*-, and *p*-phenylene-bismaleimides were prepared and copolymerized with benzalazine by the Diels-Alder reaction. Melt polymerization afforded these polymers in high yields with inherent viscosities in the range 0.13 to 0.30 and softening temperatures from 238 to 325°. Solution polymerization gave no polymers and only starting materials were isolated. Benzalazine in this reaction behaves as a double diene and undergoes a 1,3-addition with the bismaleimides to form these polymers. That this 1,3-addition occurs in the polymer formation is further verified by the basic hydrolysis of the model compounds, 4,8-diphenyl-1,5-diazabicyclo[3.3.0]octane-2,3,6,7-tetracarboxylic acid bis-anhydride (I) and 4,8-diphenyl-1,5-diazabicyclo[3.3.0]octane-2,3,6,7-bis-*n*-butylamide (II) and one of the polymers to give 4,8-diphenyl-1,5-diazabicyclo[3.3.0]octane-2,3,6,7-tetracarboxylic acid in each case.

I. INTRODUCTION

The 1,3-addition reaction of benzalazine with maleic anhydride to give 4,8-diphenyl-1,5-diazabicyclo[3.3.0]octane-2,3,6,7-tetracarboxylic acid bis-anhydride (I) in low yield has been reported.^{1,2} None of the normal Diels-Alder adduct resulting from 1,4-addition was formed.



In the reaction to form this adduct, benzalazine acts as a double diene and could therefore be expected to behave in a similar manner with a series of compounds such as the bismaleimides. It is evident however, that the particular example studied would not be suitable for polymerization reactions since the yields are far too low. It was necessary to find a system in which the adduct yield would be high enough to insure suitable yields of polymer and high molecular weight.

II. EXPERIMENTAL

Preparation of 4,8-Diphenyl-1,5-diazabicyclo[3.3.0]octane-2,3,6,7-bis-*n*-butylimide (II)

Benzalazine,² 1.86 g. (0.009 mole) and 2.998 g. (0.19 mole) of *n*-butylmaleimide³ were mixed in the solid phase and heated to 200°C. The melt

was maintained at this temperature for 10–15 min. and then allowed to cool to room temperature. The crude mixture was dissolved in acetone, the solution was decolorized with charcoal and then was cooled to 0°C. The precipitate was removed by filtration and air dried to afford 4.86 g. (100%) of II, m.p. 218–220°C.

ANAL. Calcd. for $C_{30}H_{34}N_4O_6$; C, 70.00%; H, 6.60; N, 10.92%. Found: C, 70.21%; H, 6.36%; N, 11.00%.

When this reaction was attempted in a benzene solution, only starting materials were recovered.

Bismaleimides

All bismaleimides were prepared from the corresponding bismaleamic acids, as described,⁴ except that the following modifications were adopted: A 50:1 molar ratio of acetic anhydride to bismaleamic acid and a heating time of 30 min. were employed to optimize the yield of bismaleimide. In this manner, hexamethylene- and the *o*-, *m*-, and *p*-phenylene-bismaleimides were obtained in 12, 7.5, 7.0, and 20% yields, respectively.

Polymerizations

All polymerizations were carried out by means of melt polymerization techniques. Solution polymerization did not afford polymers. The bismaleimide and benzalazine were intimately mixed, in the solid state, in 1:1 or 2:1 molar ratios, respectively. The mixtures were heated, under nitrogen, to 180–190°C., for 10–15 min., at which time the melt had either

TABLE I
Copolymerization of Benzalazine with Bismaleimides

Polymer	Mole ratio (maleimide to benzalazine)	Yield, %	M.p., °C. ^a	η_{inh}	Calculated ^c			Found		
					C, %	H, %	N, %	C, %	H, %	N, %
IVa	2:1	99	310 (s) ^d	0.195	69.79	4.08	11.63	69.15	4.34	11.60
			315							
	1:1	50		0.20						
IVb	2:1	89	450	0.13	69.79	4.08	11.63	69.02	4.47	11.77
IVc	2:1	85	325 (s) ^d	0.30	69.79	4.08	11.63	69.49	3.91	11.44
		1:1	59							
IVd	2:1	96	238 (s) ^d	0.24	68.93	5.58	11.49	68.32	5.51	11.57
			315							
	1:1	71		0.24						

^a Capillary melting point.

^b Inherent viscosities were obtained from a dimethylformamide solution of the polymer prepared by dissolving 0.25 g. of polymer in 100 ml. of dimethylformamide.

^c For polymers IVa–IVc the analysis is based on 5 recurring units plus maleimido endgroups. For polymer IVd the analysis is based on 7 recurring units plus maleimido endgroups.

^d Softening point.

resolidified or become a highly viscous mass. The crude polymer sample was washed thoroughly with chloroform and acetone to remove any unreacted monomer and then was dissolved in dimethylformamide. This solution was then stirred at room temperature with charcoal for 1 hr., the charcoal was removed by filtration, and the filtrate was poured into cold ether in order to precipitate the polymer. Two more reprecipitations afforded the polymers listed in Table I. The infrared spectra of the polymers and the infrared spectrum of the model compound (II) showed maxima (Nujol mull) at 1790, 1715, 1510, 1460, 1380, and 1187 cm^{-1} . Polymerization with 1:1 molar amounts of monomer afforded lower conversion to polymer. Sublimation of benzalazine was evident in this reaction. When the reaction was run in solution, no polymer was formed.

Basic Hydrolysis

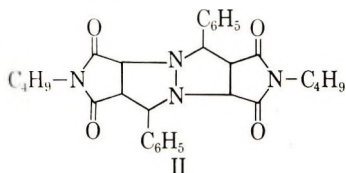
The basic hydrolysis of I, II, and IIIa were carried out under similar conditions. To the model compound or the polymer was added 25 ml. of 5–10% aqueous potassium hydroxide. The mixture was brought to the reflux temperature for 10 hr. and the resulting clear solution was cooled to room temperature, decolorized with charcoal, and then was acidified to precipitate the same tetra acid, 4,8-diphenyl-1,5-diazabicyclo-[3.3.0]-octane-2,3,6,7-tetracarboxylic acid (IV) in each case, m.p. 220–221°C. (reported,² 220–221°C.). The melting point of a mixture of these products was undepressed.

Molecular Weight of IIIId

To a 0.1862 g. sample of IIIId was added 20.80 g. of chloroform. The molecular weight of the solute was determined on a Mechrolab vapor pressure osmometer, Model 301A. The osmometer readings were interpolated by use of a standard calibration curve that gave the molecular weight of IIIId of 3396.

III. RESULTS

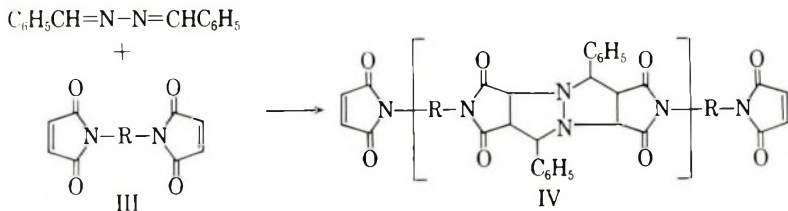
The reaction of benzalazine with *n*-butylmaleimide to give 4,8-diphenyl-1,5-diazabicyclo[3.3.0]octane-2,3,6,7-bis-*n*-butylimide (II)



in quantitative yield was undertaken to investigate the optimum reaction conditions for the polymerization of benzalazine with a series of bismaleimides and to obtain a model compound for such polymers.

When benzalazine was reacted with a series of bis maleimides (IIIa–IIIId), polymers (IVa–IVd) with inherent viscosities in the range 0.13–0.30, are

formed in high yield. The aromatic bismaleimide polymers all have softening and melting points over 300°C., while the *N,N'*-hexamethylene-bismaleimide polymer



[where R = (a) *o*-phenylene, (b) *m*-phenylene, (c) *p*-phenylene, and (d) *N,N'*-hexamethylene]

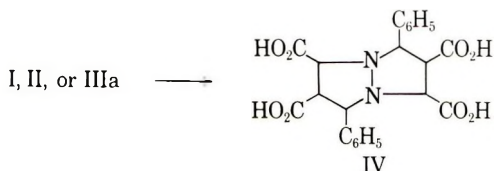
softens at 238°C. The higher softening temperatures of polymers obtained from aromatic bismaleimides is consistent with results obtained from a similar series of Diels-Alder polymers.⁵⁻⁷

The molecular weight of the *N,N'*-hexamethylene-bismaleimide polymer (IVd) was shown to be 3400, as determined on a vapor pressure osmometer. This corresponds to seven recurring units, including endgroups.

IV. DISCUSSION

In the Diels-Alder polymerization of benzalazine with a series of bismaleimides, benzalazine acts as a double diene. It is interesting to note however, that this addition cannot really be considered a true Diels-Alder reaction. It is instead of a 1,3-addition, of which there are few reported examples.

That a 1,3-addition occurs in the formation of these polymers was further verified by the basic hydrolysis of the model compounds I and II and the polymer IIIa to yield the same tetra acid (IV) in each case.



Comparison of the infrared spectra of these polymers with the spectrum of the model compound shows similar characteristic maxima.

It is surprising that even pentamers were obtained when a 2:1 monomer unbalance was employed and that the polymers were isolated in such high conversion. Since a high excess of bismaleimide is present during the reaction, the endgroups are evidently maleimido groups. Termination of the polymer by benzalazine endgroups would necessitate a 1,4-addition of benzalazine to an exposed maleimido function; a reaction which is not observed with the model compound. When exactly stoichiometric quantities of the monomers were present, higher molecular weights were not obtained.

This may be due to the fact that some benzalazine sublimed during the reaction. Lower conversions were obtained from the 1:1 reactions.

Prolonged heating of the crude polymer samples over 200°C. apparently brought about the reverse Diels-Alder reaction, as indicated by the lowering of the polymer solution viscosity. This decrease in molecular weight was also observed when the crude polymer samples were dissolved in dimethylformamide and the solution was heated at the reflux temperature for 48 hr.

We thank the Dunlop Research Center, Toronto, Canada for its generous financial support which made this investigation possible.

References

1. Wagner-Jauregg, T., *Ber.*, **63**, 3213 (1930).
2. Kovacs, J., V. Bruckner, and I. Kandel, *Acta. Chim. Hung.*, **1**, 230 (1951).
3. Metha, N. B., A. P. Phillips, F. Fu Lui, and R. E. Brooks, *J. Org. Chem.*, **25**, 1012 (1960).
4. Searle, N. E., U. S. Pat. 2,444,536 (July 6, 1948).
5. Kraimen, E. A., U. S. Pat. 2,890,206 (June 9, 1959).
6. Kraimen, E. A., U. S. Pat. 2,890,207 (June 9, 1959).
7. Chow, S. W., and J. M. Whelan, Jr., U. S. Pat. 2,971,944 (February 14, 1961).

Résumé

Les diénophiles *N,N'*-hexaméthylène-bis-maléimide et les *o*-, *m*-, et *p*-phénylène-bis-maléimides sont préparés et copolymérisés avec la benzalazine par la réaction de Diels-Alder. La polymérisation à liétat fondu fournit ces polymères à hauts rendements avec des viscosités inhérentes se rangeant de 0.13 à 0.30 et des températures de ramollissement de 238° à 325°. La polymérisation en solution ne donne pas de polymères et on n'isole que les matériaux de départ. La benzalazine dans cette réaction se comporte comme un double diène et subit l'addition 1,3 avec les bis-maléimides pour former ces polymères. Pour vérifier cette 1,3-addition dans la formation du polymère, on effectue une hydrolyse basique des composants, du même genre, le 4,8-diphényl-1,5-diazabicyclo[3,3,0]octane-2,3,6,7-tétracarboxylique acide-bis-anhydride (I) et le 4,8-diphényl-1,5-diazabicyclo[3,3,0]octane-2,3,6,7-bis-*n*-butylimide (II) et chacun des polymères donnent dans chaque cas l'acide-4,8-diphényl-1,5-diazabicyclo[3,3,0]octane-2,3,6,7-tétracarboxylique.

Zusammenfassung

Die doppelt dienophilen Substanzen *N,N'*-Hexamethylen-bismaleinimid und *o*-, *m*- und *p*-Phenylen-bis-maleinimid wurden dargestellt und mit Benzalazin durch eine Diels-Alder-Reaktion copolymerisiert. Die Polymeren wurden durch Polymerisation in Schmelze in hoher Ausbeute mit Viskositätszahlen von 0,13 bis 0,30 und Erweichungstemperaturen von 238° bis 325° erhalten. Lösungspolymerisation lieferte keine Polymeren; es konnte nur das Ausgangsmaterial isoliert werden. Benzalazin verhält sich bei dieser Reaktion als Doppel-Dien und bildet mit den Bis-maleinimiden Polymere durch 1,3-Addition. Das Auftreten einer 1,3-Addition bei der Polymerbildung wird weiters durch basische Hydrolyse der Modellverbindungen, 4,8-Diphenyl-1,5-diazabicyclo[3,3,0]octan-2,3,6,7-tetracarbonsäure-bis-anhydrid (I) und 4,8-Diphenyl-1,5-diazabicyclo[3,3,0]octan-2,3,6,7-bis-*n*-butylimid (II) und eines der Polymeren unter Bildung von 4,8-Diphenyl-1,5-diazabicyclo[3,3,0]octan-2,3,6,7-tetracarbonsäure in jedem Falle bestätigt.

Received February 8, 1963

Catalytic Polymerization of Glycine Ethyl Ester

MARY E. CARTER and O. K. CARLSON, *Exploratory Research Section, Research and Development Division, American Viscose Corporation, Marcus Hook, Pennsylvania*

Synopsis

Polyglycines have been prepared in good yields from glycine ethyl ester with a new catalyst system, aluminum isopropoxide and/or diisopropoxide aluminum chloride. A random statistical experiment was performed to optimize the bulk stage polymerization conditions. The reaction mechanism proposed begins as in the Meerwein-Ponndorf-Verley reduction with an attack by the aluminum on the carbonyl oxygen and is dependent on an amino-carbonyl entity which allows the complexed aluminum to approach a second carbonyl.

INTRODUCTION

Polypeptides have been prepared with many chemically unique monomers. The most satisfactory monomer has probably been the *N*-carboxy- α -amino acid anhydride although the α -amino acids, their esters, diketopiperazines, acyl chlorides, and azides have received considerable study through the years. The initiation of polymerization, which can be difficult for the more stable monomer, has been induced by primary, secondary, and tertiary amines, inorganic acid, bases, sodium ethoxide, heat and pressure, and water.^{1,2}

Polyglycines, usually of low molecular weights (<10,000), have been prepared by several of the above methods. Since it is the simplest polyamide possible, it is not surprising that polyglycine is also a very insoluble, untractable polymer. In its crystalline state two forms may be observed:³ form I consists of a pleated or extended state and is called the beta configuration, whereas form II can be described as a threefold screw axis with a residue translation of 3.1 Å.

The work described in this paper employs the glycine ethyl ester in the preparation of polyglycine and, as a catalyst, aluminum isopropoxide⁴ or diisopropoxide aluminum chloride. *o*-Dichlorobenzene (ODCB) dimethylformamide (DMF), and nitrobenzene, although not solvents for polyglycine, were used in many of the polymerization reactions.

EXPERIMENTAL

Materials

Glycine ethyl ester hydrochloride was purchased from Benzol Products Co., while the aluminum isopropoxide and diisopropoxide aluminum

chloride were obtained from Chattem Chemicals Co. The aluminum isopropoxide was doubly distilled; the diisopropyl chloride was Lot #SCH-V126b, Al, 14.99%; Cl, 19.94% (theo: Al, 14.94%; Cl, 19.63%).

Analytical Methods

Nitrogen determinations were made on a Coleman nitrogen analyzer. Aluminum determinations employed a modified 8-hydroxyquinoline method.

Intrinsic viscosities were determined at 30°C. in dichloroacetic acid (DCA) in a modified Cannon-Fenske viscometer. Molecular weights were obtained by the Archibald method with a Beckman Model E ultracentrifuge, using as solvent, dichloroacetic acid, 84.5 wt.-% and acetic acid, 15.5 wt.-% at 25°C.

Glycine Ethyl Ester

In preparation of glycine ethyl ester,⁵ ethyl glycinate hydrochloride (100 g.) was suspended by stirring in cold dry ether (200 ml.) and ammonia was slowly fed into the reaction flask. At the end of neutralization the ammonium chloride was removed by filtration and the ether removed on a rotary flash evaporator. The residue was then heated to 60°C. and distilled into the evaporator's rotating trap which was kept at acetone-Dry Ice temperature. The ethyl glycinate was handled in a nitrogen atmosphere and stored in vaccine bottles at -78°C.

Bulk Polymerization

The reactor consisted of a 100-ml., two-piece $\frac{3}{4}$ 45/50 Mini Lab basic assembly apparatus with an analytical still head and a 15 ml. capacity water-jacketed receiver. A dry nitrogen atmosphere was maintained in the reaction flask throughout the reaction. The monomer, an ester, was introduced, and brought to the desired starting temperature. The catalyst was introduced via a hypodermic needle and syringe. Stirring was continuous. Ethanol was distilled off as produced. The polymer was washed in a Waring Blendor in ethanol and then heated 20 min. in ethanol and dried from acetone.

Solution Polymerization

The reaction flask containing an anhydrous nitrogen atmosphere was charged with monomer, solvent, and catalyst and immersed in an oil bath at the desired temperature. Stirring was continuous. Ethanol was distilled off as produced.

The polymer was washed four times with ethanol and twice with hot water, then freeze-dried.

Two-Stage Polymerization

Monomer and catalyst were allowed to react in bulk usually until stirring became difficult. At this time, solvent was added and the reaction allowed to continue. The polymer was processed as described above.

DISCUSSION

The data in Table I show that the ethyl ester of glycine does not form a polymer in the presence of solvents used in this work. In some instances, anhydride formation did occur during the time the ester was held at an elevated temperature. It cannot be overemphasized that the purity of the glycine ester is an important factor in this study.

TABLE I
Effect of Solvents on Polymerization of Ethyl Glycinate

Mono- mer, ml.	Solvent	Solvent, ml.	Temp., °C.	Time	Polymer yield, g.	$[\eta]$, dl./g.
10 ^a			140-162	46 min.	4.1	0.113
4			140-150	90 min.	1.55	0.116
20	Pyridine	50.0	121	3 hr. 5 min.	No polymer	
15	ODCB	50.0	Room temp.	192 hr.	Trace	
25	Benzene	25.0	80	5 hr.	No polymer	
25	ODCB	28.2	100	5 hr.	No polymer	
25	Nitro- benzene	21.2	100	5 hr.	0.1	
25	DMF	25.0	100	5 hr.	No polymer	

^a Aluminum isopropylate, 0.3 ml.

Further polymerization studies with aluminum isopropoxide were carried out in *o*-dichlorobenzene. These results are given in Table II. Experiments, 4, 5, and 6 are catalyst concentration studies, and the polymer yield appears to increase with increasing catalyst concentration. As will be observed throughout this work, hot water extraction, which removes by-products such as glycine anhydride and peptides, results in an increased intrinsic viscosity.

The experiments shown in Table III employed a stronger Lewis acid catalyst, diisopropoxide aluminum chloride. Polymerization occurred in the three solvents. Aluminum retention was higher in these polymers but the insolubility of the polymer as well as the aluminum salt made complete purification difficult. However, x-ray powder diagrams of these polymers were similar to those made with aluminum isopropoxide. All polyglycines were in the form II configuration.

A random statistical experiment was carried out on the bulk polymerization stage to obtain optimum conditions for the reaction. The data collected are given in Table IV. These data were programmed for a Bendix G15 digital computer as a trivariate linear regression. The independent variables were time, temperature, and catalyst concentration. The dependent variables were (1) distillate collected, (2) bulk polymer, (3) bulk polymer viscosity, (4) hot water-insoluble polymer, and (5) viscosity of hot water-insoluble polymer. The following information was obtained

TABLE II
Ethyl Glycinate Polymerized with Aluminum Isopropoxide in ODCB

Expt. No.	Mono-mer, ml.	Catalyst, ml.	Solvent, ml.	Temp., °C.	Time	Polymer yield		[η], dl./g.	Polymer hot H ₂ O-insoluble, mole-%	Hot H ₂ O-insoluble [η] dl./g.	Al, wt.-%
						g.	Mole-%				
1	10	0.3	20	120-160	1.44	25.0	0.139				
2	19	0.4	50	138-165	24 hr.	1.20	11.1	0.150		0.163	
3	10	1.0	25	100	6 hr.	0.61	10.7	0.100	5.9	0.163	
4	10	1.0	25	100	24 hr.	2.07	36.3	0.101	6.8	0.151	0.013
5	10	2.0	25	100	24 hr.	3.51	61.4	0.118	10.7		0.014
6	10	3.0	25	100	24 hr.	2.75	48.2	0.108	9.1		0.024

TABLE III
Ethyl Glycinate Polymerized with Diisopropoxide Aluminum Chloride^a

Monomer, ml.	Catalyst, g.	Solvent	Solvent, ml.	Temp., °C.	Time, hr.	Polymer yield		Hot H ₂ O-insoluble [η], dl./g.	Al, wt.-%
						g.	Mole-%		
25.0	0.45	ODCB	28.2	100	5	3.14	22.0	0.15	1.30
25.0	0.45	Nitro-benzene	21.2	100	5	2.38	16.7	0.15	1.30
25.0	0.45	DMF	25.0	100	5	2.55	17.9		1.60

^a Catalyst added as a 1.03 molar solution in ODCB.

TABLE IV
 Polyglycine (First-Stage Variables); Charge: Ethyl Glycinate—50.0 ml.; AlCl₃(*i*-OPr)₂ in ODCB

Temp., °C.	Time, min.	Catalyst concn., × 10 ⁴ , mole/l.	Distillate collected		Polymer			Extraction with hot water				
			cc.	g.	Yield, %	[η], dl./g.	N, %	Al, %	Wt. before extrac- tion, g.	Wt. after extrac- tion, g.	Hot H ₂ O- insoluble, %	[η], dl./g.
90	422	3.43	2.2	27.6	53.6	0.107	21.3	0.056	20.92	1.61	7.7	0.134
93	198	18.9	15.0	27.6	53.6	0.114	21.0	0.079	19.0	2.62	11.9	0.161
97	142	5.6	3.2	20.8	40.4	0.066	21.3	0.10	15.1	1.05	6.9	0.145
100	96	16.3	13.5	26.5	51.5	0.112	21.0	0.16	20.0	2.28	11.4	0.148
104	30	21.4	8.8	20.7	40.2	0.124	20.6	0.28	14.6	1.38	9.4	0.156
107	310	8.59	23.7	28.8	55.9	0.107	21.3	0.088	24.5	5.58	22.8	0.128
110	478	11.2	18.9	27.2	52.8	0.107	21.4	0.22	22.15	4.90	22.1	0.131
117	254	0.085	22.4	26.6	51.7	0.119	21.9	0.40	23.47	5.81	14.6	0.132
120	534	13.7	25.3	30.2	58.6	0.107	21.2	0.12	26.32	8.28	11.5	0.130

TABLE V
 Effect of Various Reaction Conditions

Expt. No.	Ethyl glycolate, ml.	Catalyst, ml.	Solvent (ODCB), ml.	Reaction conditions	Polymer		
					Yield, g.	[η], dl./g.	Yield, %
1	44.0	2.0 ^a	250.0	Reacted at 90–155°C. 45 min., then ODCB added, heat slowly increased to 160°C., 2 hr., 20 min.	7.1	0.145	28.4
2	300.0	4.76 g. ^b	125.0	Reacted at 110°C., 10 min., then ODCB added; 2 hr., 110–160°C.	45.1	0.162	26.4
3	50.0	2.0 ^a	25.0	Heated 20 min. at 110°C. then ODCB added; 2 hr., 110–160°C.	9.22	Insoluble	32.6
4	50.0	2.5 ^c	56.0	Reacted 2 hr. 30 min., then solvent added; 3 hr. 20 min., 120–160°C.	10.67	0.141	37.7
5	50.0	2.5 ^c	56.0	Reacted for 2 hr. 30 min. at 120°C., then Waring blended and solvent added; 4 hr., 120–160°C.	10.5	0.154	37.2
6	25.0	1.5 ^c	50.0 ^d	Reacted for 3 hr. at 120°C., then Waring blended and solvent added; 5 hr., 120–160°C.	6.08	0.137	43.3

^a AlCl(*i*-OPr)₂-benzene solution, 1.0M.

^b In 30 ml. ODCB.

^c AlCl(*i*-OPr)₂-*o*-dichlorobenzene solution, 1.02M.

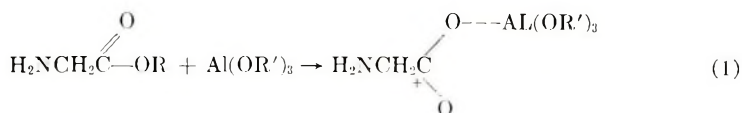
^d Hallcomid 8-10 used as solvent.

with a 95% confidence limit or better: (1) distillate was dependent on temperature, (2) bulk polymer was dependent on time, (3) bulk polymer viscosity showed no dependency, (4) hot water-insoluble polymer yield was dependent on temperature, and (5) viscosity of hot water-insoluble polymer showed dependency on time and catalyst concentration but the relationship to time was curvilinear.

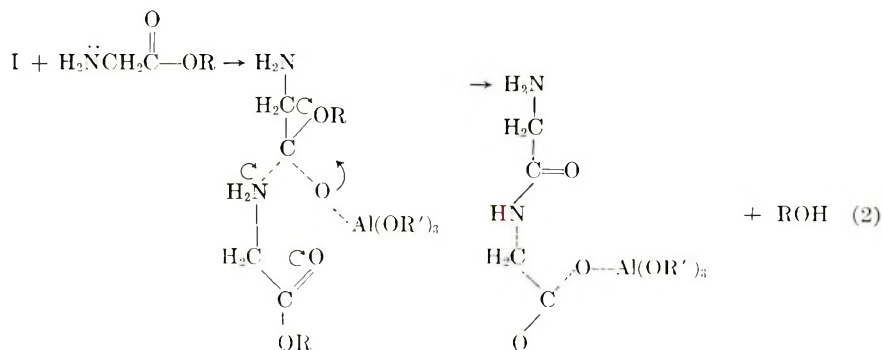
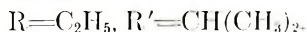
From these data a set of optimum reaction conditions was chosen for the bulk polymerization stage and are as follows: 120°C. for 150 min. with a catalyst concentration of $25.5 \times 10^{-4} M$ for 50 ml. of monomer. The bulk polymerization stage of experiments 4, 5, and 6 (Table V) was based on this conclusion. Experiments 1, 2, and 3 in this table show other variations in both the bulk and solvent polymerization stages. Archibald molecular weights for experiments 1 and 2 were 9900 and 9100, respectively.

The mechanism of the Meerwein-Pondrof-Verley reduction begins with an attack by the aluminum on the carbonyl oxygen.⁶ This type of reduction has been carried out on several aliphatic β amino aldehydes.⁷ Probably a similar attack occurred in Gheilmeth's reaction⁴ when he obtained in high yield β -*N*-diethyl-amino-ethyl-*p*-aminobenzamide from ethyl *p*-aminobenzoate and *N,N*-diethylethylenediamine. If the attack had involved the nitrogen(s), a variety of products could have been obtained.

Infrared spectra obtained immediately upon mixing glycine ethyl ester and aluminum isopropoxide showed absorption shifts that could be interpreted as an attack at the ester carbonyl oxygen. Work is continuing on the polymerization mechanism with a consideration of the various steric and electronic factors which may be involved, but in the meantime, the reaction sequence of eqs. (1) and (2) is tentatively proposed.



where



The authors wish to thank Mr. N. J. Wegemer for molecular weight determinations, Mr. N. M. Walter for x-ray powder diagrams, Dr. F. G. Pearson for the infrared spectra, and Dr. M. J. Danzig for valuable discussions.

References

1. Katchalski, E., and M. Sela, *Adv. Protein Chem.*, **12**, 243 (1959).
2. Stahmann, M. A., Ed., *Polyamino Acids, Polypeptides, and Proteins*, Univ. Wisconsin Press, Madison, Wis., 1962.
3. Crick, F. H. C., and A. Rich, *Nature*, **176**, 780 (1955); W. T. Astbury, *Nature*, **163**, 722 (1949).
4. Ghielmeth, G., *Farmaco (Pravia) Ed. Sci.*, **9** 384 (1954).
5. Baniel, A., M. Frankel, I. Friederick, and A. Katchalsky, *J. Org. Chem.*, **13**, 791 (1948).
6. Williams, E. D., K. A. Krieger, and A. R. Day, *J. Am. Chem. Soc.*, **75**, 2404 (1953).
7. Hayes, K., and G. Drake, *J. Org. Chem.*, **15**, 873 (1950).

Résumé

On a préparé des polyglycines avec de bons rendements à partir de l'ester éthylique de la glycine et d'un nouveau système catalytique, isopropylate d'aluminium et/ou chloro diisopropylate d'aluminium. Une expérience statistique a été effectuée afin de préciser les conditions optima de polymérisation en bloc. Le mécanisme de réaction proposé commence de la même manière que dans la réduction de Meerwein-Ponndorf-Verley par une attaque de l'aluminium sur l'oxygène carbonyle et dépend d'une entité aminocarbonyle qui permet à l'aluminium complexé d'approcher un second carbonyle.

Zusammenfassung

Polyglycine wurden in guter Ausbeute mit einem neuen Katalysator-system, Aluminiumisopropoxyd und Diisopropoxydaluminiumchlorid, aus Glycinäthylester hergestellt. Die optimalen Polymerisationsbedingungen in Substanz wurden ermittelt. Der angenommene Reaktionsmechanismus beginnt wie bei der Meerwein-Ponndorf-Verley-Reduktion mit einem Angriff des Aluminiums am Carbonylsauerstoff und bedarf einer Amino Carbonylgruppierung, die dem komplexierten Aluminium eine Annäherung an ein zweites Carbonyl gestattet.

Received February 27, 1963

Molecular Weight Distribution and Viscosity of Multichain Polymers in ϵ -Caprolactam Polymerization

TOMONOBU MANABE, *Nylon Department, Nippon Rayon Company, Ltd., Uji, Japan*

Synopsis

The molecular weight distribution is calculated on the basis that $x - 1$ indistinguishable monomer units are distributed in f unnumbered branches with no restrictions on the number per branch. The weight fraction of single- and multi-chain polymer mixture of polymerization degree x is for $f = 2$,

$$W_x = L(1 - p)xp^{x-1} + (Q/2)(1 - p)^2x^2p^{x-1}$$

and for $f = 3$,

$$W_x = L(1 - p)xp^{x-1} + (Q/3)[(1 - p)^3/(5 - 3p)]x^2(x + 4)p^{x-1}$$

where, p is the extent of reaction, Q the number of equivalents that reacts with one mole of monomer, and L the number of equivalents of unreacted groups per mole of monomer. When the limiting viscosity number $[\eta]$ and the melt viscosity μ are expressed as the function of the (fractionated) degree of polymerization x : $[\eta] = K_\nu x^\alpha$ and $\mu = K_\mu x^\beta$, the solution and the melt viscosities are expressed as follows:

$$[\eta] = \frac{K_\nu}{(Q + L)^\alpha} \left(1 + \frac{\alpha}{2} \frac{Q}{Q + L} \right) \Gamma(\alpha + 2)$$

$$\mu = \frac{K_\mu}{(Q + L)^\beta} \left(1 + \frac{\beta}{2} \frac{Q}{Q + L} \right) \Gamma(\beta + 2)$$

The relation among the number-average, viscosity-average, weight-average and melt viscosity-average degree of polymerization is discussed. The relation between the solution and the melt viscosities is also discussed.

INTRODUCTION

The molecular weight distribution and the viscosity of the multichain polycondensation polymers have been discussed by several authors.¹⁻⁴ When an amino acid is condensed with a small portion of a f -functional polybasic acid, $R[-COOH]_f$, the resulting polymer should have a structure



where y is the chain length of a chain. When the degree of polymerization is x , x is expressed as:

$$x = y_1 + y_2 + \dots + y_f + 1 \quad (1)$$

We should calculate the number of ways that $x - 1$ indistinguishable monomer units can be distributed in f unnumbered branches with no restrictions on the number per branch.

In the preceding theories¹⁻⁴, however, the number of ways was calculated based upon the numbered branches as:

$$(x + f - 2)! / (f - 1)! (x - 1)! \quad (2)$$

In this case some corrections have to be made.

In this paper, the molecular weight distribution is discussed theoretically in the cases of $f = 2$ and 3. The solution and melt viscosities are also discussed.

THEORY

1. Molecular Weight Distribution in $f = 2$

1.1. Relations among Variables

The following quantities are defined: $[m]_0$ = initial monomer concentration; $[a_2]_0$ = initial dibasic acid concentration; $[w]_0$ = initial water concentration; $[-CONH-]$ = concentration of $-CONH-$ groups in the condensation equilibrium; $[-NH_2]$ = concentration of $-NH_2$ groups in the condensation equilibrium; $[-COOH]$ = concentration of $-COOH$ groups in the condensation equilibrium; $[P]$ = concentration of linear polymer in the condensation equilibrium; $[w]$ = concentration of free water in the condensation equilibrium; λ = fraction of monomer converted into polymer; J = a correction factor. All concentrations are in units of moles per liter.

Among these quantities, the following relations exist.

$$[-COOH] = J ([-NH_2] + 2 [a_2]_0) \quad (3)$$

$$[P] = [-NH_2] + [a_2]_0 \quad (4)$$

$$[-CONH-] = \lambda [m]_0 - [-NH_2] \quad (5)$$

It was assumed that all the dibasic acid molecules were connected with polymer molecules in the condensation equilibrium.

If there is no decarboxylation reaction, J should be 1.

When the polymerization and the condensation are performed in a closed, one-phase system (liquid phase), the following relation is realized.

$$[w]_0 = [w] + [-NH_2] \quad (6)$$

At condensation equilibrium, the following relation is realized.

$$K = [-CONH-] [w] / [-COOH] [-NH_2] \quad (7)$$

The following, dimensionless quantities are now defined:

$$\left. \begin{aligned} L &= [-\text{NH}_2]/\lambda [m]_0 \\ Q &= 2[a_2]_0/\lambda [m]_0 \\ S &= [w]_0/\lambda [m]_0 \end{aligned} \right\} \quad (8)$$

Some of these were previously defined by Flory.¹

1.2. Molecular Weight Distribution

The extent of reaction p , i.e., the probability of reacting the $-\text{COOH}$ group with $-\text{NH}_2$ group, is expressed as:

$$p = \frac{[-\text{CONH}-]}{[-\text{CONH}-] + 2[a_2]_0 + [-\text{NH}_2]} \quad (9)$$

From eqs. (5), (8), and (9), we obtain the following eq. (10)

$$p = (1 - L)/(1 + Q) \quad (10)$$

In the condensation equilibrium, two types of linear polymer, NH_2-COOH type and $\text{HOOC}-\text{COOH}$ type, coexist. We define $M_x =$ concentration of NH_2-COOH type polymer of polymerization degree x in the condensation equilibrium, $N_x =$ concentration of $\text{HOOC}-\text{COOH}$ type polymer of polymerization degree x in the condensation equilibrium.

The concentration M_x should have the following form:

$$M_x = M_0 (1 - p)p^{x-1} \quad (11)$$

where M_0 is a constant. Considering the following condition:

$$[-\text{NH}_2] = \sum_{x=1}^{\infty} M_x \quad (12)$$

we obtain the following form for M_x :

$$M_x = [-\text{NH}_2](1 - p)p^{x-1} \quad (13)$$

Whenever we should like to determine the form of N_x , we should calculate the number of ways that $x - 1$ indistinguishable monomer units can be distributed in two unnumbered branches with no restrictions on the number per branch. Whenever the degree of polymerization is discussed, a polybasic acid is considered as a monomer unit.

The number of ways of distributing should be as given in Table I.

TABLE I

x	Number of ways of distributing ($f = 2$)
Odd (1,3,5, ...)	$(1/2)(x + 1)$
Even (2,4,6, ...)	$(1/2)x$

When we discuss a case of a higher degree of polymerization (x is large), we may consider the number of ways of distributing as $\binom{1/2}{x}$, regardless of whether x is odd or even.

According to the traditional calculation, the number of ways of distributing is as follows:

$$(x + 2 - 2)!(2 - 1)!(x - 1)! = x$$

Comparing the number of ways $\left[\binom{1/2}{x}\right]$ of distributing with the traditional one (x), we can know the difference between them.

The concentration N_x should have the following form approximately, taking the above discussions into account.

$$N_x = N_0 \binom{1/2}{x} x (1 - p)^2 p^{x-1} \quad (14)$$

where N_0 is a constant. Considering the following condition:

$$[a_2]_0 = \sum_{x=1}^{\infty} N_x \quad (15)$$

we obtain the following form:

$$N_x = [a_2]_0 (1 - p)^2 x p^{x-1} \quad (16)$$

We define R_x and W_x as: R_x = concentration of linear polymer of polymerization degree x in the condensation equilibrium, S_x = concentration of monomer units which belong to linear polymers of polymerization degree x in the condensation equilibrium. Then concentrations R_x and S_x are expressed as eqs. (17) and (18), taking eqs. (13) and (16) into account:

$$R_x = [-\text{NH}_2](1 - p)p^{x-1} + [a_2]_0(1 - p)^2 x p^{x-1} \quad (17)$$

$$S_x = [-\text{NH}_2](1 - p)x p^{x-1} + [a_2]_0(1 - p)^2 x^2 p^{x-1} \quad (18)$$

We define W_x as: W_x = weight fraction of linear polymer of polymerization degree x at condensation equilibrium; then

$$W_x = S_x / \lambda [m]_0 \quad (19)$$

We obtain the weight fraction W_x as eq. (20), taking eqs. (8), (18), and (19) into account:

$$W_x = L[(1 - p)/p]x p^x + Q[(1 - p)^2/2p]x^2 p^x \quad (20)$$

1.3. Estimation of the Molecular Weight Distribution from the Polymerization Conditions

We can estimate the molecular weight distribution by using eq. (20). In order to estimate the molecular weight distribution, we should calculate the quantities Q , L , and p from the polymerization conditions.

We can calculate Q from eq. (8).

In the case of closed, one-phase polymerization, L is calculated from the following eq. (21),

$$L = \frac{1}{2} \left[Q^2 + \frac{2}{JK} (Q + 2S) + \frac{1}{J^2 K^2} \right]^{1/2} - \frac{1}{2} \left(Q + \frac{1}{JK} \right) \quad (21)$$

where the following assumptions were made:

$$\begin{aligned} JK &\gg 1 \\ Q, S &\ll 1 \end{aligned} \quad (22)$$

We can calculate p from eq. (10).

2. Molecular Weight Distribution in $f = 3$

2.1. Number of Ways of Distributing

The number of ways that $x - 1$ indistinguishable monomer units can be distributed in three unnumbered branches with no restrictions on the number per branch is as follows.

- a. For $x = 6n + 1$ ($n = 1, 2, 3, \dots$)

$$X_x = (1/12)(x^2 + 4x + 7) \quad (23)$$

where X_x = number of ways that $x - 1$ indistinguishable monomer units can be distributed in three unnumbered branches with no restrictions on the number per branch.

- b. For $x = 3n + 1$, $x \neq 6n' + 1$ ($n, n' = 1, 2, 3, \dots$)

$$X_x = (1/12)(x^2 + 4x + 4) \quad (24)$$

- c. For $x = 2n + 1$, $x \neq 3n' + 1$ ($n, n' = 1, 2, 3, \dots$)

$$X_x = (1/12)(x^2 + 4x + 3) \quad (25)$$

- d. For $x = 2n$, $x \neq 3n' + 1$ ($n, n' = 1, 2, 3, \dots$)

$$X_x = (1/12)(x^2 + 4x) \quad (26)$$

When we discuss a case of a higher degree of polymerization (x is large), we may consider the number of ways X_x of distributing as follows, taking eqs. (23)–(26) into account.

$$X_x = (1/12)(x^2 + 4x) + \dots \quad (27)$$

According to the traditional calculation, the number of ways of distributing is as follows:

$$X_x = (x + 3 - 2)! / (3 - 1)! (x - 1)! = (1/2)(x^2 + x) \quad (28)$$

By comparing eq. (27) with eq. (28), we can know the difference between the ways of distributing.

2.2. Molecular Weight Distribution

The discussion for the case of $f = 3$ is almost the same as the case of $f = 2$. Corresponding to the case of $f = 2$, the following changes should be made:

$$[-\text{COOH}] = J(-\text{NH}_2) + 3[\mathbf{a}_3]_0 \quad (3')$$

$$Q = 3[\mathbf{a}_3]_0/\lambda[m]_0 \quad (8')$$

$$p = \frac{[-\text{CONH-}]}{[-\text{CONH-}] + 3[\mathbf{a}_3]_0 + [-\text{NH}_2]} \quad (9')$$

$$N_x = N_0 (1/12)x(x+4)(1-p)^3 p^{x-1} \quad (14')$$

$$[\mathbf{a}_3]_0 = \sum_{x=1}^{\infty} N_x \quad (15')$$

$$N_x = \frac{(1-p)^3}{5-3p} [\mathbf{a}_3]_0 x(x+4)p^{x-1} \quad (16')$$

$$R_x = [-\text{NH}_2](1-p)p^{x-1} + [\mathbf{a}_3]_0 \frac{(1-p)^3}{5-3p} x(x+4)p^{x-1} \quad (17')$$

$$S_x = [-\text{NH}_2](1-p)xp^{x-1} + [\mathbf{a}_3]_0 \frac{(1-p)^3}{5-3p} x^2(x+4)p^{x-1} \quad (18')$$

$$W_x = L \frac{1-p}{p} x p^x + Q \frac{(1-p)^3}{3p(5-3p)} x^2(x+4)p^x \quad (20')$$

where $[\mathbf{a}_3]_0$ = initial tribasic acid concentration, N_x = concentration of $-(\text{COOH})_3$ type polymer of polymerization degree x in the condensation equilibrium, R_x = concentration of polymer of polymerization degree x in the condensation equilibrium, S_x = concentration of monomer units which belong to polymers of polymerization degree x in the condensation equilibrium.

The following discussions are limited to the case of $f = 2$.

3. Average Degree of Polymerization in $f = 2$

The following average degrees of polymerization are discussed: \bar{P}_n = number-average degree of polymerization, \bar{P}_v = viscosity-average degree of polymerization, \bar{P}_w = weight-average degree of polymerization, \bar{P}_μ = melt viscosity-average degree of polymerization.

These average degrees of polymerization are defined, respectively, as follows.

$$\bar{P}_n = \frac{\sum_{x=1}^{\infty} x R_x}{\sum_{x=1}^{\infty} R_x} \quad (29)$$

$$\bar{P}_v = \left(\frac{\sum_{x=1}^{\infty} x^{1+\alpha} R_x}{\sum_{x=1}^{\infty} x R_x} \right)^{1/\alpha} \quad (30)$$

$$\bar{P}_w = \frac{\sum_{x=1}^{\infty} x^2 R_x / \sum_{x=1}^{\infty} x R_x}{\sum_{x=1}^{\infty} x R_x} \quad (31)$$

$$\bar{P}_\mu = \left(\frac{\sum_{x=1}^{\infty} x^{1+\beta} R_x / \sum_{x=1}^{\infty} x R_x}{\sum_{x=1}^{\infty} x R_x} \right)^{1/\beta} \quad (32)$$

where α and β are constant and independent of the degree of polymerization.

The discussions of melt viscosity-average degree of polymerization follow along with those of the viscosity-average degree of polymerization.

The following relations exist between $[\eta]$ and \bar{P}_v and between μ and \bar{P}_μ :

$$[\eta] = K_v \bar{P}_v^\alpha \quad (33)$$

$$\mu = K_\mu \bar{P}_\mu^\beta \quad (34)$$

where $K_v =$ constant which is related to the solution viscosity and is independent of the degree of polymerization; $K_\mu =$ constant which is related to the melt viscosity and is independent of the degree of polymerization; $[\eta] =$ limiting viscosity number (in deciliters /gram), and $\mu =$ melt viscosity (in poises).

The constants α and β are as follows:

$$0.5 < \alpha < 1.0 \quad (35)$$

$$\beta = 3.4$$

From eqs. (17), (29), (30), (31), and (32), we obtain the following equations:

$$\bar{P}_n = 1 + \frac{2(1-L)}{Q+2L} \quad (36)$$

$$\bar{P}_v = \left(\left[\frac{-1}{l_n \left(\frac{1-L}{1+Q} \right)} \right]^{\alpha+2} \frac{(Q+L)\Gamma(\alpha+2)}{(1+Q)(2+Q)(1-L)} \right. \\ \left. \times \left\{ 2L(1+Q) + Q(Q+L)(\alpha+2) \left[\frac{-1}{l_n \left(\frac{1-L}{1+Q} \right)} \right] \right\} \right)^{1/\alpha} + \dots \quad (37)$$

$$\bar{P}_w = 1 + \frac{2(1-L)}{Q+L} \left[1 + \frac{Q(1+Q)}{(Q+L)(2+Q)} \right] \quad (38)$$

$$\bar{P}_\mu = \left(\left[\frac{-1}{l_n \left(\frac{1-L}{1+Q} \right)} \right]^{\beta+2} \frac{(Q+L)\Gamma(\beta+2)}{(1+Q)(2+Q)(1-L)} \right. \\ \left. \times \left\{ 2L(1+Q) + Q(Q+L)(\beta+2) \left[\frac{-1}{l_n \left(\frac{1-L}{1+Q} \right)} \right] \right\} \right)^{1/\beta} + \dots \quad (39)$$

Whenever the average degree of polymerization is high, the following condition is realized:

$$Q, L \ll 1 \quad (40)$$

Under the above condition, eqs. (36)–(39) are simplified as follows.

$$\bar{P}_n = \frac{1}{({}^{1/2})Q + L} + \dots \quad (41)$$

$$\bar{P}_v = \frac{1}{Q + L} \left[\left(1 + \frac{\alpha}{2} \frac{Q}{Q + L} \right) \Gamma(\alpha + 2) \right]^{1/\alpha} + \dots \quad (42)$$

$$\bar{P}_w = \frac{3Q + 2L}{(Q + L)^2} + \dots \quad (43)$$

$$\bar{P}_\mu = \frac{1}{Q + L} \left[\left(1 + \frac{\beta}{2} \frac{Q}{Q + L} \right) \Gamma(\beta + 2) \right]^{1/\beta} + \dots \quad (44)$$

From eqs. (41)–(44), we obtain the following relation.

$$\begin{aligned} \bar{P}_n : \bar{P}_v : \bar{P}_w : \bar{P}_\mu = 1 : \frac{({}^{1/2})Q + L}{Q + L} \left[\left(1 + \frac{\alpha}{2} \frac{Q}{Q + L} \right) \Gamma(\alpha + 2) \right]^{1/\alpha} : \\ \frac{2[({}^{1/2})(Q + L)][({}^{3/2})Q + L]}{(Q + L)^2} : \frac{({}^{1/2})Q + L}{Q + L} \left[\left(1 + \frac{\beta}{2} \frac{Q}{Q + L} \right) \Gamma(\beta + 2) \right]^{1/\beta} \end{aligned} \quad (45)$$

Under the conditions

$$Q \ll L \quad (46)$$

eq. (45) is simplified as follows:

$$\bar{P}_n : \bar{P}_v : \bar{P}_w : \bar{P}_\mu = 1 : [\Gamma(\alpha + 2)]^{1/\alpha} : 2 : [\Gamma(\beta + 2)]^{1/\beta} \quad (47)$$

The relation expressed by eq. (47) has been obtained by Flory in his most probable distribution.

Under the condition,

$$L \ll Q \quad (48)$$

eq. (45) is simplified as follows.

$$\bar{P}_n : \bar{P}_v : \bar{P}_w : \bar{P}_\mu = 1 : \frac{1}{2} \left[\left(1 + \frac{\alpha}{2} \right) \Gamma(\alpha + 2) \right]^{1/\alpha} : \frac{3}{2} : \frac{1}{2} \left[\left(1 + \frac{\beta}{2} \right) \Gamma(\beta + 2) \right]^{1/\beta} \quad (49)$$

4. Solution and Melt Viscosities in $f = 2$

From eqs. (33), (34), (42) and (44), we obtain the following equations:

$$[\eta] = \frac{K_v}{(Q + L)^\alpha} \left[\left(1 + \frac{\alpha}{2} \frac{Q}{Q + L} \right) \Gamma(\alpha + 2) \right] \quad (50)$$

$$\mu = \frac{K_\mu}{(Q + L)^\beta} \left[\left(1 + \frac{\beta}{2} \frac{Q}{Q + L} \right) \Gamma(\beta + 2) \right] \quad (51)$$

We can obtain the solution and melt viscosities, $[\eta]$ and μ , from the analytical values, Q and L , by using eqs. (50) and (51).

5. Relation between the Solution and Melt Viscosities in $f = 2$

From eqs. (50) and (51), we obtain the relation between μ and $[\eta]$ as follows:

$$\mu = \frac{K_\mu \Gamma(\beta + 2)}{K_v^{\beta/\alpha} [\Gamma(\alpha + 2)]^{\beta/\alpha}} \frac{1 + \frac{\beta}{2} \frac{Q}{Q + L}}{\left[1 + \frac{\alpha}{2} \frac{Q}{Q + L} \right]^{\beta/\alpha}} [\eta]^{\beta/\alpha} \quad (52)$$

From eq. (52), it is clear that we can not expect a unique relation between the solution and the melt viscosities unless

$$Q/(Q + L) \ll 1 \quad (53)$$

Under the above condition, eq. (52) is simplified as follows.

$$\mu = \frac{K_\mu \Gamma(\beta + 2)}{K_v^{\beta/\alpha} [\Gamma(\alpha + 2)]^{\beta/\alpha}} [\eta]^{\beta/\alpha} \quad (54)$$

We can expect a unique relation between the solution and the melt viscosities as eq. (54) whenever the contribution Q of the multichain polymers is negligible.

CONCLUSIONS

The calculation of the molecular weight distribution should be based on the fact that the indistinguishable monomer units are distributed in the unnumbered branches with no restrictions on the number per branch.

On the above basis, some corrections are made as to the traditional molecular weight distribution.

The solution and the melt viscosities can be estimated from the analytical data or the condensation conditions.

References

1. Schaeffgen, J. R., and P. J. Flory, *J. Am. Chem. Soc.*, **70**, 2709 (1948).
2. Flory, P. J., *Principles of Polymer Chemistry*, Cornell Univ. Press, Ithaca, N. Y., 1953, p. 331.
3. Fukumoto, O., *Kobunshi Kagaku*, **18**, 22 (1961).
4. Howard, G. J., in *Progress in High Polymers*, Vol. 1, J. C. Robb and F. W. Peaker, Eds., Heywood, London, 1961, p. 187.

Résumé

On calcule la distribution des poids moléculaires sur base d'une distribution de $x - 1$ unités monomériques indistinguables en f branches non-dénombrées sans restriction quant au nombre par ramification. La fraction en poids d'un mélange de polymères à chaîne unique et à plusieurs polymères de degré de polymérisation x se présente comme suit pour $f = 2$, $W_x = L(1 - p)xp^{x-1} + (Q/2)(1 - p)^2x^2p^{x-1}$ et pour $f = 3$, $W_x = L(1 - p)xp^{x-1} + (Q/3)[(1 - p)^3/(5 - 3p)]x^2(x + 4)p^{x-1}$ où p est le degré de conversion de la réaction, Q le nombre d'équivalents qui réagit avec une mole de monomère, L le nombre d'équivalents par mole de monomère de groupes n'ayant pas réagi. Lorsque la viscosité intrinsèque $[\eta]$ et la viscosité à l'état fondu μ sont exprimées comme une fonction du degré de polymérisation (*fractionné*) x : $[\eta] = K_v x^\alpha$ et $\mu = K_\mu x^\beta$, les viscosités en solution et à l'état fondu sont exprimées comme suit:

$$[\eta] = \frac{K_v}{(Q + L)^\alpha} \left(1 + \frac{\alpha}{2} \frac{Q}{Q + L} \right) \Gamma(\alpha + 2)$$

$$\mu = \frac{K_\mu}{(Q + L)^\beta} \left(1 + \frac{\beta}{2} \frac{Q}{Q + L} \right) \Gamma(\beta + 2)$$

On discute la relation entre le degré de polymérisation moyen en nombre, moyen en viscosité, moyen en poids en moyen en viscosité à l'état fondu. On discute également la relation entre les viscosités en solution et à l'état fondu.

Zusammenfassung

Die molekulargewichtsverteilung wird auf Grundlage der Annahme berechnet, dass $x - 1$ ununterscheidbare Monomereinheiten auf f unnummerierte Zweige ohne Beschränkung der Anzahl pro Zweig verteilt werden. Der Gewichtsbruchteil an Einzel- und Vielkettenpolymergemisch vom Polymerisationsgrad x beträgt für $f = 2$, $W_x = L(1 - p)xp^{x-1} + (Q/2)(1 - p)^2x^2p^{x-1}$ und für $f = 3$, $W_x = L(1 - p)xp^{x-1} + (Q/3)(1 - p)^3/(5 - 3p)x^2(x + 4)p^{x-1}$ wo p das Reaktionsausmass, Q die Zahl der Äquivalente, die pro Mol Monomeres reagiert haben und L die Zahl der Äquivalente nichtreagierter Gruppen pro Mol Monomeres ist. Bei Darstellung der Grenzviskositätszahl $[\eta]$ und der Schmelzviskosität μ als Funktion des Polymerisationsgrades (von Fraktionen) x durch $[\eta] = K_v x^\alpha$ und $\mu = K_\mu x^\beta$ lassen sich Lösungs- und Schmelzviskosität wie folgt ausdrücken:

$$[\eta] = \frac{K_v}{(Q + L)^\alpha} \left(1 + \frac{\alpha}{2} \frac{Q}{Q + L} \right) \Gamma(\alpha + 2)$$

$$\mu = \frac{K_\mu}{(Q + L)^\beta} \left(1 + \frac{\beta}{2} \frac{Q}{Q + L} \right) \Gamma(\beta + 2)$$

Die Beziehung zwischen Zahlenmittel, Viskositätsmittel, Gewichtsmittel und Schmelzviskositätsmittel des Polymerisationsgrades wird diskutiert und ebenso die Beziehung zwischen Lösungs- und Schmelzviskosität.

Received February 27, 1963

Preparation of Poly(arylene Sulfides)*

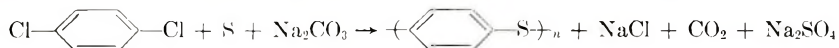
SHIGEMITSU TSUNAWAKI and CHARLES C. PRICE, *Department of Chemistry, University of Pennsylvania, Philadelphia, Pennsylvania*

Synopsis

The attempted polymerization of thiyl radicals from 4-bromothiophenol (I), 2,6-dimethyl-4-bromothiophenol (II), 2,6-dimethylthiophenol, and bis(2,6-dimethylphenyl) disulfide gave no polymer. The polymerization of lithium and sodium salts of I, II, and 2-methyl-4-bromophenol and of sodium 4-chlorothiophenoxide by refluxing in various solvents with or without copper catalyst, gave the corresponding poly(arylene sulfides). Poly(phenylene sulfide), m.p. 270–290°C. was stable at 500°C. for 2 hr. under nitrogen and showed high crystallinity by x-ray. Poly(2,6-dimethylphenylene sulfide), m.p. 160–180°C., showed little if any crystallinity by X-ray diffraction. Poly(2-methylphenylene sulfide) melted at 60–100°C.

INTRODUCTION

Aromatic polymers consisting of aromatic rings alone or of aromatic rings connected by stable linkages are expected to have a high degree of thermal and chemical inertness. Poly-(arylene sulfide) is one such aromatic polymer and its preparation has been reported. Hilditch¹ described that in addition to diphenylene disulfide, the self-condensation of thiophenol in cold concentrated sulfuric acid gives a cream-colored, insoluble, amorphous powder in a yield of about 60%, softening and decomposing at 290–295°C, and having an empirical formula of C₆H₄S. Also, Tasker and Jones² obtained an amorphous, sticky, brown material having an empirical formula of C₆H₄S, by the reaction of thiophenol with thionyl chloride. Macallum³ obtained poly(phenylene sulfide) by the reaction of *p*-dichlorobenzene with sulfur and dry sodium carbonate at 300–340°C.



The properties of the polymer varied with the ratio of sulfur and *p*-dichlorobenzene. It had empirical formulae of C₆H₄S_{1.2} to C₆H₄S_{2.3}, melting points from 255 to above 350°C., and molecular weights from 9,000 to 17,000. Lenz and co-workers^{4,5} have recently reinvestigated the Macallum polymerization and suggested a mechanism for it. They also reported the x-ray diffraction pattern, infrared spectrum, and thermal stability of this polymer compared to that of poly(phenylene sulfide) prepared by the self-polycondensation of sodium *p*-chlorothiophenoxide. The most significant

* Abstracted from the doctoral dissertation of Shigemitsu Tsunawaki, University of Pennsylvania, 1962. Supported in part by a General Tire & Rubber Co. Fellowship.

difference observed was only in the infrared spectra in the 860–900 cm.^{-1} range, which is characteristic of 1,2,4-trisubstituted benzene.

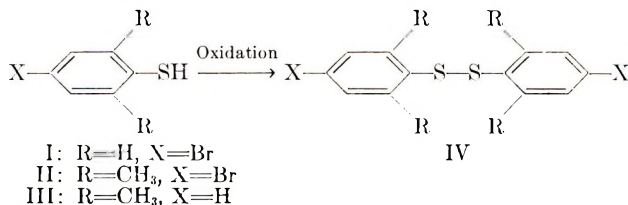
Quite recently, Lenz, Handlovits, and Smith⁶ have reported that a kinetic study of the reaction between various aryl halides and metal salts of thiophenols indicates an order of reactivity of $\text{I} > \text{Br} > \text{Cl} \simeq \text{F}$ and $\text{Li} > \text{Na} > \text{K}$ and that the polymerization of various metal salts of halothiophenoxide at 250°C. in pyridine and at 10–20°C. below their melting points without solvents, gave poly(phenylene sulfide) stable in air or nitrogen up to 450°C.

We wish here to report our work on a similar approach to the preparation of poly(arylene sulfides) as well as unsuccessful attempts at polymerization of thiyl radicals.

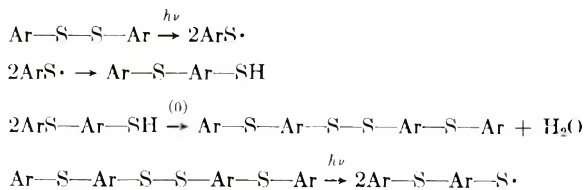
DISCUSSION

Attempted Polymerization of Thiyl Radical

Thiophenols, like phenols, are susceptible to attack by oxidizing agents. The initial step consists in abstraction of a hydrogen atom of the sulfhydryl group with formation of a free-radical containing univalent sulfur. These relatively stable radicals normally rapidly combine to form disulfides.⁷ Since the oxidation of 2,6-disubstituted phenols with oxygen in the presence of various amines and cuprous salts⁹ gives poly(arylene oxides), similar reactions of 4-bromothiophenol (I), 2,6-dimethyl-4-bromothiophenol (II), and 2,6-dimethylthiophenol (III) have been carried out, but only disulfides instead of poly(arylene sulfides) were obtained.



The homolysis of the disulfide bond by light¹⁰ is reported to produce thiyl radicals which form thiols by hydrogen abstraction.¹¹ It was considered possible, therefore, that poly(arylene sulfide) might be prepared from the disulfide by the following sequence of reactions. An analogous rearrangement has been proposed for the formation of *o*-aminodiphenyl sulfide from phenylazide and thiophenol.¹¹



Bis-(2,6-dimethylphenyl) disulfide (IV) was irradiated with ultraviolet light under oxygen, but only starting material was recovered.

Polymerization of Metal Salts of Halothiophenols

Reactive haloaromatic compounds, such as chloronitrobenzene, react easily with alkali metal sulfide or metal thiophenoxide to give the aryl sulfides. However, most aryl halides are comparatively inert, and high temperatures (300–350°C.) must be employed to produce the aryl sulfide.¹²

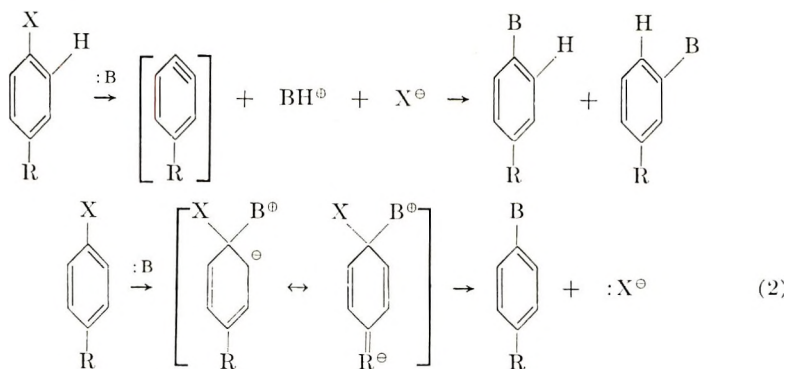
The silver salts of the thiols I and II have been prepared, but they remained unchanged after boiling in benzene or dimethyl-formamide (DMF) for three days. The results are similar to those of Hunter and Kohlhasc,¹³ who reported that the silver salt of 2,4,6-tribromothiophenol in the presence of a trace of iodine or on heating, gave only disulfide instead of polymer, although the silver salts of 2,4,6-trihalophenol gave poly(arylene oxide) under the same conditions.

We have found, however, that the lithium and sodium salts of I, II, and 2-methyl-4-bromothiophenol (V) and sodium 4-chloro-thiophenoxide can be polymerized in solvents to give the corresponding polymers. The results are summarized in Tables I–III.

From the data of these tables, the order of reactivity of metals is seemingly, Na > Li. This order agrees with that of the reactivity reported¹⁴ as K > Na > Li for nucleophilic substitution in 2,4-dinitrochlorobenzene with alkali metal methoxides. The orders of reactivity of halogens and thiophenols seem to be Br > Cl and I > V > II, respectively.

Polymer Structure

These results indicate that the polymerization consists mainly of nucleophilic attack on aryl halides by thiophenoxide anions. For the substitution of aryl halides by nucleophiles, the elimination-addition mechanism, the so-called "benzyne" mechanism¹⁵ (1), must be considered together with the usual addition-elimination mechanism of eq (2):



(Here, X = halogen, :B = nucleophile). For instance,¹⁶ *p*-bromotoluene is hydrolyzed by 1*N* sodium hydroxide at 340°C. largely through the benzyne mechanism (50% rearrangement), but at 250°C. through a combination of both mechanisms (22% rearrangement); whereas *p*-iodotoluene is hydro-

TABLE I. Polymerization of Alkali Metal *p*-Halothiophenoxides

Expt. No.	<i>p</i> -Halothio-phenoxide	Solvent ^a	Time, days	Cat- alyst ^b	Hot benzene-insoluble fraction of polymer					Hot benzene-soluble fraction of polymer			
					M.p., °C.	M.W. ^c	Yield, %	Br	C	S	M.p., °C.	M.W. ^e	Yield, %
PL17	4-Br- C ₆ H ₄ SNa	DMF	1	None	248 -255	1630	69	14.3	15.7	9.8	100	970	25
PL16		DMF	3	None	250	2810	71	25.1	37.7	10.5	100	1000	14
PL18		DPE	1	None	230 -255	1010	46	8.6	9.4	7.0	140	1050	38
PL15		DMF	1	Cu	260 -280	1490	60	12.9	12.0	13.1	120	950	27
PL14		DMF	2	Cu	270 -240	1190	48	10.2	13.6	5.8	110	970	30
PL13		DMSO	2	Cu	255 -300	10250	58	94.3	26.7		120	1040	10
PL31	4-Br- C ₆ H ₄ SLi	DMF	1	None	240 -260		8				100	550	66
PL32		DMF	3	None	240 -290		14				140	740	66
PL33		DMF	1	Cu	250 -260	1354	54	11.8	10.3	15.5	140	700	28
PL35		Pyr	7	None	230 -250		3				70	620	88
PL71	4-Cl- C ₆ H ₄ SNa	DMF	3	None	200 -206	920	25				50	500	48

^a DMF = dimethylformamide (30 ml.), b.p. 153°C.; DPE = diphenyl ether (30 ml.), b.p. 258°C.; DMSO = dimethyl sulfoxide (30 ml.), b.p. 189°C.; Pyr = pyridine (50 ml.), b.p. 116°C.

^b Catalyst, when used, was 10 mole-% of copper powder.

^c Molecular weight calculated from bromine analysis.

^d Degree of polymerization calculated from elemental analysis as follows: DP(Br) = [7991.6-80.92(%Br)]/108.16(%Br); DP(C) = 80.92(%C)/[7206.6-108.16(%C)]; DP(S) = 80.92(%S)/[3206.6-108.16(%S)].

^e Molecular weight measured by Vapor Osmometer.

TABLE II. Polymerization of Alkali Metal Salts of 2,6-Dimethyl-4-bromophenol in DMF

Expt. No.	Salt	Time, days	Catalyst ^a	M.p., °C.	M.W. ^b	Yield, %	Methanol-insoluble fraction of polymer			Pasty residue recovered from methane solution of polymer	
							Br	C	S	M.W. ^b	Yield, %
PM15	Na salt	1	None	100 -150	1200	18	—	—	—	510	61
PM12		3	None	120 -160	1500 (1380) ^d	36	9.6	8.8	9.1	900	34
PM13		7	None	160 -180	2500 (2620) ^d	49	18.7	10.8	—	700	34
PM11		4	Cu	140- -180	3100 (3900) ^d	55	28.1	—	4.8	1500	36
PM14 ^e		7	None	280	1100	40	—	—	—	480	37
PM31	Li salt	1	None	Paste	550	26	—	—	—	320	47
PM32		3	None	70 -100	860 (900) ^d	30	6.0	5.5	4.8	410	48
PM34		7	None	30 -100	740	34	—	—	—	460	46
PM33		3	Cu	90 -130	1340	33	—	—	—	530	32

^a Catalyst, when used, was 10 mole-% of copper powder.^b Molecular weight measured by Vapor Osmometer.^c Degree of polymerization calculated from elemental analyses as follows: DP(C) = 80.92(%C)/[9608.8 - 136.22(%C)]; DP(Br) = [7991.6 - 80.92(%Br)]/136.22(%Br); DP(S) = 80.92(%S)/[3206.6 - 136.22(%S)].^d Molecular weight calculated from bromine analysis.^e In pyridine solution.

TABLE III
 Polymerization of Alkali Metal Salts of 2-Methyl-4-bromophenol in DMF

Expt. No.	Salt	Time, days	Catalyst ^a	Methanol-insoluble fraction of polymer			Pasty residue recovered from methanol solution of polymer	
				M.p., °C.	M.W. ^b	Yield, %	M.W. ^b	Yield, %
PW11	Na salt	1	None	60-120	1550	49	620	41
PW12		3	None	80-120	2110	64	960	24
PW31	Li salt	1	None	50-90	1150	41	340	50
PW32		3	None	60-90	1280 ^c (1350) ^d	74	350	15
PW34		7	None paste		500	80	340	12
PW33		1	Cu	50-100	1500 ^e (1500) ^d	50	520	37

^a Catalyst, when used, was 10 mole-% of copper powder.

^b Molecular weight measured by Vapor Osmometer.

^c Degree of polymerization as calculated from elemental analysis: 10.4(Br); 11.0(C); 8.3(S).

^d Molecular weight calculated from bromine analysis.

^e Degree of polymerization: 11.6(Br); 11.6(C); 10.0(S).

lyzed at 250°C. almost completely through the addition-elimination mechanism. The infrared spectra of polymers showed that little or no positional isomerization occurred in the polymerization, indicating that the benzyne mechanism is unlikely. The results of our experiments indicate polar solvents, such as dimethylformamide, and especially dimethyl sulfoxide (PL-13, Table I), are useful as polymerization media. The use of copper catalyst¹⁷ gave only small improvements in yield or molecular weight. The generally satisfactory agreement between molecular weights calculated from bromine and from sulfur analyses indicate little if any Ullmann-type biaryl condensation.

A regular structure is also supported by the high crystallinity of poly(phenylene sulfide) as determined by x-ray diffraction powder patterns. For example, sample PL17A (M.W. 1630) showed crystal spacings corresponding to 4.67(m), 4.29(s), 3.83(m), 3.49(w), 3.20(w), 2.75(w), and 2.46-(vw) Å, but that of poly(2,6-dimethylphenylene sulfide) (PM13B, M.W. 1190) showed only broad spacings at about 6.33, 3.79, and 2.80 Å. The melting points of polymers are 270–290°C. for poly(phenylene sulfide), 80–120°C. for poly(2-methylphenylene sulfide), and 160–180°C. for poly(2,6-dimethylphenylene sulfide). Evidently the order of melting point is based mainly on the symmetry of the unit structures. The amorphous, soluble character of the methylated polymers has enabled us to measure their number-average molecular weight in solution, which was not possible for the unmethylated polymer.⁶

Thermal Stability

High thermal stability for poly(arylene sulfides) was observed, as may be expected.⁶ The weight losses of poly(phenylene sulfide) (PL15A and PL16A) after heating for 1 hr. at various temperatures up to 600°C. under reduced pressure are summarized in Table IV. From the melting points of residues, poly(phenylene sulfide) is seemingly stable up to 500°C., but at 600°C. some crosslinking may occur to give infusible, insoluble materials. After 2 hr. at 500°C. the molecular weights of residue and sublimate indicate only fractional distillation had occurred. The weight loss at 500°C. therefore does not indicate thermal degradation.

With low molecular weight poly(phenylene sulfide), thermal treatment at 250°C. merely resulted in fractionation of polymers, since again the average molecular weight of the residues and sublimed substance were found to agree with the molecular weight of starting polymers. Similar results were observed for poly(2,6-dimethylphenylene sulfide) and poly(2-methylphenylene sulfide).

EXPERIMENTAL

The ultraviolet and infrared spectra were obtained using a Process and Instruments Model R53, and a Model 21 Perkin-Elmer Spectrophotometer and a Perkin-Elmer Infracord Spectrophotometer, respectively. Micro-

TABLE IV
Thermal Stability Evaluation of Poly(arylene Sulfoxides)

Polymer	M.W.	Temp., °C.	Time, hr.	Yield, %	Residue in flask (R)			Sublimate on condenser surface (S)		
					M.W.	M.p., °C.	M.W. ^b	Yield, % ^a	M.W.	M.W. ^b
PL32B	740	250	1/2	90.3	1420	150-230	9.7	310	800 ^c	
PL32B	740	250	1/2	89.6	1440	160-170	10.4	320	770 ^c	
PL12B	1050	250	1/2	88.2	1290		11.8	450	1050	
PL15A	1490	250	1	99.5		250-280	0.5			
PL15A	1490	300	1	97.3		250-280	2.7			
PL15A	1490	400	1	92.0		250-280	8.0			
PL15A	1490	500	1	71.7		260-280	28.3			
PL15A	1490	500	2	60.8	6000 ^d	260-280	39.7	770 ^d	1640	
PL15A	1490	600	1	38.6		300	61.4			
PL16A	2810	300	1	97.3		260-280	2.7			
PL16A	2810	400	1	95.2		270-280	4.8			
PL16A	2810	500	1	76.3		270-280	23.7			
PL16A	2810	600	1	46.2		300	53.8			
PL17B	980	250	1	86.9	1400		13.1	330	980	
PM33B	1040	250	1	82.6	2100	150-160	17.4	400	1190	
PM13B	2580	250	1	95.5	1890	150-160	4.5	520	1710	
PW32B	1280	250	1	72.0	1240	60-100	28.0	310	610	
PW33B	1500	250	1/2	81.0	2020	90-110	8.6	350	1560	

^a Calcd. as $\frac{(\text{weight of polymer}) - (\text{weight of residue (R)})}{(\text{weight of polymer})} \times 100$.

^b Calcd. as $100 / \left(\frac{\text{yield}(\%) \text{ of R}}{\text{M.W. of R}} + \frac{\text{yield}(\%) \text{ of S}}{\text{M.W. of S}} \right)$.

^c Calcd. as $100 / \left(\frac{\text{yield}(\%) \text{ of R}}{\text{M.W. of R}} + \frac{\text{yield}(\%) \text{ of S}}{(\text{M.W. of S})^{1/2}} \right)$ (assuming R to be poly(phenylene sulfides) containing one disulfide bond).

^d Calcd. from elemental analysis.

analyses were done by the Galbraith Laboratories, Knoxville, Tennessee. Molecular weights were measured by a Mechrolab Vapor Pressure Osmometer, Model 301, using benzene as the solvent. Melting (or softening) points were determined by the capillary method. Solvents were dried and redistilled before use.

2,6-Dimethylthiophenol (III) was prepared from 2,6-dimethylaniline.¹⁸

2,6-Dimethyl-4-bromothiophenol (II) was synthesized by the modified method of Bortkus¹⁹ from 2,6-dimethyl-4-bromoaniline.²⁰ II, b.p. 76–77°C./0.3 mm., n_D^{25} 1.6140, was obtained in a yield of 91%. Treatment of the thiol II with 2,4-dinitrochlorobenzene produced a yellow solid which, after recrystallization from benzene, yielded 4-bromo-2,6-dimethyl-2',4'-dinitrodiphenyl sulfide as yellow plates, m.p. 191–192°C.

ANAL. Calcd. for $C_{14}H_{11}N_2O_2SBr$: C, 43.88%; H, 2.89%; Br, 20.85%. Found: C, 43.76%; H, 2.78%; Br, 20.75%.

Treatment of 1.1 g. of thiol II in 50 ml. of 1% aqueous sodium hydroxide with 15 ml. of 3% hydrogen peroxide gave a yellow solid. After recrystallization from ethanol, it yielded white needles of bis(2,6-dimethyl-4-bromophenyl) disulfide, m.p. 129–130°C; yield, 3.82 g (76%).

ANAL. Calcd. for $C_{16}H_{16}Br_2S_2$: C, 44.48%; H, 3.78%; Br, 36.85%. Found: C, 44.51%; H, 3.75%; Br, 36.73%.

2-Methyl-4-bromothiophenol (V) was also synthesized by the modified method of Bortkus¹⁹ from 2-methyl-4-bromoaniline;²¹ the thiol V, b.p. 94–95°C./15 mm., n_D^{25} 1.6205, was obtained in a yield of 86%. Treatment of the thiol V with 2,4-dinitrochlorobenzene produced a yellow solid which, after recrystallization from benzene, yielded 4-bromo-2-methyl-2',4'-dinitrodiphenyl sulfide as yellow plates, m.p. 165–166°C.

ANAL. Calcd. for $C_{13}H_9N_2O_4SBr$: N, 7.59%; S, 8.69%; Br, 21.64%. Found: N, 7.40%; S, 8.66%; Br, 21.54%.

The thiol V (1.0 g.) oxidized as described above gave bis(2-methyl-4-bromophenyl) disulfide, m.p. 86–87°C., yield 0.73 g.

ANAL. Calcd. for $C_{14}H_{12}Br_2S_2$: C, 41.61%; H, 2.99%; Br 39.54%; M. W., 404. Found: C, 41.42%; H, 2.87%; Br, 39.53%; M. W., 400.

Silver salts were prepared by the method of Hunter.¹³

Sodium salts were prepared by reaction of an equivalent amount of sodium methoxide with thiophenols in benzene followed by concentration *in vacuo*.

Lithium salts were prepared by reaction of an equivalent amount of lithium hydroxide with thiophenol in aqueous methanol followed by removal of water as its azeotrope with benzene and then by drying *in vacuo*.

Attempted Polymerization of Thiyl Radicals

The thiol III (1.4 g.) was oxidized by the method of Hay,⁹ using 0.05 g. of cuprous chloride and 40 ml. of pyridine. The product was bis(2,6-dimethylphenyl) disulfide (IV).

The disulfide IV (2.74 g., 0.01 mole) dissolved in 20 ml. of pyridine was stirred with a magnetic stirrer for 10 days at room temperature in a quartz flask, while irradiated with ultraviolet light. After pouring into water, the resulting yellow precipitate was filtered, washed with water, and recrystallized from methanol, yielding 2.5 g. (91%) of white needles, m.p. 102–104°C. (authentic sample), m.p. 103–104°C.

4-Bromothiophenol (5.67 g., Evans Chemetics Inc.) was treated by the method of Staffin and Price,⁸ using 100 ml. of benzene, 100 ml. of 0.6*N* aqueous potassium hydroxide, and 0.987 g. of potassium ferricyanide, but the products were bis(4-bromophenyl) disulfide (m.p. 93–95°C., 30% yield) and unchanged 4-bromothiophenol (m.p. 72–74°C., 67% recovery). The thiol (2.17 g.) was also treated in the same way, but the products were bis(2,6-dimethyl-4-bromophenyl) disulfide (m.p. 129–133°C., 23% yield) and unchanged thiol II (55% recovery).

Polymerization of Metal Salts of Thiophenols

The metal salts of thiophenols (0.01 mole) were warmed in solvents under nitrogen. After refluxing for a fixed time, the mixture was concentrated to 10 ml. *in vacuo* and then poured into 100 ml. of 50% methanol. The precipitate was collected by centrifugal separation, washed by resuspending in 50 ml. of water and extracted with hot benzene. The residue was fraction A. The benzene solution was added to 100 ml. of methanol. The second precipitate was collected by centrifugal separation, dissolved in benzene and freeze-dried to give the second residue, fraction B. The methanol solution was concentrated *in vacuo*, dissolved in benzene, washed with water and freeze-dried to give the third residue, fraction C.

In cases where a catalyst was used, the residue A was suspended in 100 ml. of 2% nitric acid at room temperature for 1–7 days, collected by filtration, and washed with water, in order to remove catalyst.

The conditions and results are summarized in Tables I–III.

In reactions of the silver salts of thiols I and II, both the residues A, m.p. > 333°C., were the unchanged starting salts, since treatment of the residues A with 2% nitric acid gave the corresponding disulfides.

Thermal Stability

Thermal stability of poly(arylene sulfide) was evaluated by heating a known weight of the polymer (about 0.1 g.) in a vacuum sublimation flask with a finger type condenser at a fixed temperature for a fixed time *in vacuo*. The conditions and results are summarized in Table IV.

References

1. Hilditch, T. P., *J. Chem. Soc.*, **97**, 2579 (1910).
2. Tasker, H. S., and H. O. Jones, *J. Chem. Soc.*, **95**, 1910 (1909).
3. Macallum, A. D., *J. Org. Chem.*, **13**, 154 (1948); U. S. Pats. 2,513,188 (1950) and 2,538,941 (1951).
4. Lenz, R. W., and W. K. Carrington, *J. Polymer Sci.*, **41**, 333 (1959).
5. Lenz, R. W., and C. E. Handlovits, *J. Polymer Sci.*, **43**, 167 (1960).
6. Lenz, R. W., C. E. Handlovits, and H. A. Smith, *J. Polymer Sci.*, **58**, 351 (1962).
7. For instance, F. R. Mayo and C. Walling, *Chem. Revs.*, **27**, 387 (1940).
8. Staffin, G. D., and C. C. Price, *J. Am. Chem. Soc.*, **82**, 3632 (1960).
9. Hay, A. S., H. S. Blanchard, G. F. Endres, and J. W. Eustance, *J. Am. Chem. Soc.*, **81**, 6335 (1959).
10. Schaafsma, Y., *Chem. Weekblad*, **54**, 61 (1958); Y. Schaafsma, A. F. Bickel, and E. C. Kooyman, *Tetrahedron* **10**, 76 (1960).
11. Takebayashi, M., T. Shingaki, and T. Mitsuyama, *Osaka Univ. Sci. Repts.*, **10**, 35 (1961).
12. Mauthner, F., *Ber.*, **39**, 1347, 3593 (1906).
13. Hunter, W. H., and A. H. Kohlhasse, *J. Am. Chem. Soc.*, **54**, 2425 (1932).
14. Reinkeiner, J. D., W. F. Kieffer, S. W. Frey, J. C. Cochran, and E. W. Barr, *J. Am. Chem. Soc.*, **80**, 164 (1958).
15. Wittig, G., G. Pieper, and G. Fuhrmann, *Ber.*, **73**, 1193 (1940).
16. Bottin, A. T., and J. D. Roberts, *J. Am. Chem. Soc.*, **79**, 1458 (1957).
17. Mauthner, F., *Ber.*, **37**, 3593 (1906).
18. Campaigne, E., and S. W. Osborn, *J. Org. Chem.*, **22**, 561 (1957).
19. Bortkus, E. A., E. B. Holtelling, and M. B. Neuworth, *J. Org. Chem.*, **22**, 1185 (1957).
20. Noelting, E., A. Braun, and G. Thesmar, *Ber.*, **34**, 2242 (1901).
21. Bamberger, E., *Ann.*, **441**, 304 (1925).

Résumé

Les essais de polymérisation de radicaux thiyles, obtenus à partir du 4-bromothiophénol (I), du 2,6-diméthyl-4-bromothiophénol (II), du 2,6-diméthylthiophénol et du disulfure de bis(2,6-diméthylphénylène) n'ont pas donné lieu à la formation d'un polymère. On a pu obtenir les polysulfures d'arylène correspondants en polymérisant les sels de lithium ou de sodium de (I), (II), du 2-méthyl-4-bromothiophénol, et du 4-chlorothiophénoxyde de sodium à température de reflux dans divers solvants, avec ou sans catalyseurs de cuivre. Le polysulfure de phénylène, p.f. 270-290°C., est stable à 500°C pendant deux heures sous atmosphère d'azote, et possède un degré de cristallinité élevé, observé par diffraction des rayons-X. La diffraction des rayons-X démontre l'absence presque totale de structures cristallines dans le polysulfure de 2,6-diméthylphénylène. Le polysulfure de 2-méthylphénylène fond entre 60 et 100°C.

Zusammenfassung

Versuche zur Polymerisation von Thiylradikalen aus 4-Bromthiophenol (I), 2,6-Dimethyl-4-bromthiophenol (II), 2,6-Dimethylthiophenol und Bis(2,6-dimethylphenyl)-disulfid lieferten kein Polymeres. Die Polymerisation der Lithium- und Natriumsalze von I, II und 2-Methyl-4-bromphenol und von Natrium-4-Chlorthiophenoxyl durch Rückflusskochen in verschiedenen Lösungsmitteln mit oder ohne Kupferkatalysator lieferte die entsprechenden Polyacrylensulfide. Polyphenylensulfid, Schmp. 270–290°C., war bei 500°C unter Stickstoff durch zwei Stunden beständig und zeigte hohe Röntgenkristallinität. Poly-(2,6-Dimethylphenylensulfid), Schmp. 160–180°C, zeigte, wenn überhaupt, dann nur geringe Kristallinität. Poly(2-methylphenylensulfid) schmilzt bei 60–100°.

Received February 1, 1963

Revised March 1, 1963

Determination of Molecular Weights of Polymers by Procedure X in Stress Relaxation

HIROSHI SOBUE and KENKICHI MURAKAMI, *Department of Industrial Chemistry, Faculty of Engineering, University of Tokyo, Tokyo, Japan*, and HIROYUKI HOSHINO, *Mitsubishi Rayon Co. Ltd., Tokyo, Japan*

Synopsis

τ_m , defined as the maximum relaxation time, was shown in previous papers to be one of the elements characterizing the "box" type curve in the rubbery region of a linear amorphous polymer, and a new procedure called procedure X was proposed to obtain τ_m . The relation among τ_m , weight-average chain length \bar{n}_w , temperature T , and characterized temperature T_i (glass transition temperature T_g , WLF temperature T_s , or Tobolsky's temperature T_d) was indicated by an equation, with which constant values of $\log A$ depending on the kind of polymer were obtained for several polymers in the regions of $M \gg M_c$. For polymers in the vicinity of M_c , another set of constant values of $\log A'$ was obtained. Finally, the effect of τ_m on temperatures for a polymer was studied.

Introduction

It is generally known that the "box" type curve is depicted in the rubbery region of the relaxation spectrum of a linear amorphous polymer. Three parameters, τ_e , τ_m , and E_0 are defined as the minimum relaxation time, the maximum relaxation time, and the height in the "box" curve function, respectively, as shown in Figure 1.

One of these characterizing factors, τ_m was shown to be a function of molecular weight and temperature in a quantitative form for polymers by Tobolsky and Andrews,¹ and later by Tobolsky and Murakami.² The method of obtaining the value of τ_m by Tobolsky and Andrews, however, seems less natural than that used by Tobolsky and Murakami,³ which is the so-called procedure X in the previous papers,^{2,4} the possibility of measuring the molecular weights by procedure X was briefly described for some amorphous polymers such as polyisobutylene, polyvinyl acetate, and polystyrene.

This paper deals with such a new procedure for polymethyl methacrylate in more detail.

Theoretical

The relaxation modulus $E_r(t)$ is generally expressed as follows, assuming the continuous distribution of relaxation times $E(\tau)$:

$$E_r(t) = \int_0^{\infty} E(\tau) \cdot e^{-t/\tau} d\tau \quad (1)$$

or

$$E_r(t) = \int_{-\infty}^{\infty} H(\tau) \cdot e^{-t/\tau} d(\ln \tau) \quad (2)$$

Here,

$$H(\tau) = \tau E(\tau)$$

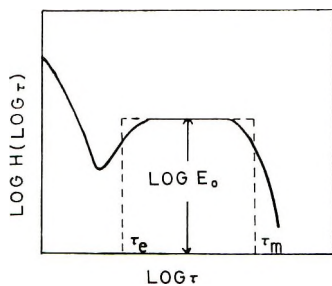


Figure 1.

If the distribution of relaxation times in the rubbery flow region is expressed as a discrete distribution, we have

$$E_r(t) = E_a e^{-t/\tau_a} \dots + E_{m-1} e^{-t/\tau_{m-1}} + E_m e^{-t/\tau_m} \quad (3)$$

For the region of $t > \tau_m$, eq. (3) becomes eq. (4):

$$E_r(t) = E_m e^{-t/\tau_m} \quad (4)$$

or

$$\log E_r(t) = \log E_m - (t/2.303\tau_m) \quad (5)$$

So a plot of $\log E_r(t)$ versus t should approach a straight line indicated as eq. (5) for $t > \tau_m$, if a maximum relaxation time truly exists. The slope of the line is $1/2.303 \tau_m$, and the intercept of the line is $\log E_m$. A straight line is indeed approached when $\log E_r(t)$ is plotted against t for amorphous polymers such as polyisobutylene, polyvinyl acetate, and polystyrene as already mentioned in the other papers.^{3,4} The method mentioned above is called procedure X.

The relation among a maximum relaxation time τ_m , weight-average chain length \bar{n}_w , temperature T , and the glass transition temperature T_g or WLF temperature T_s , or Tobolsky's temperature T_d is indicated as follows.^{2,4,5} $\log A$ is the constant which is dependent on the kind of polymer. Here τ_m is in seconds.

$$\log \tau_m = \log A_g - 17.44 \frac{T - T_g}{51.6 + T - T_g} + 3.4 \log \bar{n}_w \quad (6a)$$

$$\log \tau_m = \log A_s - 8.86 \frac{T - T_s}{101.6 + T - T_s} + 3.4 \log \bar{n}_w \quad (6b)$$

$$\log \tau_m = \log A_d - 16.14 \frac{T - T_d}{56 + T - T_d} + 3.4 \log \bar{n}_w \quad (6c)$$

Experimental and Discussion

The samples of polymethyl methacrylate were prepared from monomers purified by means of vacuum distillation in a stream of nitrogen. The polymers were prepared in the presence of varying concentrations of the initiator 2-azobisisobutyronitrile at 60°C., to a low conversion (around 10%). The radical-initiated polymers thus obtained were found to have a heterogeneity index of 1.92, for which the results of calculation are mentioned in the appendix. The number-average molecular weights of these samples were determined in chloroform at 20°C. by use of the relation proposed by Baysal and Tobolsky⁶ as follows.

$$\log \bar{P}_n = 3.261 + 1.256 \log [\eta] \quad (7)$$

Table I shows the experimentally obtained results by us.

The values of $1/\bar{P}_n$, the reciprocal of the number-average degree of polymerization degree against the polymerization rate are all shown in Table I and are plotted in Figure 2 as a monoradical line.

Stress relaxation data for these nine samples from about $\bar{DP} = 900$ to 6000 were measured at 170° C. in the region of rubbery flow. The techniques of stress relaxation used here were essentially the same as those used in other studies.^{2,3} From data of this kind, master curves of $E_r(t)$ were constructed for these samples on the basis of the time-temperature position principle. Two master curves for samples of 14 and 20 (the extreme cases of molecular weights) are shown in Figure 3.

By procedure X for the master curves of these samples, the values of τ_m were obtained as shown in Figure 4. It is apparent that the portions of straight lines appear at least after 2×10^2 sec., though the slopes of straight lines become flat with increasing molecular weight. All data thus obtained are shown in Table II.

TABLE I
Polymerization of Methyl Methacrylate (Catalyst: 2-Azobisisobutyronitrile, 60°C.)

Sample No.	$1/\bar{P}_n$	t , sec.	Conversion		$R_p \times 10^5$, mole l. ⁻¹ sec. ⁻¹	\bar{M}_w/\bar{M}_n
			%	mole/l.		
13	1.09×10^{-3}	7.86×10^2	10.27	0.960	122	1.92
14	7.25×10^{-4}	1.02×10^3	10.01	0.963	98.0	1.92
15	5.78×10^{-4}	1.32×10^3	11.63	1.090	82.5	1.92
16	4.76×10^{-4}	1.58×10^3	10.65	0.977	61.8	1.92
17	3.58×10^{-4}	1.98×10^3	9.32	0.872	44.0	1.92
18	3.47×10^{-4}	2.40×10^3	12.20	1.141	47.5	1.92
19	3.03×10^{-4}	2.97×10^3	9.16	0.857	28.8	1.92
20	2.02×10^{-4}	4.15×10^3	9.99	0.935	22.5	1.92
21	1.73×10^{-4}	4.38×10^3	8.29	0.798	18.2	1.92

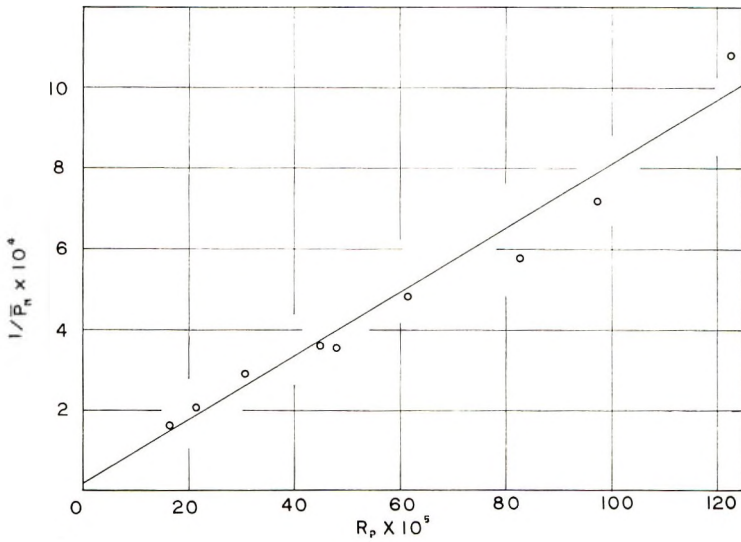


Figure 2

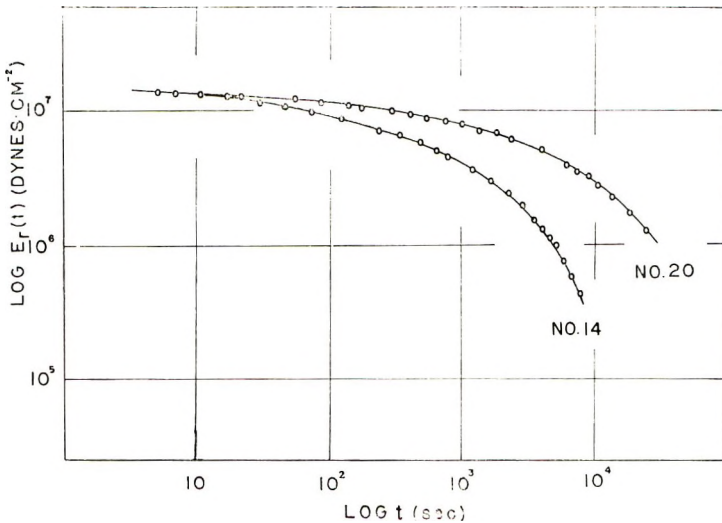


Figure 3.

If the values of $\log \tau_m$ are plotted against those for $\log \bar{P}_n$ from Table II, we have Figure 5.

It is clear from Figure 5 that the slope of this straight line has the value of 3.4 in the range of $\log \bar{P}_n \geq 3.4$, or about $\bar{P}_n = 2500$, and has a value of approximately unity in the range of $\log \bar{P}_n \leq 3.4$. It is a matter of interest to consider that the inflection point for these two straight lines may be closely related to the critical molecular weight M_c , though this point seems to be somewhat higher than M_c of polymethyl methacrylate.

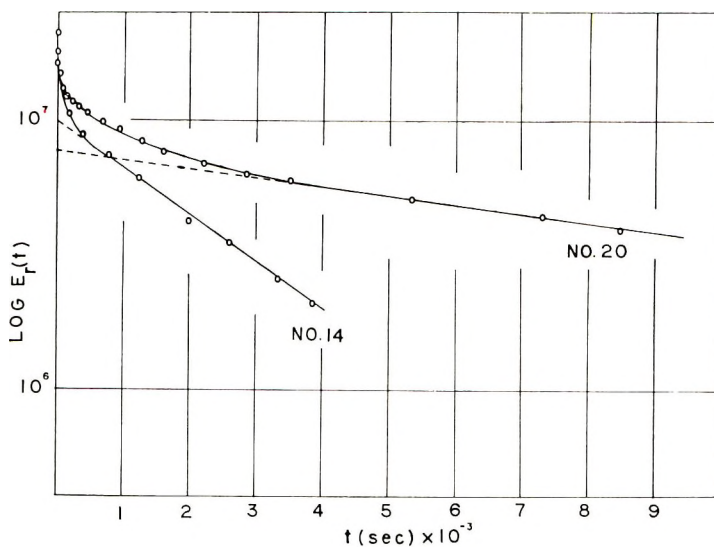


Figure 4.

TABLE II

Sample No.	\bar{P}_n	$\log \bar{P}_n$	τ_m , sec.	$\log \tau_m$
13	9.20×10^2	2.96	4.00×10^3	3.60
14	1.38×10^3	3.14	4.76×10^3	3.68
15	1.73×10^3	3.24	5.54×10^3	3.74
16	2.10×10^3	3.32	7.07×10^3	3.85
17	2.79×10^3	3.44	1.17×10^4	4.07
18	2.88×10^3	3.46	1.44×10^4	4.16
19	3.30×10^3	3.52	2.03×10^4	4.30
20	4.94×10^3	3.69	6.00×10^4	4.78
21	5.76×10^3	3.76	8.80×10^4	4.95

If the value of $\log \tau_m + 17.44 [(T - T'_\theta)/(51.6 + T - T'_\theta)]$ is plotted against that of $\log \bar{n}_w$ for polymethyl methacrylate for the data in Table III, Figure 6 can be obtained; this figure includes also data for polyisobutylene, polyvinyl acetate, and polystyrene which appeared elsewhere.⁵

As in Figure 5, the inflection point of the two straight lines appears around the value of $\log \bar{n}_w = 4.00$ in the case of polymethyl methacrylate in Figure 6. While the slope of the straight line for polymethyl methacrylate is approximately unity in the range \bar{n}_w less than the inflection point, that of the straight line above the inflection point at $\bar{n}_w = 4.00$ is approximately 3.4. From the intercept of the straight line having a slope of unity, we have

$$\log A'_v = 11.34$$

$$\log A'_s = 0.95$$

$$\log A'_d = 8.42$$

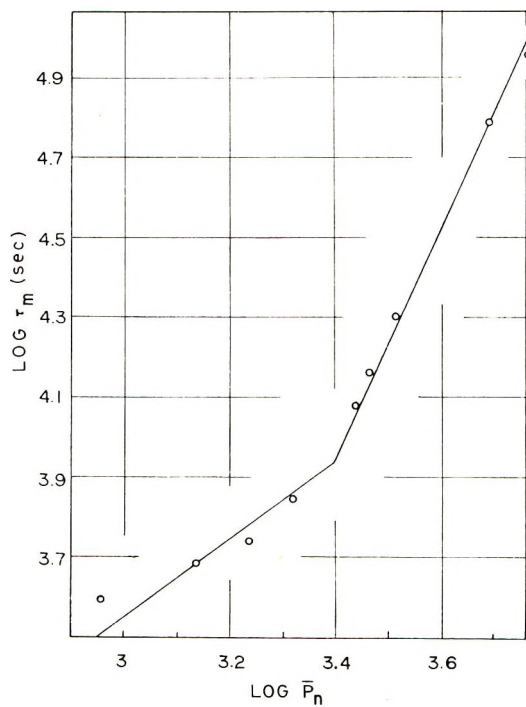


Figure 5.

TABLE III

Sample No.	$\log \bar{P}_n$	$\log \bar{n}_w$	$\log \tau_m$	$\frac{\log \tau_m + 17.44}{T - T_g}$
				$51.6 + T - T_g$
13	2.96	3.54	3.60	14.80
14	3.14	3.72	3.68	14.88
15	3.24	3.82	3.74	14.94
16	3.32	3.90	3.85	15.05
17	3.44	4.02	4.07	15.28
18	3.46	4.04	4.16	15.36
19	3.52	4.10	4.30	15.50
20	3.60	4.27	4.78	15.98
21	3.76	4.34	4.95	16.15

From the intercept of the straight line having a slope of 3.4, we have

$$\log A_g = 2.25$$

$$\log A_s = -8.16$$

$$\log A_d = -0.67$$

Table IV shows the constant values of $\log A$ for several polymers having molecular weights over M_c .

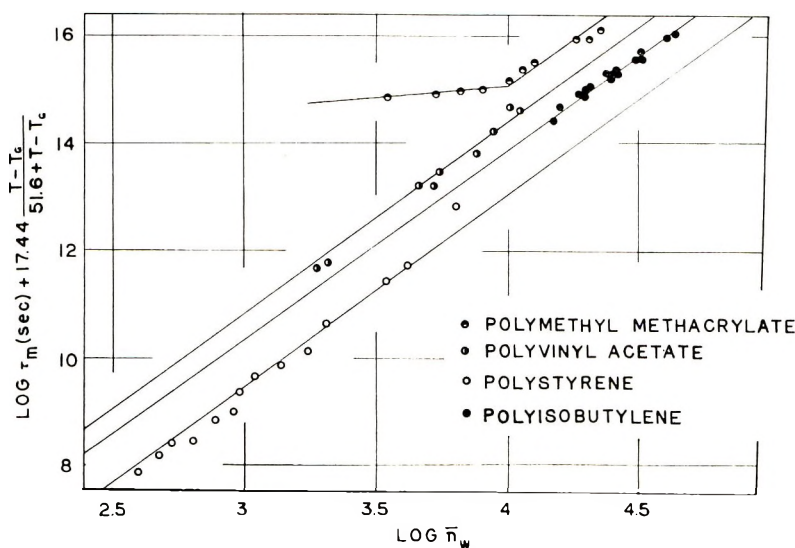


Figure 6.

TABLE IV

Sample	$\log A_{\theta}$, sec.	$\log A_s$, sec.	$\log A_d$, sec.
Polymethyl methacrylate	2.25	-8.16	-0.67
Polyisobutylene	-0.52	-7.57	-0.01
Polystyrene	-0.70	-9.45	-3.64
Polyvinyl acetate	0.86	-8.41	-0.39

Next, the dependency of τ_m on temperatures was studied for polymethyl methacrylate having $\log \bar{n}_w \leq 4.0$ (slope is unity). For these methyl methacrylate polymers, the following eq. (8) is obtained,

$$\log \tau_m = \log A_s' - c_1 \frac{T - T_s}{c_2 + T - T_s} + \log \bar{n}_w \quad (8)$$

$$\log \frac{\tau_m}{\bar{n}_w A_s'} + c_1 = \frac{c_1 c_2}{c_2 + T - T_s}$$

Then

$$\log \left(\log \frac{\tau_m}{\bar{n}_w A_s'} + c_1 \right) = \log c_1 c_2 - \log (c_2 + T - T_s) \quad (9)$$

Here, c_1 and c_2 are the WFL coefficients corresponding to T_s .

The values of τ_m for polymethyl methacrylate sample 14 were measured, at temperatures varying from 165 to 180°C.

The relation between τ_m and temperature is tabulated in Table V, and theoretical line representing eq. (9) for the polymethyl methacrylate sample.

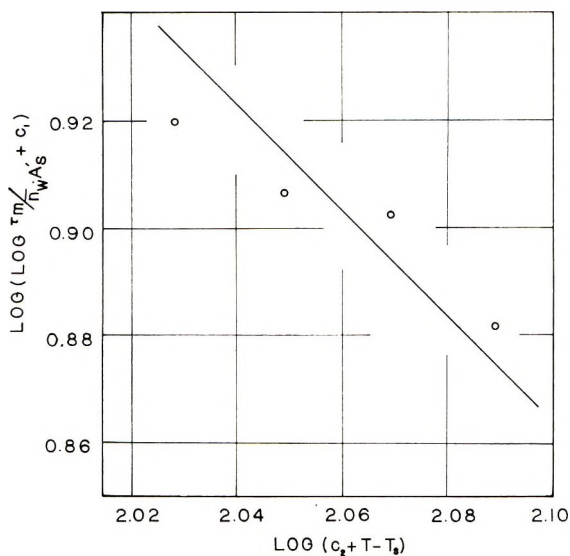


Figure 7.

The four points obtained experimentally in Figure 7 fit pretty well on the theoretical line.

In conclusion, the new method of measuring molecular weight by procedure X was found applicable for polymethyl methacrylate, and the constant value of $\log A$ for polymethyl methacrylate was obtained. Finally, the shear viscosity η was calculated from the stress relaxation data by using the equation proposed by Fujita:⁸

$$\eta_{\text{shear}} = \frac{1}{3} \int_0^{\infty} E_r(t) dt \quad (10)$$

The value of $\log \eta_{\text{shear}}$ thus obtained was plotted against $\log \bar{M}_w$ in Figure 8, and a straight line having a slope of approximately 3.4 was obtained for polymethyl methacrylate of sufficiently high molecular weight.

TABLE V

T , °K.	$\log \tau_m$, sec.	$\log \left(c_1 + \log \frac{\tau_m}{\bar{n}_w \cdot A_s'} \right)$	$\log (c_2 + T - T_g)$
438	3.92	0.9196	2.0278
443	3.68	0.9089	2.0476
448	3.60	0.9025	2.0668
453	3.23	0.8820	2.0849

Appendix

It was shown previously by Baysal and Tobolsky⁶ that for radical-initiated polymerization of styrene carried to low conversions, the ratio of weight-average molecular weight to number-average molecular weight was

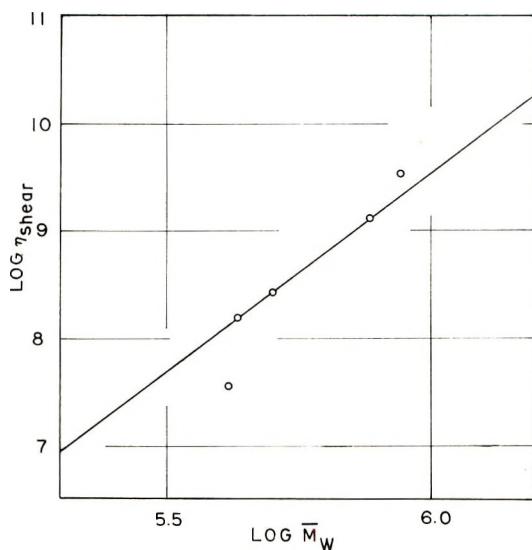
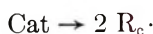


Figure 8.

$\bar{M}_w/\bar{M}_n = 1.5$. Recently Yamada⁷ found that the more reasonable value for this ratio lay approximately between 1.6 and 1.7 by his improved calculation. Here in order to obtain a reasonable value of the ratio of weight-average molecular weight to number-average molecular weight for polymethyl methacrylate polymerized under the same conditions as mentioned above, the following treatment was done.

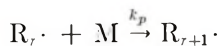
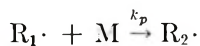
In polymerization of radical-initiated methyl methacrylate, we have the following reactions.

Initiation:

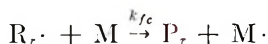
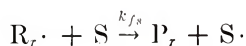


where the velocity of propagation of $R_1 \cdot$ is I .

Propagation:

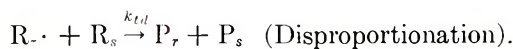


Chain transfer:



where S and M are solvent and monomer, respectively.

Termination:



If the concentration of radicals during polymerization is constant, or in the steady state,

$$d[\text{R}_1\cdot]/dt = I - k_p M [\text{R}_1\cdot] + (k_{fs}S + k_f M) [\text{R}\cdot] - (k_{fs}S + k_f M) [\text{R}_1\cdot] - (k_{tc} + k_{td}) [\text{R}_1\cdot] [\text{R}\cdot] = 0 \quad (1)$$

$$d[\text{R}_r\cdot]/dt = k_p M [\text{R}_{r-1}\cdot] - k_p M [\text{R}_r\cdot] - (k_{fs}S + k_f M) [\text{R}_r\cdot] - (k_{tc} + k_{td}) [\text{R}_r\cdot] [\text{R}\cdot] = 0 \quad (2)$$

$$-dM/dt = I + k_p M [\text{R}\cdot] + k_f M [\text{R}\cdot] \doteq k_p M [\text{R}\cdot] \quad (3)$$

Here, $[\text{R}\cdot]$ means the concentration of total radicals, and is given as follows.

$$[\text{R}\cdot] = [I/(k_{tc} + k_{td})]^{1/2} \quad (4)$$

From eqs. (1)–(4),

$$[\text{R}_1\cdot] = \left(\frac{I}{k_{tc} + k_{td}} \right)^{1/2} \frac{k_{fs}S + k_f M + [I(k_{tc} + k_{td})]^{1/2}}{k_p M + k_{fs}S + k_f M + [I(k_{tc} + k_{td})]^{1/2}} \quad (5)$$

$$[\text{R}_r\cdot] = [\text{R}_{r-1}\cdot] \frac{k_p M}{k_p M + k_{fs}S + k_f M + [I(k_{tc} + k_{td})]^{1/2}} \quad r \geq 2 \quad (6)$$

$$-dM/dt = k_p M [I/(k_{tc} + k_{td})]^{1/2} \quad (7)$$

The rate of forming a polymer having a degree of polymerization r , is given by

$$dP_r/dt = (k_{fs}S + k_f M) [\text{R}_r\cdot] + 1/2 k_{tc} \sum_{n=1}^{r-1} [\text{R}_n\cdot] [\text{R}_{r-n}\cdot] + k_{td} [\text{R}_r\cdot] [\text{R}\cdot] \quad (8)$$

Equations (5) and (6) can be written as the following eqs. (9) and (10), respectively:

$$[\text{R}_1\cdot] = \left(\frac{I}{k_{tc} + k_{td}} \right)^{1/2} (1 - \zeta) \quad (9)$$

$$[\text{R}_r\cdot] = \zeta [\text{R}_{r-1}\cdot] = \left(\frac{I}{k_{tc} + k_{td}} \right)^{1/2} (1 - \zeta) \zeta^{r-1} \quad r \geq 2 \quad (10)$$

Here,

$$\zeta = k_p M / \{ k_p M + k_{fs}S + k_f M + [I(k_{tc} + k_{td})]^{1/2} \} \quad (11)$$

From eqs. (8), (9), and (10),

$$\begin{aligned} \frac{dP_r}{dt} = & \left(\frac{I}{k_{tc} + k_{td}} \right)^{1/2} (1 - \zeta) \zeta^{r-1} \left[k_{fs}S + k_f M \right. \\ & \left. + \left(\frac{I}{k_{tc} + k_{td}} \right)^{1/2} \left(\frac{(r-1)k_{tc} \{ k_{fs}S + k_f M + [I(k_{tc} + k_{td})]^{1/2} \}}{2k_p M} + k_{td} \right) \right] \end{aligned} \quad (12)$$

For the polymers in the initial stage,

$$\begin{aligned} P_r &= (dP_r/dt)t \\ \Delta M &= (-dM/dt)t \end{aligned} \quad (13)$$

Accordingly,

$$\begin{aligned} P_r &= \frac{\Delta M}{k_p M} (1 - \zeta) \zeta^{r-1} \left[k_{fs} S + k_f M \right. \\ &\quad \left. + \left(\frac{I}{k_{tc} + k_{td}} \right)^{1/2} \left(\frac{(\gamma - 1) k_{tc} \{ k_{fs} S + k_f M + [I(k_{tc} + k_{td})]^{1/2} \}}{2k_p M} + k_{td} \right) \right] \end{aligned} \quad (14)$$

Then the moments of distribution of degree of polymerization are given by eqs. (15), (16), and (17) as follows:

$$\sum_{r=1}^{\infty} P_r = \frac{\Delta M}{k_p M} \left[k_{fs} S + k_f M + \left(\frac{I}{k_{tc} + k_{td}} \right)^{1/2} \left(\frac{k_{tc}}{2} + k_{td} \right) \right] \quad (15)$$

$$\sum_{r=1}^{\infty} r P_r = \Delta M \quad (16)$$

$$\begin{aligned} \sum_{r=1}^{\infty} r^2 P_r &= \frac{2k_p M \cdot \Delta M}{\{ k_{fs} S + k_f M + [I(k_{tc} + k_{td})]^{1/2} \}^2} \\ &\quad \left[k_{fs} S + k_f M + \left(\frac{I}{k_{tc} + k_{td}} \right)^{1/2} \left(\frac{3}{2} k_{tc} + k_{td} \right) \right] \end{aligned} \quad (17)$$

In the case of the termination process consisting of combination and disproportionation without chain transfer,

$$k_f = k_{fs} = 0 \quad (18)$$

When $X = k_{td}/(k_{tc} + k_{td})$ is substituted into eqs. (15)–(17) with eq. (18), we have

$$\sum_{r=1}^{\infty} P_r = \frac{1}{2} \frac{\Delta M}{k_p M} (Ik_{tc})^{1/2} \frac{(1 + X)}{(1 - X)^{1/2}} \quad (19)$$

$$\sum_{r=1}^{\infty} r P_r = \Delta M \quad (20)$$

$$\sum_{r=1}^{\infty} r^2 P_r = \frac{k_p M \cdot \Delta M}{(Ik_{tc})^{1/2}} (1 - X)^{1/2} (3 - X) \quad (21)$$

$$\begin{aligned} \bar{M}_w / \bar{M}_n &= \left(\sum_{r=1}^{\infty} r^2 P_r / \sum_{r=1}^{\infty} r P_r \right) / \left(\sum_{r=1}^{\infty} r P_r / \sum_{r=1}^{\infty} P_r \right) \\ &= \frac{1}{2} (1 + X)(3 - X) \end{aligned} \quad (22)$$

On the other hand, from the results of Schulz and his co-workers⁹ for bulk polymerization of methyl methacrylate, $k_{tc}/k_{td} = 0.40/0.60$; thus on substitution of $X = 0.60$ into eq. (22), $\bar{M}_w/\bar{M}_n = 1.92$ is obtained.

References

1. Andrews, R. D., and A. V. Tobolsky, *J. Polymer Sci.*, **7**, 221 (1951).
 2. Tobolsky, A. V., and K. Murakami, *J. Colloid Sci.*, **70**, 282 (1960).
 3. Tobolsky, A. V., and K. Murakami, *J. Polymer Sci.*, **45**, 443 (1959).
 4. Sobue, H., and K. Murakami, *J. Polymer Sci.*, **40**, S14 (1961).
 5. Sobue, H., and K. Murakami, *Kogyo Kagaku Zasshi*, **64**, 2055 (1961).
 6. Baysal, B., and A. V. Tobolsky, *J. Polymer Sci.*, **3**, 171 (1952).
 7. Yamada, N., private communication (1961).
 8. Fujita, H., and K. Ninomiya, *J. Polymer Sci.*, **24**, 233 (1957).
 9. Schulz, G. V., G. Henrici-Olivé, and S. Olivé, *Makromol. Chem.*, **31**, 88 (1959).
- (The value of k_{tc}/k_{td} for polymethyl methacrylate is still different among the literature available, but this didn't cause any unfavorable results in the study.)

Résumé

Nous avons décrit dans nos articles précédents que τ_m , par définition le temps de relaxation maximum est un des éléments caractérisant la courbe du type "boite" dans la région caoutchouteuse d'un polymère linéaire amorphe et qu'un nouveau procédé nommé "procédé X" est proposé pour obtenir ϵ_m . La relation contenant τ_m , \bar{n}_w , la longueur de chaîne moyenne en poids, T , la température, la température caractéristique T_i (T_g , température de transition vitreuse, T_i WLF température ou T_α température de Tobolsky) sont indiquées par l'équation, $\log A$ dépendant de la nature du polymère. Les constantes ont été obtenues pour différents polymères dans la région $M \gg M_c$. Pour des polymères dans le voisinage de M_c , d'autres valeurs constantes de $\log A'$ ont été obtenues. Finalement, on a étudié l'effet de τ_m sur les températures pour un polymère donné.

Zusammenfassung

In früheren Mitteilungen wurde die als maximale Relaxationszeit definierte Grösse τ_m als Element zur Charakterisierung der Kurve vom "Box"-Typ in Kautschukbereich eines linearen amorphen Polymeren herangezogen und ein neues Verfahren, Verfahren X genannt, zur Ermittlung von \bar{n}_w angegeben. Die Beziehung zwischen τ_m , dem Gewichtsmittel der Kettenlänge \bar{n}_w , der Temperatur T und charakteristischen Temperatur T_i (Glasumwandlungstemperatur T_g , WLF-Temperatur T_s oder Tobolsky-Temperatur T_α) wurde durch eine Gleichung angegeben, mit deren Hilfe in Abhängigkeit von der Art des Polymeren konstante $\log A$ -Werte für einige Polymere in Bereich von $M \gg M_c$ erhalten wurden. Für Polymere in der Nachbarschaft von M_c wurde ein anderer Wert der Konstanten, $\log A'$, erhalten. Schliesslich wurde der Einfluss von τ_m auf die Temperaturwerte für ein Polymeres untersucht.

Received March 8, 1963

BOOK REVIEWS

N. G. GAYLORD, Editor

An Introduction to Polymer Chemistry, W. R. MOORE, Aldine Publishing Company, Chicago, 1962, 270 pp., \$7.50. Available from University of London Press Ltd., 35s.

This book may best be reviewed by comparing it with *Textbook of Polymer Science*, by F. W. Billmeyer, Jr. (Interscience Publishers, 1962, 601 pp., \$12.75). Both books are intended primarily for usage in first courses in polymer chemistry at the senior or graduate level, and secondarily, as broad surveys on this subject for chemists and engineers working in the polymer field. Both require no previous knowledge of polymer chemistry, and both attempt to cover the fundamentals of polymerization reactions and the structure and properties of polymers. In such a comparison, Billmeyer's book is slightly superior in most respects to Moore's treatment. This comment, however, is not meant as a serious criticism of Moore's book, which is a fine, comprehensive review of the subject, having the advantage of being both complete in treatment and inexpensively priced.

The book is divided approximately equally between the general areas of organic chemistry and physical chemistry of synthetic organic polymers. In addition, there is a chapter on inorganic and "semi-inorganic" polymers, and a chapter on natural organic polymers. The latter contains a good introductory coverage of the chemistry of cellulose and is a valuable addition. The former will undoubtedly confuse the uninitiated into believing that the preparation and characterization of inorganic polymers is at a more advanced state than it actually is today. This uncritical treatment of the preparation and properties of inorganic polymers is unfortunate.

Nevertheless, the treatment of polymerization reaction mechanisms in this book is somewhat more complete than Billmeyer's although the coverage of anionic and cationic polymerization of olefinic monomers is less than satisfactory. The physical chemistry section is thorough in its treatment of the fundamentals, but it is not as up to date as one could desire. For example, there is no reference to single-crystal formation or the lamellar structure of polymer crystals, both of which are covered in detail by Billmeyer.

One major criticism of this book is the lack of adequate documentation of each subject. In this respect, both this book and Billmeyer's book are far inferior to *Introduction to Polymer Chemistry*, by J. K. Stille (Wiley, 1962, 248 pp., \$6.95) which, however, is almost completely lacking in a treatment of the physical chemistry of polymers for a one-semester, introductory course.

In spite of these shortcomings, this book more than adequately fulfills the purposes for which it is intended. It is both a fine, basic text for a one-semester, survey course on the entire field of polymer chemistry and a readable discussion of the fundamentals for workers in the field.

Robert W. Lenz

Fabric Research Laboratories, Inc.
Dedham, Massachusetts